Top-Down In-Situ Combustion in Heavy Oil Reservoirs Having Strong Bottom Aquifer Support

Mohammed Omar Salim Al Manahali

BSc, MSc Petroleum Engineering

A thesis submitted for the degree of Doctor of Philosophy
Institute of Petroleum Engineering, Heriot-Watt University,
Edinburgh, Scotland.

May 2010

Abstract

The underlying sustained demand for oil despite fluctuations in the oil price, and the requirement to replace dwindling reserves, both encourage oil companies to consider developing heavy oil reservoirs through implementation of EOR methods. Injection of air into the reservoir and initiation of a fire front causes the reservoir temperature to increase with a resulting decrease in the viscosity of the oil; this results in higher production rates and a better recovery factor.

The main objective of this study is to investigate numerically the potential for applying the combustion process using a combination of real field data (from the Nimr field) and data from the literature, and to evaluate the overall process performance. This entails using a 2D cross-sectional model, which is constructed based on available field properties, to enable a detailed investigation of the fire front behaviour. The optimum operating conditions for the in-situ combustion process are determined by conducting a suite of sensitivity calculations. These sensitivity calculations are divided into two groupings, classified as well configurations and reservoir heterogeneities. Under both groupings, the modelling of the combustion process also considered the presence of the strong bottom water aquifer support.

The results of this study suggest that the application of in-situ combustion in the heavy oil reservoir with strong bottom water aquifer is a technically viable proposition. The appropriate choice of well configurations is considered to be a vital component in the successful implementation of the combustion process, and leads to better process performance in terms of increasing the recovery factor. The presence of aquifer support should be regarded as a challenge to the initiation and sustaining of the fire front, and hence a carefully selected well placement plan (e.g. top-down) could make the difference between success and failure of the process. Depending on the well configurations selected, the impact of reservoir heterogeneities on the combustion process varied significantly. The combustion process recovery factor decreased as the fire front velocity changed, which is due to the large volume of coke been produced and deposited. This modelling study demonstrated the main approaches to optimise the combustion process performance, and while some data is field specific, the modelling results are generic.

to my

Parents, Brothers, Sisters and Fiancée

for their

Prayers, Love, Support, Patience and Encouragement

Acknowledgement

In The Name of Allah, The Most Gracious, The Most Merciful

Praise be to Allah (God), the one who blessed me with the spirit and his great bounties which enabled me to carry out this research and complete my PhD thesis.

My sincere gratitude and thanks go to my supervisor, Dr. Eric Mackay. With his enthusiasm, his inspiration and his great efforts to explain things clearly and simply throughout my thesis work and writing period. He provided encouragement, sound advice, good teaching and lots of great ideas. I would have been lost without his valuable feedback. I also would like to thank Dr. Suat Bagci for his contribution on early stages of my research. I would like to thank Dr. Ann Muggeridge and Dr. Karl Stephen for spending time reading and examining my thesis. Also, I would like to thank CMG support team for their great help throughout the study.

I would like to thank Petroleum Development Oman (PDO) through its financial support to my scholarship and also I would like to thank John VanWunnik and David Brooks for their precious discussions and time spent with me when I visited PDO. My deep gratitude to Khalid Rawahi and Hamed Hadhrami, for thier great support.

Without the companionship of my colleagues and friends, the time spent doing this work would have been much difficult. I would like to thank Yusuf Zaabi and Yasser Tabook who always stood for me when I needed them mostly. I would like to thank everyone helped me to be at this point at this time. Thank you all.

Finally, and most deeply, I thank my parents, brothers, sisters and friends back home for their patience, encouragement and prayers. My Special thanks go to Uncle Ali for his support and valuable advice throughout the years of my studies. Thank you all for everything.

Academic Registry

Research Thesis Submission

Name*:*	Mohammed Omar Salim Al Manahali		
School/PGI:	IPE		
Version: *(i.e. First, Resubmission, Final)*	First	Degree Sought *(Award and Subject area)*	PhD

Declaration

In accordance with the appropriate regulations I hereby submit my thesis and I declare that:

1) the thesis embodies the results of my own work and has been composed by myself
2) where appropriate, I have made acknowledgement of the work of others and have made reference to work carried out in collaboration with other persons
3) the thesis is the correct version of the thesis for submission and is the same version as any electronic versions submitted*.
4) my thesis for the award referred to, deposited in the Heriot-Watt University Library, should be made available for loan or photocopying and be available via the Institutional Repository, subject to such conditions as the Librarian may require
5) I understand that as a student of the University I am required to abide by the Regulations of the University and to conform to its discipline.

* *Please note that it is the responsibility of the candidate to ensure that the correct version of the thesis is submitted.*

Signature of Candidate*:*		Date:	

Submission

Submitted By *(name in capitals):*	Mohammed Omar Salim Al Manahali
Signature of Individual Submitting:	
Date Submitted:	

For Completion in Academic Registry

Received in the Academic Registry by *(name in capitals):*			
Method of Submission *(Handed in to Academic Registry; posted through internal/external mail):*			
E-thesis Submitted (mandatory from January 2009)			
Signature:		Date:	

Table of Contents

List of Tables

List of Figures

Nomenclature

Abbreviation:

EOR = enhanced oil recovery

API = American petroleum institute

IFT = interferential tension

PV = pore volume

ppm = part per million

MMP = minimum miscibility pressure

OOIP = original oil in place

FCM = first contact miscible

LPG = liquid petroleum gas

MCM = multiple contact miscible

WAG = water alternating gas

CSS = cyclic steam stimulations

SAGD = steam assisted gravity drainage

CMG = Computer Modelling Group

K_v/K_h = vertical permeability to horizontal permeability ratio

USSR = Union of Soviet Socialist Republics

U.S. = United States

COFCAW = combination of forward combustion and water flooding

AOR = air oil ratio

GOR = gas oil ratio

COSH = combustion override split-production horizontal

2D = two dimensions

3D = three dimensions

THAI = toe-to-heel air injection

MOZ = mobile oil zone

THSF = toe-to-heel steam flood

VI = vertical injector

VP = vertical producer

HI = horizontal injector

HP = horizontal producer

1D = one dimension

LDOD = long distance oil displacement

SDOD = short distance oil displacement

LTO = low temperature oxidation

HTO = high temperature oxidation

OIIP = oil initially in place

H/C = hydrogen to carbon ratio

ARC = accelerating rate calorimetre

RTO = ramped temperature oxidation

STOIIP = stock tank oil initially in place

PDO = Petroleum Development Oman

STARS = steam, thermal and advanced reservoir simulator

HO = heavy oil

LO = light oil

FDP = field development plan

PVT = pressure, volume and temperature properties

Soi = initial oil saturation

Swi = initial water saturation

Sgi = initial gas saturation

SCAL = special core analysis data

Krw = water relative permeability

Kro = oil relative permeability

Krg = gas relative permeability

Krog = oil/gas relative permeability

CPU = central processing unit

BC = base case

ICV = inflow control valve

Symbols:

t = time (day)

μ = viscosity (cp)

D = depth (ft)

h = thickness (ft)

Tr = reservoir temperature (°F)

Ø = porosity (ft^3/ft^3)

k = permeability (mD)

Pr = reservoir pressure (psi)

So = oil saturation (ft^3/ft^3)

T = temperature (°F)

Soi = initial oil saturation (ft^3/ft^3)

Swi = initial water saturation (ft^3/ft^3)

Sgi = initial gas saturation (ft^3/ft^3)

Chapter 1

Overview

1.1 Introduction

As conventional oil fields reach maturity and global demand for oil increases, there is a shift to production from non-conventional oil reservoirs. They have recently become an important resource as conventional oil reservoirs are in decline. Heavy oil reservoirs are considered to be non-conventional oil reservoirs, and are sometimes ignored as a source of oil because of the difficulties and cost involved in their development, which reduces their economic viability.

The increase in oil prices over the past decades has increased the viability of applying enhanced oil recovery (EOR) methods to recovery from non-conventional oil reservoirs. The main objective of an EOR method is to achieve higher overall oil recovery and higher production rates. The low recovery for heavy oil is mainly due to its high viscosity, i.e. too viscous to flow through the formation to the producer wells at rates sufficient to support an economic operation. Thermal EOR methods are required for production from heavy oil reservoirs, where hot fluid or air for combustion is injected with the aim of increasing the reservoir temperature to reduce the viscosity of the heavy oil. The oil production rate increases as the reservoir temperature increases; this is due to the dramatic effect of temperature on the viscosity of heavy oil. Moreover, horizontal well technology has contributed significantly to improving light oil as well as heavy oil recovery. By combining advanced horizontal well concepts with EOR methods this results in enhancement to fluid flow in a heavy oil reservoir which is radically different to that occurring in a conventional EOR method when vertical wells are used.

1.2 Heavy oil

It is known that hydrocarbon resources remain very extensive; worldwide there are extraordinary reserves of heavy oil and bitumen. This is true in the sense that we will never produce the last barrel, according to the available production technologies. However, most agree that the time of conventional oil, oil that was easy and cheap to find and produce, is coming to an end. The easy availability of petroleum resources supported the high level of economic growth that has been experienced over the last 150 years and helped sustain the six-fold increase in population growth. This high growth period was fuelled by light oil, which is mostly above 20°API. Around 70% of these reserves come from about 300 giant oil fields with reserves greater than 500 million barrels (Lanier, 1998).

The available oil for future production is identified by how much oil has been produced so far, the estimate of oil reserves in place, and a forecast of oil that is yet to be discovered. Production rates are readily available because production and sales volumes are metered. Reserves are more difficult to estimate. Forecasting future discoveries presents challenges because analysis requires backdating reserve additions to the date the field was discovered versus the date the reserve estimates were modified. There are many forecasts for future oil reserves, but most agree that conventional oil will be a much smaller portion of future energy resources. As for oil demand, the International Energy Agency (IEA) projects that the global energy demand will increase by 1.7 to 2% per year in the period between 2000 to 2030. On the other hand, the supply of energy in the form of cheap conventional oil is declining by 3% (Gaviria et al, 2007). This means that the non-conventional oil production will have to fill the gap, of which a majority will be heavy oil. The impact of non-conventional oils may be significant, but only if the technology is available to ensure heavy oil asset values are realised.

1.2.1 Crude oil classifications

According to the American Petroleum Institute (API) classification heavy oil is defined as oils which have API gravities fall between 10.0° and 22.3°. Moreover, extra heavy

oils are defined as having API gravities less than 10.0° API (Hinkle et al., 2006). Table 1.1 shows the API classifications, which use both the API gravities and viscosities to distinguish between the different types of crude oils. The difference between extra heavy oil and bitumen is the crude viscosity, where the former has a viscosity less than 10,000 mPa.s, and the later has a viscosity grater than 10,000 mPa.s (Nasr et al., 2005).

Classification	API^{o}	In-Situ Viscosity (mPa.s)
Light	>31.1	
Medium	22.3 – 31.1	
Heavy	10 – 22.3	
Extra Heavy	<10	<10000
Bitumen	<10	>10000

Table 1.1: *API classifications of crude oils (Nasr et al., 2005)*

1.2.2 Heavy oil distribution

Heavy oil/bitumen is found worldwide, with both Canada and Venezuela dominating resource potential. The true resource base is believed to be much larger since heavy oil discoveries are not often well defined or documented unless developable in the current market environment (Lanier, 1998). Around 7 trillion barrels of oil in place have been attributed to those heaviest hydrocarbons reservoirs worldwide (Albahlani et. al., 2008). This is more than three times the amount of combined world reserves of conventional oil and gas. Figure 1.1 shows heavy oil reservoirs distribution around the world. The heavy oil deposits of Canada and Venezuela together may account for about 55–65% of the known < 20° API oil deposits in the world (Hinkle et al., 2006). As an example of Canadian massive bitumen reserves, the province of Alberta holds the world's largest reserves of bitumen as shown in Figure 1.2, which compares Alberta bitumen reserve with some of the world proven oil reserves (Nasr et al., 2005).

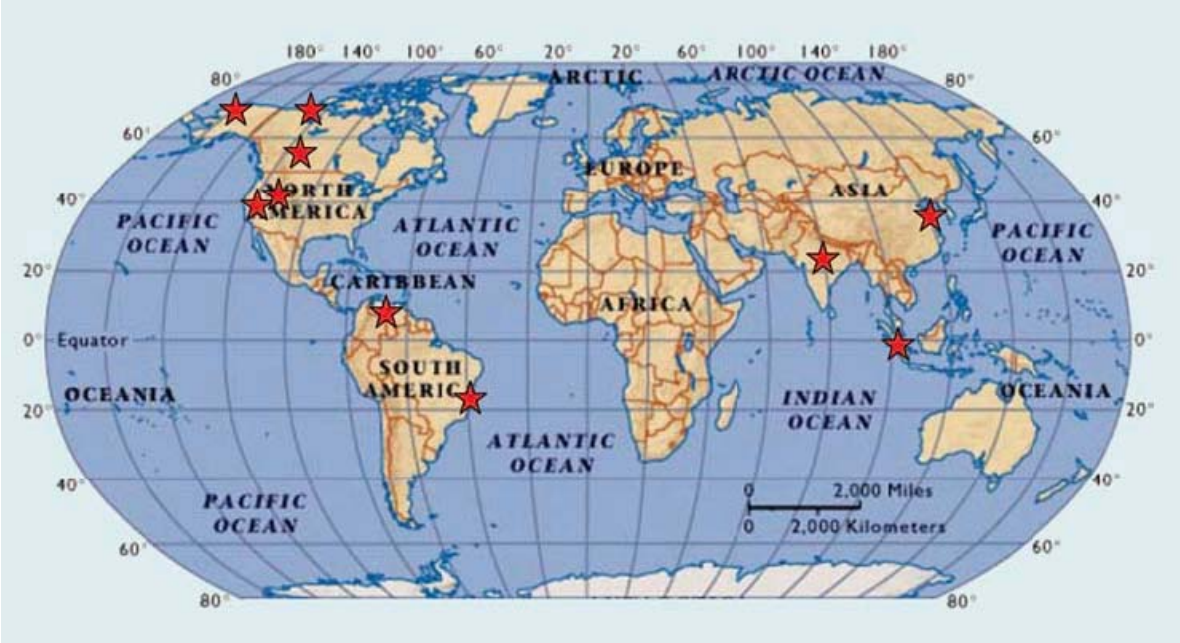

Figure 1.1: *Distribution of heavy oil reservoirs around the world (Hinkle et al., 2006)*

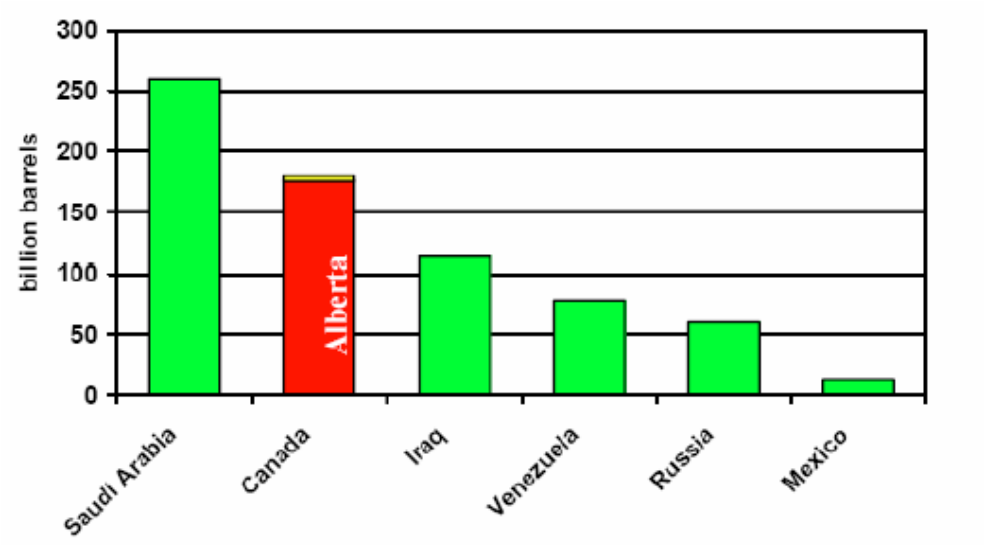

Figure 1.2: *Comparison of Alberta's proven reserves of bitumen and the proven reserves of some of the conventional oil producers' countries (Nasr et al., 2005)*

1.3 Enhanced oil recovery (EOR)

1.3.1 EOR definition

By one definition, enhanced oil recovery (EOR) means the extra recovery of liquid hydrocarbons from known oil or tar sand reservoirs not technically or economically feasible when using conventional methods (Perry, 1981). Also, it can be defined as oil recovery by the injection of materials not normally presents in the reservoir (Lake, 1989). EOR is the application of different techniques with the objective to increase the amount of oil that can be extracted from an oil bearing formation. It requires the injection of fluids and energy into known oil reservoirs to produce additional oil.

Oil recovery operations have been subdivided into three stages, according to a typical reservoir development plan: primary, secondary, and tertiary stages. Historically, these stages described the production from a reservoir on a sequential basis. Primary production, the initial production stage, resulted from the naturally existing energy within the reservoir itself. It is oil recovery by natural drive mechanisms, solution gas, water flux, gas cap drive, or gravity drainage. Secondary recovery, the second production stage, usually was implemented after primary production decreased. Conventional secondary recovery methods are waterflooding, pressure maintenance, and gas injection. Tertiary recovery, the third stage of production, is implemented after the secondary recovery. Tertiary methods use miscible gases, chemicals and thermal energy to recover extra oil. The decision to progress from stage to stage in the reservoir development plan is taken based on the economical oil production rate that can be achieved during the pervious recovery stage. The added increment may be tertiary, but may be primary or secondary, depending on the reservoir and the oil in place. A well known example is the production of the heavy oils that occurs throughout much of the world. If the crude is extremely viscous, it may not flow at economic rates under natural drive mechanisms, so primary production would be negligible. For such reservoirs, waterflooding would not be feasible; therefore, the use of thermal recovery methods might be the only option to recover an economically significant amount of oil. In this case, a method of recovery considered to be a tertiary method in a normal, chronological

depletion sequence, would be used as the first method of recovery. Because of such situations, the use of “tertiary recovery” terminology fell into disfavour in petroleum engineering literature and the designation of “enhanced oil recovery” become more acceptable and popular.

EOR occurs principally where there is the injection of gases or liquid chemicals and the use of thermal energy. Hydrocarbons gases, carbon dioxide, nitrogen, and flue gases are among the gases used in EOR methods. A number of liquid chemicals are commonly used, including polymers, surfactants, and hydrocarbons solvants. Thermal methods typically consist of the use of steam, hot water, or in-situ generation of thermal energy through oil combustion in the reservoir rock. The injected fluids and injection process supplement the natural energy present in the reservoir to displace oil to a producing well. In addition, the injected fluids interact with the reservoir rock and fluids to create conditions favourable for oil recovery. These interactions might, for example, result in lower interferential tension (IFT), oil viscosity reduction, wettability modification, etc. The interactions are attributable to physical and chemical mechanisms and to the injection or production of thermal energy. Most EOR methods involve the injection of more than one fluid. In a typical case, a relatively small volume of an expensive chemical may be injected to mobilise the oil. This small volume is displaced with a larger volume of a relatively inexpensive chemical. The purpose of following such procedures is to reduce the total expense of the operation (Green & Willhite, 1998; Lake, 1989).

1.3.2 EOR methods

The main EOR methods can be categorised into three principal groups: chemical, gas injection (miscible), or thermal methods. Chemical methods are those in which certain chemicals, such as surfactants or alkaline agents, are injected to use a combination of phase behaviour and IFT reduction to displace oil. In gas injection methods, the objective is to inject fluids that are directly miscible with the oil or that generate miscibility in the reservoir through composition alteration. Phase behaviour changes are a major factor in the application success of such processes (more details about Chemical EOR and Gas injection methods are presented in Appendix A). Thermal methods rely

on the injection of thermal energy or the in-situ generation of heat to improve oil recovery. Reduction of oil viscosity and chemical reaction is the primary mechanisms leading to improved oil recovery (Lake, 1989; Green & Willhite, 1998).

Thermal EOR methods: Thermal methods account for the biggest share of the world's enhanced oil production (Taber et al, 1996). All thermal recovery processes tend to reduce the reservoir flow resistance by reducing the viscosity of the crude as shown in Figure 1.3 for a sample of Athabasca bitumen. Thermal recovery methods, such as steam flooding, in-situ combustion, and cyclic steam stimulation are effective in lowering the oil viscosity and enhancing its recovery. The thermal recovery processes used today fall mainly into two categories: those in which a hot fluid is injected into the reservoir (i.e. steam injection) and those in which heat is generated within the reservoir itself. The latter are known as in-situ processes, an example of which is in-situ combustion or fireflooding. Thermal recovery processes also can be classified as thermal drives or stimulation treatments. In thermal drives, fluid (e.g. hot water injection) is injected continuously into a number of injection wells to displace oil and obtain production from other wells. The pressure required to maintain the fluid injection also increases the driving forces in the reservoir, increasing the flow of crude. Thus, a thermal drive not only reduces the flow resistance but also provides a force that increases flow rates. In thermal stimulation treatments, only the reservoir near the production wells is heated (i.e. cyclic steam stimulation). Driving forces present in the reservoir such as gravity, expansion of solution gas, and natural water drive improve the recovery rates once the flow resistance is reduced. Stimulation treatments also can be combined with thermal drives, in which case the driving forces are both natural and imposed. In thermal stimulation treatments, the reduction in flow resistance also may result from the removal of organic or other solids from openings in the casing, the liner, the screen, and even from the pores of the reservoir rock (Prats, 1982; Nasr et al, 2005).

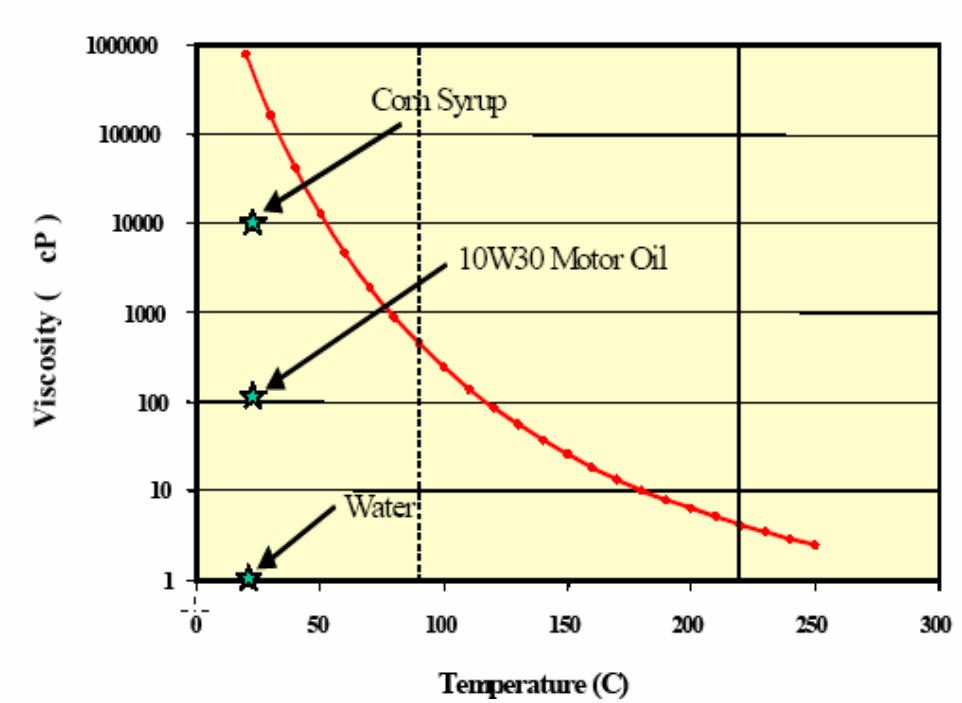

Figure 1.3: *A typical viscosity versus temperature profile of Athabasca bitumen (Nasr et al, 2005)*

There are four main thermal related EOR processes applied in heavy oil fields.

Hot water injection: Hot water flooding is said to be almost as old as conventional waterflooding, although early operations have not been documented adequately. In this process, the water is filtered, treated to control corrosion and scale, heated, and if necessary, treated to minimize the swelling of clays in the reservoir. The primary role of the heated water is to reduce the oil viscosity to improve the displacing efficiency over that obtainable from a conventional waterflood. The design and operation of hot water drives have many elements in common with conventional waterflooding. In hot water floods, the gravity separation usually is accentuated by the increased density difference between water and oil as temperatures increase. Because of this buoyancy and other factors, the contours of equal temperature and saturation are not vertical within the reservoir (Prats, 1982).

Steam injection: It is also called steam drive or steamflood. Steam injection is more effective than hot water drive due to latent heat of vaporization that can be accounted for from the steam. In this method, steam is injected through injection wells and the

fluids are displaced toward production wells that are drilled in specified patterns, as shown in Figure 1.4.

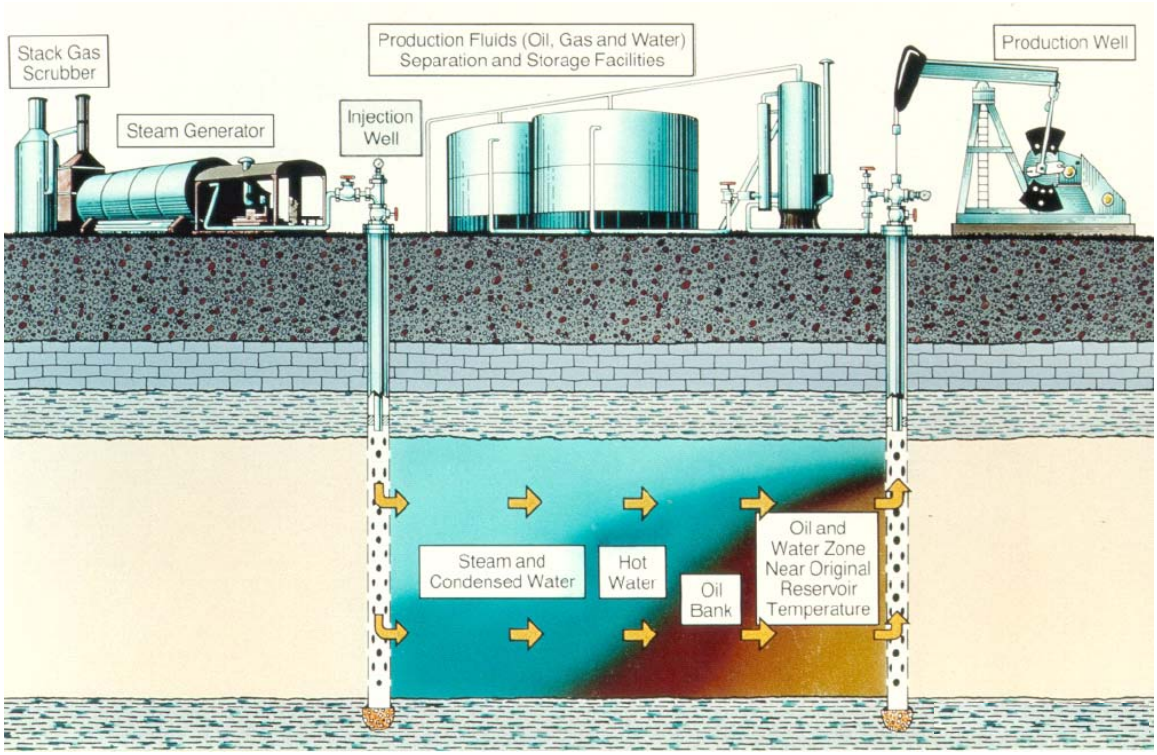

Figure 1.4: *Steam injection process (U.S. DOE, 1986)*

Recovery mechanisms in this method are based on viscosity reduction, steam stripping, and steam vapour drive. As the steam loses energy in its movement through the reservoir, condensation to liquid water occurs. Therefore, the process consists of a hot waterflood in the region of condensation followed by steam displacement. The process has been applied primarily to low API gravity, high viscosity oils but is also applicable to lighter crudes (Green & Willhite, 1998). Steam injection, also, promotes the formation of a low viscosity oil bank near the condensation front. It usually yields low residual oil saturations, and improves the effective mobility ratio of the displacing process. In the steam stripping process, steam removes relatively light components from the crude, much as a dry current of air passing over a pool of water lowers the vapour pressure and picks up moisture. Steam stripping removes a larger fraction of the crude than would be suggested by its boiling point distribution. For example, the boiling point distribution of particular crude might indicate that 20% of the crude boils at 400°F (ca. 200°C), but when the vapour pressure is maintained at a low level by the flowing

vapour, more than 20% of the crude would be removed (Prats, 1982). As the steam condenses, most of the stripped components in the steam also condense, and these light ends condensing at the steam condensation front help to improve the displacement efficiency. The mixing of the condensing light ends with crude reduces the viscosity of the crude contacted by a subsequent advance of the condensation front. Eventually, the oil bypassed by the advancing condensation front is so light and distillable that it shrinks significantly as steam continues to pass by. Such shrinkage of the bypassed oil can result in very low ultimate values for the residual oil in steam drives. In addition, the condensation phenomenon itself, quite apart from any distillation effects, results in more favourable effective mobility ratios than would have been expected on the basis of viscosity ratios alone.

A major problem with steam processes is that the steam density is much lower than that of oil and water and therefore the steam tends to move to the top of a reservoir, overriding a large part of the oil body. This is compensated for partially by heat conduction away from the zone of actual contact by the steam, however, and the heated portion of a reservoir can be a high percentage of total reservoir volume. The heated volume depends significantly on the reservoir structure. Mobility control is also a problem with the steamflood process because steam viscosity is small compared with the viscosities of liquid water and oil. Other points of concern include heat losses, equipment problems from operating at high temperatures, and pollutant emissions resulting from surface steam generation (Green & Willhite, 1998).

Cyclic steam stimulation (CSS): This process is known by a number of names: steam soak, steam stimulation, huff ‘and’ puff, and cyclic steam injection. In CSS recovery process, high temperatures steam is injected into a production well for a specified period (Figure 1.5). The well is then closed in for a while, the so-called "soak" part of the process. The well is next opened for production, which continues until flow rates diminish to a point when the entire procedure is repeated. A typical well may go through several cycles, with the effect of the steam gradually diminishing with continued applications. The pressure dilates or fractures the formation and the heat reduces the viscosity of the oil. The heated oil is then pumped up to the surface, from the same injection well (Green & Willhite, 1998; Nasr et al., 2005).

In CSS, production is increased through a combination of mechanisms, including viscosity reduction, steam flashing and steam stripping. The cumulative effect of these mechanisms is greatest for heavier oils with high viscosities. CSS is popular because the production response is obtained earlier and the amount of recovered oil per amount of steam injected is often higher than in thermal drives. Also, relatively small steam boilers can be used, and they can be moved from well to well. Wells can be steam soaked several times, the main requirements being natural driving forces, such as solution gas or gravity drainage, and sufficient oil near the wells (Prats, 1982).

The drawback is the recovery of CSS as percentage of the OOIP, which is much lower than other thermal recovery processes, especially in conventional CSS that uses only vertical wells for heavy oil (Nasr et al., 2005).

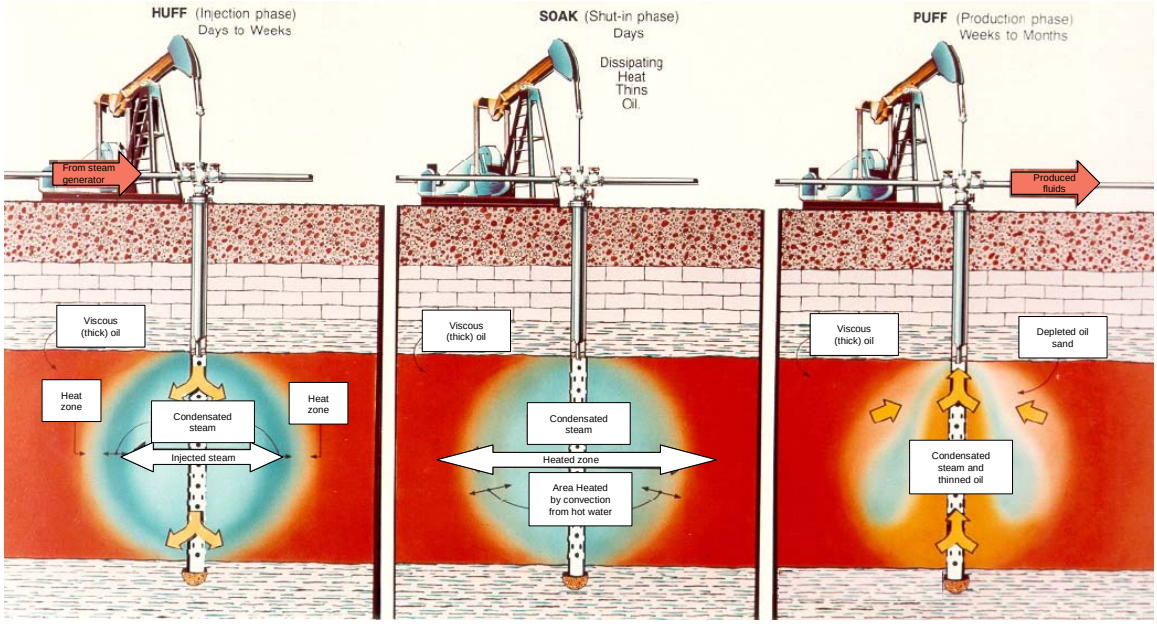

Figure 1.5: *Cyclic steam stimulation process (U.S. DOE, 1986)*

In-situ combustion: It is also known as fireflooding and Figure 1.6 illustrates the combustion process. In this process, thermal energy is generated in the reservoir by combustion, which may be initiated with either an electric heater or gas burner or may be spontaneous. Air is by far the most common way to introduce oxygen into a reservoir. It is compressed at the surface and continuously injected. In the heating and combustion that occur, the lighter components of the oil are vaporized and moved ahead. Depending on the peak temperature attained, thermal cracking may occur, and

vapour products from this reaction also move downstream. Part of the oil is deposited as a coke like material on the reservoir rock, and this solid material serves as the fuel in the process. Thus, as oxygen injection is continued, a combustion front slowly propagates through the reservoir, with the reaction components displacing vapour and liquids ahead toward production wells (Green & Willhite, 1998; Prats, 1982).

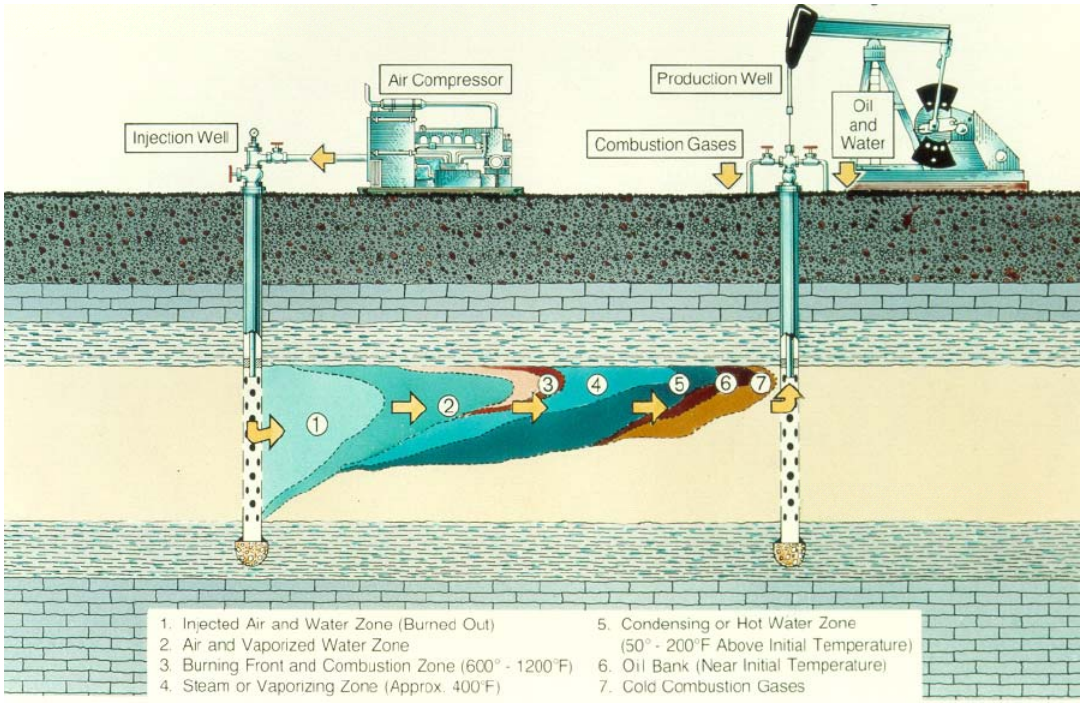

Figure 1.6: *In-situ combustion process (U.S. DOE, 1986)*

There are three different types of in-situ combustion. Dry in-situ combustion exists where air (oxygen) is the only injectant into the well. In wet combustion, water is injected along with air. The water effectively picks up energy in the burned zone behind the front. In the third type, not often applied, the combustion is carried out in a reverse manner. Combustion is started at the production wells. Oxygen is still injected at injection wells and so the combustion zone moves in the direction opposite to the fluid flow (Green & Willhite, 1998).

Recovery mechanisms include viscosity reduction from heating, vaporization of fluids, and thermal cracking. Injected gases and water, from both the water of combustion and recondensed formation water, pick up energy as they pass through the burned zone and move toward the combustion front. Ahead of the combustion front, a steam plateau

exists (i.e., a region of condensing steam in which the temperature is almost constant at the steam saturation temperature) corresponding to the reservoir pressure. A hot waterflood essentially exists in this region, much in the same manner as in a steam injection process. Ahead of the steam plateau, the temperature decreases to the original reservoir temperature (Green & Willhite, 1998; Al-Wadhahi et. al., 2005).

In in-situ combustion the wellbore near the pay zone, or for that matter any part of the injection well that might come in contact with free oxygen and fuel (crude), should be designed for high thermal stresses. Crude is likely to enter the well bore by gravity drainage where the air enters the formation preferentially over a short segment of a large open interval having adequate vertical permeability. This crude inflow may be increased as the reservoir temperature near the wellbore increases as a result of the heat generated either by the ignition system used in the wellbore or by the combustion process itself, including reverse combustion following spontaneous ignition a short distance into the reservoir. In designing injection wells, precautions should be taken against any likelihood of combustion in the wellbore. Injection wells generally require special design considerations since they are specifically vulnerable to the fire front process. Production wells, on the other hand, can be expected to be affected by corrosion, erosion, and high temperature from the producing interval to the wellhead, the most severe conditions being at the producing interval. The standard well equipment, therefore, must be modified accordingly. The degree of modification depend on the crude and water in the reservoir, the friability of the sand, the steel used in the tubing and casing, the method of well completion, the amount of heat and free oxygen, and the type of in-situ combustion process or control measures used (Prats,1982).

In-situ combustion as a thermal EOR method has the following main advantages compared to other thermal EOR methods (Taber *et al*, 1996):

- it utilizes the two cheapest and most plentiful of all EOR injectants: air and water.
- for fuel, it burns about 10% of the least desirable fraction of the oil, and may upgrade the rest.
- it works over a wider range of field conditions than steam injection.

- it involves a combination of advantages of various recovery methods such as hot water flooding, carbon dioxide flooding, miscible gas injection and steam injection.
- it is thermally efficient since heat is generated in-situ in the formation. Whereas in a steam injection process, heat is generated at the surface and extensive heat loss occurs when steam is transported to the formation, especially in deep formations.
- it can be applied as a sequel to other EOR processes, such as steam and water flooding.
- the total recovery factor of the combustion process is generally higher than other heavy oil recovery methods.

A major problem with in-situ combustion methods is control of the movement of the combustion front. Depending on reservoir characteristics and fluid distributions, the combustion front may move in a nonuniform manner through the reservoir, with resulting poor volumetric contact. Also, if proper conditions are not maintained at the combustion front, the combustion reaction can weaken and cease completely. The process effectiveness is lost if this occurs. Finally, because of the high temperatures generated, significant equipment problems can occur at the wells. Further details of the in-situ combustion recovery method and its various forms will be provided and discussed in Chapter 2 of this thesis.

1.3.3 EOR screening guide

Screening of the technical criteria is a good starting point for evaluating potential EOR methods for candidate reservoirs. It is vital to evaluate the reservoir characteristics, fluid properties, and reservoir rock fluid properties for the success of the EOR project. A suitable way to show EOR methods is to arrange them by oil gravity as Taber *et al.* (1996) suggested, and as shown in Figure 1.7. The size of the arrows representing the method is intended to show the relative importance of each of the EOR methods in terms of the incremental in oil production.

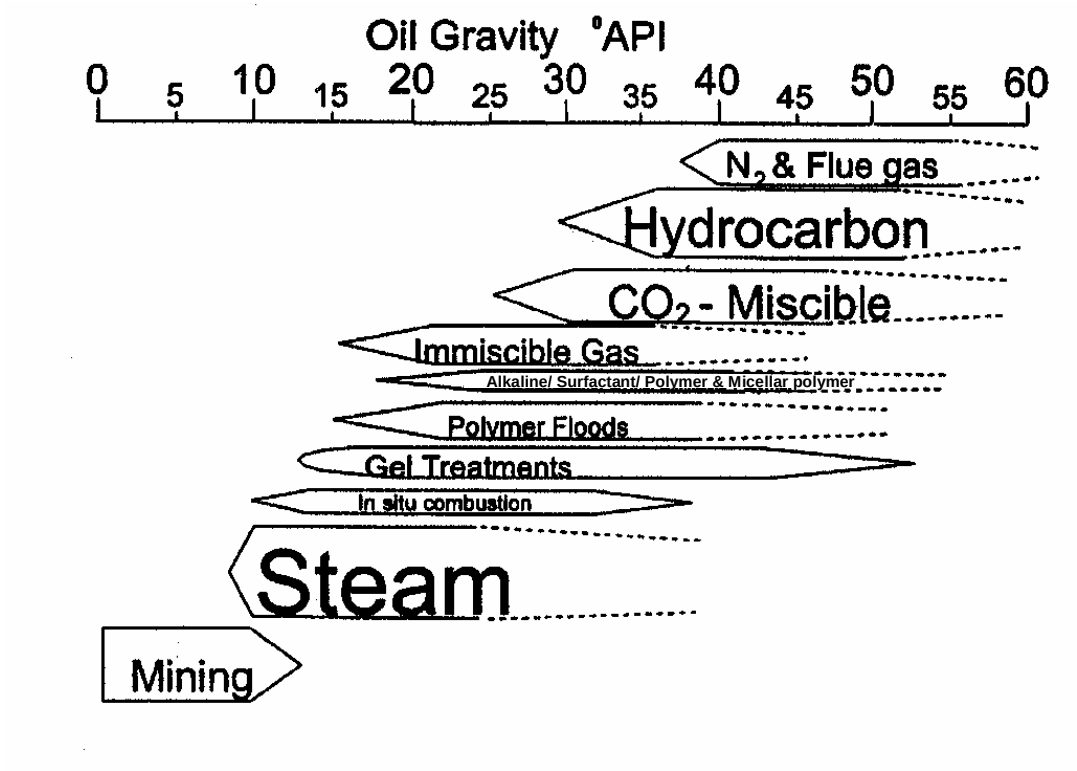

Figure 1.7: *Oil gravity range of oil that is most effective for EOR methods (Taber et al, 1996)*

Selecting and implementing an EOR method requires several steps (Figure 1.8). Initially, with a basic knowledge of reservoir properties and formation fluid characteristics a screening guide is consulted for judging the possible applicability of a particular method. This is followed by crude oil characterization, and reservoir rock property characterization. After selection of candidate methods, basic static tests are carried out. Methods which appear to be promising are then subjected to flow studies in porous media where a semi-realistic environment is introduced. The data resulting from these tests are often used as input variables for numerical simulators which have provisions for considering such properties as reservoir heterogeneity. Pilot projects demonstrate the viability of the selected method. Finally, assuming success at the lower screening levels, an EOR project is implemented in the field. It is essential to note that economic studies and evaluation are conducted throughout all these screening steps (Goodlett et al, 1986; Al-Wadhahi et. al., 2005).

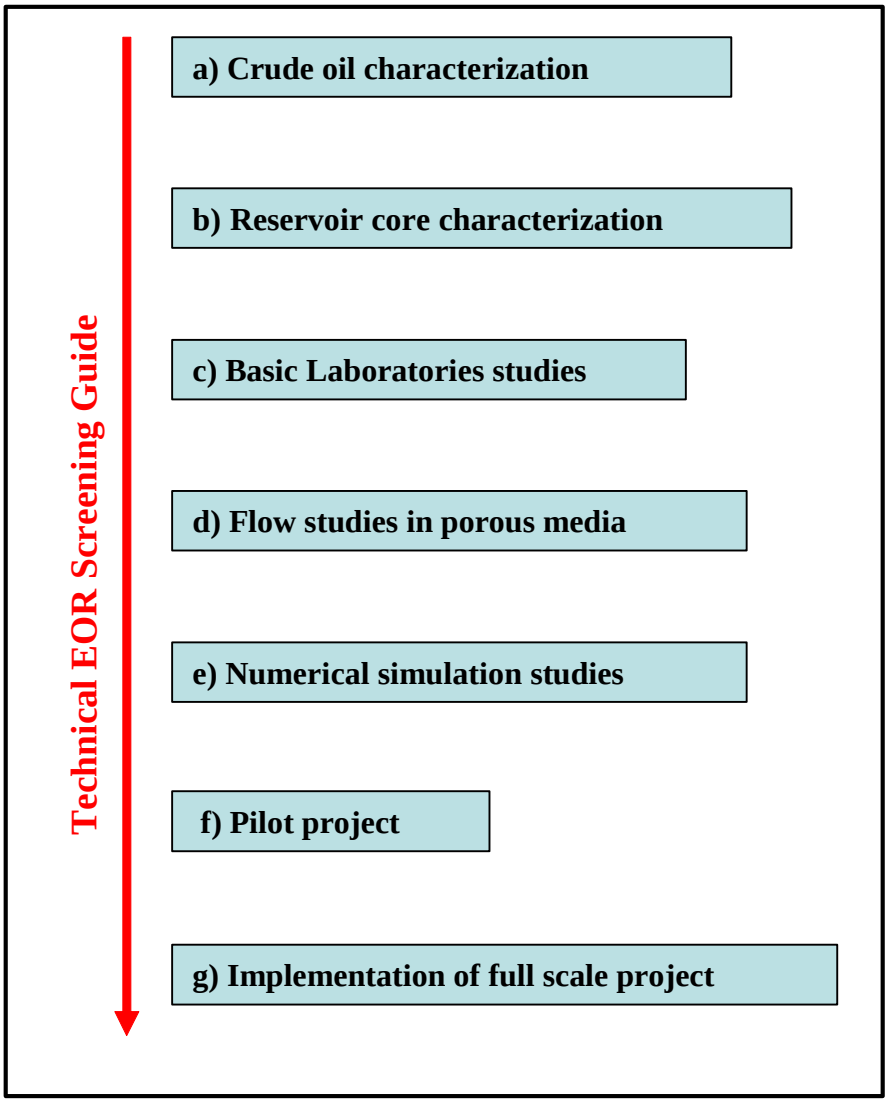

Figure 1.8: *Technical screening guide describing steps in development of filed EOR application (adapted from Goodlett et al, 1986)*

There are general technical criteria available in the literature which can be used to evaluate the applicability of EOR methods. These criteria reflect current estimates of the range of oil and reservoir properties over which the different processes are applicable. Green & Willhite (1998) provided some oil and reservoir characteristics for successful EOR methods, as shown in Table 1.2. Restrictions on the application of the processes exist. For example, the carbon dioxide miscible process is limited to reservoirs with sufficient depth to obtain the miscibility pressure and to oils that have relatively high API gravity because of miscibility pressure and/or mobility problems. Steam injection has reservoir depth limitations because of heat losses and the steam temperatures obtainable. Surfactant and polymer processes are generally limited because of salinity

and temperature and the associated difficulty of designing stable surfactant and polymer systems. The screening criteria shown in Table 1.2 are only approximate. Also, as the technology develops, the limitations will be relaxed to reflect new knowledge about known processes, variations of known processes, or even new processes (Taber et al, 1996).

	Oil Properties			Reservoir Characteristics					
EOR Method	Gravity°API	Viscosity (cp)	Composition	Oil Saturation (% PV)	Formation Type	Net Thickness (ft)	Average Permeability (md)	Depth (ft)	Temperature (°F)
Gas Injection Methods (Miscible)									
Nitrogen (& Flue Gas)	>35↗48↗[1]	<0.4↘0.2↘	High % of $C_1 - C_7$	>40↗75↗	Sandstone or Carbonate	Thin unless dipping	N.C.[2]	>6,000	N.C.
Hydrocarbon	>23↗41↗	<3↘0.5↘	High % of $C_2 - C_7$	>30↗80↗	Sandstone or Carbonate	Thin unless dipping	N.C.	>4,000	N.C.
Carbon Dioxide	>22↗36↗	<10↘1.5↘	High % of $C_5 - C_{12}$	>20↗55↗	Sandstone or Carbonate	(Wide range)	N.C.	>2,500	N.C.
Chemical									
Micellar/-Polymer, Alkaline/-Polymer (ASP), and Alkaline Flooding	>20↗35↗	<35↘13↘	Light, intermediate. Some organic acids for alkaline floods	>35↗53↗	Sandstone preferred	N.C.	>10↗450↗	<9,000↘3,250	<200↘80
Polymer Flooding	>15-<40	<150,>10	N.C.	>70↗80↗	Sandstone preferred	N.C.	>10[3]↗800↗	<9,000	<200↘140
Thermal									
Combustion	>10↗16→?	<5,000→1,200	Some asphaltic components	>50↗72↗	High porosity sand/ sandstone	>10	>50[4]	<11,500↘3,500	>100↗135
Steam	>8-13.5→?	<200,000↘4,700	N.C.	>40↗66↗	High porosity sand/ sandstone	>20	>200[5]	<4,500↘1,500	N.C.

1. Underlined values represent the approximate mean or average for current field projects. ↗ indicates higher value of parameter is better.
2. N.C. = not critical.
3. >5 md from some carbonate reservoirs.
4. Transmissibility >20 md ft/cp.
5. Transmissibility >50 md ft/cp.

Table 1.2: *Summery of screening criteria for EOR methods (Green & Willhite, 1998)*

1.4 Horizontal wells

The technology of horizontal wells for the production of crude oil from conventional and heavy oil reservoirs and tar sands has been implemented successfully in many fields. Horizontal wells provide a larger area of contact with the reservoir than do vertical wells and, in addition, they provide means for the lateral transportation of fluid. Thus, for example, a 1000m (ca. 3300ft) horizontal well in a reservoir 10m (ca. 33ft) thick has an area of contact 100 times larger than that of a vertical well completed through the depth of the reservoir. Often one horizontal well can replace several vertical wells which can be considered economic even though a single horizontal well may cost

more to drill and complete than a vertical well. In some cases, horizontal wells make recovery economic in situations where conventional wells would be impractical (Greaves et al, 1993).

In many cases, the most important factor limiting the production of oil from a reservoir is the tendency for water from an underlying aquifer, or gas from a gas cap, to be drawn vertically to the production well. Horizontal wells can have substantial advantages in such reservoirs. The conventional way of reducing the effect of coning is to complete the vertical well over a limited vertical distance to maximize the standoff from the water or gas cap, as the case may be. In these circumstances, the contact of the vertical well with the reservoir is reduced even further than it would be for a full height completion. The effect of reservoir thickness on the relative performance of a horizontal well is much smaller. Because of its extended contact with the reservoir, a horizontal well usually has less pressure drawdown for a given production rate than does a vertical well. This reduced drawdown reduces the tendency for the coning of water or gas with the produced oil. Thus, for example, horizontal wells may be operated at the same rate as conventional wells but with less coning. In some cases, production without coning may be economic using horizontal wells, where it would be prohibitively slow with vertical wells (Butler, 1994; Joshi, 1991a).

Horizontal well technology is now being used in EOR projects, especially in thermal oil recovery. Although horizontal wells have been used in miscible and waterflood projects, the main EOR applications to date are in steam projects. The main advantages of the use of horizontal wells are improved sweep efficiency, enhanced producible reserves, increased steam injectivity, and a decrease in the number of wells required for field development. This last point is especially important in thermal oil recovery projects, where several closely spaced vertical wells are required for economic development. However, the main disadvantage of horizontal wells is their initial cost. Horizontal well technology has contributed significantly to improving heavy oil recovery, by combining advances in horizontal well concepts with thermal EOR methods. The use of this technology in heavy oil production is based on the important increase of well productivity, better sweep efficiencies, and better control when a method of thermal recovery is used, and on the use of gravitational drainage mechanisms in low pressure

reservoirs. For example in a CSS process, a horizontal well is used as both injector and producer, with alternating injection and production cycles and a possible soak period. Compared with vertical wells, more steam can be injected into horizontal wells, which results in a significantly higher recovery. Another useful example of horizontal well technology application in EOR is the steam assisted gravity drainage (SAGD) method. Here, horizontal steam injectors and oil producers are located close to each other, with the injector located above the production well (Figure 1.9). A minimum pressure differential, close to the gravity head differential, is desirable between the injection and production wells. The injected steam travels upward, and hot displaced oil and condensate are collected in a bottom horizontal well, which is pumped off. The main advantage of the process over conventional steam injection is that hot oil is produced by gravity drainage as soon as it is displaced from the formation. Also, the steam chamber expands vertically upward initially and then sideways, significantly enhancing sweep efficiency (Joshi, 1991b; Cunha, 2005).

Implementation of horizontal wells concept in the combustion process, either as producer or injector, can improve the in-situ combustion front performance. For example, the use of horizontal producer can result in reduction of the pressure drawdown exerted by the producer in the reservoir and can help in establishing a uniform combustion front movement across the reservoir, which improve the sweep efficiency of the fire front. Also, the use of horizontal injector well, instead of the conventional vertical injector well, in the combustion process can initiate a wider combustion front, which enhances the process performance and would result in better recovery factor and shorter recovery time of the oil in the reservoir.

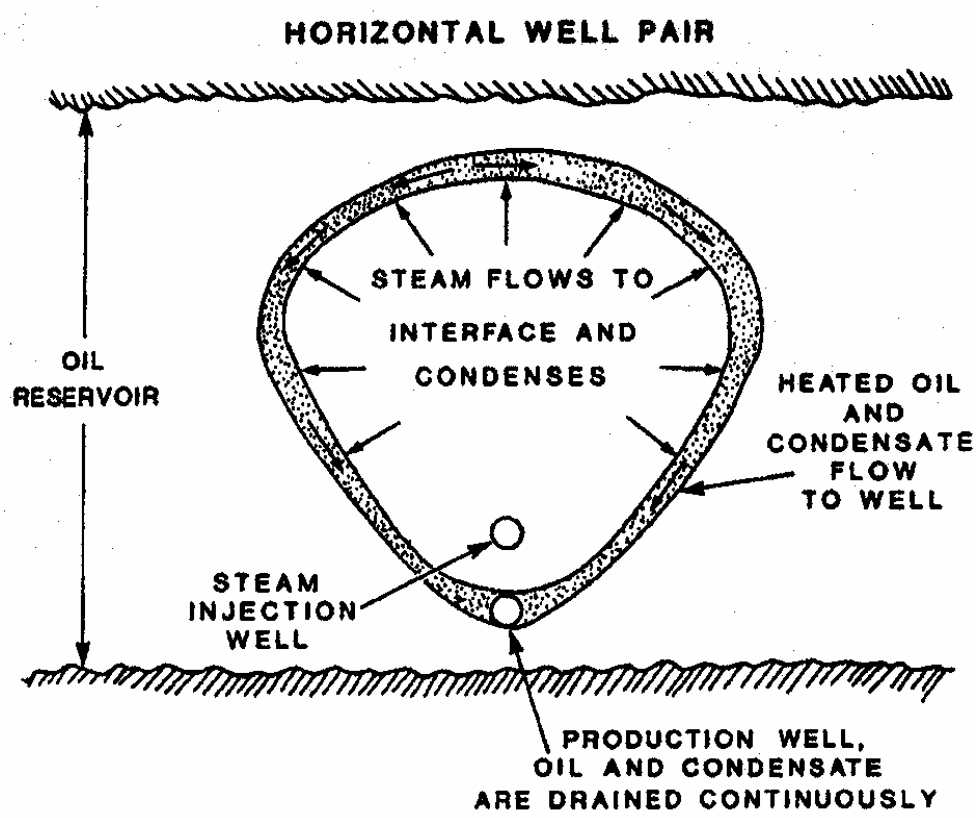

Figure 1.9: *Schematic of steam assisted gravity drainage (Joshi, 1991b)*

1.5 Objectives of this study

The main objective of this work is to perform a numerical simulation study of the top-down in-situ combustion process using the Computer Modelling Group simulator suite (CMG), and evaluate the performance of the process as a recovery method. The specific reservoir simulator used is STARS, which in purpose built to handle temperature changes and chemical reactions, such as those that occur during the in-situ combustion processes. The study is performed using data from the the Nimr field, which is located in the South of Oman, where real reservoir rock and fluid properties are used. The model construction relies on the available combustion data from the field, and for unavailable data the best practice data from the literature is used in the model.

Other secondary objectives include:

- Successfully initiate and sustain the fire front in the Nimr reservoir model, and optimise the combustion process,

- Investigate the effect of different well configurations, types, number, spacing, and completion on the fire front behaviour and process performance,
- Evaluate the effect of strong bottom aquifer support on in-situ combustion,
- Optimise the top-down well configuration uses in the model to maximise the combustion process recovery,
- Investigate several reservoir heterogeneity effects in the model.

1.6 Thesis contents

This thesis is developed in six further chapters. Chapter 2 presents a literature review on the main in-situ combustion topics that relate to this study. It mainly covers; combustion process types, new in-situ combustion processes, combustion recovery mechanisms, experimental and simulation studies, field applications and the main kinetics chemical reaction models. Chapter 3 concentrates mainly on data preparation and model development. This chapter includes an overview of the field used in the study, model parameters under investigation, and sensitivity analysis to manage successful initiation and progress of the fire front. Also, the main in-situ combustion simulation challenges, including numerical dispersion effects and the application of dynamic gridding are investigated. Finally, the base case model is defined. Chapter 4 investigates the use of several well configurations in the combustion process. Well types, completions, locations and numbers are evaluated and their effect on in-situ combustion is presented. Moreover, optimisation of well lengths and spacing are carried out in this chapter to provide the optimum model scenario in order to maximise the recovery factor of the fire front. In Chapter 5, strong bottom water aquifer support is introduced to the base case model and the combustion process performance is evaluated where several well scenarios are used. Chapter 6 presents further investigation of the successful application of in-situ combustion with the presence of several types of reservoir heterogeneities. The main reservoir heterogeneities investigated in this chapter are: Kv/Kh ratio, multiple permeability layers, discontinuous impermeable shale layers and shaley sand layer scenarios. Finally, Chapter 7 summarises the work carried out in this thesis and presents the conclusions that are drawn from it. Also, recommendations for future work

are presented in this chapter. It should be highlighted that while this study used some specific field data, the modelling results are considered to be generic.

Chapter 2

Literature Survey of In-Situ Combustion

2.1 Introduction

In situ is Latin for "in place". Thus, in-situ combustion is simply the burning of fuel where it exists in reservoir rocks. A classical definition of in-situ combustion is “the propagation of a high temperature front for which the fuel is a coke-like substance laid down by thermal cracking reactions” (Moore et al., 1999). It is a displacement process in which an oxygen containing gas is injected into a reservoir where it reacts with the crude oil to create a high temperature combustion front which is propagated through the reservoir. The heat generated then is used to help recover crude oil in place. In most cases, the injected gas is air which contains 21% of oxygen; however, in some cases an enriched gas is used where a higher concentration of oxygen is injected. The fuel consumed by the combustion front is a residuum produced by a complex process of cracking, coking, and steam distillation that occurs ahead of the combustion front. In-situ combustion is possible if the crude oil combination produces enough fuel to sustain the combustion front. In-situ combustion field tests have been carried out in reservoirs containing API gravities from 9° to 40° API (Green & Willhite, 1998).

Combustion is started in the formation by injecting air that is heated to 400-1200°F (ca. 200-650°C), depending primarily on the reservoir initial temperature and the temperature oxidation characteristics of the crude oil being ignited. Usually the air is preheated at the sand face of the injection well by a gas burner, electrical heater, or some other convenient method. However, in some reservoirs, the oil ignites spontaneously after air has been injected over some time. Since the combustion reactions are temperature sensitive and deep formations have high initial temperatures, this results in the occurrence of spontaneous ignition whenever air is injected to very deep formation. However, in shallow formations the combustion process initiation

requires several weeks of continuous heating, and in some cases the crude might never ignite, depending on the oil reactivity. When ignition occurs near the injector well, the burning front moves radially from the injection well at a rate governed principally by the type and amount of fuel burned, the air injection rate, and the oxygen content of the injected air (White et al, 1983).

2.2 Early history of in-situ combustion

The oldest known means of introducing heat into reservoirs is downhole heaters. The primary purpose of downhole heaters is to reduce the viscosity and increase the production rate of viscous crudes, but occasionally they also are used to maintain the crude at temperatures above the pour point as the crude moves to the surface, and to remove or inhibit the formation and deposition of organic solids such as paraffin and asphaltenes. Since the use of bottom hole heaters and equivalent hot fluid circulation systems can affect only the production borehole and its immediate vicinity, the practice is associated with stimulation, remedial, and preventive treatments.

The first means of in-situ combustion of reservoir crudes probably occurred during air injection projects used in the early 1900's to enhance oil recovery. In 1917, analyses of gas samples were carried out from several air injection projects in which the oxygen concentrations were deficient relative to those of nitrogen. Although carbon dioxide concentrations also were low, possibly indicating an oxygenation of the crude rather than active combustion, such oxygenation methods do produce heat. However, the generation of heat in those cases does not constitute an example of a thermal recovery process, for there was no apparent intent to generate and use heat in the reservoir.

As early as 1920, some key elements of underground combustion processes in oil reservoirs were recognised, including injection of air to burn part of the crude to generate heat and reduce the crude viscosity while providing a driving force to displace the oil. The first published large scale field operations of the underground combustion process were carried out in the USSR in 1933. Those tests, however, were carried out in coal seams in what is now known as an in-situ coal gasification process. The first

attempt at an application to oil reservoirs is also Soviet in origin and occurred in 1934. Beyond the initial attempt, however, the process does not appear to have been pursued further until about a decade later.

In the U.S., the first field applications of the combustion process are probably those starting in 1942. Although the intent was to radiate heat at 900°F (ca. 480°C) from a bottomhole heat exchanger into a watered out reservoir, rather than to inject the heated air into the formation, the early response at distant wells strongly suggests that hot air was injected into the formation. Increased production at several nearby wells was accompanied by increased gas flow rates, increased crude gravities, and increased temperatures, all typical of a combustion process. By the mid-1940s, the concept of burning a portion of the oil in the reservoir for the purpose of enhancing oil production began receiving serious attention from major oil companies in the U.S. The companies started investigating the process in the laboratory to learn about the parameters controlling the process. After that, the application of the process in field pilots began and proved to be technically successful and introduced a way to rapid development of this oil recovery technology (Prats, 1982; Sarathi, 1998; Breston, 1958)

2.3 Types of combustion processes

There are three known types of in-situ combustion process. Those are: dry forward combustion, wet forward combustion, and reverse combustion. The most commonly used form of in-situ combustion is dry forward combustion. In dry forward combustion, the combustion front is initiated and moves out from the injection well as air injection is continued. The combustion front moves in the same direction as the air. Wet combustion, also known as COFCAW (combination of forward combustion and waterflooding), uses water injection during the combustion process to recover the heat from the burned zone. In this process, the ratio of injected water to air is used to control the rate of advance of the combustion front, the size of the steam zone, and the temperature distribution. The reverse combustion process occurs when the combustion front moves in a direction opposite that of the injected air. Reverse combustion is

achieved by igniting the oil near a production well while temporarily injecting air into it. Upon continuation of the normal air injection program from the injector well, the combustion front moves toward the injection wells (Prats, 1982; Chu, 1977).

Laboratory experiments, numerical simulations and field tests have been widely used to investigate the in-situ combustion process. The results of these investigations have confirmed that the complex in-situ process has a number of distinct transient zones of varying physical and chemical importance. These zones, starting from the injection end, are the burned zone, combustion zone, cracking region, evaporation and visbreaking region, steam plateau, water bank, oil bank and initial zone, as Figure 2.1 shows. As the name suggests, the burned zone is the area where combustion had already taken place. If the combustion is completed efficiently, the burned zone should contain no residual oil or coke. The combustion zone is where reaction between oxygen and fuel takes place generating heat. Ahead of the combustion zone there is a cracking zone where high temperature generated by the combustion process cause some thermal cracking of the oil which produces the coke to be burnt in the combustion process. Further ahead lies the evaporation and visbreaking zone. The combustion gases, after loosing some of their heat in the cracking zone, enter this zone at somewhat lower temperature, and as such cause evaporation, which results in the creation of a steam plateau and visbreaking, which is a form of mild cracking. Some coke is also formed in this process and immediately ahead of this zone is the hot water bank zone resulting from the condensation of the steam. This is followed by the oil zone, which contains the light hydrocarbon fraction generated in the cracking and visbreaking zones, and finally the initial zone which is yet to be affected by the in-situ combustion process (Wu et al., 1971; Islam et al., 1989).

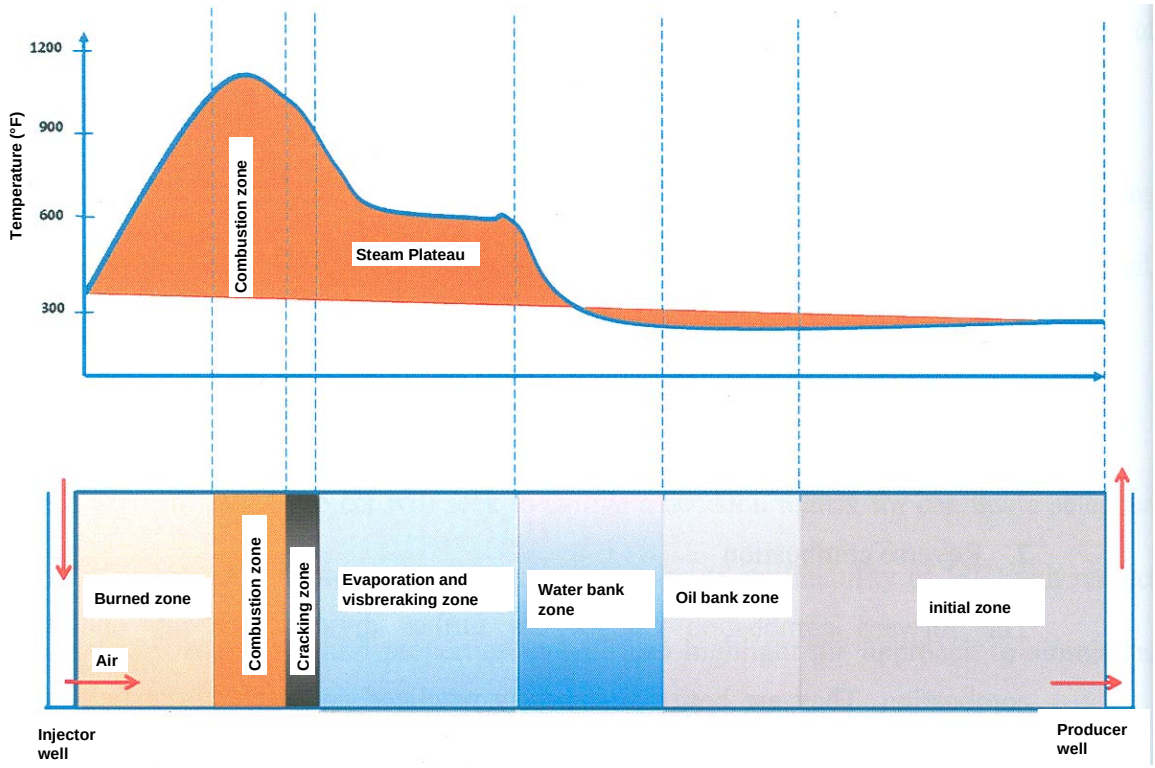

Figure 2.1: *In-situ combustion zones (adapted from Opata, 2008)*

In a fully developed front, hot combustion gases strip light ends from the crude oil flowing ahead of the front as a result of the high mobility of gas compared with that of liquids. Hydrocarbons stripped by the hot combustion gases and water vapour condense to form a small steam plateau of hot water and light hydrocarbon banks. The oil saturation that remains after steam stripping is subjected to thermal cracking as the combustion front approaches, leaving a residual deposit on the sand grains that is rich in carbon. This residuum becomes the fuel for the process. Typical equivalent oil saturations burned within the burned region are in the range of 6% to 12%; the rest of the crude is displaced (Green & Willhite, 1998; Prats, 1982).

The hydrocarbon products and other compounds released by the cracking process (SO_2, carbon monoxide, CH_4. and hydrogen) join the combustion gases and are either absorbed by crude oil ahead of the front or are produced in the effluent. It is necessary that fuel is consumed in order for the combustion front to advance. Thus, the rate of frontal advance is controlled by fuel availability and the rate that oxygen is delivered to the burning front.

2.3.1 Dry forward combustion

Dry forward combustion is a type of in-situ combustion in which the burning front moves in the same direction as the injected air. As air is continuously supplied at the injection well, the fire ignited at this location moves toward the production wells. In this process, the combustion front acts as a piston which pushes ahead of it the unburnt crude fractions from the swept zones. The heavier fractions are transformed into a carbonaceous deposit with a low hydrogen content, which is often improperly called "coke". This deposit is burned with the oxygen from the injected gas. In the case of efficient combustion process, the region swept by the combustion front usually no longer contains any organic compounds.

Temperature levels in dry forward combustion are affected by the amount of fuel (coke) burned per unit bulk volume of reservoir rock. The temperature levels in turn affect the displacement, distillation, stripping, cracking, boiling of the crude, and formation of fuel downstream of the combustion front. Temperatures in the range of 650 to 1,500°F (ca. 340 to 815°C) have been observed frequently both in the laboratory and in the field (Prats, 1982). At high temperatures, the combustion zone width is very small. At moderate temperatures, the combustion reaction proceeds slowly enough to allow significant leakage of free oxygen in the direction of flow, thus increasing the thickness of the reaction zones. At lower temperatures, a smouldering reaction with the bypassed air may occur over distances of several feet. This usually happens when unheated air is injected into oil reservoirs; the ensuing smouldering reaction generates heat and ultimately causes spontaneous ignition. Air bypassing may also occur in any part of the reservoir if the local air flux is very great, even when fuel is present and temperatures are high.

There are four main combustion zones in dry forward combustion as Figure 2.2 shows. These zones are numbered in the direction from the injector to the producer (Latil, 1980, Burger et al., 1985):

*Zone (*1) combustion process has already taken place and the formation in this zone is completely cleared of water and oil, which were consumed or displaced ahead of the front when the combustion front passed through this zone. Any further injected air is

heated by flowing through the hot matrix of this zone and part of the combustion energy is recovered in this way.

*Zone (*2) is called the combustion zone where oxygen is consumed by combustion reactions involving the hydrocarbons and the coke remaining on the rock surface. The temperature reached in this zone depends essentially on the nature of the solids, liquids and gases present per unit formation volume.

*Zone (*3) the coke formation zone: The heavy oil fractions which have been neither displaced nor vaporized undergo pyrolysis where large hydrocarbon molecules are broken into smaller molecules. These reactions may occur in the presence of oxygen if it manages to bypass the combustion zone.

*Zone (*4) where the temperature has fallen sufficiently, there are no further significant chemical changes. This zone is swept by the combustion gases and displaced fluids, and the following phenomena take place:

(a) In the downstream region nearest the reaction zone, successive vaporization and condensation of the light oil fractions and water take place. This tends to accelerate the downstream heat transfer.

(b) In the region where the temperature is lower than that of water condensation, a zone with a water saturation higher than the initial water saturation exists (water bank) which pushes a zone with an oil saturation higher than original (oil bank). If the oil is highly viscous this may result in plugging of the formation. In every case, these two banks are a zone of high pressure loss. Beyond the oil bank the formation progressively approaches its original conditions.

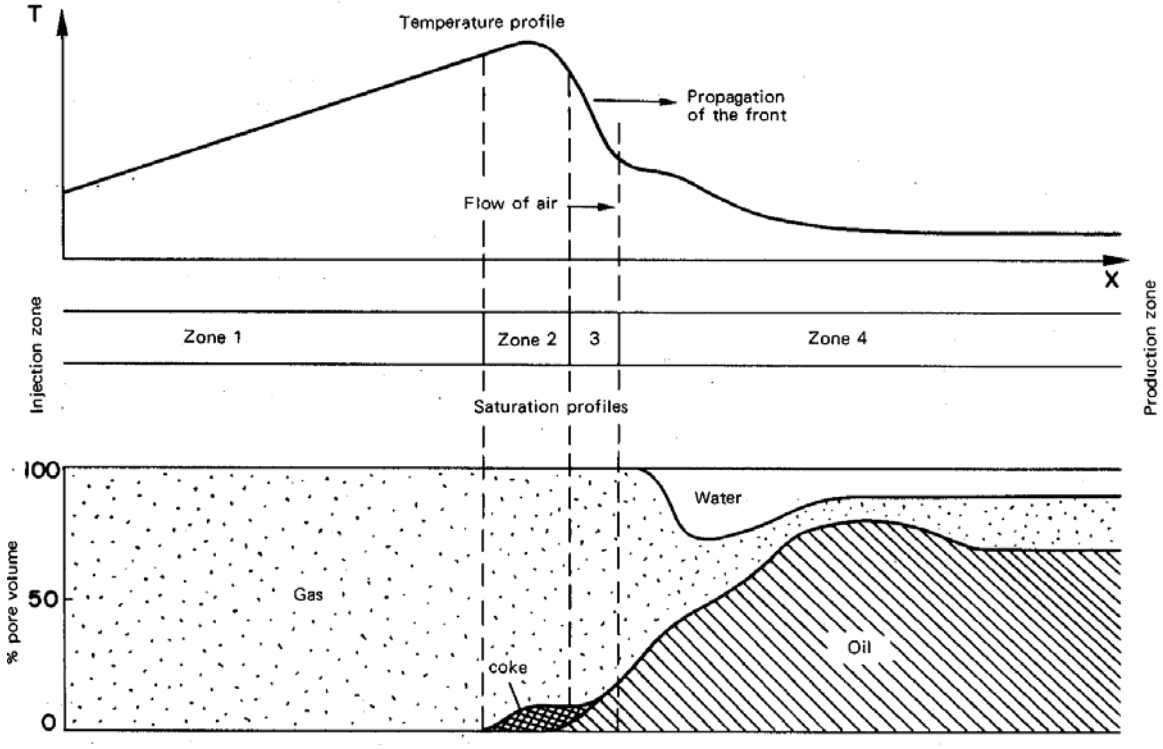

Figure 2.2: *Dry combustion temperature and saturation profiles (Latil, 1980)*

Reservoir characteristics have a direct effect on the dry in-situ combustion process performance. For example, when the reservoir is relatively thin, the displacement process behaves like a frontal advance process with the temperature and saturation distribution. A narrow combustion zone forms where temperatures may be very high. The injected air is preheated to combustion temperature as it flows through the rock behind the combustion zone. Combustion products, primarily water (as water vapour), carbon dioxide, and carbon monoxide, flow ahead of the slowly moving (0.125 to 1.0 ft/d) (0.038 to 0.3 m/d) front (Green & Willhite, 1998). Oxygen not consumed by the combustion front and nitrogen also flows with the combustion gases. On the other hand, when the reservoir is thick and has good vertical permeability, gravity segregation or override occurs. The combustion front migrates to the top of the reservoir where it stretches out across the reservoir. The combustion front expands horizontally and vertically in a complicated manner. The same process mechanisms are present when gravity segregation occurs, but front movement is influenced by the complex multiphase flow pattern inherent in a combustion front that expands both vertically and horizontally. The reservoir under the combustion front is heated by conduction, which is

particularly important in heavy oil reservoirs where large changes in oil viscosity occur with relatively small changes in temperature.

During forward combustion, the temperature behind the burning front is high, indicating a great amount of heat stored in the formation matrix. The injected gas (air) heats on contact with the matrix and recovers only a small amount of the heat, with considerable losses to the surrounding formations. For this reason, water sometimes is used during or after the combustion process to help transfer the heat from the burned zone and to use it efficiently downstream, where the oil is. Another drawback of dry forward combustion is the presence of a highly viscous oil zone surrounding the production well. The fluid in this zone remains at the original reservoir temperature and its forward displacement by the heated oil is normally difficult. Breakthrough of the combustion front into a production well is a major problem and it occurs in most projects. In thin reservoirs, most of the oil displaced by the combustion front is produced before breakthrough. In reservoirs where the combustion front does not burn the entire vertical cross section, large amounts of oil have been produced from hot wells by cooling the production well by injecting water down the casing annulus or by shutting the well in for a period of time after the arrival of the combustion front. The latter practice allows heating of the reservoir by conduction from the combustion zone (Green & Willhite, 1998; Prats, 1982).

2.3.2 Wet forward combustion

With dry forward combustion, any heat generated and stored in the formation rock which is not used to preheat the injected gas is lost by conduction to the overburden and under burden. Better thermal efficiency is achieved when water injection is combined with the injection of air. The advantage of injecting water in this process is that the great enthalpy difference between the liquid water injected and the steam formed upon contact with the hot formation to recover the thermal energy accumulated behind the front to transport it to ahead of the front area.

Wet combustion can be defined as an in-situ combustion technique in which water is injected simultaneously or alternately with air into a formation. It actually refers to wet

forward combustion and is developed to use the great amount of heat that would otherwise be lost in the formation. Addition of water is considered as an advantage to the process since it enhances the production of steam. This leads to that the steam zone ahead of the combustion front being larger and, thus, the reservoir is swept more efficiently than with air alone. The improved displacement from the steam zone results in lower fuel availability and consumption in the combustion zone, so that a greater volume of the reservoir is burned for a given volume of air injected.

In low permeability reservoirs, it may be difficult to inject both air and water simultaneously at the desired rates. In that case, the water and air may be injected alternately, each phase being injected for a few days at a time. The duration of the air and water injection periods is controlled to achieve the desired average water/air ratio. The water/air ratio also is controlled to obtain required improvements in combustion front velocities or temperature levels. At low water/air ratios, all the water that reaches the combustion front already has been converted to steam. If the water/air ratios are kept sufficiently high, most of the water reaching the combustion front still will be in the liquid phase. This reduces the maximum temperature level, in some cases to that corresponding to the partial pressure of steam in the steam/gas mixture. Usually, such temperatures are adequate for thermal drives.

Gravity segregation between water and air does influence the wet combustion process. In extreme cases, water may not reach the upper part of the sand intervals, so that only dry combustion with its relatively poor heat recovery takes place. In the lower parts of the interval, combustion may not be sustained because of the presence of too much water and too little air; in the centre section, wet combustion may occur at some unknown water/air ratio. Laboratory scale experiments in gravity dominated systems indicate that the average performance of wet combustion has the claimed advantages even under such adverse conditions of gravity segregation (Prats, 1982).

In order to simplify the main combustion zones, the wet forward combustion can be divided into five main zones (Figure 2.3) (Latil, 1980; Burger et al., 1985):
Zone (1) this zone, having already been swept by the combustion front, contains little or no hydrocarbons. However since the temperature is below the water liquid/vapour

equilibrium temperature, two-phase flow exists. Since there is a saturation of liquid water, a large quantity of the injected water never reaches the vaporization front.

Zone (2) the water in this zone is in the vapour phase, so the pores are saturated with the injected air and water vapour. The vaporization front of the injected water is at the boundary between the first and second zones, where the temperature gradient is very steep between these two zones.

Zone (3) the combustion zone: the oxygen is used up in the combustion of the coke in place.

Zone (4) the vaporization condensation zone: the temperature here is little different from the vaporization temperature of water. The water vapour produced either from the injected water or from the combustion undergoes a progressive condensation in this zone. The light and intermediate oil fractions are vaporized and carried toward the producer. At a sufficient thermal level certain chemical reactions may also take place.

Zone (5) in this zone a sharp pressure drop is observed which is due to the existence of the water bank and then the oil bank. Further on, the formation gradually regains its initial characteristics.

In the wet in-situ combustion process, as the water/air ratio increases, the energy given off by the combustion and built up in the formation is no longer sufficient to vaporize all the injected water which reaches the vaporization front. The high temperature region (zones 2 and 3 in Figure 2.3) becomes more and more narrow and eventually disappears completely (Islam et al., 1989).

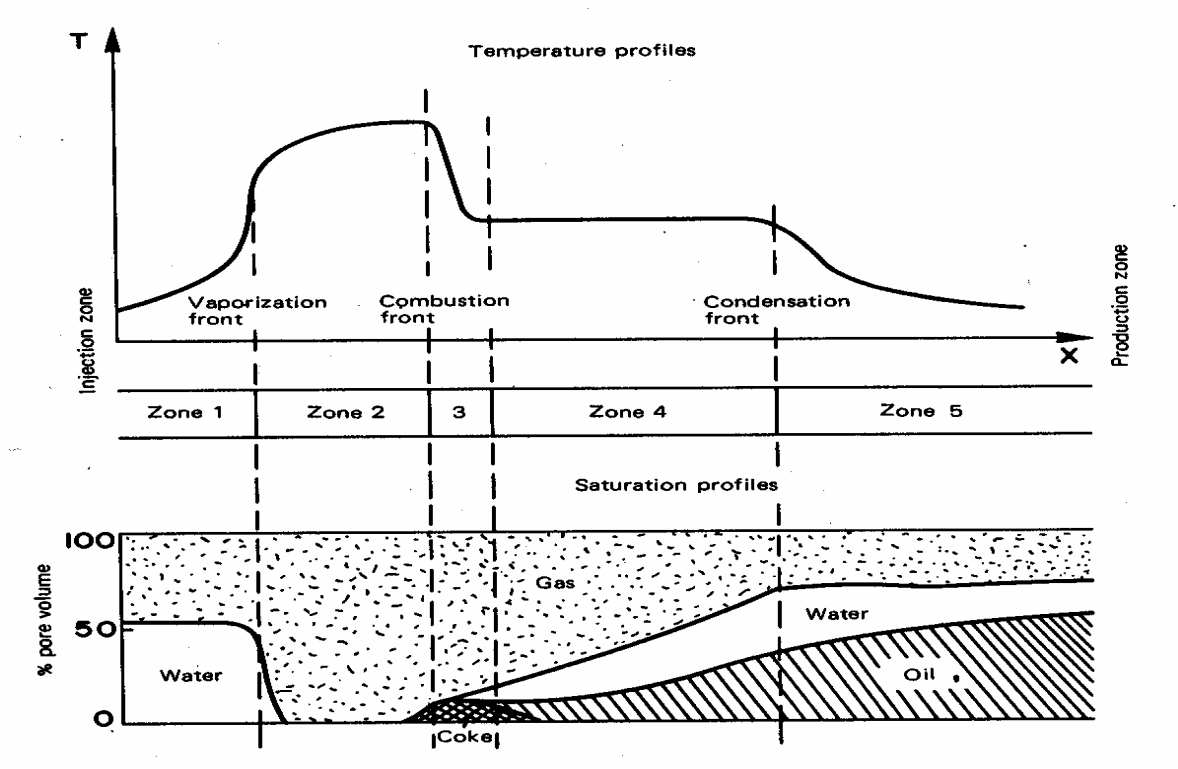

Figure 2.3: *Wet combustion temperature and saturation profiles (Latil, 1980)*

2.3.3 Reverse combustion

Reverse combustion is a type of in-situ combustion in which the burning front moves in an opposite direction to the injected air. It actually refers to dry reverse combustion, and is used to recover extremely viscous oil or tar. In reverse combustion the combustion front is initiated at the production well. The crude ahead of the front near the producer well tends to flow through the front toward the producer. As the crude and the high temperature combustion front come together, the crude is cracked severely and a relatively large amount of coke is formed and deposited. The large amount of fuel formed in reverse combustion operations is responsible for the relatively large amount of equivalent oil saturation burned in the process. Thus, the amount of displaceable oil in this type of in-situ combustion is lower what can be produced by the two other types of combustion processes. On the other hand, the API gravity of the recovered product is increased significantly by extensive cracking within the combustion and burned zones. Also, because the more volatile pyrolysis products flow through the hot burned zone, no oil bank builds up and the resistance to flow is fairly low.

There are four main zones which can be distinguished in a reverse combustion process. Figure 2.4 below shows the zones starting from the injector and moving to the producer (Latil, 1980, Burger et al., 1985):

Zone (1) in this zone the porous medium has its initial characteristics. However it is being swept by the oxygen containing gas so that certain oxidation reactions can take place, if the temperature of the layer is high enough and the oil is easily oxidizable.

Zone (2) the temperature begins to increase due to conduction from the hot zone. The beginning of oxidation also causes the temperature to rise. The following phenomena occur: vaporization of water, distillation of the light oil fractions and oxidizing cracking of some of the hydrocarbons.

Zone (3) the combustion zone where the temperature reaches its maximum. The oxygen left over from previous zones is used up in the oxidation and combustion reactions of the more reactive hydrocarbon molecules.

Zone (4) the unburned coke remains behind in the porous medium. The fluids in their gaseous or liquid states flow towards the producer.

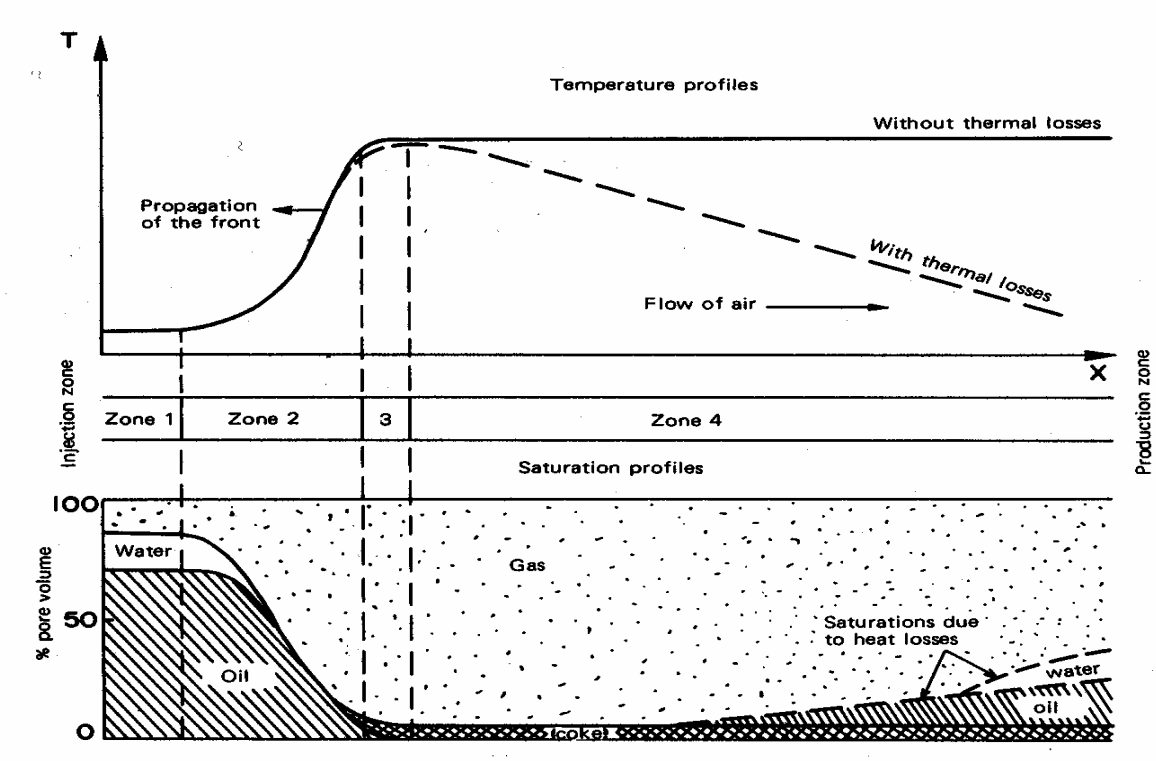

Figure 2.4: *Reverse combustion temperature and saturation profiles (Latil, 1980)*

A major difficulty with this process is that of keeping it going for a longer time. The continuation of air injection into an unheated reservoir generally leads to spontaneous ignition near the injection well. Since the oxygen is depleted not far from the injection well, reverse combustion cannot be maintained. In most cases, a reverse combustion operation cannot be expected to last for more than a few weeks, and usually for only a matter of days (Prats, 1982). The time required for spontaneous ignition to occur is governed primarily by two factors: the reactivity of the crude and the initial reservoir temperature. Another drawback is that reverse combustion is not as efficient as dry forward combustion because lighter fractions of the oil are burned and heavier fractions are left behind the burning front. Furthermore, the fact that the efficiency of the method depends on the air flux makes the process difficult to control. The optimum flux is very high and extremely difficult to achieve, except if the well spacing is very small. For all these reasons, reverse combustion has scarcely been applied in the field; although this process has sometimes been claimed to be feasible in certain shallow tar sand deposits (Burger et al., 1985).

To fulfil the objectives of this study, dry forward combustion is the recovery method chosen to be applied in the Nimr field. This is mainly because of the field properties, in terms of the reservoir thickness, crude viscosity and the naturally existing aquifer support, which all make the dry forward combustion process the most suitable for application in the Nimr case.

2.3.4 Field applications

The motivation for developing thermal recovery processes is the existence of major reservoirs all over the world that are known to contain billions of barrels of heavy oil and tar sands that cannot be produced with conventional techniques. In many reservoirs, the oil viscosity is so high that primary recovery on the order of a few percent of original oil in place (OOIP) is common. In some reservoirs, primary recovery is negligible. According to the Oil and Gas Journal's biannual EOR survey in 1998, about 1.3 million bbl/d of oil was being produced worldwide using thermal methods, which was about 2% of the world's oil production that year (Sarathi, 1998).

In-situ combustion, as one of the thermal techniques, has been tested extensively in a variety of reservoirs with mixed results. Daily production from in-situ combustion in 1993 was approximately 22,000 bbl/d (Green & Willhite, 1998). At the beginning of 1998, worldwide oil production from in-situ combustion projects was estimated to have risen to 28,900 bbl/d. Of this, the U.S. accounted for 5,200 bbl/d from 8 projects and Canada 6,250 bbl/d from 3 projects (Sarathi, 1998). Although steam injection and in-situ combustion have been used successfully in the same reservoir, steam injection has been the process of choice for reasons other than process efficiency. In-situ combustion is the only thermal recovery process that can be used in deep, high pressure reservoirs. Green & Willhite (1998) summarised the criteria for both stream injection and in-situ combustion processes which are shown in Table 2.1. These criteria are to be used as a guide in selecting candidates for thermal recovery processes. Exceptions to the criteria may be found in specific reservoirs.

Screening Parameters	In-Situ Combustion	Steam
Oil gravity , ^{o}API	9 to 40	10 to 34
In-situ oil viscosity, μ (cp)	≤ 5000	≤ 15000
Depth, D (ft)	≤ 11500	≤ 3000
Pay-zone thickness, h (ft)	≥ 20	≥ 20
Reservoir temperature, T_r (^{o}F)	not specified	not specified
Porosity, Ø (fraction)	≥ 0.20	≥ 0.20
Average permeability, k (mD)	35	250
Transmissibility, kh/μ (mD-ft/cp)	≥ 5	≥ 5
Reservoir pressure, P_r (psi)	≤ 2000	≤ 1500
Minimum oil content at start of process, S_o (fraction)	≥ 0.08	≥ 0.10
Salinity of formation brine (ppm)	not specified	not specified
Rock type	Sandstone or carbonate	Sandstone or carbonate

Table 2.1: *Screening parameters for thermal recovery processes (Green & Willhite, 1998)*

Many of the criteria are identical for steam and in-situ combustion. Consequently, it is not uncommon to find that a reservoir that can satisfy the criteria for both processes. Three criteria where there are significant differences include depth, reservoir pressure, and average reservoir permeability. Steam processes are limited to depths on the order of 3,000ft (ca. 1,000m) because wellbore heat losses can become excessive. Although the depth limitation for in-situ combustion is suggested to be 11,500ft (ca. 3,500m), this is not a process limitation if air can be injected at the reservoir pressure and the crude oil deposits sufficient fuel to sustain the combustion front. Reservoir pressure is the second criterion where the two processes differ. In steam injection projects, the fraction of energy transported as latent heat decreases as pressure increases. The temperature of steam increases with pressure, as does the heat loss to the surroundings. Consequently, under the same conditions, the volume of the reservoir that can be swept by steam decreases with injection pressure. This makes the reservoir pressure to become a limiting factor in the application of steam injection processes. It is not practical to inject steam in the field near the critical pressure of steam, which is 3,206.2psi (22,106kPa) (critical temperature is 705.4°F (374.1°C)). Although steam has been injected at pressures of 2,500psi (17,237kPa) in field projects, most successful steam injection projects operate at pressures on the order of 1,500psi (10,342kPa) or lower (Green & Willhite, 1998). Reservoir pressure is not limited by a similar mechanism in the in-situ combustion process. Reservoir pressure for in-situ combustion projects is affected by air compression costs and injection rates. Permeability of the reservoir is the third criterion where there are substantial differences between steam injection and in-situ combustion. In-situ combustion can be applied in reservoirs that have lower permeability than the permeability limit for steam injection because the air injection rates are sufficient to sustain the combustion front. In contrast, the steam zone can advance only as long as heat losses from the steam zone to the surrounding formations can be maintained by the steam injection rate. In low permeability reservoirs, it is not possible to inject steam at sufficient rates to propagate a steam zone appreciable distances into the reservoir. Implementing in-situ combustion instead of steam injection provides a rapid result for the thermal process in terms of immediate increase in the reservoir temperature, since the heating process is produced in-situ. It also eliminates the cost and disadvantages of generating energy at the surface (heat loss in the surface facilities and the high carbon

dioxide footprint) as occurs with steam injection (Hart Energy, 2006; Zwart et al., 2008).

In-situ combustion has been extensively field tested in a variety of reservoirs. These include reservoirs that are too thin and too deep to use other thermal process (i.e. steam injection). Most in-situ combustion field projects have been in progress since the early 1960's or 1970's. In this section some of the well known in-situ combustion projects will be presented as examples for the potential of the process. The first example is the world's largest in-situ combustion project, which is still under operation until today. It is the Suplacu de Barcau field in Romania. The second example is the MOCO zone reservoir in Midway Sunset field, USA. This example presents the possibility for applying the in-situ combustion process in a multiple sands reservoir, which is considered to be a complex geological system. The third example is the West Heidelberg Cotton Valley Sands, USA. It is probably the world's deepest in-situ combustion project, with an average depth of 11,400ft (3,475m).

Suplacu de Barcau field: It is located in North West Romania, and it is the site of the world's largest in-situ combustion project. The Suplacu de Barcau oil reservoir, shown in Figure 2.5, is a monocline with an average dip of 5° north. It contains unconsolidated, slightly shaly sands and is located at a depth of 165ft (50m) at the south end of the monocline and 656ft (200m) at the north end. Table 2.2 presents reservoir and fluid properties. Net-pay thickness is 33ft (10m), with an average porosity of 32%. Permeability of the sand ranges between 1,700 and 2,000mD. The reservoir oil has a viscosity of 2,000cp at the reservoir temperature of 64.4°F (180°C). OOIP was estimated to be 295 million bbl. Due to the low reservoir energy, the final recovery factor by primary methods and pumping was evaluated at 9%. The reservoir conditions led to the use of thermal recovery methods quite soon after the discovery of the field in 1957 (Burger et al., 1985; Green & Willhite, 1998).

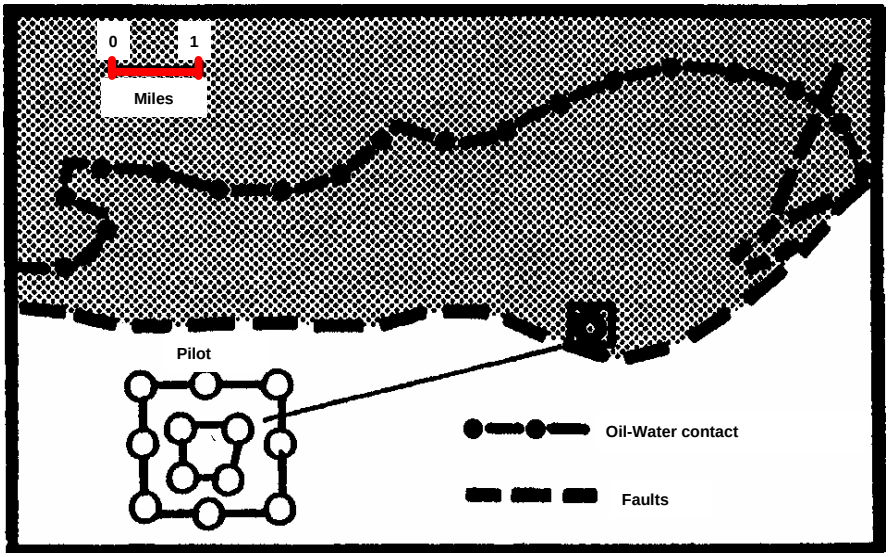

Figure 2.5: *Suplacu de Barcau field (Green & Willhite, 1998)*

Suplacu de Barcau Reservoir and Fluid Properties	
Average depth (ft)	400
Average net pay (ft)	33
Porosity (%)	32
Average permeability (mD)	1850
Initial water (%)	15
Oil Gravity (°API)	16
Oil Viscosity (cp)	2000
Oil density (lb/ft^3)	59.9
OOIP (million STB)	295

Table 2.2: *Suplacu de Barcau reservoir and fluid properties (Carcoana, 1990)*

A dry in-situ combustion pilot was initiated in 1964 on the area at the top of the structure, as indicated in Figure 2.5. The experimentation on dry combustion began on a 1.25 acre inverted five-spot patent. The production rate of some wells increased from 19 to 630bbl/d. These encouraging results led to the expansion of the pattern to a 5 acre nine-spot using the same injection well. The pilot main results are given in Table 2.3. The high recovery and the low air/oil ration (AOR) are due to the fact that a high amount of oil coming from outside the pattern was produced (Gadelle et al., 1981). Between 1967 and 1971, eight 9.9 acre nine-spot patterns were pilot tested. These were located directly east and south of the initial pilot pattern. Expansion continued in the

upper part of the reservoir in the east and west directions until the patterns merged to form a linedrive patern. Figure 2.6 shows the combustion front and the burned region. The combustion front was estimated to be 5 miles (8km) in length by 1990. At that time, 120 MMscf/d of air was being injected into 100 injection wells (Green & Willhite, 1998).

Total air injected (MMscf)	1870
Total gas produced (MMscf)	1700
AOR (Mscf/bbl)	5
Air requirement (Mscf/bbl)	2-2.1
Oil consumed as fuel (lbm/ft^3)	2.2
Recovery (%)	85
Average combustion front velocity (ft/d)	0.3

Table 2.3: *Suplacu de Barcau pilot test results (Gadelle et al., 1981)*

The development plan in Suplacu de Barcau pilot was to displace the combustion front down dip. The linedrive was maintained by converting production wells to injectors when the combustion front breaks into the production well. The conversion process is illustrated in Figure 2.7, which is a cross section between Wells 426 and 428 showing conversion of Well 428 into an air injection well after the combustion front arrives. Observation wells drilled behind the combustion front revealed that the top half of the pay zone was burned. This region was separated from lower unburned zone by a coke layer. Gravity segregation is prominent in this field, as indicated by core analyses and the illustration of the combustion process in Figure 2.7 where the front moves in the formation upper area. A pilot test of wet combustion was conducted and expanded to 20 wells during 1976-79. However, the project remains primarily a dry in-situ combustion project. This is because the water injection required to transfer the heat through the combustion front does not appear to have been part of the operation. (Carcoana, 1990; Green & Willhite, 1998; Prats, 1982).

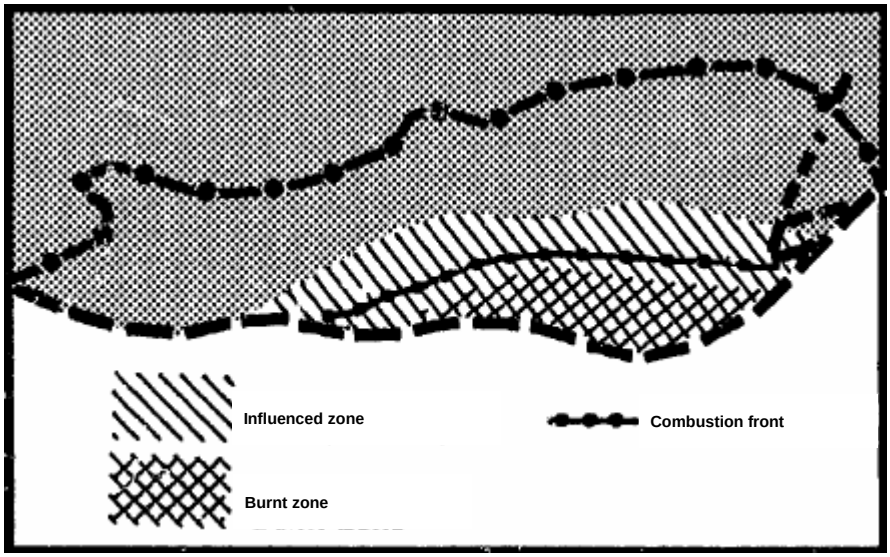

Figure 2.6: *Area affected by combustion front (Carcoana, 1990)*

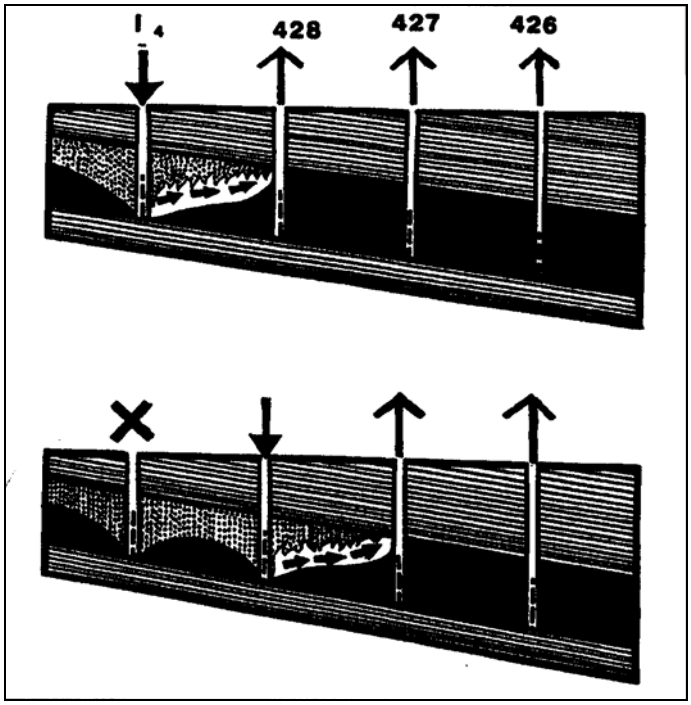

Figure 2.7: *Maintenance of linedrive combustion front by conversion of a production well to air injection well after breakthrough of combustion front (Green & Willhite, 1998)*

The results of applying in-situ combustion in Suplacu de Barcau (1961 to 1982) are summarised in Figure 2.8. It shows the project air injection, oil production, and the AOR. In 1987, oil production was 10,400 bbl/d with about 600 wells affected by in-situ combustion. The average AOR ranged between 9.5 and 11.3 Mscf/bbl during 1973 to

1979 and increased to 14.2 Mscf/bbl after 1985 (Green & Willhite, 1998). In 2005, there are nearly 800 wells with total production of about 7,900 bbl/d of crude oil. The cumulative extracted crude in 35 years was about 117 million barrels, which corresponds to a recovery factor of 44.6% (Panait-Patica et al., 2006). The ultimate oil recovery is expected to be 52% OOIP (Green & Willhite, 1998).

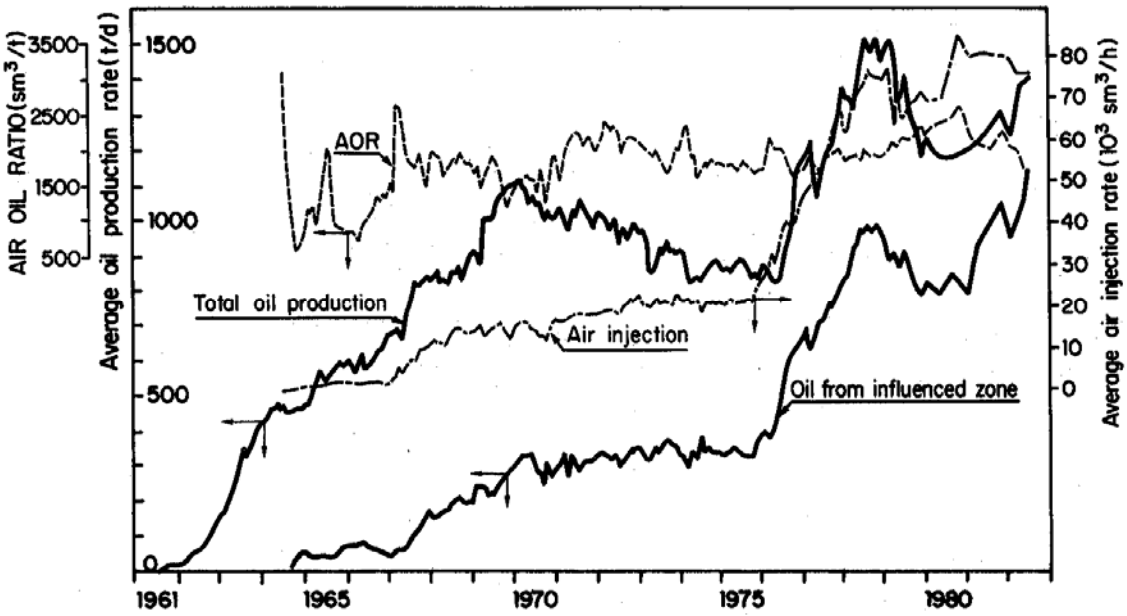

Figure 2.8: *Air injection, oil production, and AOR profiles of the Suplace de Barcau combustion operations (Burger et al., 1985)*

MOCO zone reservoir-Midway Sunset Field: The MOCO zone reservoir, located in the Midway Sunset field, California, was discovered in 1957. The reservoir is a small anticline with six major sands. Structure contours and the areal extent of the six sands are shown in Figure 2.9. The sands generally are separated by interbedded shales and to the east become thin and disappear and to the west some of the sands merge. The sands were separately identified, correlated, isopached, and designated M1 through M6. This permitted an appropriate design of air distribution in the injection wells, which have various combinations of sands open. In the development of the reservoir all oil sands present at a particular location were opened to production. Cross section E-E' in Figure 2.10 shows that sands M1 through M6 are correlated across the field, as well as separated by shale zones. The dip in the reservoir is up 45° to the north and 20° to the south. Reservoir characteristics are summarised in Table 2.4. The reservoir originally

contained 38 millions bbl of 14.5°API gravity oil (Gates et al., 1971; Green & Willhite, 1998).

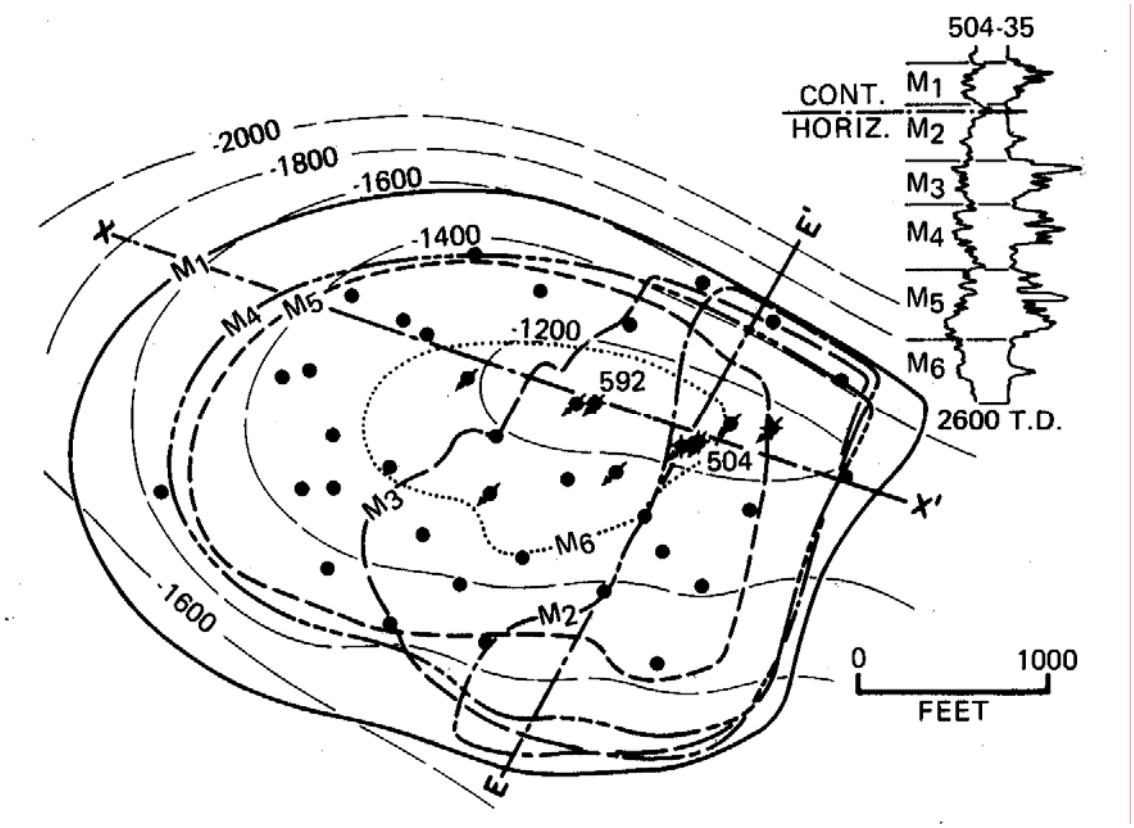

Figure 2.9: *MOCO zone sand distribution and structure (Boberg, 1988)*

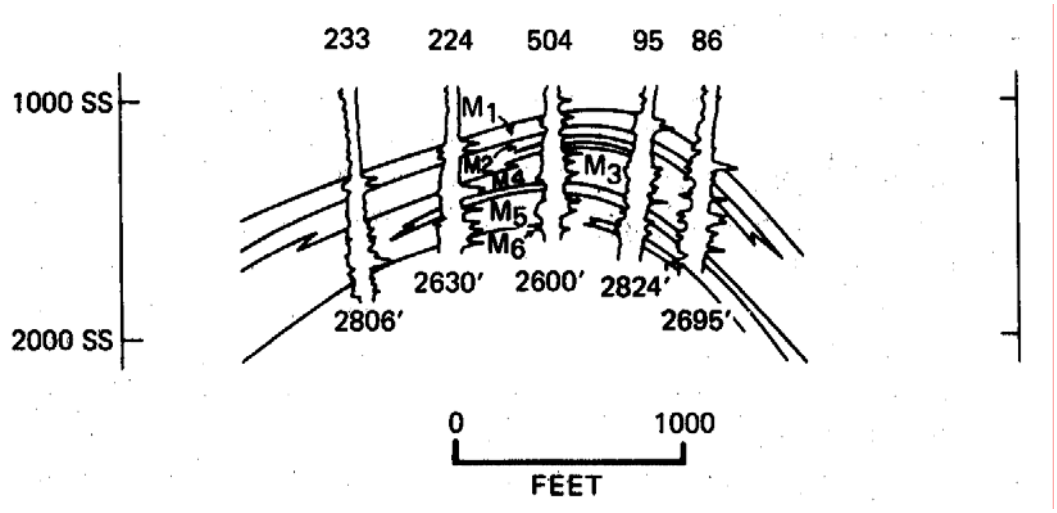

Figure 2.10: *Cross section E-E' MOCO zone (Boberg, 1988)*

Productive area (acres)	150
Average depth (ft)	2100 to 2700
Gross formation thickness (ft)	500
Average net sand thickness (ft)	129
Porosity (%)	36
Oil saturation (%)	75
Water saturation (%)	25
Formation volume factor (rb/stb)	1.06
Initial oil in place (bbl/acre-ft)	1980
Initial oil in place total (millions bbl)	38
Permeability (mD)	1575
Initial formation pressure (psi)	1000
Reservoir temperature (^{o}F)	125
Oil gravity (^{o}API)	14.5
Oil viscosity at formation temperature (cp)	110
Sand Character	Unconsolidated

Table 2.4: *Reservoir and fluid properties MOCO zone (Gates et al., 1971)*

The MOCO reservoir was developed partially after its discovery in 1957. However, because there was no demand for the heavy crude, it was essentially shut in until November 1959. It was expected that without fluid injection of some kind there would be a rapid decline in oil production rate. Although there were multiple sands present, the reservoir properties of the MOCO zone appeared favourable for in-situ combustion. The cumulative primary production amounted to only 0.5% of original oil in place at the beginning in-situ combustion in the reservoir (Chu, 1982).

In-situ combustion was initiated in January 1960. Air injection was initiated at the top of the structure in well (MOCO 504), in order to fully utilise gravity in the recovery of the highly mobile hot crude affected by the combustion process. The air injection rate was 1000 Mcf/d and at a pressure of 950 psi. Spontaneous ignition occurred about 18 days after the start of air injection. Production response was immediate following air injection, with production rates increasing to 2,850 bbl/d in February 1960 in response to the high volume of air injection. Peak oil rate was reached in 1964 at 4,200 bbl/d. Air

injection was increased to an average rate of 8,000 Mscf/d in early 1964. In 1976, the air injection rate was reduced to 5,500 Mscf/d and remained at this rate thereafter. Declines in oil production rates correlate with declines in air injection in 1963, 1967, and 1973. Four additional injection wells were added to improve distribution of the air between zones. Figure 2.11 shows the MOCO zone reservoir performance and air injection rates over the life of the project. As of 1989, the cumulative oil produced was 14 million bbl and the cumulative air injected was 59.5 Bscf. The oil production rate as of 1989 was 1,040 bbl/d from 34 active wells. The project's AOR has remained at 4 to 4.3 Mscf/bbl, with a producer to injector ratio of 6:1 (Gates et al., 1971; Green & Willhite, 1998).

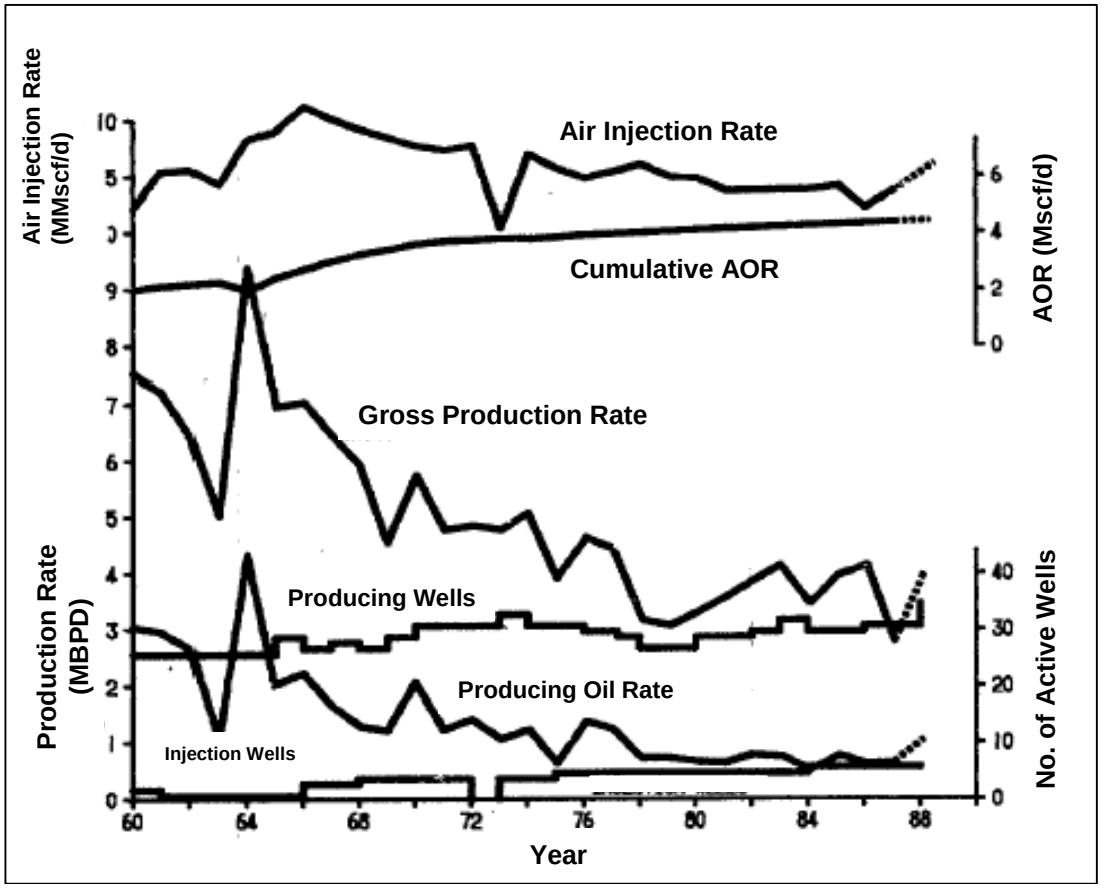

Figure 2.11: *MOCO zone production and injection history (Curtis, 1989)*

The combustion front behaviour in this project appeared to be overriding in several of the individual sand members, strongly supported by gravity segregation and the steep dip of the reservoir. Consequently, the combustion process resembles a gravity stabilized frontal advance displacement. Based on the reservoir performance, Curties

(1989) estimated the ultimate recovery will reach 50 to 57% original oil in place at a cumulative air injection volume of 85 to 90 Bscf. Also, he estimated the remaining producing life for the MOCO reservoirs to be 12 to 15 years at an average air injection rate of 5,000 Mscf/d.

The West Heidelberg Cotton Valley field: The West Heidelberg Cotton Valley Sands Unit in Jasper County, USA (Figure 2.12) is the location of what is probably the world's deepest in-situ combustion project. It was discovered in January 1944. The Cotton Valley sands are of Jurassic age, occurring at an average depth of 11,400ft (3,475m). Fourteen sands are identifiable in the Cotton Valley, but only eight are productive. Of these eight, Sands 4 and 5 are the major oil reservoirs. Structurally, the Cotton Valley lies on the flank of a salt dome and dips about 8° from east to west. The eastern updip limit is the salt intrusion, and the western downdip limit is an essentially immobile tar or asphalt deposit (Huffman et al., 1983; Burger et al., 1985).

Table 2.5 gives average reservoir data. Both Sand 4 and Sand 5 reservoirs have very similar characteristics. The average porosity is 15%, and air permeability is 65md. Initial oil and water saturations were 85% and 15%, respectively and oil gravity is 26°API. However, oil gravity near the tar deposit is 15°API. The initial reservoir temperature was 220°F (104°C), and the initial reservoir pressure was 5,100psi (35,163kPa). The reservoir pressure at the start of air injection was 1,500psi (10,342kPa). The OOIP was about 18 million bbl where 1.1 million bbl (or 6.1% OOIP) was produced by primary production.

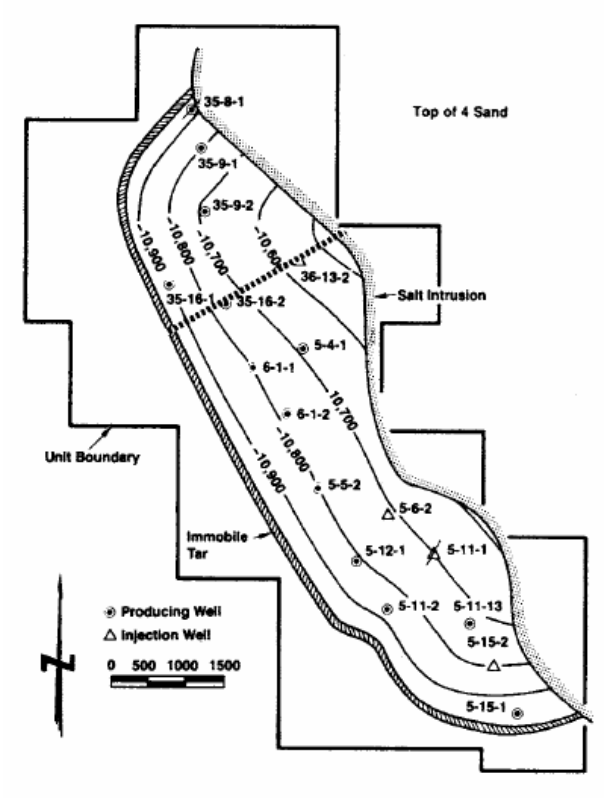

Figure 2.12: *West Heidelberg filed unit map (Kumar, 1991)*

Productive area (acres)	350
Net pay for the two sands (ft)	62
Porosity (%)	15
Air permeability (mD)	65
Initial oil saturation (%)	85
Initial water saturation (%)	15
Gravity (^{o}API)	26
Reservoir temperature (^{o}F)	220
Reservoir pressure (psi)	(Original) 5100
	(At start of air injection) 1500
OOIP (MMstb)	18

Table 2.5: *West Heidelberg average reservoir data (Kumar, 1991)*

Because of the low primary recovery, studies were initiated to determine how the large volume of remaining oil could be recovered. To avoid high lifting costs and because the relatively unfavourable water/oil mobility ratio indicated probable poor recovery by

waterflooding, a decision was made to install a pressure maintenance project that relies on air injection for in-situ combustion. Air injection started in Sand 5 in December 1971 at the rate of 1 MMscf/d. Spontaneous combustion occurred as anticipated. Production response to air injection was noticed in 3 months. Project performance is shown in Figure 2.13. At the 1 MMscf/d air injection rate, oil production increased to about 500 bbl/d by the end of 1973 and continued at a 300 to 500 bbl/d rate until early 1977, when production started declining. Cumulative oil produced from the Cotton Valley project since air injection was started is 2.9 million STB as of August 1982. The ultimate oil recovery from this project is estimated at 7.4 million STB or 41% of the 18 million STB OOIP (Huffman et al., 1983; Kumar, 1991).

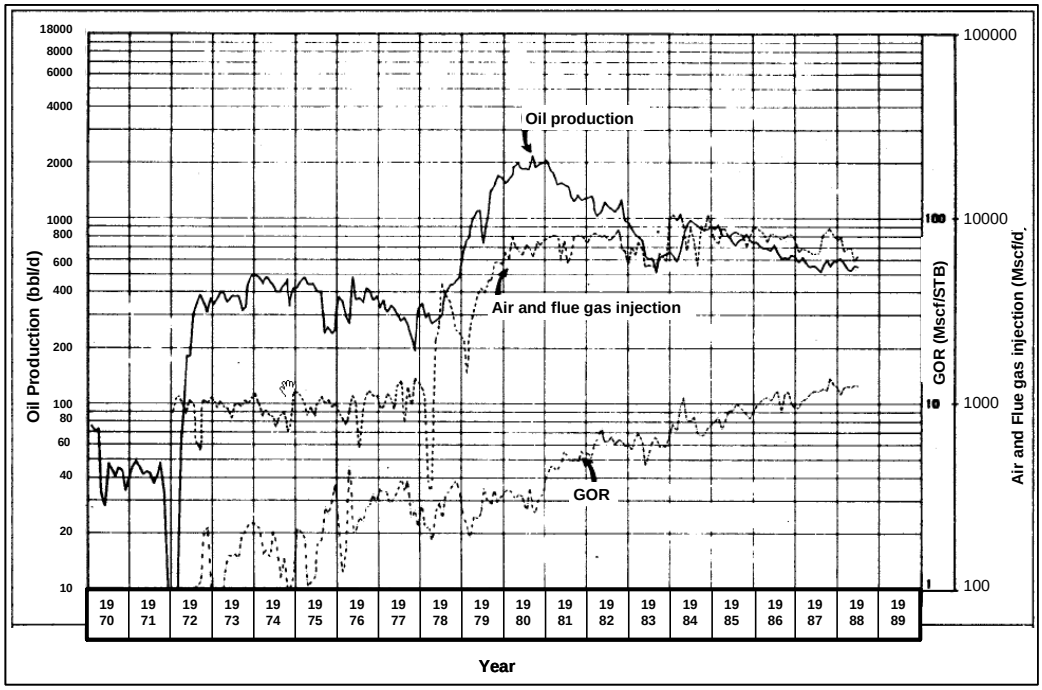

Figure 2.13: *Performance of West Heidelberg Cotton Valley in-situ combustion project (Kumar, 1991)*

There are many examples in the literature which show a variety of reservoir properties and field locations worldwide in which in-situ combustion is applied. Table 2.6 shows some of the known distribution of in-situ combustion projects in the world and their oil production. However, there are several key factors that need to be considered in order to ensure a successful application of the in-situ combustion process. These key factors are summarised below (Ursenbach et al., 2010):

- Selection of the right reservoir with the right crude oil reactivity to allow the initiation of the combustion front. The crude reactivity can be tested through the conduction of laboratory experiment such as ramped temperature oxidation (RTO) and accelerating rate calorimetry (ARC). There are a few cases where the reservoir is not suitable for the application of the combustion process, for example in reservoirs with very high conductivity thief zones, or in reservoirs with a valuable gas cap under production.
- Design of the right process by determining the appropriate air injection requirements. Also, the need to identify the natural advantages of the reservoir which may include dip, areal extent, pay thickness, existing wells, etc. and include those advantges in the design process.
- Use the right air compressor to ensure a sustainable fire flood. This is important as a poorly designed compressor can result in reduced process performance or even lead to failure in the combustion process due to pump downtime and limited injection capacity for further field development.
- Provide the right ignition at the process start in order to avoid quenching of the fire front at early stages.
- The right amount of air should be injected to maintain sufficient combustion process reactions.
- The need to continuously monitor the development of the process and the need to make the appropriate correction to the process parameters.

Country	**Project name**	**Operator**	**Date Initiated**	**ISC Type**	**Oil Gravity, °API**	**No. Injector**	**No. Producer**	**AOR, Mscf /bbl**	**Produc--tion bbl/d**
USA									
1	Bellvue, LA	Bayou State	1970	Wet	19	15	85	12	400
2	Midway Sunset, CA	Texaco	1960	Dry	14.5	10	47	4	1000
3	Medicine Pole Hill Unit, ND	Contin--ental Resources	1985	Dry	39	7	17	7.2	725
4	Buffalo, SD	Contin-ental Resources	1979	Dry	30	12	21	10.5	550
5	W. Buffalo, SD	Contin-ental Resources	1987	Dry	30	6	15	10.9	365

Country	Project name	Operator	Date Initiated	ISC Type	Oil Gravity, °API	No. Injector	No. Producer	AOR, Mscf /bbl	Produc--tion bbl/d
6	S. Buffalo, SD	Contin-ental Resources	1983	Dry	30	19	40	9.3	1420
7	W. Hackberry, LA	Amoco	1995	Dry	33			15.6	280
8	Mt. Poso, CA	AERA	1997	Dry					
9	Horse Creek Field, ND	Total Minatome	1996	Dry	32.2	3	11	10	400
Canada									
1	Battrum Saskatchewan	Mobile Canada	1966	Wet	18	15	94	10	3700
2	Battrum Saskatchewan	Mobile Canada	1967	Wet	18	7	35	10	1200
3	Battrum Saskatchewan	Mobile Canada	1965	Wet	18	3	22	10	1350
4	Wabaska W Alberta	Amoco Canada	1994	Dry	14	1	2		260
Albania	Kasnice		1973	Dry	12				130
Azerba--ijan	Balakhany Sabunchi		1988	Wet	16	6	35		600
China	Kerxing--nemangu	CnPc Nemangu	1996	Dry	29				
Hungary	Demjen--kelet		1976	Wet	39	3	9	14	270
India									
1	Balol	Oil & Nat'l Gas Corp	1990	Wet	15.6	1	4		190
2	Lanwa	Oil & Nat'l Gas Corp	1992	Wet	13.5	1	4		165
3	Balol	Oil & Nat'l Gas Corp	1996	Dry	15.6				
4	Santhal	Oil & Nat'l Gas Corp	1996	Dry	17				
5	Bechraii	Oil & Nat'l Gas Corp	1996	Dry	15.6				
Kazakh--stan	Karazhan bas		1981	Wet	22.3	78	364	7.2	4150
Romania									

Country	Project name	Operator	Date Initiated	ISC Type	Oil Gravity, °API	No. Injector	No. Producer	AOR, Mscf /bbl	Produc--tion bbl/d
1	Saplacau de Barcau		1964	Dry /Wet	16	132	507	12.3	8800
2	W. Videle		1980	Dry	19	19	50	17	610
3	E. Videle		1979	Dry	19	33	89	21	660
4	W. Balaria		1975	Dry	19	22	60	24.5	820
5	E. Balaria		1987	Dry	16	15	47	22.5	550
Russia	Okha				17.4				180

Table 2.6: *Statistics of world's active in-situ combustion projects (Sarathi, 1998)*

According to the most recent survey available in the literature, there are four active commercial in-situ combustion projects worldwide (Turta et al., 2007). Two of the projects, the Balol and Santhal projects, are in India, one is in Romania (the Suplacu de Barcau project) and the fourth is the Bellevue project in USA. A detailed study, which covered the application of in-situ combustion process to the Balol field is presented by Dayal et al. 2010. The total amount of heavy oil which is produced using in-situ combustion process worldwide is 16200 bbl/d, which represents the total production of those four projects. Three of the current projects are operated using line drive well configurations, where the combustion front is initiated in the uppermost part of the reservoir and then propagates towards the lower part of the reservoir approaching the producer well. Thus top-down combustion should be considered in any generic study of in-situ combustion such as this one. One of the common features of all four combustion projects is that the fire front tends to propagate in the top section of the reservoirs, due to the gas override effect. This is a permanent feature of almost any conventional fire flood process applied to heavy oil reservoirs. Another common feature is difficulty to predict the arrival of the fire front to the production well. The only way to identify the front arrival is when the bottomhole temperature of the producer increases (Turta et al., 2007). However, in numerical studies it is possible to present temperature maps (as we show in this study), which can be used not only to identify front arrival, but also the temperature distribution throughout the entire system.

2.4 New in-situ combustion processes

Conventional in-situ combustion processes were used in the field applications in the past. In these processes, vertical well configurations for both injectors and producers were implemented. Lateral oil displacement was achieved by combustion front propagation between air injectors and oil producers. The application of conventional in-situ combustion caused some operational problems, which affected the overall performance of the combustion process. As a result, more studies have been conducted to overcome the conventional combustion problems and new in-situ combustion processes have been developed. These new processes are discussed briefly below:

2.4.1 COSH

The word COSH is the short form of Combustion Override Split-production Horizontal well. The COSH process is performed to combine the beneficial features of gravity drainage and horizontal production wells. It is considered based on the importance of gravity drainage as an efficient recovery mechanism together with the combustion process. Gravity drainage is the principal mechanism for moving heated oil to the horizontal production well in the COSH process. Typical combustion operational problems such as slow production response, difficulty in sustaining combustion, early oxygen breakthrough, severe sanding, corrosion, and scaling are minimized by using a novel well arrangement to segregate and control the fluid flows. This process is perceived to work very well in a wide variety of reservoirs (Lau et al., 1995; Bagci et al., 2000).

In the COSH process, gas containing oxygen is injected via rows of vertical injection wells as shown in Figure 2.14. The gas is generally injected in the upper part of the formation. Remote gas production wells are used to collect the gases generated by the combustion process (Figure 2.15). These wells are completed near the top of the payzone initially. Although the main function of these wells is to collect combustion gases, they may also be used to produce oil at times. The gas production wells can be horizontal or vertical. A horizontal production well is placed near the base of the

formation beneath each row of vertical gas injection wells to collect hot liquids generated by the combustion process at each injection well. A horizontal well near the base of the formation provides a higher recovery efficiency of heated oil than would be possible with vertical wells. Gas production in the horizontal well is monitored and controlled at low rates to prevent the combustion temperatures from reaching the well. A hot gas chamber is formed around each vertical well similar to the steam chamber in the steam assisted gravity drainage (SAGD) process. Whereas in the SAGD steam chamber the gas phase is primarily steam, the COSH hot gas chamber consists of steam, injected gas, and combustion gases. In both processes, gravity drainage is the principal mechanism for moving heated oil or bitumen to the horizontal production well (Kisman et al., 1994; Bagci et al., 2000).

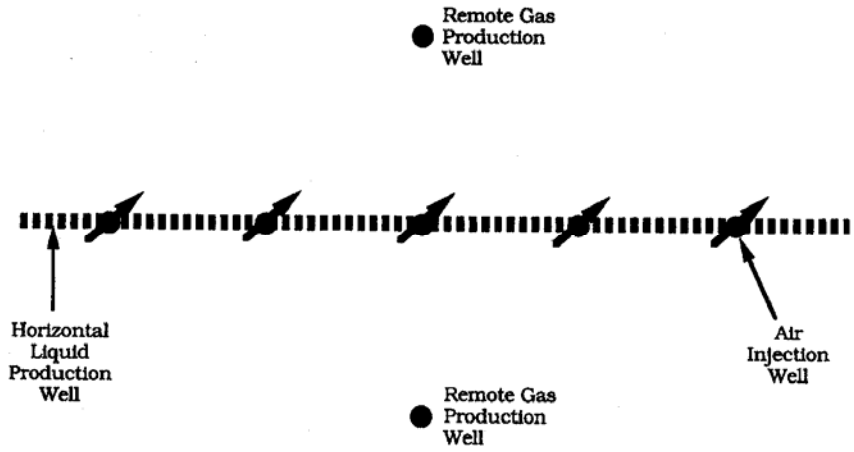

Figure 2.14: *COSH schematic well layout diagram (Kisman et al., 1994)*

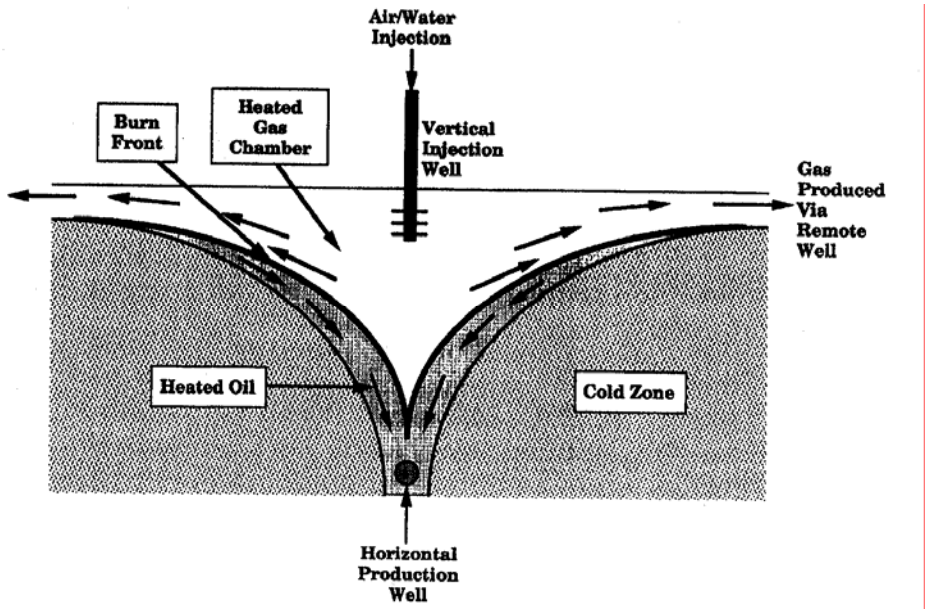

Figure 2.15: *Schematic COSH process diagram (Kisman et al., 1994)*

The COSH process is expected to have many operational advantages compared to other combustion processes. For example, it reduces problems related to oxygen breakthrough, because both gas and liquid flow is segregated for the most part toward different production wells. Also, it should be easier with the COSH process to maintain a stable combustion front. This is because the region between the combustion front and the oil production well is short and there are no problems driving oil long distances and maintaining oil mobility ahead of the combustion front as required for conventional combustion processes. In addition, the horizontal oil production well is readily protected from combustion damage and corrosion by limiting its gas production rate which can be easily controlled. Gravity segregation of fluids in the reservoir makes it difficult for oxygen to reach the horizontal well because gases entering the horizontal well flow down through a hot liquid head where any oxygen content in the gas is consumed.

COSH experimental and numerical studies: Kisman et al. (1994) conducted a numerical study in how the COSH process combined the high recovery potential of gravity drainage with the energy efficiency of the combustion process while minimising problems associated with combustion operations. In this study, 2D and 3D rectangular models have been used. The 3D model (Figure 2.16) was used to generate production forecasts and the 2D model was used to study the process mechanisms. The numerical simulation study indicated that the COSH process has technical performance

approaching that of the highly rated SAGD process, and had significantly lower energy costs. The COSH process is applicable to medium oil reservoirs, heavy oil reservoirs, and oil sand reservoirs where gas communication can be established between injection wells and gas production wells. Because of its low energy costs and lack of heat losses in the injection wells, the COSH process can be applied in thinner and deeper reservoirs than is possible with steam processes.

Chenghui et al. (1998) used experimental and numerical simulation techniques to study the feasibility of developing the Leng 41 Block in the Liaohe oil field in China with the COSH method. The study addressed COSH mechanism and applicability by studying the effect of formation thickness and operational parameters in gas injection, gas production, and horizontal oil production well. The study showed that by keeping constant gas injection pressure and decreasing the bottomhole pressure in the gas production wells and in the horizontal wells, it is possible to increase the oil rate during the early stages of the COSH process. Also, the formation thickness has a great effect on the initiation of the COSH process and the oil rate in the horizontal well after the COSH process starts.

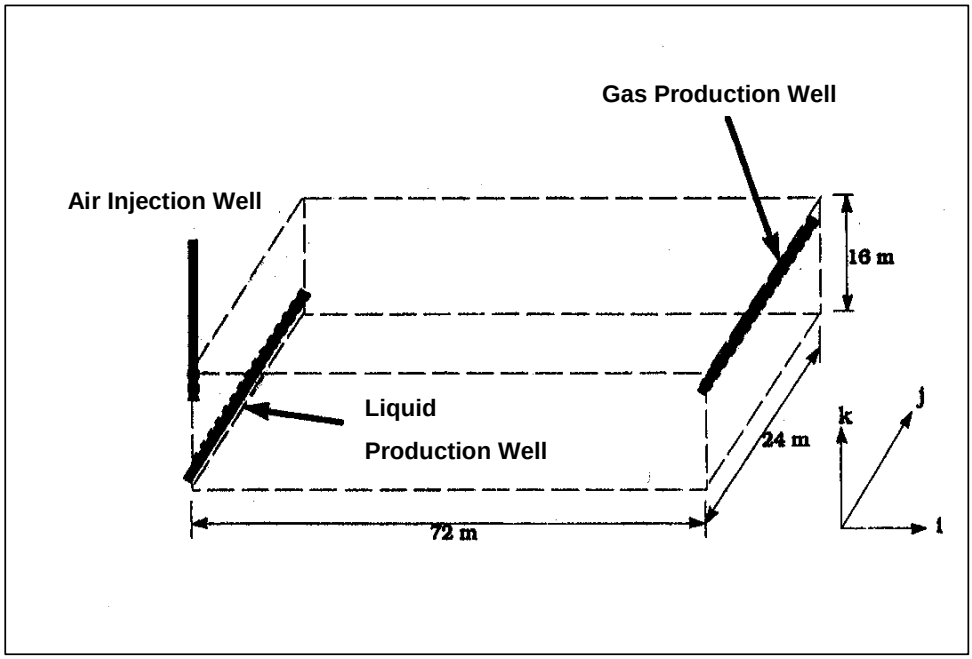

Figure 2.16: *3D COSH simulation model (Kisman et al., 1994)*

Bagci et al. (2000) conducted experimental work to study the COSH process. The study aimed to investigate the high recovery potential of gravity drainage with the efficiency of combustion processes and to examine the effect of various well configurations, horizontal and vertical sweep efficiency and oil recovery. A 3D physical model was used to perform the experiment. The model was a rectangular box with dimensions of 18cm by 54cm by 12cm. The vertical well was used as an air injection well and the top horizontal well was used to collect the gases generated by the combustion process (Figure 2.17). A horizontal production well was placed near the base of the model to collect crude oil and water. A total of eight experiments were conducted: six of dry combustion and two of wet combustion. The study revealed that higher oil recoveries were achieved with COSH process compared to that achieved with a vertical injection-vertical production well configuration case. A horizontal well near the base of the formation provides a higher recovery efficiency of heated oil than is possible with vertical wells. Also, it was possible to maintain a stable combustion front with the COSH process because the region between the combustion front and the oil production well was short and hot. Furthermore, the areal sweep efficiencies were higher in the case of the COSH process with horizontal production wells because of their larger contact area.

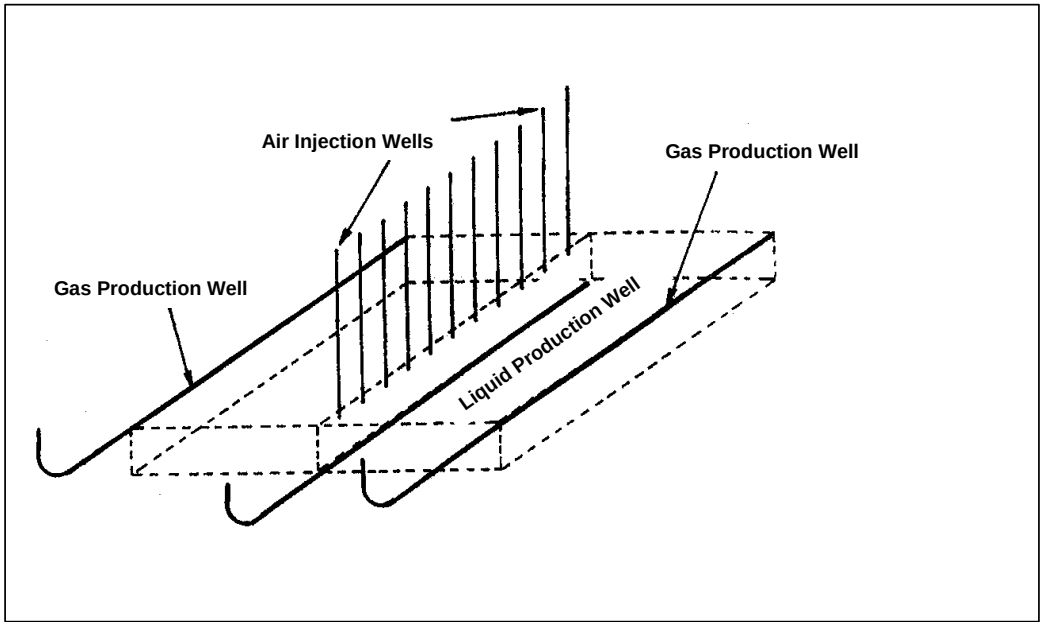

Figure 2.17: *Well pattern design for COSH process (Bagci et al., 2000)*

2.4.2 THAI

THAI 'Toe-to-Heel Air Injection' is a new thermal EOR process, which integrates in-situ combustion and advanced horizontal well concepts to achieve potentially very high recovery of heavy oil. It uses a horizontal producer well instead of a vertical producer well (conventional in-situ combustion). Furthermore, the injection well and horizontal producer well are arranged in line drive. The combustion front propagates along the horizontal well, from the 'toe' to the 'heel' position (Figure 2.18). THAI is able to achieve very high recoveries from heavy oil and tar sand bitumen reservoirs, due to the efficient sweep of the reservoirs by the combustion and hot gas fronts. An important advantage of THAI for heavy oil and tar sand bitumen application is its ability to realise very substantial in-situ upgrading by thermal cracking, producing upgraded oil to the surface. The process operates in a gravity stabilised manner by restricting drainage to a narrow mobile zone. This causes the flow of mobilised fluids to enter directly into the exposed section of a horizontal production well. The process can be operated on primary production or as a follow up to existing technologies where the advantages of high thermal efficiency are required. This is achieved by concentrating the energy required for oil mobilisation, recovery and thermal upgrading in the reservoir (Xia et al., 2001; Greaves et al., 1999).

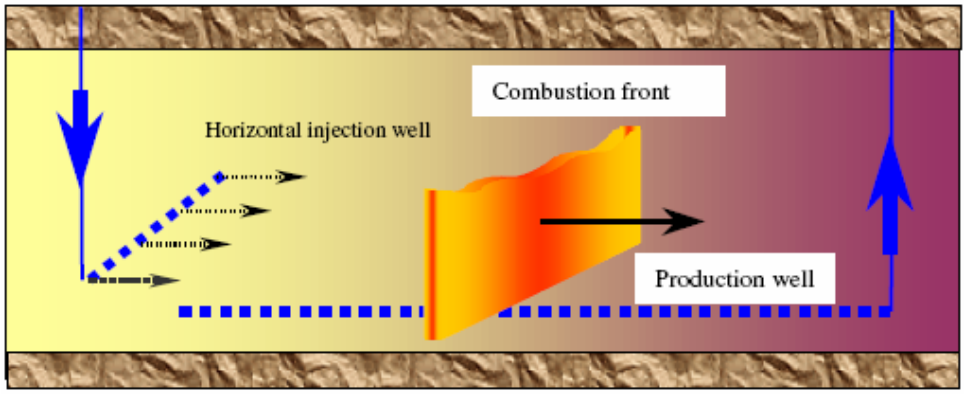

Figure 2.18: *Concept of THAI process using horizontal injector (Greaves et al, 2000)*

One of the most important features of the THAI process is the creation of a mobile oil zone (MOZ) ahead of the combustion front as shown in Figure 2.19. In a heavy oil reservoir, because of the high oil viscosity in the cold region of the reservoir, the heavy oil has an extremely low mobility. The cold oil provides a natural seal along the

horizontal well and preventing any gas bypassing. In addition, the cold heavy oil creates a viscous barrier and resists gas displacing into the near producer oil region. The creation of the MOZ allows the combustion process to be operated efficiently (Xia et al., 2000; Greaves et al, 2000).

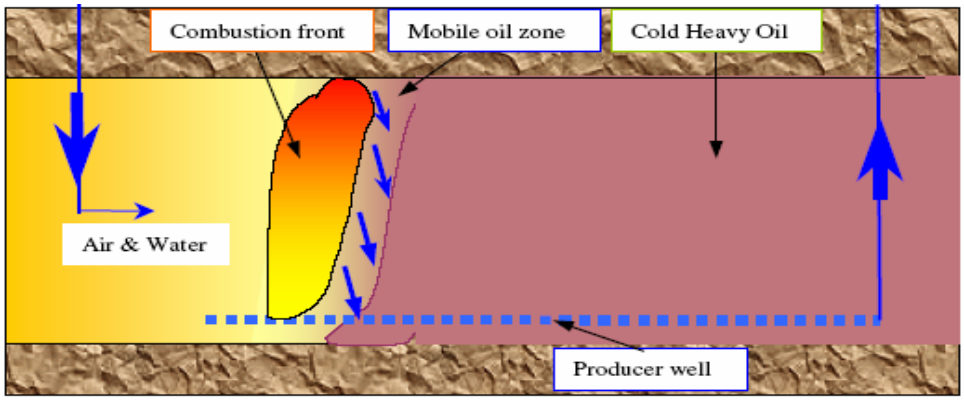

Figure 2.19: *Mobilised oil draining from narrow zone into exposed section of horizontal producer well (Greaves et al, 2000)*

By placing the injection well and horizontal producer well close to the top and bottom, respectively, of the oil layer, the flow of gas, water and oil occurs only in a MOZ ahead of the combustion front, and it is flowing from top to bottom under gravity drainage. The short flow path associated with the MOZ has a controlling effect on gas overriding. This ensures that there is a stable propagation of the combustion front through the reservoir. Furthermore, this property of concentrating the oil displacement in the MOZ effectively makes the process less sensitive to global reservoir heterogeneity effects. The high temperature in MOZ ahead of the combustion front provides not only for very efficient thermal sweeping of the oil layer, but also optimal conditions for thermal cracking of heavy residual, and hence thermal upgrading. Thermal cracking of heavy molecular weight components ahead of the combustion front produces the fuel for combustion reactions, sustaining stable combustion front propagation. The short distance oil displacement mechanism allows thermal upgraded oil to be drawn down into the exposed section of the horizontal producer, immediately below. In conventional in-situ combustion (using vertical injector vertical producer wells configuration), the mobilised oil is caused to bank-up in the cold region ahead of the front which leads to many operational problems, such as emulsion blocking and loss of air injectivity. Thus, THAI is able to capture and preserve the full extent of thermal upgrading produced by

thermal cracking reactions (Xia et al., 2002). The main benefits of THAI process are listed in Table 2.7 below:

Gas override is controlled and a good in-situ combustion front initiation
All mobilised liquids and combustion gases are drawn down into exposed section of horizontal producer well
High sweep efficiency, related to the absence of any gas coning (channelling) in the producer
Unique enhanced mobility oil zone downstream of the in-situ combustion front reduces sensitivity (preferential advancement) to reservoir heterogeneity in the virgin zone, mainly for extra heavy reservoirs
Fluid injectivity is increased due to higher permeability in the burned out zone and production mostly of upgraded and heated oil, immediately downstream of in situ combustion front
Front tracking capability via its "toe-to-heel" propagation with tight control of propagation
No extensive prior steaming or heating of oil layer necessary for injector producer communication development; this is achieved during in-situ combustion ignition phase and initiation of the linear front using vertical wells
For a commercial line drive operation, for a fixed well pattern, the number of wells is reduced to almost half due to their use first as producers and then as injectors
Creates ideal conditions for downhole catalytic upgrading, via the novel CAPRI^{TM} in-situ upgrading of heavy oils process, displaying enhanced upgrading, similar to surface upgrading

Table 2.7: *Benefits of THAI process for heavy oil recovery and upgrading (Greaves et al, 2000)*

THAI experimental and numerical studies: In 2000, Greaves et al. conducted experimental and numerical studies. The aim was to understand the mechanisms governing the high oil recovery and thermal upgrading achieved by THAI and to compare this process with other thermal EOR process. A 3D combustion cell was used and Wolf Lake crude was used as a representative heavy oil. In order to avoid heat losses from the cell, an improved control system was used in the experimental set up to

achieve near adiabatic condition. The numerical simulation of the process was carried out using CMG-STARS reservoir simulator. Because a 3D cell was used as the physical model for the experiments, it was necessary to build a 3D reservoir simulation model. The authors identified that THAI is a highly efficient method of heavy oil recovery. The very high oil recoveries achievable (up to 85%) make it a very attractive EOR method. Also, the thermal sweep is the main driving force for heavy oil recovery, assisted by forced flow into the horizontal producer well. Thermal cracking plays an essential part in the THAI process to maintain stable combustion, achieving high oil recovery and upgrading of heavy oil. Furthermore, the preliminary numerical simulation using CMG-STARS showed that THAI is a stable combustion process. Finally, compared to other thermal EOR methods to recover heavy oil, THAI has the advantage of a providing more robust process, reduces the effect of reservoir heterogeneities, which leads to higher ultimate oil recovery.

Xia et al. (2000) presented an experimental study using 3D combustion cell. The main aim of the study was to compare in-situ combustion (THAI) against steam flooding (Toe-to-Heel Steam flood) THSF. The 3D physical model experiments were conducted on virgin Athabasca tar sand bitumen. The authors concluded that Athabasca Tar Sand bitumen gave excellent ignition, and very stable combustion propagation was achieved during primary oil recovery with THAI using the 3D physical model. Very high oil recoveries were achieved (>80%) using THAI process as a primary production, and also as a follow up in a partially depleted reservoir, previously produced by steam injection (THSF). The oil produced was substantially upgraded, achieving an increase in API gravity averaging 8 points. Finally, the viscosity of the produced oil by THAI is reduced by over four orders of magnitude, compared with oil produced by steam injection.

In 2002, Xia et al. investigated the effect of the ignition and start-up periods of the experiments on the overall performance of the THAI process. In this study, a series of six 3D combustion cell tests were carried out using different combinations of the injection and production wells (Figure 2.20) for heavy oil (Wolf Lake) and bitumen recovery (Athabasca Tar Sand). The experiments showed that with electrical ignition, fast initial oil production was achieved for both Wolf Lake crude oil and Athabasca Tar Sand bitumen. When hot air was used for ignition, there was a substantial delay in oil

production, depending on initial reservoir temperature. Therefore, the delay in initial oil production seems to depend on the temperature level and the amount of heat injected during communication phase and ignition phase. The study found once high temperature was attained and combustion stabilised, the combustion front propagated through the sandpack in a 'toe-to-heel' manner, no matter what injector producer well configurations (i.e. HIHP, VI2HP…) was used.

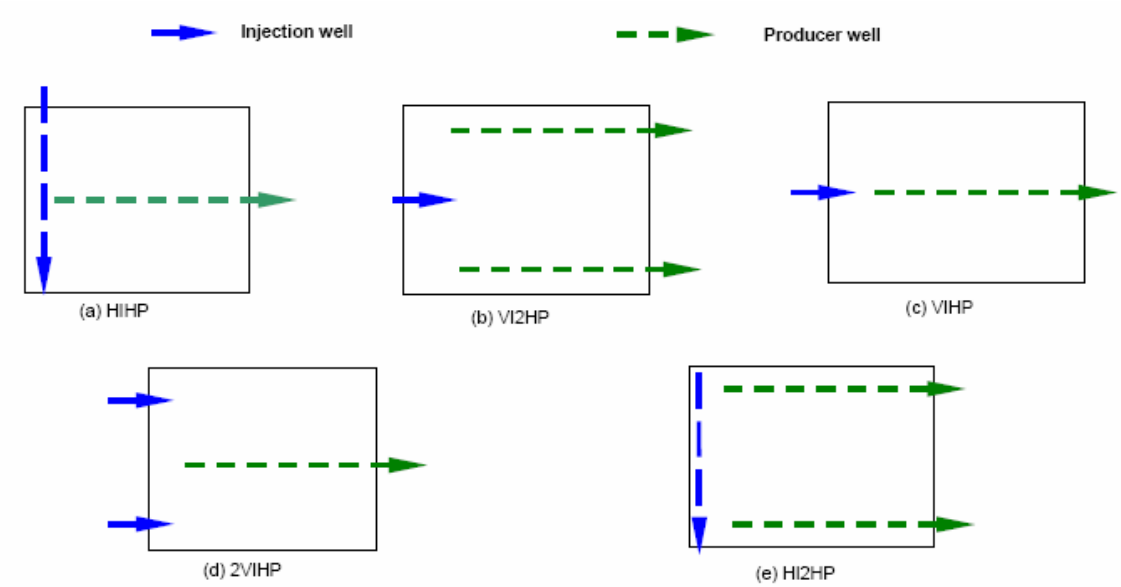

Figure 2.20: *Injector producer well combinations in THAI (Xia et al., 2002)*

In the case of bottom aquifer support, the use of the THAI process could be limited by high water cut at the heel with instantaneous air bypassing through the bottom water in the toe region (Turta et al., 2009). This might risk the stability of the combustion process because the THAI process was not designed for reservoirs with strong bottom water. However, the process THAI could be modified to delay watering of the heel and decrease air bypassing in the toe region, but this requires more investigations to be performed. Turta et al. (2009) believed that the process might still work for very weak bottom aquifer support where the aquifer thickness is very small (<10%) compared to the oil zone.

Rojas et al. (2010) conducted a numerical simulation study to investigate the impact of both the well configurations and reservoir heterogeneity in the fire flood recovery process using THAI well scenarios. The study results showed that the combination of

horizontal injector and two horizontal producers proved to be the best well pattern proposed out of all the well configurations they tested. Also, introduction of reservoir heterogeneity to the THAI process affected the recovery factor, but did not significantly impact the fire front initiation and propagation throughout the model.

2.4.3 Basal combustion

Many heavy oil reservoirs are underlain by thick bottom water aquifer. Very few of these reservoirs are commercially exploitable by conventional cold production or thermal technologies because of the high water mobility. The aquifer can act as a strong water source, which causes too early breakthrough in the production wells, or as strong energy sink that takes away most of the injected heat energy. As a result, the reservoirs are generally not attractive to produce, regardless of the huge oil resources contained in them. Basal combustion, which is a novel in-situ combustion process, can be considered as a solution to produce such reservoirs. Observations from field operations and numerical simulation studies indicated that when air is injected into a bottom water heavy oil reservoir most of it will flow along the upper part of the water zone and form a basal air layer underneath the heavy oil zone. Thus basal combustion utilises the high mobility bottom water and the density effect of air to introduce an air layer at the oil water contact, as Figure 2.21 shows. Depending on pressure distribution in the reservoir, this basal air layer will guide and spread the air flow. Since oxygen is contained in the air injected, this basal air layer is an extremely good in-situ combustion site. The reasons for the potential of in-situ combustion in this basal air layer are that the oxygen rich gas is in direct contact with hydrocarbon in place, and once ignited, this combustion layer will heat the oil zone from below (or hot plate heating mechanism) to mobilise and upgrade the oil in place above it. The potential benefits of basal combustion to heavy oil development can be very significant (Lau, 2001).

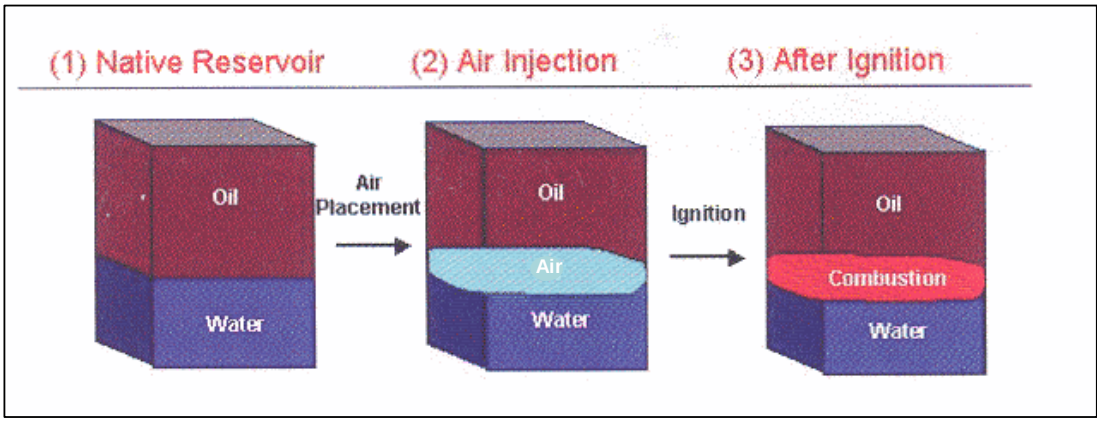

Figure 2.21: *Concept of basal combustion (Lau, 2001)*

The schematic of the basal combustion process with subsequent vertical displacement is provided in Figure 2.22. Initially a lateral displacement is made mainly through the aquifer using a vertical injector and a vertical producer, although the combustion front may have some lateral displacement within the oil layer itself. A horizontal well is located at the top of the formation, and it is kept closed during the lateral displacement through the aquifer. Thus, according to Figure 2.22, the process involves four phases:

- Preliminary air injection at the oil water contact to link the wells,
- Ignition of the formation in the injector well and propagation of the fire front almost up to the breakthrough in the vertical producer,
- A long period of soaking to allow conduction of heat upwards,
- Production of the oil through the horizontal producer while the vertical producer is closed.

The last phase is a vertical displacement due to the strong bottom water pushing the heated oil towards the horizontal producer. It is relatively stable, since water is heavier than oil, although the heated oil may not displace cold oil in a completely stable manner.

There are some limitations to basal combustion. The most important limitation is the loss of some oil in the aquifer which results in low oil recovery from this process. Also, it requires a very long soak period for effective conductive heating of the upper oil zone in order to establish stable vertical displacement which results in a delay in oil production. Another drawback of this process is the higher water cut due to the process location near to the aquifer (Coates et al., 2004; Lau, 2001, Turta et al., 2009).

Basal combustion experimental and numerical studies: Lau (2001) studied the possibility of developing and producing heavy oil reservoirs, which have underlying bottom aquifers. He addressed the application of in-situ combustion in the form of the new basal combustion concept. The study was conducted by first establishing a numerical model to simulate the combustion effects observed in the laboratory combustion test. This model was then modified in steps into a field scale 3D model to investigate the feasibility of applying basal combustion in a 63000cp oil viscosity reservoir. The simulation results show that in-situ combustion may work very well in bottom water reservoirs, because the water zone can be utilised as: (1) mass and energy transport media, (2) an effective heating generation zone. Also, high recovery of upgraded oils can be expected if basal combustion is applied in oil sands, and high energy efficiency can be expected if it is applied in mobile heavy oil reservoirs.

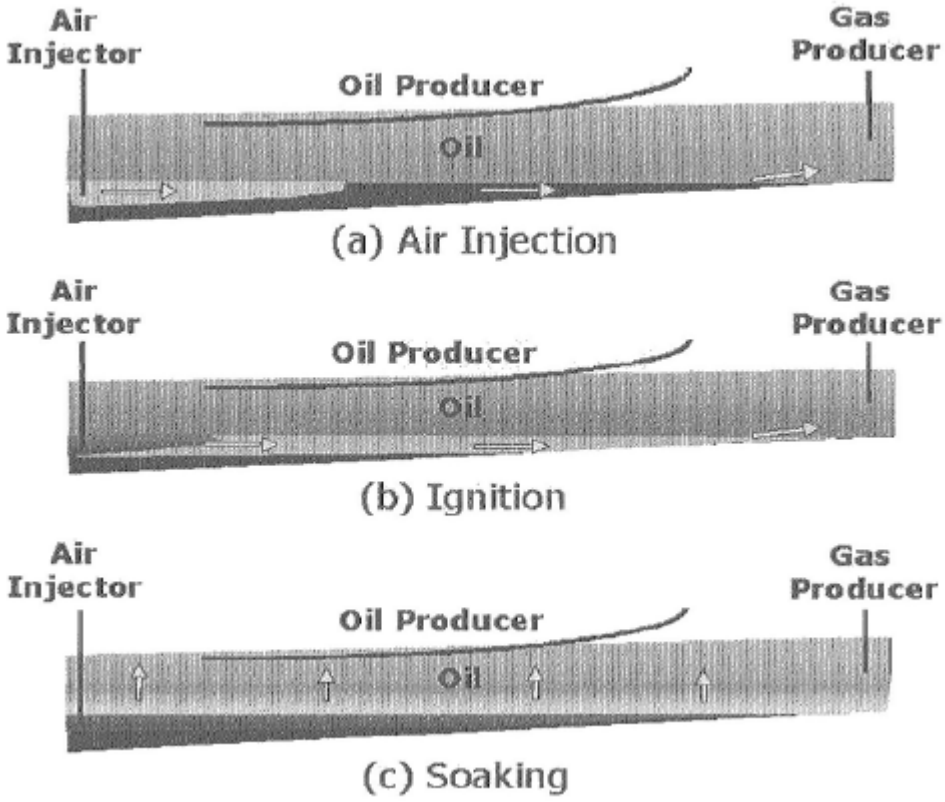

Figure 2.22: *Basal combustion with vertical displacement (Coates et al., 2004)*

2.4.4 Top-down in-situ combustion

Top-down is an in-situ combustion process, in which the combustion front is started and maintained by injecting air at the top of the reservoir, with drainage of the mobilised oil by gravity to a bottom horizontal well. It is developed with the aim of overcoming some of the problems that have restricted the successful application of conventional in-situ combustion processes in oil reservoirs and heavy oil formations. Previous in-situ combustion field projects, however, have been less successful than steam, primarily because of the difficulty in controlling the combustion front propagation. The conventional in-situ combustion operations of the past involved the injection of air into a central vertical injection well surrounded by a number of vertical production wells (typically as part of a larger pattern of injection and production wells). Combustion is initiated near the injection well and horizontally propagated radially outwards, aiming to drive the mobilised oil towards the production wells. The problem frequently encountered is that the combustion fronts tend to advance irregularly with the vertical sweep constrained by gravity override of the displacing gas and the areal sweep reduced by preferential flow to one well of the pattern. Injected air overriding the combustion zone, created problems at the production end and the overriding hot steam and combustion gases are not efficient to heat the formation ahead of the burn zone (fire front). The displacement geometry of the process requires that the mobilised oil be displaced ahead of the combustion front into the colder immobile oil increasing oil saturation and further reducing mobility with the limited productivity of the vertical production wells unable to improve the situation (Cunha, 2005; Coates et al., 1995)

The schematic of the top-down process is provided in Figure 2.23. A number of vertical injection wells are completed at the top of the oil zone and they are spaced immediately above a horizontal well located at the bottom of the oil zone. Combustion is initiated at the injectors and is propagated downward with the mobilised oil draining by gravity to the lower production well.

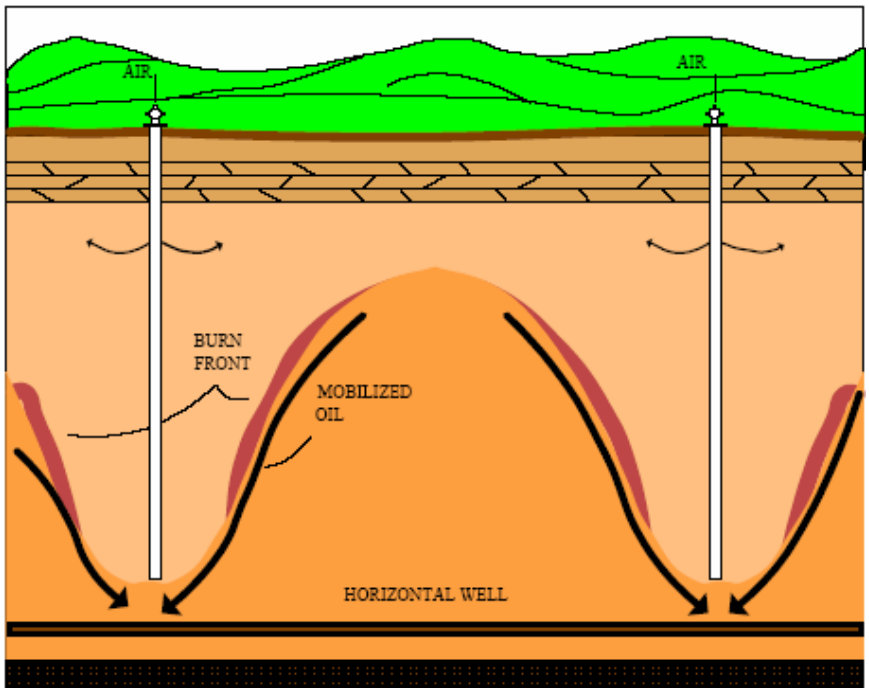

Figure 2.23: *Top-down in-situ combustion process (Coates et al., 2004)*

The conceptual strategy of the top-down process involves the stable propagation of a high temperature combustion front from the top to the bottom of a heavy oil or oil sand reservoir. Combustion is initialised and maintained by injection of an oxygen containing gas at the top of the reservoir, with mobilised oil draining to a lower horizontal producer well. Most of the injected oxygen is consumed in the high temperature combustion reactions at the combustion front. Oxygen that passes unreacted through the combustion front, reacts in lower temperature reactions to produce a layer of coke which is subsequently burned as the combustion front moves through. Hot combustion gases and thermally cracked light ends mix with the oil ahead of the high temperature front, which result in heating, upgrading and driving the oil by a top down gas drive. Gravitational forces help drain the oil to the horizontal producer.

The top-down in-situ combustion process design is best when considered for thick high viscosity reservoirs where vertical flow channel can be established between the injector and producer to provide an initial path through which the mobilised oil can travel. By considering such a design the advantages and potential of this process are that it should be relatively easy to control with fewer operational issues because of the gravity stability and less oxygen channelling to the production well. Recovery from the top-

down combustion scenario is high and because of gravitational drainage less air is required to enhance the combustion process. In the case where oxygen enriched air is used, this may help in improving the performance of the process by allowing lower injection rates. Also, the development of an overlying gas cap helps drive the oil to the producer. In the case of a bottom water aquifer being present, if the operating pressure is matched to the aquifer pressure this process should reduce water influx into the oil zone, which makes the top-down in-situ combustion process a potential recovery method that could be applied in oil reservoirs with strong bottom aquifer support (Turta et al., 2009).

Some of the challenges of the top-down in-situ combustion process are that the amount of oil available is controlled by the thickness of the pay, therefore the thicker the pay the better. The high bitumen saturation and viscosity of virgin heavy oil reservoirs must be overcome to obtain initial injectivity. Finally, this process has not been tested in the field and any field pilot will be fairly substantial, requiring a large upfront investment (Coates et al., 2004; Coates et al., 1995).

Top-down experimental and numerical studies: In 1995, Coates et al. investigated the possibility of applying top-down process in heavy oil reservoirs as a new in-situ combustion process. A 3D physical model was used to conduct the experimental work. The model was built using experience gained from pervious work in 1D combustion experiments and numerical model predictions. In order to verify the experimental study, numerical simulations were preformed using CMG-STARS by incorporating a reaction model for in-situ combustion of Athabasca bitumen. The authors concluded that employing a suitable air injection flux is essential to obtaining a gravity stable combustion front. The injection flux must be sufficient to supply enough oxygen to initiate and sustain combustion but not too high as to lead to channelling. Furthermore, the time to reach ignition after commencing air injection is highly dependent on the degree of pre-heating. If pre-heating is accomplished by steam injection, the ignition time will take longer because of the increased water saturation in the formation. In addition, wet combustion shows the potential to increase production rate if it is commenced before the sand pack has become depleted. Finally, provision of a vertical communication path aids in establishing initial injectivity; however, selecting the proper

path depends on the formation permeability distribution as a combustion front can rapidly advance along a high permeability path.

In the previous study (Coates et al., 1995), the effect of well configurations was not investigated and their impact on the in-situ combustion process is currently not known. Also, the combustion process performance in the case where a strong bottom aquifer support exists needs to be examined. In order to investigate these points, this study will be conducted to numerically consider the application of in-situ combustion with different well configurations and with/without the presence of strong bottom aquifer support. Moreover, the effect of reservoir heterogeneity will be studied and its impact on the fire front process will be presented.

2.4.5 Long and short distance oil displacement

In many EOR processes, a long distance oil displacement (LDOD) scenario may occur where a long distance separates injector and producer wells involved in the process. The LDOD has the ability to increase microscopic displacement efficiency (immiscible and miscible methods) in the invaded zone and to increase the sweep efficiency by suitably modifying the mobility ratio. For example, during polymer flooding, an increase in viscosity of the injected water occurs in the invaded zone. However for thermal methods, a decrease in viscosity occurs just ahead of the displacement front, and the average oil viscosity is a weighted average of the cold oil and heated mobilised oil viscosity. It is this average which strongly influences the propagation of the displacement front in layers with different permeabilities. Unfortunately, this average is closer to cold oil viscosity rather than heated oil viscosity over much of the life of these projects. Consequently, because the heated oil is forced to flow through the cold region, the mobility ratio between injectant and oil still remains very high, which reduces the thermal process efficacy when a LDOD configuration is used. As a result, another well configuration group is developed which is called short distance oil displacement (SDOD). For the application of thermal EOR methods, there are thus two broad categories of well configurations which occur:

- Short distance oil displacement (SDOD) configuration
- Long distance oil displacement (LDOD) configuration

The LDOD processes are schematically illustrated in Figure 2.24. The application of in-situ combustion in an LDOD configuration is representative of conventional lateral in-situ combustion, where the oil is displaced laterally by an in-situ combustion front (Figure 2.24). In many situations, due to the high viscosity of oil, its displacement to producers located a long distance away from an injector is neither practical nor profitable. In these cases, if the oil reservoir consists of a thin and relatively homogeneous pay section and if no channelling or override develops, the required injection pressure may be too high (due to large pressure gradients). Therefore, such a process cannot sustain reasonable injection rates. The process can lead to either an exceedingly high injection pressure or a direct channelling of the in-situ combustion front, which is associated with very poor volumetric sweep efficiency. In both situations the process performance is low and a low recovery factor is typically achieved (Coates et al., 2004; Turta et al., 2004).

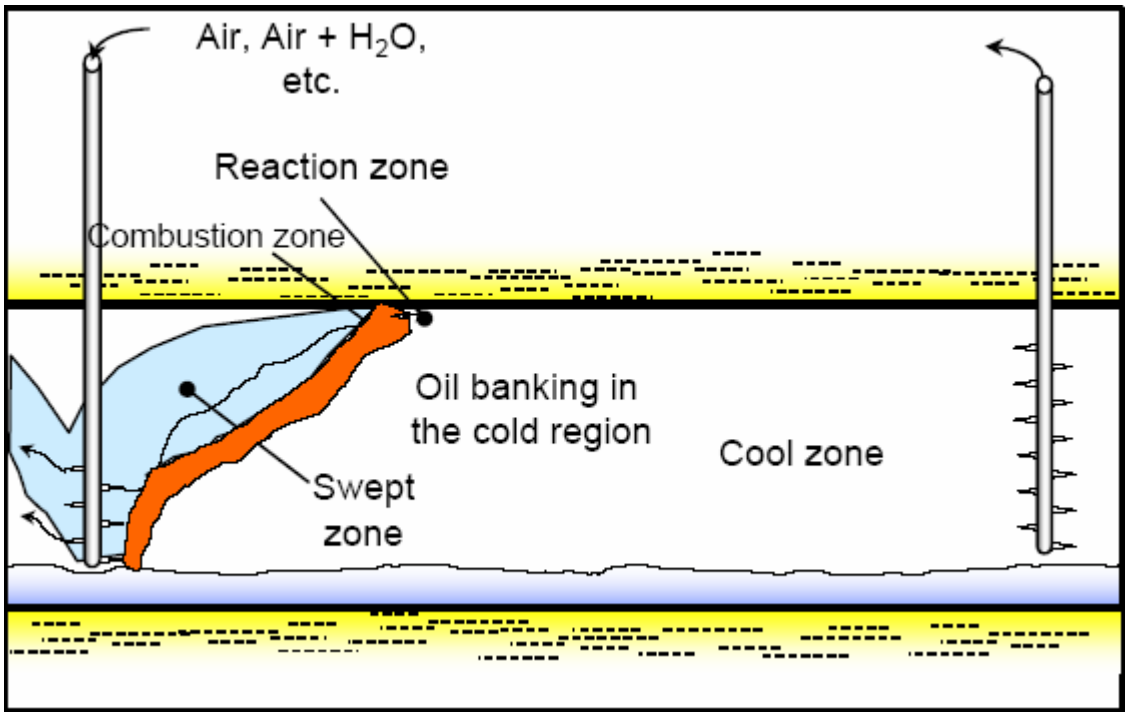

Figure 2.24: *Conventional lateral in-situ combustion process (Coates et al., 2004)*

With the arrival of horizontal well technology, a new approach to improve recovery of heavy oil is becoming popular, from moving mobilised oil in a pattern or line drive flood over long distances (of the order of hundreds of metres) to short distance oil displacement, which typically occurs over a few metres or tens of metres using the short

distance oil displacement processes. Generally, the SDOD processes use horizontal producers and injectors, or combinations of horizontal producers and vertical injectors. An important feature of SDOD processes is the mitigation of the heterogeneity effect. The negative effects of heterogeneity are decreased, mainly due to the use of the horizontal well. Also, these processes utilise gravity segregation as an advantage. The application of the in-situ combustion in an SDOD configuration is shown in Figure 2.25 (A) for SAGD and (B) for THAI. The distance travelled by oil is significantly shorter, and oil is no longer flowing through the cold region; instead it flows through a MOZ created adjacent to a heated chamber formed during the process. Also, SDOD is implemented in the other in-situ combustion processes, such as COSH, and basal in-situ combustion with subsequent vertical displacement. In the case of top-down combustion, the oil is partially displaced and flows through the cold oil region (which is a feature of LDOD), however top-down is considered to be an SDOD process. This is because the distance that oil is displaced in the SDOD processes is much smaller (thickness of layer) compared to the distance in the LDOD processes. An important advantage of the SDOD processes is their ability to preserve the upgraded oil (which is a product of the in-situ combustion process) and to produce it without delay (Coates et al., 2004; Turta et al., 2004).

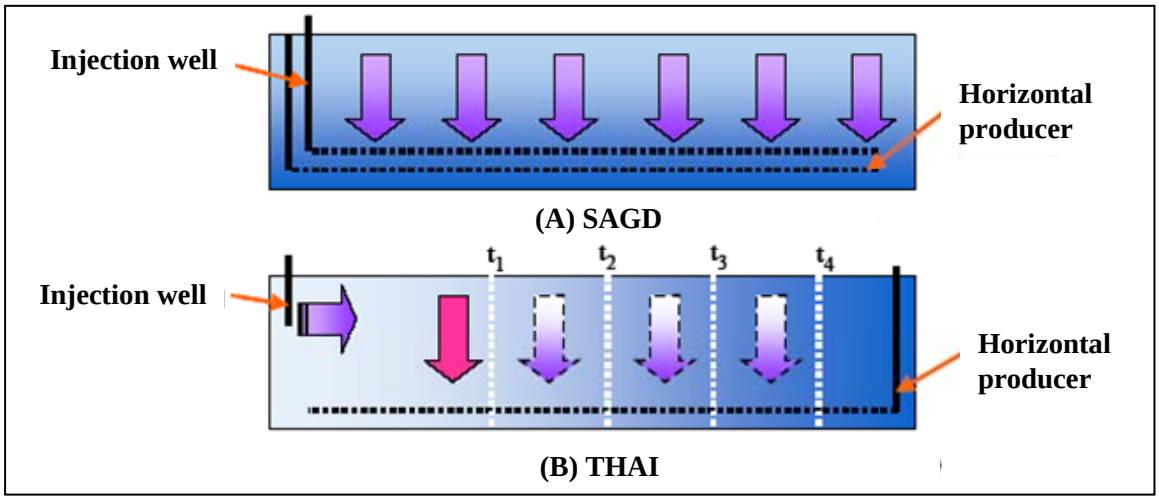

Figure 2.25: *Short distance oil displacement processes (Coates et al., 2004)*

2.5 In-situ combustion oil displacement mechanisms

Thermal EOR methods rely on several displacement mechanisms to recover oil. The relative importance of each mechanism depends on the type of oil being displaced and the related recovery process. For in-situ combustion processes, the mechanisms are closely related to the thermal and temperature effects of the reservoir rock and fluid properties. In this process the oil displacement results from (1) viscosity reduction of oil, (2) thermal expansion of the reservoir fluids and rocks, thus reducing their densities, (3) distillation and thermal cracking of oil, (4) a solution gas drive from produced gas that facilitates the flow of fluids within the reservoir toward the production wells, (5) increased pressure gradient imposed by the injected air and generated gases, and (6) gravity drainage. Mechanisms such as distillation drives and thermal expansion of the heated oil add to recovery as crude distillation tends to reduce residual oil saturation. Lighter oil fractions vaporise providing a miscible flood front in advance of the thermal front. However, thermal processes mainly rely on crude viscosity reduction due to temperature increases as the most important recovery mechanism (Jha et al., 1986, Marique, 1996).

Viscosity reduction: This is the most important mechanism in thermal EOR processes. Since the aim of applying thermal processes to a reservoir is to increase the reservoir temperature, as a result oil viscosity decreases dramatically. This significant reduction in oil viscosity results in increased oil flow rate and efficient oil displacement in the reservoir. Figure 2.26 shows the viscosity reduction for different API gravity crudes 12°, 20°, and 30° with temperature. When the temperature is higher than 350°F (ca. 177°C), the crude oils have a viscosity less than 7cp. As the temperature increases from 100 to 350°F (ca. 38 to 177°C), the 12°API crude has an approximately 265 fold reduction in oil viscosity; 35 fold for the 20°API crude; and 11 fold for the 30°API crude (Wu, 1977).

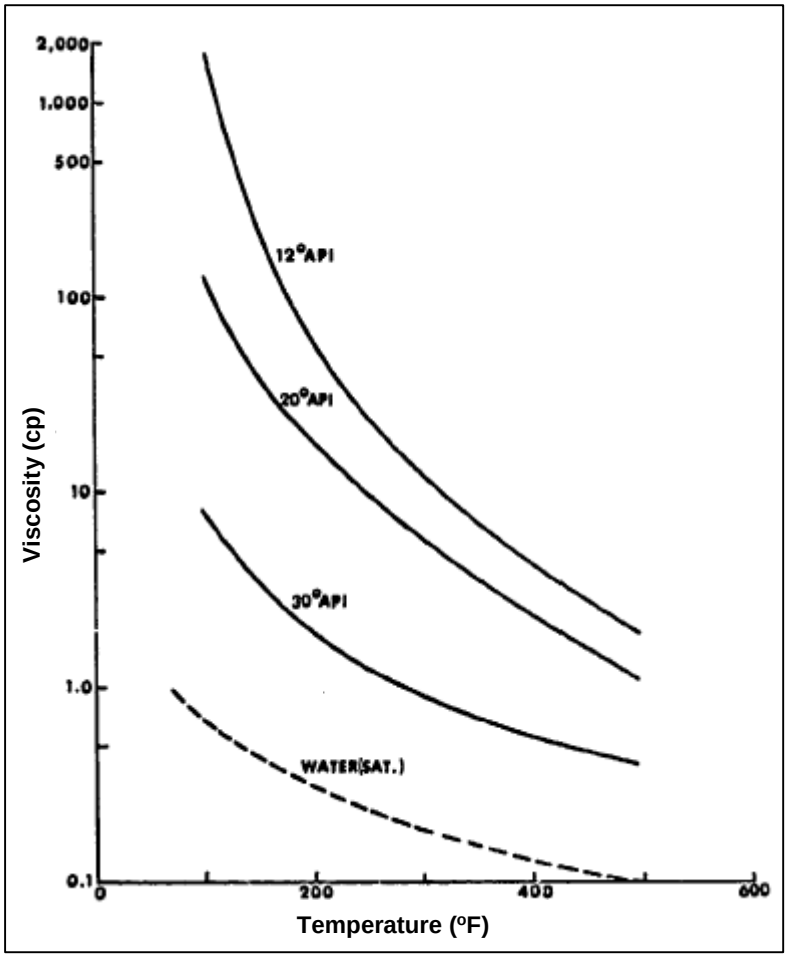

Figure 2.26: *The effect of temperature on crude oil viscosity (Wu, 1977)*

Thermal expansion: This is also a very important mechanism for oil recovery. By providing the reservoir with heating energy, the temperature increases and allows the expansion of the reservoir contents. As a result of this expansion, the oil flow rate is increased due to the increase in oil saturation.

Distillation and thermal cracking of oil: In in-situ combustion, steam is produced from the vaporisation of initial water saturation and from water produced as a result of combustion reactions. The steam works as an important driving mechanism to recover crude oil, this mechanism is called steam distillation. Steam distillation is a process of separating (vaporising) the light ends from the crude oil by the action of steam. In general, it involves three phases: two immiscible liquid phases and a vapour phase. At equilibrium conditions, each of the immiscible liquid phases contributes its vapour pressure to the system pressure at a given temperature. When the system pressure is equal to, or less than, the sum of the vapour pressures, the liquid mixture boil and give

off component vapours. Since the vapour pressure of each liquid depends only on the temperature, it is evident that, at a given pressure, the boiling temperature of the liquid mixture always is lower than the boiling temperature of either phase alone (Wu et al., 1971). Rapid vaporization of water in the steam plateau should in principle enhance the efficiency of steam distillation since the mixing of the two liquid phases is improved by the resulting disturbance. This rapid phase change should also help expel a portion of the oil from the smaller pores because of the expansion of the water vapour.

Thermal oil cracking is another driving mechanism in the combustion process. It occurs in the high oxidation reactions zone of the combustion process, where the maximum temperature of the reaction can be achieved. This mechanism allows the breaking of the chemical bond in the heavy ends of the crude oil. As a result, more light ends are produced, which increase the API gravity of the oil and allows for the production of more valuable oil.

Miscible and gas drives: Hydrocarbon gases develop from normal distillation mix with the hydrocarbon gases formed in the cracking reaction. The combined streams blend and condense in the oil bank ahead of the combustion front. This blending reaction and the heat imparted to the oil when the gases condense make the oil more mobile and improve oil displacement. Another effective drive mechanism is formed during the burning process. The combustion gases generated at the burning front move ahead of the combustion front, which transfers heat to oil in the downstream region. Carbon dioxide is one of the produced gases from the combustion reaction. It partially dissolves in the oil and reduces the oil viscosity (White et al., 1983).

Gravity drainage: The gravity drainage mechanism is one of the most efficient ways of producing an oil reservoir. Unfortunately, most heavy oil reservoirs cannot be produced economically under freefall gravity alone because the effective oil permeability is too low, the oil viscosity is too high, or the dip of the formation is too small. The new in-situ combustion processes such as COSH, THAI, and top-down developed to make use of gravity drainage recovery mechanisms. For example, in top-down combustion, the injector is placed in the top and the horizontal producer is located in the bottom of the

reservoir. By using this well configuration the heated oil flows to the producer in the bottom under gravity drainage drive.

For the previously discusses recovery mechanisms, the reservoir characteristics and the fluid properties are the main factors which define the dominant recovery mechanism in the system.

2.6 In-situ combustion having bottom water

Bottom water drive is considered to be one of the natural drive mechanisms, which enhances oil production from a reservoir. The drawback of this mechanism is the possibility of water coning. Water coning is considered the biggest problem during oil production from a reservoir with bottom water. The occurrence of water coning is due to pressure gradients (pressure drawdown) resulting from well production from the pay zone. The pressure gradients result in a water cone rising toward the bottom of the producing interval. The tendency of the water to cone is offset or partially offset by gravity forces since the water has a higher specific gravity than the oil. A dynamic balance exists between the gravitational forces and the pressure gradients caused by well production. If the pressure gradient exceeds the gravitational force, water coning to the wellbore will occur (Ju et al., 2005). It is very difficulty to control water coning, especially for heavy oil reservoirs with bottom water since the difference in specific gravities of oil and water is very small. Most of the available literature is focused on the prediction of critical production rates and water coning processes for production. For a heavy oil reservoir, generally, the critical production rate is too small to gain a profit based on operating costs. If the operator maintains a production rate above the critical production rate, water coning results in a high water cut is observed. This means that the application of in-situ combustion is affected by the presence of bottom water, which tends to divert a significant portion of the injected air, thereby reducing the heat input in the oil zone. Depending on the extent of the bottom water, this process may be uneconomical under such circumstances. Moreover, for a given set of conditions, it may be economically feasible to conduct an in-situ combustion project in spite of a bottom

water zone. The role of bottom water on in-situ combustion can be quite complex, depending on the oil viscosity and oxidation characteristics of the crude oil. In such cases the injected air may flow near the upper part of the water zone, forming a vertical gas saturation gradient. To a first approximation, the amount of air channelling through the water is independent of the water zone thickness. Naturally, it will vary as the fire front advances through the oil zone. A complicating factor is the production of the bypassed air through the oil zone in the vicinity of the producer. If oxygen is not consumed by any oil present in the water zone, it may cause spontaneous ignition, creating a combustion surface near the producer. This type of behaviour has been observed in the field as well as in numerical simulations (Farouq Ali, 1983). In general, the presence of bottom water in in-situ combustion reservoir leads to high AOR; however, the process may still be feasible in thick water zones.

Application of in-situ combustion in presence of bottom water aquifer: Turta et al. (2009) conducted a detailed review of both field and laboratory tests for the applications of in-situ combustion in heavy oil reservoirs which are underlined by bottom water support. The studies based on available published information from pilot test or experimental work which covers implementation of air injection as a thermal EOR method. The review of the pilot tests showed that when applying in-situ combustion to a reservoir with the presence of aquifer support, the overall process parameters in terms of design, implementation, operation, monitoring and evaluation should be made differently than those used for conventional in-situ combustion process (without an aquifer present). This is mainly because the aquifer support leads to unstable propagation of the fire front and the main symptoms observed were a decrease in the oxygen utilization with time. Another issue with the application of in-situ combustion in bottom water support reservoirs was that the injected air bypasses the fire front through flowing into the water zone. This results in unpredictable and uncontrollable combustion front propagation. Moreover, Turta et al (2009) reviewed the laboratory work which showed that designing and conducting meaningful and representative experiments for in-situ combustion in the presence of bottom aquifer support were challenging and more complex than normal combustion test experiments. However, the available experimental work did manage to capture the movement of the fire front

between the oil and water zones, which could contribute to the understanding of similar future laboratory and field projects.

Zwart et al. (2008) conducted a numerical modelling study in a medium heavy oil reservoir to investigate the affect of strong aquifer presence on the efficiency of implementing thermal EOR methods. They used both in-situ combustion and high pressure steam injection in their modelling study. The main aim of the study was to utilise the aquifer presence to enhance the oil recovery from the reservoir when implementing thermal EOR. In the in-situ combustion scenario where a 2D cross sectional model was used, air was injected from the model top and the fire front initiated and then moved toward the producer which was located near the oil water contact. This well configuration allowed the influx from the aquifer to drive the reduction in viscosity; heated oil heated the producer which improves the aquifer displacement of the oil. As a result, more oil was mobilised and produced and a better oil recovery was achieved.

A numerical study of the application of in-situ combustion where bottom aquifer support exists was conducted by Brooks et al. (2010) as a part of the main study to evaluate the viability of applying EOR methods into medium heavy oil reservoirs. A 3D simulation model was used and the combustion process reactions were represented with a single reaction, which was the high temperature oxidation reaction. This was done to simplify the modelling process and reduce the calculation time and the modelling process complexity. This is in contrast to our study, where six chemical reactions were used. The thermally assisted aquifer drive (TAAD) concept was used to ensure a successful combustion process where the fire front moved downwards in the model (instead of the lateral movement under the gas override effect) and the aquifer influx was controlled in order to achieve an improved sweep efficiency. The study results suggested that well placement and configurations are a critical factor in the success of the combustion process, and thus these should be considered in any comprehensive simulation study (Chapter 4 of the present work considers these is detail). Also, the use of three vertical injectors completed in the top and two horizontal producers completed in the middle of the model resulted in an optimum fire flood process. Implementation of in-situ combustion in this study resulted in an increase of 17.3% in the cumulative oil

produced from the model. The third dimension used in this study led to some variation in the overall combustion process results when compared to what has been done in this thesis. For example, this study considered well numbers and locations in greater detail than could be addressed in the 2D model used in this thesis.

2.7 Chemistry of in-situ combustion:

Since the techniques of in-situ combustion are essentially based on the existence of chemical reactions occurring within the porous medium. A qualitative and quantitative analysis of these reactions is crucial to an understanding of these methods. The basic knowledge related to the nature and rates of these reactions is important as well as to the heating effects they induce to the system. They are generally studied in the laboratory either at a constant temperature or by submitting the samples to a programmed temperature increase in order to simulate an approaching combustion front. The heat of combustion can be calculated provided that the composition of the reactants and the products is known. Though extensive research has been done at the application level, it is equally important to understand the underlying chemistry of the phenomenon of in-situ combustion so that the kinetics can be described and modelled. The combustion front propagation and air requirements are controlled by the exothermic oxidation reactions (Burger et al 1972). Moreover, the peak temperature which is the temperature at which the rate of the reaction is maximum, is related to the heat released by oxidation and combustion reactions. This draws a need to quantitatively estimate the different parameters that relate to the chemistry of the process. The physical phenomena which occur during hot fluid injection also contribute to the efficiency of in-situ combustion. Some of these phenomena may even have greater intensity due to the higher thermal level. Other effects may intervene, considering the composition of the fluids and the thermodynamic conditions involved.

In this section, the main chemical reactions and the kinetics which are believed to exist in in-situ combustion processes are briefly presented. Also, other chemical factors which have an impact on the in-situ combustion process are discussed.

2.7.1 The chemical reactions

There are three major chemical reactions groups considered in the in-situ combustion process. Two are oxidation reactions which are (1) low temperature oxidation of liquid phase hydrocarbons (LTO) and (2) high temperature oxidation (HTO) of solid hydrocarbons residue. The third reaction is the thermal cracking (pyrolysis), which is the main producer of combustion process coke (Le Thiez et al, 1990; Belgrave et al., 1993). When in-situ combustion process operated in high temperature oxidation mode, the following reactions are expected to take place (Xia et al., 2001):

- Thermal cracking:

$$Crude\ heavy\ ends \rightarrow Crude\ light\ ends + Coke \qquad \textbf{2.1}$$

- Oxidation of Coke:

$$Coke + Oxygen \rightarrow CO + CO_2 + H_2O \qquad \textbf{2.2}$$

- Oxidation of Heavy residual:

$$Crude\ heavy\ ends + Oxygen \rightarrow CO + CO_2 + H_2O \qquad \textbf{2.3}$$

HTO: occurs due to the oxidation of fuel deposited in the rock matrix achieving the maximum temperature in the in-situ combustion process (peak temperature). It takes place in the combustion front and provides the maximum heating energy to the reservoir. At temperatures more than about 932°F (500°C), the oxidation reaction between oxygen and coke result in the formation of carbon dioxide, carbon monoxide, and water as the principle reaction products. The HTO reaction removes carbon from the fuel by breaking the fuel chain. The stoichiometry of the HTO process is given by equation (2.4) when the sulphur, nitrogen, and oxygen contents of fuel are ignored.

$$CH_x + (1 - 0.5m' + 0.25x)O_2 \rightarrow (1 - m')CO_2 + m'CO + \frac{x}{2}H_2O \qquad \textbf{2.4}$$

Here *x* is the average number of hydrogen atoms per carbon atom, known as the atomic H/C ratio, and m' is the mole ratio of carbon monoxide to (carbon monoxide+carbon dioxide) (Prats, 1982; Mamora, 1995). In addition to hydrocarbon gases, the presence of nitrogen, carbon dioxide, carbon monoxide, oxygen, water, hydrogen, argon, and H_2S are found in the analysis of produced gas in combustion field operations. As related to the combustion process, nitrogen, oxygen, and argon are considered to come from the injected air. The carbon oxides and water are considered to be the products of HTO. Hydrogen is considered to be released by thermal cracking of the crude just downstream

of the combustion front, and any sulphur in excess of the associated with naturally occurring hydrogen sulphide is considered to arise from desulfurisation reactions. Analyses of produced carbon oxides and free oxygen often are used to determine the type and amount of fuel burned (Prats, 1982). The fuel availability under the conditions of the HTO reaction is usually determined from the analysis of laboratory combustion experiments where the reservoir rock and crude oil are used. The most common experiment is to curry out a material balance on the effluent gases collected during a combustion tube experiment (Green & Willhite, 1998).

LTO: takes place upon air injection either before or after ignition, when the oxygen is available downstream from the combustion front. This may result from (1) incomplete oxygen consumption in the high temperature combustion zone, (2) air channelling around the combustion front, or (3) a tilted combustion front surface (Fassihi et al, 1980a). LTO reactions are exothermic reactions which are characterised by either no carbon oxides or low level of carbon oxides in the produced gases. In other words, more oxygen reacts with the oil than can be found in produced gases (Fassihi et al, 1980a). The reactions occur with the oxygen dissolved in the whole volume of the dispersed oil phase. When the oil phase is highly dispersed in a porous medium, diffusion may be faster than oxidation. The main product of the LTO reactions are oxygenated compounds such as carboxylic acids, aldehydes, ketones, alcohols, and peracids, (Fassihi et al, 1980a; Green & Willhite, 1998).

Mamora (1995) conducted combustion tube experiments to investigate the factors that cause LTO and its effect on the combustion process and properties of the produced oil. The experiments showed that LTO occurred due to the low fuel concentration, which resulted in a reaction front temperature of only 572ºF (350ºC), and oxygen channelling ahead of the combustion front.

Thermal cracking (Pyrolysis): is the main chemical reaction that deposits fuel (coke) in reservoir matrix, which is required to initiate and sustain the in-situ combustion process in a reservoir. Several terms are used to describe this process, for example “coke formation,” “fuel laydown,” “cracking,” and “fuel deposition”. Fuel deposition occurs in reservoirs as a result of various physical and chemical changes inflicted upon

the reservoir oil, mainly distillation and thermal cracking (Abu-Khamsin et al., 1988). The amount of fuel deposited is a critical parameter in the combustion process. If the fuel concentration is too low, the amount of heat generated may be insufficient for a self sustaining combustion front. In contrast, a high fuel concentration may result in a low combustion front velocity, severe temperature profile and high air requirements, resulting in high air compression costs. The way the maximum amount of oil recovery is determined is by subtraction of the amount of fuel consumed from the OIIP (Mamora, 1995).

In order to model fuel deposition, the sequence of events that leads to it has to be characterised and related. Ahead of the combustion front, the displacement of light hydrocarbons followed by steam drive reduces the oil saturation to the residual with substantial distillation of light ends. The approach of the combustion front causes temperature to rise steadily with time, which results in more distillation and triggers mild oil pyrolysis. Then, immediately before the arrival of the front, severe pyrolysis of the trapped hydrocarbons causes fuel deposition. According to the sequence of events, two classes of pyrolysis reactions can exist, based on the reaction temperature evolved in standard processes of thermal treatments of crude oil: visbreaking and coking. Visbreaking reactions are preformed under mild temperature to reduce permanently the oil's viscosity and specific gravity. On the other hand, coking reactions are performed under severe thermal cracking conditions to produce a solid residue at low H/C ratio (Abu-Khamsin et al., 1988).

Several studies were carried out to investigate the factors affecting fuel deposition in in-situ combustion. Experimental studies found that the fuel deposition increased with initial oil saturation, oil viscosity and the residue, and decreased with increasing atomic H/C and API gravity of the oil. Also, reservoir lithology has an effect in the fuel deposition process (Alexander et al., 1962; Gates et al., 1980). Subsection (2.7.3) illustrates the impact of clays and metal ions on the in-situ combustion process.

2.7.2 Kinetics of the chemical reactions

Kinetics deals with the dynamics of reaction processes. It is important to study in-situ combustion kinetics to obtain modelling parameters, such as the Arrhenius activation energy, order of reaction, and pre-exponential factor. Such values are needed for numerical modelling studies and also can be used to calculate ignition energy requirements or the ignition duration. Kinetics is also important to identify the reaction regimes of a particular crude oil by distinguishing between LTO and HTO and to determine the possibility of spontaneous ignition if the crude oil is kept in contact with air at reservoir conditions (Yannimaras et al., 1995).

Laboratory combustion and oxidation tests can provide important and relatively inexpensive insight into the behaviour of in-situ combustion for a given reservoir system. The needs for those experiments are for three main reasons:

- To have a better understanding of the oxidation behaviour for the oil and rock systems;
- To have the ability to estimate kinetic parameters of the relevant combustion reactions,
- To better understand and have a more quantitative idea of the expected recovery performance of the combustion process when applied to a particular reservoir.

However, due to the complexity of the combustion process, there is still not a single experiment that can provide all the required data. Therefore, different experiments are required to obtain a complete picture of the in-situ combustion process (Gutierrez et al., 2009).

The combustion tube experiment is used to determine the main kinetic parameters for the in-situ combustion process (Figure 2.27). This experiment helps to obtain the main in-situ combustion parameters such as fuel requirements, air requirement, reaction peak temperature, oxygen utilisation, front advancement rate…etc (Abolhoseini, 2004). Figure 2.28 shows effluent gas analysis of a combustion tube experiment for 27°API gravity crude. The concentration of carbon dioxide and carbon monoxide in the effluent gas is measured, as is the concentration of oxygen consumed while air is passed through a mixture of crude and sand being subjected to a linearly increasing temperature. There are two sets of concentration peaks. The first at about 485°F (ca. 252°C) corresponds to

a LTO of the crude, one in which relatively little carbon dioxide is formed even though oxygen consumption is high. It is noted that the amount of oxygen consumed exceeds that recovered as carbon oxide gases. The second peak, which is at about 750°F (ca. 399°C) corresponds to the combustion of a fuel with a low H/C ratio (Prats, 1982). Almost all the oxygen consumed at high temperatures can be accounted for by the produced carbon oxide gases. Since the production of carbon oxide gases represents the removal of carbon, the reactions associated with the second peak are controlled by the simultaneous availability of fuel and oxygen at high temperatures. The fuel is said to be burning when conditions associated with the second peak exist. This means that the amount of oxygen consumed is essentially balanced by the amount in the produced carbon oxide gases. In the LTO, the fuel is being oxygenated rather than burned as discussed previously.

In order to study the oxidation kinetics of the combustion process, both accelerating rate calorimeter (ARC) and ramped temperature oxidation (RTO) experiments are required. The ARC test is capable of providing kinetic parameters by following the reaction adiabatically. It also can determine those parameters over an extended pressure range. This enables an accurate determination of the combustion process reaction; Arrhenius activity energy, pre-exponential factor and reaction order at the reservoir pressure (Yannimaras et al., 1995). The purpose of RTO experiment is to study oxidation behaviour and reaction kinetics under controlled conditions, with the end goal of providing realistic reaction data which could be used in thermal reservoir simulators. The RTO tests involve the controlled heating from 36 to 72°F/hour (20 to 40 °C/hour) of an oil-rock mixture in a reactor while preheated air is flowed through (Cristofari et al., 2006). The heating is continued until the system target temperature is reached and then held at that temperature for the remainder of the experiment. The RTO provides the reactivity and oxidation characteristics of the oil and helps to estimate the ignition heating rate and time needed to initiate the combustion process in the reservoir. This test has proven to be extremely useful at defining the different oxidation regimes and understanding their impact on oil recovery (Gutierrez et al., 2009). In the work carried out in the current study, the kinetic reaction model uses combustion tube test, ARC and RTO experimental data.

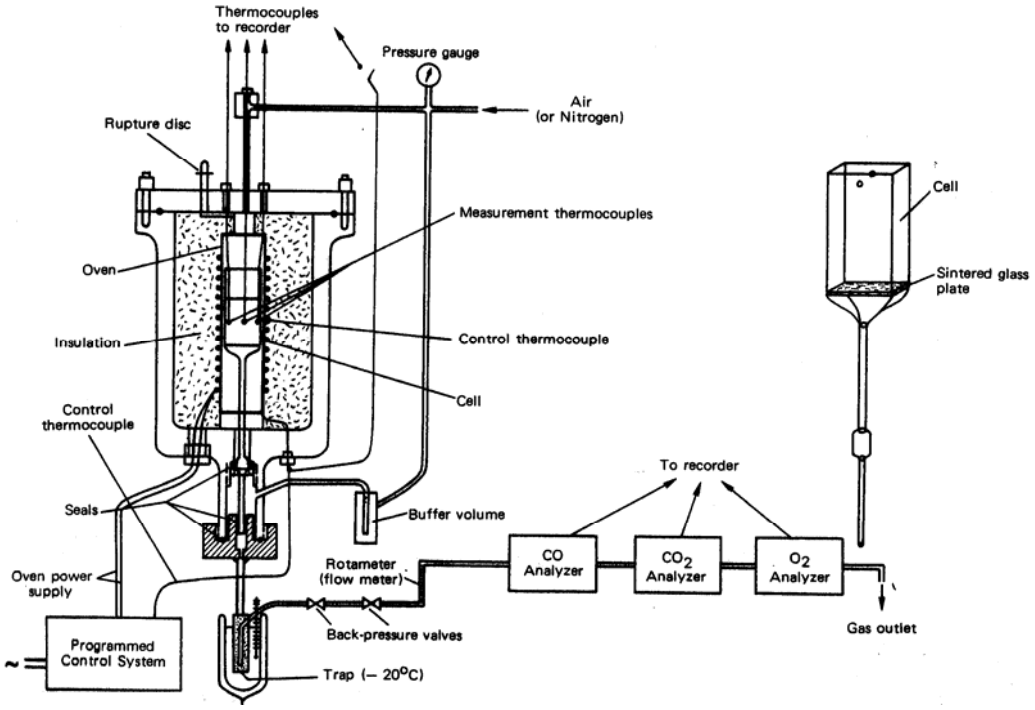

Figure 2.27: *Schematic of combustion tube (Latil, 1980)*

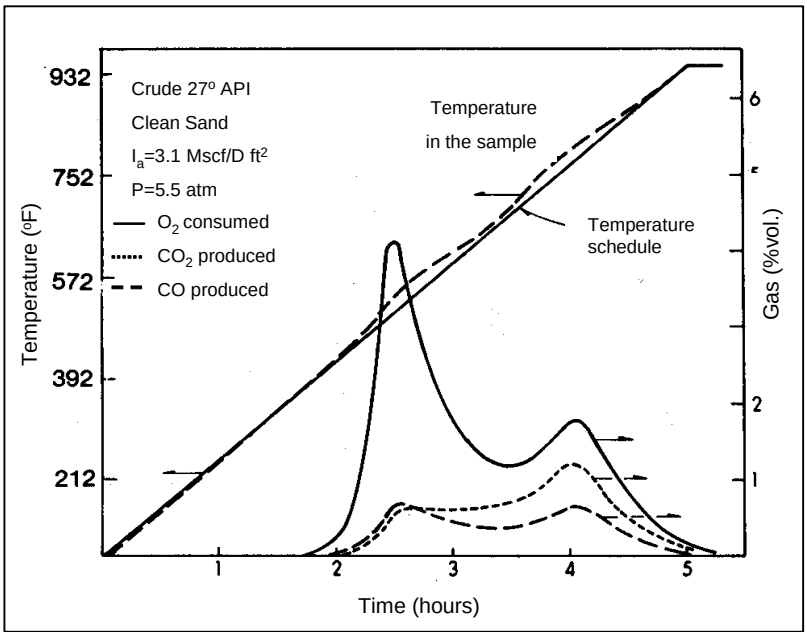

Figure 2.28: *Oxidation of crude oil in clean sand (Prats, 1982)*

The main interest in studying the kinetics of in-situ combustion is to determine the conditions required to achieve ignition and to maintain combustion. The rate of oxygen reacted per unit mass of fuel, K, can be written as (Prats, 1982):

$$-\frac{1}{m_o}\frac{dm_{O_2}}{dt} = K = p_{O_2}^{n} A_c e^{-E/RT_{ab}} \qquad \textbf{2.5}$$

where m_{O2} is the mass of oxygen consumed per unit bulk reservoir volume, m_o is the mass of oil per unit bulk reservoir volume, P_{O2} is the partial pressure of oxygen (atm), E is the activation energy (Btu/lbm mol), R is the universal gas constant (= 1.986 Btu/^{o}R.lbm mol), T_{ab} is the absolute temperature (^{o}R), A_c is the pre-exponential constant (sec^{-1} atm^{-n}), and n is the order of the reaction with respect to oxygen. Reported values of the constants A_c, n, and E obtained experimentally from literature have been summarised in Table 2.8. The kinetics parameters in Table 2.8 are for low and intermediate temperatures. The activation energy (E) ranged from 30,300 to 36,400 Btu/lbm mol, with an average value of 32,200 Btu/lbm mol. Values of the pre-exponential constant A_c vary widely, and the order of the reaction n ranges from 0.31 to 0.75. Surface area and type of mineral in the rock matrix influence oxidation and combustion kinetics and appears to have a strong effect on the amount of fuel burned (Fassihi et al, 1980a; Fassihi et al, 1980b; Vossoughi et al., 1982).

Crude (^{o}API)	Ac (sec^{-1} atm^{-n})	E (Btu/lbm mol)	n	Temperature Range (^{o}F)
27	310	30,800	0.65	194 to 300
18	16,580	36,400	0.60	174 to 284
22	1,200	30,400	0.60	122 to 284
19.9	not available	30,300	0.50	270 to 475
27.1	not available	31,350	0.75	250 to 450
27.1	not available	31,360	0075	250 to 450

Table 2.8: *Kinetic parameters for oxidation and combustion of crudes (Prats, 1982)*

2.7.3 Factors affecting the chemical reactions

Thermal cracking of petroleum hydrocarbons can be highly affected by catalysts. Clays and metallic additives present in the sand exert a catalytic influence on the reaction. Therefore, their presence in reservoir lithology can influence the kinetic parameters as well as the overall in-situ combustion parameters.

Effect of clay: Several experimental studies were conducted to investigate the effect of clay on the in-situ combustion process. Some experiments were run with either the original reservoir cores or a mixture of sand and clay cores. The main findings of these studies are summarised here.

Fassihi et al (1980b) conducted experimental runs using 5% clay added to the sand pack in their kinetic studies of the in-situ combustion process. The LTO oxygen consumption peak was found to be higher than the corresponding peaks in the no clay case (Figure 2.29). This implies that in the presence of clay more fuel is available for oxidation reactions. In 1982, Vossoughi et al preformed experimental work using adiabatic combustion tube and thermal analysis methods to investigate the effect of clay on the combustion process. They found that clay content of the sand mixture influenced the amount of fuel deposited on the sand. Increasingly more fuel was deposited as the clay content of the sand was increased. As a result, the heat of combustion per unit volume of sand also increased, and higher combustion peak temperatures were observed. They concluded that the large surface area of the clays is a major contributor to the fuel deposition process. Bagci (2005) studied the effect of clay content on the combustion reaction parameters. He used a reaction cell packed with a mixture of limestone, Bati Roman crude oil (12.9^{o}API) and water. He concluded that the addition of clay to the limestone matrix causes: (1) more fuel deposition and an increase in the combustion peak temperature (Figure 2.30), which suggests that in the presence of clay, a stable combustion is possible in a larger range of conditions. These effects are attributed to catalytic and large specific surface area of clays; (2) the activation energy of all three major reactions (LTO, thermal cracking, and HTO) involved in combustion process decreased, which is indicative of catalytic properties of clay.

One of the latest experimental studies was conducted by Chicuta & Trevisan (2009) on the impact of clay content in the in-situ combustion process using Brazilian heavy oil properties. They determined that the presence of clay proved to play a key role in fuel deposition and consequently in propagation of the fire front. In the case of using clean sand in their experiment, the combustion front was quenched, while in the presence of 4.5-10% clay in the sand, a longer front sustainability and higher recovery were

achieved. However, in the present study clay has not been considered because its effect is relatively minor compared to the other parameters considered.

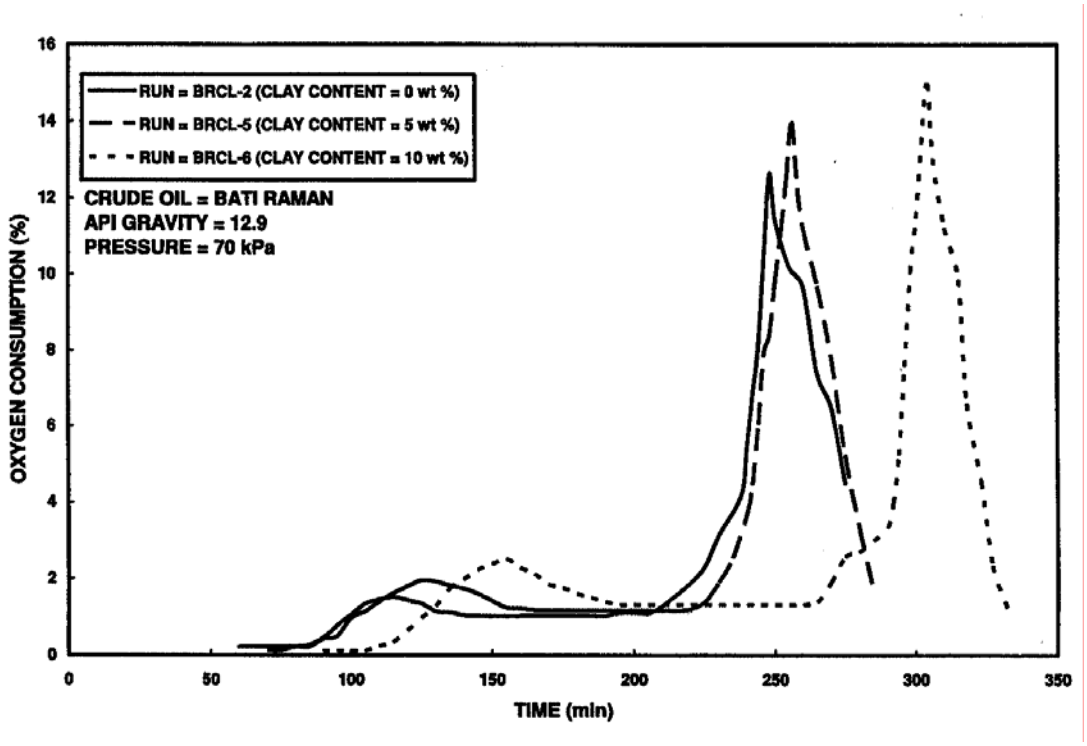

Figure 2.29: *Oxygen consumption as a function of time for different clay content values (Bagci, 2005)*

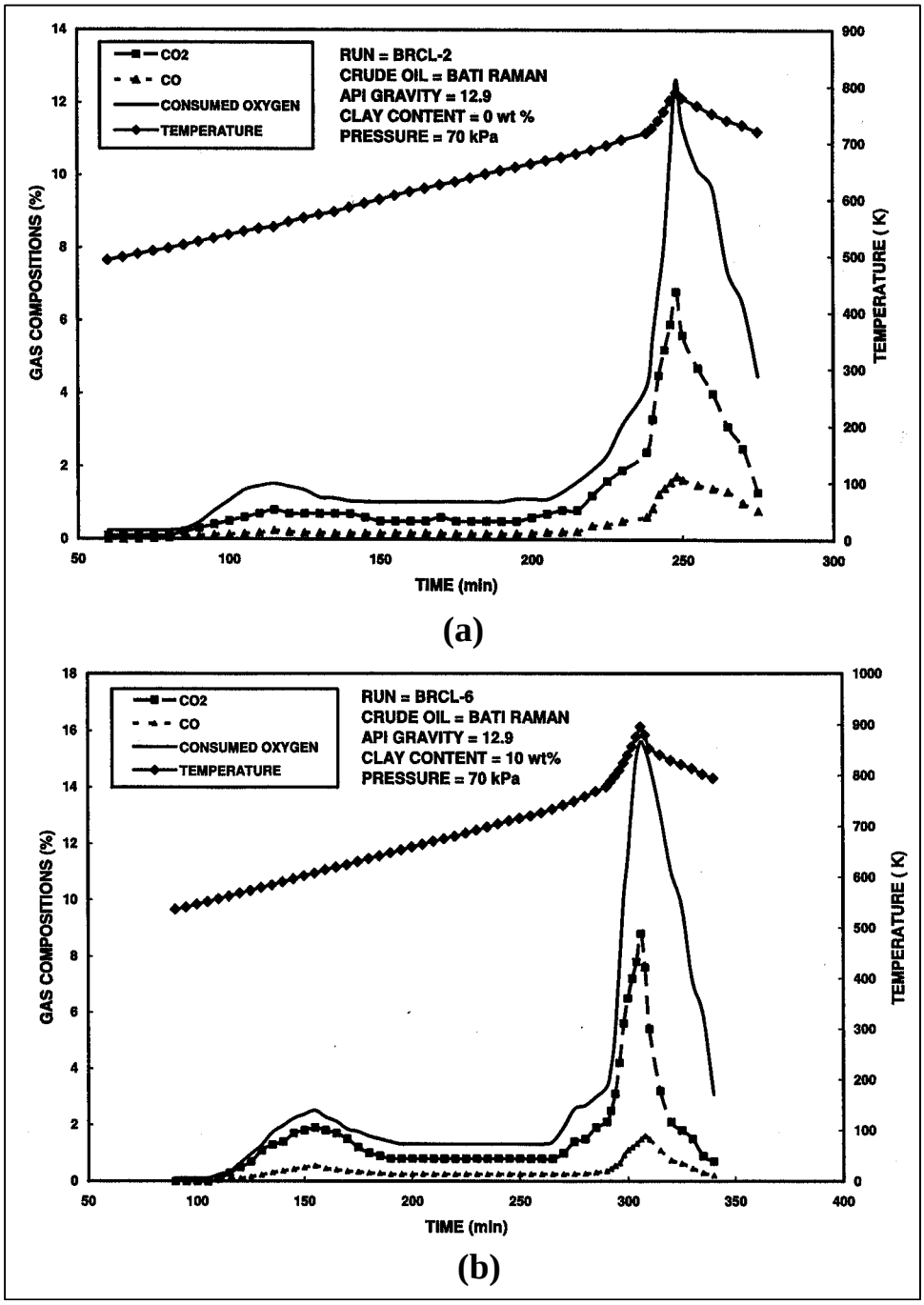

Figure 2.30: *Gas composition and temperature profiles as a function of time (a) without clay content, and (b) with 10% clay content (Bagci, 2005)*

Effect of metallic additives: The presence of metallic additives such as copper, iron, nickel, vanadium, iron etc. create a catalytic effect that lowers the temperature at witch the combustion reaction occurs (Fassihi et al., 1980b). This is because of the fact that the reaction activation energy is reduced in the presence of additives. The presence of additives either in the oil or in the matrix has been shown to promote the oxidation

reactions. A typical set of experimental results is presented by Burger et al (1972) shown in Figure 2.31a through Figure 2.31c. The results in Figure 2.31a show the extent of the oxidation reactions when the crude and sand are free of any additive, whereas a copper derivative was added to the oil (= 2,000 ppm Cu) for the test in Figure 2.31b and 1% nickel oxide was added to the sand in the case of Figure 2.31c. Two main observations result from the comparison of Figure 2.31a through Figure 2.31c. In the presence of additives: (a) the oxidation reactions are observable at a lower temperature which can be explained by an increase of the oxidation rate when a catalyst is present (lower activation energy), and (b) the area of the second peak is increased. This is because of the formation of a more significant quantity of coke; therefore, the fuel availability and air requirement in combustion must increase. The influence of metallic additives on the fuel availability may have a great importance for the success of the in-situ combustion technique applied to heavy oil reservoirs. The fuel availability of such oils may be sufficient to support the propagation of a forward combustion front in a natural matrix containing metallic additives, whereas it can be too low in clean sand.

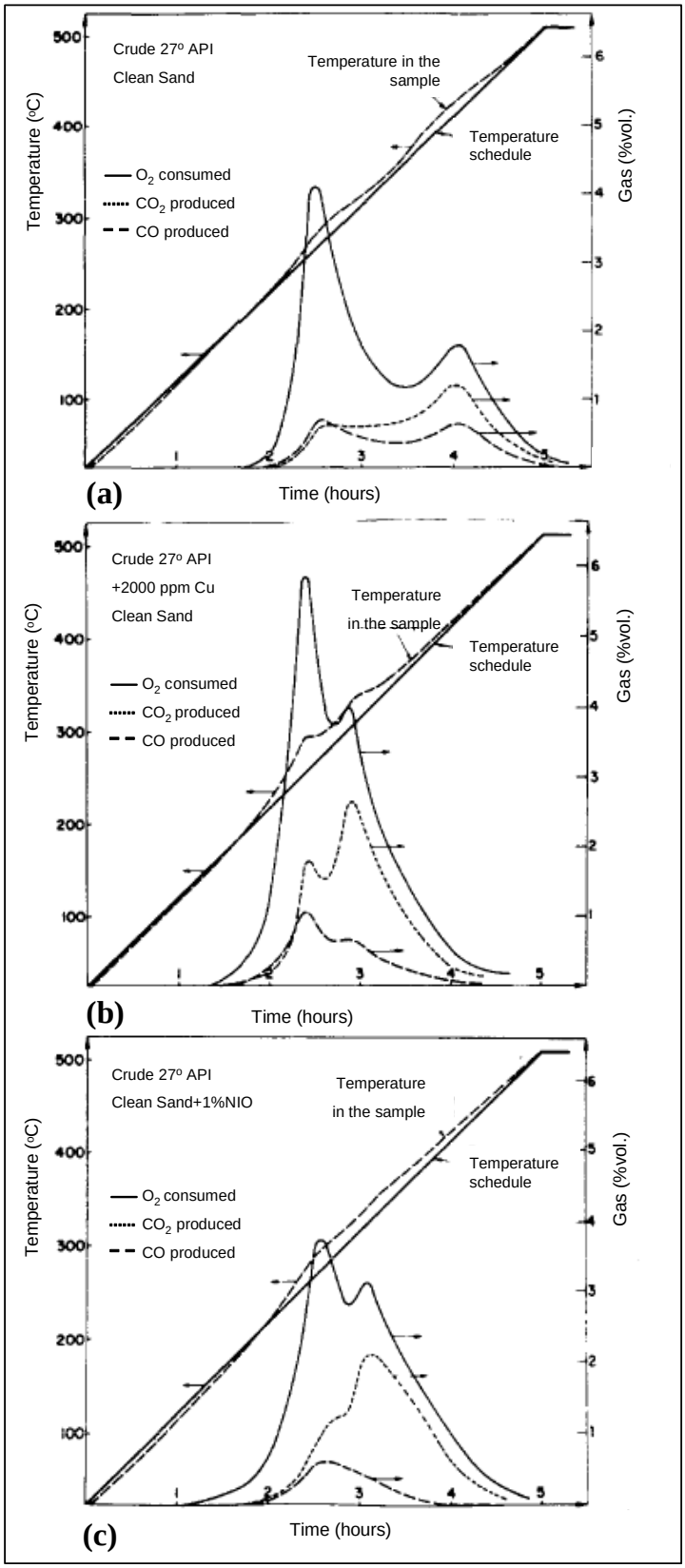

Figure 2.31: *Oxidation of (a) a crude oil in a clean sand, (b) a crude oil contain a cooper additive in a clean sand, (c) a crude oil in a clean sand with addition of nickel oxide (Burger et al.,1972)*

2.8 Motivation of this study

The literature review conducted in this chapter presents an overview of recent studies that investigated the application of in-situ combustion as a thermal EOR method. However, there are some gaps in the current research, which will need further investigation. For example, the studies conducted by several researchers such as Bagci et al. (2000), Greaves et al. (2000); and Xia et al. (2002) did not provide a detailed investigation of well configuration effect in the combustion process. Hence, in this study the impact of using diverse well configurations (type, number, spacing, completion, etc) on the in-situ combustion process performance are investigated. Moreover, the fire front behaviour under the presence of strong bottom aquifer support needs to be investigated where different well configurations are used. Also, there is a need to study in detail the ways to optimise implementation of the combustion process by optimising the well locations in the reservoir in the presence of bottom aquifer support. A comprehensive evaluation of the potential of using top-down in-situ combustion in thick heavy oil reservoirs with aquifer support is considered in this study, since the currently available studies (such as the Coates et al., 1995 study) do not cover this area of research. Furthermore, reservoir heterogeneity effects on the application of in-situ combustion has not been addressed yet. In this study, several types of reservoir heterogeneity will be investigated using the simulation model developed, and their impact on the fire front behaviour and performance will be presented. For example, the effect of discontinuous shale layers and multiple permeability layers on the in-situ combustion process performance will be addressed, where different well configurations are used with/without the presence of strong bottom aquifer support. The need to consider and address these issues is the motivation for this work, since the impact of these processes may make the difference between technical successes together with economic viability, and the failure in scenarios such as the one proposed for the Nimr field.

Chapter 3

Field Overview and Simulation Model Development

3.1 Introduction

This chapter provides an overview of the rock and fluid properties, which are based on the Nimr field properties, and used in the development of the simulation model for this study. It also explains the use of numerical simulation and its challenges when modelling EOR and specifically the in-situ combustion process. The methodology of model development, starting with 1D combustion tube test model, and upscaling to a 2D pilot size model is discussed. Furthermore, the main phases of model development are highlighted and ways of optimizing the main criteria of in-situ combustion are presented. More sensitivities are conducted to investigate grid numerical dispersion effects in in-situ combustion simulation. Following, the use of 2D cross sectional model is justified to further investigate in-situ combustion application in heavy oil reservoirs. Moreover, the dynamic gridding option in the simulation process is used. The base case model is defined after the 2D model has been enlarged, and it will be used to carry out more sensitivity calculations in the coming results chapters.

3.2 In-situ combustion simulation

Numerical modelling is an important tool in oil industry research to study and investigate the application of new techniques for recovery from oil reservoirs. This valuable tool allows engineers to mimic the reservoir rock and fluid properties in order to predict and evaluate reservoir behaviour and its oil recovery performance before applying the technique in the real case. However, the use of simulation should be carefully implemented, especially with consideration to the input parameters in the

model, since the accuracy of the rock and fluid properties can decisively affect the output results of the simulation.

Thermal EOR methods used to extract heavy oil are expensive, require taking risks and need considerable advanced planning. Therefore, dealing with expensive methods requires putting a great effort into predicting their viability to a high degree of accuracy using the available reservoir simulators. Numerical modelling of thermal EOR methods is complicated when compared with black oil and compositional modelling. This is as a result of the need to consider and solve all the flow and energy equations involved in such systems. The presence of heavy oil in the reservoir introduces issues due to high density and viscosity and the complicated physics to the simulation process. Therefore, the simulator is required to capture all the thermal conduction and convection between the reservoir fluids and rock and the thermal effects of vaporisation and condensation of fluids (Youngren, 1980). In the case of in-situ combustion, the complexity of the simulation process is increased due to the introduction of exothermal kinetic reactions into the model with the formation of coke and the oxidation of coke and hydrocarbons. These result in the difficulties to accurately predicting the in-situ combustion performance through numerical simulation. One reason why such a process is challenging to simulate accurately is that the temporal and spatial scales of the important physical processes in this system vary widely. For example, scales associated with heat conduction are typically much larger that those governing chemical reactions, which in turn are considered larger than the scales associated with the transfer of components between phases (Kristensen et al., 2008). Moreover, the number of components present in the model (i.e. water, hydrocarbons, coke…) and their phases, and the need to handle large variations in saturations and temperatures add to the difficulty of modelling such cases. This means that modelling of in-situ combustion requires a high quality description of all the model components in order to represent the real reservoir behaviour.

The current advancement in thermal reservoir simulation and high performance computing are enabling the development of larger and more representative heavy oil reservoir models. Modern reservoir simulators can accurately model the complex

physics of heavy oil in-situ combustion processes and all other heavy oil recovery methods.

For the scope of this study STARS (Steam, Thermal and Advanced processes Reservoir Simulator), a software package from Computer Modelling Group (CMG) was used to investigate application of in-situ combustion to the Nimr field. This software is one of the leading available thermal reservoir simulators. It has the advanced capability of modelling in-situ combustion and identifies all the possible driving mechanisms, components, low and high temperature oxidations and kinetic reactions. It also takes into account the heat losses from the model to the over/under burden (STARS Manual, 2006).

3.3 Nimr field overview

Nimr is a mature field producing medium heavy oil with API gravity of 21°. It is located in South Oman (
Figure ***3.1***) and it extends over an area of approximately 77.2 mile2 (Al-Kharusi, 1997). It is producing under strong bottom water drive. It was discovered in 1980 and is the second largest oil field in Oman (Kragas et al., 2002). It has been on production since 1985. The field contains over 2.5 billion barrels of STOIIP (Al-Wadhahi et al., 2005). It consists mainly of sandstone with an average porosity of 28% and permeability between 0.5 to 5 Darcy (Leemput et al., 1997). The initial reservoir temperature was 123°F and the initial pressure was 1507psi (Al-Abri et al., 2004). The Nimr reservoirs (shown in Figure ***3.1***) are dominated by Aeolian sequences which are called Amin Formation. These Cambrian sands extend about 3281 ft below the oil water contact which allows the existence of strong bottom water aquifer. The top of the formation is defined by a major composite erosional unconformity. After an interval of around 220 million years, sedimentation resumed with the deposition of Permo-Carboniferous glacial sequences (Al Khlata Formation) on a structurally complex paleo-topography modified by additional glacial valley erosion (Figure 3.2). The glacial valleys contain a heterogeneous mixture of sand, shale and diamictite. In some locations, the valley fill

has good reservoir properties. However, in other cases the valleys act as seals due to their heterogeneous mixture, which results in the formation of six major accumulations A, B, C, E1, E2, and G with slightly different oil-water contacts (Leemput et al., 1997).

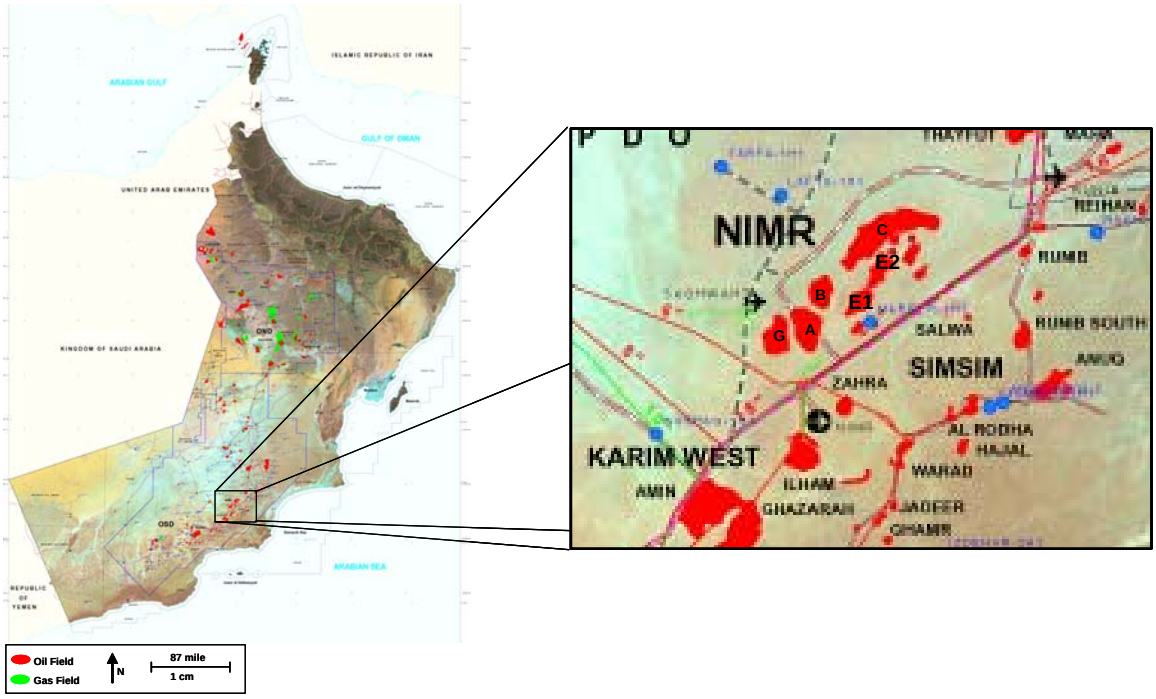

Figure 3.1: *Location of Nimr field in Oman shown various reservoir units (Raghunathan et al., 2006)*

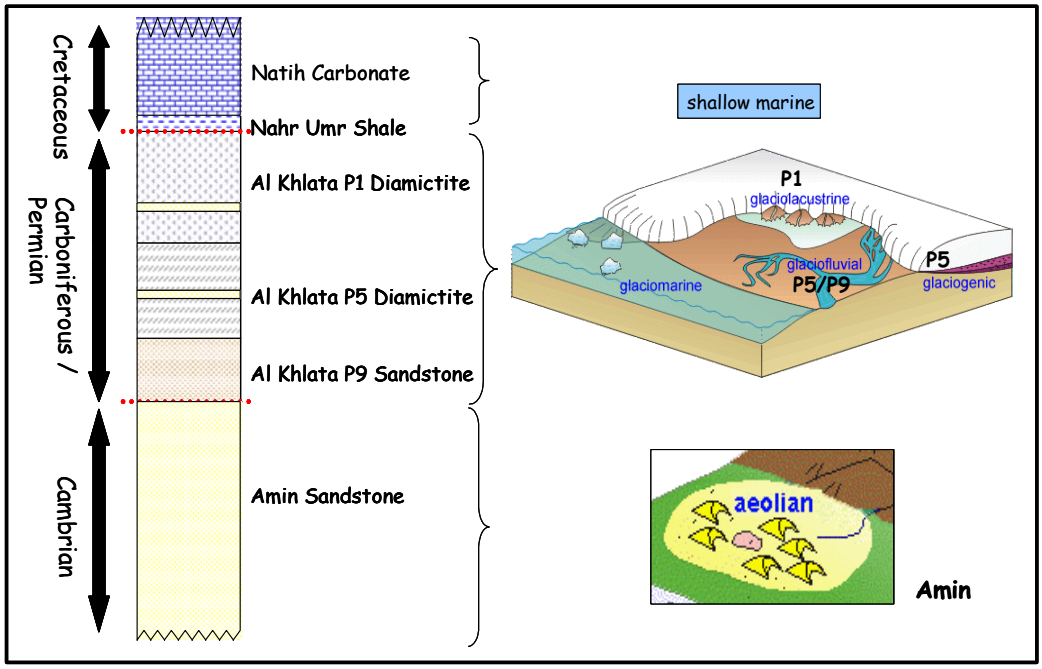

Figure 3.2: *Stratigraphy and depositional environment of reservoir and seal formations in the Nimr E area (Raghunathan et al., 2006)*

Initial field development plans were via vertical wells, but since the mid-1990's development has been primarily by horizontal wells. Combined production from the Nimr field accounts for more than 10% of Petroleum Development Oman (PDO) oil production, and it is produced from around 500 active wells at a present field water cut of about 93% (Medeiros et al., 2004). The presence of a combination of unstable displacement, strong bottom aquifer drive, high oil to water viscosity ratio, complex geological setting and non-matrix permeability events (low permeability laminations, fractures and continuous layers of varying permeability) has resulted in the typical mature field problems of water movement and its impact on sweep and recovery. To overcome these problems, PDO is planning to apply in-situ combustion as a novel recovery method for heavy oil reservoirs that are subjected to strong bottom water drives. The Nimr E (both E1 and E2) reservoir is going to be considered for the study and application of in-situ combustion (Figure 3.3) and later on, if the study is successful in-situ combustion could be used to improve oil recovery factors in other Nimr reservoirs. Table 3.1 summarises some of Nimr E data and reservoir properties. The Nimr E reservoir is chosen because of its shallower depth, which enhances the economies of applying in-situ combustion. Furthermore, Nimr E despite there being no water injection, is currently producing at high water cut compared to other Nimr reservoirs which indicates the need for immediate action to reduce the operational cost in handling the water produced, as well as increasing the ultimate recovery. The preference of choosing in-situ combustion as a thermal EOR process instead of steam injection is as a result of the high initial Nimr pressure. High pressure is considered to be a favourable factor for in-situ combustion operations unlike for steam injection. More details of the comparison between the criteria to choose between steam injection and in-situ combustion were presented in Chapter 2 of this thesis.

Applying in-situ combustion in Nimr E with the current high water cut is considered as a challenge. This is due to the high water influx in the oil zone which could prevent any attempt to initiate the fire front. In order to overcome this problem, the field current watered out producers needed to be shut off, to allow reduction of the water cones near the producers. Moreover, a new well configuration is required to be considered where the air injectors should be completed near the reservoir top away from the current water cones. This placement of the injectors should maximise the distance between the wells

and the water aquifer and enable successful initiation of the combustion front at an early stage of the process. The fire front will continue to propagate in the reservoir as long as there is enough fuel in place. Also, the flu gases which are produced as a result of the combustion process help to reduce the amount of water influx approaching the front through exerting a high pressure profile ahead of the front.

Fluids and Rock properties	
Depth	2133 ft
Formation type	Sandstone
Clay content	Low
Water salinity	6000ppm
Horizontal permeability	4000 mD
Vertical permeability	2000 mD
Oil viscosity* (cp)	707
Oil density* (kg/m^3)	929
Oil compressibility* (kPa^{-1})	2.4 E-07
Production data	
Original oil in place (MM bbl)	786
Cumulative produced oil (MM bbl)	79.9
Total recoverable reserve (MM bbl)	164.8
Net pay thickness	131 ft
Oil rate (bbl/day)	21014
Water cut	95%
Number of producer wells	148 (of which 21 wells are vertical)
Number of injector wells	0
* at 123°F and 1507psi	

Table 3.1: *Nimr E Data (Coates & Turta, 2004)*

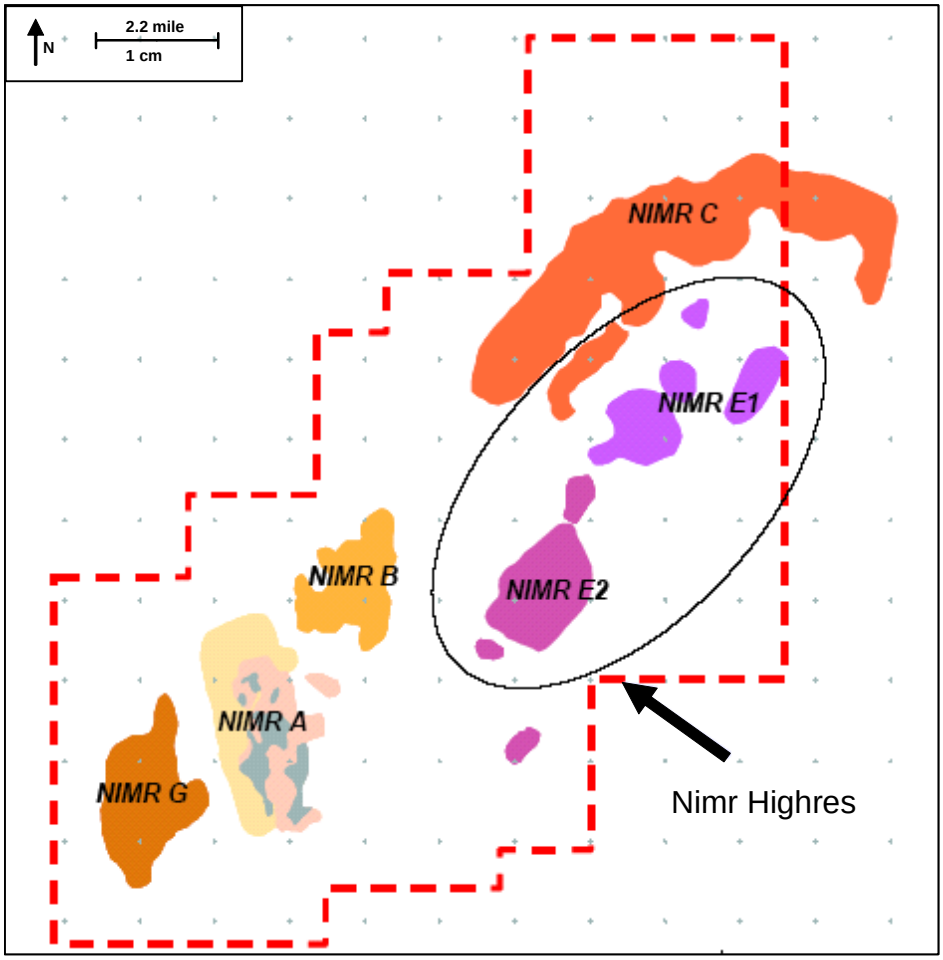

Figure 3.3: *Location of Nimr E reservoir (Coates & Turta, 2004)*

3.4 In-situ combustion 1D model development

3.4.1 Kumar's 1D model

As a start in this study, a template STARS simulator data set, supplied by CMG, was used to build up and develop the simulation model. The template was designed for the simulation of a dry combustion tube test experiment. It was originally developed by Kumar (1987) to history match laboratory combustion tube results. It was a 1D model with a total of 12 grid blocks (Figure 3.4). It had a relatively small total volume of 0.07ft3 with grid block dimensions of 0.1602 ftX0.1602ftX0.2205ft in the x, y, and z directions, respectively. The model defined and used six components: water, heavy oil (HO), light oil (LO), oxygen, inert gas (carbon monoxide+carbon dioxide+nitrogen) and

coke. Hence, hydrocarbons were represented in the model as three components, two of which were pseudo components and the third was a solid phase. The use of two pseudo components (oil heavy ends and light ends) to represent the hydrocarbons portion of the reservoir fluids in this study could be considered as a limitation due to the reduction in the accuracy of modelling in-situ combustion process. However, this approach was considered because the individual chemical reactions for each component of the hydrocarbons mixture were not available at this point. Also, the simulation process complexity increases as the number of defined components increases due to extra chemical reactions and thermal questions needed to be solved. All non-condensable gases except oxygen (such as nitrogen, carbon monoxide, carbon dioxide) were represented as a single inert gas to reduce the number of equations to be solved and to reduce the simulation calculation time.

In-situ combustion chemical kinetic reactions in the combustion tube experiment were represented with four reactions in the simulation model of this study (the flow equations solved by STARS were presented in Appendix B1). One of these kinetic reactions was thermal cracking of the heavy oil pseudo component, as equation (3.1) shows. This reaction was considered to be suitable for thermal cracking of crude oil which was represented in the simulation model as two or more pseudo components (Lin et al., 1984), as was the case in this study. The stoichiometric coefficient and reaction rate parameters of the cracking reaction were originally determined from a series of cracking experiments (Kumar, 1987).

$$HO \rightarrow 3.71\,LO + 7.13\,COKE \qquad \textbf{3.1}$$

The other three kinetic reactions were the combustion reactions of: light oil, heavy oil and coke as shown in equations (3.2), (3.3), and (3.4) (Kumar, 1987).

$$HO + 56.99\,O_2 \rightarrow 51.53\,CO_x + 28.34\,H_2O \qquad \textbf{3.2}$$

$$LO + 13.32\,O_2 \rightarrow 11.96\,CO_x + 6.58\,H_2O \qquad \textbf{3.3}$$

$$COKE + 1.11\,O_2 \rightarrow CO_x + 0.55\,H_2O \qquad \textbf{3.4}$$

The1D model had a permeability of 12,700 mD and a porosity of 41.4%. The initial pressure and temperature of the model were 2014.7 psi and 100°F respectively. The initial saturations were 65.4%, 17.8%, and 16.8% for oil, water, and gas respectively.

The oil used in the combustion model was 26° API gravity, and the air injection rate was 0.554 scf/hr according to the combustion tube test.

This 1D model was used at the beginning of the study to provide the knowledge required to understand the concept of in-situ combustion modelling. It helped to provide and highlight the important criteria to look for when simulating in-situ combustion such as: air injection rate, heating duration and heating rate at the beginning of the process.

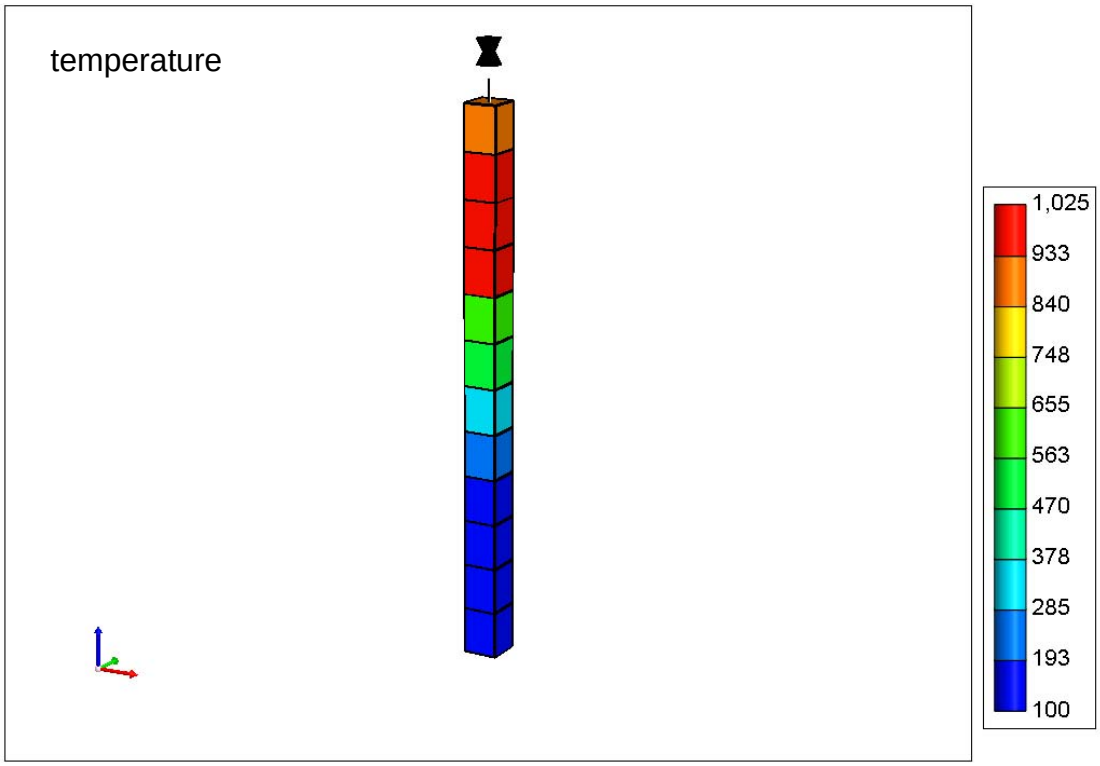

Figure 3.4: *1D model temperature profile (°F)*

3.4.2 Choice of kinetic model

In order to simulate in-situ combustion for a specific field, a kinetic model was needed to be developed and used in the flow simulation model. This kinetic model would be considered to be reliable if it represents and predicts the outcome of the in-situ combustion process in the field. Usually for a field study the kinetic model is developed by evaluating the combustion behaviour of the crude using a combustion test experiment in the laboratory. For the scope of this study, as already mentioned, the

simulation is for application of in-situ combustion in the Nimr field. However, currently there is no kinetic model available for this field. As a result, the only way to simulate in-situ combustion in Nimr currently was by applying the available kinetic models in the literature. Of the models developed previously, Kumar's (1987) kinetic model was used here. Another useful kinetic model in the literature is the Belgrave et al. (1993) model. This model basically defined and used seven components which are water, asphaltenes (heavy ends), maltenes (light ends), oxygen, nitrogen, inert gas (carbon monoxide+carbon dioxide) and coke. The kinetic model consisted of a total of six reactions, three thermal cracking reactions, two low oxidation (LTO) reactions and one high oxidation reaction (HTO). The model kinetics was based on Athabasca bitumen. Like Kumar's model, the hydrocarbons were represented in the model as three components, two of which are pseudo components (asphaltenes and maltenes) and the third was a solid phase. The three thermal cracking reactions are shown in equations (3.5), (3.6), and (3.7) below. Maltenes by far were the most reactive components of the hydrocarbons in the model. As a result, as soon as the temperature increased, maltenes started to crack and produce asphaltenes. As the temperature continued to increase in the combustion model, the asphaltenes were thermally cracked to produce more coke which fuelled the combustion process and also produced inert gases (Belgrave et al., 1993).

$$Maltenes \rightarrow 0.372\, Asphaltenes \qquad \textbf{3.5}$$

$$Asphaltenes \rightarrow 83.223\, Coke \qquad \textbf{3.6}$$

$$Asphaltenes \rightarrow 37.683\, Gas \qquad \textbf{3.7}$$

The unreacted oxygen which flowed through the fire front oxidised the hydrocarbons ahead of the front in the lower temperature zone. This led to more coke being deposited (equation (3.8)) and at the same time increases the amount of asphaltenes at the expense of maltenes (equation (3.9)). Those two reactions represent the LTO reactions in the Belgrave et al. (1993) kinetics model. The coke combustion was demonstrated by equation (3.10) in the kinetic model.

$$Asphaltenes + 7.513\, O_2 \rightarrow 101.539\, Coke \qquad \textbf{3.8}$$

$$Maltenes + 3.431\, O_2 \rightarrow 0.4726\, Asphaltenes \qquad \textbf{3.9}$$

$$Coke + 1.232\, O_2 \rightarrow CO_x + 0.565\, H_2O \qquad \textbf{3.10}$$

In order to investigate the effect of different kinetic models on in-situ combustion, Kumar's kinetic model was replaced by Belgraves's model in the 1D simulation model. The simulation results of both Kumar's and Belgarve's models are shown below. The average model temperature (Figure 3.5a) for the case of Belgarve's model was lower than in the case of Kumar's model over most of the model run time. This is because a lower amount of coke was produced in Belgarve's model compared to the rapid increase of coke in Kumar's model (Figure 3.5b). The reason for the difference was thought to be the way Belgrave defines coke production in the three cracking reactions, which delay the onset of coke formation (Belgrave et al., 1993) and helped more oil to be recovered instead of converting it to fuel for the combustion. The recovery factor of the Belgrave model was higher (82%) compared to the Kumar model (76%); Figure 3.6a shows the cumulative oil produced from both models. The acceleration of oil production and the reduction in oil saturation (Figure 3.6b) in Belgrave's model indicate that the fire front for this model was more efficient at recovering oil and the front propagation through the model was excellent. Based on the comparison between the two kinetics models, Belgrave's model showed more comprehensive cracking and oxidation reactions. This detailed reactions scheme was capable of predicting the experimentally determined fire front propagation velocity, air requirements and the fuel requirements (Belgrave et al., 1993) and it therefore helped to capture the in-situ combustion process behaviour in the model. For the aim of this study, Belgrave's kinetic model will be used in the simulation of in-situ combustion.

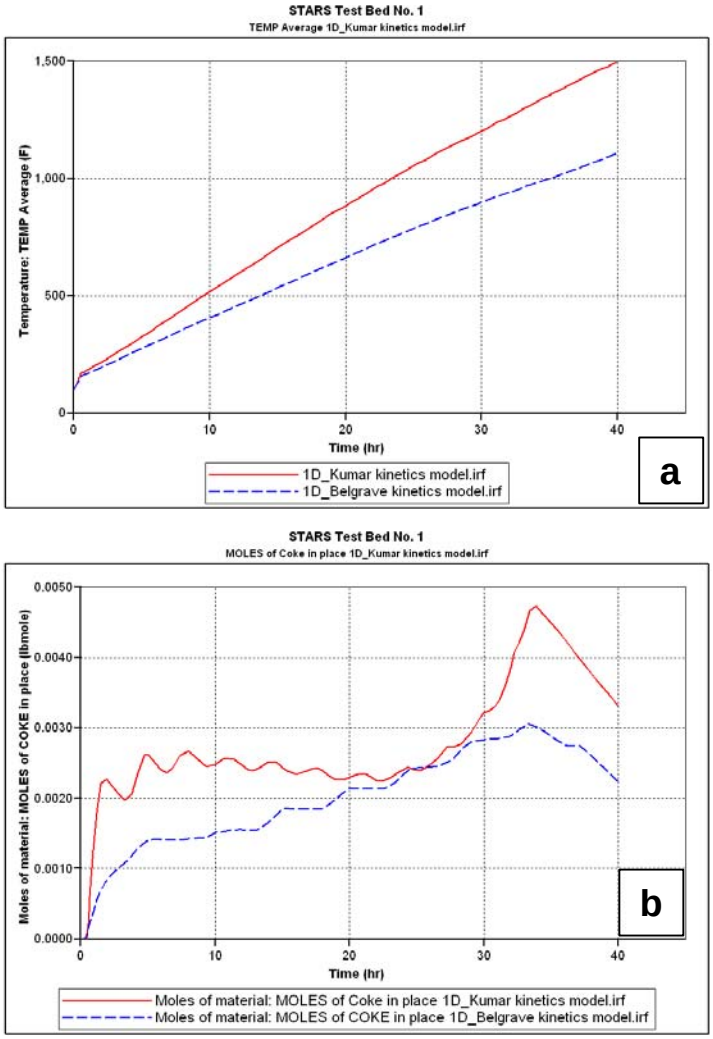

Figure 3.5: *Simulation results comparison between Kumar's model versus Belgrave's model: (a) average model temperature, and (b) net coke in place.*

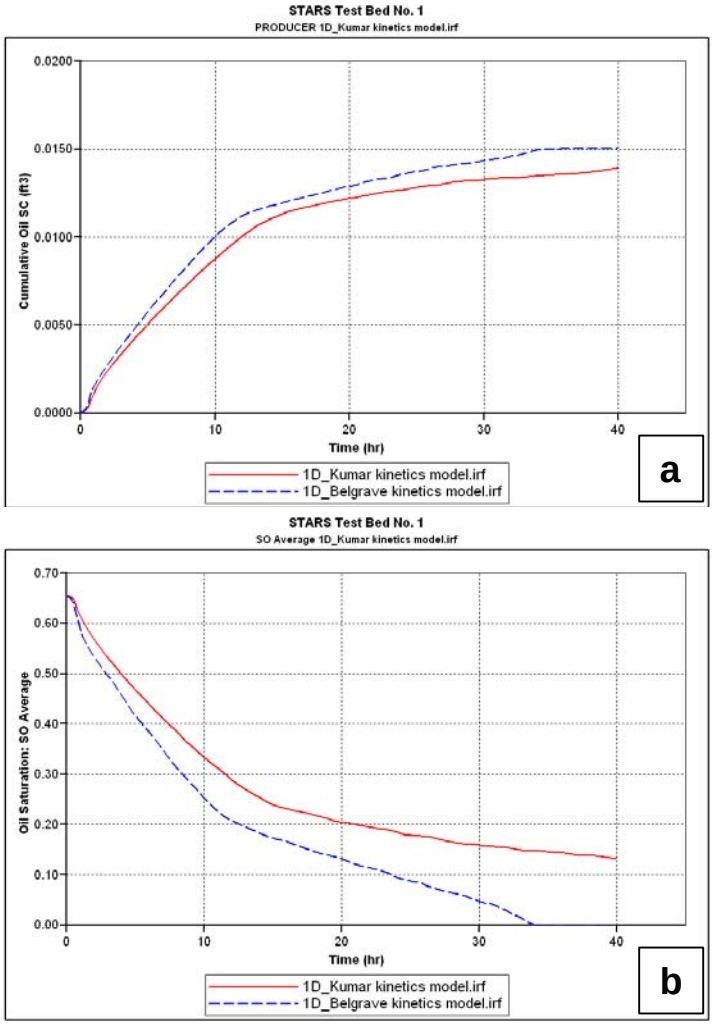

Figure 3.6: *Simulation results comparison between Kumar's model versus Belgrave's model: (a) cumulative oil produced, and (b) oil saturation.*

3.4.3 Inclusion of Nimr field data in the model

So far in this study, the model development had used properties that were taken mainly from the literature and from a template included with the CMG software installation. It was important to transfer and replace the model properties using the available properties of the Nimr field. Much of the properties were either available through publications (i.e. SPE papers) or through PDO reports (i.e. FDP, PVT reports). The main properties to be replaced in the current model by Nimr properties were rock porosity and permeability and initial reservoir condition, relative permeability curves, oil viscosity, and k-values of pseudo components.

Both porosity and permeability of the simulation model were changed to be 28% and 4,000md respectively. The initial reservoir pressure was changed to 1507 psi instead of 2,014psi and the initial reservoir temperature was 123°F. The initial oil saturation was 82% in Nimr and the water saturation was 18% (gas initial saturation is zero). Also, Nimr crude consisted mainly of 99.851% mole fraction maltenes and the remaining 0.149% as asphaltenes, according to the compositional analysis of the crude. Table 3.2 shows the change of these rock and initial reservoir properties from the previously developed model and the current updated Nimr model.

Properties	Previous model	Nimr model
Porosity (%)	41.4	28
Permeability (mD)	12700	4000
Soi (%)	65.4	82
Swi (%)	17.8	18
Sgi (%)	16.8	0
Initial temperature (°F)	100	123
Initial pressure (psi)	2014.7	1507
Maltenes mole fraction (%)	74.4	99.851
Asphaltenes mole fraction (%)	25.6	0.149

Table 3.2: *Main rock and initial conditions of Nimr field*

The large variation in the mole fractions of asphaltenes from the pervious model (25.6% asphaltenes) to the Nimr updated model (0.149% asphaltenes) should not affect fuel availability in the simulation model. This was because Belgrave's kinetic reactions model (which was used in the simulation) allowed for more asphaltenes to be produced from both the maltenes thermal cracking (equation 3.5) and maltenes oxidation reactions (equation 3.9). This means more coke was available for the fire front to consume, even though the original asphaltenes contents of Nimr crude was initially low.

Two phase water/oil relative permeability had been modelled for Nimr via Corey functions based on Nimr special core analysis data (SCAL). However, some degree of uncertainty was attached to this set of relative permeability data, principally due to an overall uncertainty in the wettability of the system (Al-Abri et al., 2004). The water/oil

relative permeability curves are shown in Figure 3.7. The gas/liquid relative permeability for Nimr was not available since there was not initially any gas in the reservoir. However, in the in-situ combustion process the involvement of gas flow in the system is an important factor of the overall process and gas/liquid relative permeability should be provided to allow simulation of the process. Hence, the use of the literature data set of gas/liquid relative permeability was used in this study (Figure 3.8).

In order to evaluate the uncertainty of using literature data set of gas/liquid relative permeability in the combustion process for Nimr case, a sensitivity calculation was conducted in Appendix B2 where two different sets of gas/ liquid relative permeabilities were used. The main outcome when different gas relative permeability curves were used was that the fire front managed to initiate and propagate with some minor variations as the results showed when both curves were used in the simulation model. For more details of this sensitivity refer to Appendix B2.

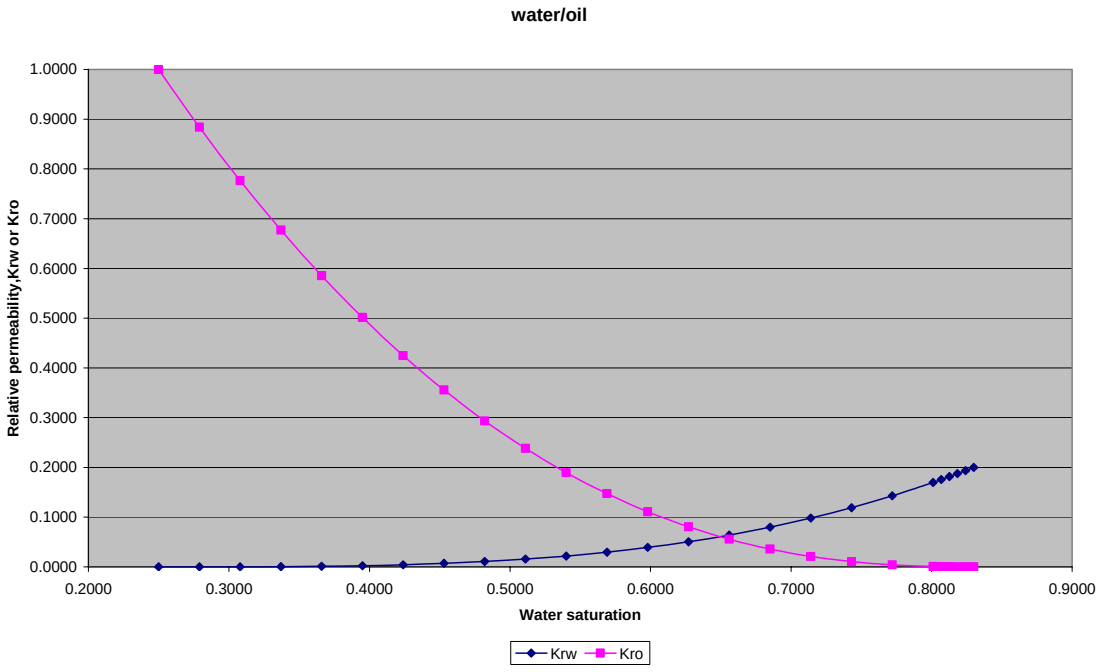

Figure 3.7: *Water/oil relative permeability curves (Al-Abri et al., 2004)*

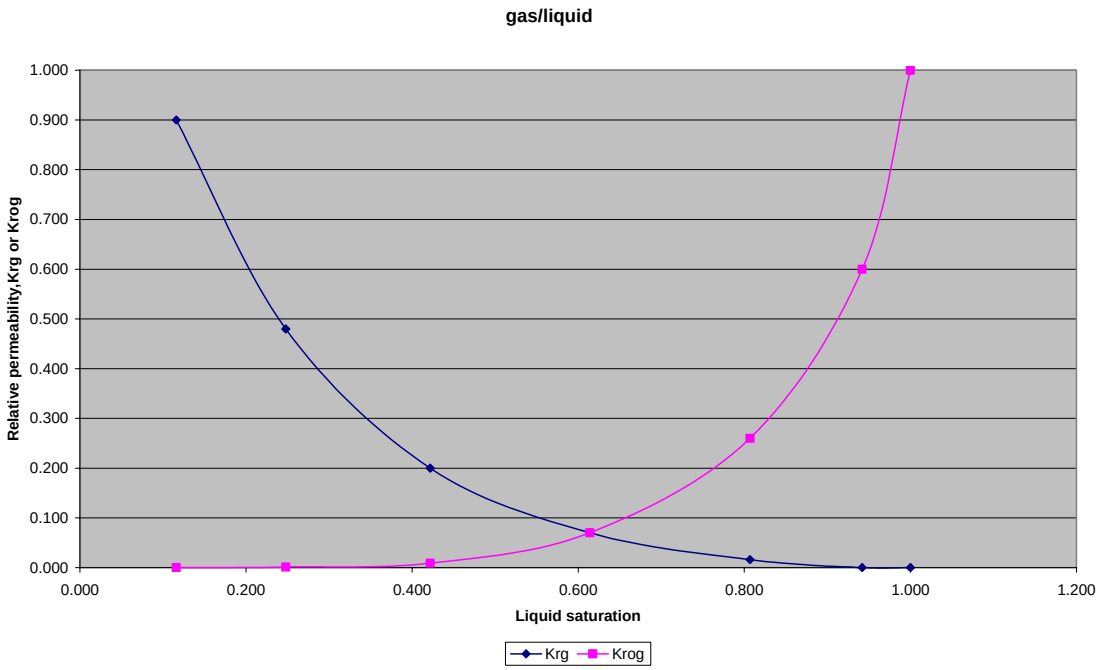

Figure 3.8: *Gas/liquid relative permeability curves (Koederitz)*

In many heavy oil recovery processes the oil viscosity versus temperature function contains much of the nonlinearity in the flow equations. This is because oil viscosity can decrease by several orders of magnitude over only a modest temperature increase. Therefore, it was crucial that the temperature dependence of oil viscosity be represented adequately. In STARS, oil viscosity could be represented in two ways. These are: either as a correlation or as a viscosity versus temperature table. The former approach was most suitable for use in the case of Nimr, because of the uncertainty associated with the first PVT samples of Nimr in the early stages of its discovery. Also, defining oil viscosity in the simulation model using the correlation approach helped to provide oil viscosity for a wider range of temperature instead of using a table with a limited range of temperature values. The correlation used is shown in equation (3.11):

$$vis\cos ity = a \times EXP^{\left[\frac{b}{T}\right]} \qquad \textbf{3.11}$$

where T is in absolute degrees (STARS Manual, 2006). In order to calculate the two coefficients (a, b), two measurements of Nimr oil viscosity were used from well NIMR-5 (Raghunathan et al., 2006). The viscosity of both hydrocarbons components (maltenes and asphaltenes) in this model was assumed to be the same as the crude oil. Figure 3.9

shows oil viscosity versus temperature for Nimr crude using the correlation in equation (3.11).

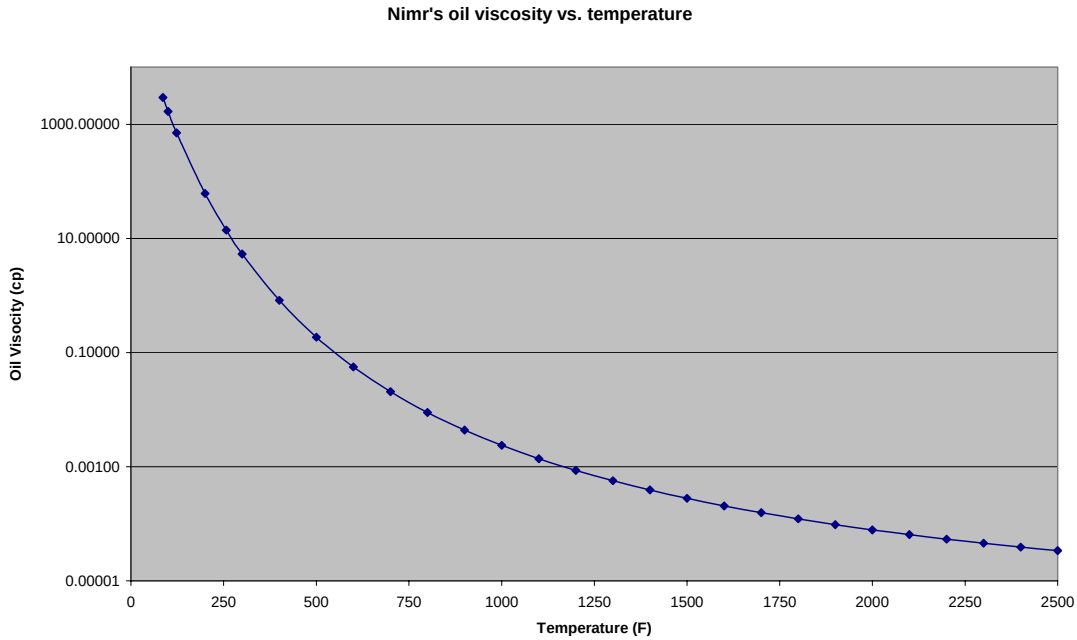

Figure 3.9: *Nimr's oil viscosity versus temperature.*

The phase equilibrium k-values (vapour to liquid ratio of the component at specific temperature and pressure) of both pseudo components were adapted from Kumar's (1987) model. Using the Kumar approach, various k-values were produced and used in the simulation model. This provided a range of k-values for each component at different temperature and pressure. Table 3.3 presents k-values values for both maltenes and asphaltenes at 1500psig and temperatures from 77°F to 927°F.

Temperature (°F)	Maltenes	Asphaltenes
77	1.96E-04	3.21E-09
127	6.12E-04	2.85E-08
177	1.64E-03	1.96E-07
227	3.88E-03	1.09E-06
277	8.27E-03	5.00E-06
327	1.61E-02	3.36E-05
377	2.28E-02	1.07E-04
427	2.95E-02	3.09E-04
477	3.76E-02	5.24E-04
527	4.43E-02	7.52E-04
577	5.10E-02	1.13E-03
627	5.78E-02	2.12E-03
677	6.45E-02	3.63E-03
727	7.25E-02	4.97E-03
777	8.06E-02	7.12E-03
827	8.86E-02	9.80E-03
877	9.80E-02	1.34E-02
927	1.13E-01	2.28E-02

Table 3.3: *Phase equilibrium k-values at 1500psig (adapted from Kumar, 1987)*

The simulation model had two vertical wells, an injector and a producer. The injector was completed in the top block of the model, whereas the producer was completed in the bottom block. This way of completing both wells was chosen to fulfil the aim of this study of investigating top down in-situ combustion process. The injector well was controlled by air injection rate, which was usually determined by running several sensitivities to optimise the rate for each model developed in this study. The producer was controlled using bottom hole pressure constraint mode, which made the choice of this constraint value crucial. If a high value of bottom hole pressure was used (e.g. 1,200psi), this will limit the fire front advance in the model, and result in less efficient sweep by the in-situ combustion process and a low recovery factor. However, if a low bottom hole pressure value (e.g. 200psi) was used, this result in a significant difference between the upstream and downstream pressure, which leads to that injected air being

able to bypass the fire front. As a result, early break through of air occurs and the performance of the fire front decreased significantly.

3.4.4 Numerical dispersion effect (using 1D model)

Modelling of the in-situ combustion process is very sensitive to the model's grid dimensions. This is because of numerical dispersion effects caused by the dramatic variations in temperature and saturation that occur at the combustion front. Numerical dispersion is a well known problem which can cause serious difficulties in the simulation process, and can lead to poor prediction results. It is an error that results from the use of grid block approximation to solve the simulation equations, such as the flow and the thermal equations (Camy and Emanuel, 1977). It can be reduced and controlled by implementing finer grids blocks in the simulation model. The smaller the grid blocks the smaller the dispersion error. Also, increasing the grid resolution of the model greatly increases the precision and accuracy of sweep volume estimates, and clarifies the interactions between the different phases in the combustion front, as well as helping to better capture of temperature profile (Albahlani and Babadagli, 2008). In other words, the higher the grid resolution the more representative is the model and the more accurate are the results. However, having fine grids in the model will increase run time and, depending upon the CPU capability, the equations may not converge. This means that for the simulation of the in-situ combustion process a compromise between model accuracy and computer time is usually required.

In this study, different grid resolutions were investigated to optimise the run time while capturing the physical behaviour of the process. For the given 1D model developed in this study, which had the following dimensions of 0.1602ft by 0.1602ft by 2.646ft (air injection rate of 0.554 scf/hr), different grid resolutions were used. Initially, five different resolutions were tested: a total of 12 grid blocks, 20 grid blocks, 40 grid blocks, 80 grid blocks, and 120 grid blocks. Table 3.4 shows the block dimensions for each of those models. To compare and investigate the effect of grid resolution on the in-situ combustion process, all the model properties (including the air injection rate and both heating rate and duration) were kept the same in the various resolution models. The simulation results for the comparative resolution sensitivities showed that the model

with higher grid resolution (fine grids i.e. 120 blocks) allowed faster combustion front propagation in the model from the injector to the producer and resulted in slightly shorter recovery time required to sweep the oil in the model (Figure 3.10a). The reason for this was that, with the implementation of smaller grids, the grid blocks ahead of the fire front were exposed for a short period of time to the front high temperature. This results in a lesser amount of coke being produced (Figure 3.10b), and when the front approached those blocks, it consumed the coke so fast and then it moved to the next grid blocks. This contrasted with the case where larger grid blocks were used (i.e. 12 blocks) where the large block dimensions led the front advancement rate and increased the exposure time of the blocks ahead of the front to the high temperature (Marjerrison et al., 1992) and led to larger amount of coke produced and deposited. As a result, both the model's porosity and permeability were reduced. This acted as a factor in slowing the front advancement, and also decreased the amount of oil available to be recovered by the process.

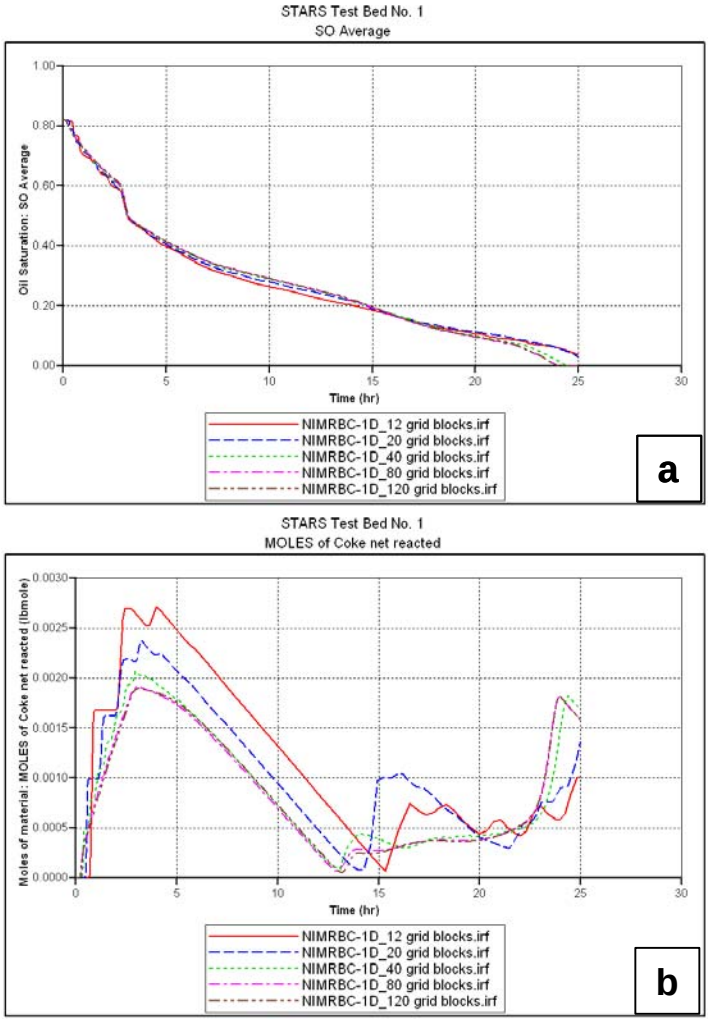

Figure 3.10: *Simulation results for grid resolution models: (a) average oil saturation, and (b) net coke in place.*

Model name	Total number of grid blocks	Grid block dimensions (ft)	Grid blocks in x, y, z directions
12 grid blocks	12	0.1602X0.1602X0.2205	1X1X12
20 grid blocks	20	0.1602X0.1602X0.1323	1X1X20
40 grid blocks	40	0.1602X0.1602X0.0662	1X1X40
80 grid blocks	80	0.1602X0.1602X0.0331	1X1X80
120 grid blocks	120	0.1602X0.1602X0.0221	1X1X120

Table 3.4: *Grid resolution models*

The comparison of the total oil produced by the five models (Figure 3.11a) showed that as the grid resolution increases, the cumulative oil produced increases. In the lower

resolution models, the cumulative oil produced was less as a result of the larger amount of oil, which was converted to coke in the coarser models, which reduced the oil saturation without increasing the recovery factor from such models. Furthermore, the peak temperatures increased with finer grid resolutions because of the reduced numerical dispersion effects (Figure 3.11b). Also, the smaller the blocks the earlier the peak temperature occurred as a result of the faster front advancement. This means the finer grids were more accurate in representing the actual temperature front because of the reduction of the averaging error in each grid block. With larger grids models, there was more coke available for the fire front to consume and a higher peak temperature might be expected compared to the fine grid models. However, due to the numerical dispersion error experienced in larger blocks models this was not the case. Thus the coarser simulation results should be considered as unreliable. This error may have a very significant impact on the feasibility of implementing in-situ combustion process for such cases (Rangel-German et al., 2006). Finally, the model with 120 grid blocks took over 12 times as long to run as the 12 grid blocks model. This indicated that a balance was required between the model grid resolution and how representative of the process it was, and the CPU time required.

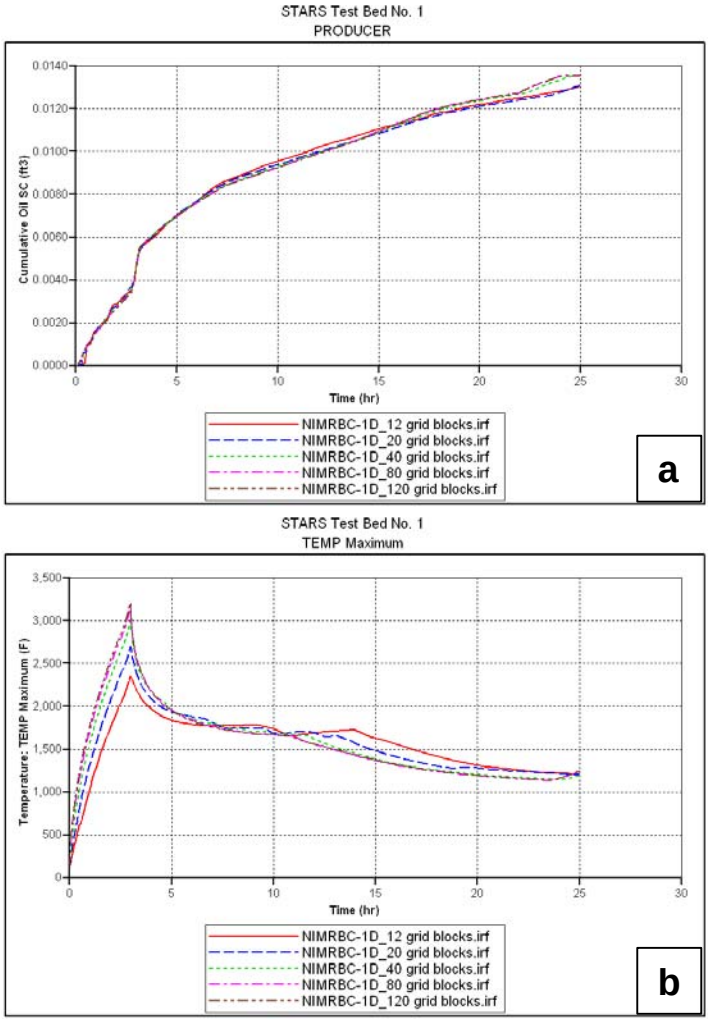

Figure 3.11: *Simulation results for grid resolution models: (a) cumulative oil produced, and (b) peak temperature.*

3.4.5 Modelling of combustion tube test experiment using the 1D model

The aim for this section is to present a comparison of the in-situ combustion process behaviour between the combustion tube test experiment and the 1D simulation model, which was developed for this study. The comparison should help to identify the main differences to expect in the combustion process performance when literature data were used to define the kinetic model in the numerical simulation study. The 1D simulation model was originally developed using most of the available Nimr data, which are the reservoir rock and fluid properties. However, all of the required combustion process variables used in the modelling of the fire flood are not yet available for this field. A very important and necessary part of the field process is represented by the kinetic

model. This model includes all the chemical reactions (thermal cracking, high and low temperature oxidations), for which the dependence variables are: reaction activation energy, reaction order and reaction coefficients. Also, there is a need to identify fuel availability, the air requirements, air oil ratio, recovery factor and the analysis of the produced gases in order to be able to model the combustion process. Since PDO is interested in application of in-situ combustion in the Nimr field, there are already plans to determine all the required in-situ combustion variables. As a start, a set of combustion tube tests (detailed explanation of the combustion tube test was presented in Chapter 2) were conducted by the University of Calgary with, cooperation from the Sultan Qaboos University. The results of one dry combustion tube test were available (Hammawa et al., 2007a) when this study was conducted. The main outputs from the combustion tube test experiment were fuel requirements, air requirements, hydrogen to carbon ratio (H/C), oxygen utilization, maximum temperature, recovery factor, frontal advancement rate, [(carbon monoxide+carbon dioxide)/carbon monoxide] and [(carbon monoxide+carbon dioxide)/nitrogen] ratios. Variations between these variables were expected since some of the 1D model properties were not matching with the actual combustion tube test properties (i.e. kinetic model), even though similar initial and operating parameters were used in both approaches (Table 3.5). The reason for performing such a comparison was to qualitatively understand the difference between both the true measurement (CTT) and its representation (1D simulation model), and what caused those variations. It also helped to identify the range of variation we should expect when using literature input combustion data in the simulation model.

Initial and operating conditions	Dry Combustion tube test (Hammawa et al., 2007a)
Porosity (%)	40.8
Permeability (D)	27.14
Pressure (MPa)	10
Temperature (°C)	55
Feed gas (mole%)	O2:20.66 + N2: 79.34
Soi (%)	86.3
Swi (%)	13.7
Sgi (%)	0

Table 3.5: *Initial and operating conditions of the combustion experiment.*

Most of the combustion properties were obtained from the 1D model by developing a spreadsheet into which the BC simulation results were exported. All the simulation output variables were obtained at the same time step of the simulation run, which was where the average oil saturation was equal to zero at the end of the run. This approach was considered to be very optimistic when compared to the real field case where different criteria define the optimum cut off value such as the water cut or cumulative oil produced. When required, the cut off control value can be redefined and the simulation combustion output variables can be determined according to the new cut off value. Equation 3.12 was used for the determination of the fuel requirement value from the simulation model results and was equals to 32 kg/m^3 for the simulation model.

$$\text{Fuel requirement} = (\text{STOIIP} - \text{cum. oil produced} - \text{remaining oil [as net coke in place]} - \text{remaining oil in place [as liquid phase]})/\text{total reservoir volume} \quad \textbf{3.12}$$

Also, the percentage of oil in place which was converted to fuel and consumed equals 9.9% (equation 3.13).

$$\text{Fuel consumed out of the STOIIP} = (\text{STOIIP} - \text{cum. oil produced} - \text{remaining oil [as net coke in place]} - \text{remaining oil in place [as liquid phase]})/\text{STOIIP} \quad \textbf{3.13}$$

Both values were higher than what the combustion process consumed in the combustion tube experiment (Table 3.6). This was because of the numerical dispersion effect where the large grid dimensions in the simulation model led to more fuel being produced. As a result the peak temperature of the 1D model was double the value of the peak temperature in the combustion tube test. Figure 3.12 shows the STOIIP, the cumulative oil produced, the net coke in place and the total fuel consumed for the simulation model. The difference between the first three curves (STOIIP, cumulative oil produced and net coke in place) produced the curve of the total amount of fuel consumed. The recovery factor for the model was obtained by the division of the cumulative produced oil by the total model STOIIP. In order to calculate the air requirement, the total air injected in the model was divided by the total reservoir rock volume. In the combustion tube test the frontal velocity was determined by following the 350°C temperature profile propagation throughout the core sample until the end of the experiment. A similar approach was

used for the simulation model to determine the fire front advancement rate. The front velocity of the 1D simulation model was slightly slower than the front propagation in the combustion experiment. This was as a result of the large amount of coke produced in the numerical model, which led to the fire front requiring a longer duration to consume and propagate through the model. The H/C and [(carbon monoxide+carbon dioxide)/carbon monoxide] combustion variables could not be obtained for the model. These two variables could only be determined through the implementation of the combustion tube test. Table 3.6 summarises the main variables of the combustion process for both the combustion tube test and the 1D model results. There were some matches of the results between the experiment and the simulation model. However, properties such as peak temperature and total fuel consumed were not matching and they were higher in the simulation model compared to the experimental values. The reason for the differences between the two cases was, as already mentioned, as a result of the fact that some of the simulation model properties were not specifically Nimr field properties. Also, due to effect of numerical dispersion when using the large grid blocks in the simulation model, despite the previous efforts to minimise this effect in this study, a completely accurate match between experimental and simulated results will never be achieved. The larger grid blocks allowed for more fuel formation and deposition ahead of the front, and therefore increased the fuel requirement. Furthermore, as the fuel availability increases the maximum temperature profile increased. The recovery factors of both the combustion experiment and the 1D combustion model were almost the same.

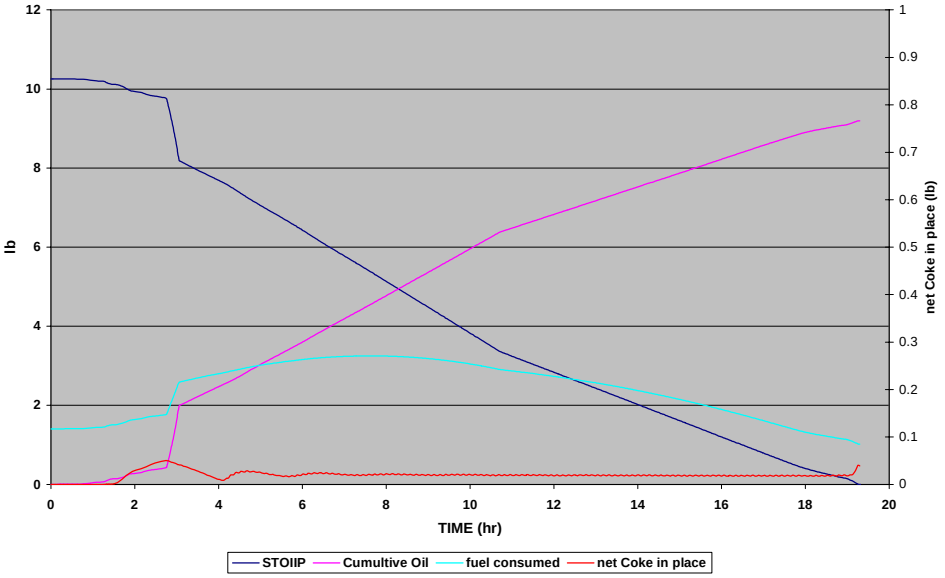

Figure 3.12: *The 1D simulation model STOIIP, the cumulative oil produced, the net coke in place and the fuel consumed curves.*

Combustion variables	Dry Combustion tube test (Hammawa et al., 2007a)	1D combustion tube test simulation using the 1D model properties (So=0)
Fuel requirement (kg/m^3)	18	32
Air requirement (m3/m^3)	212.7	269
H/C	2.02	Not applicable
O2 utilization (%)	96.3	100
Fire front velocity 350°C (m/h)	0.139	0.105
Maximum temperature (°C)	569	1192
Recovery factor (%)	88.3	89.7
Fuel consumed out of STOIIP (%)	<5	9.9
(CO2+CO)/CO ratio	5.06	Not applicable
(CO2+CO)/N2 ratio	0.18	0.57

Table 3.6: *Main combustion variables of the combustion tube experiment and the 1D combustion tube simulation model*

3.5 In-situ combustion 2D cross sectional model development

3.5.1 2D model

In the development of 2D cross section model, a larger model was built (Figure 3.13). The 2D cross sectional model had dimensions of 100ft by 3.3ft by 100ft, to provide a clear reliable in-situ combustion modelling process that was able to run using the available resources. It had two wells, a vertical injector which was completed in the top 25ft and a vertical producer which was completed in the bottom 25ft on the other side of the model. The total number of grid blocks used in this model was 1,024, with 32 blocks in both the x and z directions, and one grid block in the y direction. The grid block dimensions were 3.125ft, 3.3ft, and 3.125ft in the x, y, and z directions respectively. All the other model properties (i.e. porosity, permeability… etc) were kept the same as in the previous developed 2D model. The model enlargement led to the need for investigate and evaluate the required amount of air to be injected in order to initiate and start the in-situ combustion process in the model. Many runs were conducted to determine the optimum air injection rate as well as the heating rate, and the heating duration for the producer in the model as the following subsection illustrate.

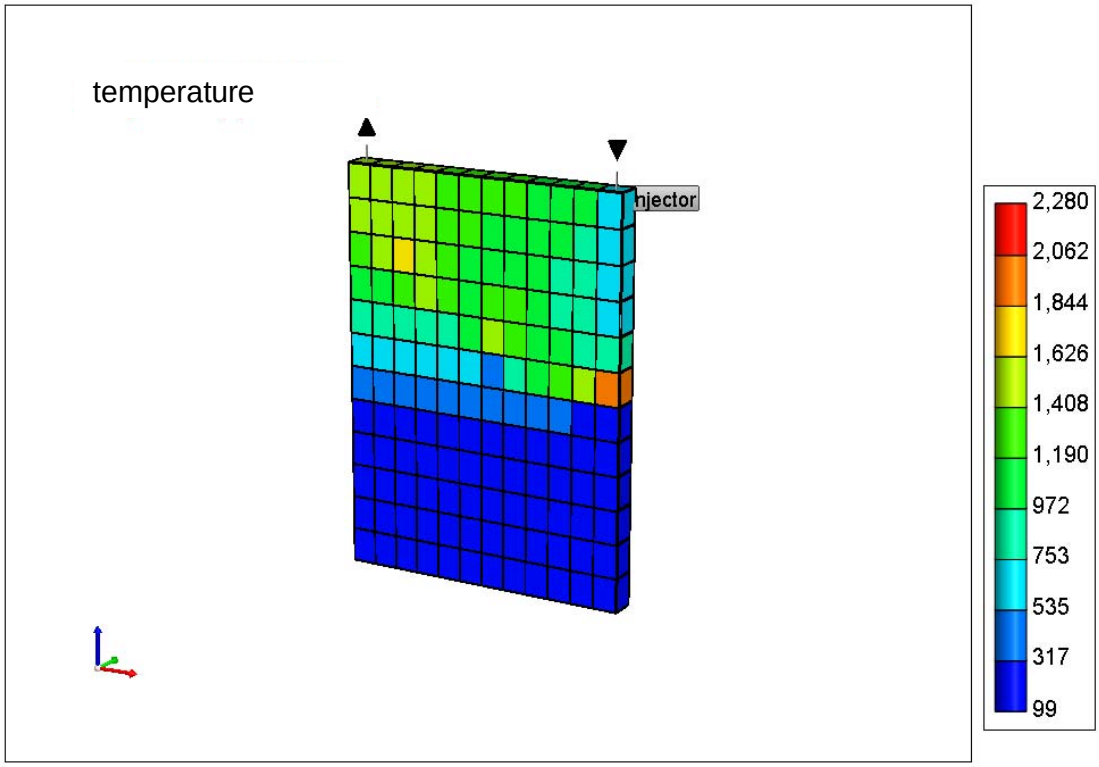

Figure 3.13: *2D cross sectional model temprture profile (°F)*

3.5.2 Optimization of air injection rate, ignition heating rate and duration of ignition period

For in-situ combustion, identification of the critical operating parameters was important. The determination of the optimum model input parameters such as air injection rate, ignition heat rate, and ignition duration was crucial. This can be done by study of each individual parameter through several sensitivities runs. Using the updated 2D model, these parameters were determined and evaluated and the results showed the optimum values for each parameter. This optimisation process needed to be carried out for each model developed in this study because when changing any input parameter in the model the result could be a failure to initiate or sustain in-situ combustion process in that model. Moreover, optimization of the critical parameters usually helped to enhance the economics of the in-situ combustion process by increasing the recovery factor of the process or by reducing the capital and operating cost of investing in this enhanced recovery method.

Air injection rate: This was an important criterion for in-situ combustion modelling. In the case where a high air injection rate was used, this usually led to the model being overpressurised and could damage the formation if it exceeded formation fracture pressure. Also, a higher injection rate could affect the project feasibility by increasing the capital cost of investment in more air compression that the process required. However, a low air injection rate, below the optimum value could result in the in-situ combustion not being initiated or perhaps delayed, which would lead to a poor recovery factor. Also, it would result in a much longer project life and delay in the income from the investment. To investigate and find the optimum air injection rate for the updated 2D model, several sensitivities run were conducted. A wider range of injection rates was used from 50 ft^3/hr (1,200ft^3/day) to 200 ft^3/hr (4,800ft^3/day) to evaluate the effect of changing air injection rate on in-situ combustion. Figure 3.14 shows some of the main results of changing air injection rate in the model. The first thing to highlight was that both the average model temperature (Figure 3.14a) was proportionally increased as air injection rate increases. This increase in the average model temperature was mainly due to a larger amount of oxygen being available at higher injection rates, which corresponded to a larger amount of coke being burned (Tabasinejad, et al., 2006). The average oil saturation decreased as air injection rate increased (Figure 3.14b). This was because most of the oil was recovered at the higher air injection rates and also because more oil was converted to coke at higher air rates. Figure 3.15a shows the cumulative oil production, which indicated higher oil production with higher air injection rates. This increase in air rate helped to accelerate oil production (Kumar, 1987) as the steepness of each cumulative oil production curve shows. This meant a higher air rate led to a higher recovery factor, and enhances the economics of applying in-situ combustion, since large amounts of oil were produced in the early years of project life. The amount of oil converted to coke was increased as the air injection rate increased (Figure 3.15c). Additionally, with a high air injection rate, there was limited time available for all the moveable oil ahead of the front to be displaced before the front arrived. This resulted in more oil (movable oil left ahead of the front) was converted to coke and consumed by the fire front (Onyekonwa, et al., 1986). Figure 3.16 shows the front advancement for an air injection rate of 50ft3/hr (a), and for 200ft^3/hr (b), at the same time step (300 days) using the temperature profile to represent the front movement. It was clear that the rate of advancement of the combustion front increased

as the injection rate was increased (Kumar, 1987). In other words, the front advancement velocity was almost directly proportional to the air injection rate in the model. For field-like conditions, the rate of advance was mainly controlled by the air injection rate. Therefore, in general, higher air injection rates will result in faster recovery as a result of faster front propagation rate (Kumar, 1987). From the comparison between the air injection rates, the optimum air injection rate for this specific 2D model was chosen to be $100ft^3$/hr (2,400 ft^3/day), even though this rate gave a lower recovery factor when compared to the 200 ft^3/hr rate. The reason for choosing the 100 ft^3/hr rate because for in-situ combustion process, there is a minimum rate of frontal advancement, which is required to sustain the high temperature combustion (Nelson & McNeil, 1961). For dry forward in-situ combustion process the suggested minimum propagation rate was equal to 0.125 ft/day (Northrop et al., 1994). In the 2D model, the $100ft^3$/hr injection rate managed to achieve 0.2 ft/day frontal propagation rate, which was well above the minimum advancement rate. This was important to ensure better combustion process performance and that the high temperature combustion was sustained throughout the process duration. Another reason to choose this optimum injection rate was because at higher air injection rate (i.e. $200ft^3$/hr), fracture could develop in the formation near the injector well. These fractures would work as conduit for air flow and led to air bypassing the fire front and quenching the combustion front. Also higher air rate would result in more oil lost by convertion to coke. The coke was consumed by the front and resulted in excessive temperatures (when higher amount of coke is available) which could damage the well completions. In addition, the choice of an injection rate of $100ft^3$/hr would improve the economics of the project by reducing the number of compressors required to inject the air by one third compared to the $200ft^3$/hr case. It should be noted that a detailed evaluation of economics was not considered in this project.

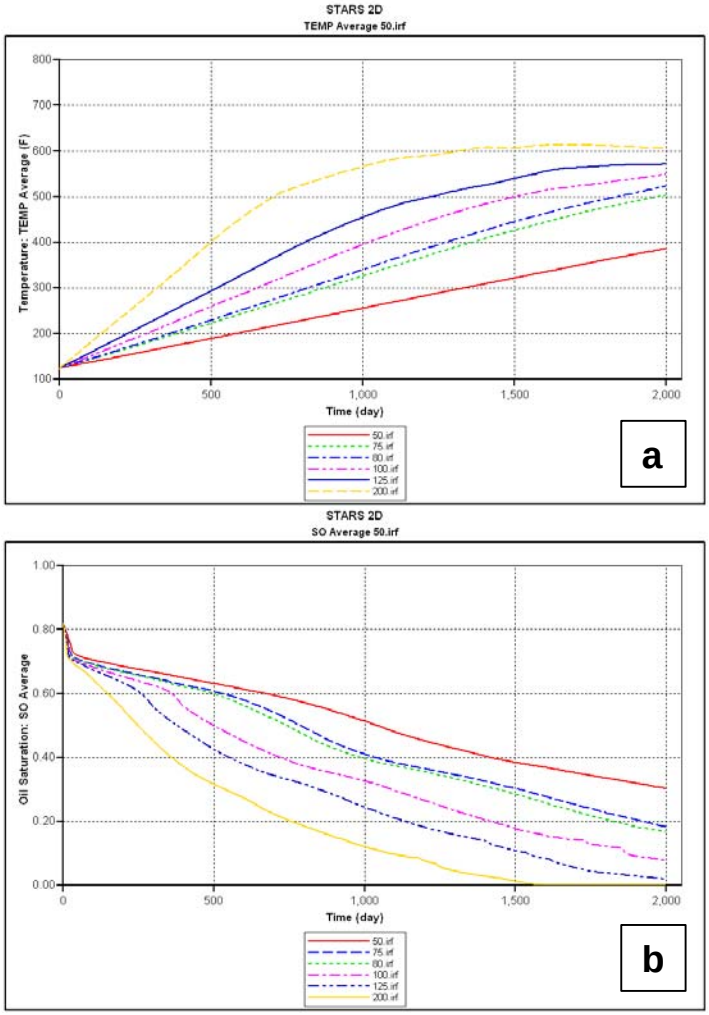

Figure 3.14: *Simulation results for the air injection sensitivities: (a) average model temperature, and (b) average oil saturation.*

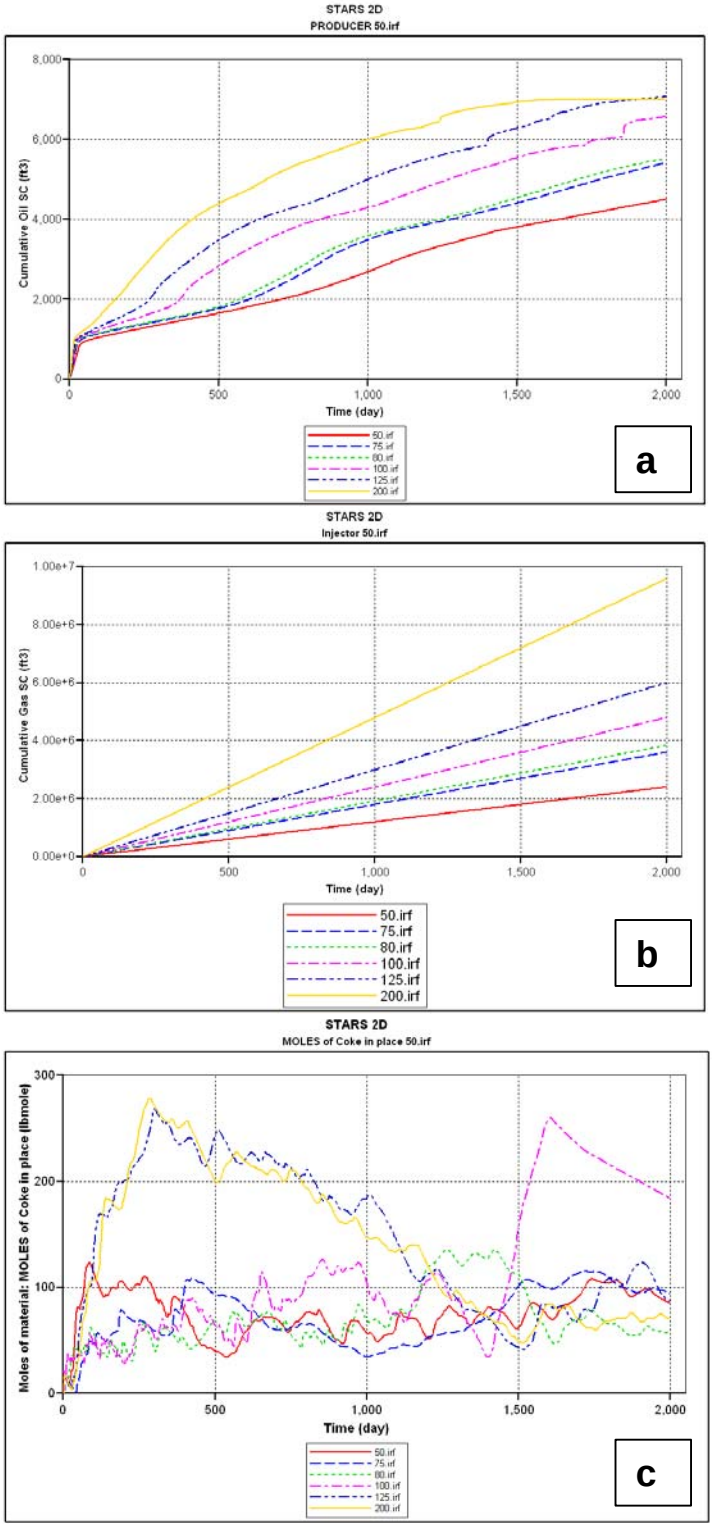

Figure 3.15: *Simulation results for the air injection sensitivities: (a) cumulative oil production, (b) cumulative air injection, and (c) net coke in place.*

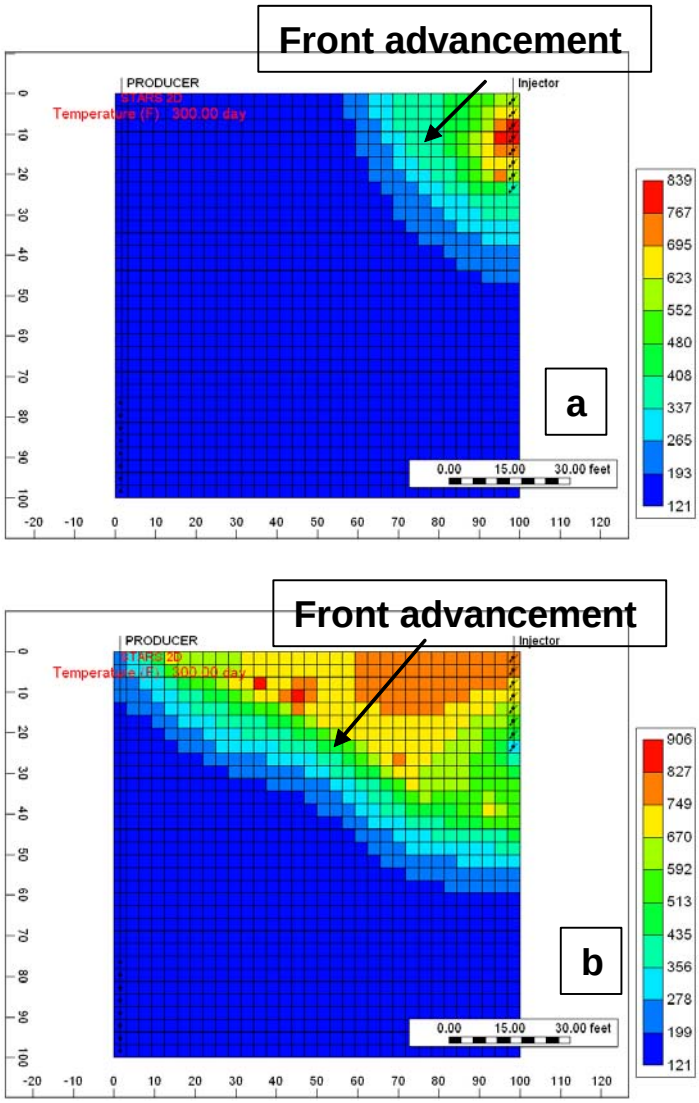

Figure 3.16: *Coke concentration which indicates the front movement in the model two different air injection rates at the same time step: (a) air injection rate 100ft^3/hr, (b) air injection rate 200ft^3/hr.*

Ignition heating rate: in order to start in-situ combustion, a form of ignition was required. Depending on the crude oil reactivity and the formation temperature, spontaneous ignition could occur as soon as air is injected into the formation. However, most in-situ combustion was usually initiated by using external heaters: either electrical heaters or gas burners. According to the initial compositional analysis of Nimr crude samples, and the combustion tube tests which were conducted by University of Calgary, on behalf of Sultan Qaboos University in corporation with PDO, the oil reactivity for Nimr was not enough to start spontaneous ignition at the current formation temperature. The study showed that Nimr crude ignited at 350°C (662°F), which supposed that

external heaters were required to start the combustion in the formation (Hammawa, et al., 2007a; Hammawa, et al., 2007b). To start in-situ combustion in the 2D model, an analysis of the required ignition heating rate was needed. Different heating rates were used in this sensitivities analysis, from as low as 10,000 Btu/hr to as high as 120,000 Btu/hr (Figure 3.17a). From the comparison of these sensitivities results, it was clear that the main difference between the various heating rates was when the fire front was ignited. The higher the heating rate supplied by the heaters in the formation, the earlier the in-situ combustion process was initiated in the formation (Figure 3.17b). Figure 3.18a and Figure 3.18b, show that there was no significant difference in the model average temperature or the cumulative oil production as the ignition heating rate changes. From this comparison, it was clear that the need for a sufficiently high heating rate in the beginning of the in-situ combustion process was crucial to start the fire front at an early stage of the process, and avoid delaying oil recovery. The amount of heating required varies from case to case, depending in the crude oil and formation properties. For this specific model a heating rate of 40,000 Btu/hr was chosen to be an optimum rate because the fire front was not delayed, as in lower heating rate (10,000 Btu/hr), and at the same time it was cheaper than supplying excessive heat for the higher ignition rates (i.e 120,000 Btu/hr).

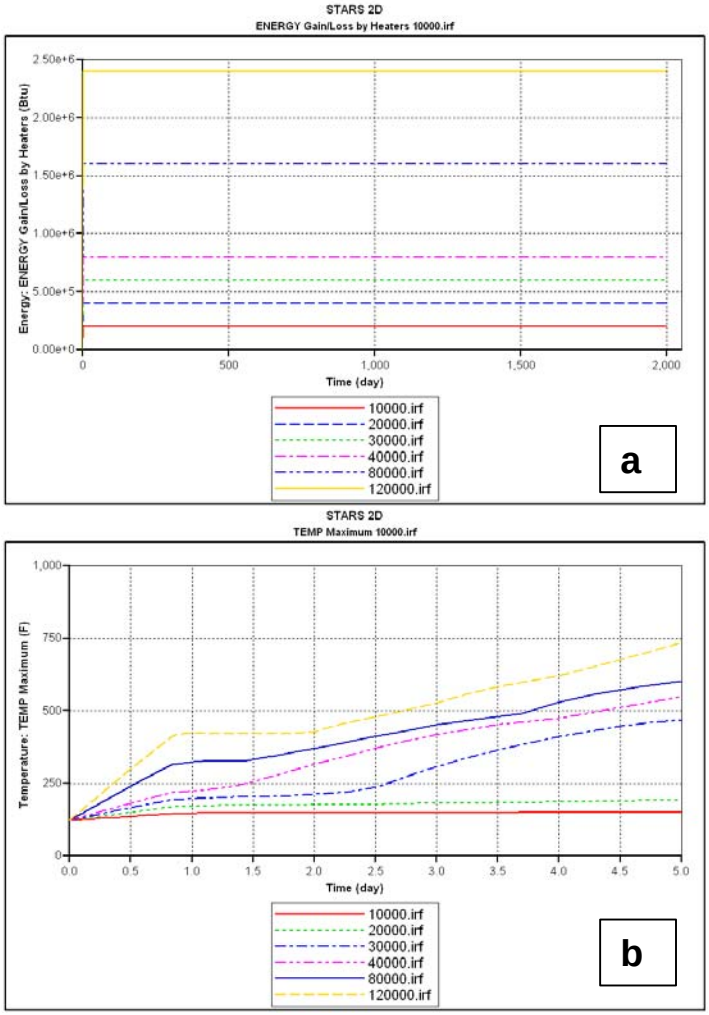

Figure 3.17: *Simulation results for the ignition heating rate sensitivities: (a) energy provided by heaters, and (b) peak temperature.*

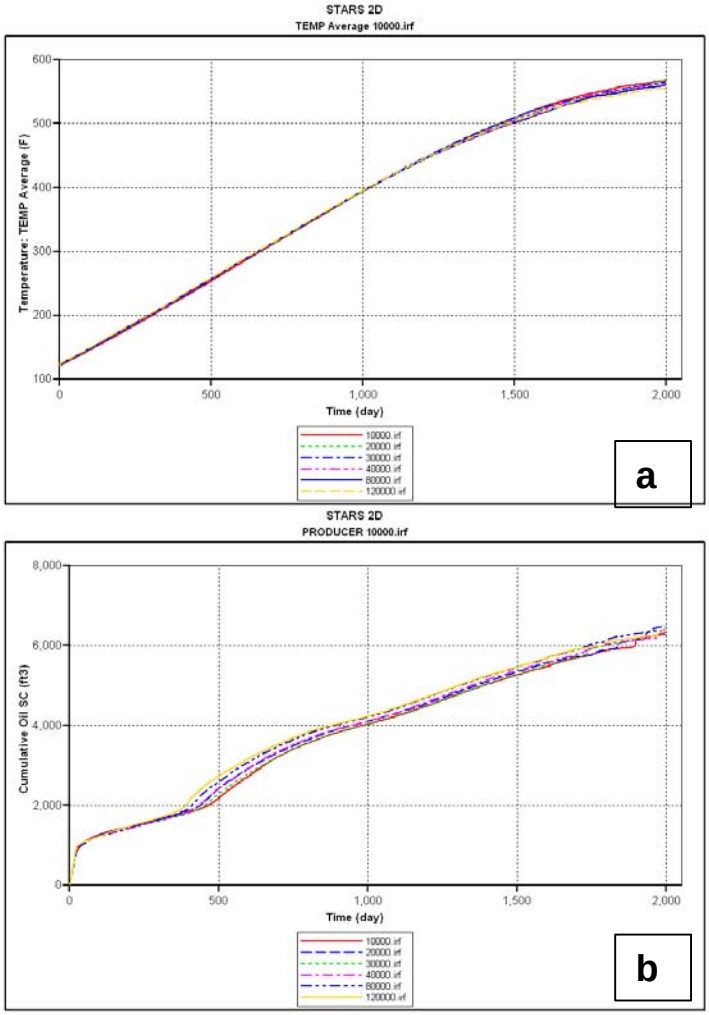

Figure 3.18: *Simulation results for the ignition heating rate sensitivities: (a) average temperature, and (b) cumulative oil produced.*

Duration of ignition period: The need to initiate the fire front in in-situ combustion usually depends on both the amount of heat which is supplied to the formation and the total duration over which the external heaters are used. From the pervious sensitivities; the optimum air injection rate and the ignition optimum period for the 2D model were calculated. With the aim of determining the optimum heating period in mind, several sensitivity runs were conducted, each with different heating periods. The significance of determining such an important input parameter for the in-situ combustion process was that if the heaters were switched on for only a short period, the fire front might not be ignited, which would result in a failure or delay of the process. In the case of using the heaters for a longer period, this would result in energy wastage, and the high temperature values near the heaters might also damage the injector well completion.

Figure 3.19 and Figure 3.20 show the simulator results from running the 2D model for 5 different heating periods. Figure 3.19a shows the total energy gained by the formation from the heaters. The observations from this sensitivity were the same as previous observations from the heating rate sensitivity in terms of the fact that the change in heating duration only affected the early fire front ignition time. Delayed front ignition occurred for shorter heating periods such as only 1 day heating period. However, the longer heating duration results in almost the same time for fire front ignition; this meant that if a heating period of 3 months or 6 months were used, both will enable the in-situ combustion front to initiate in the same time range (Figure 3.19b). However, the 6 months heating period would cost much more and there was not much improvement or difference in the process outcome. Both Figure 3.20a and Figure 3.20b show the overall differences between the different heating durations in this model, and the impact on cumulative oil produced and average oil saturation. It was important to choose the right heating period to provide sufficient front ignition, but also save time and money in terms of energy consumption if the heaters were still in use after the front was initiated. The optimum heating duration from these sensitivity calculations for this 2D model was found to be 1 month. This value, when compared to other shorter ignition periods did provide relatively early ignition time and when compared to longer ignition periods it provided a slightly lower recovery factor, but with some energy saving (Figure 3.20a).

The variation of the three input parameters discussed here showed the different effects on the in-situ combustion process. From the results, air injection rate was the most sensitive parameter, and any variation in it would result in a critical variation in the process performance. However, both the heating rate and the ignition duration did have an effect, although any changes in these had a limited impact on the combustion process. This was due to the fact that as soon as the fire front has been initiated, there existence was not essential for the process to sustain unlike the air injection parameter.

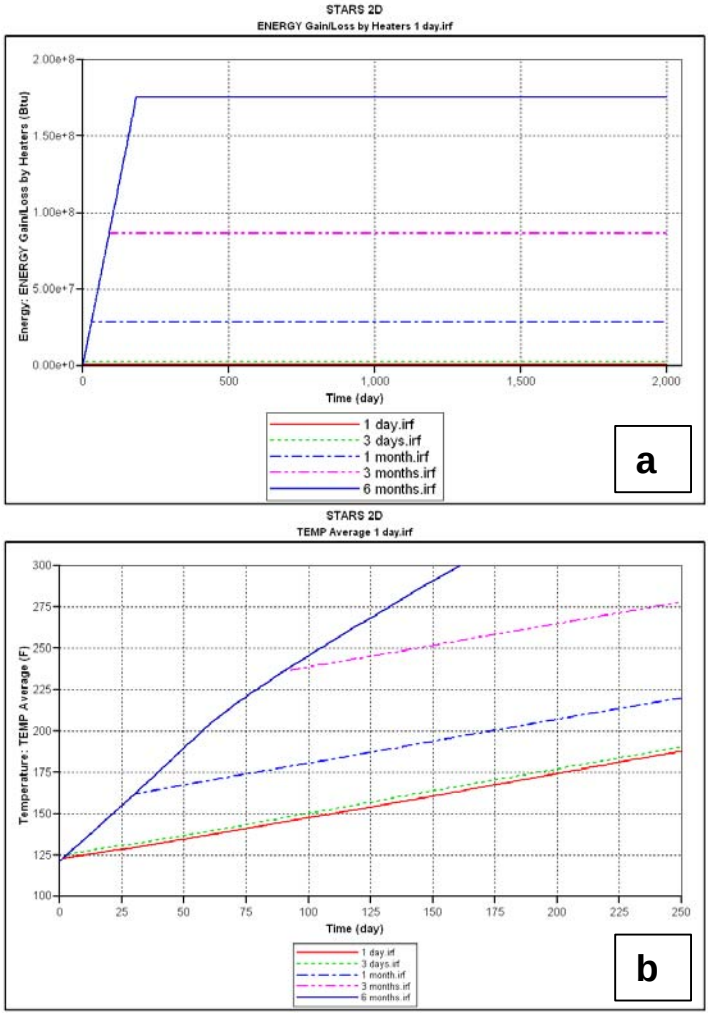

Figure 3.19: *Simulation results for the ignition heating duration sensitivities: (a) energy provided by heaters, and (b) average temperature.*

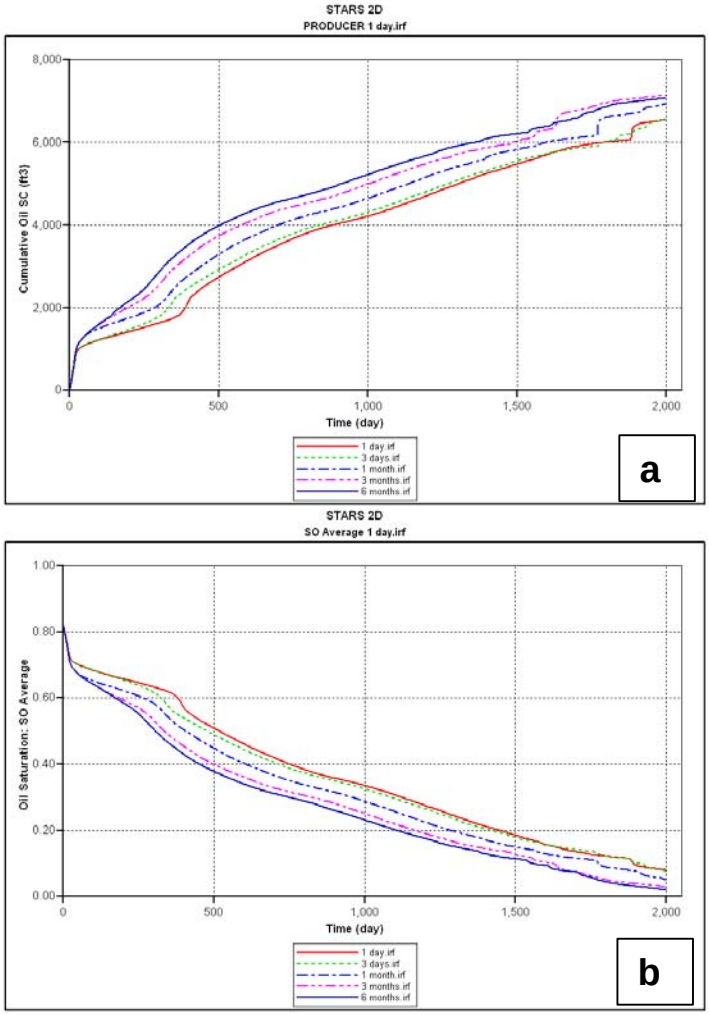

Figure 3.20: *Simulation results for the ignition heating duration sensitivities: (a) cumulative oil produced, and (b) average oil saturation.*

The previous sensitivity calculations helped to optimise the 2D cross sectional model and it was found that the optimum air injection rate of 2,400 ft^3/day and heating rate of 960,000Btu/day were required for a total heating duration of one month. Figure 3.21a shows the average model temperature, which increased steadily as a result of the successful initiation and progression of the fire front. The increase in the model temperature led to a rapid decrease in oil viscosity decrease (Figure 3.21b) as time proceeds. The recovery factor for this model was 83% with a total cumulative oil produced of 6,290 ft3 (Figure 3.22a). This recovery factor was considered to be high and was a consequence of the choice of 2D geometry. It was a small homogenous model with very fine grid blocks, which helped to capture the localised impact of the fire front

temperature. The combustion process reduced the average oil saturation from 82% in the start of the in-situ combustion process to 9% (Figure 3.22b).

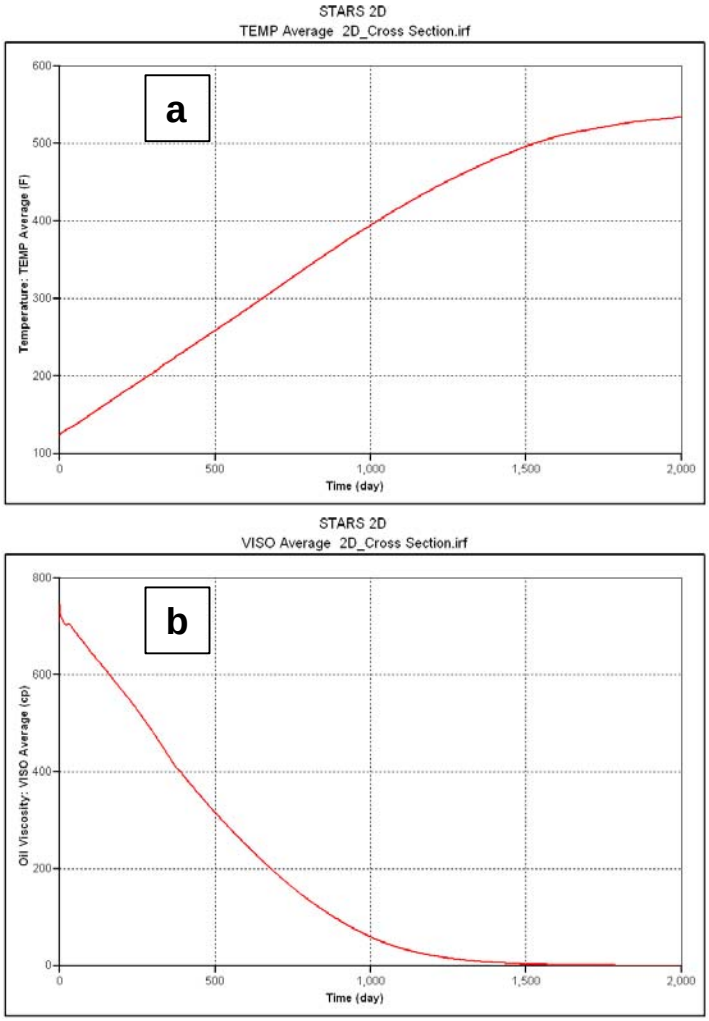

Figure 3.21: *Simulation results for 2D cross sectional model: (a) average model temperature, and (b) average oil viscosity.*

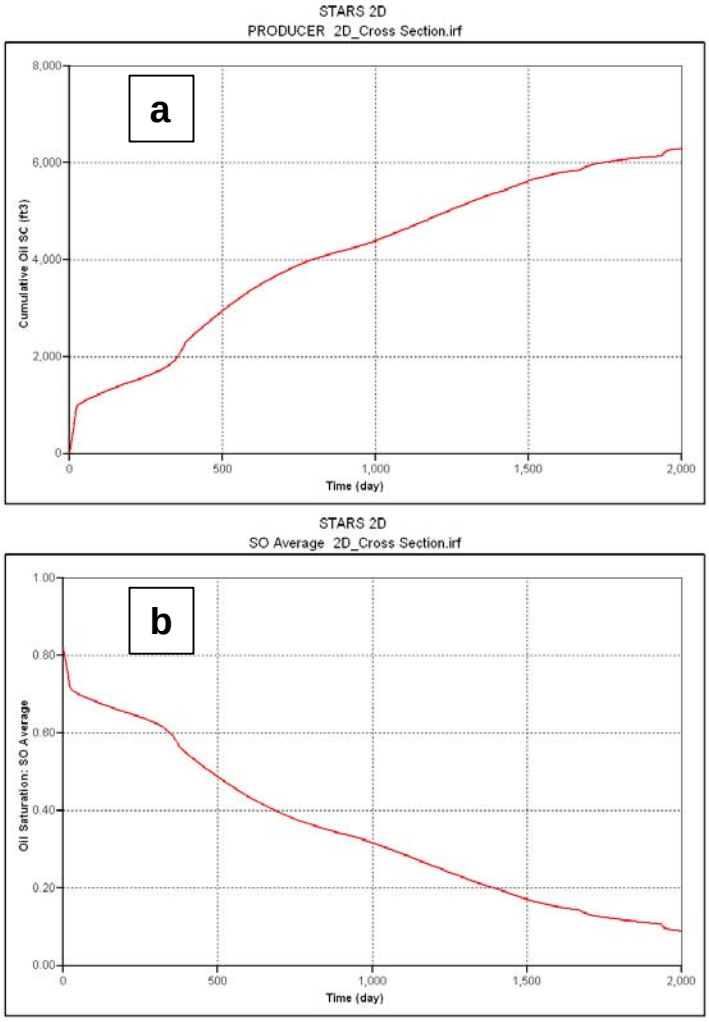

Figure 3.22: *Simulation results for 2D cross sectional model: (a) cumulative oil produced, and (b) average oil saturation.*

The temperature profile at 485 days of the process is shown in Figure 3.23a and the ternary saturations plot are shown in Figure 3.23b. The combustion front was initiated at the top of the model and then it started to propagate in both lateral and vertical directions. The front advancement laterally was faster than its propagation vertically. This was due to the gravity segregation effect where the injected air tended to flow across the top of the model until it reached the other end of the model. After that, it started to move vertically downwards and approached the top producer well perforation. This highlighted how critical it is to efficiently locate the wells and complete them in such a challenging recovery process.

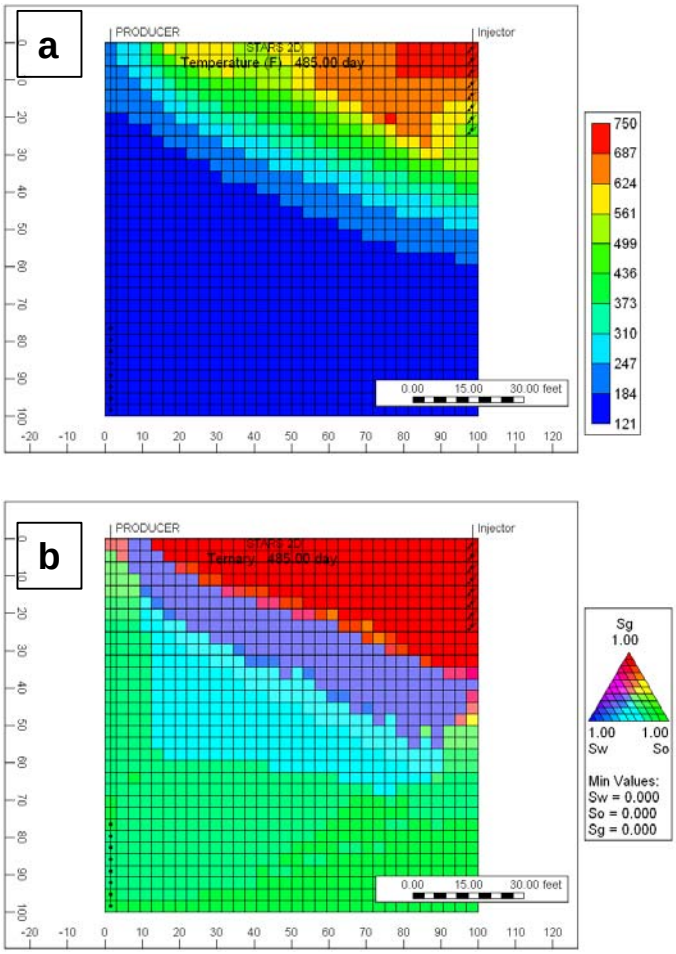

Figure 3.23: *Simulation results for 2D cross sectional model at 485 days: (a) temperature profile, and (b) ternary saturation plot.*

3.5.3 Optimization of grid block resolution (using 2D cross sectional model)

Optimisation of grid resolution was required for the 2D model (as it was essential in the 1D model) in order to be able to capture the combustion process in a time frame that allowed multiple sensitivity calculations. The 2D model grid dimensions in both x and z directions were 3.125ft. Three more models were used to determine the optimum grid resolution; their details are shown in Table 3.7.

Model name	Total number of grid blocks	Grid block dimensions (ft)	Grid blocks in x, y, z dimensions
3.125ft	1024	3.125X3.3X3.125	32X1X32
6.25ft	265	6.25X3.3X6.25	16X1X16
12.5ft	64	12.5X3.3X12.5	8X1X8
25ft	16	25X3.3X25	4X1X4

Table 3.7: *2D cross sectional model grid resolution optimisation*

The comparison of the main results from the 2D cross sectional models showed that as the grid block size increased, the amount of coke produced increased (Figure 3.24a), and the cumulative oil produced decreased (Figure 3.24b). The fire front advancement velocity in the low grid resolution models was slower when compared to the high resolution models (Figure 3.25). All of these results for the 2D cross sectional models match the same effect observed for grid resolution in the 1D combustion tube test models. However, the average temperature showed an increase in temperature as the grid block size increase (Figure 3.26). This was because of the dramatic increase of coke produced in the larger grid models, which was consumed by the fire front and increases the temperature profile.

From the comparison of 2D grid resolution, the optimum grid dimension chosen was the 6.25ft scenario. The results from both the 3.125ft and the 6.25ft cases (Figure 3.24) were almost matching. However, the 6.25ft model had an advantage over the 3.125 model, which was that it required only 6% of the CPU time to run and it required less than 30% of the storage memory needed for the 3.125ft model.

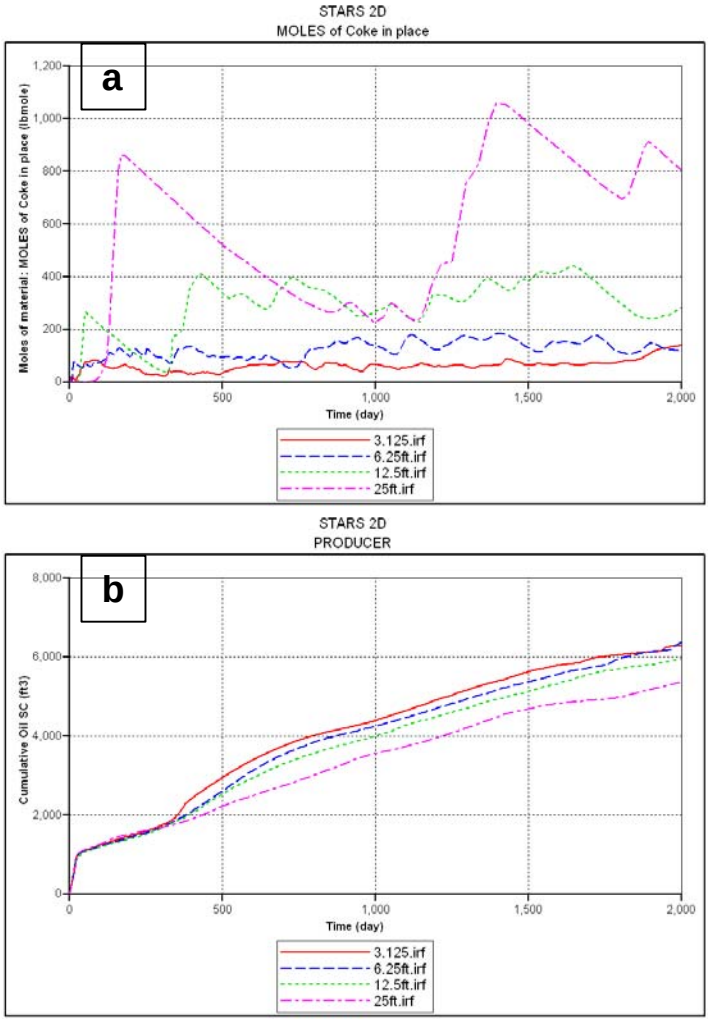

Figure 3.24: *Simulation results for grid resolution of the 2D cross sectional models: (a) net coke in place, and (b) cumulative oil produced.*

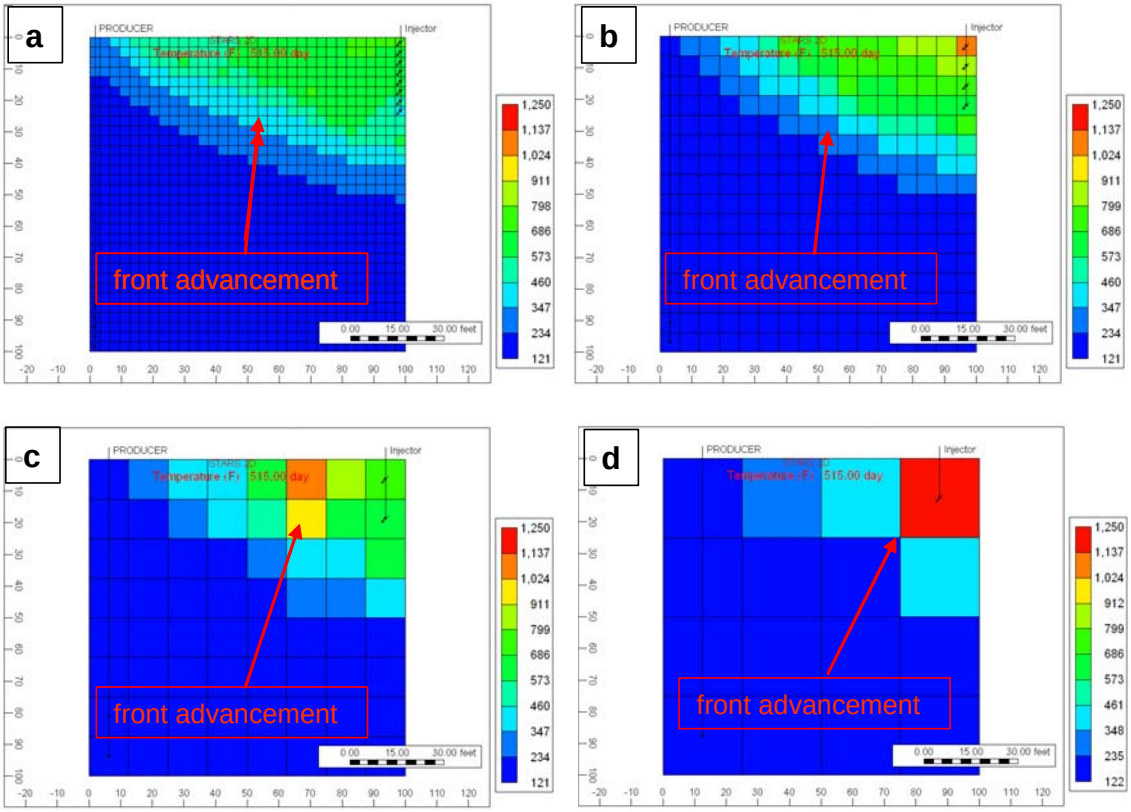

Figure 3.25: *Temperature profile at 515 days (a) 3.125ft model, (b) 6.25ft model, (c) 12.5ft model, and (d) 25ft model.*

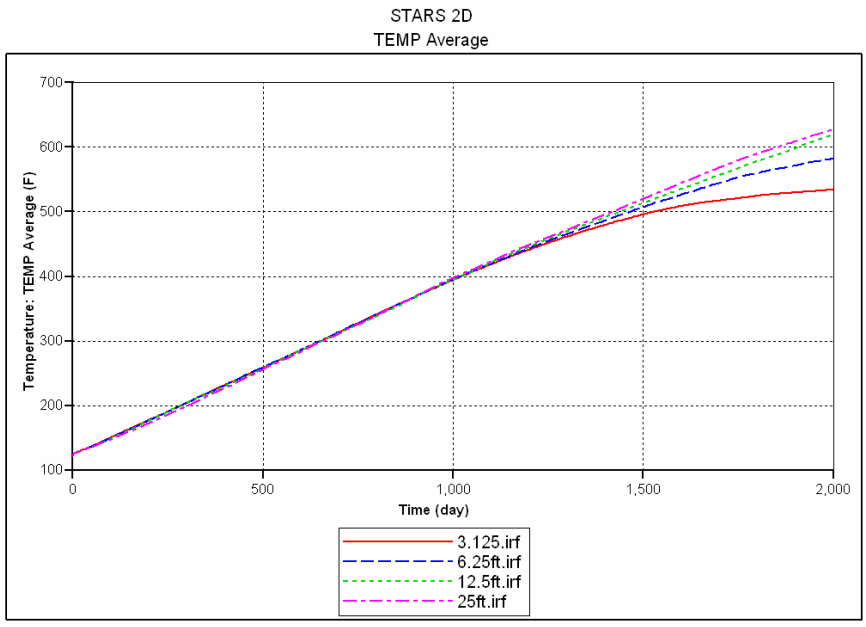

Figure 3.26: *Average temperature of the 2D cross sectional models*

3.5.4 Dynamic gridding implementation in 2D cross sectional model

In in-situ combustion process, the fire front is located between the mobilised reduced viscosity oil and the more viscous oil which has yet to be contacted by the heat. This interface region is usually thin when compared to normal grid block sizes used to model the combustion process at the field scale or even the pilot scale. As a consequence, the reliability of the results generated by the simulation can be poor because of the failure to accurately represent the combustion process, since the fire front properties were being averaged over grid blocks that were much larger than the interface region. The dynamic gridding feature in the STARS software is designed to enable the model to capture the fire front details as well as to save computing time during the simulation by reducing the number of grid blocks used in the model (STARS Manual, 2006; Sammon, 2003). This feature can be implemented in the model either as grid refinement process or as grid amalgamation (Figure 3.27a), which place fine grid blocks in the model *when* and *where* required (at the fire front interface), and leave the coarse grids as they are throughout the rest of the model. By activating this feature, there can be a several fold (up to 10 times) decrease in run time while leaving the results unchanged (Christensen et al., 2004 and Alghufaili, 2008). The dynamic gridding process is activated in the simulator based on user provided threshold values for any or all the following properties: saturations, phase mole fraction and temperature. For this study, temperature was used as the threshold because of the need to capture and follow the propagation of combustion front throughout the model. Also, the dynamic amalgamation option was preformed in all the time steps of the modelling process. Figure 3.27b shows the dynamic grid amalgamation for the 2D cross sectional model at different time steps.

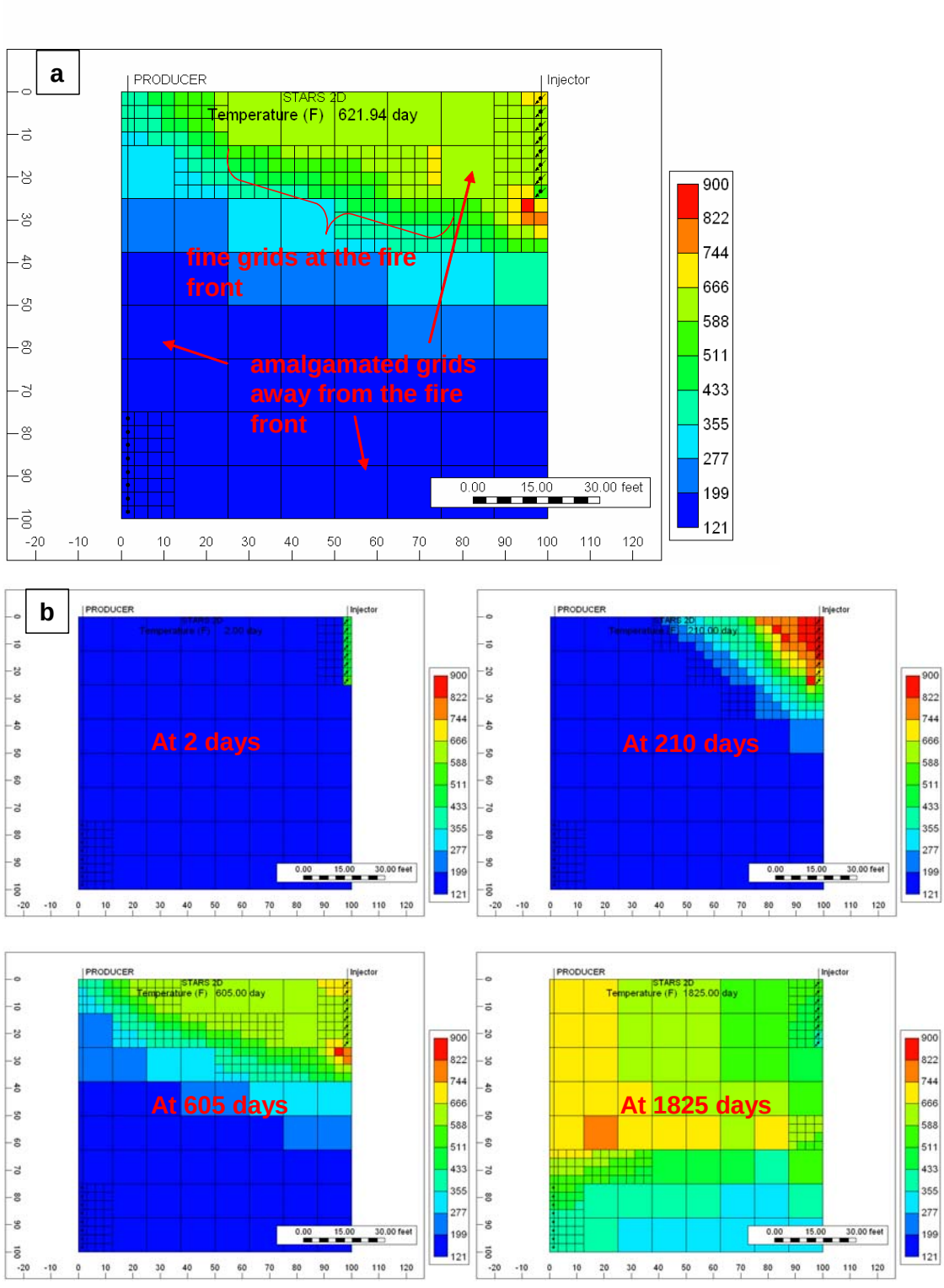

Figure 3.27: *(a) illustration of dynamic grid amalgamation for the 2D cross sectional model, and (b) dynamic grid amalgamation at different time steps.*

Dynamic gridding was used in the 2D cross sectional model to improve the run time. The dynamic gridding option was used to amalgamate 4 grid blocks in both x and z

directions if the temperature in the region changes to a value less than the threshold value. The temperature threshold (Δt) was set to be 10°C (50°F) following the CMG guidelines. Implementation of the amalgamation option in the 2D model resulted in almost a 7 times decrease in the computing time when compared to the refined 2D cross sectional model. The fire front advancement velocity of both models was almost the same as Figure 3.28 shows. However, there were variations between the two models results. Figure 3.29, shows the variations of (a) average model temperature, (b) coke in place and (c) the cumulative oil produced. These differences were due to the dynamic gridding amalgamation using larger grids in the regions away from the fire front interface. This led to the conclusion that the use of dynamic amalgamation did affect the results, and a similar variation of results was identified as previously in the comparison of fine grid models and a coarse grid models. In order to reduce the variations in the results while using the amalgamation option, the amalgamation ratio needed to be redefined. Instead of using a ratio of 4 in the x and z direction, it was preferable to use a ratio of 2. As a result, the variations between the results of the refined and amalgamated model (with ratio of 2) were smaller when compared to the larger amalgamation ratio model (ratio of 4) as Figure 3.30 shows. Another possible way to reduce the difference in results was by reducing the threshold temperature value from 10°C. A lower temperature threshold means smaller variations of results compared to the 2D cross sectional model results as Figure 3.31 shows. This was because the lowering of the threshold value allowed for the amalgamation rule to become more sensitive in terms of amalgamating the grids or not according to the smallest change in the temperature profile while the combustion front was propagating. However, a limitation must be considered when reducing the temperature threshold, because the lower the value the longer the computing time was required. The comparison of the values of threshold used here showed that a threshold value of 5°C that was suitable in the amalgamation of the 2D cross sectional model for the aim of this study.

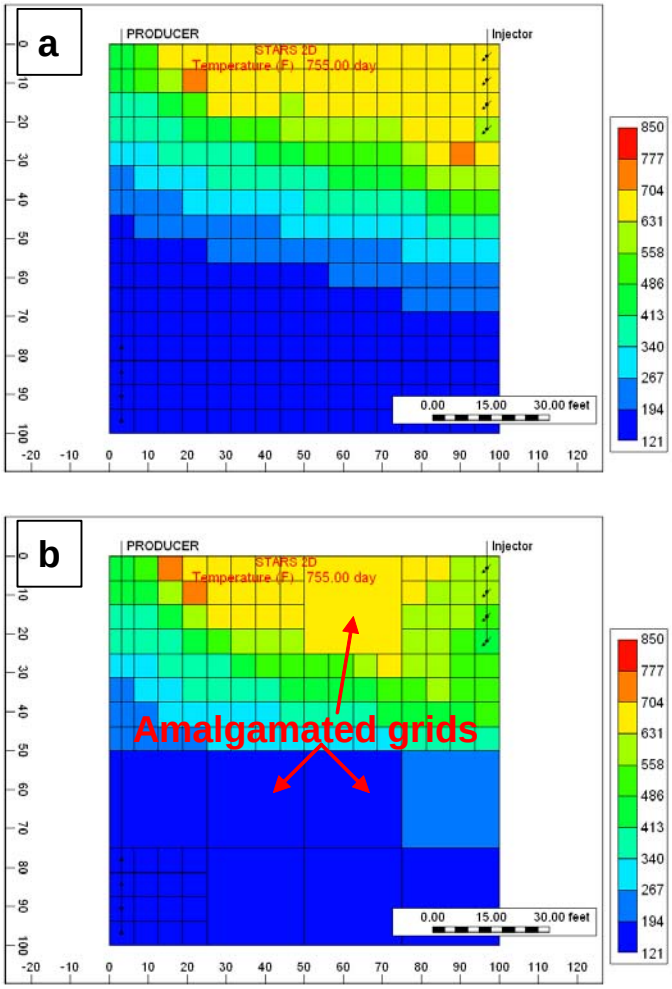

Figure 3.28: *Comparison of use of dynamic grid amalgamation or not in the 2D cross sectional model. (a) without amalgamation, (b) with amalgamation.*

The use of dynamic gridding gave a very significant improvement in the simulation of in-situ combustion in terms of reducing the computing time and providing relatively reliable results when compared to a refined model. However, the selection of both amalgamation ratio and the temperature threshold should be done carefully. This was important to avoid using values which would result in unreliable predictions. It was recommended to conduct several sensitivities in order to choose the most feasible values which provided reliable results and saved computing time.

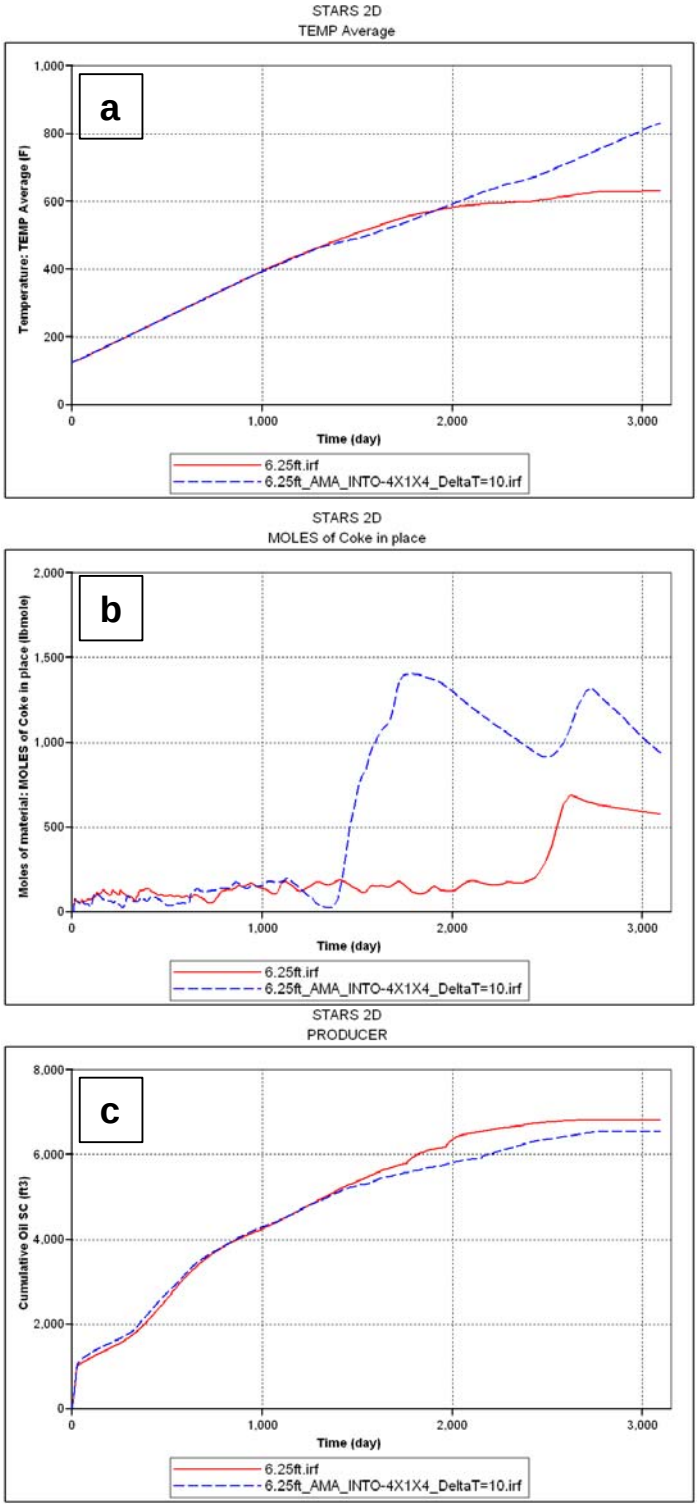

Figure 3.29: *Simulation results for dynamically amalgamated (blue) or unchanged (red) 2D cross sectional models: (a) average temperature (b) net coke in place, and (c) cumulative oil produced.*

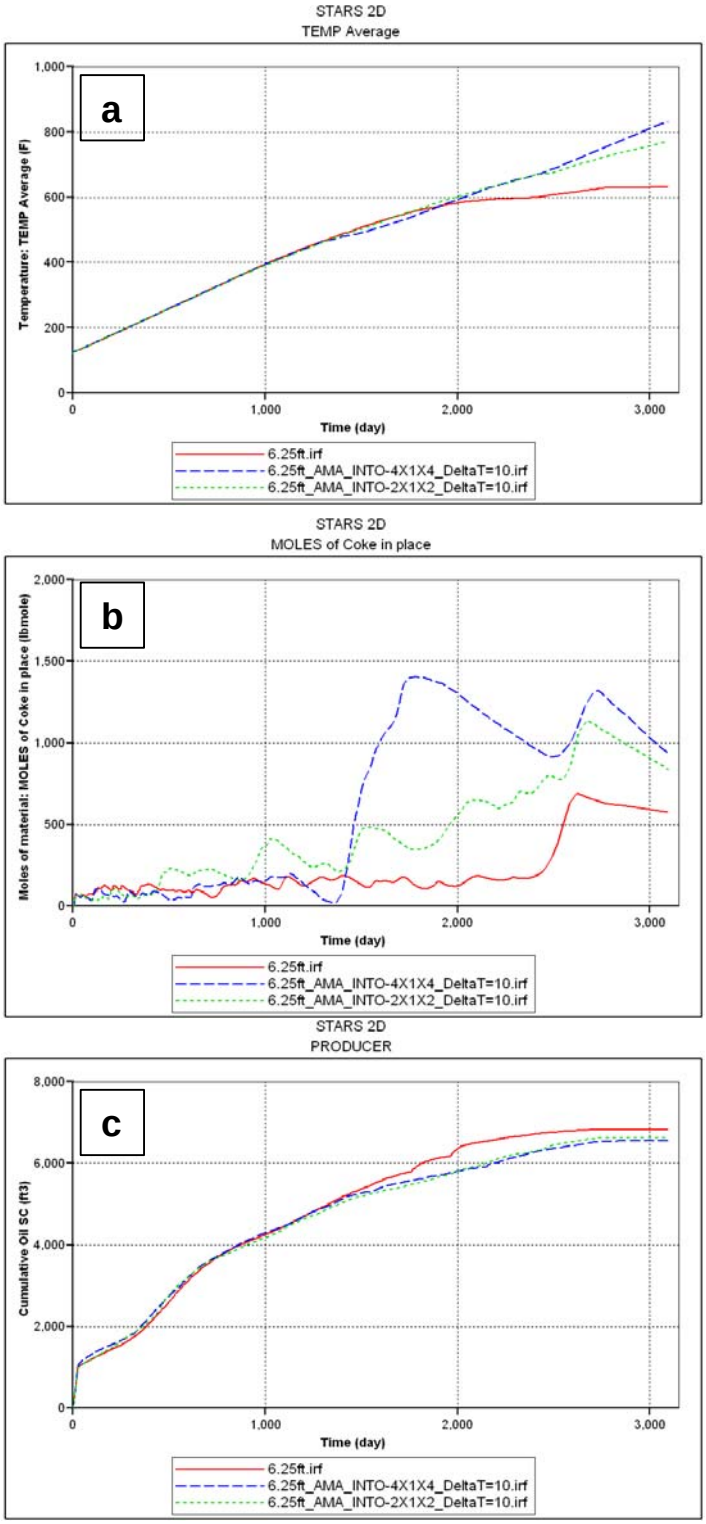

Figure 3.30: *Simulation results for variation in the amalgamation ratio of the 2D cross sectional models: (a) average temperature (b) net coke in place, and (c) cumulative oil produced.*

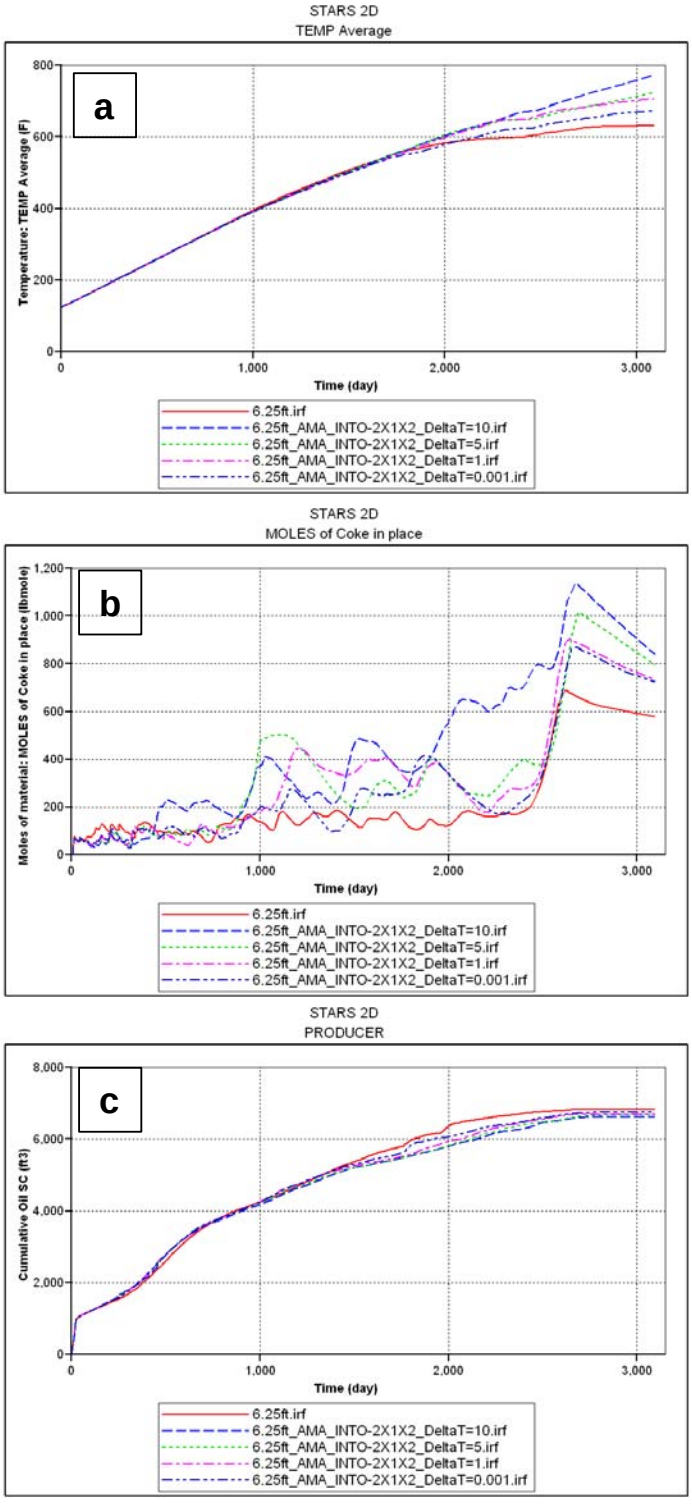

Figure 3.31: *Simulation results for variation in the amalgamation temperature threshold of the 2D cross sectional models: (a) average temperature (b) net coke in place, and (c) cumulative oil produced.*

3.5.5 Model enlargement and definition of the Base Case model

The developed 2D cross sectional model with amalgamated gridding was enlarged to represent a pilot scale model size. The enlargement was essential to enable a more representative view of in-situ combustion recovery mechanisms. The model enlargement was achieved by increasing the model x dimension from 100ft to 325ft. In order to have accurate in-situ combustion modelling results, similar grid resolutions was used in this larger model (6.25ftX3.3ftX6.25ft) as was used in the smaller model. This resulted in the number of grid blocks being increased from 256 (16X1X16) to 832 (52X1X16), which led to a dramatic increase in the model run time. The large oil volume in the new large 2D model required an increase in the air injection rate to allow the fire front to initiate and be sustained. An air injection rate of 7,200ft^3/day for the first 240 days was used, and after that it was increased to 14,400ft^3/day. These rates were determined from sensitivity analysis of the optimum air injection rate for the enlarged model. Use of the lower injection rate at the beginning avoided pressurisation of the system in the initial stages of the fire front development, but after 240 days the fire front was well established, and any further increase in air injection rate could increase burning and enhanced the process without overpressurising the system.

As the number of grid blocks increased in the large model, the amalgamation ratio of 2 made the model take a long time to run. To overcome this problem, the amalgamation ratio was changed to 4, which resulted in shorter computing time without causing major variations in the results. The temperature threshold was kept as 5°C (9°F) (the same value as in the small 2D cross sectional model). Figure 3.32 shows both the small 2D cross sectional model and the enlarged one. This large 2D model was considered to be the Base Case (BC) model to represent a pilot scale of in-situ combustion process using some of the Nimr field properties (the BC data file was presented in Appendix B3). It will be used in the remainder of this study for further evaluation of the combustion process. For the purpose of this research, the simulation model was run for 3095 days (over 8 years). This long run time helped to evaluate the process and identify how long the combustion front could be sustained. Also, it was used to show the ultimate expected recovery factor of such a homogenous combustion model. Figure 3.33 shows some of the 2D BC model results: (a) average temperature profile, (b) average oil saturation and viscosity, and (c) the cumulative oil produced. The temperature profile

shows a steady increase from the start of the process. This indicated a successful initiation and propagation of the front. Both the average oil saturation and viscosity showed how the increase of temperature led to a rapid reduction in oil viscosity, which enhanced the oil mobility and resulted in a dramatic reduction in the average oil saturation. The recovery factor calculated from this homogenous BC model was 80.1%.

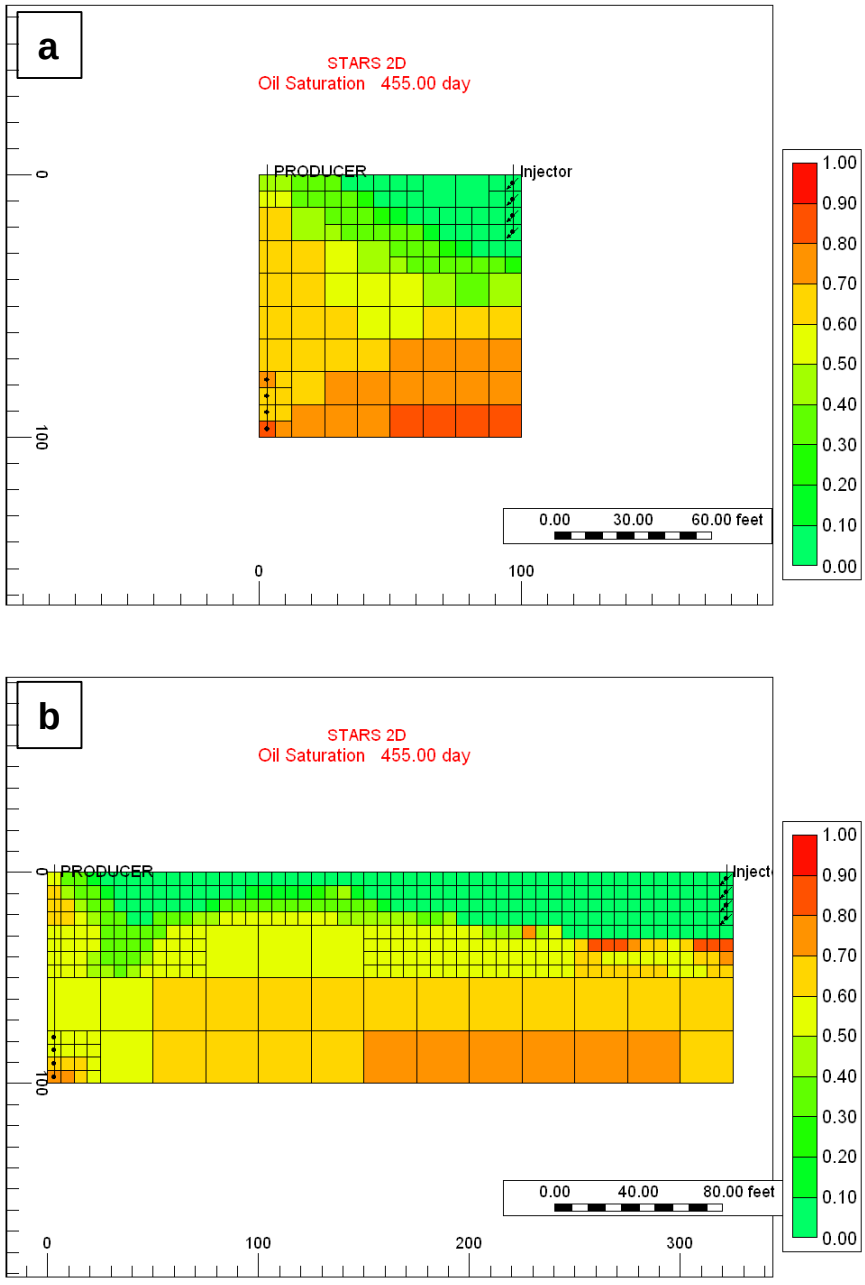

Figure 3.32: *2D cross sectional model enlargement: (a) small model, and (b) large model.*

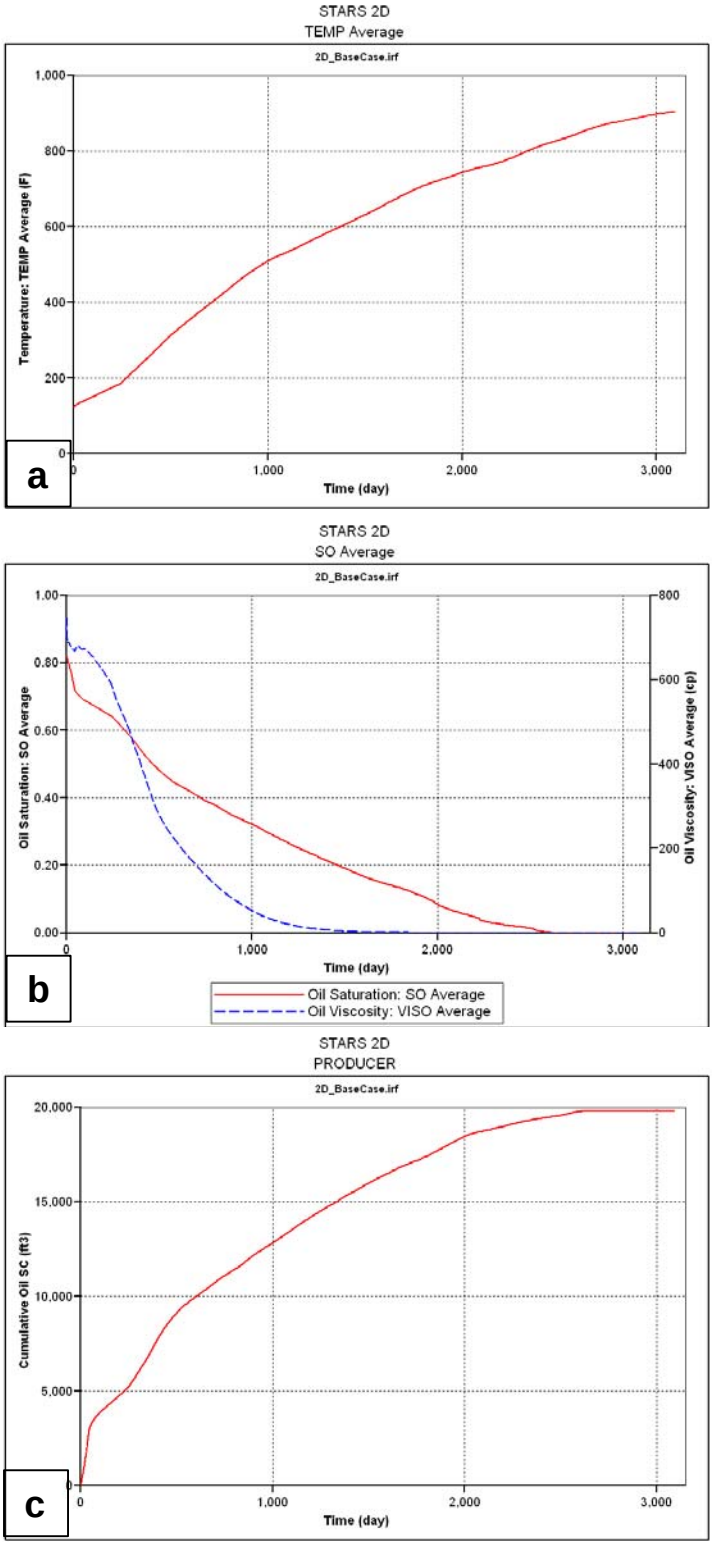

Figure 3.33: *Simulation results for the 2D Base case model: (a) average temperature (b) average oil saturation and viscosity, and (c) cumulative oil produced. [The time is presented in days and the results are plotted for the total simulation duration of 3095 days in this figure and the subsequent figures].*

3.6 Summary

In this chapter, various topics were discussed and evaluated, starting with the main challenges faced in numerical modelling of EOR methods generally, and in-situ combustion specifically. An overview of the Nimr field and its properties was provided. After that, the simulation model development for the in-situ combustion process from 1D to 2D was presented. This showed the need to use both the field properties and the data available in the literature for modelling the process. Moreover, the main simulation parameters were determined and optimised in the simulation model to be able to initiate the fire front and to allow it to be sustained and propagate to sweep the entire model. The air injection rate found to be the critical parameter in such a delicate and sensitive simulation process.

Numerical dispersion effects were investigated in both 1D and 2D models, and the way that increasing grid resolution can reduce this effect was explored. However, it came at a price, which was the increase in computing time. In order to achieve this study's objectives and to cope with the limitation of the available resources, 2D cross sectional models were chosen, in order to allow for more sensitivity analyses to be conducted using the available computer resources. Furthermore, the use of the dynamic gridding option in the in-situ combustion process simulation helped to provide as reliable results as the fine grid models, but with much reduced computing time. As a result, model enlargement to represent an actual pilot size system was able to be achieved using dynamic gridding. Consequently, a BC model was defined to be used in the remainder of this study, in the main results chapters (4, 5, and 6).

Chapter 4

Simulation of In-Situ Combustion with Diverse Well Configurations

4.1 Introduction

Application of various well configurations and their effect on the performance of in-situ combustion was investigated in this chapter. The BC simulation model which was developed throughout chapter 3 was used here as a starting point for this chapter (Table 4.1 provides a summary of the model's well controls throughout chapter 4). Most of the studies in the literature which dealt with well configuration evaluation for thermal EOR methods concentrate on steam flooding. The effect of well configuration in the sweep efficiency during in-situ combustion is one of the most important process parameters, but has not been extensively evaluated and is least well understood. Most investigations were conducted experimentally through the use of combustion tubes which used a vertical well arrangement and which cannot provide information on the sweep efficiency because of their 1D geometry. Another experimental approach which can evaluate the process from a well configuration point of view was the 3D physical scale model experiment (Coates et al., 1995; Bagci et al., 2000; Greaves et al., 2000; Xia et al., 2002). In this experiment some of the well configurations have been investigated and the results were used to predict the process performance in the field and also to validate simulator models. However, the result outcomes from those small scale experiments did not give the overall performance of the process and they were limited to the number of well configurations to be used and could be considered costly and time consuming. The use of simulation models can provide much valuable insight into the process and to show the stability of the combustion front when applying different well configurations. Hence, in this chapter the aim was to evaluate in-situ combustion performance using the 2D pilot size BC cross sectional model of the Nimr field under

the implementation of different well configurations. The simulations enabled a more general evaluation and investigation of the effect of well locations; well types, well completions, numbers of wells and well spacing distance on the behaviour of in-situ combustion. To achieve that, over 40 sensitivity runs were presented in this chapter and they were categorised into 10 groups to make it easier to compare and present. Each group will be presented as a main section in this chapter with all the observations and results. The main criteria used to choose the best performing model for each group respectively were: the recovery factor, time required to achieve the recovery factor, oxygen break through and the final average oil saturation value. These four criteria were chosen to represent the main factor which could be used to evaluate the economic feasibility of the in-situ combustion process. Also, the use of oxygen break through was because of its important effect on the process performance, as the results will show. In each section, the results and the observations were presented using both tables and figures to show the variations of the results and to highlight the important outcomes of the combustion process.

Injector well	Air injection rate of 7,200ft^3/day for the first 240 days and 14,400 ft^3/day thereafter
Producer well	Bottom hole pressure of 500psi
Simulation duration	3095 days

Table 4.1: *Summary of the model's well controls (no pressure limit on injector well)*

4.2 Horizontal producer application in in-situ combustion.

The BC model used had two wells, a vertical injector which was completed in the top 25ft of the model and a vertical producer which was completed in the bottom 25 ft of the model. The total horizontal distance between the two wells was 312.5 ft (Figure 4.1a). The BC model dimensions were 325ft in the x, 3.3ft in the y, and 100ft in the z directions. The implementation of horizontal wells offers the prospect of better performance over vertical wells. This improved performance was due to the longer

contact area between the model and the well. More details about the use of horizontal wells were presented previously in Chapter 1.

The 2D BC model vertical producer was replaced by a horizontal producer at the bottom of the model, and it was perforated over the entire model length (Figure 4.1b). All the BC model properties were kept the same in the new model to be consistent in the comparison between the results throughout this chapter. From the first results comparison between the two models (BC vs. VI_Edge-HP_100Perecent-perf), the combustion process performance and the recovery factor (74.9%) of the new model were lower. The main reason for this low performance was the inappropriate location of the vertical injector at the edge, which led to the limitation in terms of making the most of the horizontal producer, as well as the early oxygen break through as a result of the shorter distance between the two wells. As a result, the vertical injector was moved from the edge to the centre of the model (Figure 4.1c), the new model was called (VI_Center-HP_100Perecent-perf). The changing of injector location helped to optimise and maximise horizontal producer performance.

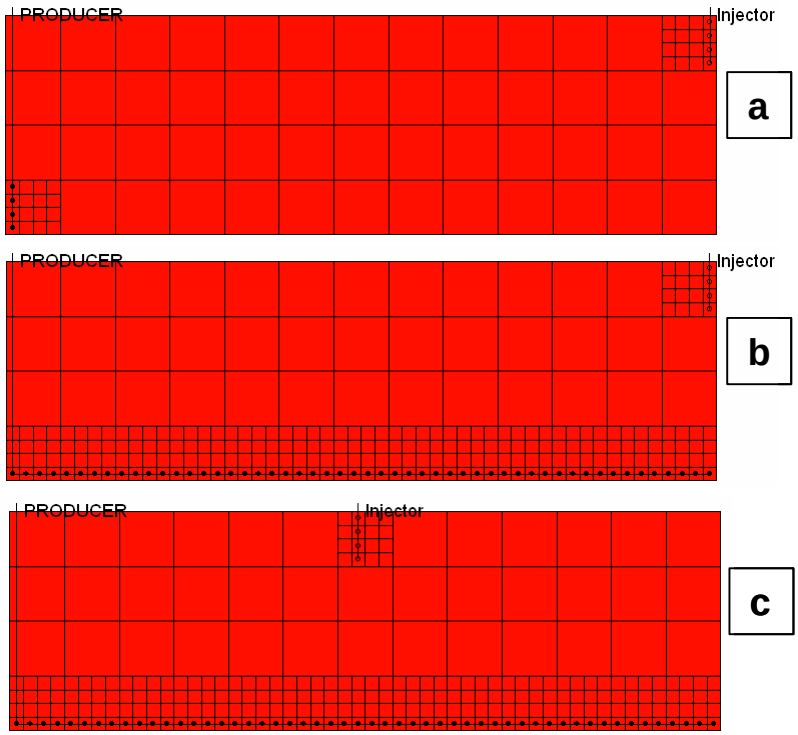

Figure 4.1: *Well configurations: (a) Base case model, (b) VI_Edge-HP_100Perecent-perf, and (c) VI_Center-HP_100Perecent-perf*

Gas override effect was reduced when the horizontal producer was used and located at the model bottom, as Figure 4.2b and Figure 4.2c shows, when compared to the BC model (Figure 4.2a). In the horizontal producer models, when the fire front was initiated, the system experiences two different driving forces: gravity segregation of gases (gas override effect), and lower pressure gradient change near the bottom of the model (horizontal producer), which was the dominate force in this model and controlled the front propagation and produced a piston like displacement. Furthermore, oxygen break through to the horizontal producer occurred earlier compared to the BC model (Figure 4.3a).This was as a result of the shorter distance between the vertical injector and the nearest horizontal well perforation. When oxygen break through occurred too early in the in-situ combustion process, the oxygen utilization ratio was decreased and the oxygen started to circulate from the injector to the producer and bypasses the fire front, which reduced the combustion front velocity. This resulted in more air being required and a longer time was required to sweep the model. On the other hand, if oxygen break through occurred too late, this also reduced the fire front propagation velocity as a result of the huge amount of oil banking ahead of the front before it broke through to the producer well, as in the BC model. In order to improve the performance of the in-situ combustion process, it was very important to optimise and control the oxygen break through timing by selecting the appropriate well configurations and the implementation of appropriately designed well completions.

The temperature profile of the BC model was higher than average temperature of the models with a horizontal producer (Figure 4.3b). This was because the amount of coke produced in the BC was dramatically more than the amount of coke in the horizontal producer models (Figure 4.3c). This means that more fuel was available for the combustion front to consume and resulted in higher temperature. Having a lower temperature profile in the in-situ combustion process can help to reduce the risk of damaging downhole equipment in both wells, as long as it does not affecting the overall process performance. The lower amount of coke produced in the horizontal producer model was as a result of two main factors. The first reason was the introduction of the mobile oil zone (MOZ) which allowed the reduced viscosity mobile oil to be produced instantaneously under the effect of gravity drainage. Figure 4.4 shows an illustration of the mobilized oil in the vertical injector and horizontal producer well configurations. In

the BC model the mobile oil flowed ahead of the front, and as time progress the oil accumulated and formed banks which reduced the fire front propagation before it could be produced. Whereas, in the case of the horizontal producer, the MOZ allowed for the production of the oil and helped to reduce the resistance facing the fire front while it propagated to sweep the entire model (Figure 4.3b and Figure 4.3c). Another advantage of having the MOZ was it helped to preserve the upgraded oil as a result of the thermal cracking due to the combustion process by producing it immediately. This will help to enhance the economics of the project by having a portion of the produced oil with higher API gravity. The second reason for the lower mass of coke produced in the horizontal well models was that the use of a *horizontal* producer removed the oil without the creation of any extensive mobile flow path in the colder oil region, whereas, because of the flow geometry, a greater volume should be burned to create a flow path between a *vertical* injector and producer (in the BC model) within which the oil could flow.

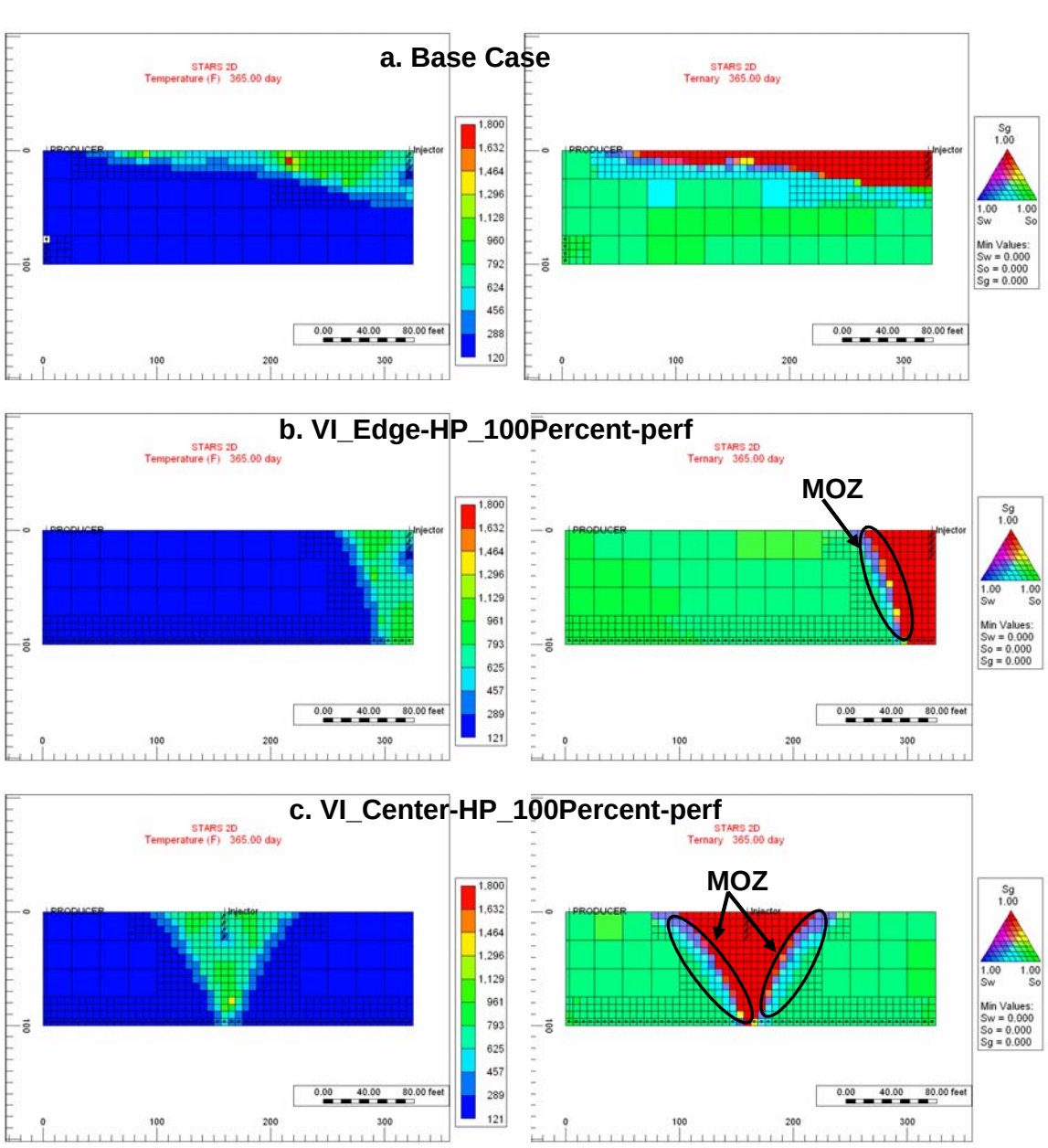

Figure 4.2: *Simulation results showing both temperature and saturations by ternary plots at 365days: (a) base case model, (b) VI_Edge-HP_100Perecent-perf, and (c) VI_Center-HP_100Perecent-perf*

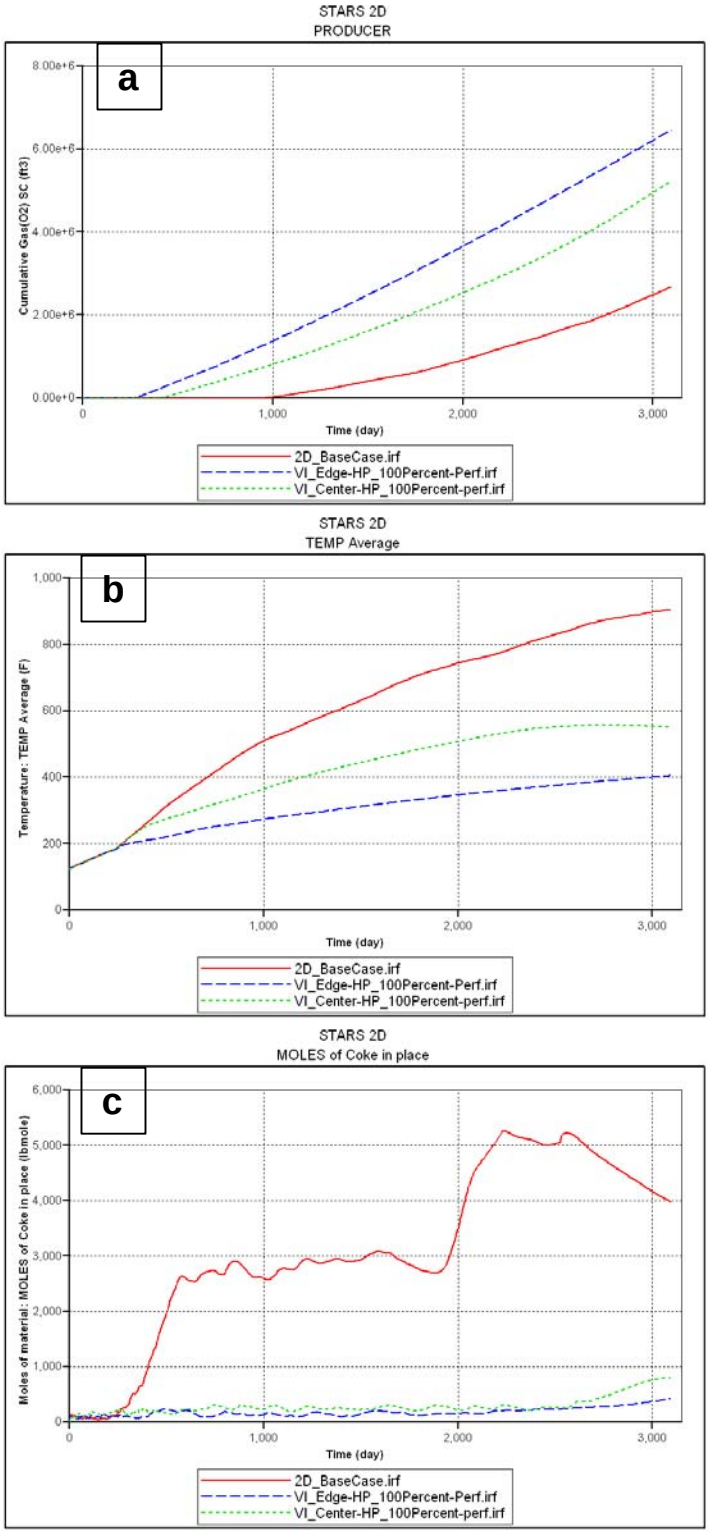

Figure 4.3: *Simulation results of application of horizontal producer: (a) cumulative oxygen produced, (b) average temperature, and (c) net coke in place.*

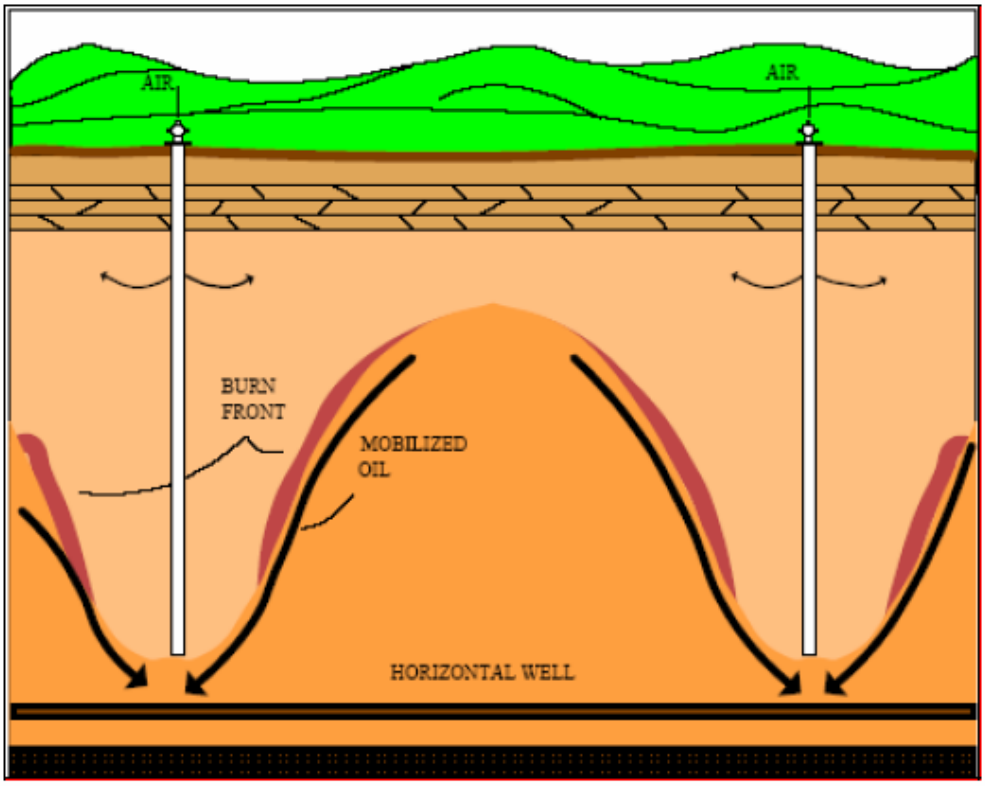

Figure 4.4: *Mobile oil zone in in-situ combustion process (from Coates et al., 2004)*

The cumulative oil produced by the vertical injector on the edge of the model with the horizontal producer (VI_Edge-HP_100Perecent-perf), was lower than the BC model (Figure 4.5). The reason for that, as already mentioned, was the early oxygen break through to the producer which reduced the performance of the combustion process by increasing the required time to sweep the entire model. However, when we change the vertical injector well to the middle of the model (VI_Center-HP_100Perecent-perf), the oxygen break through was delayed, and the initial fire front split into two fire fronts, each with a MOZ (Figure 4.2c). The way these two fronts propagated results in more cumulative oil being produced for this model compared to the other two models. Table 4.2 summarises the main simulation results of the three models. The (VI_Center-HP_100Perecent-perf) model has 91.6% as a recovery factor (obtained using the spreadsheet developed in Chapter 3), which was a very high value when compared to actual field cases. This high recovery value could be used only as an *indictor* of how the process was affected when utilizing the horizontal well for such homogenous cases. The BC model took less time to be fully swept (2611 days) compared to the other models due to the delayed oxygen break through in this model.

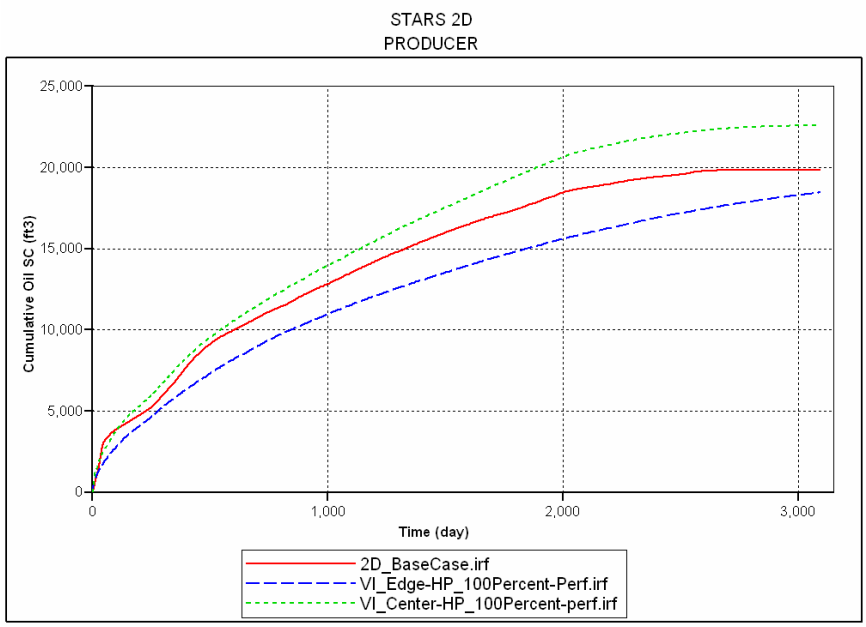

Figure 4.5: *Cumulative oil produced using a horizontal producer compared to a vertical producer*

Model name	Recovery factor (%)	Time to achieve this recovery factor (days)	Oxygen break through (days)	Final average oil saturation (fraction)
Base case	80.1	2611	885	0
VI_Edge-HP_100Perecent-perf	74.9	3095	260	0.16
VI_Center-HP_100Perecent-perf	91.6	3095	362	0

Table 4.2: *Simulation results of horizontal well application for in-situ combustion*

4.3 Impact of horizontal producer location and length

Application of a horizontal well for the in-situ combustion process led to a better efficiency when compared to the use of a vertical producer well in the previous section. The primary aim in this section was to investigate the effect of the horizontal section length of the horizontal producer in the combustion process and to determine the

optimum length for the current model. The horizontal producer length in the (VI_Center-HP_100Perecent-perf) model was 100% of the model length, which was 325ft. Two further simulation runs were conducted in this sensitivity category, in the first model the horizontal producer length was 50% (162.5ft) of the original horizontal producer length, and the horizontal well length in the second model was 25% (81.25ft). However, before evaluating the effect of the horizontal producer, the producer location needed to be investigated, in order to optimise the performance of the combustion process.

4.3.1 Horizontal producer location

In this sensitivity, two models were developed, both having a vertical injector in the middle of the model and a 162.5ft (50%) length horizontal producer completed in the bottom model layer. In the first model (VI_Center-HP_50Perecent-perf), the middle of the horizontal producer was placed directly under the vertical injector (Figure 4.6a), whereas in the second model (VI_Center-HP_50Perecent-perf_Offset) the middle of the horizontal well was offset by 81.25ft from the vertical injector (Figure 4.6b).

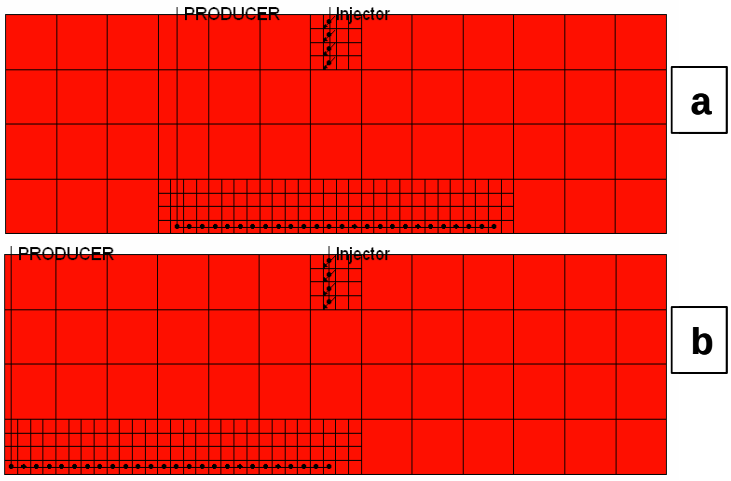

Figure 4.6: *Well configurations: (a) VI_Center-HP_50Perecent-perf, and (b) VI_Center-HP_50Perecent-perf_Offset*

Figure 4.7a and Figure 4.7b show both the temperature profile and the ternary saturation plot at 290 days for both model runs. When comparing both models, the temperature profile distribution of the offset model was non-symmetric. This was because of the way

the horizontal producer was placed in the offset model. Also, the amount of net coke in place was large in the offset model (Figure 4.8a), hence the higher average temperature profile (Figure 4.8b). The cumulative oil produced by the centred horizontal producer model was more by 7% compared to the offset model (Figure 4.8c). As a result, for the horizontal well length sensitivity it was preferable to locate the horizontal producer well in the middle of the model while having the vertical injector in the centre.

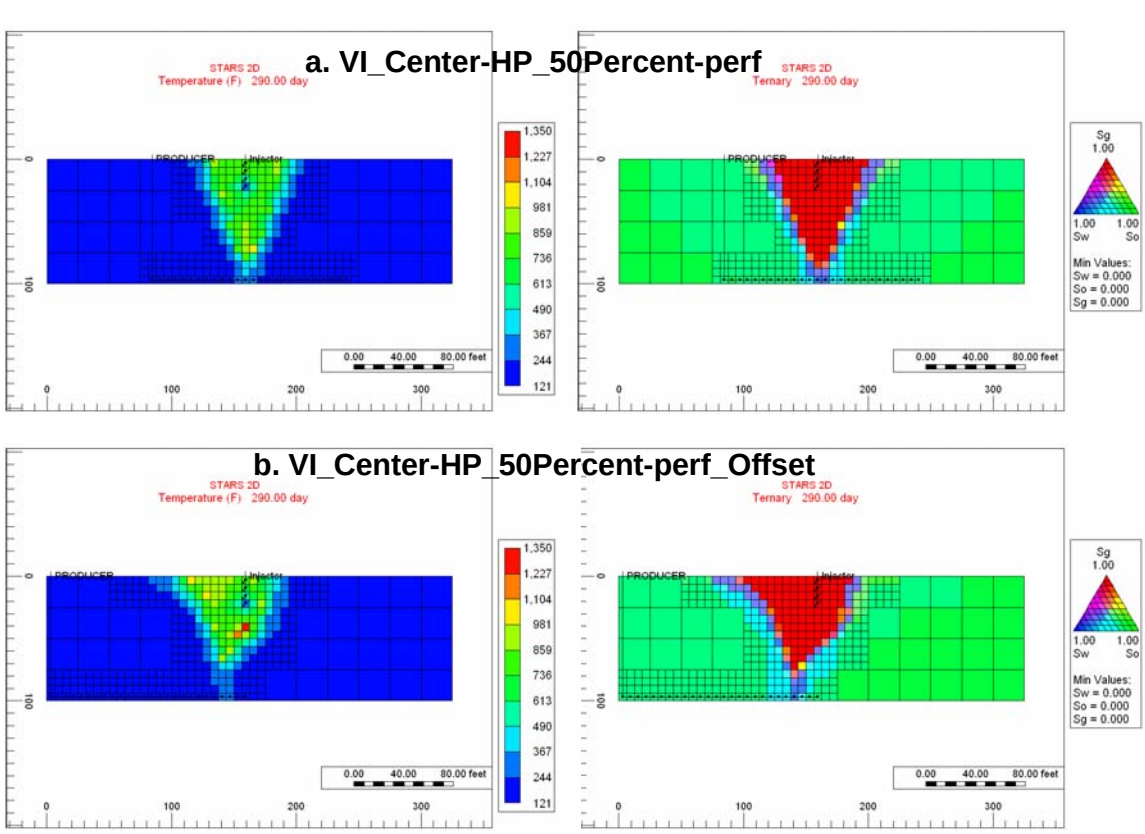

Figure 4.7: *Simulation results of both temperature and ternary saturation plot at 290 days: (a) VI_Center-HP_50Perecent-perf, and (c) VI_Center-HP_50Perecent-perf_Offset. Note the non symmetry in the front temperature profile for the offset horizontal producer scenario (b).*

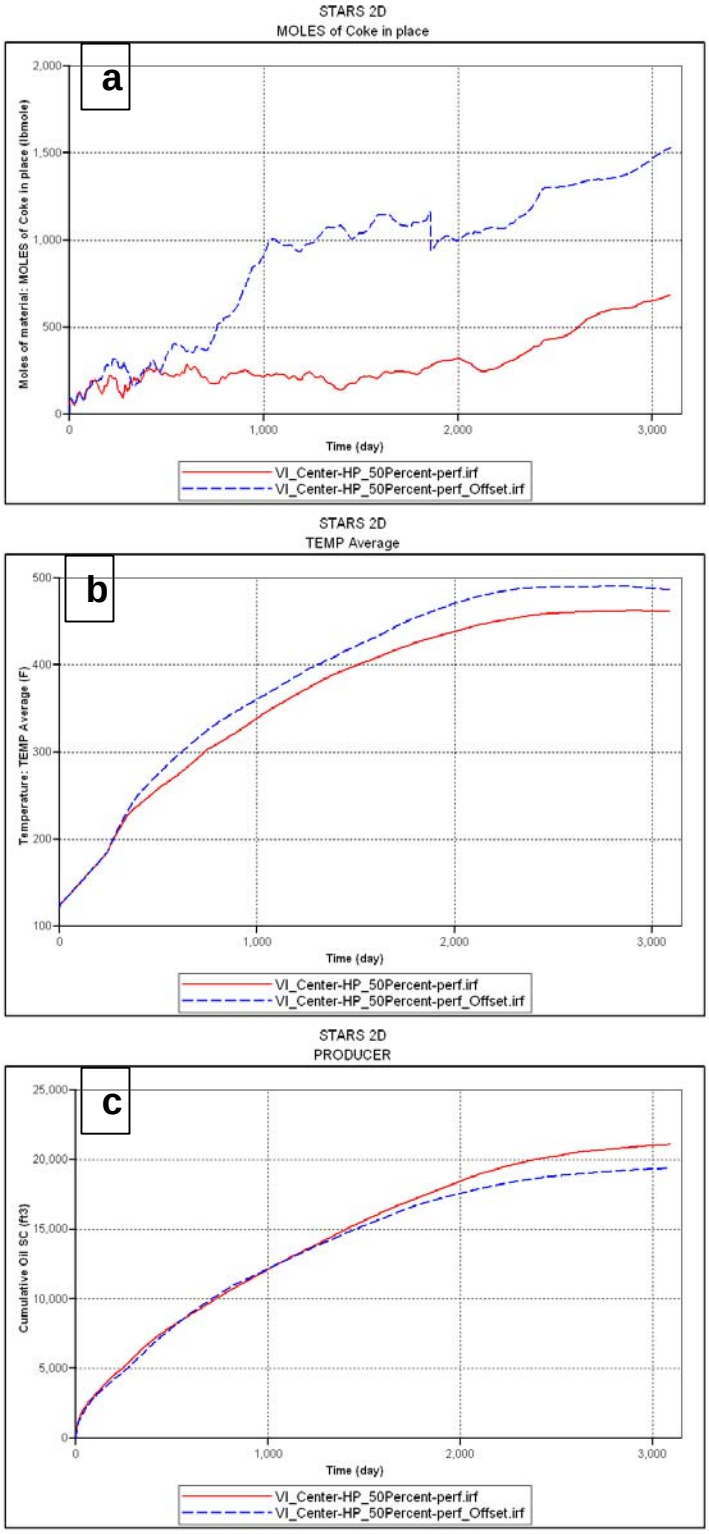

Figure 4.8: *Simulation results of horizontal producer placement: (a) net coke in place, (b) average temperature, and (c) cumulative oil produced.*

4.3.2 Effect of length of the horizontal producer well

The three models used in the horizontal length sensitivity were shown in Figure 4.9. The temperature distribution for the three models (Figure 4.10) at 200 days shows the fire front advancement profile. In the 25% horizontal producer well model, oxygen break through occurred earlier than was the case in the two other models. This was as a result of the intensive pressure depletion per each perforation of this short horizontal producer compared to the longer wells. This dominate depletion force enhanced the fire front propagation vertically (Figure 4.10c) faster than its lateral movement until the oxygen break through occurred and all the fuel near the producer was consumed. After that, the fire front started to move laterally but very slowly since it was moving away from the producer well (against the pressure depletion force). As a result of this resistance the front velocity was reduced and this allowed more time for the oil ahead of the front to be converted to coke, which explained the higher amount of coke for this model, especially the increase that stars at around 1250 days (Figure 4.11a).

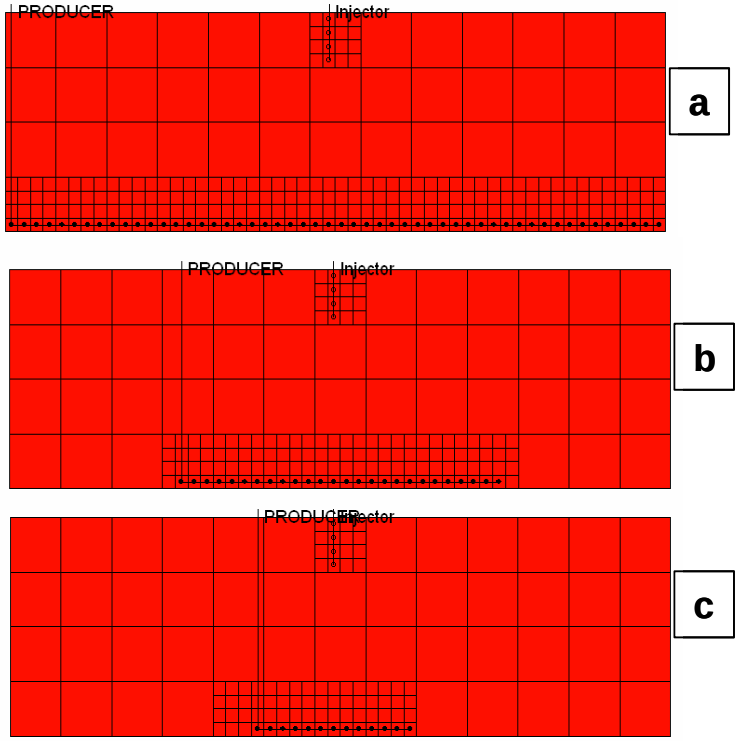

Figure 4.9: *Well configurations: (a) VI_Center-HP_100Perecent-perf, (b) VI_Center-HP_50Perecent-perf, and (c) VI_Center-HP_25Perecent-perf*

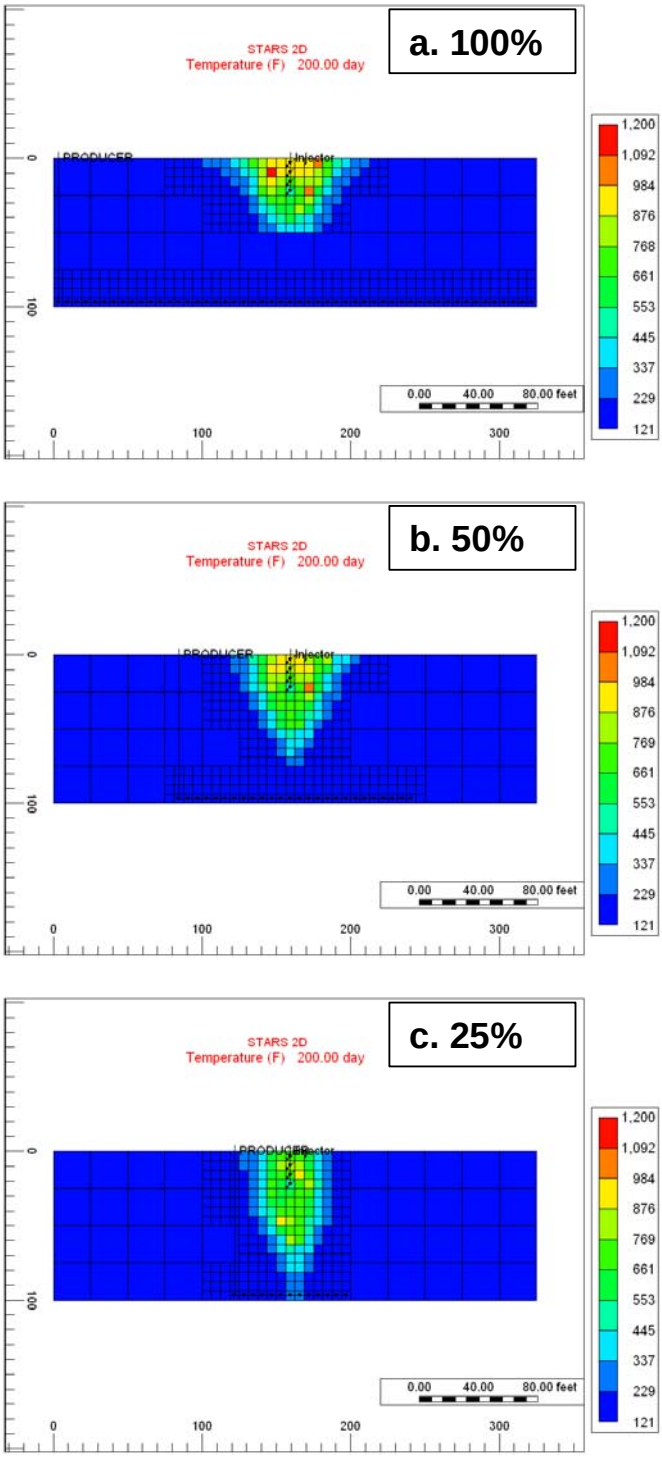

Figure 4.10: *Simulation results of temperature at 200 days: (a) VI_Center-HP_100Perecent-perf, (b) VI_Center-HP_50Perecent-perf, and (c) VI_Center-HP_25Perecent-perf*

From the sensitivities in the previous section, usually the model which produced more coke in place was expected to have a higher average temperature profile. This was not

the case in this sensitivity, since the 25% horizontal well length model had a low average temperature profile (Figure 4.11b), even with its large amount of coke produced (Figure 4.11a). This was because there was not enough air (oxygen) available to feed the fire front to be able to consume the coke and increase the temperature. The main reason for the shortage of air supply was that the air tended to flow through the path of least resistance, which was directly from the injector well to the producer well, and kept circulating without being able to divert and support the fire front, which started to move laterally away from the producer well. This meant that for this model, in order for the fire front to be able to sweep the entire model area, a much large amount of air was required, and the model needed to be run for a longer time. The model with the 100% completed horizontal well produced more oil as a result of the better sweep efficiency and the large contact area between the formation and the well. Figure 4.12 shows the temperature profile of all the three models at the final time step (3095 days), and it was clear that the longer horizontal producer was able to direct the fire front to every corner of the model and almost recover all the oil. On the other hand, in the shorter horizontal well models, some of the bottom formation zones have not efficiently been swept and this was one of the reasons which caused less oil to be produced from those models (Figure 4.11c). Table 4.3 summarises the main simulation outcome results of this section. The highest recovery factor (91.6%) was achieved by using the longer (100%) horizontal producer. However, the recovery factor of the 50% horizontal producer length was only 6% less than the long horizontal producer model result. In a field case, the decision which horizontal section length to use can be made by comparing the cost of drilling and completing an extra 50% of the well length and the gained profit from the extra 6% recovery factor achieved by the longer well. The option chosen will be determined by economics.

Model name	Recovery factor (%)	Time to achieve this recovery factor (days)	Oxygen break through (days)	Final average oil saturation (fraction)
VI_Center-HP_100Perecent-perf	91.6	3095	362	0
VI_Center-HP_50Perecent-perf	85.6	3095	343	0.06
VI_Center-HP_25Perecent-perf	78.0	3095	319	0.1
VI_Center-HP_50Perecent-perf_ Offset	78.6	3095	394	0.08

Table 4.3: *Simulation results of horizontal producer length effect in in-situ combustion*

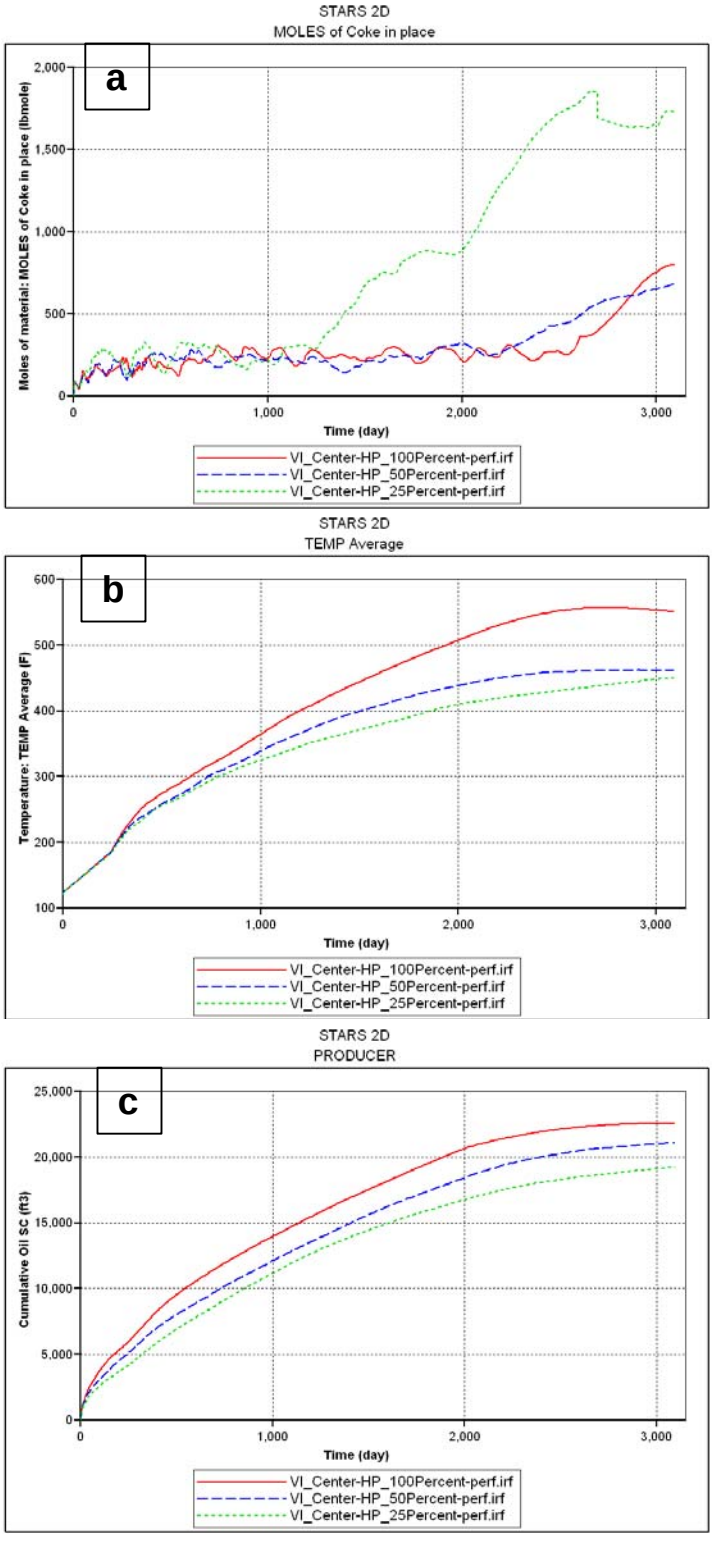

Figure 4.11: *Simulation results of horizontal producer length: (a) net coke in place, (b) cumulative oil produced, and (c) average temperature*

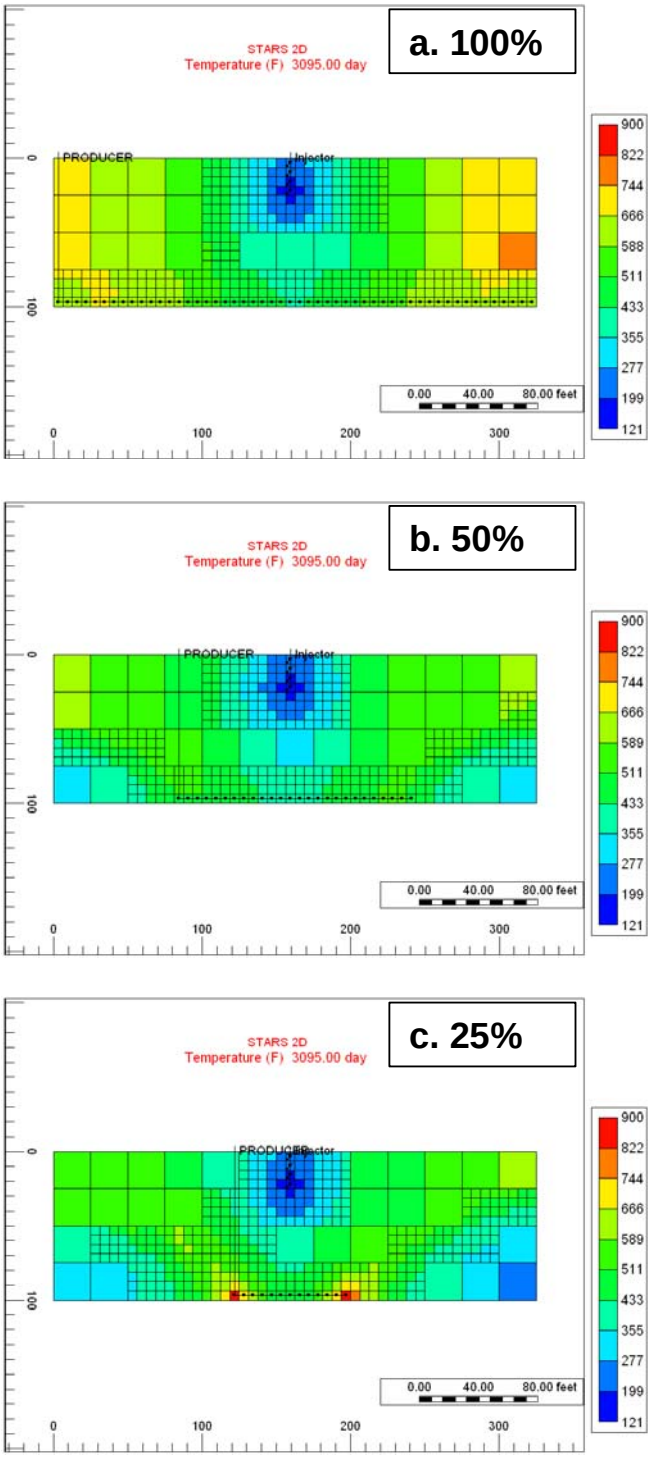

Figure 4.12: *Simulation results of temperature at 3095 days: (a) VI_Center-HP_100Perecent-perf, (b) VI_Center-HP_50Perecent-perf, and (c) VI_Center-HP_25Perecent-perf*

4.4 The effect of vertical distance between the vertical injector and horizontal producers of varying lengths

4.4.1 Vertical distance between vertical injector and horizontal producer

Well placement plays an important rule in the development of any reservoir. Depending on the development plan, wells are usually located to maximise the recovery factor from the formation. For in-situ combustion, both the lateral and vertical spacing between wells are critical to sustain the fire front and to efficiently sweep the formation volume. In this section, the vertical distance between a vertical injection well and a horizontal producer was investigated, and its effect on the in-situ combustion process was discussed. Firstly, the 100% horizontal producer length model was used, where the well was completed at the model bottom, 75ft below the vertical injector's lowest perforation (Figure 4.13a). Two other models were developed with distance of 50ft and 25ft between both wells (Figure 4.13b and c). From the simulation results, the first thing to notice was that the fire front was developed near the vertical injector and then moved downward to approach the horizontal producer. After that, it reached the producer, and then it moved laterally along both sides of the horizontal producer until it reached the model boundaries. The oxygen break through occurred earlier in the 25ft spacing model because of the short distance between the wells. An important observation was that in both the 50ft and 25ft models the horizontal producer acted like a barrier which prevented the front from propagating to the other end (the bottom) of the model (Figure 4.14). Moreover, the slight increased in temperature in the area below the horizontal producer could be as a result of the heat conduction from the area above the producer (Figure 4.14b and c), since most of the heated fluid was produced instantaneously. The result of this was that the oil saturation was almost unchanged in that area (Figure 4.14b and c). Thus placing a horizontal producer near the vertical injector results in poor areal sweep of the formation. Figure 4.15a shows the average temperature profile of the three models, and it was clear that the model with the 75ft vertical spacing between the wells generates higher temperature. This was because the fire front was able to sweep the entire model and was sustained for longer period. On the other hand, the fire front in both the 50 ft and the 25ft models was quenched as soon as all the oil was recovered

from the area above the horizontal producer, and it did not have access to the oil in the area below the producer. This was reflected in the lower cumulative oil produced in these two scenarios (Figure 4.15b), as well as the high average oil saturation in both models at the end of the simulation (Figure 4.15c). For this specific case study, it was recommended to maximise the vertical spacing between both the vertical injector and the horizontal producer to ensure the fire front was sustained as long as possible, leading to a higher recovery factor and better in-situ combustion performance. Table 4.4 summarises the simulation results from the three models.

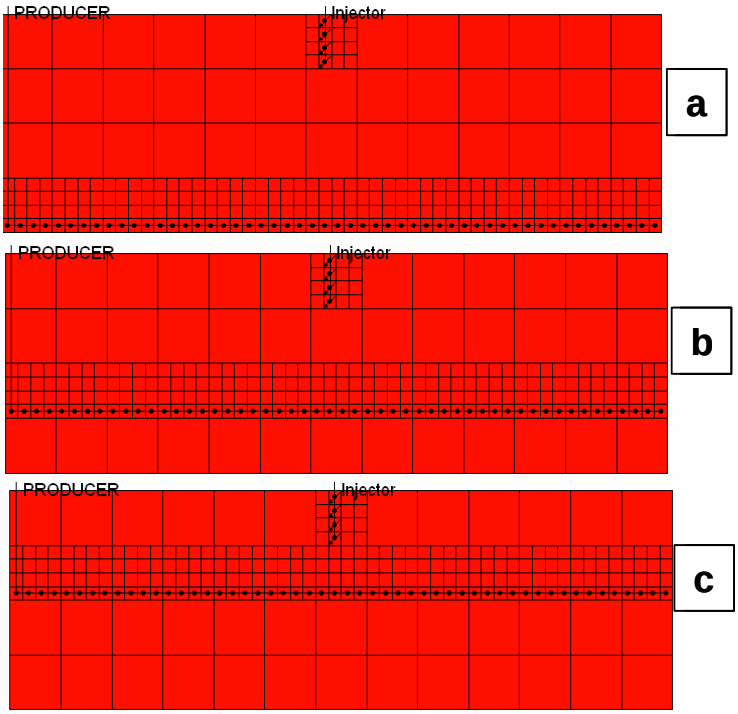

Figure 4.13: *Vertical distance between the vertical injector and the horizontal producer wells: (a) VI_HP_75ft, (b) VI_HP_50ft, and (c) VI_HP_25ft*

Model name	Recovery factor (%)	Time to achieve this recovery factor (days)	Oxygen break through (days)	Final average oil saturation (fraction)
VI_HP_75ft	91.6	3095	362	0
VI_HP_50ft	69.8	3095	260	0.19
VI_HP_25ft	42.0	3095	145	0.44

Table 4.4: *Simulation results of vertical distance between the vertical injector and the horizontal producer wells*

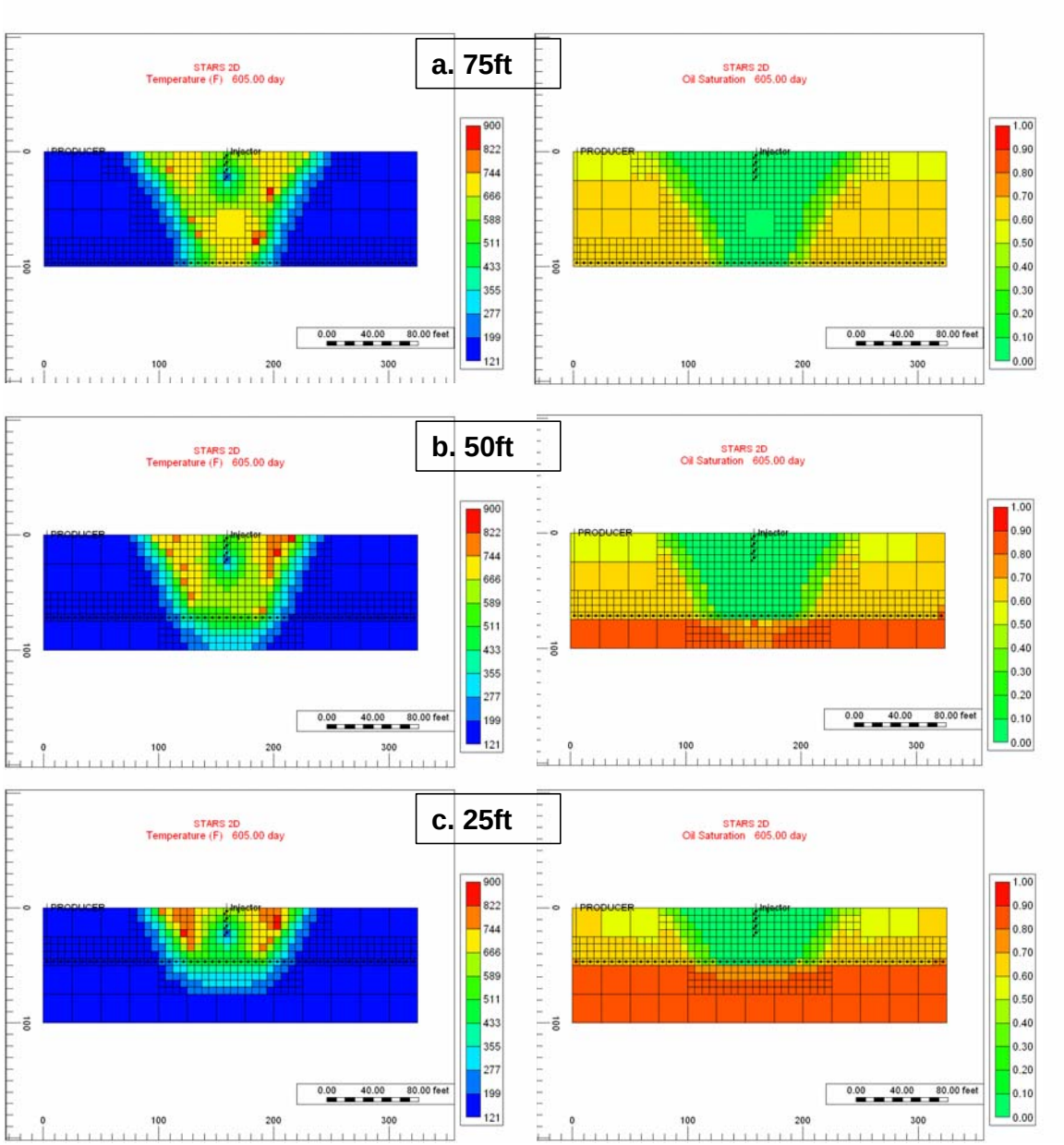

Figure 4.14: *Simulation results of temperature and oil saturation at 605 days: (a) VI_HP_75ft, (b) VI_HP_50ft, and (c) VI_HP_25ft. Note the front limitation to access the area below the horizontal producer in both cases b and c.*

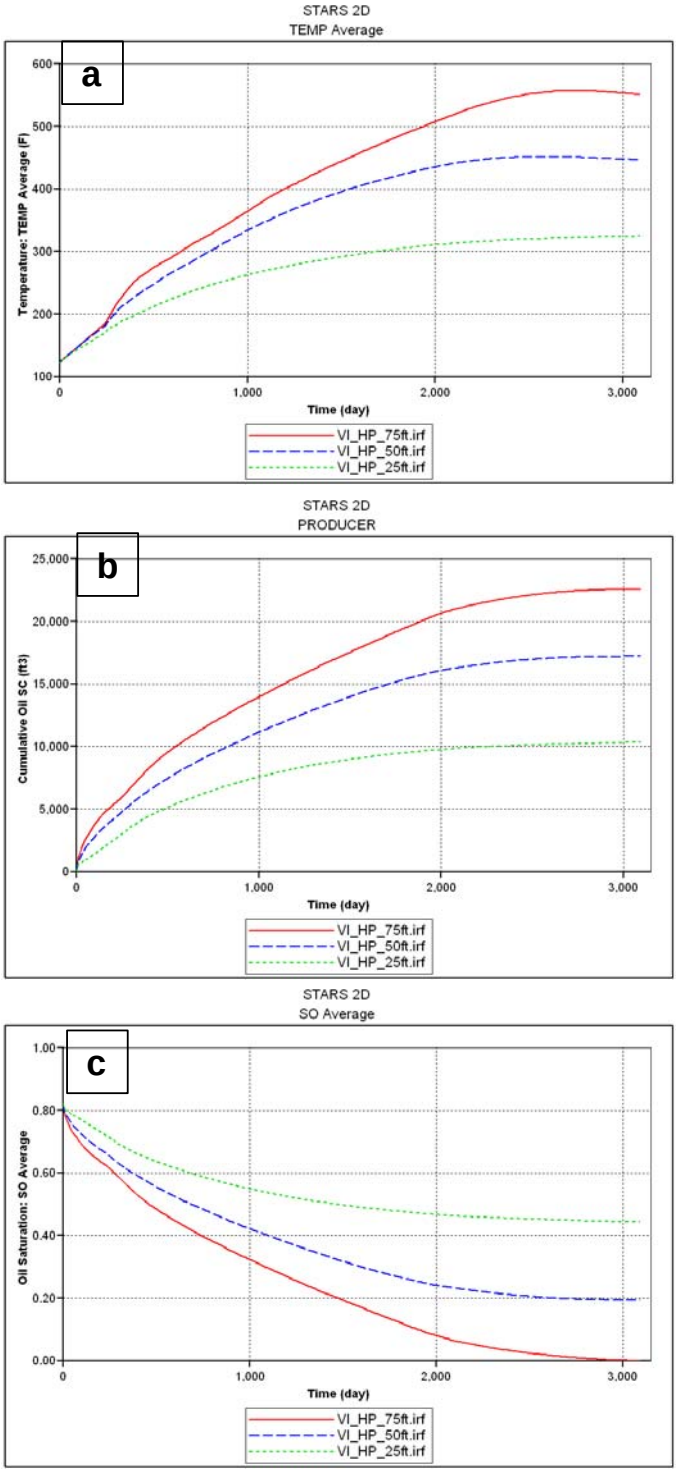

Figure 4.15: *Simulation results of vertical distance between the vertical injector and the horizontal producer wells: (a) average temperature, (b) cumulative oil produced, and (c) average oil saturation*

4.4.2 Impact of vertical distance between vertical injector and horizontal producer with 100% and 50% section lengths

The previous subsection showed the need to maximise the vertical spacing between the vertical injector and the horizontal producer in order to enhance the in-situ combustion and increase the recovery factor. In this subsection, an investigation was conducted to evaluate the possibility of the fire front being able to sweep the area below the 50% horizontal producer well length if it was placed just 25ft vertically away from the injector. The 100% horizontal producer (Figure 4.16a) produced the lowest recovery factor in the previous sensitivity because it acted as a barrier and restrained the fire front from propagating to the bottom of the model area. For the 50% horizontal producer model (Figure 4.16b) communication between the upper and lower areas was possible around the sides of the well. This *might* allow the fire front to propagate around the producer edges and recover the oil in that area and reduce the barrier effect observed in the 100% horizontal producer model.

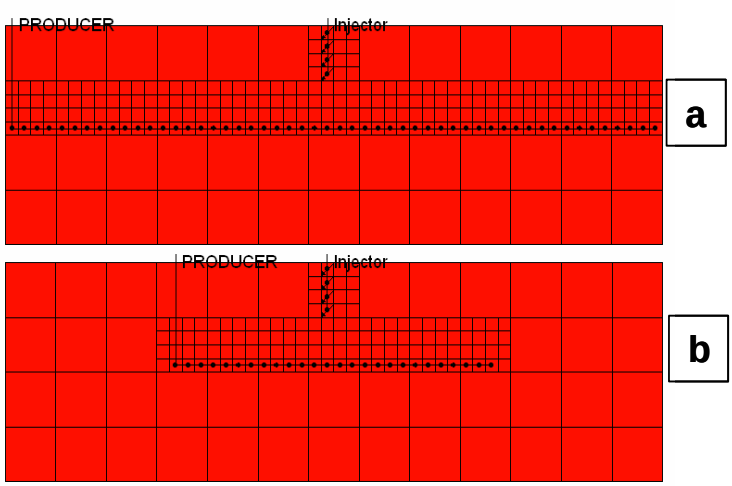

Figure 4.16: *Vertical distance effect between vertical injector and horizontal producer with 100% and 50% horizontal section lengths: (a) VI_HP-100%_25ft, and (b) VI_HP-50%_25ft*

The simulation results showed that the combustion front for the 50% horizontal producer model did not manage to recover the oil in the bottom (Figure 4.17) of the model, even though there was access to that area around both sides of the producer. The most plausible explanation for this was that the pressure depletion gradient near the

producer was dominant, and the air injected was recycled directly by the producer instead of supporting the front around the edge of the producer. This affected the fire front propagation velocity and made it impossible for the combustion front to advance and recover the oil from the bottom of the model area. This explained the high oil saturation and the low temperature profile in the lower area. This may be observed even by the last time step (3095 days), as shown the oil saturation and temperature distribution map in Figure 4.17. The average temperature profile was lower in the 50% horizontal well producer model as Figure 4.18a shows. This was mainly due to the poor frontal sweep efficiency, and as a result of the front being quenched earlier in this model due to the lack of fuel. The cumulative oil produced was higher in the 100% producer model because the longer production interval allowed recovery of more oil (Figure 4.18b), and it helped to sustain the combustion for a longer period of time, which resulted in a lower average oil saturation at the end of the calculation (Figure 4.18c).

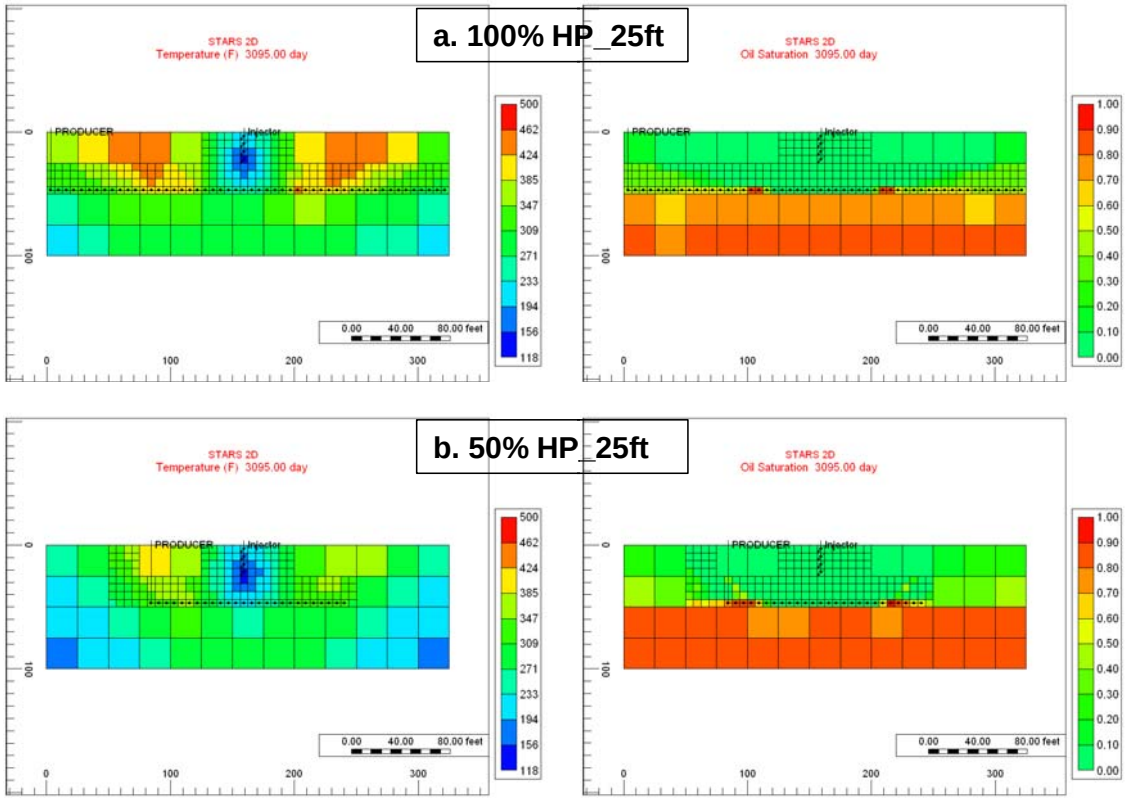

Figure 4.17: *Simulation results of temperature and oil saturation at 3095 days: (a) VI_HP-100%_25ft, and (b) VI_HP-50%_25ft. Note the largely unrecovered oil beneath the horizontal well at the end of the calculation in both cases.*

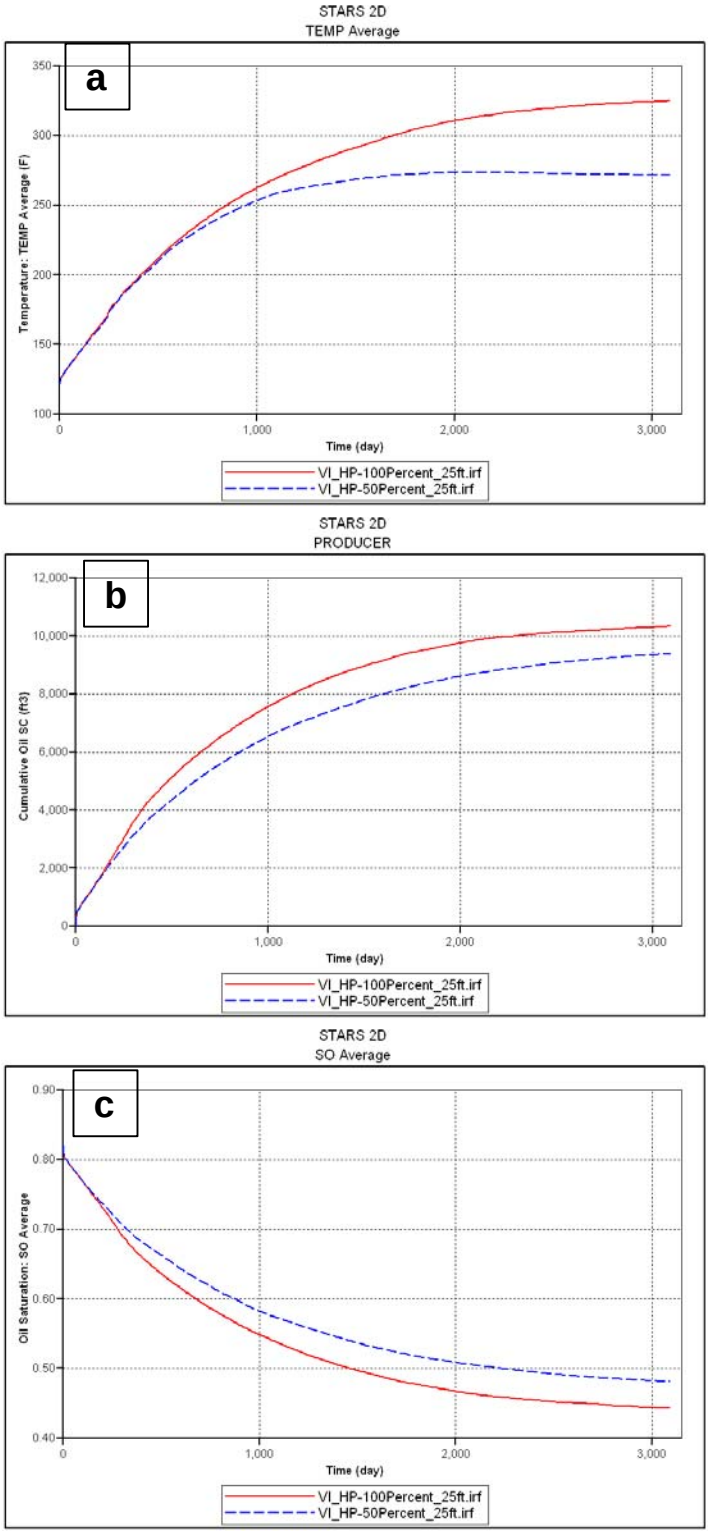

Figure 4.18: *Simulation results of vertical distance effect between vertical injector and horizontal producer with 100% and 50% horizontal section lengths: (a) average temperature, (b) cumulative oil produced, and (c) average oil saturation*

4.5 Effect of length of completion interval in vertical injector

In-situ combustion modelling was sensitive to the variation of many of the model parameters, with changes to input parameters potentially resulting in major changes in the process performance. In all the previous cases the vertical injector was completed in the top (25ft) section of the model (Figure 4.19a). The change to the perforation interval of the vertical injector will result in a change in the pattern of the fire front propagation. In order to evaluate the effect of the injector completion intervals on the overall combustion process performance, three models were developed and compared with the model with the vertical injector completed at the top. In all the models a horizontal producer was used and it was completed in the bottom layer for the entire length of the model (100%). Also, all the model parameters were kept the same in order to achieve a coherent comparison between the cases. The vertical injector in the first model was completed in the middle 4 layers (25ft) of the model (Figure 4.19b). The second model had the vertical injector completed in the bottom 25ft, and it was thus just 6.25 ft away from the horizontal producer (Figure 4.19c). Finally, in the third model the well was perforated over all the 87.5ft vertical interval (Figure 4.19d).

The temperature maps at 250 days and 1825 days for all the four models were shown in Figure 4.20. For the top perforated vertical injector model (Figure 4.20a), the front was initiated in the top layers and then it moved along the top of the model as a result of gas override, which controlled the frontal advancement, and gave it a triangular shape after 250 days. Figure 4.20b shows the initial shape of the fire front for model where the vertical injector was completed in the middle. The fire front started in the middle of the model and from the beginning it was influenced by two forces: the pressure depletion toward the producer well and the gravity segregation which caused the gas to migrate towards the upper area of the model. This results in a fire front shape that looks like a mushroom during the early stages (250 days). However, the frontal advance was changed at a later time (1825 days), when it moved to the upper area and swept the model. The front initiation and propagation for both the bottom perforated vertical injector (Figure 4.20c) and the fully perforated injector well (Figure 4.20d) was almost the same. The fire front starts in the bottom of the model with a circular shape, and then

it pushed its way to the top of the model as a result of gas override. The only difference between those two models was that the front movement in the all perforated model was slightly faster than the case of the bottom completed injector model. This was as a result of that when combustion front moved upward in the all perforated injector well model the air was supplied from the nearest perforated layer to the front unlike the bottom perforated injector case where the air needed to be injected through the bottom perforations and then travelled upward to supply the front.

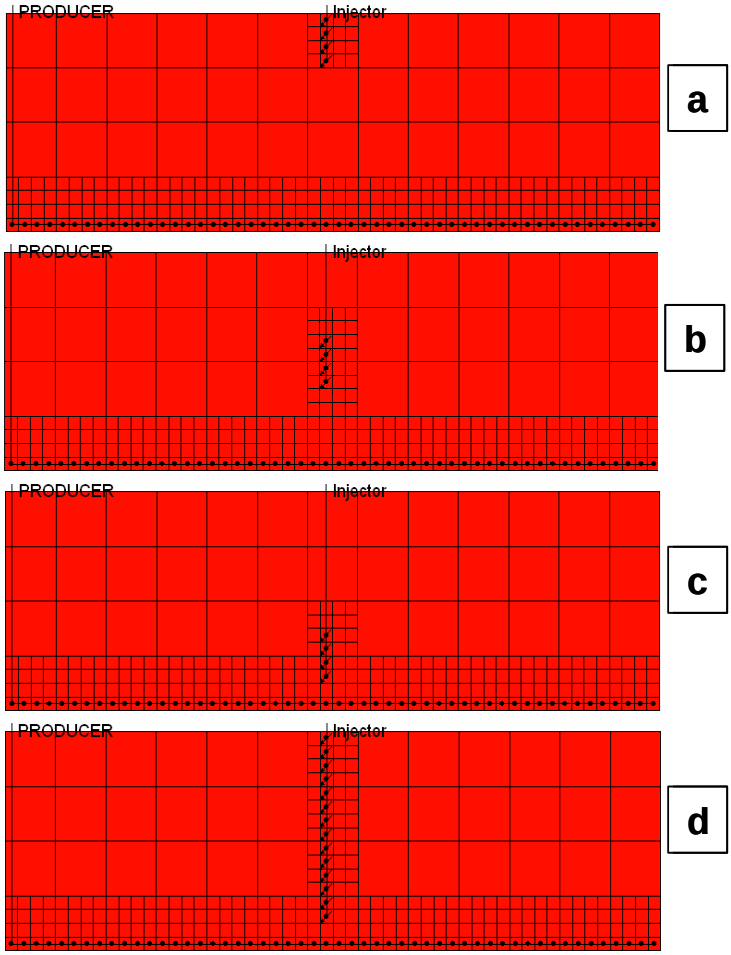

Figure 4.19: *Vertical injector perforation intervals: (a) VI_topPerf, (b) VI_middPerf, (c) VI_bottomPerf, and (d) VI_allPerf*

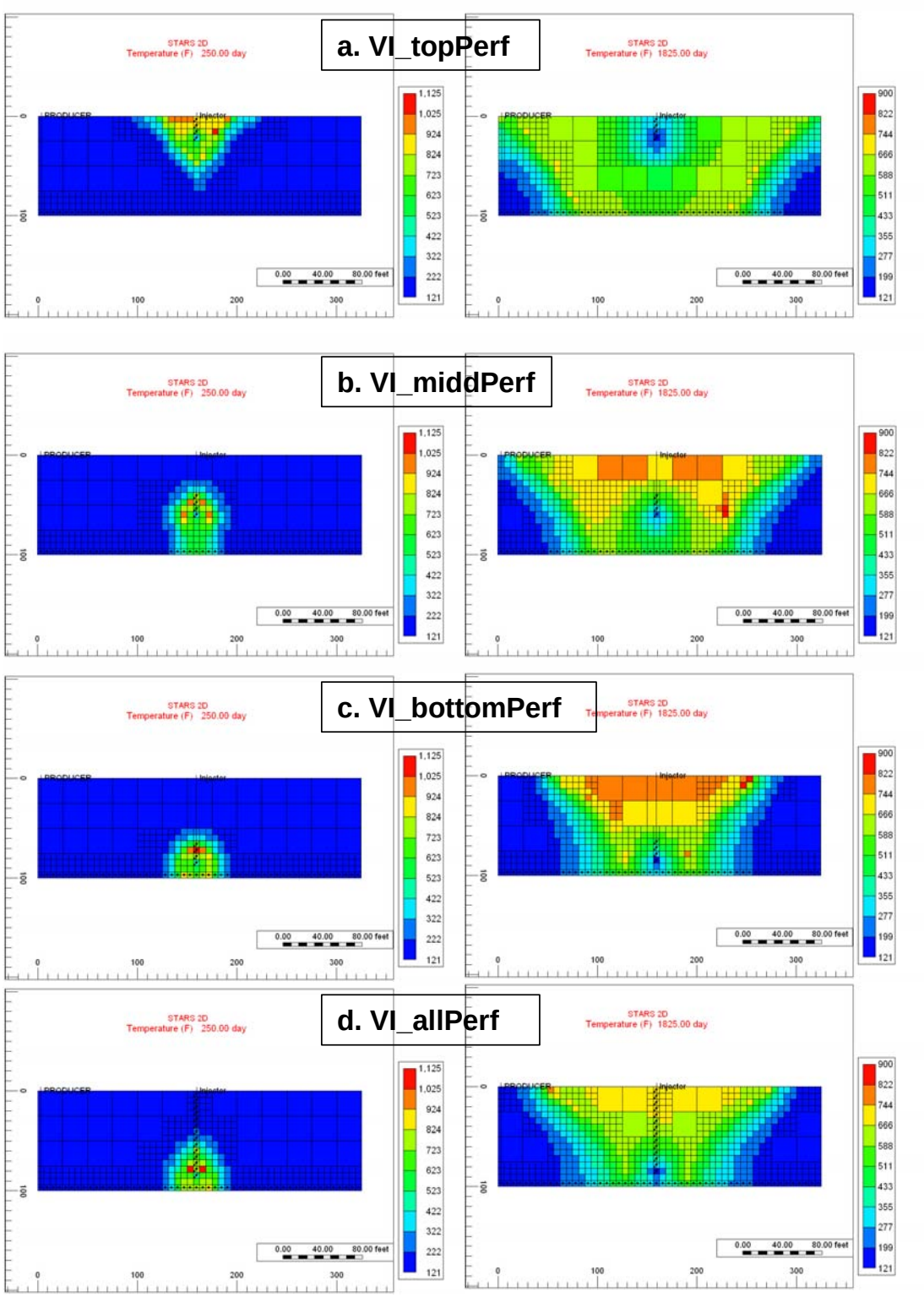

Figure 4.20: *Simulation results of temperature at 250 and 1825 days: (a) VI_topPerf, (b) VI_middPerf, (c) VI_bottomPerf, and (d) VI_allPerf*

Figure 4.21 shows the saturation ternary plot for all phases for all four of the models. It was clear that the top perforated injector model was able to sweep the entire formation,

whereas the other three scenarios had some areas, especially the bottom corners of the model, unswept. Similar results were observed for the average oil saturation at the end of the calculation (Figure 4.22a). The highest cumulative oil produced (Figure 4.22b) was when the vertical injector was completed in the top layers compared to the other three models. The main reason behind the lower recovery factor in those three cases was the location where the fire front was initiated. For example, for the middle completed vertical injector model, the fire front was initiated in the middle layers and it started to moves upward against the gravity drainage force, which resulted in slowing of the frontal velocity, and led to more oil being converted to coke as Figure 4.22c shows. For this case it was clear for the first 800 days that the model was producing a large amount of coke as a result of the upward movement of the front, and as soon as it approached the top of the model, the net coke produced decreased dramatically, until it almost matched the amount of coke in place for the top perforated vertical well model at around 1200 days. Similar observations were made for the two other models (VI_bottomPerf and VI_allPerf), with more oil being converted to coke because of the longer time the front needed to move from the bottom to the top of the model. Table 4.5 shows the results of the four models and it were noticeable that oxygen break through occurred earlier in the cases where the distance between the vertical injector perforations and the horizontal producer was shorter. This sensitivity showed the impact of the vertical injector perforation on in-situ combustion efficiency. Hence, as a best practice it is recommended that vertical injector wells be completed in the top layers away from the producer well.

Model name	Recovery factor (%)	Time to achieve this recovery factor (days)	Oxygen break through (days)	Final average oil saturation (fraction)
VI_topPerf	91.6	3095	362	0
VI_middPerf	89.0	3095	140	0.02
VI_bottomPerf	82.0	3095	30	0.08
VI_allPerf	83.0	3095	22	0.08

Table 4.5: *Simulation results of vertical injector perforation intervals*

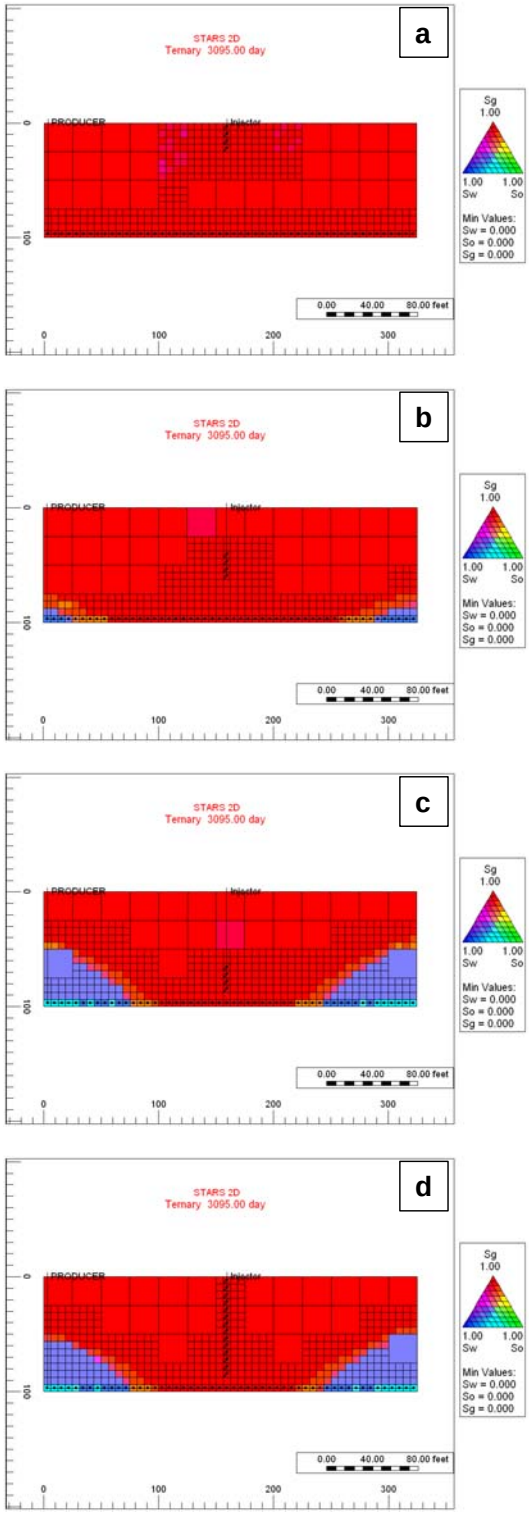

Figure 4.21: *Simulation results showing ternary saturation plots at 1825 days: (a) VI_topPerf, (b) VI_middPerf, (c) VI_bottomPerf, and (d) VI_allPerf*

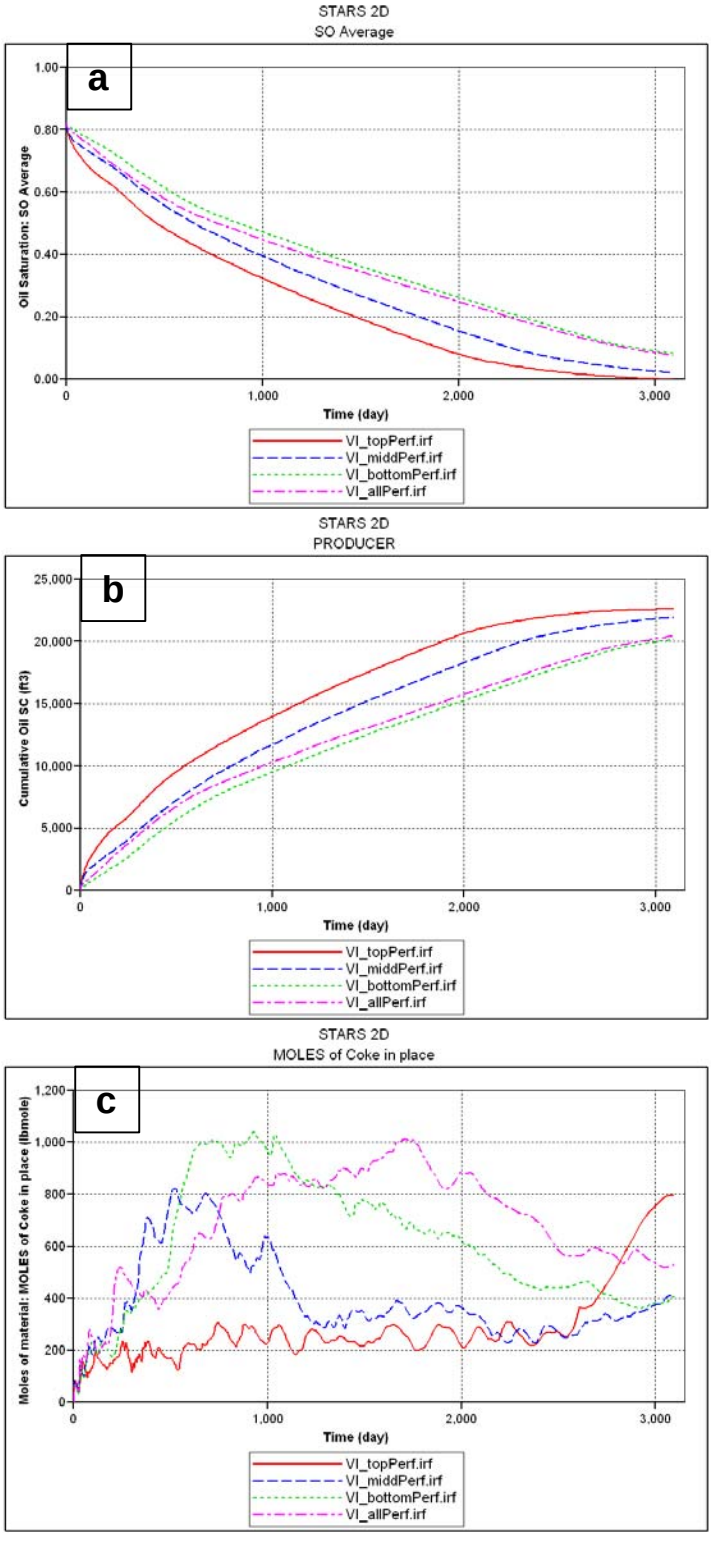

Figure 4.22: *Simulation results of vertical injector perforation intervals: (a) average oil saturation, (b) cumulative oil produced, and (c) net coke in place*

4.6 Impact of number of vertical injectors

In the forward in-situ combustion process, the fire front was initiated from the injector and then propagated to sweep the formation. If more than one vertical injector was used in the process, this will result in the initiation and development of two fire fronts (compared to a single front) which might enhance the process performance. In order to investigate this issue, a new model was developed with two vertical injector wells (Figure 4.23a). This model had the same properties as the single vertical injector model (Figure 4.23b), with the exception that each injector well injects half the total injection rate in the single well case.

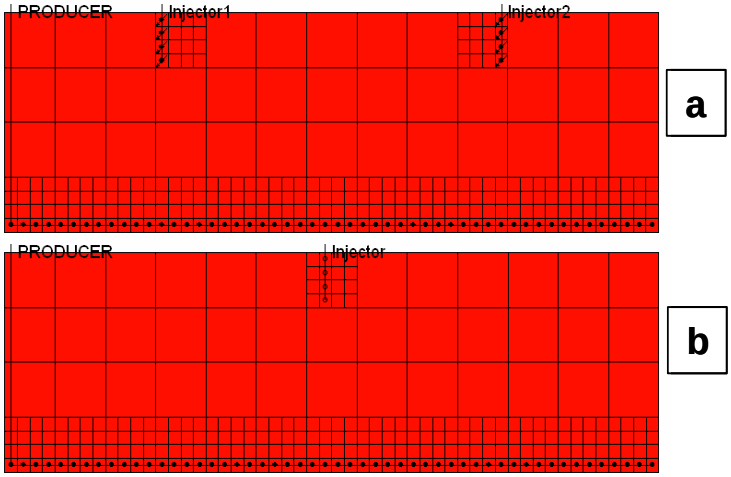

Figure 4.23: *Number of vertical injectors: (a) 2VI and (b) 1VI*

The model with two vertical injectors managed successfully to initiate two fire fronts as Figure 4.24a shows. The temperature distribution shows the shape of the fire fronts in both models, and their changes with time at 300 days and 1025 days (Figure 4.24). For the single vertical injector model, the front spread faster in both the lateral and vertical directions as a result of the higher air injection rate. However, this high rate resulted in early break through of oxygen into the horizontal producer at 362 days compared to 631 days in the two vertical injector model (Figure 4.25a). In the case of the two vertical injectors, the two fronts started efficiently to sweep the model and as time progressed they managed to sweep almost the entire model volume in a much shorter time when compared to the single injector model. Figure 4.25b shows the cumulative oil produced

from both models. It was clear that both models gave almost the same recovery factor. However, the two vertical injector model did accelerate the recovery factor and managed to reach the maximum factor in just 1692 days compared to the single vertical injector model (3095days). As a result, increasing the number of injectors did not increase the recovery factor; it only enhanced the combustion process by having various fire fronts and therefore reduced the recovery time.

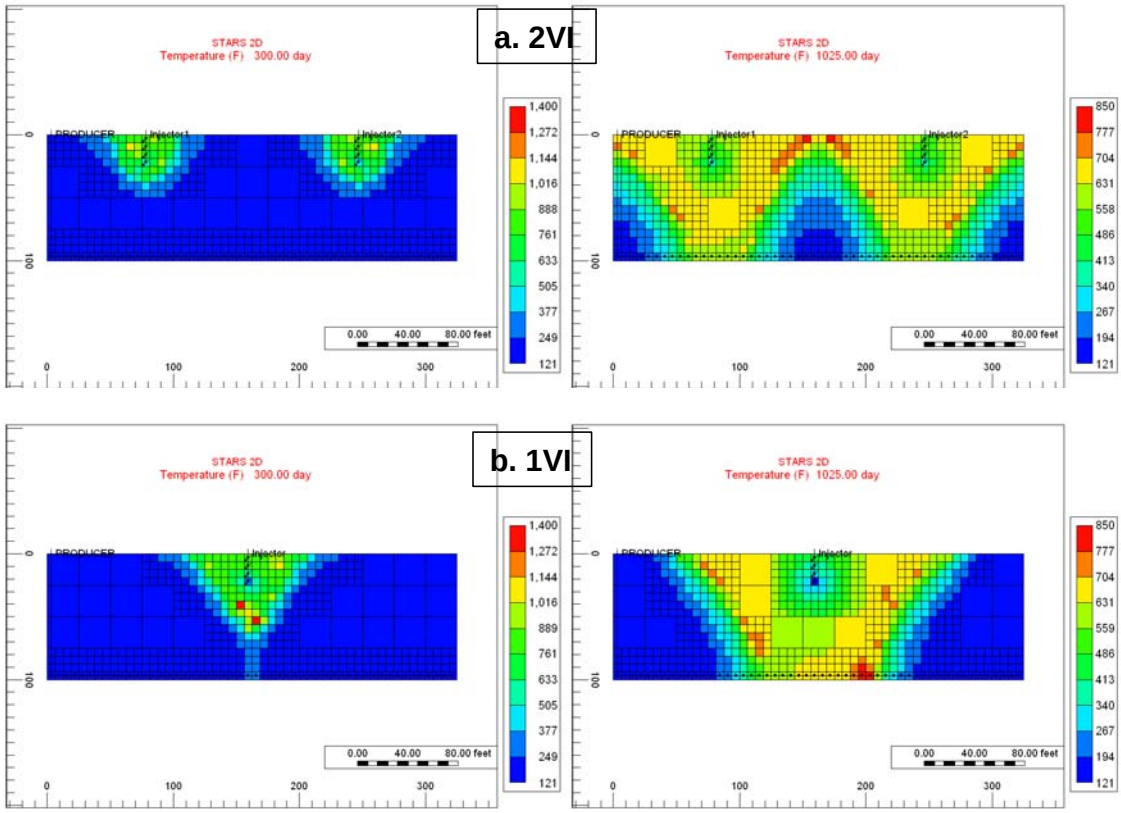

Figure 4.24: *Simulation results of temperature at 300 days and 1025 days: (a) 2VI and (b) 1VI*

The amount of coke produced by the two vertical injector model was much greater, as Figure 4.26a shows. This was as a result of the fact that two fronts allowed far more fuel to deposit and both fronts needed higher total fuel requirements in order to be sustained and progress. This also resulted in higher average temperature in the two vertical injectors model (Figure 4.26b). In this sensitivity, since the in-situ combustion performance was not much affected by the number of the vertical injectors used, the decision to increase the number of vertical injectors should be taken purely based on the project economics. Drilling more vertical injector wells will enhance the project

feasibility by reducing project time and by having more oil in earlier stages of the project development. However, both the drilling and operating cost of the wells needs to be considered before making such a decision.

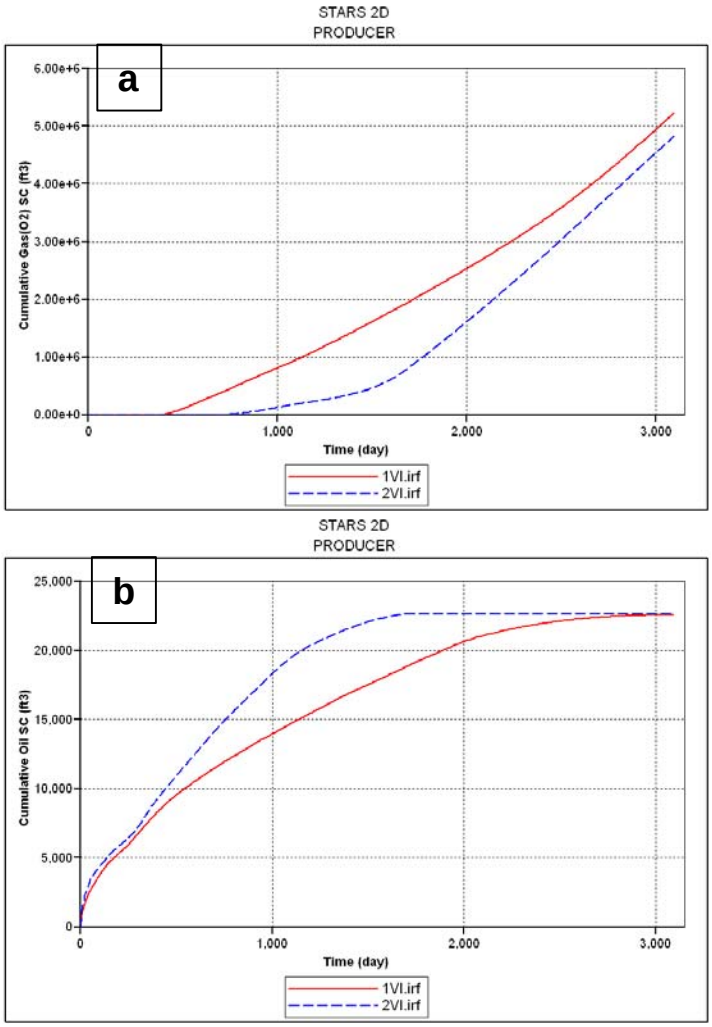

Figure 4.25: *Simulation results of number of vertical injectors: (a) cumulative oxygen produced and (b) cumulative oil produced*

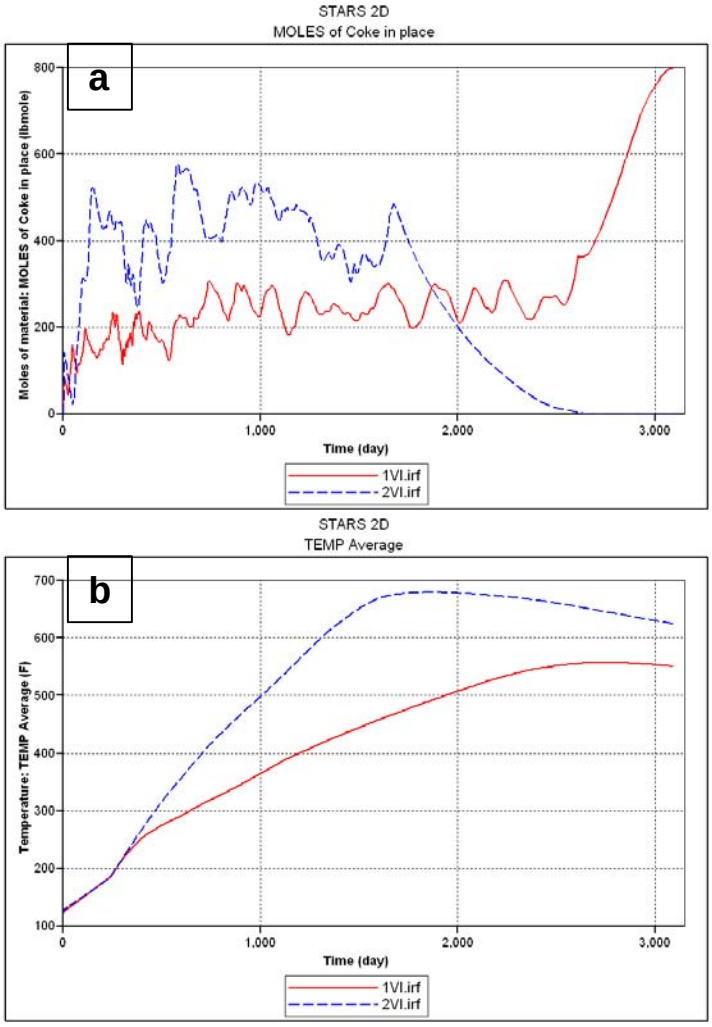

Figure 4.26: *Simulation results for a number of vertical injectors: (a) net coke in place and (b) average temperature*

4.7 Effect of using two sided horizontal producer

Akin et al. (2000) conducted an experimental study to investigate the combustion process performance when using various well configurations. They used a 3D scaled physical model and various well configurations were introduced to the model. One of the configurations used in their study was to have two horizontal wells with a right angle between them and a vertical injector in the opposite corner of the 3D experimental model. This configuration resulted in recovering of the highest amount of oil when compared to the other configurations used in their study. In order to represent the same

well configurations in a 2D cross sectional model, a two sided horizontal well could be used. In other words, the horizontal section of the horizontal producer was perforated to allow tubing flow and the vertical section of the producer well was perforated to allow annular flow between the tube and the well casing. The aim in this sensitivity was to investigate the use of a two sided horizontal producer well with a vertical injector in the opposite corner, and its effect on the combustion process. Another objective was to evaluate the impact of the length of two sided horizontal producer.

The 2D cross sectional model was developed with three different scenarios in mind. The first scenario was to complete the total vertical and horizontal sections (100%) of the two sided horizontal producer (Figure 4.27a). In the second model only half (50%) of the vertical section was perforated and also half of the horizontal section was completed (Figure 4.27b). In the third model the horizontal producer was completed over 25% of its vertical and horizontal length (Figure 4.27c). The remainder of the model properties and combustion parameters were kept the same in all three models.

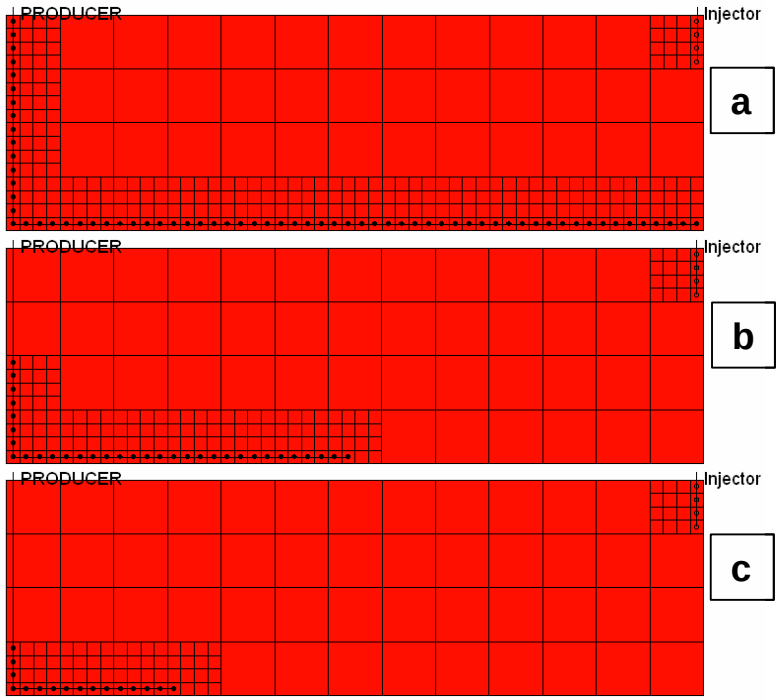

Figure 4.27: *Two sided horizontal producer length: (a) 2Sided_HP-100%, (b) 2Sided_HP-50%, and (c) 2Sided_HP-25%*

The combustion front behaviour in these three different scenarios was shown in the temperature distribution maps at 425 days and 995 days (Figure 4.28). The two sided 100% completed horizontal producer allowed for early oxygen break through in its horizontal section due to the short distance between the vertical injector and the closest horizontal section perforation. After that, the front continued to sweep the model top due to the gas override effect, until it reached the top perforation of the vertical section (Figure 4.28a). For the 50% and 25% two sided horizontal producer models, the behaviour was similar in terms of the pattern the fire front followed. However, the only difference was in the timing of the frontal advance rate, due to the different well lengths. In these two models, the fire front initiated in the vertical injector and mainly started to sweep the top area of the model (Figure 4.28b and c at 425 days) only, until it reached near one end of the horizontal section of the well (i.e. middle of the model for the 50% length model), where the front movement was split in two different directions. The first part of the fire front continues sweeping the top area of the model until it approached the top perforation of the vertical section of the two sided horizontal producer, and the second part of the fire front started moving downward to reach the first perforation of the horizontal section of the producer well (Figure 4.28b and c at 995 days). The common behaviour of the combustion fronts in all three models was to break through the horizontal section first due to the shorter distance between the vertical injector and the horizontal section of the horizontal producer (Figure 4.29a). After that, the front continued sweeping the model volume until break through in the top perforation of the vertical section of the producer, shown in Figure 4.29a by the change of slope in production for each model, albeit at different times. The peak temperature profiles of the models shows (Figure 4.29b) some temporary increased in the temperature at the time when oxygen broke through to the vertical section of the horizontal producer, and the amount of oxygen produced temporarily decreased at the same time as oxygen break through occurred in the vertical section (Figure 4.29c). This could be explained as follows: when the oxygen broke through into the vertical section (which was the nearest part of the producer to the top of the model), the injected air (including oxygen) started to move very fast from the moment it was injected through the top of the model until it reached the top vertical section perforation to be produced and recycled again. This fast movement of the air acted as a fan which blew oxygen into the fire front, which helped and increased the front peak temperature temporarily

(Figure 4.29b). More oxygen was consumed at that moment, and as a result the oxygen production rate was temporarily decreased (Figure 4.29c).

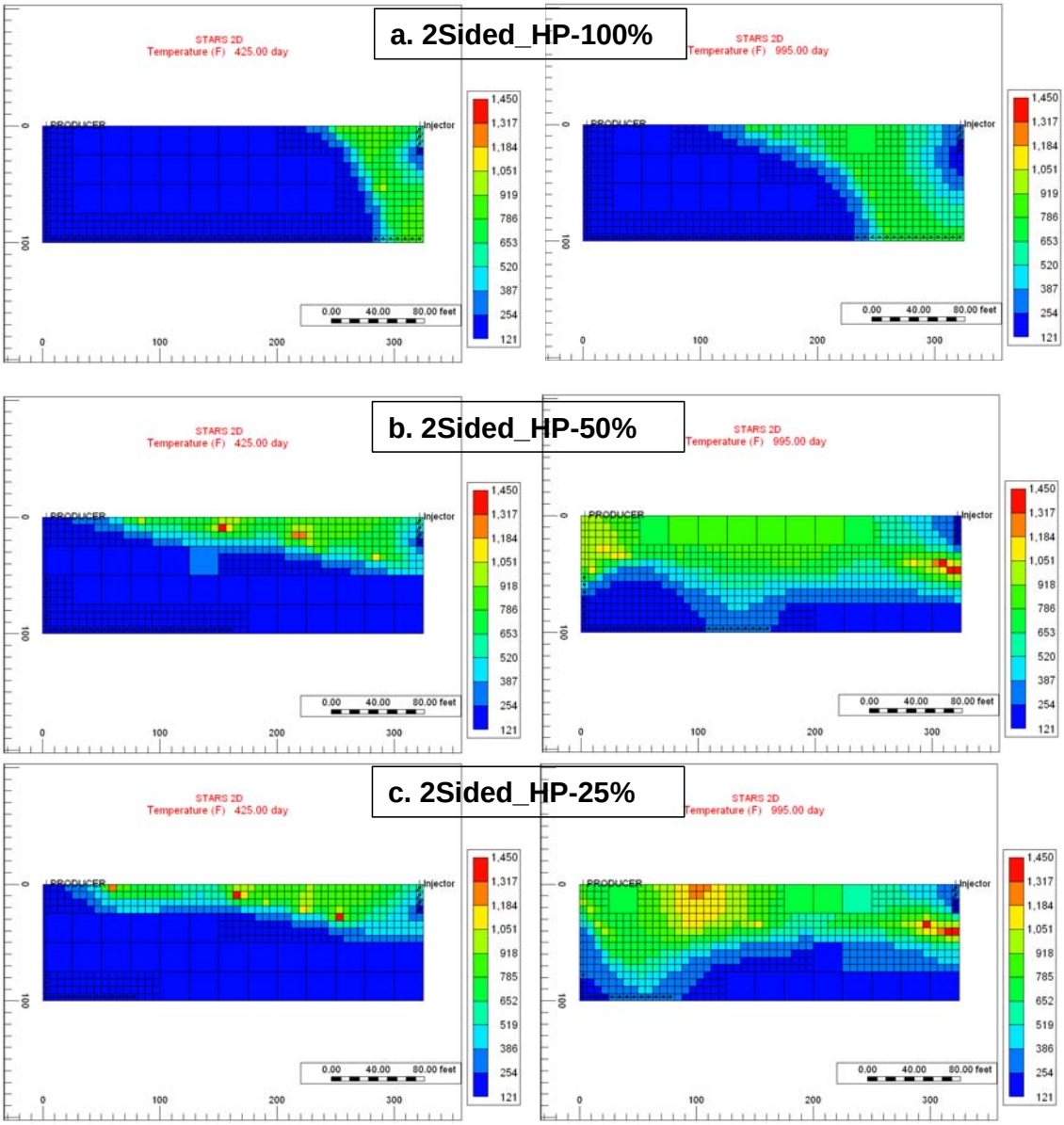

Figure 4.28: *Simulation results showing temperature at 425 days and 995 days: (a) 2Sided_HP-100%, (b) 2Sided_HP-50%, and (c) 2Sided_HP-25%*

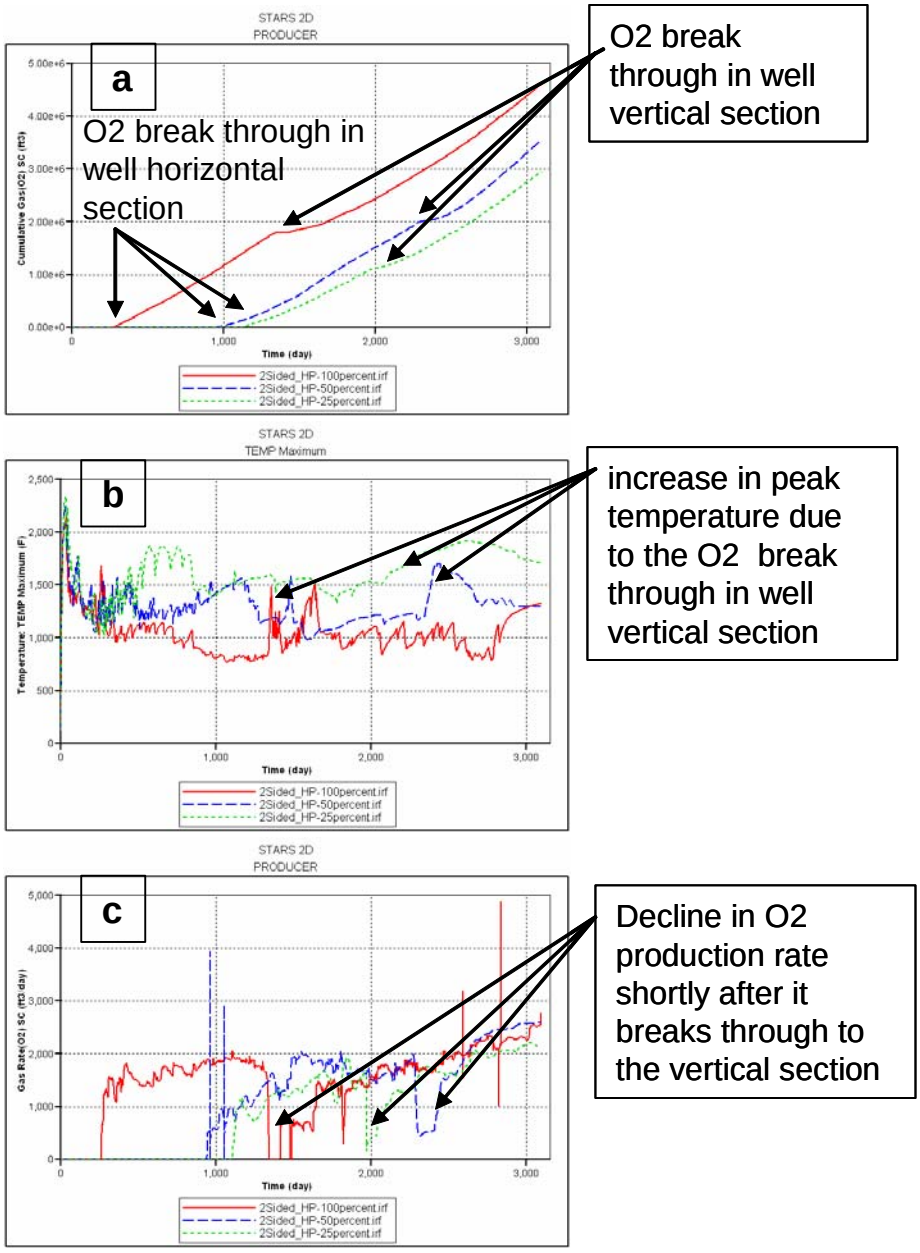

Figure 4.29: *Simulation results of two sided horizontal producer length: (a) cumulative oxygen produced, (b) peak temperature, and (c) oxygen production rate*

The occurrence of early oxygen break through in the 100% completed two sided horizontal producer resulted in low cumulative oil produced (Figure 4.30a) as a result of the poor areal sweep of the fire front. However, for both the 50% and 25% length cases, the delay of oxygen break through allowed the combustion front to sweep a large area of the model and resulted in a higher recovery factor (Figure 4.30a) and shorter recovery time as the average oil saturation Figure 4.30b shows. This highlighted the importance of carefully designing the in-situ combustion process to allow a larger area

of the model to be swept before oxygen break through occurred. Table 4.6 below summarises the general results out of the two sided horizontal producer sensitivity.

Model name	Recovery factor (%)	Time to achieve this recovery factor (days)	Oxygen break through (days)	Final average oil saturation (fraction)
2Sided_HP-100%	70.0	3095	265	0.01
2Sided_HP-50%	82.9	2445	902	0
2Sided_HP-25%	83.9	2276	1065	0

Table 4.6: *Simulation results of two sided horizontal producer length*

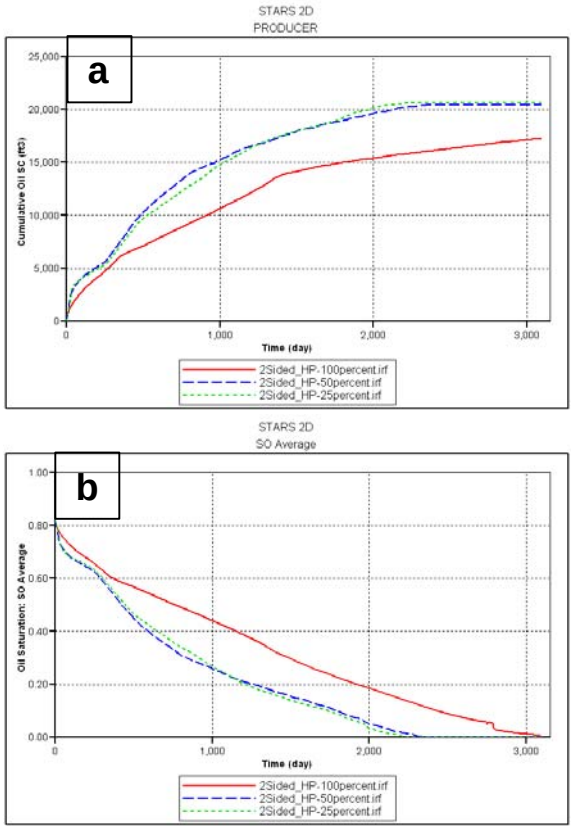

Figure 4.30: *Simulation results of two sided horizontal producer length: (a) cumulative oil produced, and (b) average oil saturation*

4.8 Effect of using a horizontal injector and impact of variations in horizontal producer location

Most injector wells used in heavy oil recovery methods were horizontal. In the application of thermal stream injection for the steam assisted gravity drainage (SAGD) methods, a pair of horizontal wells were generally used. In this method the horizontal injector was located above the horizontal producer to allow the injected steam to soak the heavy oil above the injector, and in the area between the injector and the producer, which resulted in a reduction of the crude viscosity and enabled its production. In this section the horizontal injector concept was introduced to the in-situ combustion simulation process using the 2D cross sectional model. The effect of the horizontal injector well length on combustion will be investigated. Also, the injector location relative to the producer will be evaluated in order to assess the combustion performance under the various horizontal injector well configurations.

4.8.1 Impact of horizontal injector length when horizontal producer on bottom

This approach was investigated since it could be considered as the most likely to be applied in the Nimr field. This was because of the Nimr reservoir depth and the fact that drilling a horizontal injector instead of several vertical injector wells will save drilling money and enhances the project feasibility. Also, according to the Nimr field development plan, most of the current producer wells in Nimr were horizontal producers, and they were located in the reservoir top away from the aquifer (to avoid high water cut). When in-situ combustion was approved to be used in Nimr, those producers could be converted to horizontal injectors, which will result in time savings and a reduction in the capital cost of implementing in-situ combustion in the field.

The aim of this sensitivity was to evaluate the horizontal injector length effect on the combustion process when the injector was located at the top of the model and the horizontal producer was placed in the bottom of the model. Three models were developed with three different horizontal injector lengths: the first with 100% (Figure

4.31a) injector length, the second had 50% (Figure 4.31b) and the third model with 25% (Figure 4.31c) injector length.

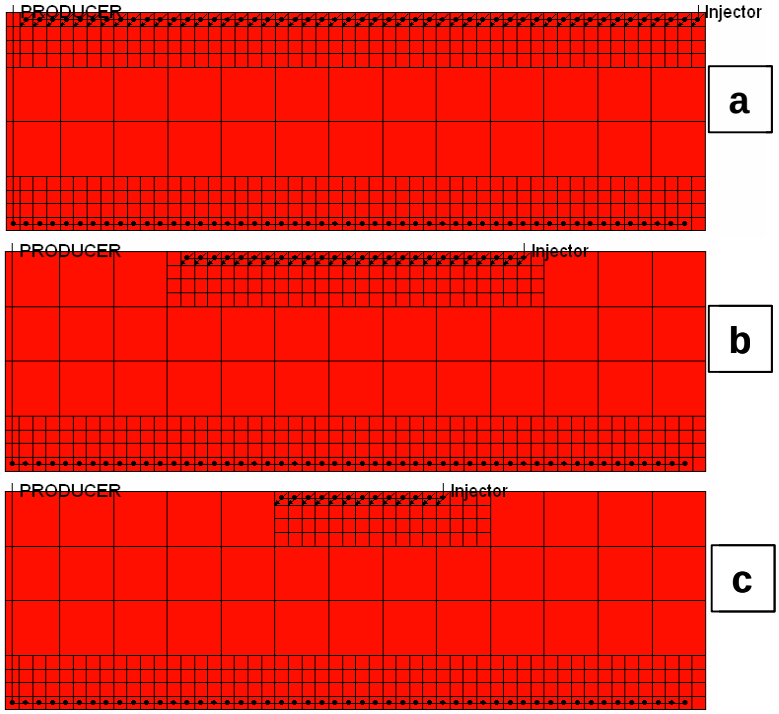

Figure 4.31: *Top horizontal injector lengths and bottom horizontal producer: (a) HI_Top_100%, (b) HI_Top_50%, and (c) HI_Top_25%*

Both the temperature distribution and the three phase saturation ternary at 665 days (Figure 4.32) show the front development and propagation for each of the three models. Figure 4.32a shows that for the 100% length horizontal injector the combustion front started at the top and then moves typically as a piston like displacement from the top of the model until it approached the horizontal producer at the bottom of the model. This behaviour led to a delay in the fire front and oxygen break through (Figure 4.33a) in this model. As a result, the oil banking effect exists ahead of the front and resulted in a reduction in the fire front velocity and allowed more coke deposition (Figure 4.33b), which led to an increase in the model average temperature profile (Figure 4.33c). In the two other cases where the horizontal injector lengths were shorter (50% and 25%), the frontal behaviour was different compared to the 100% horizontal injector case, as Figure 4.32b and c show. For the shorter horizontal injector well the amount of air injected per unit perforation was much higher than the case of a longer well, since similar air injection rate was used in all the models. This resulted in the width of the fire

front being smaller, which made it easier to propagate faster through the layers to approach the producer. The smaller the horizontal injector length the faster the fire front propagates as Figure 4.38 illustrates, and the earlier the oxygen break through occurred (Figure 4.33a), which led to less oil banking and less coke being produced for those short horizontal injector models (Figure 4.33b).

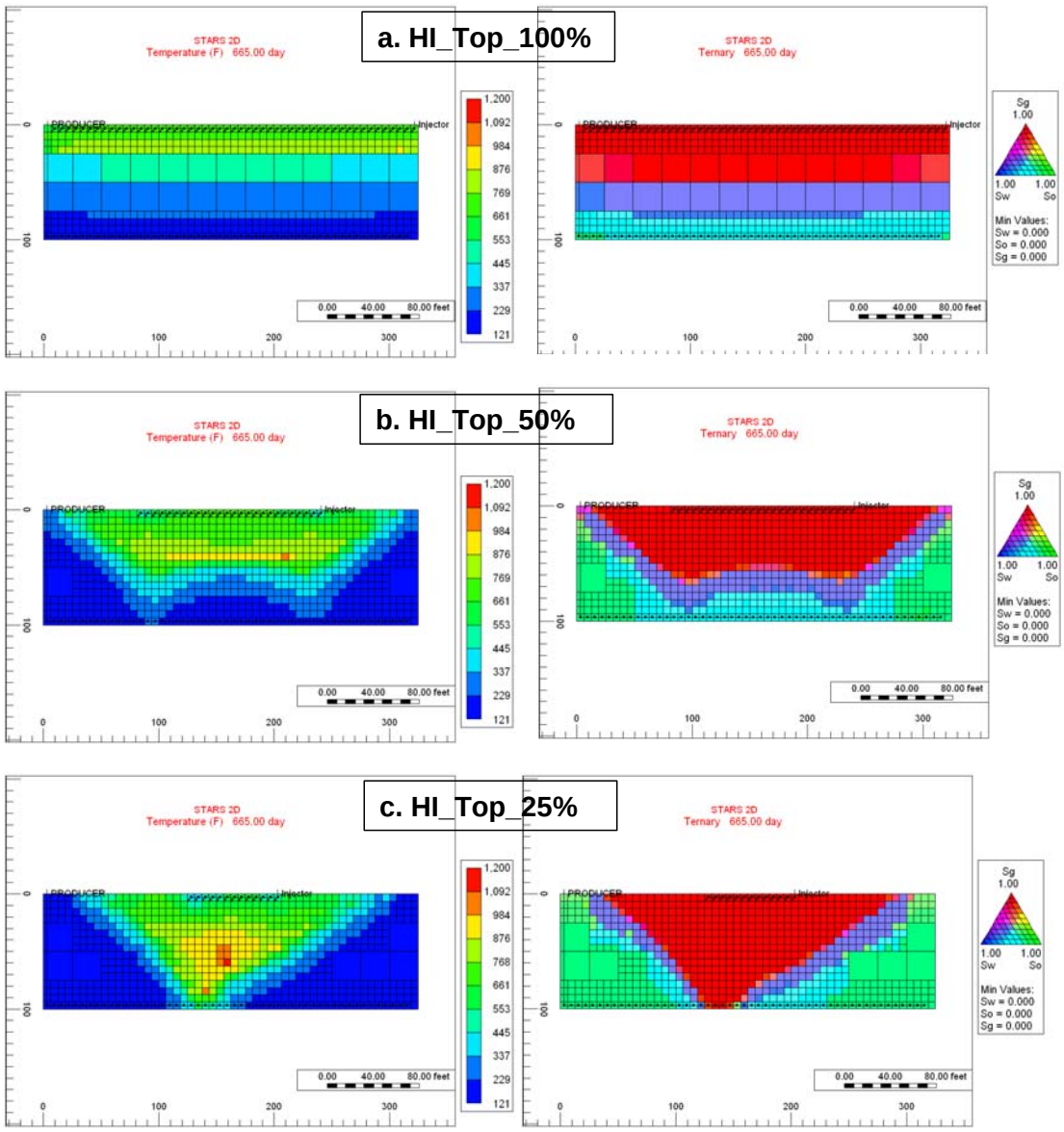

Figure 4.32: *Simulation results of temperature and ternary saturation plots at 665 days: (a) HI_Top_100%, (b) HI_Top_50%, and (c) HI_Top_25%. Note the piston like frontal movement in case (a) compared to the frontal movement in the other two cases (b and c)*

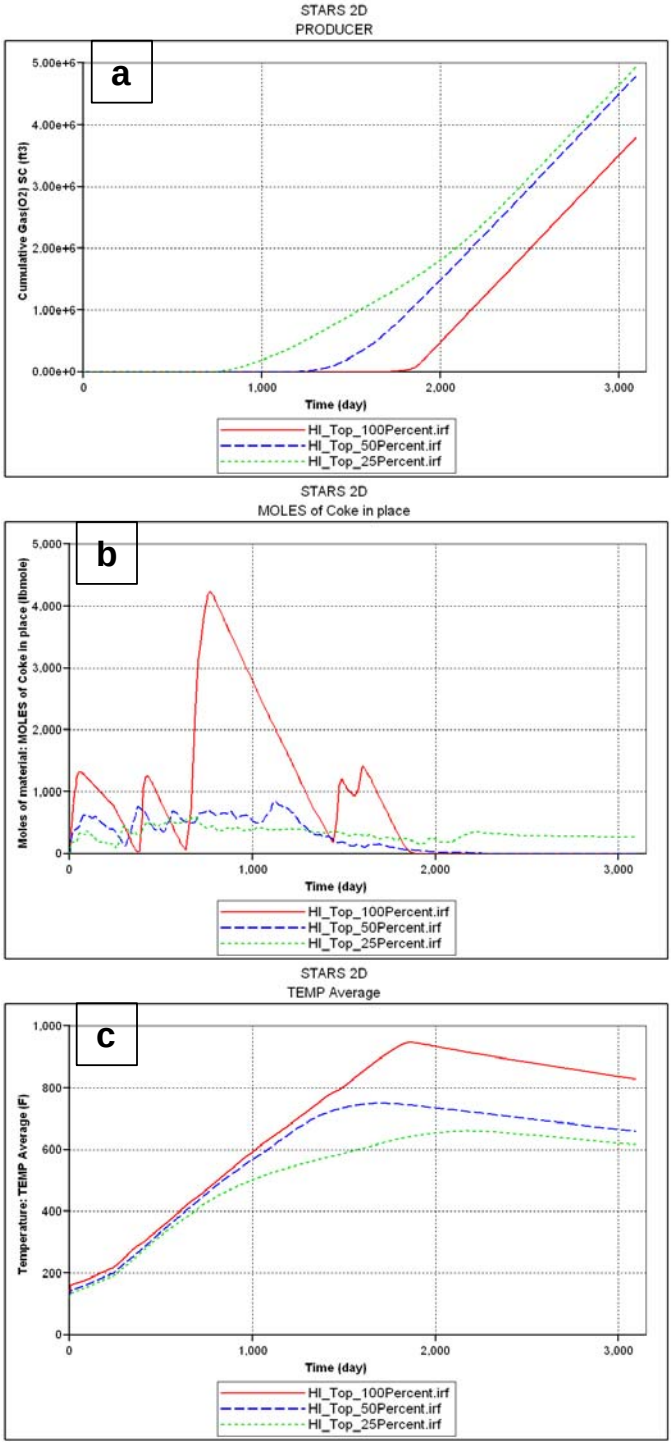

Figure 4.33: *Simulation results of top horizontal injector lengths and bottom horizontal producer: (a) cumulative oxygen produced, (b) net coke in place, and (c) average temperature profile. Note the larger amount of coke deposited (b) for the 100% long HI case as a result of slow frontal movement.*

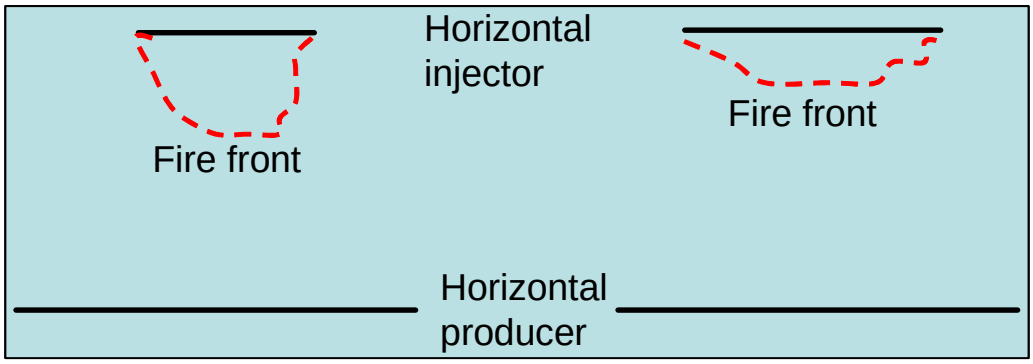

Figure 4.34: *Schematic of the fire front propagation shapes when using different horizontal injector well lengths*

The 100% horizontal injector length model produced a lower total amount of oil (Figure 4.35) as a result of the large amount of oil which was converted to coke. However, the near perfect piston like displacement of this model managed to reduce the recovery time, as Table 4.7 shows, when compared to the other two cases. The 25% horizontal injector model was the more feasible option when using top horizontal injector well for the in-situ combustion process as a result of the higher recovery factor achieved and the lower development cost of a short well length.

Model name	Recovery factor (%)	Time to achieve this recovery factor (days)	Oxygen break through (days)	Final average oil saturation (fraction)
HI_Top_100%	89.4	1656	1625	0
HI_Top_50%	91.7	1760	1105	0
HI_Top_25%	91.8	2282	665	0

Table 4.7: *Simulation results of top horizontal injector lengths and bottom horizontal producer*

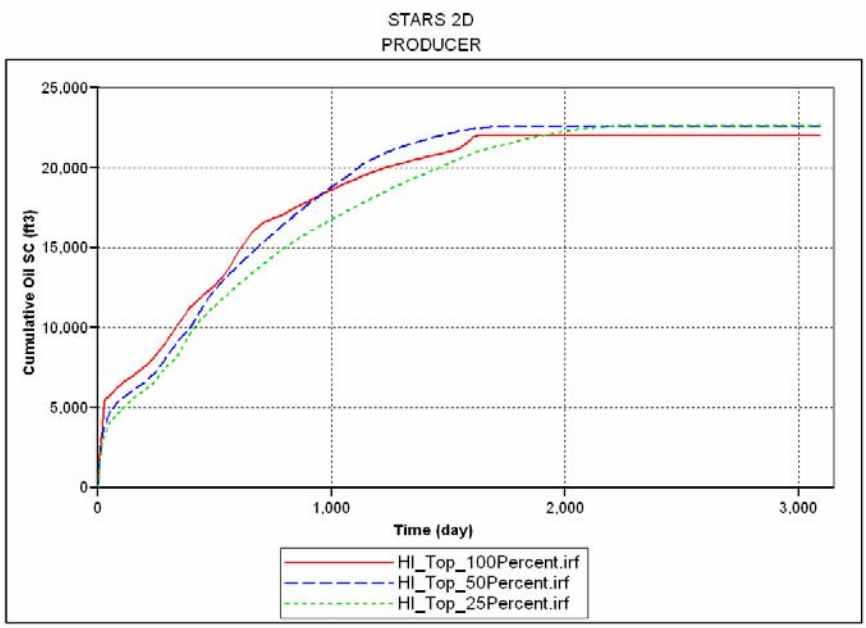

Figure 4.35: *Simulation results of top horizontal injector lengths and bottom horizontal producer cumulative oil produced*

The temperature map of the 25% horizontal injector model (Figure 4.36a) shows a non-symmetric combustion front shape and the reason for that might be the injector placement offset for the model centre, or it could be a numerical simulator averaging error which caused the non-symmetric front. To clarify the issue a model was developed and the horizontal injector was placed exactly in the model centre, which was achieved by reducing the well length by one grid block. This resulted in a symmetric front shape (Figure 4.36b), which answered the question and shows how sensitive the modelling of the in-situ combustion process was to any minor change in the model properties.

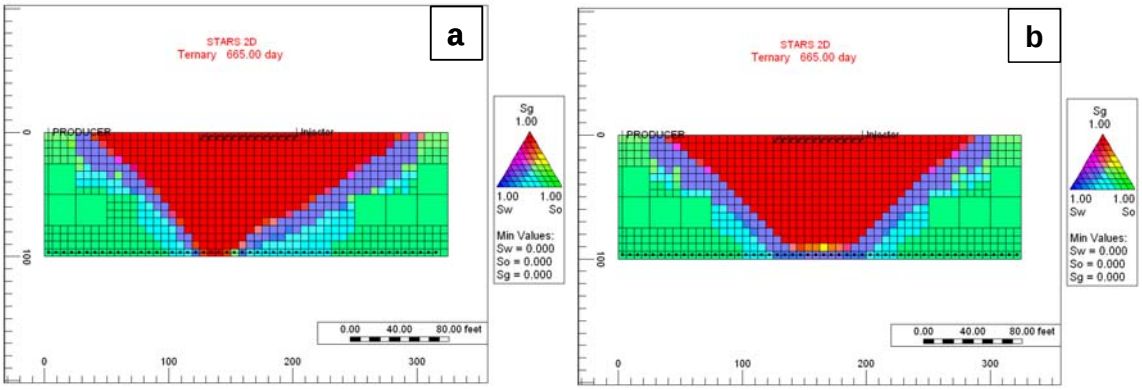

Figure 4.36: *Simulation results of ternary at 665 days: (a) HI_Top_25%, and (b) Symmatric_HI_Top_25%*

4.8.2 Bottom horizontal injector and top horizontal producer

Changing the horizontal injector from being on top of the model to being on the bottom will impact the combustion process performance. In order to evaluate the change in performance a new model was used, and the 50% length horizontal injector was used in this subsection (Figure 4.37a). The 100% length horizontal well was completed in the model top. From the temperature map results of the 50% bottom horizontal injector models (Figure 4.38a), the front behaviour was totally different from the 50% top horizontal injector model (Figure 4.38b). The front was initiated in both ends of the horizontal injector and then propagated upward very slowly in two separate circular shapes. The reason for having this shape instead of the smooth piston like displacement which existed in the top horizontal injector model was that in the bottom horizontal injector scenario the front and all of its fluids were moving upward against the force of gravity to approach the horizontal producer. It was easier for the front to be initiated at ends of the horizontal injector because of the availability of oil at the ends of the well and it was easier to move sideward instead of moving upward from the beginning of the process. The front movement from the bottom to the top of the model, against gravity, results in a slow frontal velocity and non-uniform front shape (Figure 4.38a at 965 days). Significant volumes of coke were formed (Figure 4.39a) and high temperatures were observed in the model (Figure 4.39b) because of the slow velocity of the front. Figure 4.39c shows the total oil produced from both models. The recovery factor of the bottom horizontal injector model was 35.7% (Table 4.8) because of the oil which was lost as a result of it been converted to be fuel, and also as a result of the poor front sweep efficiency. The main conclusion from this sensitivity was that it was better to avoid placing a horizontal injector well in bottom of the reservoir unless there were other forces at play (e.g. strong bottom aquifer).

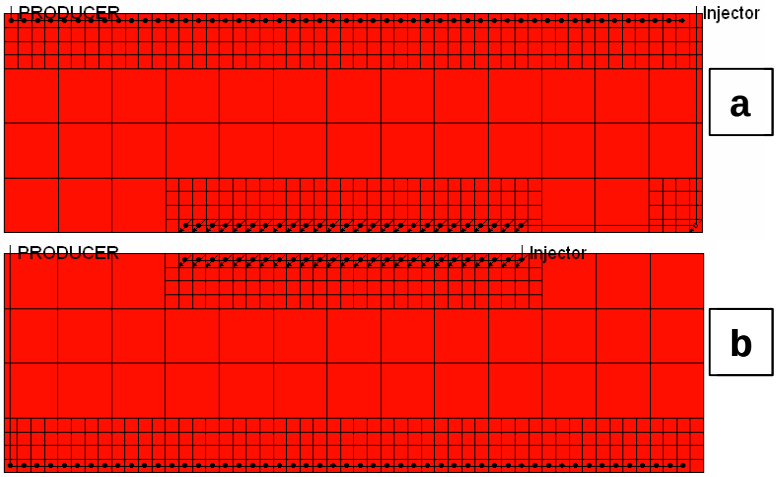

Figure 4.37: *Bottom horizontal injector and top horizontal producer: (a) HI_ Bottom _50%, and (b) HI_Top_50%*

Model name	Recovery factor (%)	Time to achieve this recovery factor (days)	Oxygen break through (days)	Final average oil saturation (fraction)
HI_Bottom_50%	35.7	3095	1225	0.03
HI_Top_50%	91.7	1760	1105	0

Table 4.8: *Simulation results of bottom horizontal injector and top horizontal producer*

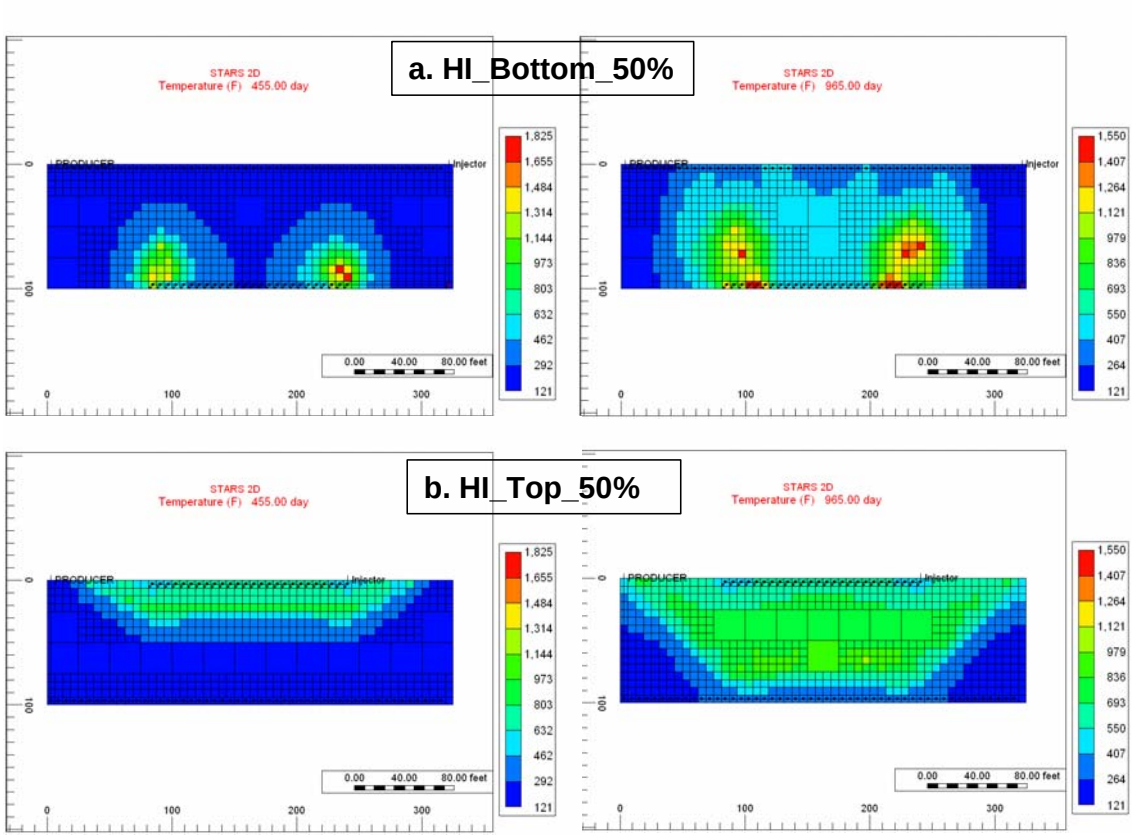

Figure 4.38: *Simulation results of temperature at 455 days and 965 days: (a) HI_ Bottom _50%, and (b) HI_Top_50%*

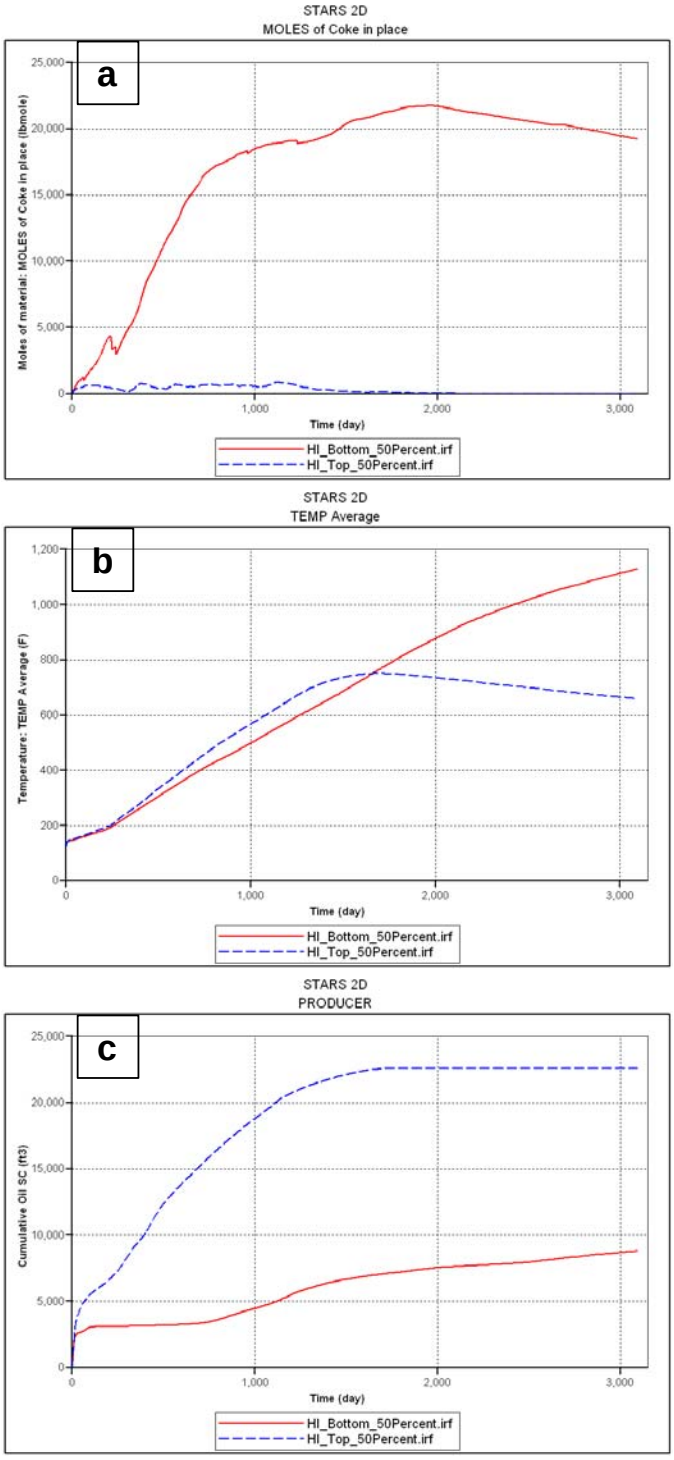

Figure 4.39: *Simulation results of bottom horizontal injector and top horizontal producer: (a) net coke in place, (b) average temperature profile, and (c) cumulative oil produced. For the bottom completed HI case, the high amount of coke formation and deposition (a) result in lower amount of oil production (c).*

4.9 Application of partially completed horizontal injector

4.9.1 Partially completed horizontal injector

The use of a horizontal injector well for the in-situ combustion process did enhance the process performance, mainly when the horizontal injector was placed in the top of the model, as shown in the previous section, where the entire injector length was completed. This section focused on the use of a partially perforated horizontal injector well in the combustion process. This method of completion will result in variations in the way the fire front is initiated, and then propagates, which will lead to some variations in the efficiency of the in-situ combustion process. In order to evaluate this effect four scenarios where the horizontal injector was partially completed were developed (all the wells had the same air injection rate), as Figure 4.40 shows. Each completion interval in the horizontal injector had a total of 18.75ft of length.

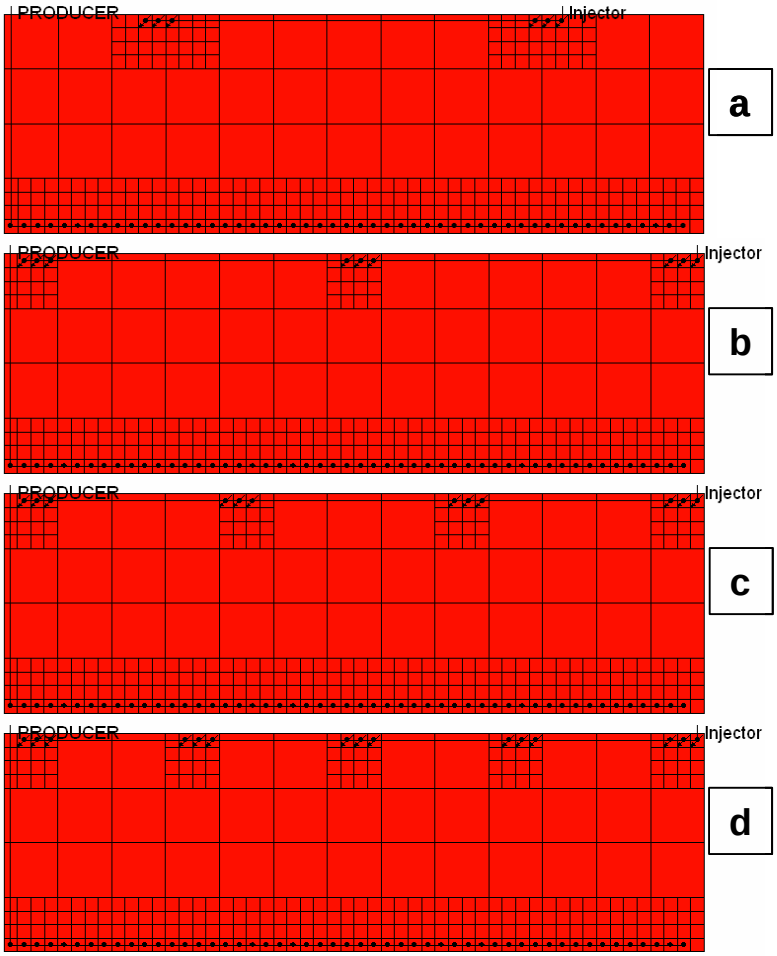

Figure 4.40: *Partially completed horizontal injector: (a) HI_2parts, (b) HI_3parts, (c) HI_4parts, and (d) HI_5parts*

The comparison of the average temperature profiles (Figure 4.41a) showed that the cases with more perforation intervals had the highest overall average temperature. This was as a result of the fact that as the number of perforation intervals increased, the fire fronts developed in the model merged together shortly after they initiated (Figure 4.43), and they formed a piston like front displacement (as with the case of the 100% length horizontal injector model-Figure 4.32a).This combustion shape resulted in a delay of both the fire front and oxygen break through, which increased the oil banking effect, and slowed the frontal propagation velocity. As a result more coke was produced (Figure 4.43b) and this led to the overall model temperature increased. Moreover, Figure 4.43 shows the temperature and saturation ternary plot at 485 days for the four models. It was noticeable that as the number of perforation intervals increased, the combustion front shape became more uniform because of the shorter distance separates

the intervals, which allowed for fronts to merge together. All four of the horizontal completion scenarios produced almost the same recovery factor as Table 4.9 shows. The two parts horizontal injector model produced slightly a higher amount of oil because of the lesser amount of coke (Figure 4.41b). Figure 4.42 shows both cumulative oil and oxygen produced. The total recovery time was reduced as the number of completion intervals increased (Table 4.9). This was because of the oil banks which developed ahead of the piston like displacement front in those models (i.e. five parts). When they broke through to the horizontal producer they managed to produce all the moveable oil and reduced the recovery time. The previous observations in this section highlight that to use the two parts horizontal injector model for in-situ combustion was the optimum option for development. This was because of the higher recovery factor achieved by this well completion and the lower amount of investment required to complete two intervals compared to other scenarios.

Model name	Recovery factor (%)	Time to achieve this recovery factor (days)	Oxygen break through (days)	Final average oil saturation (fraction)
HI_2parts	92.1	1631	855	0
HI_3parts	91.9	1582	640	0
HI_4parts	91.6	1395	1250	0
HI_5parts	91.3	1375	1303	0

Table 4.9: *Simulation results of partially completed horizontal injector*

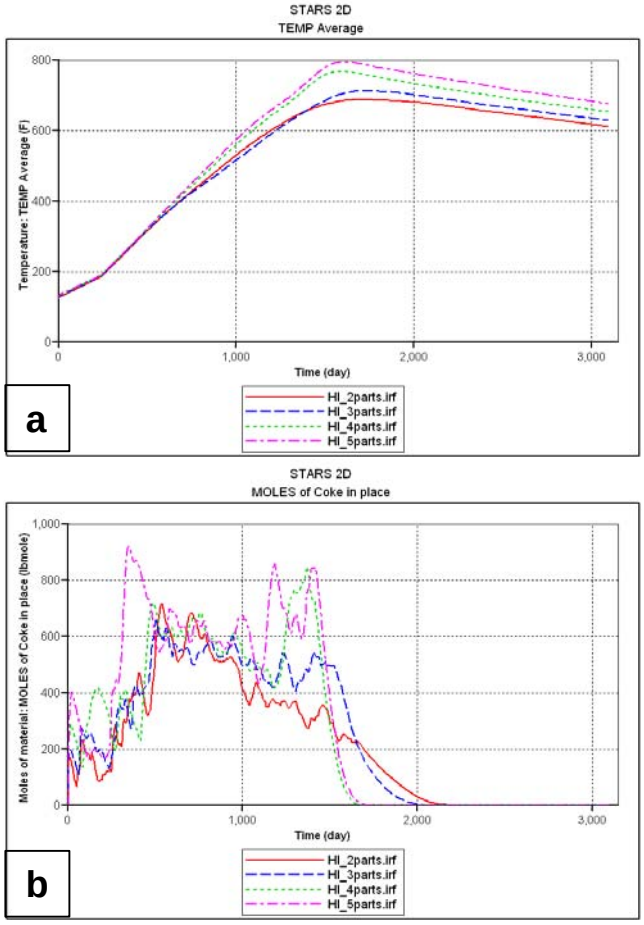

Figure 4.41: *Simulation results of partially completed horizontal injector: (a) average temperature profile, and (b) net coke in place. Note that as the completion intervals increase, the more coke was produced by the combustion front (i.e. five parts case).*

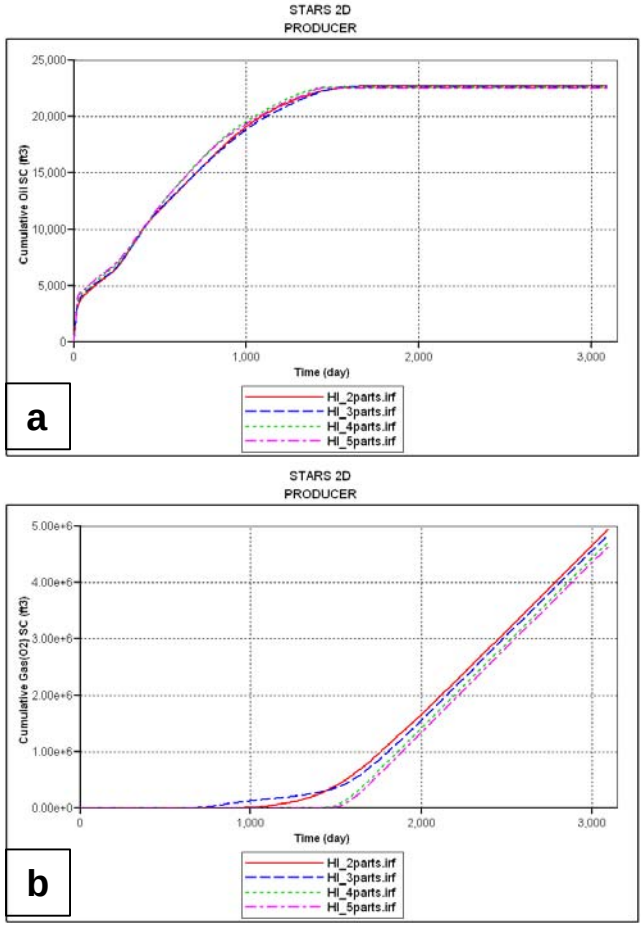

Figure 4.42: *Simulation results of partially completed horizontal injector: (a) cumulative oil produced, and (b) cumulative oxygen produced.*

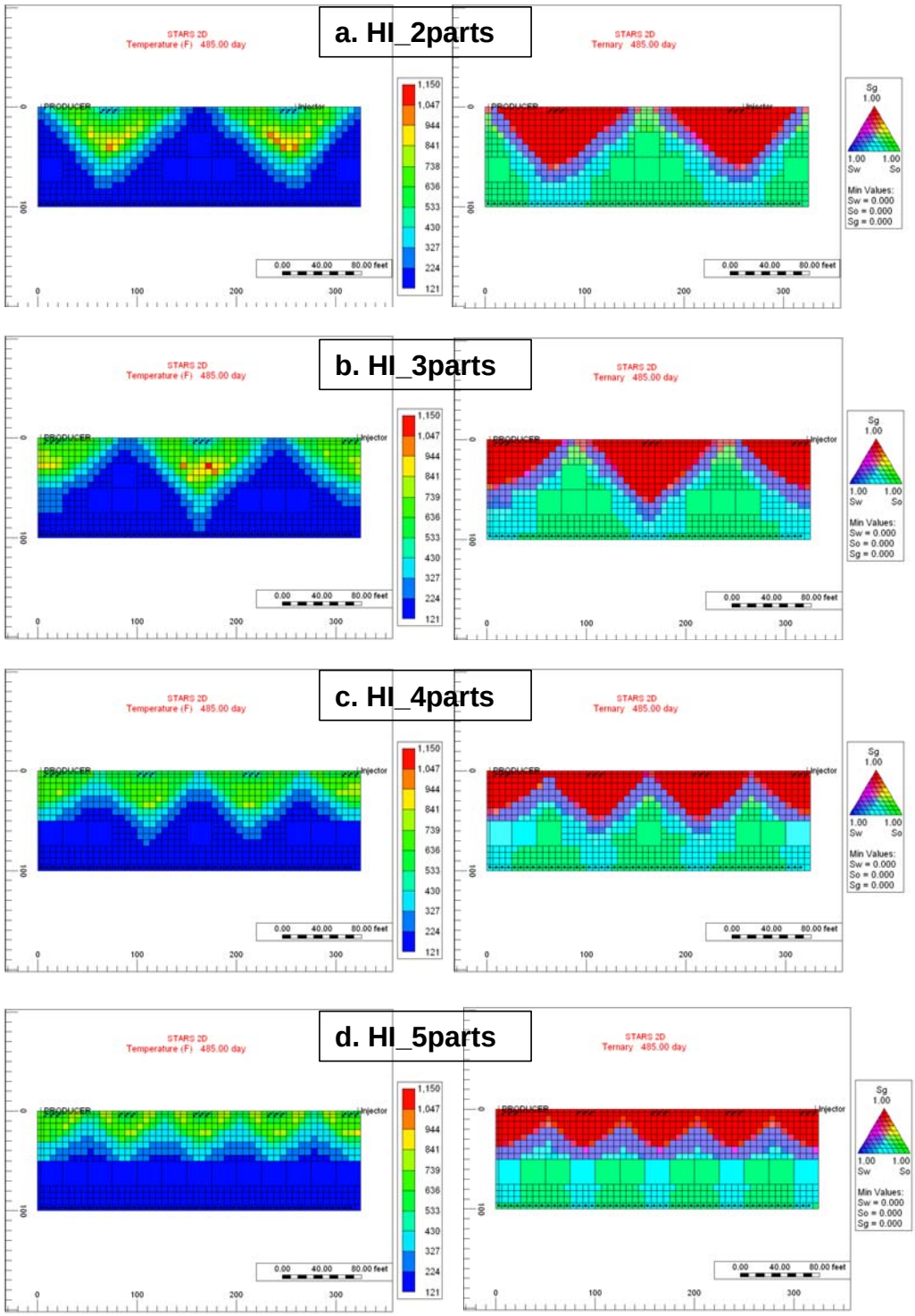

Figure 4.43: *Simulation results of temperature and ternary saturation plots at 485 days: (a) HI_2parts, (b) HI_3parts, (c) HI_4parts, and (d) HI_5parts*

4.9.2 Comparison between the use of a partially completed horizontal injector with four intervals and the use of four vertical injectors

The aim here was to compare the performance of the in-situ combustion process when using a horizontal injector with four completion intervals relative to the use of four individual vertical injector wells. This comparison should provide a clear idea of which type of injectors are able to enhance the fire front propagation and recovery factor. A new model was developed which had four vertical injectors (Figure 4.44), each located at the exact same position as the centre of each of the perforation intervals in the horizontal injector (Figure 4.40c).

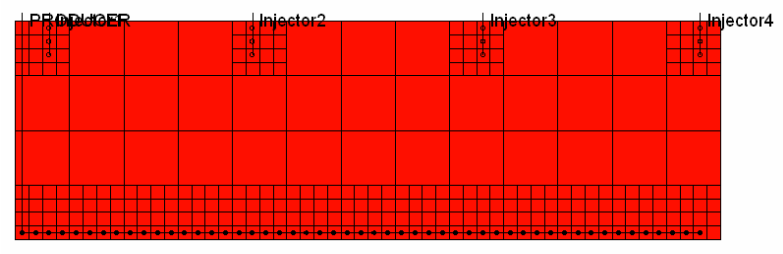

Figure 4.44: *Model with four vertical injector wells*

The fire fronts started from each vertical injector well, propagated and spread vertically more than laterally because of the vertical orientation of the vertical injector perforations, whereas for the four parts horizontal injector the fronts started to spread laterally more than vertically (Figure 4.45). Overall the two models' combustion performance could be considered similar in the respect that both models produced almost the same total amount of oil (Figure 4.46a). The average temperature profile of the four vertical injector model was slightly higher compared to the four parts horizontal injector model (Figure 4.46b). This was as a result of the amount of coke produced by the four vertical injectors fire fronts (Figure 4.46c) being higher. The oxygen break through occurred almost twice as fast in the four vertical injectors model (635 days) as in the four parts model (1250 days). This was because of the faster vertical front propagation in the four vertical injectors model as a result of the way the injectors were completed. The cost of developing and maintaining one horizontal injector should be much less than the cost of drilling four vertical injectors, especially for deep reservoirs

such as Nimr. As a result, the decision to choose the appropriate injector type will depend on the economic evaluation of any combustion project design.

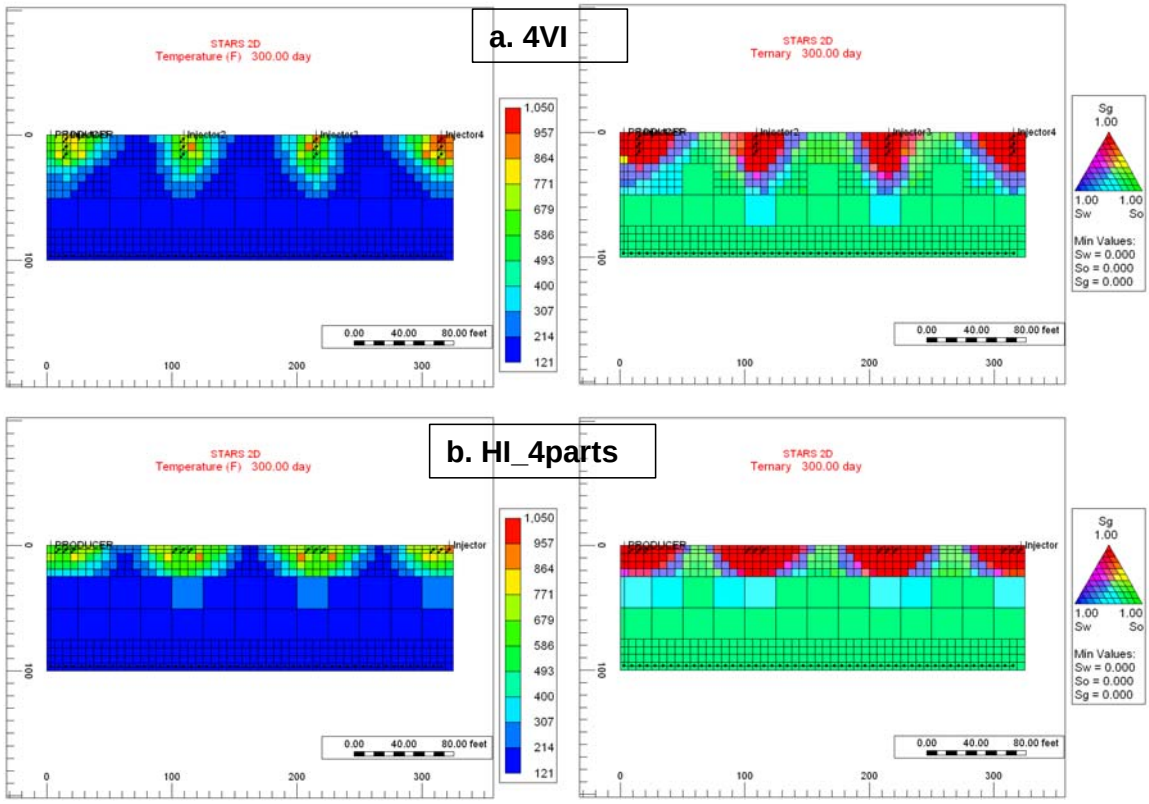

Figure 4.45: *Simulation results of temperature and ternary at 300 days: (a) 4VI, and (b) HI_4parts*

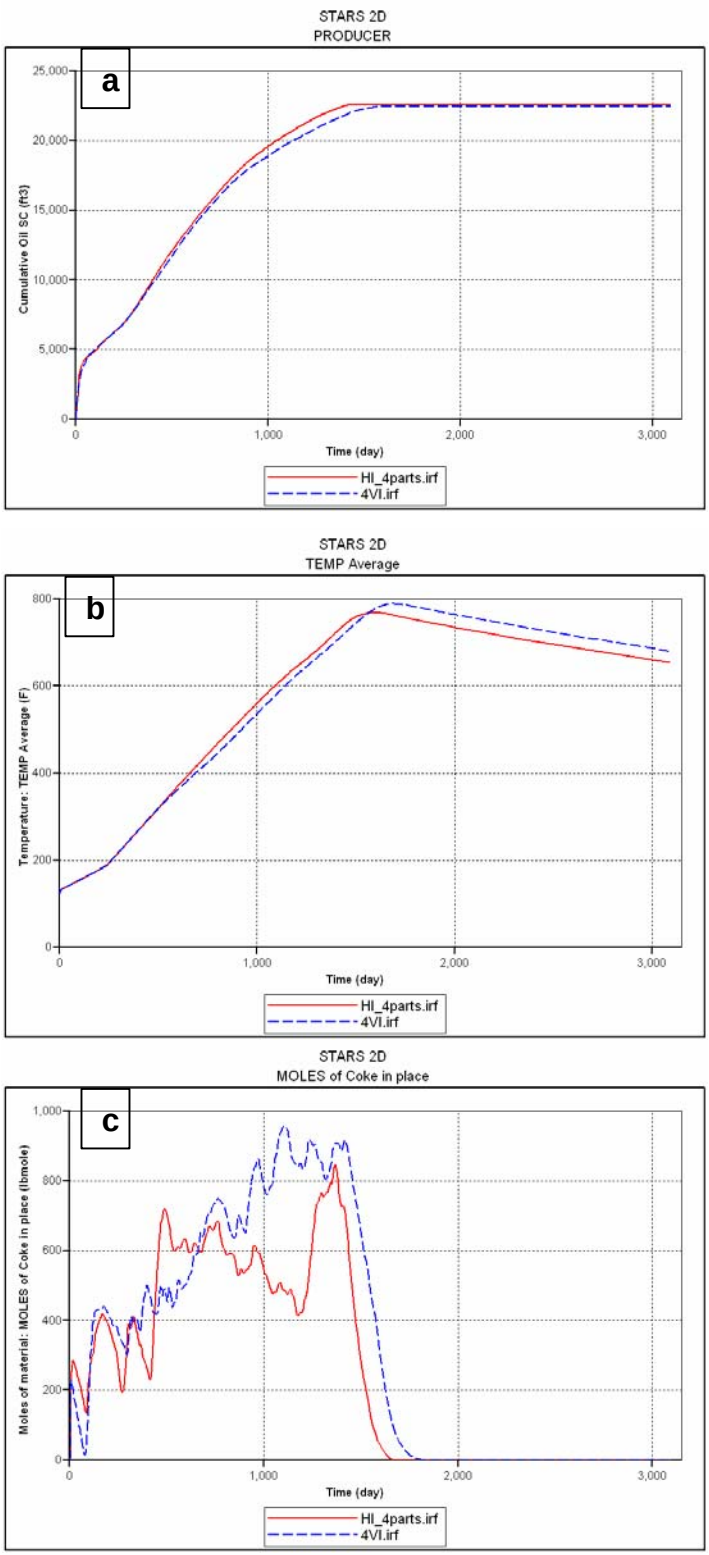

Figure 4.46: *Simulation results of comparison between the four parts horizontal injector and the four vertical injectors model: (a) cumulative oil produced, (b) average temperature profile, and (c) net coke in place.*

4.9.3 Effect of length of completion intervals for partially completed horizontal injector

The completion interval length used in the previous sensitivity runs was 18.75ft. In this sensitivity run, the effect of the completion interval length of the partially completed horizontal injector well was investigated. The previously developed three parts horizontal injector model (Figure 4.40b) was used here to develop a new model which had a three parts horizontal injector well, but where each completed interval length was now 31.25ft long (Figure 4.47).

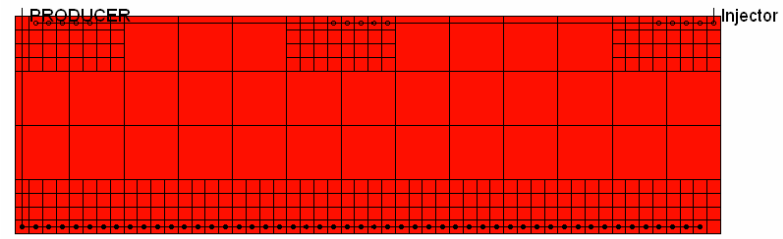

Figure 4.47: *31.25ft long completion intervals in the partially completed horizontal interval*

Table 4.10 summarises the comparison between the two models. The main observation was that the combustion process performance was the same in both models, and the change of the perforation interval length did not make any major difference in the recovery factor. The only observed difference between the two cases was the variation in the average temperature profile (Figure 4.48a), where the long perforations interval (31.25ft) model had a slightly higher overall average temperature. This was because the longer completed intervals result in initiation of three wide fire fronts at the initial stage of the process, which later on merged together to form a larger fire front compared to the smaller one developed by the 18.75ft perforation intervals model. This result in slightly more coke being deposited (Figure 4.48b), and results in an increase in the average model temperature profile.

Model name	Recovery factor (%)	Time to achieve this recovery factor (days)	Oxygen break through (days)	Final average oil saturation (fraction)
31.25ft-interval	91.9	1582	640	0
18.75-interval	91.6	1590	645	0

Table 4.10: *Simulation results of perforation interval length of partially completed horizontal injector*

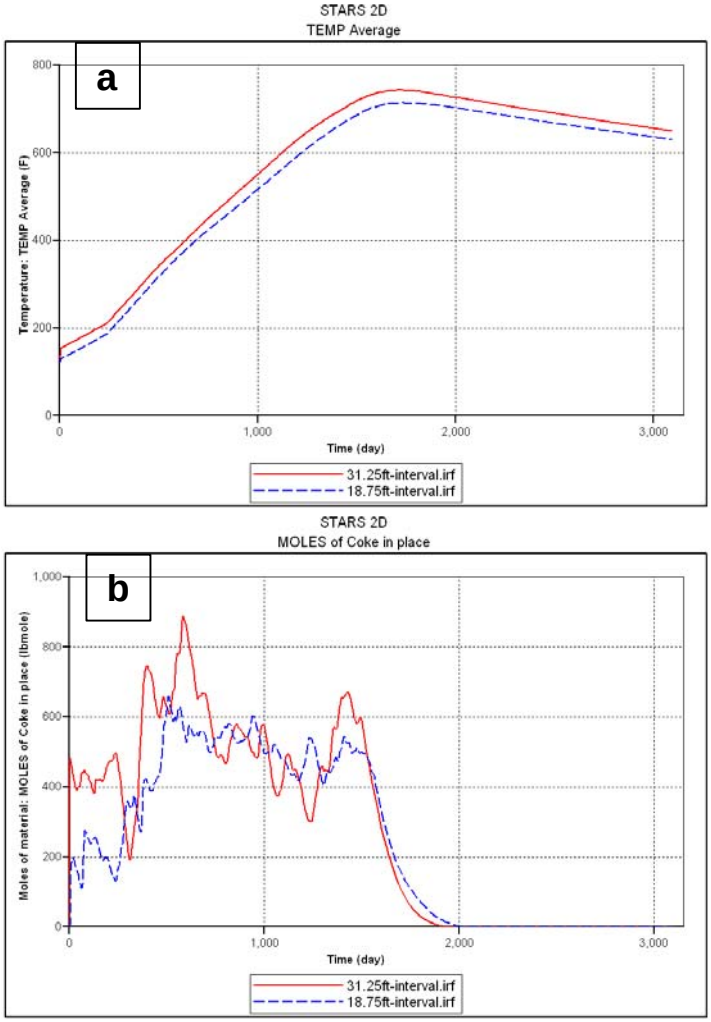

Figure 4.48: *Simulation results of perforation interval length of partially completed horizontal injector: (a) average temperature profile, and (b) net coke in place*

4.10 Application of multi lateral horizontal producer wells

Multi-lateral wells were used widely in the oil industry mainly to improve oil recovery. Such wells help to accelerate the oil production and reduce production cost (Gharsalla et al., 2008). This technology provides a commercially feasible method to develop lower grade reservoirs in terms of enhancing the cost effectiveness of such reservoirs (Roberts et al., 1997). Multi-lateral wells were largely applied in thin reservoirs under conventional drive mechanisms, and their application in heavy oil reservoirs could result in improvements in the recovery factor when a combustion process was used. In this section, a new model was developed that had two multi-lateral horizontal producers. Each well had two horizontal lateral sections and the vertical spacing between the two sections was 50ft. The horizontal lateral section length was 81.25 ft. A vertical injector was used and it was completed in the top 25ft of the model (Figure 4.49a). The results of this model were compared with the results from the 100% horizontal producer length (325ft) model (Figure 4.49b) since the total length of all the lateral sections of the multi lateral horizontal producers was 325ft.

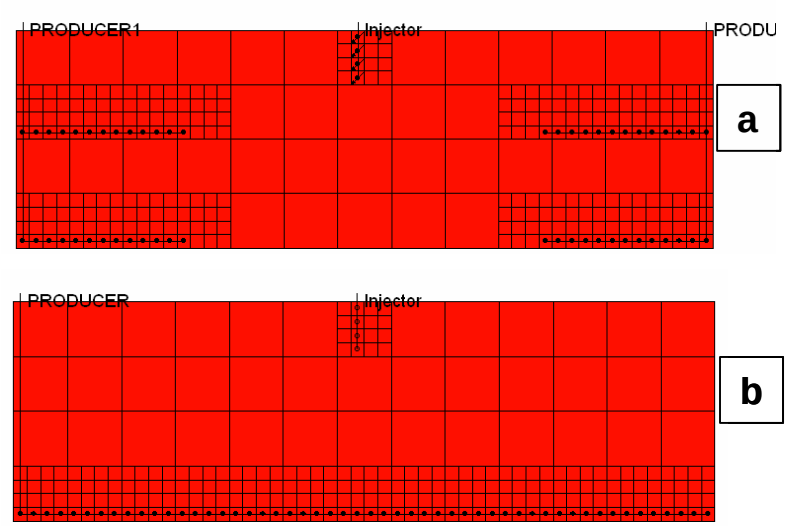

Figure 4.49: *Multi-lateral horizontal producers: (a) Multi-HP_50ft_Spacing, and (b) HP-100%*

Figure 4.50 presents the temperature distribution maps of both models at 330 days and 1095 days. The fire front development in the multi-lateral model initially was spreading

laterally in the top of the model, while moving to approach the first perforations of the upper sections of the multi-lateral producers (Figure 4.50a at 330 days). On the other hand, in the 100% horizontal producer model the fire front propagated vertically faster than it moved laterally because of the location of the horizontal producer in the bottom of the model (Figure 4.50b). At 1095 days, the combustion front managed to sweep almost all the area between the top of the model and the upper sections of the multi lateral producers (Figure 4.50a at 1095 days). However, the area between the upper section and the lower section of the multi-lateral wells was poorly swept. This was because as soon as the fire front reached the upper section, most of the injected air was been produced and circulated between the injector and the producers, which resulted in shortage of air supplies to the fire front. This led to a dramatically reduced frontal velocity, and resulted in a large mass of coke being deposited (Figure 4.51a) ahead of the front, especially after 2000 days. Moreover, the cumulative oil produced by the multi-lateral model was lower than the 100% horizontal producer case (Figure 4.51b). This was as a result of the amount of oil which was converted to coke, as well as the poor sweep efficiency of the combustion front on this model (Figure 4.51c), especially in the lower area.

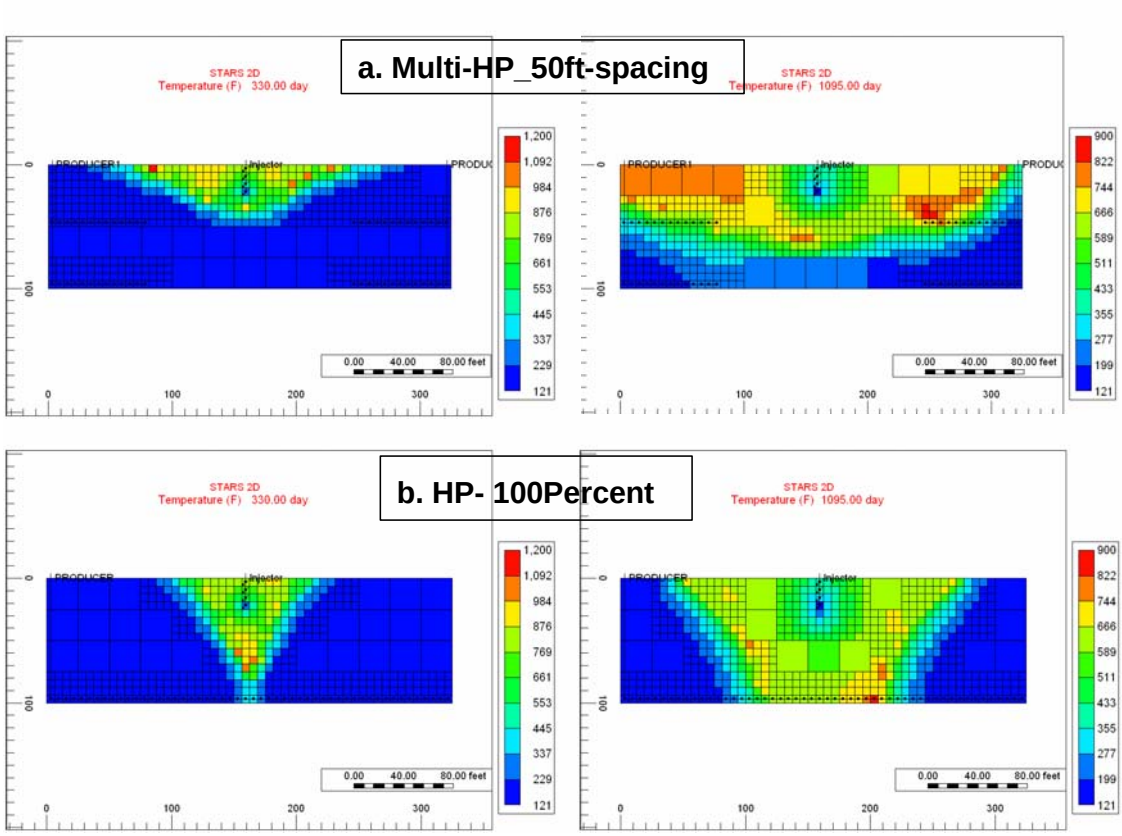

Figure 4.50: *Simulation results of temperature 330 days and 1095 days: (a) Multi-HP_50ft_Spacing, and (b) HP-100%*

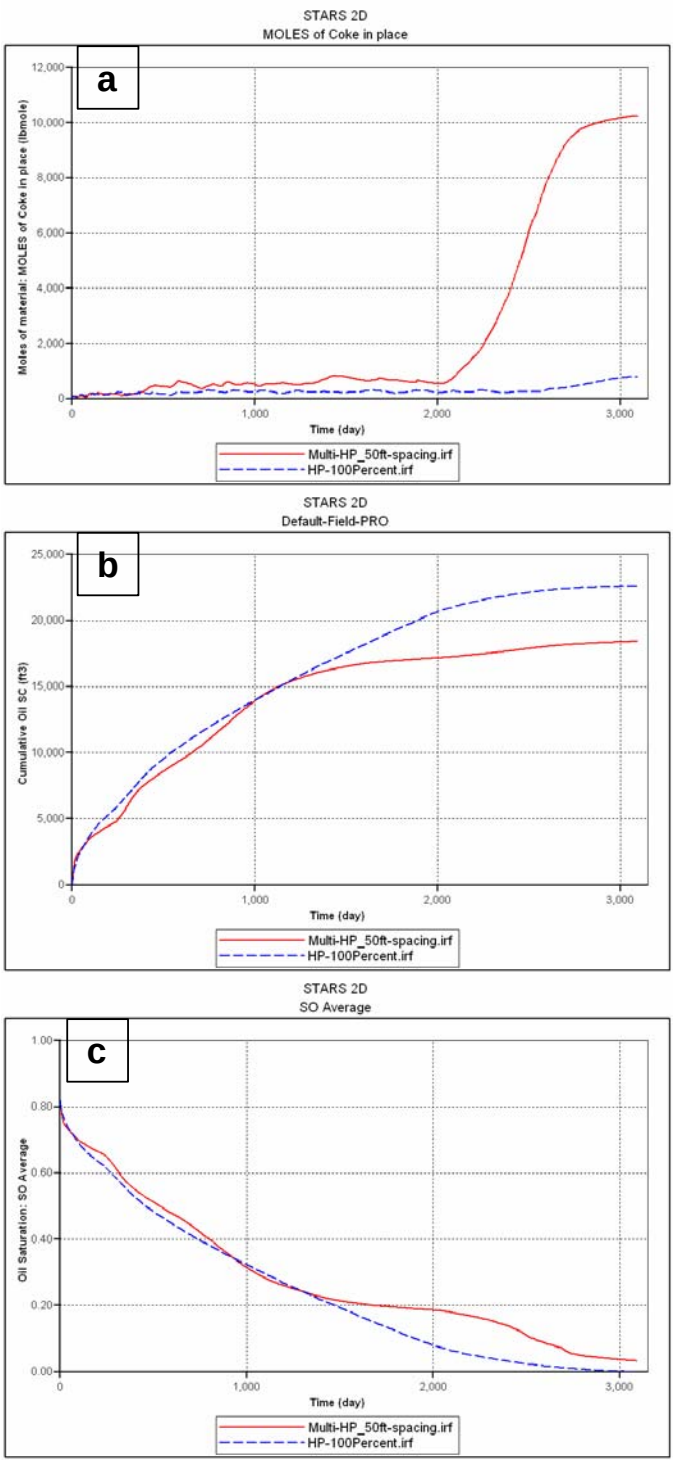

Figure 4.51: *Simulation results of multi-lateral horizontal producers: (a) net coke in place, (b) cumulative oil produced, and (c) average oil saturation. Note the rapid increase of coke deposition (a) after 2000 days of the run for the multi-lateral wells case.*

In order to mitigate the poor front efficiency in the lower area of the multi-lateral wells model, the model was run again, but this time the upper section perforations were closed when the fire front reached them at around 1600 days (Figure 4.52). This allowed the combustion front to propagate further and deeper into the model, which resulted in an improvement in the cumulative oil produced (Figure 4.53a). This was as a result of the improvement in the front velocity since air was not produced from the upper sections, which led to better front velocity and a reduced amount of coke was produced (Figure 4.53b). Table 4.11 summarises the results from the three models. The recovery factor was increased by 11.5% when the upper sections of the multi-lateral horizontal producers were closed after the front reaches them. However, even with this improvement in the recovery factor for the multi-lateral model, it was still less efficient than the performance of the in-situ combustion process when using the 100% length horizontal producer. The main outcome of this sensitivity was that the use of multi-lateral producer did not improve the recovery factor of this specific combustion process when using the 2D cross sectional model of the Nimr field.

Model name	Recovery factor (%)	Time to achieve this recovery factor (days)	Oxygen break through (days)	Final average oil saturation (fraction)
Multi-HP_50ft_Spacing	74.8	3095	443	0.03
HP-100%	91.6	3095	362	0
Multi-HP_50ft_Spacing_upper SHUT	86.3	3095	443	0.02

Table 4.11: *Simulation results of multi lateral horizontal producers comparison with the 100% horizontal producer length*

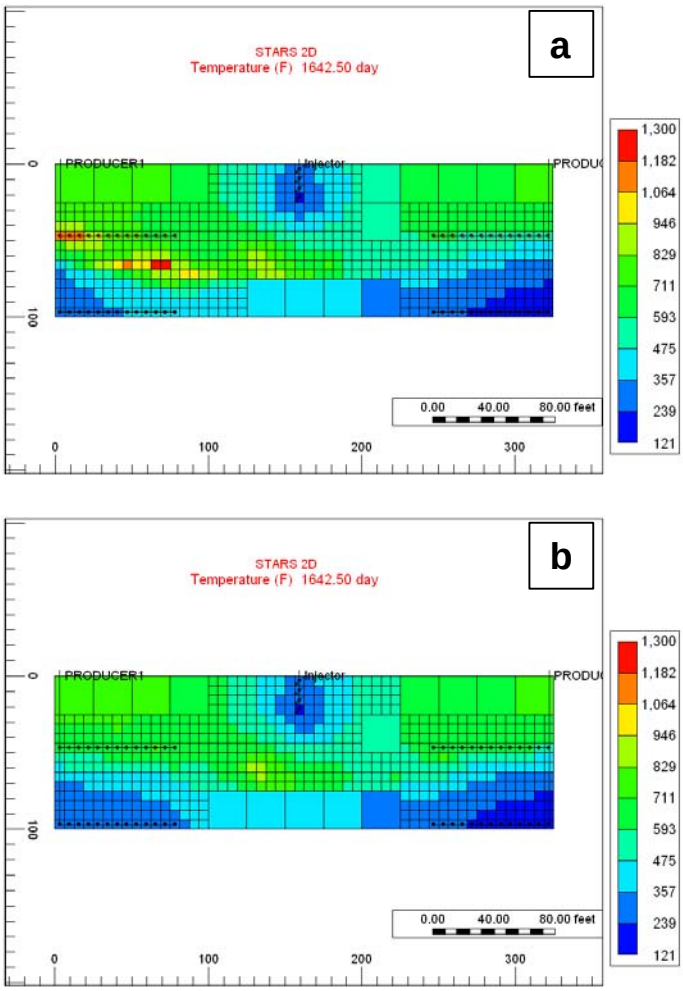

Figure 4.52: *Simulation results of temperature 1642.5 days: (a) Multi-HP_50ft_Spacing_upperSHUT, and (b) Multi-HP_50ft_Spacing*

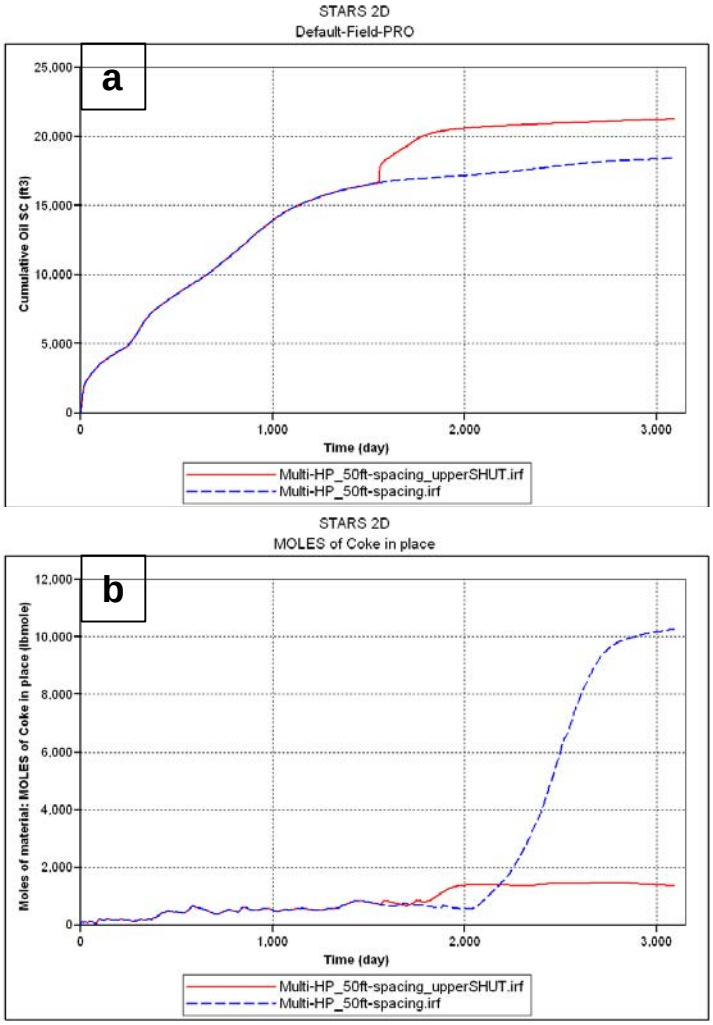

Figure 4.53: *Simulation results of multi-lateral horizontal producers when the upper section was closed: (a) cumulative oil produced, and (b) net coke in place. Note the improvement in the cumulative amount of oil production (a) as the upper section perforations of the multi-lateral well were closed.*

4.11 Application of intelligent wells for the in-situ combustion process

Akram (2008) conducted a numerical study applying intelligent wells for SAGD for Athabasca oil sands. The application of such technology helps to optimize the steam injected and enhance the economic feasibility. The key properties of using intelligent well systems were the ability to monitor and to remotely control the well completion intervals. This allows for the ability to quickly respond to any unexpected changes in the reservoir performance (Sun et al., 2008). One of the main tools used in the

completion of intelligent wells was the inflow control valve (ICV), which was a choking valve installed in the horizontal well completion, and aims to maximise recovery after unwanted fluid break through occurs. Field experience has shown the potential of ICVs, to extend the horizontal well life by extending the plateau period, minimising both water and gas coning and increasing recovery (Alkhelaiwi et al., 2007). The current advancement in technology enables the manufacturing of new types of ICVs which are designed to operate and withstand high temperature working environments (up to 500°F). This allows the implementation of intelligent well completion into thermal heavy oil recovery mechanisms such as SAGD and in-situ combustion (Halliburton, 2009).

In order to evaluate the benefits of applying intelligent completion in in-situ combustion a sensitivity analysis was conducted. The aim of this sensitivity was to test the idea of using smart completions as an in-situ combustion recovery method using the Nimr 2D cross sectional model. The main idea of implementing smart completion was to close the perforation sections of the horizontal producer when the fire front broke through to the producer. This should help to redirect the fire front to other non-swept area of the model and enhance the combustion process performance. Closing the perforations will result also in a reduction in the amount of air bypassing the front and being produced, and will increase the oxygen utilisation ratio. In this study, a vertical injector and horizontal producer well configuration was used. The vertical injector was placed in the centre of the model and completed in the top 25ft. The horizontal producer was located in the bottom layer and completed over the entire model length (325ft), as Figure 4.54 shows. The result from this model was compared with a similar model which had a normal horizontal producer.

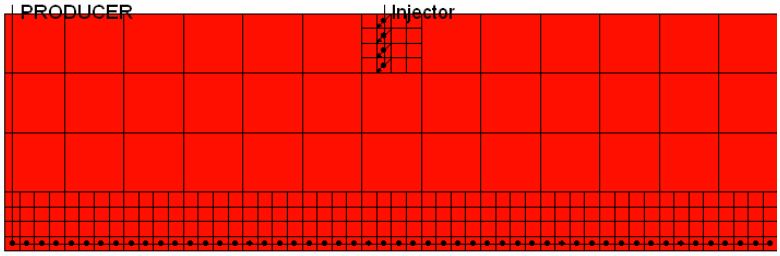

Figure 4.54: *Application of intelligent well completion for in-situ combustion*

The comparison of results for both models showed that they predicted a similar total amount of oil produced (Figure 4.55a). However the intelligent producer model managed to recover all the mobile oil in the system in 26% shorter time compared to the model with the normal horizontal producer. This was because closing the perforations when the fire front broke through led efficiently to redirect the front to other areas of the model to recover remaining oil. Figure 4.56 shows the temperature map at 1460 days for both models. For the intelligent well model (Figure 4.56a), the fire front moved to the model boundaries faster, and the temperature profile was higher in this model compared to the normal horizontal producer model (Figure 4.56b). This was as a result of closing of perforations in the middle of the producer which helped to supply air to the combustion front, which then consumed more coke and increased the temperature (Figure 4.55b). Table 4.12 shows the main simulation results of this sensitivity. The recovery factor for the intelligent well model was 0.4% less that the model with the normal horizontal producer. However, the intelligent well model managed to sweep the entire model area in much shorter time (2278 days), which saved the operating cost of further running of the normal horizontal producer for over two years for an extra 0.4% recovery. As a result of this sensitivity, the application of intelligent wells in horizontal producer model helped to accelerate the oil production and reduces the required recovery time to drain the oil in place.

Model name	Recovery factor (%)	Time to achieve this recovery factor (days)	Oxygen break through (days)	Final average oil saturation (fraction)
Intelligent - HP	91.2	2278	362	0
HP_100%	91.6	3095	362	0

Table 4.12: *Simulation results of application of intelligent well completion in in-situ combustion*

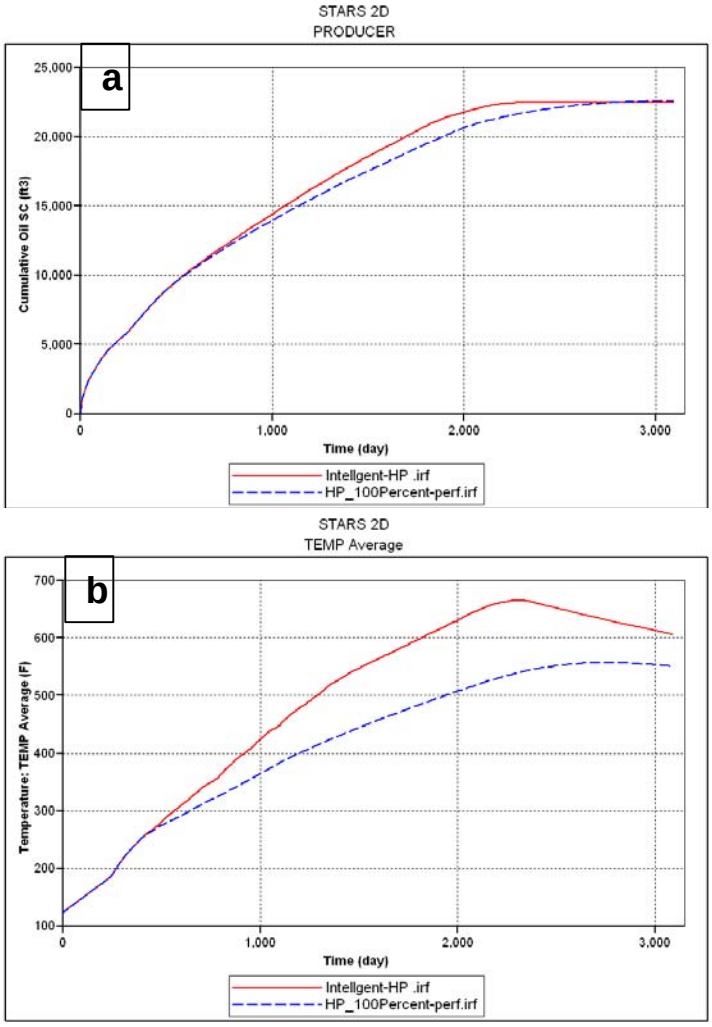

Figure 4.55: *Simulation results of application of intelligent well completion in in-situ combustion: (a) cumulative oil produced, and (b) average temperature profile*

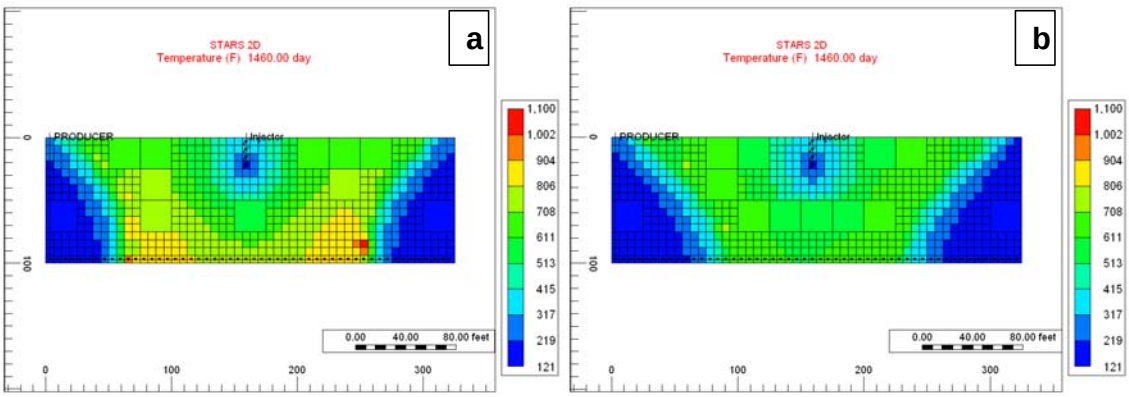

Figure 4.56: *Simulation results of temperature at 1460 days: (a) Intelligent-HP, and (b) HP_100%*

4.12 Summary

In this chapter, the performance of in-situ combustion process was investigated under various possible scenarios of well types, number of wells, well configurations, well spacing and well completions. Any change to well locations or control led to variations in the combustion process because of the sensitive nature of this type of thermal recovery method. The use of a horizontal producer introduced the mobile oil zone (MOZ) to the system, which resulted in higher recovery factors and accelerated oil production rates. Also, it helped to instantaneously produce and preserve the upgraded fraction of the oil, which resulted in a higher API gravity oil being produced. The sensitivity to the horizontal producer length showed that longer horizontal sections led to a more stiable pressure depletion gradient, which enabled the fire front to sweep the entire model area, and gave a higher recovery factor.

An essential criterion for planning in-situ combustion was well spacing. The investigation of this criterion in this chapter concluded that the shorter the distance between the injector and the producer, the faster oxygen break through occured, and the lower was the total cumulative oil production. Moreover, the well placement plan should consider the possible fire front propagation path, in order to avoid limiting fire front movement and allow access to all the oil volume. When a vertical injector well was used, it was preferable to complete the well at the top of the formation. This was to enable the fire front initiation in the top of the formation to avoid excessive coke production as a result of the fire front moving upwards under the gas override effect. Furthermore, implementation of two vertical injectors allowed for two fire fronts to be initiated, which resulted in accelerated oil production. However, it did not result in a higher recovery factor.

A horizontal well was used as an injector in this study to initiate a wider fire front. The sensitivity indicated that locating the horizontal injector in the top of the formation was preferable, as it enabled the fire front to propagate as a piston like displacement, which enhanced the recovery factor. Moreover, the length of the horizontal injector was evaluated, and it was found that the shorter horizontal injector well managed to avoid

the formation of oil banks ahead of the front, which resulted in more oil being produced and lower development costs for the injector. The use of partially completed horizontal injector resulted in several fire fronts in the formation, which resulted in a higher recovery factor. This way of completing the horizontal injector helped to achieve an economically feasible development of the in-situ combustion process, instead of having several vertical injector wells, especially in deeper reservoirs.

Numerical modelling of in-situ combustion using multi-lateral horizontal producer wells resulted in poor recovery factors. This was as a result of the air being produced and circulated out of the upper sections of the multi-lateral wells without the combustion front sweeping the bottom area of the formation. Furthermore, the use of intelligent well completions in the combustion process resulted in accelerated oil production, and a reduction in the recovery time. This was because closing the perforations led to improved propagation of the fire front to unswept regions.

The comparisons of the recovery factor of some of the main sensitivities conducted in this chapter are shown in Figure 4.57. The model which had a horizontal injector completed with two partially perforated intervals in the formation top and a horizontal producer in the bottom gives the highest recovery factor (92.1%). The model with five completion intervals in the horizontal injector, according to the results which were shown from Table 4.2 to Table 4.12, managed to achieve the shortest recovery time of 1375 days.

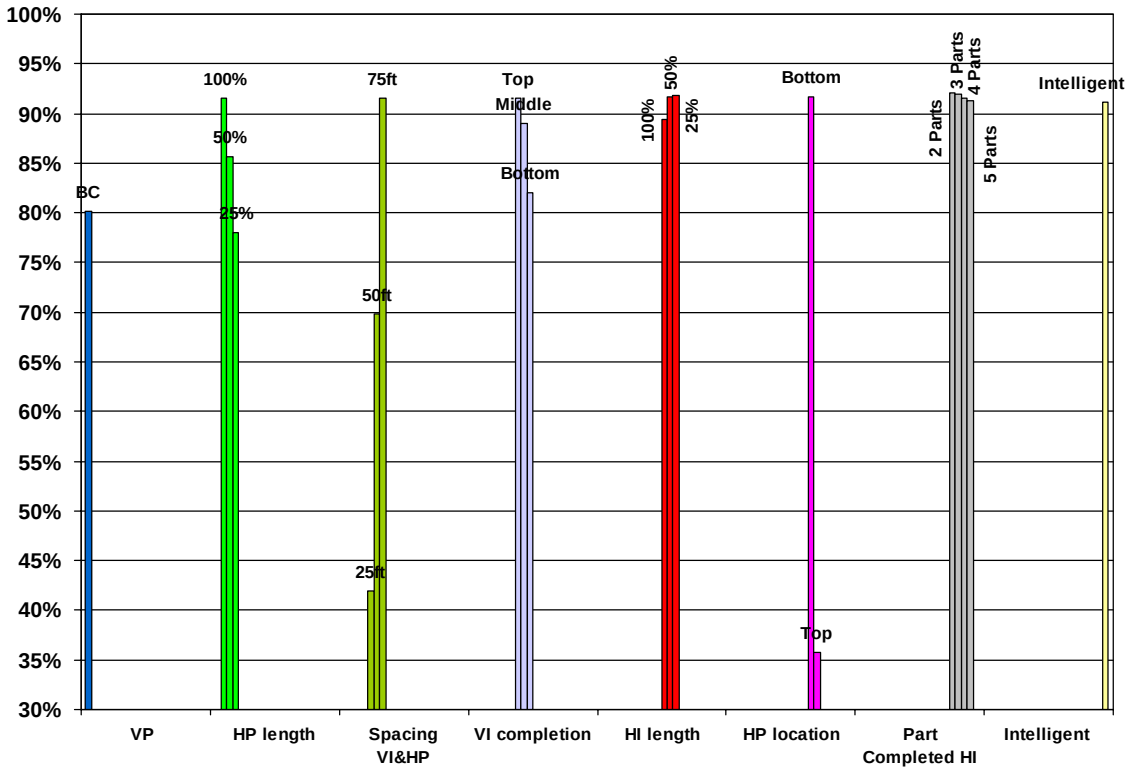

Figure 4.57: *Summary of the recovery factors achieved by some of the main scenarios which were considered in this chapter.*

Chapter 5

In-Situ Combustion Modelling of Nimr with Strong Aquifer Support

5.1 Introduction

Introducing a strong bottom water aquifer to the Nimr 2D cross sectional model will result in the introduction of a new driving force into the system. While using the in-situ combustion process to recover the oil in place, the aquifer flux will affect the performance of the combustion front. This effect could lead to variations in the process behaviour, such as changes to the fire front propagation path, the amount of fuel consumed, the front velocity, and in some cases the water flux could result in quenching of the combustion front. In this chapter, the effect of a strong bottom aquifer drive on in-situ combustion will be investigated and evaluated. Various scenarios of wells types, spacing, placement and configurations will be developed to assess the efficiency of in-situ combustion under a strong water drive mechanism. The aim was to utilise the strong pressure support from the aquifer without quenching the fire front, in order to enhance the recovery factor and improve the performance.

5.2 Aquifer drive

While a strong aquifer is considered to be a favourable drive mechanism in conventional light oil reservoirs, this is not necessarily the case in heavy oil reservoirs. This is because of the poor primary recovery of heavy oil reservoirs which are supported by strong aquifers. The recovery of heavy oil at feasible rates without producing large quantities of water is considered a primary challenge for operators of such reservoirs where a strong aquifer exists. A high rate of pressure depletion drives

fluids to the production wells, and results in upward coning of water. After water break through, the well produces oil with large volumes of water, and the water cut increases rapidly. The dramatic increase in water cut usually led to an un-profitable well operation, and results in shut in of the well. In order to mitigate this problem, the producer well should be operated under a critical oil production rate to prevent the pressure drawdown requirement from exceeding an unrealistic value. Unfortunately, in heavy oil reservoir the critical production rate may be too small to make the process feasible, due to the poor oil/water viscosity ratio and the existence of strong water aquifer support leading to excessive water production (Qin et al., 2009). Usually, in heavy oil reservoirs the critical oil production rate is very low compared to otherwise similar light oil reservoirs. This results in more water being produced in heavy oil reservoirs when the critical rate is exceeded. This means the producer well would produce heavy oil without water for just a very short time, and then the water cut increases rapidly due to the adverse mobility ratio.

5.2.1 Aquifer representation in STARS

According to the STARS manual, an aquifer can be represented numerically or by either of Carter-Tracy or Fetkovitch analytical approaches. Selection of the right aquifer water flux calculations purely depends on the actual aquifer properties. For example, since the Nimr aquifer is considered to provide a strong drive mechanism, this means that the way to define it should be as an infinite acting aquifer, to mimic the large pressure support due to the large water influx expected. Hence, a Fetkovitch analytical aquifer cannot be used here because this approach is only able to model finite aquifer systems. The numerical aquifer is one of the more accurate methods, since it provides a probable geological description of the real case. However, the drawback of using this method is the additional use of computer storage and CPU time. For larger aquifers, like Nimr, a big number of large grid blocks would be required to accurately represent the aquifer. The Carter-Tracy approximation method provides and accurate solution for this aquifer scenario. This approach also counts for both flow of oil from the reservoir to the aquifer, and, in the reverse direction, the flow of water and energy from the aquifer to the reservoir.

5.2.2 Nimr aquifer properties

Heavy oil reservoirs that have strong water aquifer support, such as Nimr, are difficult to produce. The standard development consists of producing from long horizontal wells which are usually completed in the top of the reservoir, but even with such precautions, the aquifer water will quickly cone towards the producers, the quicker the more viscous the oil is. Recovery factors are therefore low (Al-Abri et al., 2004). The main aquifer properties of the Nimr reservoir are shown in Table 5.1.

Aquifer parameter	Value
Salinity	5000 ppm
Surface density	1006 kg/m^3
Reservoir density*	1002 kg/m^3
Compressibility*	0.44e-6 /kPa
Viscosity*	0.54 cp
Length	16 km
Width	16 km
Height	800 m
Porosity	27%
Permeability	1000 mD
*at 10300 kPa, 123°F	

Table 5.1: *Nimr aquifer properties*

In order to represent the aquifer flux of a strong bottom aquifer in the 2D cross sectional Nimr simulation model, an analytical aquifer was attached to the bottom of the model. The analytical aquifer used was based on the Carter-Tracy approximation, and all its properties are summarised in Table 5.1. In order to quantify the amount of oil that could be pushed below the original oil water contact during the combustion process, some aquifer grid blocks were included in the model, as Figure 5.1 shows. Some input parameters in the 2D cross sectional model of Nimr originally developed in chapter 3 were changed to enable introduction of the aquifer in the model. Principally, the producer well completion interval was moved from being originally in the bottom of the model to being in the middle section of the model (Figure 5.1) in order to reduce water

production. Also, the bottom hole pressure (BHP) control of the producer needed to be increased from the original 500psi in the BC model. In order to change this parameter, a sensitivity calculation was conducted using the aquifer model where the producer BHP value changed from 500psi to 1,300psi. The reason for considering a higher BHP value was to reduce the pressure difference between the upstream and downstream of the model and reduce the overall drawdown in the system. This will help to avoid rapid increase of the water influx into the model and rise in water out. Figure 5.2 presents both the temperature profiles and the ternary saturation plots for both BHP models at 455 days. The main observation was that in the lower BHP (500psi) case, the fire front propagated faster than the case where higher BHP was used, this resulted in earlier front break through into the producer well. This was due to the large pressure drawdown in the 500psi scenario. However, this large drop in pressure in the model between the injector and producer resulted in the fire front being quenched at an earlier time (around 715 days), which was due to the significant amount of water influx in the oil zone (Figure 5.2). The quenched time can be determined from the net coke in place and it was indicated when the curve remained straight as shown in Figure 5.3a. Furthermore, the lower BHP case managed to produce around 30% more cumulative oil than the higher BHP case as shown in Figure 5.3b. However, this came at a price, which was that the model with 500psi BHP produced eight times more cumulative water than the case in the 1,300psi BHP model (Figure 5.3c). This sensitivity showed the importance of choosing the right BHP to allow a modest pressure drawdown in the system, in order to avoid quenching of the combustion process and to avoid producing significant amount of water. For the purpose of this study 1,300psi BHP was used in the aquifer model as the producer well control mode. This model will be considered as a base case cross sectional model of the Nimr field for the remainder of this chapter and the well controls are shown in Table 5.2.

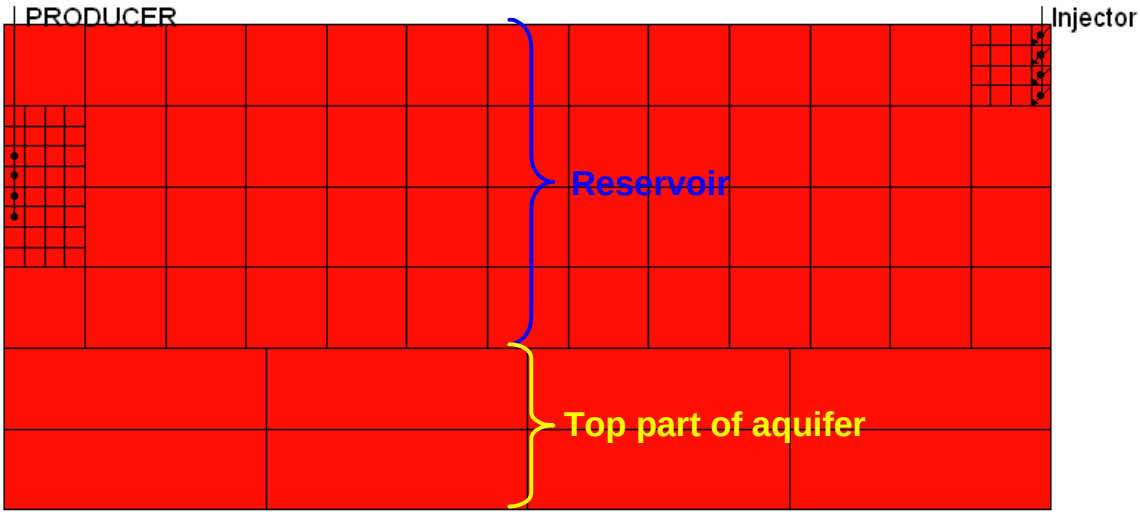

Figure 5.1: *2D cross sectional Nimr aquifer base case model*

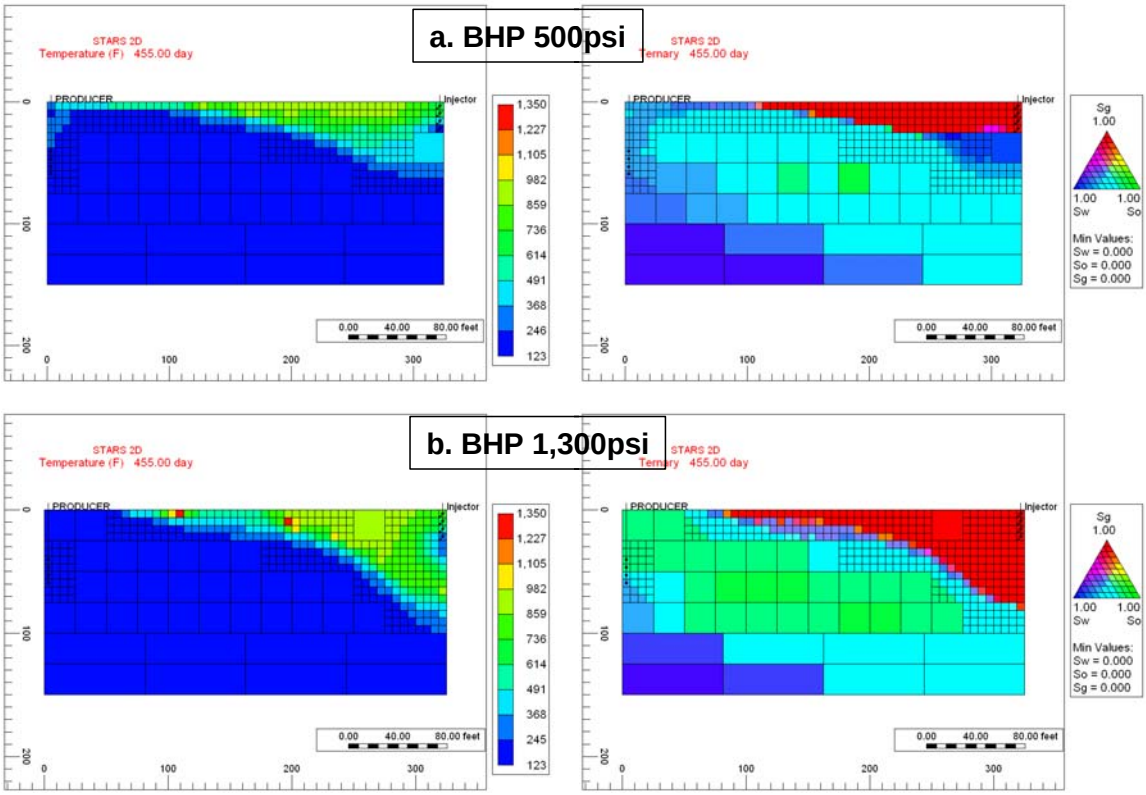

Figure 5.2: *Simulation results of temperature and ternary saturation plots at 455 days: (a) producer with BHP 500psi, and (b) producer with BHP 1,300psi*

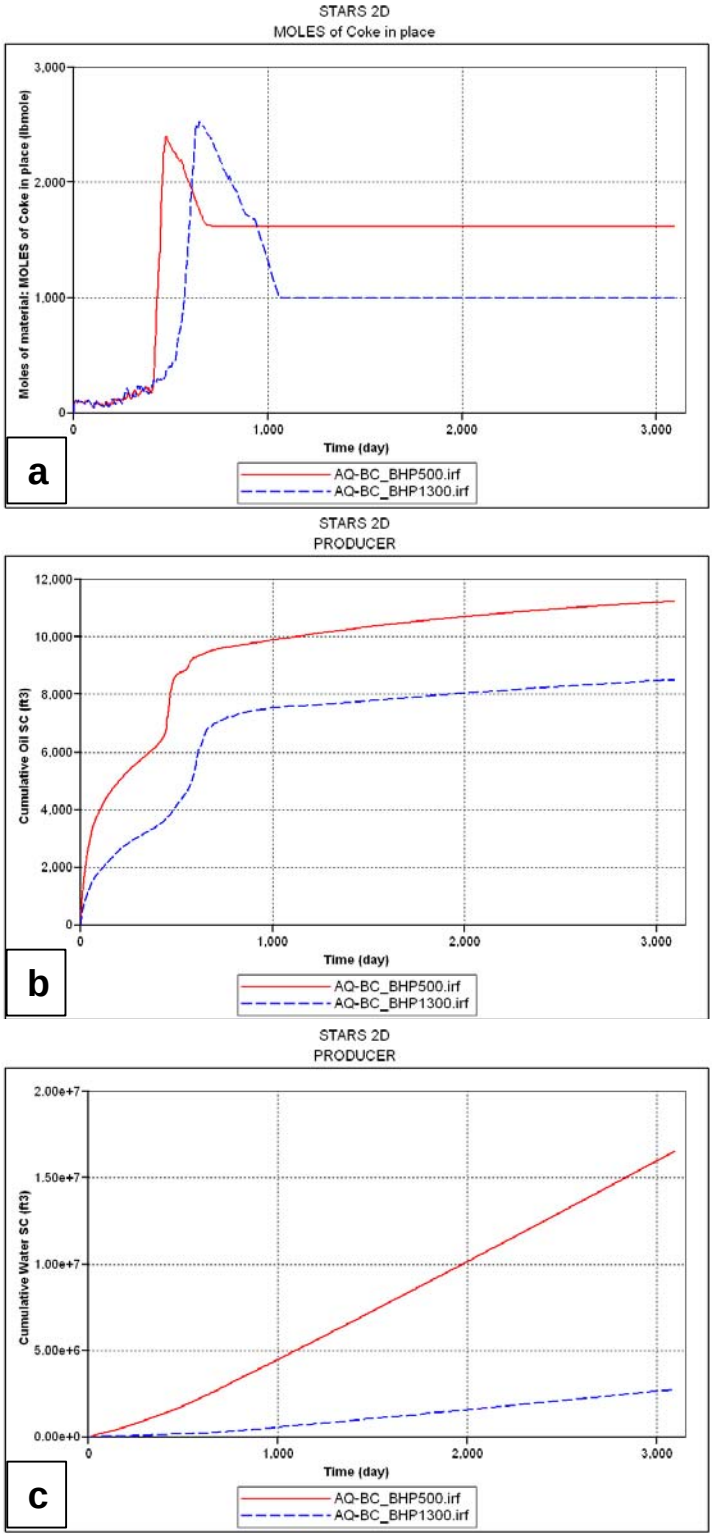

Figure 5.3: *Simulation results of producer well control (BHP): (a) net coke in place, (b) cumulative oil produced, and (c) cumulative water produced.*

Injector well	Air injection rate of 7,200ft^3/day for the first 240 days and 14,400 ft^3/day thereafter
Producer well	Bottom hole pressure of 1,300psi
Simulation duration	3095 days

Table 5.2: *Summary of the Aquifer BC model's well controls (no pressure limit on injector well)*

5.3 Effect of vertical injector and producer completion intervals

The fire front initiation and propagation was affected by the way both the injector and producer wells were completed, as observed in the previous chapter. Introducing the aquifer to the in-situ combustion process in the simulation model led to a change in the balance of forces in the model, which directly affected the combustion process performance. In this section, the effect of changing both vertical injector and producer wells on the performance of in-situ combustion where there is strong aquifer support was investigated.

5.3.1 Effect of vertical injector completion when vertical producer is completed only in middle

The base case model used in this chapter had two vertical well configurations (Figure 5.1). The producer was completed in the middle 25 ft of the model to delay water break through, whereas the vertical injector was completed in the top 25ft of the model. In order to evaluate the effect of the vertical injector completion on the behaviour of the fire front, two more models were developed, where the vertical injector was completed in the middle (Figure 5.4b) and in the bottom (Figure 5.4c) in the second model.

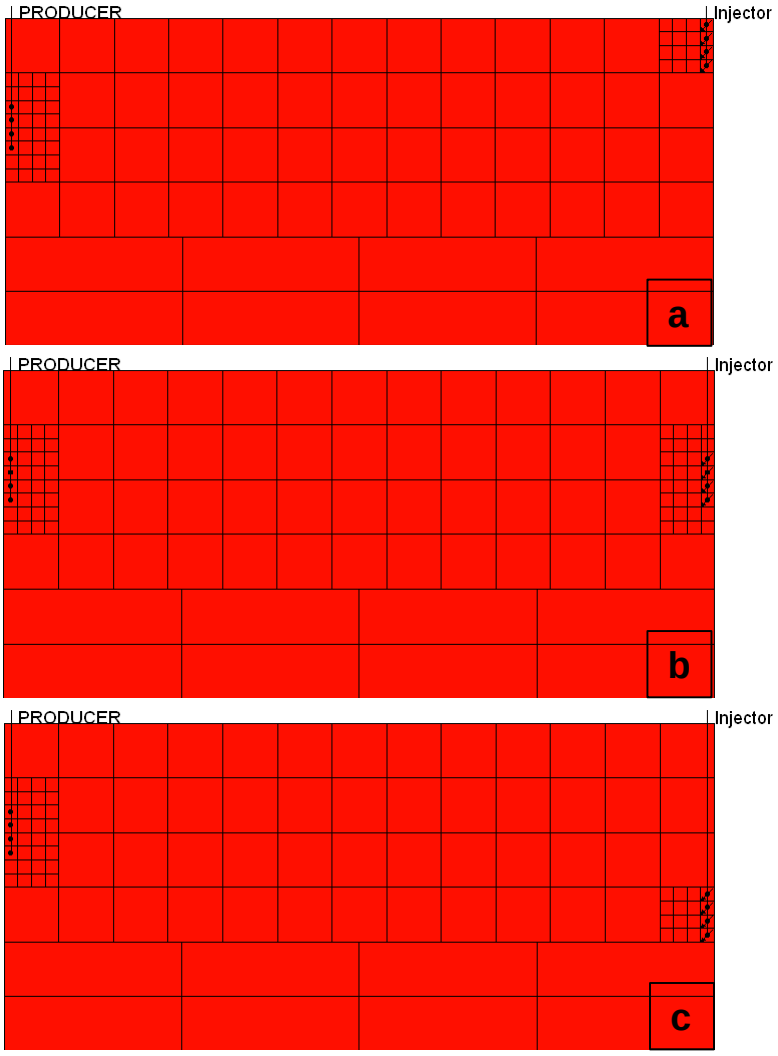

Figure 5.4: *Vertical injector well completion intervals: (a) VI-TopPerf, (b) VI-MiddPerf, and (c) VI-BottPerf*

There were several common observations from this sensitivity. In all the three models, the fire front was successfully initiated, and then it started to propagate vertically due to both the gas override effect and the massive water influx from the aquifer, as Figure 5.5 shows. The high water saturation ahead of the front was noticeable from the saturation ternary map (Figure 5.5), and it was as a result of two factors. First, the water produced from the oxidation combustion reactions increased the water saturation ahead of the front, which resulted in an increase in the relative permeability to water. The second factor was that after the relative permeability of water increased, water became more mobile, which allowed the aquifer influx to flow ahead of the front.

Generally in all the three models, the fire front was quenched as soon as the fire front broke through to the vertical producer well, because after that time the fire front could not propagate downwards against the large aquifer influx. The quenching time varies from model to model because of the way the vertical injector was completed. However, the net coke in place curve (Figure 5.6a) can be used to determine the approximate quenching time for each model, which occurred when there were no more changes in the net coke produced. For example, in the bottom completed vertical injector model, the fire front managed to be sustained for a longer time (1334 days) compared to the other two models. This was because the fire front was ignited at the bottom of the model and then it took a longer time to propagate to the model upper area because its movement against gravity reduced the front velocity and resulted in more coke been produced (Figure 5.6a), which allowed for longer front sustainability.

The total produced oil (Figure 5.6b) from each model was mostly as a result of the combination of both the fire front and the aquifer influx. However, when the fire front was quenched, further oil production was mainly due to the aquifer drive. The aquifer water flowed into the oil zone and started to sweep oil from that area under the pressure drawdown of the vertical producer. Also, the water influx swept some of the areas behind the fire front, which resulted in convertion of the water into steam, as in the case of the wet in-situ combustion process. This steam usually helped to recover the heat stored in the formation rocks behind the front, and led to extra energy being available to reduce crude viscosity. However, unlike the wet in-situ combustion process where the amount of injected water is controlled, here the strong aquifer drive resulted in more water flowing and led to quenching the fire front which reduced the overall model temperature and no more steam was generated.

Table 5.3 shows the main results of this sensitivity. The recovery factor of the middle completed vertical injector model was the highest compared to the other two cases. This was because of the way the fire front was initiated in the middle of the model, and then propagated throughout the model, managing to sweep the entire area of the model and at the same time produced less coke in place. Hence, for these specific configurations, it was preferable to complete the vertical injector in the middle section of the model.

Model name	Recovery factor (%) @ 3095 days	Recovery factor @ quenched time (%)	Front quenched time (days)	So @ 3095 days (fraction)	So @ quenched time (fraction)
VI-TopPerf	34.6	30.9	1133	0.31	0.33
VI-MiddPerf	47.0	33.7	1095	0.26	0.33
VI-BottPerf	45.3	40.9	1334	0.23	0.25

Table 5.3: *Simulation results of vertical injector completion intervals sensitivity*

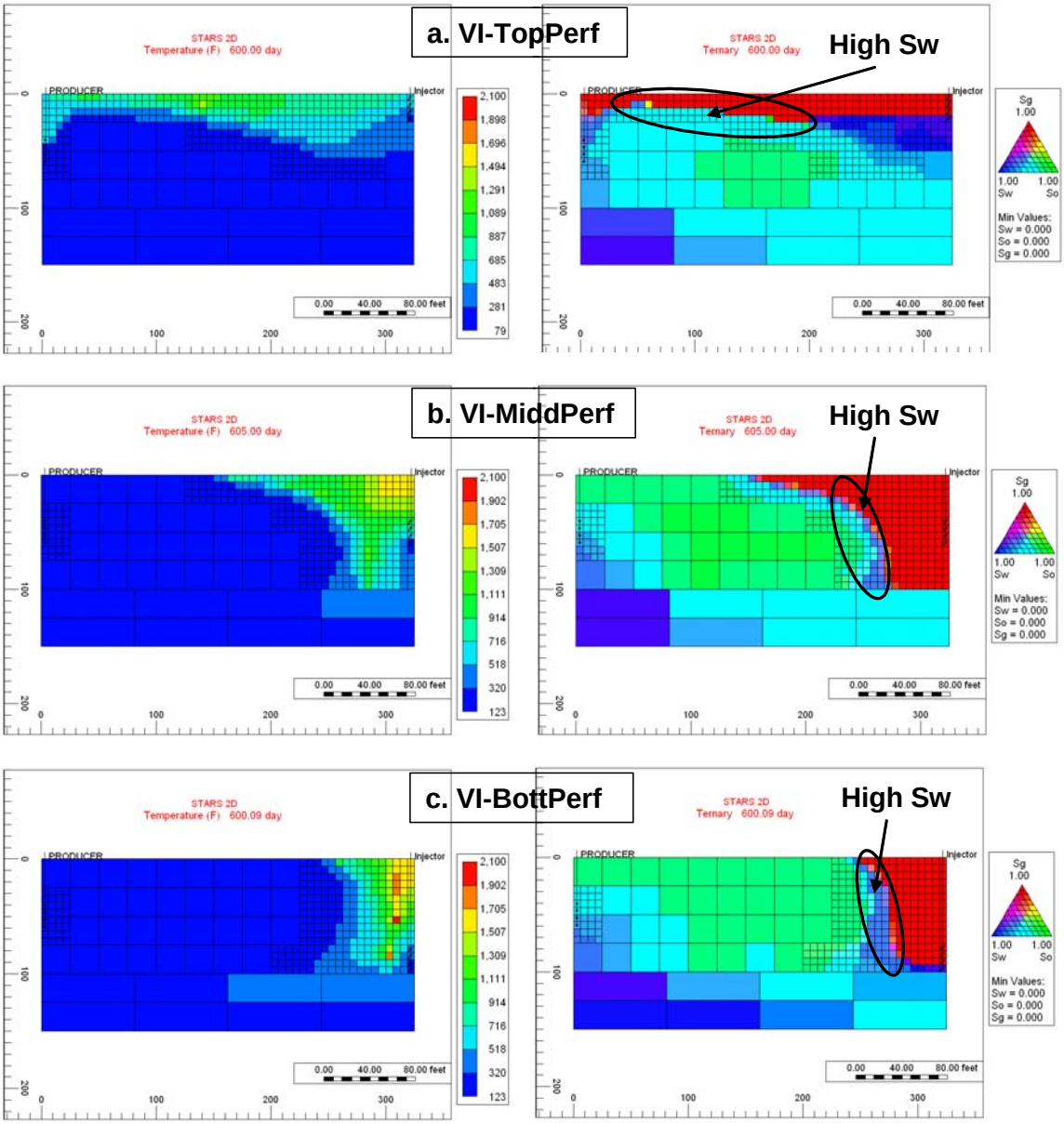

Figure 5.5: *Simulation results of temperature and ternary saturation plot at 600 days: (a) VI-TopPerf, (b) VI-MiddPerf, and (c) VI-BottPerf. Note the variation in the combustion front shapes as the vertical injector completion intervals changes.*

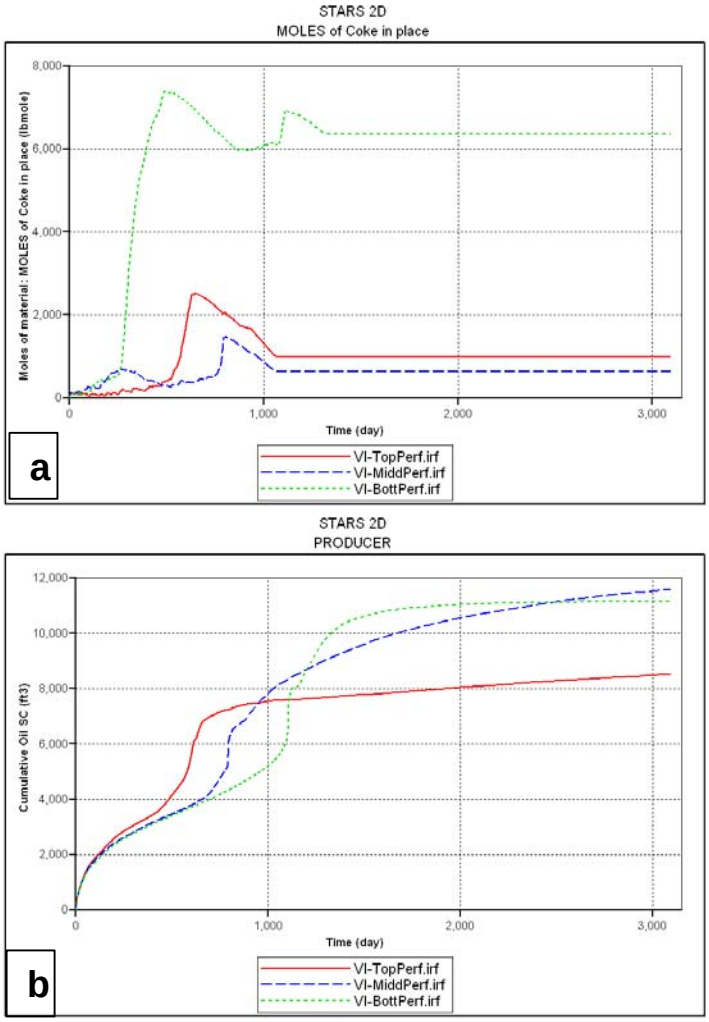

Figure 5.6: *Simulation results of vertical injector completion intervals: (a) net coke in place, and (b) cumulative oil produced.*

5.3.2 Effect of vertical producer completion when vertical injector is completed only in middle

This sensitivity aimed to investigate the effect of the vertical producer completion interval on the combustion process. The previous sensitivity showed that to complete the vertical injector in the middle of the model resulted in better front sweep efficiency while having the vertical producer completed in the middle of the model as well (Figure 5.7a). Here, a new model was developed where the vertical producer was completed on the top of the model (Figure 5.7b) to evaluate fire front performance.

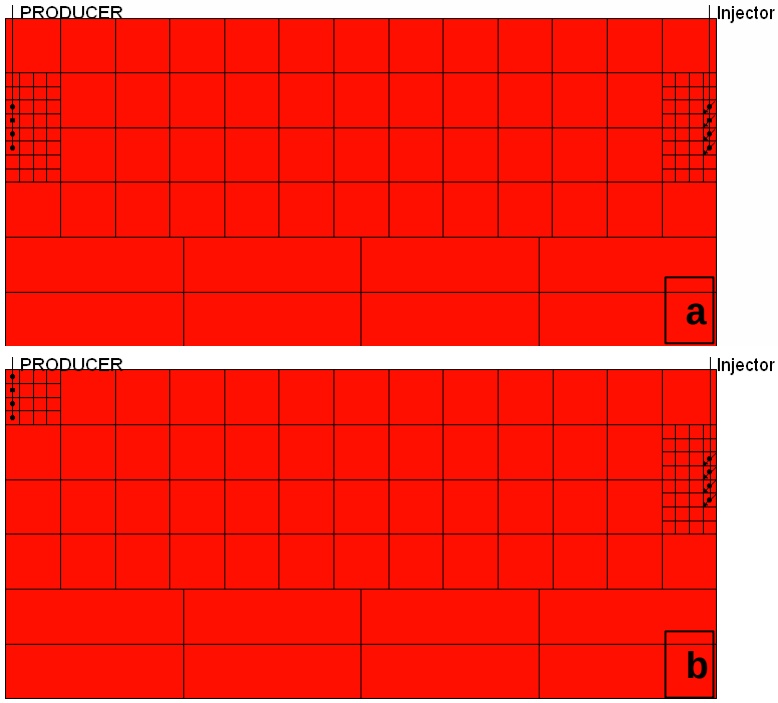

Figure 5.7: *Vertical producer well completion intervals: (a) VP-MiddPerf, and (b) VP-TopPerf*

Figure 5.8 shows the temperature distribution of both models at 665 days and 803 days. The fire front propagation plots for both models were identical at 665 days. This was because both fronts were ignited in the middle sector of the model. However, at a later time step (803 days) the advance of the combustion fronts for both models were totally different. This was as a result of the fire front on the top completed vertical producer model breaking through earlier to the producer, which resulted in quenching of it at around (773 days). Whereas, for the middle completed vertical producer model, the front was sustained for a longer time, and the break through was delayed because of the front needed to move downward to reach the top perforations of the producer. Since the movement was against the water influx from the aquifer, it resulted in a slowing of the fire front velocity and led to larger amounts of net coke in place being produced (Figure 5.9a). The total recovered oil from both models was shown in Figure 5.9b and the middle completed producer model had produced slightly more oil because the front managed to be sustained for longer time and swept larger areas. However, the total amount of water produced by the middle completed vertical producer model was twice the amount produced by the top completed producer model (Figure 5.9c). This was mainly due to the shorter distance between the middle completed producer and the

aquifer. This also resulted in early water break through occurring. Table 5.4 summarises the main results of this sensitivity.

Model name	Recovery factor (%) @ 3095 days	Recovery factor @ quenched time (%)	Front quenched time (days)	So @ 3095 days (fraction)	So @ quenched time (fraction)
VP-MiddPerf	47.0	33.7	1095	0.26	0.33
VP-TopPerf	46.2	31.7	773	0.27	0.34

Table 5.4: *Simulation results of vertical producer completion intervals sensitivity*

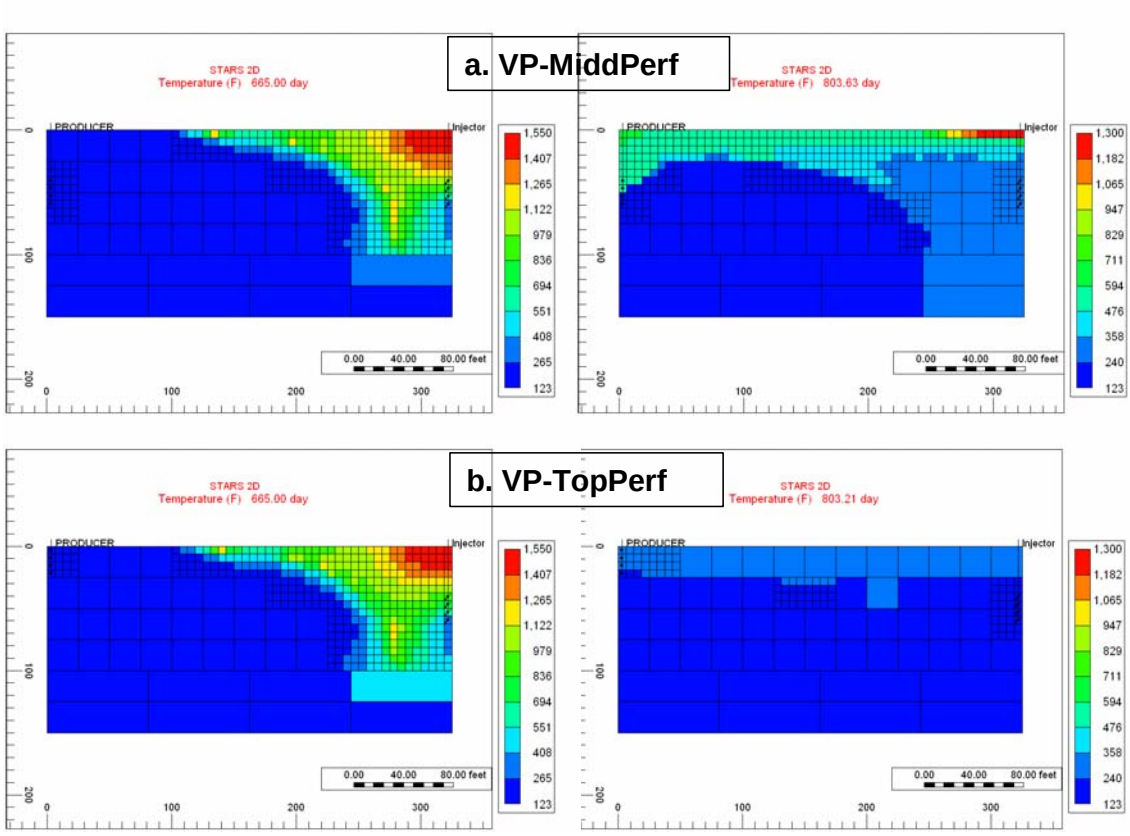

Figure 5.8: *Simulation results of temperature at 665 and 803 days: (a) VP-MiddPerf, and (b) VP-TopPerf*

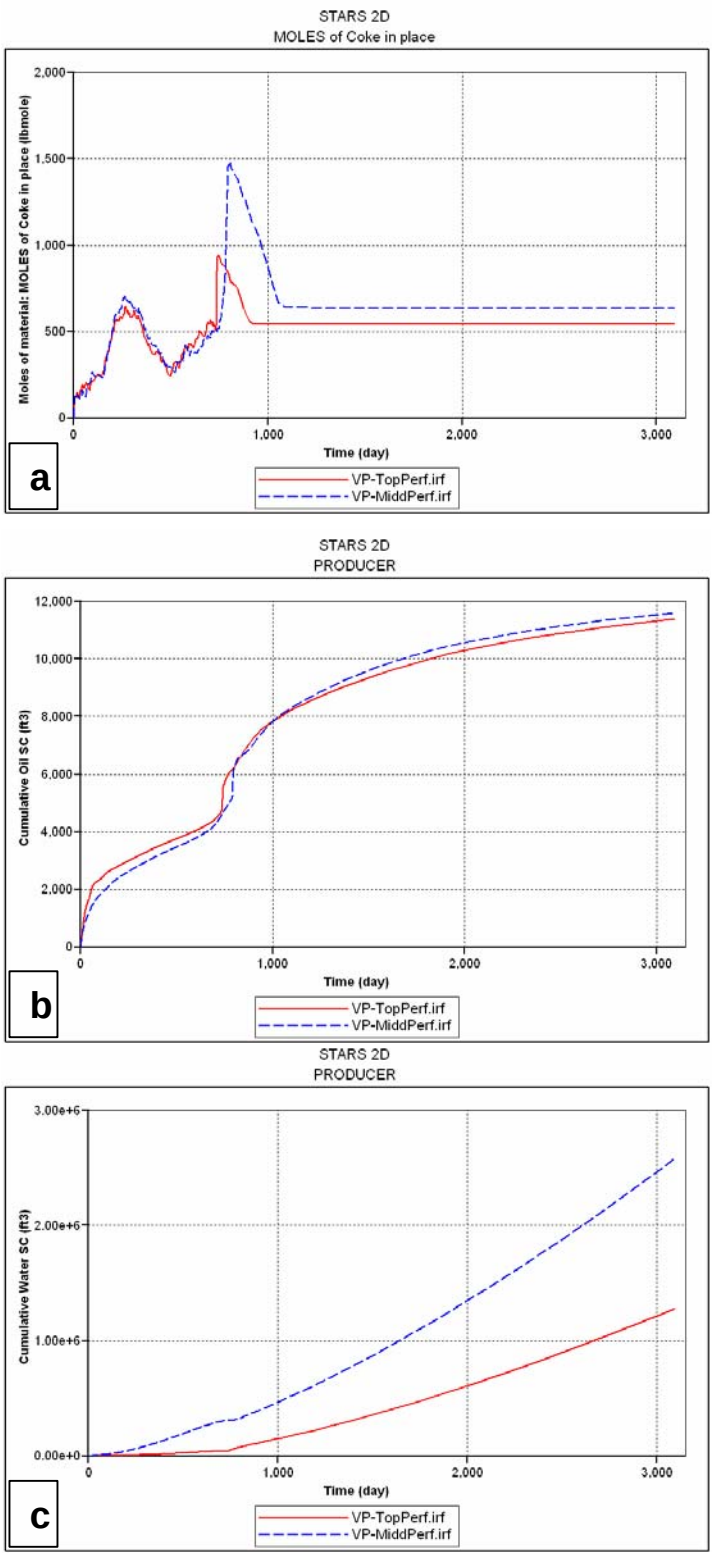

Figure 5.9: *Simulation results of vertical producer completion intervals: (a) net coke in place, (b) cumulative oil produced, and (c) cumulative water produced.*

5.4 Horizontal producer application

The chapter of this thesis that addresses well configurations (chapter 4) showed that using a horizontal instead of a shorter vertical producer enhanced the combustion process in terms of introducing a more gradual pressure gradient change in the model, especially in the 100% long horizontal producer case, which allowed the fire front to sweep a larger area and resulted in a higher recovery factor. In this section, a horizontal producer was introduced to the combustion process when a strong bottom aquifer existed, while using a vertical injector completed in the model's bottom section. The effect of using such a producer will be investigated, and later on in this section the optimisation of the horizontal producer length will be performed.

5.4.1 Effect of using horizontal producer completed at top

For this section two models were developed. The first model had a vertical producer which was completed in the top 25ft of the model (Figure 5.10a) and the second model had a 312.5 ft long horizontal producer completed in the extreme top layer of the model (Figure 5.10b). The reason of completing both producer wells in the top of the model was to delay the water break through as much as possible to allow for much earlier oil production.

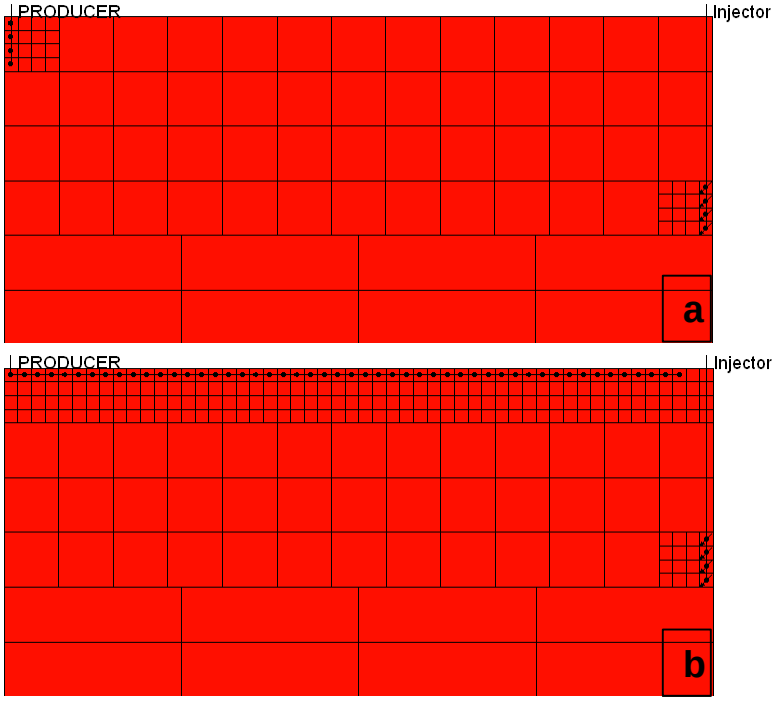

Figure 5.10: *Comparison between both horizontal and vertical producer wells: (a) VP-TopPerf, and (b) HP-100Top*

The simulation results for this sensitivity showed that as soon as the fire front was ignited in the horizontal producer model, it managed to be sustained for just 150 days, as the net coke in place Figure 5.11a shows. After that, the front was quenched because it started to propagate upwards to break through to the nearest horizontal producer perforations due to the short distance between the vertical injector and the toe of the horizontal producer. Figure 5.12 shows the temperature maps of both models at 40 days and 695 days. For the horizontal producer case at 40 days, the fire front was initiated and then started moving upward, whereas at 665 days the model temperature was the same as the initial temperature, since the front was quenched around 150 days. For the vertical producer model, the front was sustained for a much longer time because of the longer distance between both the injector and the producer wells, and continued until broke through into the producer at around 1260 days. There were two main reasons for the combustion front being quenched when it broke through to the producer. The first reason was that large volumes of water presented around the producer, mainly due to the water influx from the aquifer, and this occurred as a result of the pressure drawdown in the model. This high water saturation results in the front being quenched. The second reason was the shortage of air supply to the fire front when it moved away from the

producer after break through occurred. This was because air followed the path of least resistance, which was from the injector to the producer perforations, and then it continued to circulate between the wells instead of supporting the front movement away from the producer. Figure 5.11b shows the cumulative oil produced by both models. The horizontal producer model managed to produce more oil and had a recovery factor of 42.6% (Table 5.5) just on 150 days before the front quenched. On the other hand, the recovery factor of the vertical producer model reached 36.1% in the total 1260 days before the front was quenched. The higher recovery factor of the horizontal producer model was due to the larger contact area between the horizontal well and the formation when compared to the vertical producer. The ultimate recovery factor for the horizontal producer at the end of the model run at 3095 days was 70.6%, which indicates the opportunity to use horizontal producer in such a combustion process, even when a strong aquifer exists. However, the horizontal producer scenario did produce a large volume of water over five times the case where the fire front was sustained in the vertical well scenario (Figure 5.11c). It would be better if the combustion front could be sustained for a longer time in the horizontal producer case. This would enable larger areas of the model to be swept by the front and a higher recovery factor could be achieved, and at the same time the amount of water produced would be decreased. This is mainly due to an increase of gas saturation ahead of the front toward the producer well as a result of the flu gases being produced by combustion process which will reduce the water influx propagation toward the producer. To achieve this, the horizontal producer should be carefully located and completed far away from the vertical injector. This sensitivity calculation showed that the high recovery factor achieved by the horizontal producer did come at a price, which was the large volume of water produced, and the cost of treating and handling such a large amount of water. This issue should always be considered when planning to use horizontal producers in such systems.

Model name	Recovery factor (%) @ 3095 days	Recovery factor @ quenched time (%)	Front quenched time (days)	So @ 3095 days (fraction)	So @ quenched time (fraction)
VP-TopPerf	46.4	36.1	1260	0.23	0.28
HP-100Top	70.6	42.6	150	0.16	0.31

Table 5.5: *Simulation results of comparison between both horizontal and vertical producer wells*

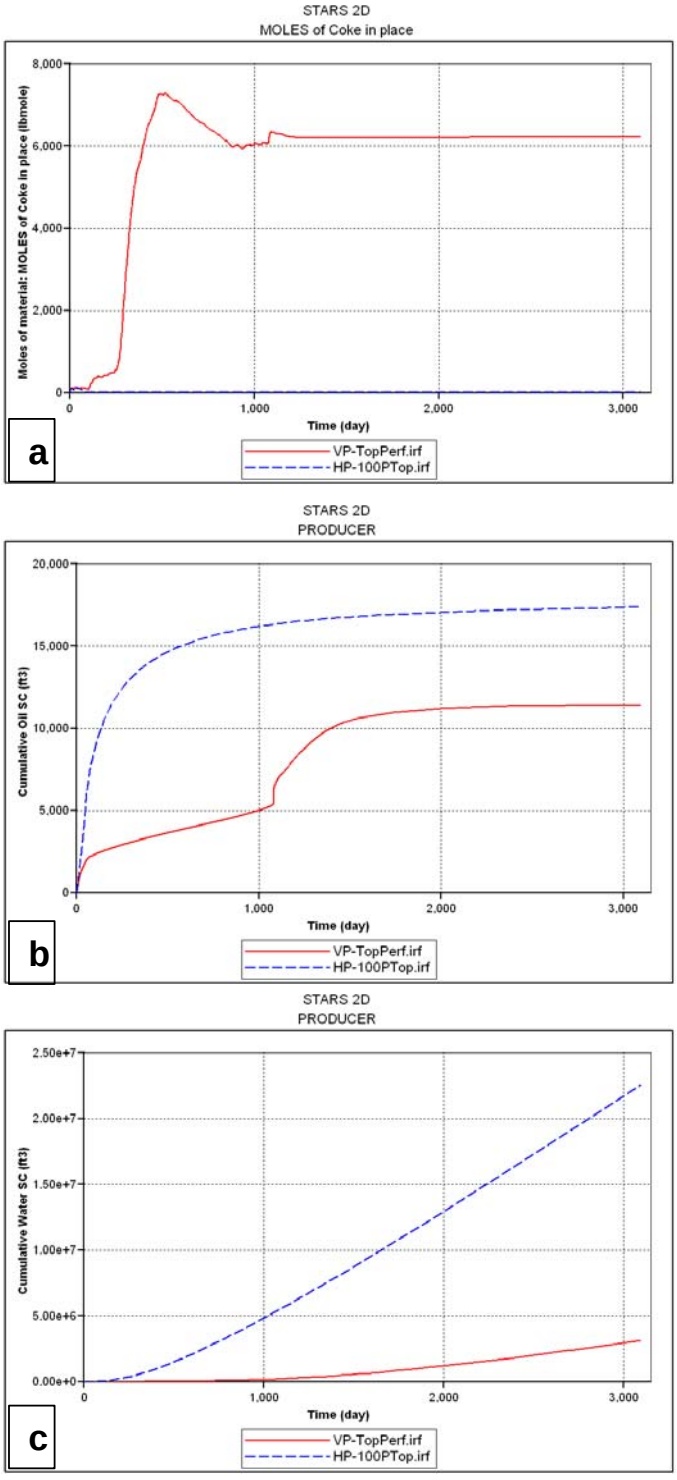

Figure 5.11: *Simulation results of comparison between both horizontal and vertical producer wells: (a) net coke in place, (b) cumulative oil produced, and (c) cumulative water produced.*

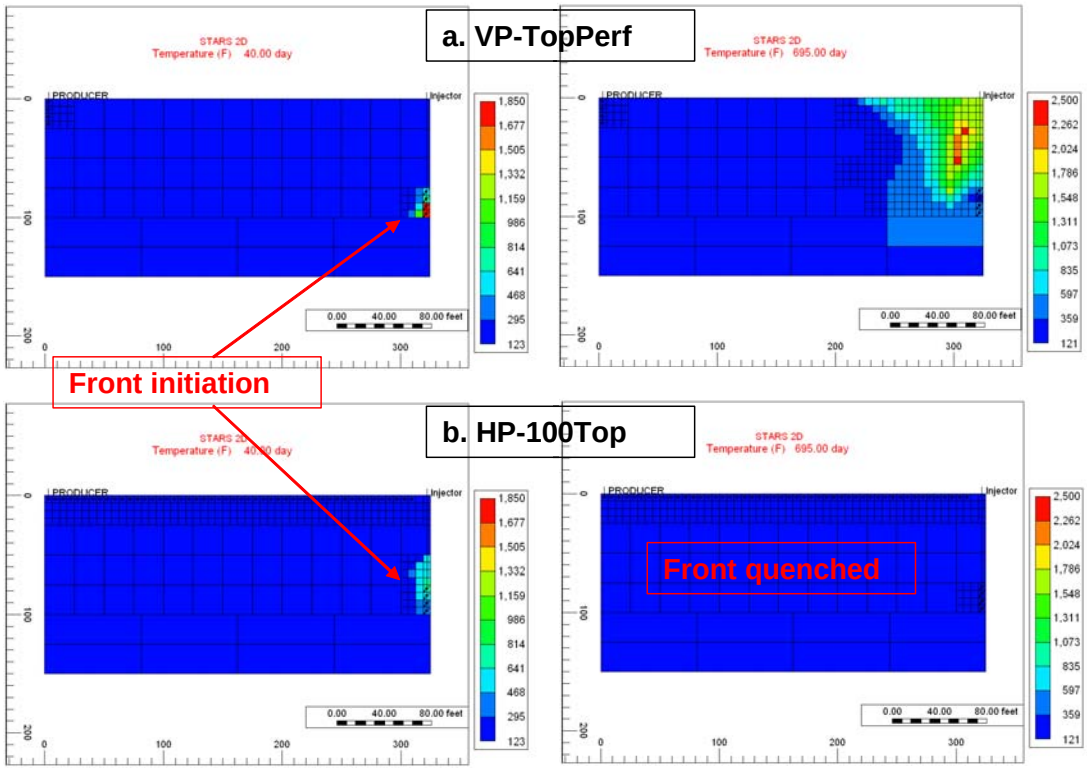

Figure 5.12: *Simulation results of temperature at 40 and 695 days: (a) VP-TopPerf, and (b) HP-100Top*

5.4.2 Optimisation of length of horizontal producer completed at top while using vertical injector

The use of a horizontal producer which was completed in the top of the model results in a high recovery factor compared to the vertical producer case. However, it also led to a shorter life for the combustion front. In order to further investigate the effect of using a horizontal producer well in the combustion process, and to obtain the optimum horizontal section length, two new models were developed. The first model had a 162.5 ft long horizontal producer (HP-50%Top) and the second model a 81.25 ft horizontal well length (HP-25%Top), as Figure 5.13 shows.

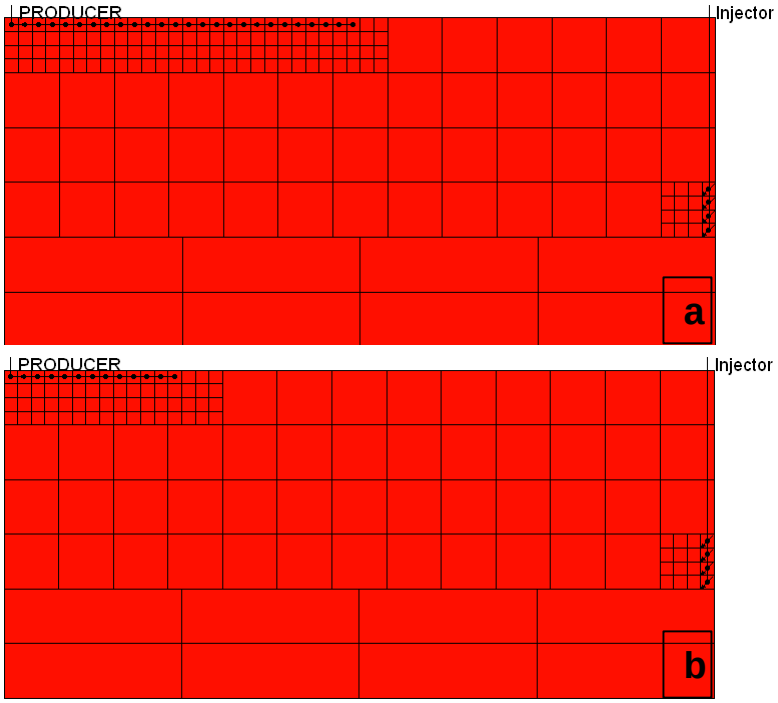

Figure 5.13: *Optimisation of horizontal producer wells length: (a) HP-50%Top, and (b) HP-25%Top*

This sensitivity results showed that the longer the horizontal producer the faster the fire front moved and the earlier the combustion front break through occurred. This was because the distance between the injector and the producer was shorter when the horizontal producer was longer, which led to the pressure drawdown being induced earlier in the area near the vertical injector, resulting in a faster fire front velocity, which was also affected by the water influx from the aquifer. This behaviour of the combustion fronts were shown in Figure 5.14, which presented the temperature of the three models at 60 days and 515 days. Moreover, it was noticeable that the combustion front of the 100% length horizontal producer model managed to break through very fast (at 150 days) compared to the other two cases (Figure 5.15a). Also, the fire front of the 50% horizontal producer propagated faster than the case of a 25% horizontal producer model, as shown in Figure 5.14 at 515 days. In other words, the shorter the horizontal producer, the longer the fire front was sustained, which resulted in larger areas being swept by the combustion front, but lower cumulative oil being produced, as Figure 5.14b shows. This occurred because of the larger amount of oil converted to coke (Figure 5.14a) as a result of the slow fire front propagation in the shorter horizontal producer case. This was due to the long distance which separated the injector from the

producer, and also because of the fire front needed to force its way to the horizontal producer when it moved laterally through the zone affected by the high water influx from the aquifer.

For both the 50% and 25% horizontal producer models, the front was quenched at around 725 days and 995 days respectively (Table 5.6). The cumulative oil produced Figure 5.15b for both 50% and 25% horizontal producer models shows steep change in the slope of the curve for both cases, and both changes occurred slightly before the fire fronts were quenched. This was as a result of the oil bank ahead of the fire front breaking though to the producer just prior to the front breaking through and being quenched, which led to a higher oil production rate at that moment in time. Also, similar behaviour was observed in Figure 5.16 which presents the relationship between the cumulative oil produced by each scenario and the water cut of each case. When the oil bank broke through to the producer the water cut in both models (50% and 25%), which was by this stage already very high, reduced sharply at that point from a value greater than 95% to a value in the range 75% to 90%. As soon as the bank of oil is produced the water cut returns to the original trend. The 100% horizontal producer model produced the highest recovery factor (Table 5.6), but it also produced a large volume of water (Figure 5.15c), which may affect the project feasibility due to the need for investment in water treatment facilities to handle such large volumes of water. However, the 50% horizontal producer case achieved a recovery factor of 58.2%, while producing 60% less water compared to the 100% horizontal producer model. The requirement to complete only half the length, and the lower water handling costs, would have to be weighted up against the reduction in oil production rate in the economic analysis of using a horizontal producer for in-situ combustion in scenarios where there was strong bottom aquifer support. Figure 5.16 could be used to define the economic limit for the combustion process using those various scenarios.

Model name	Recovery factor (%) @ 3095 days	Recovery factor @ quenched time (%)	Front quenched time (days)	So @ 3095 days (fraction)	So @ quenched time (fraction)
HP-100Top	70.6	42.6	150	0.16	0.31
HP-50Top	58.2	51.4	725	0.20	0.24
HP-25Top	50.3	44.9	995	0.22	0.25

Table 5.6: *Simulation results of optimisation of horizontal producer wells length*

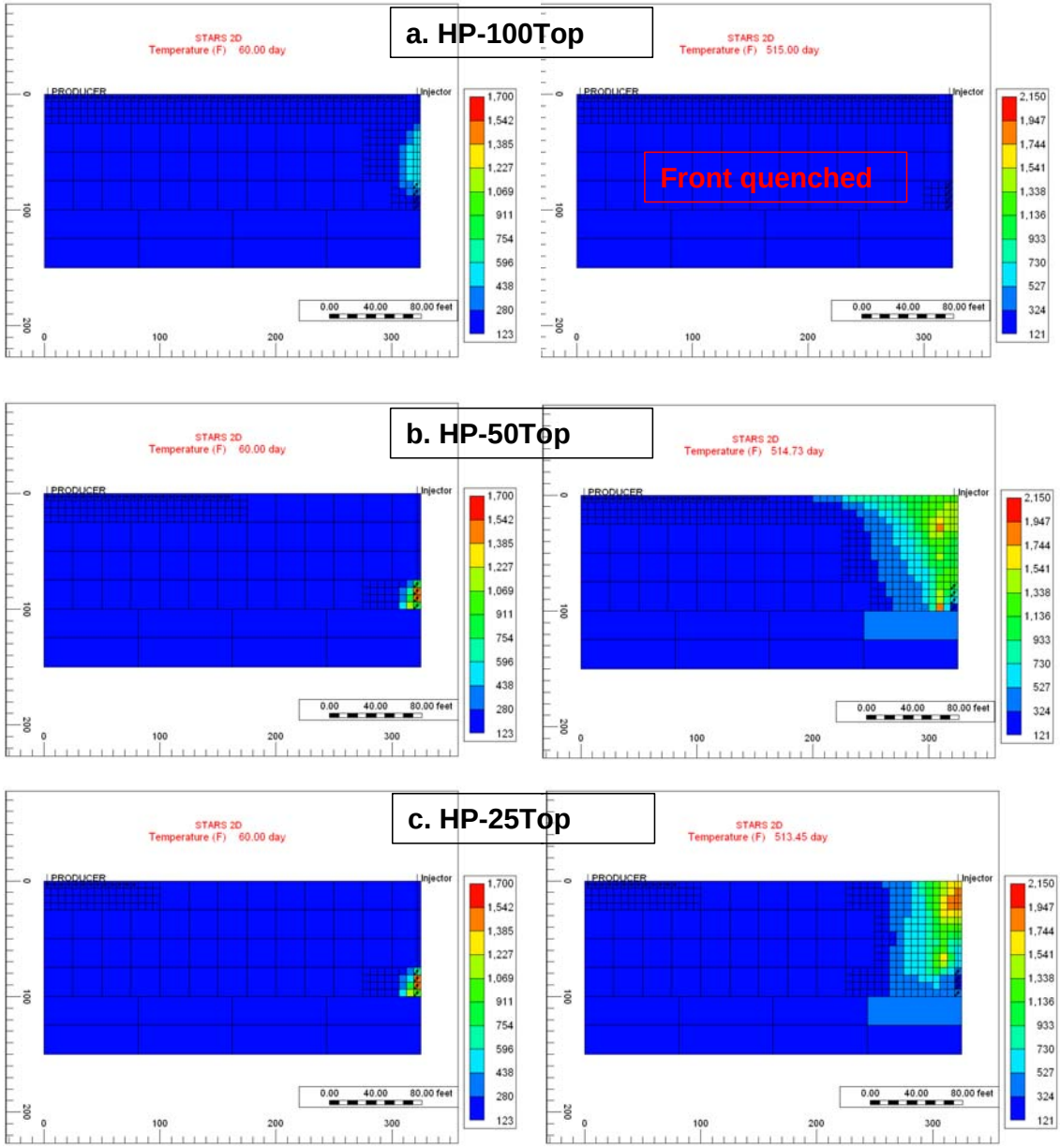

Figure 5.14: *Simulation results of temperature at 60 and 515 days: (a) HP-100Top, (b) HP-50%Top, and (c) HP-25%Top. Note that for the 100% long horizontal producer case, the fire front quenched earlier than the other two cases as part (a) of this figure shows at 515 days.*

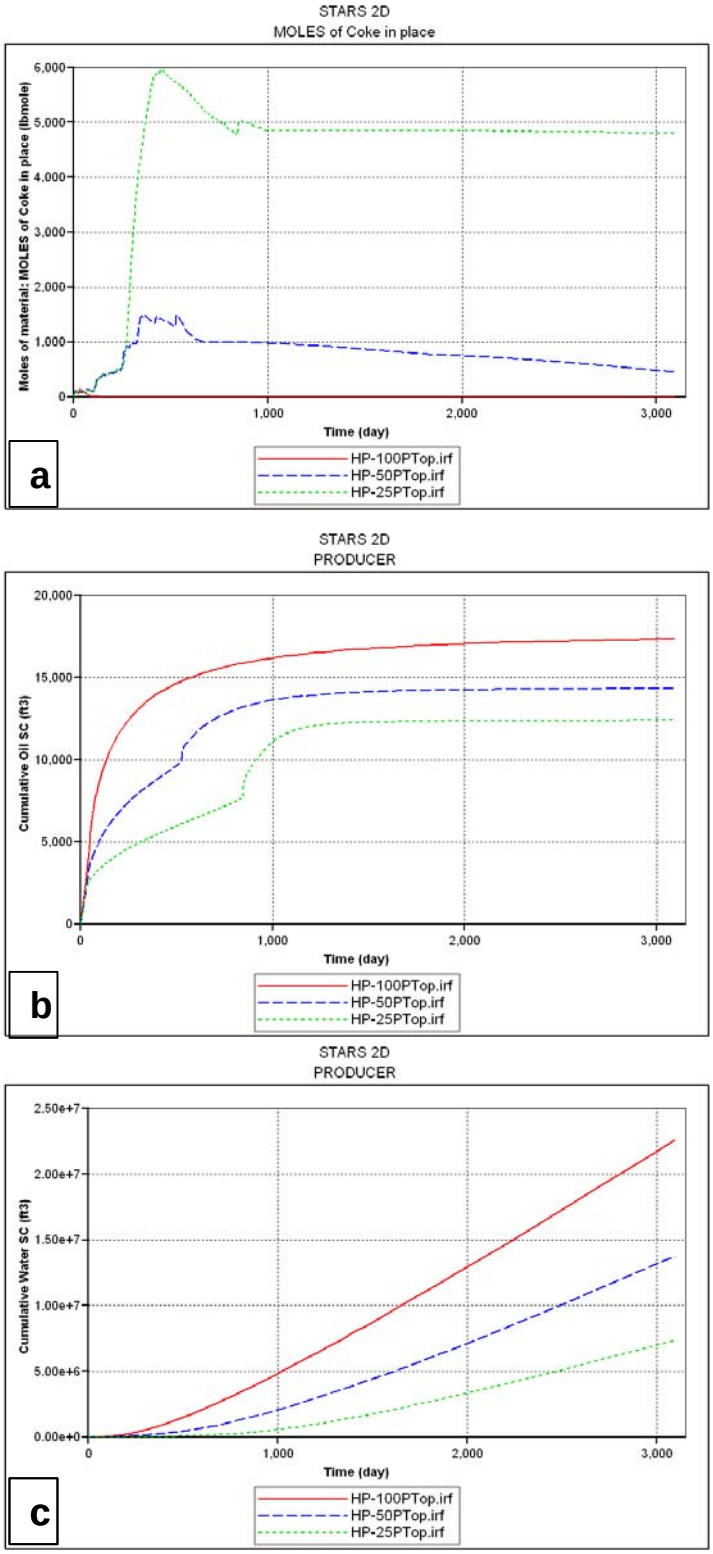

Figure 5.15: *Simulation results of optimisation of horizontal producer wells length: (a) net coke in place, (b) cumulative oil produced, and (c) cumulative water produced.*

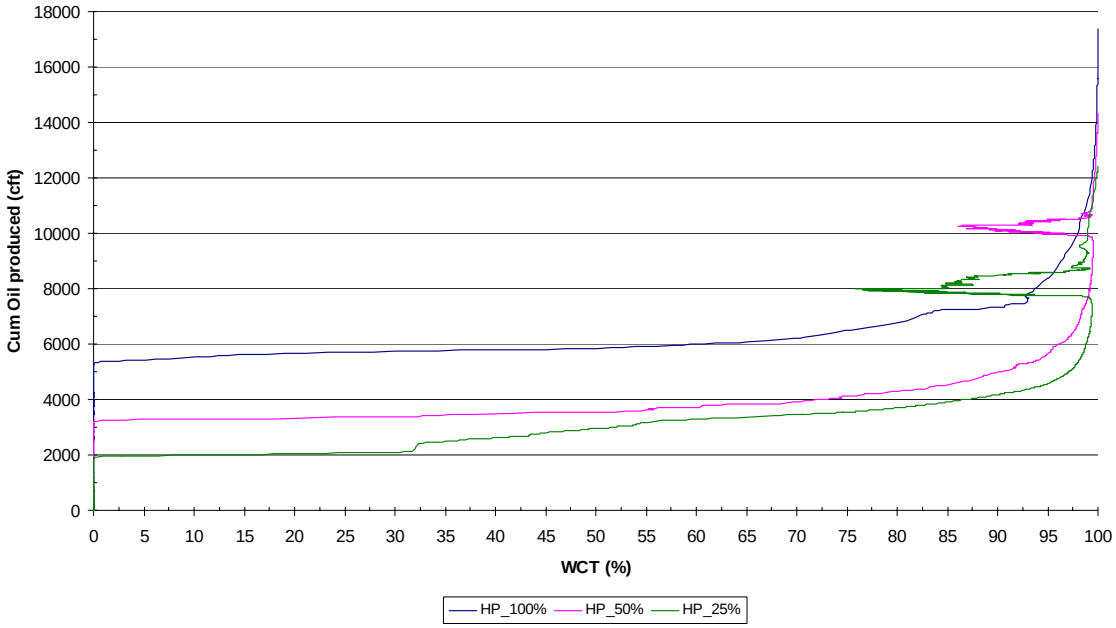

Figure 5.16: *Cumulative oil produced versus water cut.*

5.5 Effect of horizontal producer placement using a vertical injector completed at bottom

From the results presented this far, the use of horizontal producer in the in-situ combustion process enhanced the recovery factor where there was strong bottom aquifer support. In all the previous sensitivities, the horizontal producer was completed in the top of the model to maximise the distance to the aquifer, in order to reduce the total amount of water produced. In this section, the aim was to study the effect of changing the horizontal producer completion location from the top to the middle of the model. As a result, a new model was developed where the 162.5ft (50%) long horizontal producer was completed in the middle of the model (Figure 5.17), and the results of this model were compared with the results from the case where the horizontal producer was completed in the top of the model (Figure 5.13a), as in the previous sensitivity.

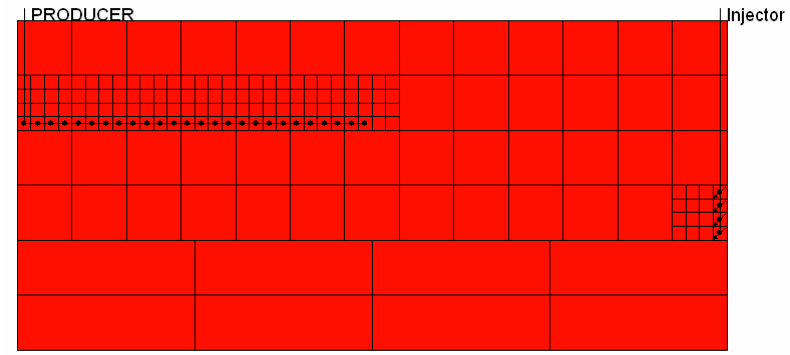

Figure 5.17: *Horizontal producer placement (HP-MiddPerf)*

Model name	Recovery factor (%) @ 3095 days	Recovery factor @ quenched time (%)	Front quenched time (days)	So @ 3095 days (fraction)	So @ quenched time (fraction)
HP-TopPerf	58.2	51.4	725	0.20	0.24
HP-MiddPerf	58.6	58.6	3095	0.19	0.19

Table 5.7: *Simulation results of horizontal producer placement*

Table 5.7 summarises all the main results from both models. The main observation from this sensitivity was that the fire front was sustained for the entire model run where the horizontal producer was completed in the middle of the model. This was because having the horizontal producer in the middle prevented water influx from quenching the front while the combustion front propagated through the area above the producer, as Figure 5.18 at 815 days shows. The temperature maps at 360 days (Figure 5.18) for both models show similar front propagation patterns. However, the fire front in the top horizontal producer model was quenched as soon as it broke through into the producer (at 725 days), whereas, for the middle completed horizontal producer model, the combustion front continued to propagate slowly in the top of the model (Figure 5.19) even after it broke through to the producer. Also, the recovery factor of the middle completed producer model was slightly higher (Table 5.7), mainly due to the optimum combination of both the combustion process and the aquifer drive. However, due to the shorter spacing between the horizontal producer and the aquifer in this case, the total

water produced was over twice the total amount produced by the top completed horizontal producer model (Figure 5.20). This sensitivity demonstrated that the choice of placement of the horizontal producer in such a system was crucial, due to the effect it had on the overall process performance. It showed how the combustion front could be sustained for a longer time when there was a strong bottom aquifer influx, by placing the horizontal producer in the middle of the model. However, even when the front was sustained for a longer time, there was no significant change in the overall recovery factor. Hence, it was recommended that the horizontal producer be completed on the top of the system, away from the aquifer, especially when using a vertical injector completed lower down in the formation.

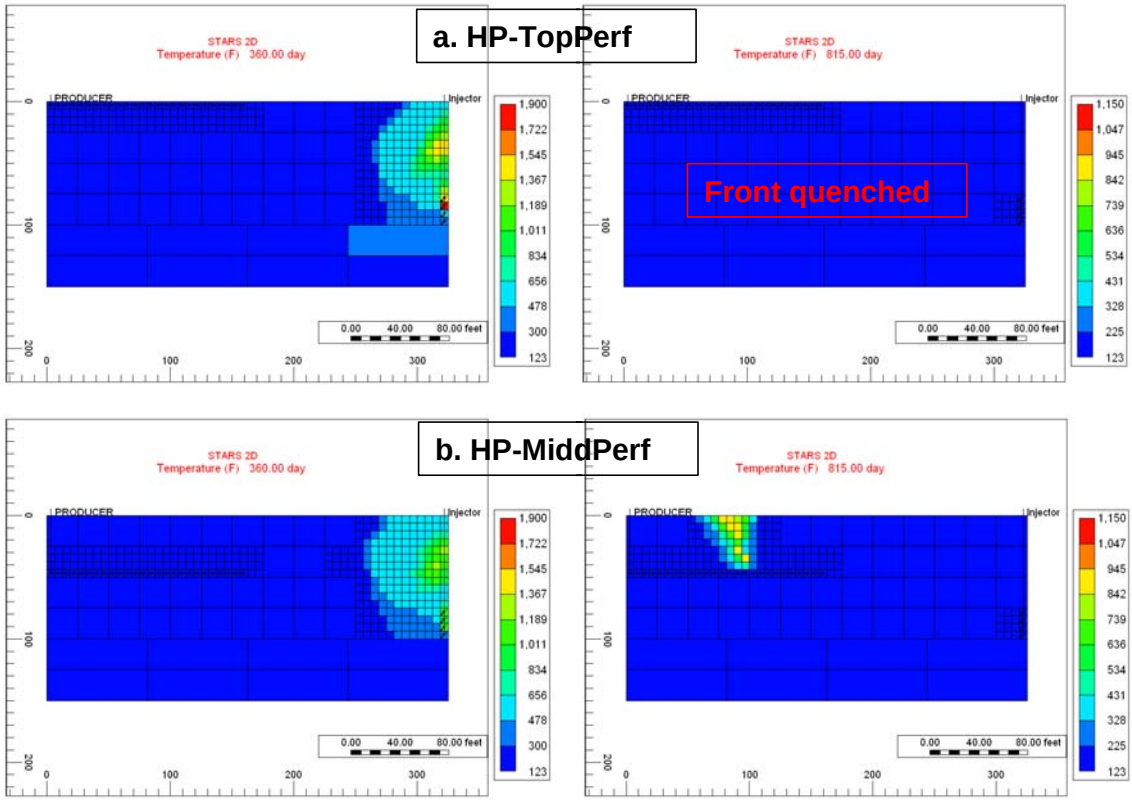

Figure 5.18: *Simulation results of temperature at 360 and 815 days: (a) HP-TopPerf, and (b) HP-MiddPerf*

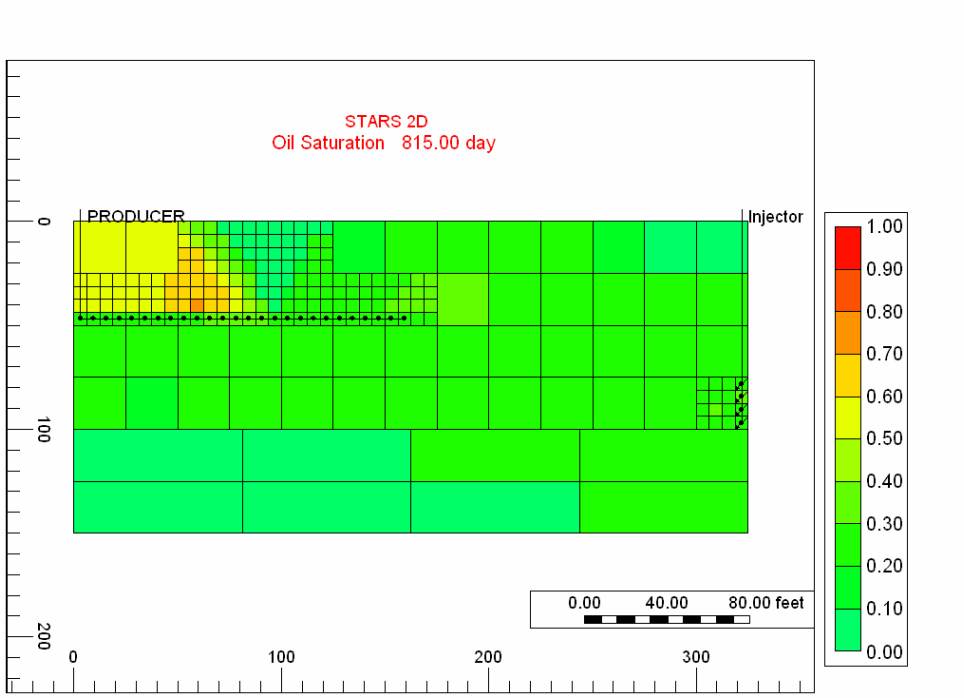

Figure 5.19: *Simulation results of oil saturation at 815 days for the HP-MiddPerf, which show the high oil saturation in the model top above the producer*

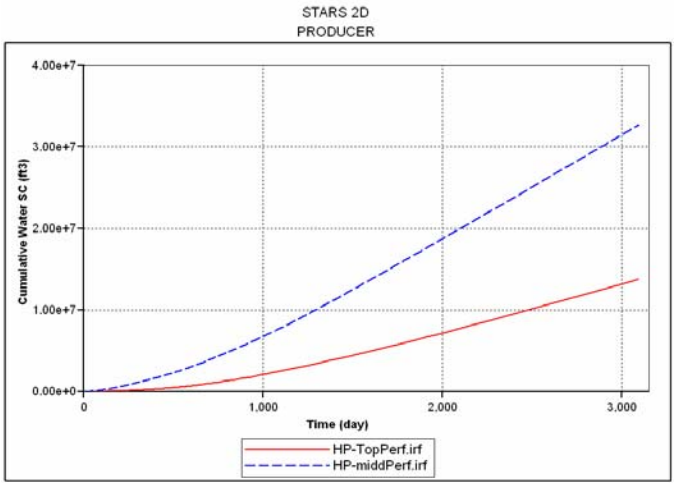

Figure 5.20: *Simulation results of cumulative water produced as a function of horizontal producer placement. The cumulative oil produced plot for this sensitivity had the same profile as in Figure 5.15b (for HP_50%) and the recovery factor was presented in Table 5.7. Also, the temperature maps were shown in Figure 5.18 for two different time steps.*

5.6 Horizontal injector application

The use of horizontal producer, as demonstrated in this chapter, changed the recovery performance, and resulted in an increasing recovery factor due to both the combustion process and the aquifer drive. The objective of this section was to evaluate the possibility of using a horizontal well as an injector when strong aquifer support also existed. The performance of the combustion process was investigated, and the optimum horizontal injector length was obtained. Moreover, well placement was examined for both horizontal injectors and producers in the Nimr simulation model.

5.6.1 Effect of using horizontal injector

In order to evaluate the effect of a using horizontal injector on the combustion process, a new model was developed. The horizontal injector was initially located in the middle of the model (Figure 5.21a), by placing it between the horizontal producer (top) and the aquifer. This might restrict the aquifer water from approaching the horizontal producer, and result in a reduction in the total amount of water producer from the model. In this sensitivity, a horizontal injector length of 325 ft (100% entire model length) was used. Later, the optimum injector length will be evaluated. The results from this model were compared to the simulation results of a vertical injector model (Figure 5.21b), where the vertical injector was completed in the middle 25ft of the model.

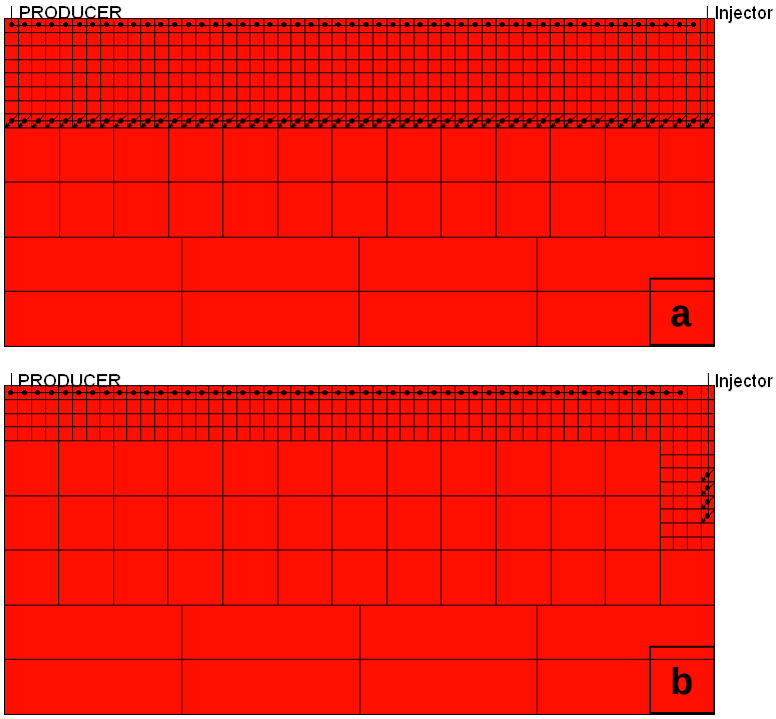

Figure 5.21: *Comparison between the use of horizontal and vertical injector wells: (a) HI, and (b) VI*

The main observations from the temperature distribution maps (Figure 5.22) for both models at 20 days was that the fire front for the horizontal injector model was initiated along the well length, because of the way the horizontal injector was completed and heaters were installed in each perforation of the well. For the vertical injector, the fire front was ignited near the well and then propagated upward until it broke through into the producer after a relatively short time (130 days), and was quenched. The wide fire front initiation in the horizontal injector model helped to sustain the fire front for a long time (470 days) as a result of delaying the front break through. However, this led to more net coke in place being produced (Figure 5.23a) in the horizontal injector model because of the long sustained period of burning, and also as a result of the wide fire front which was moving slowly upwards against gravity. The cumulative oil produced in the vertical injector model (Figure 5.23b) was higher than for the horizontal injector case due to two reasons. The first was the greater amount of oil that was converted to coke. The second reason was that the placement of the horizontal injector between the aquifer and the producer limits the influx of aquifer water into the producer. This resulted in the water being unable to efficiently sweep the area between the injector and

the producer, which resulted in a higher oil saturation remaining in that area (Figure 5.24), even at the last time step of the simulation, unlike for the vertical injector model. Moreover, the placement of the horizontal injector has an advantage in terms of reducing the total amount of water produced (Figure 5.23c) compared to the vertical injector case, which produced over 50% more water. This sensitivity showed that the horizontal injector when, completed in the middle of the model, could be used, and it did help to sustain the combustion front for a longer time. It also reduced the amount of water produced. However, this well configuration produced a lower recovery factor (Table 5.8), and also resulted in a higher final average oil saturation (17%) because of the way the horizontal injector restricted the water influx and prevented a better sweep efficiency in the model after the fire front was quenched.

Model name	Recovery factor (%) @ 3095 days	Recovery factor @ quenched time (%)	Front quenched time (days)	So @ 3095 days (fraction)	So @ quenched time (fraction)
HI	62.7	52.9	470	0.17	0.22
VI	71.7	40.7	130	0.15	0.32

Table 5.8: *Simulation results of comparison between horizontal and vertical injector wells*

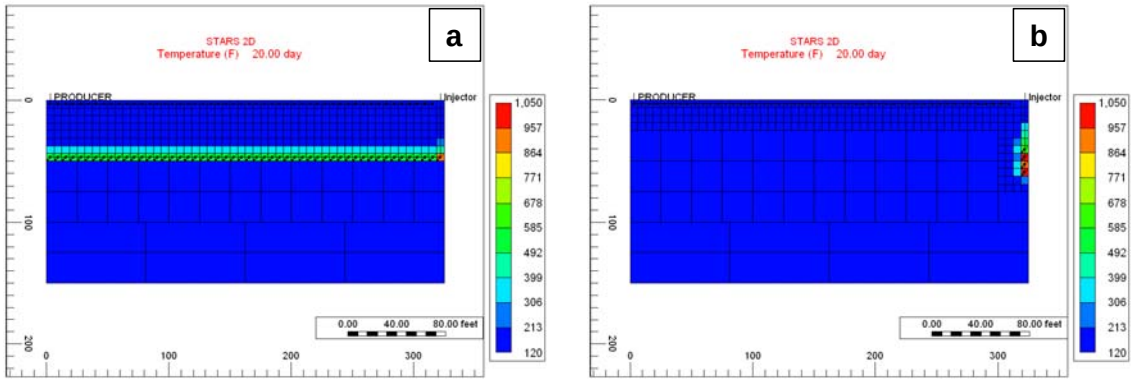

Figure 5.22: *Simulation results of temperature at 20 days: (a) HI, and (b) VI*

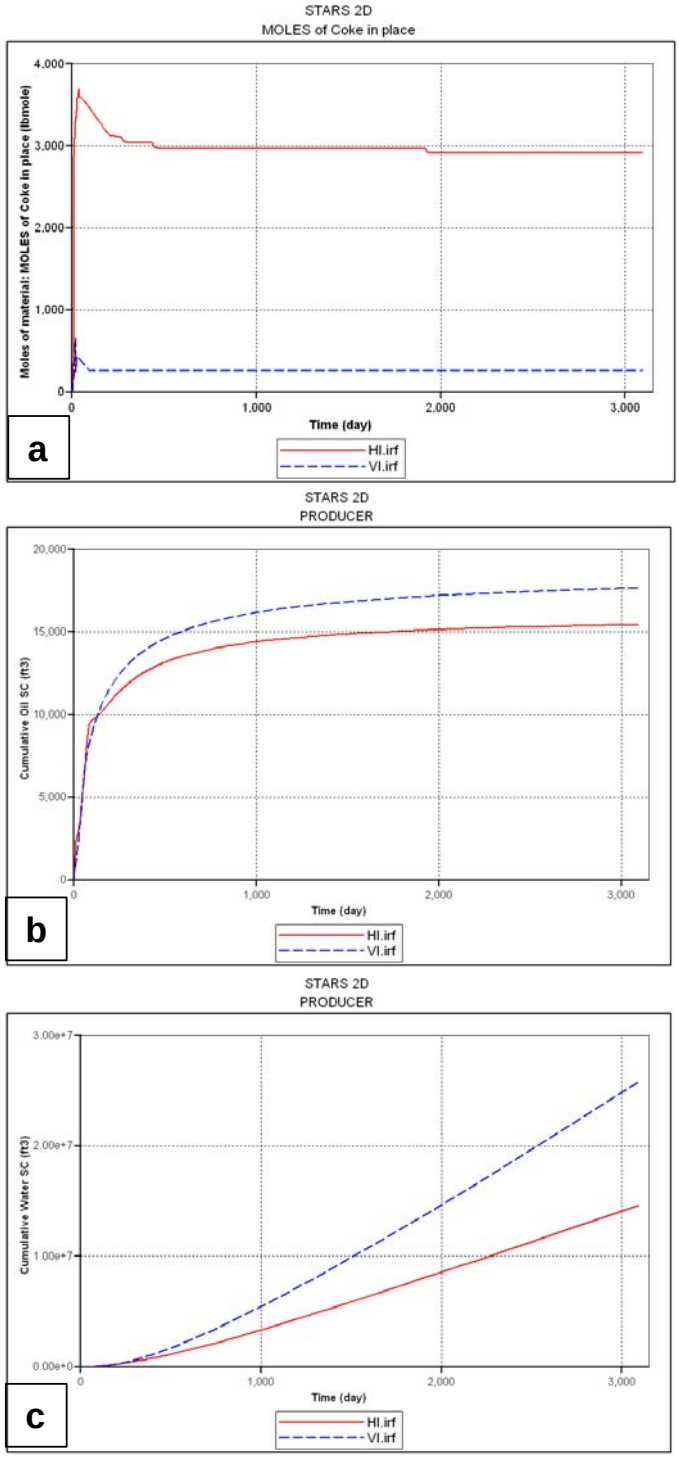

Figure 5.23: *Simulation results of comparison between horizontal and vertical injector wells: (a) net coke in place, (b) cumulative oil produced, and (c) cumulative water produced.*

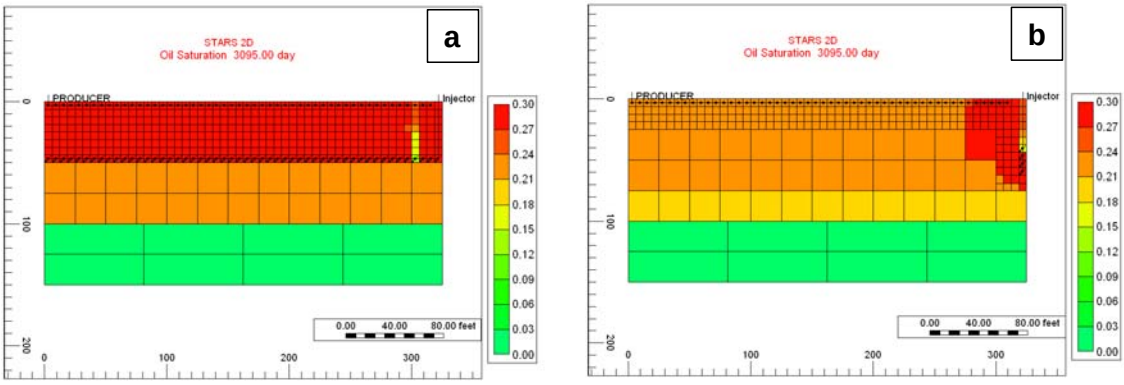

Figure 5.24: *Simulation results of oil saturation at 3095 days: (a) HI, and (b) VI. The smoothness of the saturation profile in the lower layers was due to the uniform sweep in the vertical directions from the aquifer to the producer well.*

5.6.2 Optimisation of horizontal injector length

This sensitivity was focusing on an evaluation of the horizontal injector length. Changing the injector length may help to overcome some of the drawbacks observed when using the 100% horizontal injector (Figure 5.21a). In order to optimise the horizontal injector length, two new models were developed. The first has 162.5 ft (50%) horizontal injector length (Figure 5.25a) and the second model has 81.25 ft (25%) horizontal section length (Figure 5.25b).

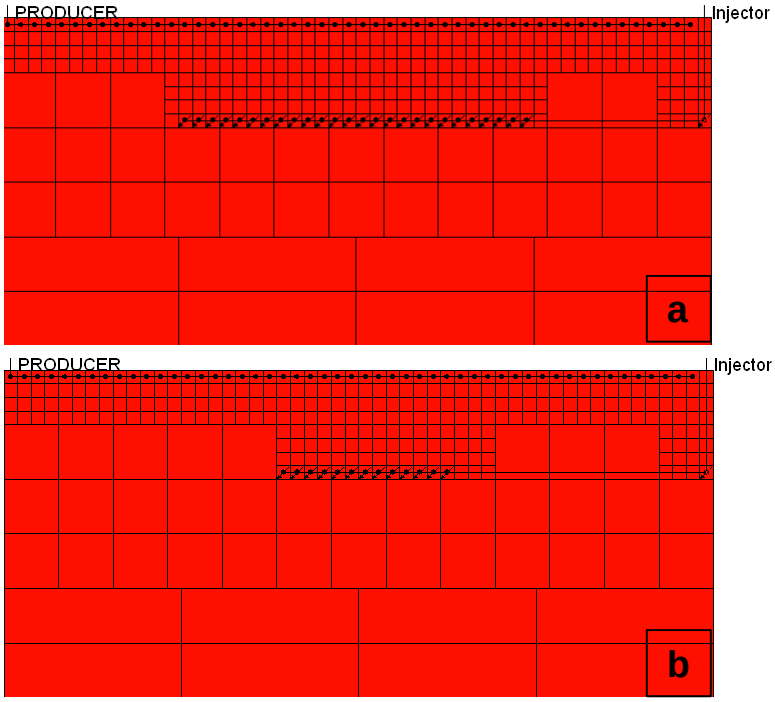

Figure 5.25: *Optimisation of horizontal injector length: (a) HI-50%, and (b) HI-25%*

Figure 5.26a shows that the 25% length horizontal injector model produced more cumulative oil. This was as a result of less coke being produced by this model (Figure 5.26b), due to the early extinguishing of the front (at 350 days). Another reason for the greater volume of oil produced by the 25% horizontal injector model was that more water was allowed to flow around the edge of the horizontal injector and recover the oil from the area between the injector and the producer. This also explained the greater volume of cumulative water produced by this model compared to the other two models (Figure 5.26c). The use of a shorter horizontal injector allowed for better sweep efficiency by the aquifer drive, even when the combustion front was quenched, and also led to a lower volume of oil left in place in the model, as Figure 5.27 shows. However, it was clear that the 100% horizontal injector was acting as a barrier to prevent the aquifer water from sweeping the area between the injector and the producer wells, which resulted in higher oil saturations. Figure 5.28 presents the temperature maps of the three models. For the 100% horizontal injector case (Figure 5.28a), the combustion front was ignited along the total well length, and was then mainly propagated upward towards the toe of the horizontal producer. This may be because of the greater fuel availability in the last uncompleted grid block near the toe of the producer. The fire fronts for both the 50% (Figure 5.28b) and 25% (Figure 5.28c) horizontal length models

were initiated along the entire well length. After that, the front propagated upward from the centre of horizontal injector. This was as a result of the fire front near the ends of the horizontal injector being quenched because of the water influx around the injector. Table 5.9 summarises the results from this sensitivity. The main observations for this specific well configuration were that the shorter the horizontal injector, the higher the recovery factor from the process. Also, the earlier the front was quenched, the more water that was produced from the model.

Model name	Recovery factor (%) @ 3095 days	Recovery factor @ quenched time (%)	Front quenched time (days)	So @ 3095 days (fraction)	So @ quenched time (fraction)
HI-100%	62.7	52.9	470	0.17	0.22
HI-50%	65.0	53.1	395	0.16	0.23
HI-25%	67.6	53.1	350	0.16	0.24

Table 5.9: *Simulation results of optimisation of horizontal injector length*

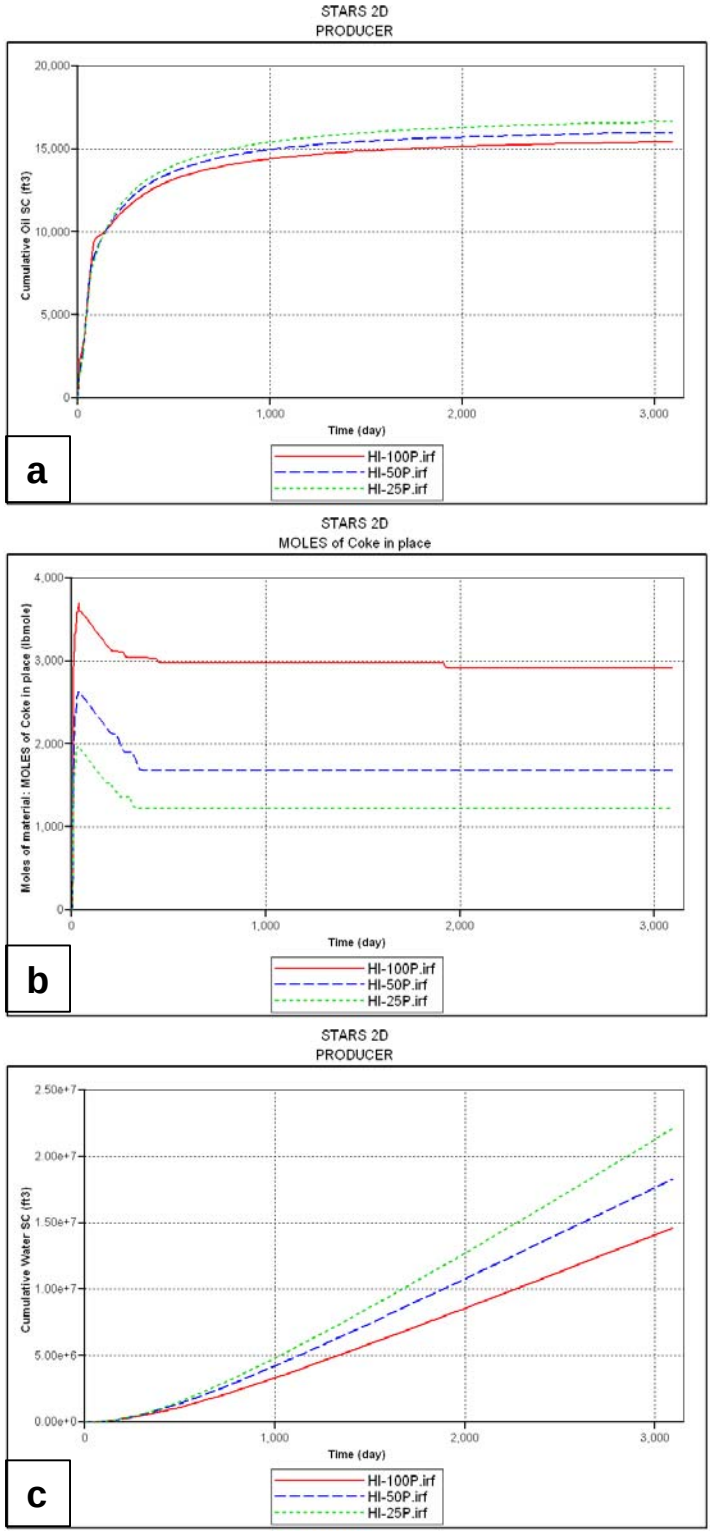

Figure 5.26: *Simulation results of optimisation of horizontal injector length: (a) cumulative oil produced, (b) net coke in place, and (c) cumulative water produced.*

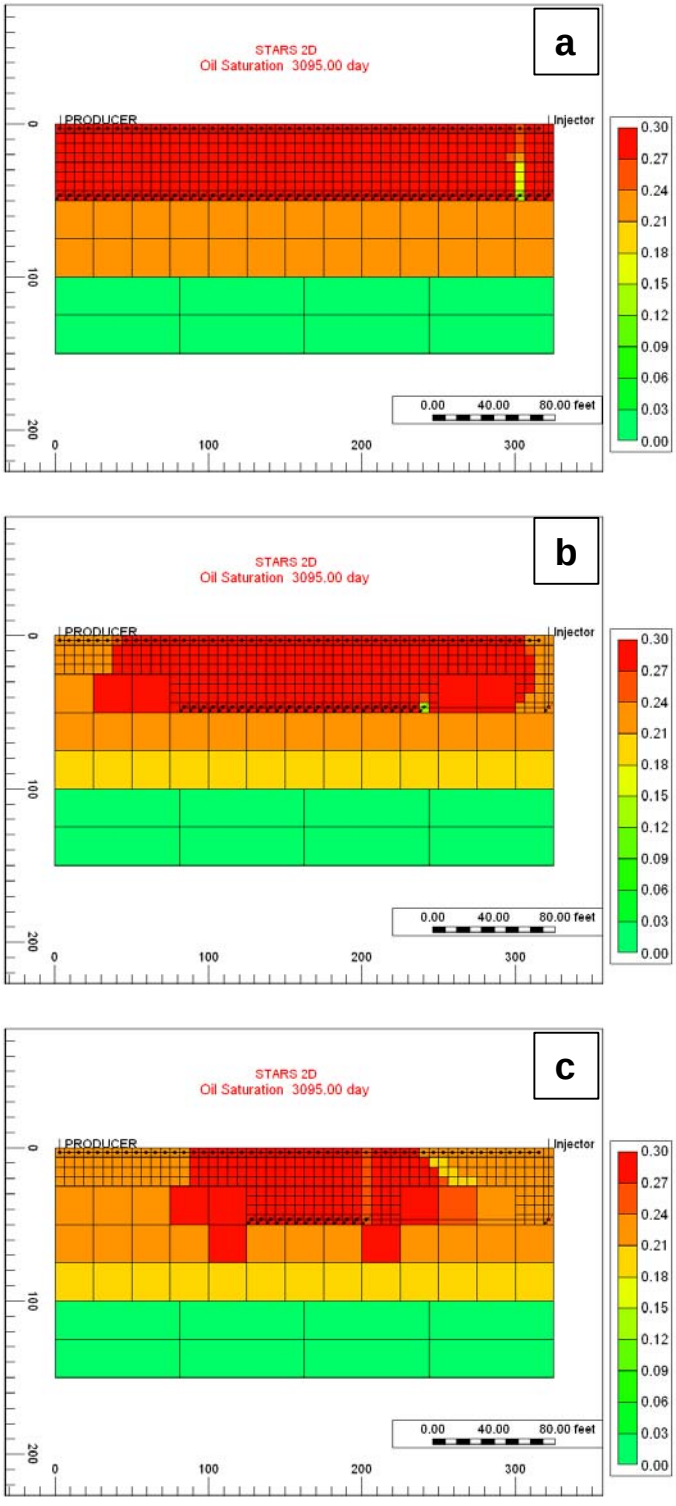

Figure 5.27: *Simulation results of oil saturation at 3095 days: (a) HI-100%, (b) HI-50%, and (c) HI-25%. Note the difference in oil saturations between the three cases especially in the area between the producer and the injector*

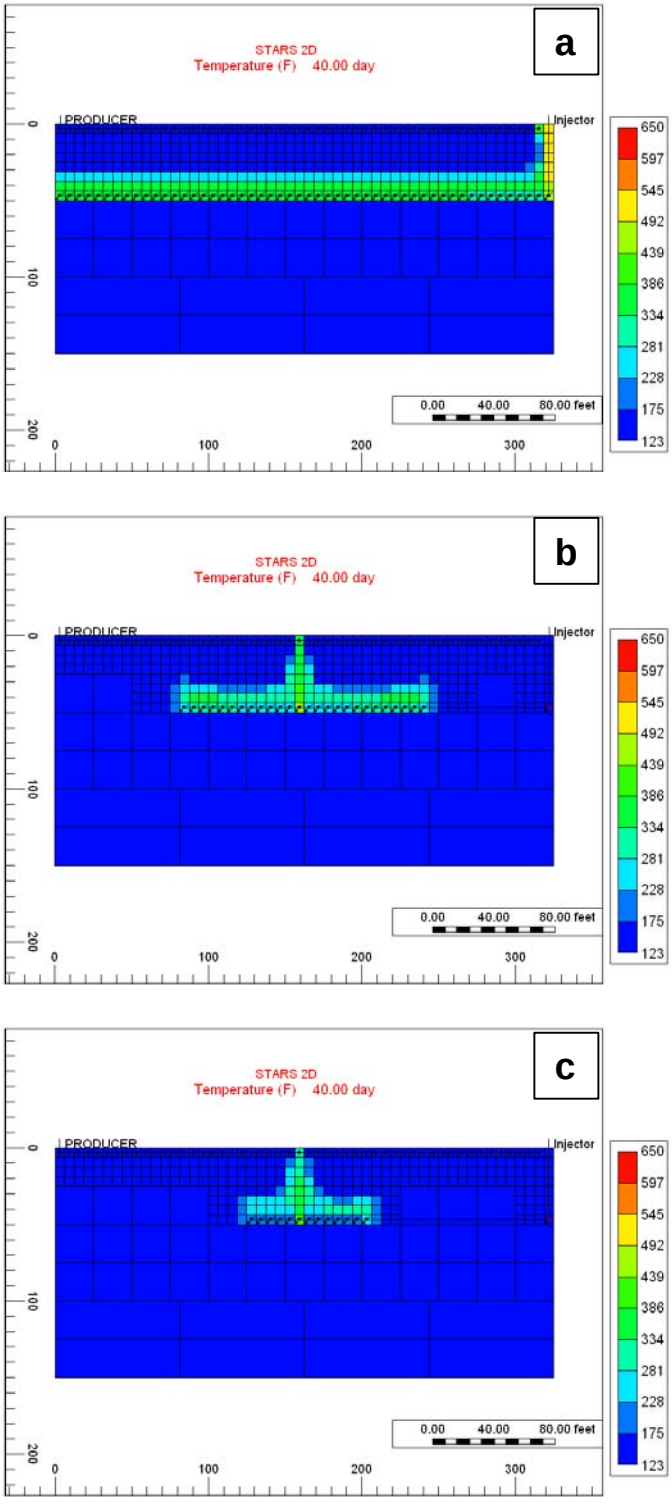

Figure 5.28: *Simulation results of oil temperature at 40 days: (a) HI-100%, (b) HI-50%, and (c) HI-25%*

5.6.3 Horizontal injector placement relative to the horizontal producer

In order to develop the top-down in-situ combustion process using the horizontal injector and horizontal producer well configurations, the injector was relocated at the top of the model. This will allow for the initiation of the fire front in the top of the model, and it then propagates from top to bottom and approaches the horizontal producer. Also, the new location of the horizontal injector will maximise the distance to the aquifer, and delay or even prevent the front from been quenched by the aquifer water. As a result, more oil can be recovered by the fire front, especially from the upper reservoir area between both wells. In this sensitivity, two models were used. Both had the horizontal producer completed over 100% of the model length and the horizontal injector was 81.25ft (25%). In the first model (Figure 5.29a), the horizontal injector was completed in the middle of the model, and in the second model (Figure 5.29b) the injector was completed in the top of the model.

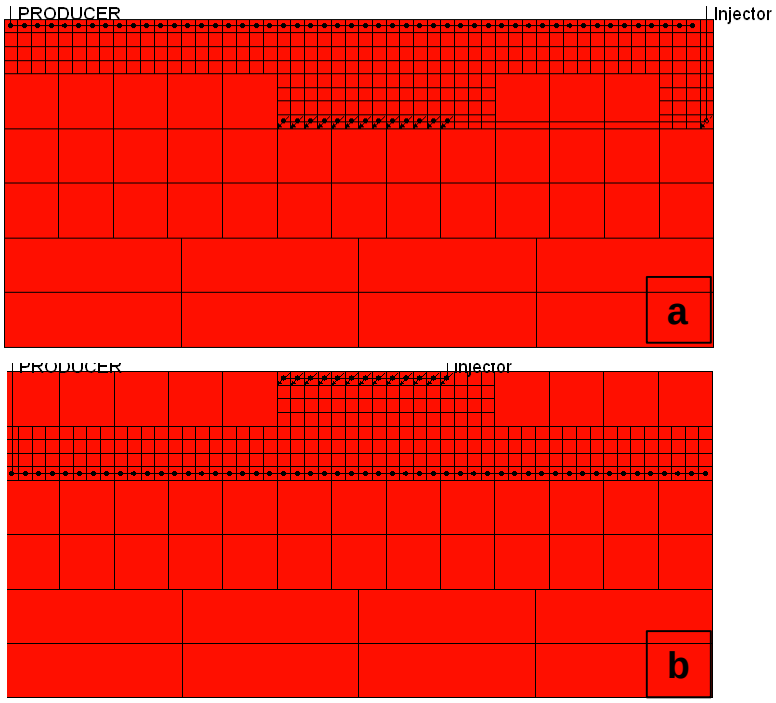

Figure 5.29: *Horizontal injector placement: (a) HI-Middle, and (b) HI-Top*

According to both model temperature maps (Figure 5.30), the fire fronts were initiated near the horizontal injector perforations (Figure 5.30 at 20 days), and after that they propagated to approach the producer. For the model with the horizontal injector

completed at the top, after 365 days (Figure 5.30) the fire front had spread laterally in the top of the model, and also moved vertically to approach the horizontal producer. It was sustained for the total model duration (3095 days). This was because the aquifer water sweep was blocked by the horizontal producer in the middle section of the model, and all the water flowed to the producer and did not contact the combustion front. On the other hand, in the middle completed horizontal injector model, the fire front was quenched early, at around 350 days, as a result of the water flux. The total amount of oil produced by the horizontal injector model was higher than for the middle horizontal injector model (Figure 5.31a), and the top horizontal injector model achieved a 9.4% higher recovery factor (Table 5.10) than the middle completed injector model. This was mainly as a result of the lower volume of oil converted to coke in the top completed horizontal injector model (Figure 5.31b) due to the downward movement of the combustion front with gravity. Also, the higher recovery in the top competed horizontal injector was due to the sustaining of the fire front for the entire duration of the model run, which allowed for a greater area being swept by the front and more oil being recovered. The only drawback of using this top-down well configuration (horizontal injector completed in the top of the model) was the large volume of water produced by this model (Figure 5.31c), which was mainly as a result of the shortened distance between the horizontal producer and the aquifer.

This sensitivity showed that the top-down combustion process, when achieved by completing the horizontal injector in the top of the model and the producing well was located in the middle section of the model, results in the highest recovery factor (77%) of all the scenarios presented so far in this chapter. As mentioned previously, in Chapter 4, almost all the current horizontal wells were completed in the top of the Nimr reservoir. This will make top-down in-situ combustion more attractive for PDO in terms of feasibility and economics.

Model name	Recovery factor (%) @ 3095 days	Recovery factor @ quenched time (%)	Front quenched time (days)	So @ 3095 days (fraction)	So @ quenched time (fraction)
HI-Middle	67.6	53.1	350	0.16	0.24
HI-Top	77.0	77.0	3095	0.10	0.10

Table 5.10: *Simulation results of horizontal injector placement*

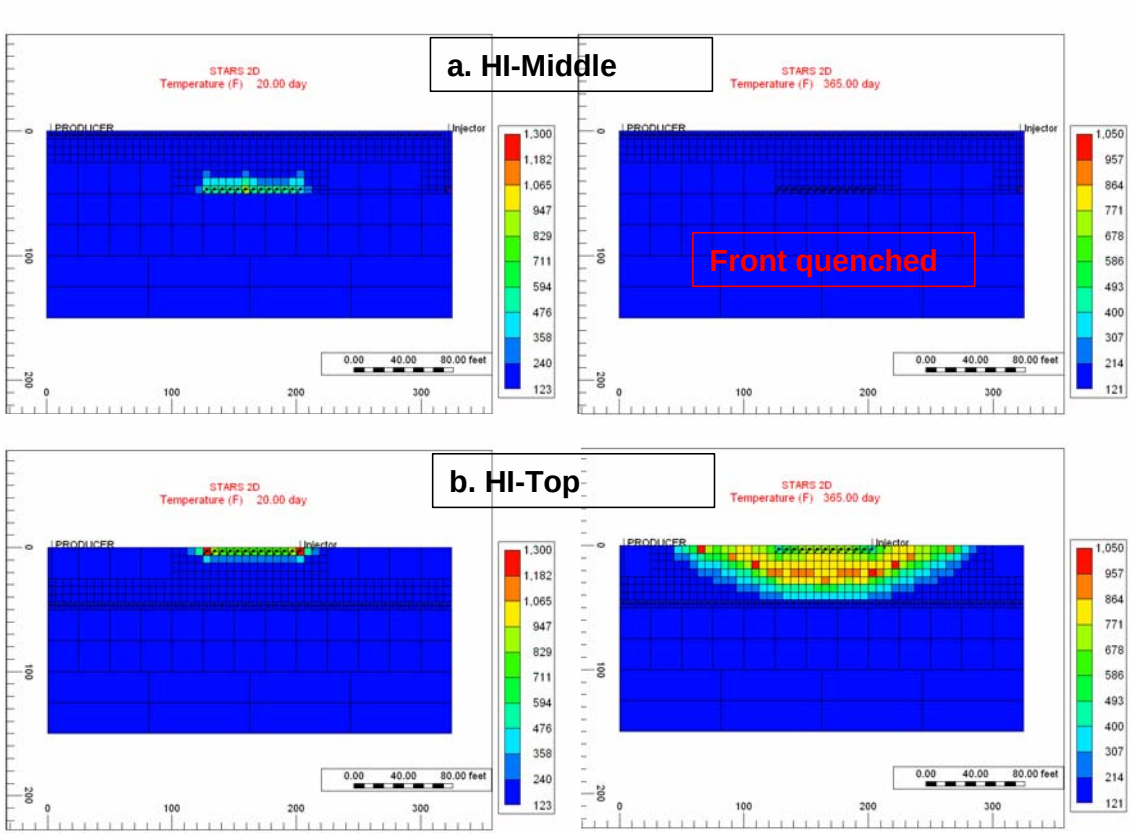

Figure 5.30: *Simulation results of oil temperature at 20 days and 365 days: (a) HI-Middle, and (b) HI-Top*

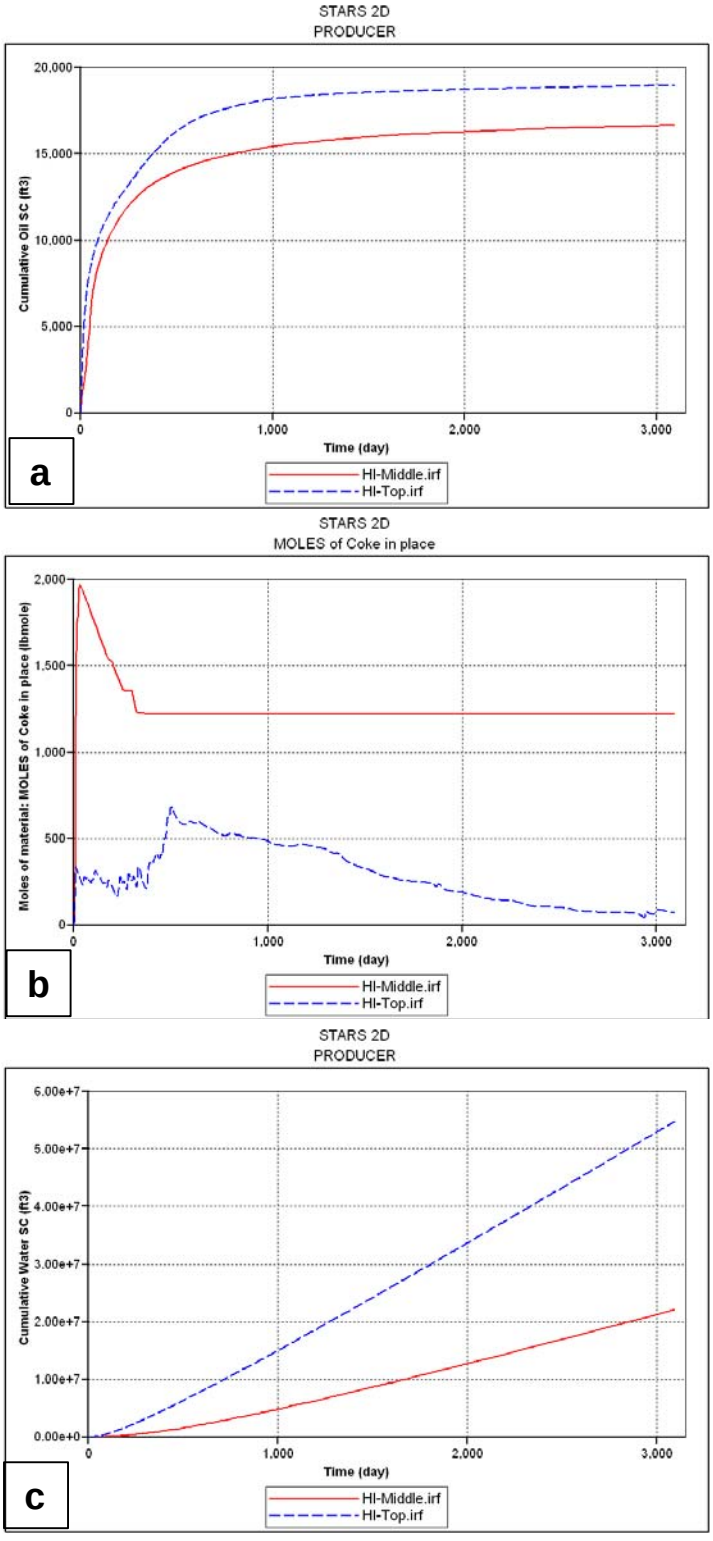

Figure 5.31: *Simulation results of horizontal injector placement: (a) cumulative oil produced, (b) net coke in place, and (c) cumulative water produced.*

5.7 Effect of spacing between horizontal producer and the aquifer

The use of the top-down well configuration resulted in a longer duration of the fire front, and allowed for a higher recovery factor to be achieved. Previously, in the top-down scenario considerably the horizontal producer was located in the middle of the model, which made it approximately 50ft away from the aquifer, as Figure 5.32a shows. The aim of this section was to investigate the effect on the overall recovery process of the spacing between the horizontal producer and the aquifer. To achieve this objective, two new models were developed. In the first model, the horizontal producer was located 18.75 ft away from the aquifer (Figure 5.32b). The horizontal producer in the second model was located in the lowest layer of the oil zone, almost at the aquifer (Figure 5.32c). Lowering the location of the horizontal producer in the model resulted in an increase in the area between the horizontal injector and producer, which increased the potential area to be swept by the combustion front.

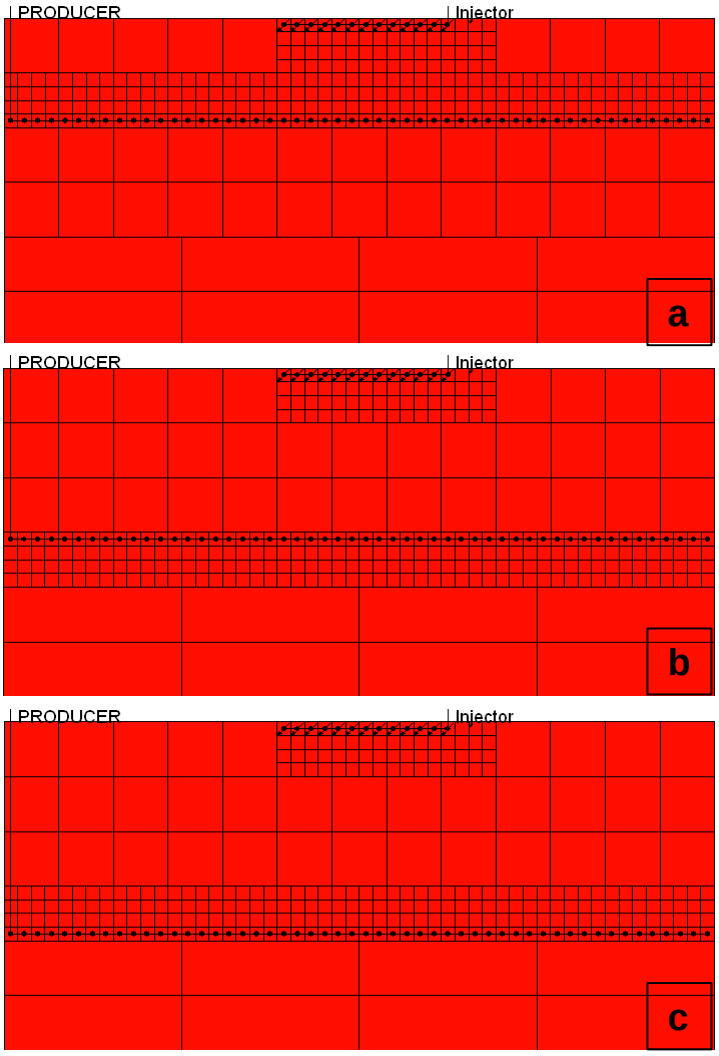

Figure 5.32: *Effect of spacing between horizontal producer and aquifer: (a) 50ft-from-AQ, (b) 18.75ft-from-AQ, and (c) at-AQ*

To begin with, the fire fronts in all three models were sustained until the end of the simulation (3095 days), which highlighted the importance of using these well configurations (top-down) were a successful in-situ combustion process, was possible in the presence of strong bottom water aquifer. Moreover, as the distance between the horizontal producer and the aquifer decreased, this resulted in more cumulative oil being produced by the combustion front, as Figure 5.33a shows. This was mainly because the fire front was able to sweep larger areas without being quenched, and thus more oil was recovered. Furthermore, the total water produced by each model was increased as the distance between the horizontal producer and the aquifer decreased, as Figure 5.33b shows. For example, in the case where the horizontal producer was placed just above the aquifer, the model produced over two and a half times the volume water

compared to the amount produced by the case where the horizontal producer was located 50ft away. This meant that in order to achieve a higher recovery factor the system may need to produce much more water, which could affect decisions around well configurations and the overall feasibility of the process. The temperature maps and the ternary plot of oil, water, and gas saturations for all three models at 575 days were shown in Figure 5.34. The way the fronts develop in all the models were almost identical, except that both the oxygen (Table 5.11) and fire front breakthrough occurred faster in the cases where the distance between the injector and the producer was shorter. Also, for the case where the horizontal producer was 50 ft away from the aquifer, there was an acceleration in the rate of oil production as the steep slope in the plot of the cumulative oil produced (Figure 5.33a) shows. This was because of the smaller area to be swept in this case, which resulted in oil banks being able to break through into the producer earlier when compared with the other two cases. Table 5.11 summarises all the main simulation results for the comparison between the three models. This sensitivity showed the potential of using top-down well configurations to sustain the combustion process for longer time, even when a strong aquifer existed. Also, it showed that the shorter distance between the horizontal producer and the aquifer in the top-down wells scenario resulted in a higher recovery factor and higher cumulative water being produced. As a result, the choice of the optimum spacing between the producer and the aquifer depends on the maximum capacity of the treatment facility to handle the water produced in the field.

Model name	Recovery factor(%) @ 3095 days	Oxygen break through (days)	So @ 3095 days (fraction)
50ft-from-AQ	77.0	454	0.10
18.75ft-from-AQ	80.7	922	0.06
at-AQ	83.8	1315	0.03

Table 5.11: *Simulation results of effect of spacing between horizontal producer and aquifer*

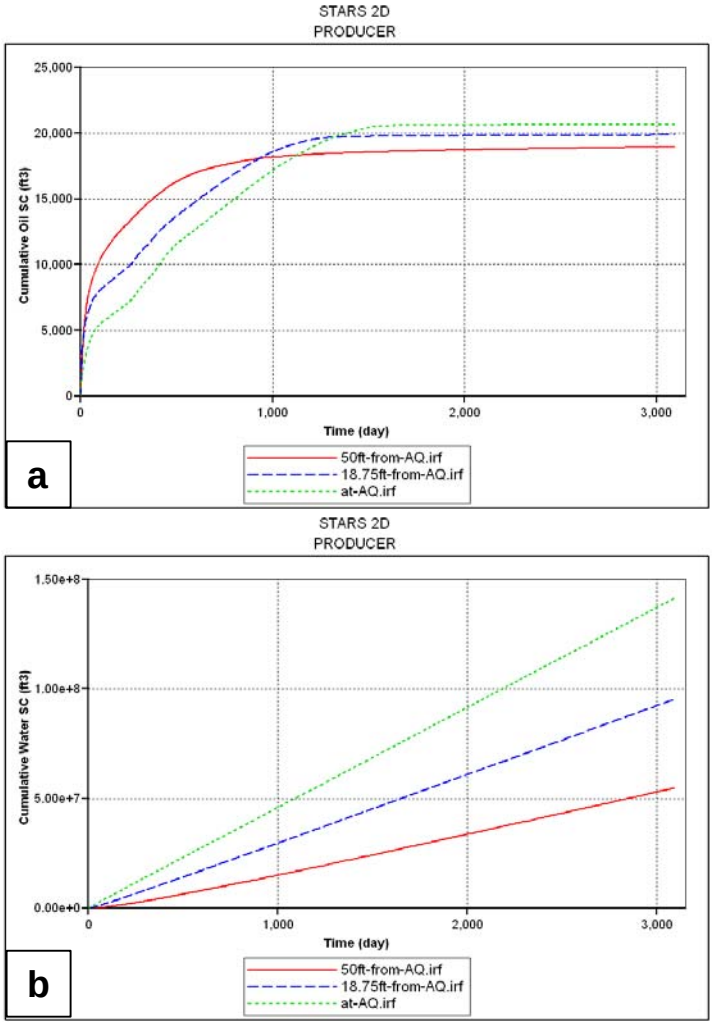

Figure 5.33: *Simulation results of effect of spacing between horizontal producer and aquifer: (a) cumulative oil produced, and (b) cumulative water produced. Note the large difference in the volumes of water produced by each case (b).*

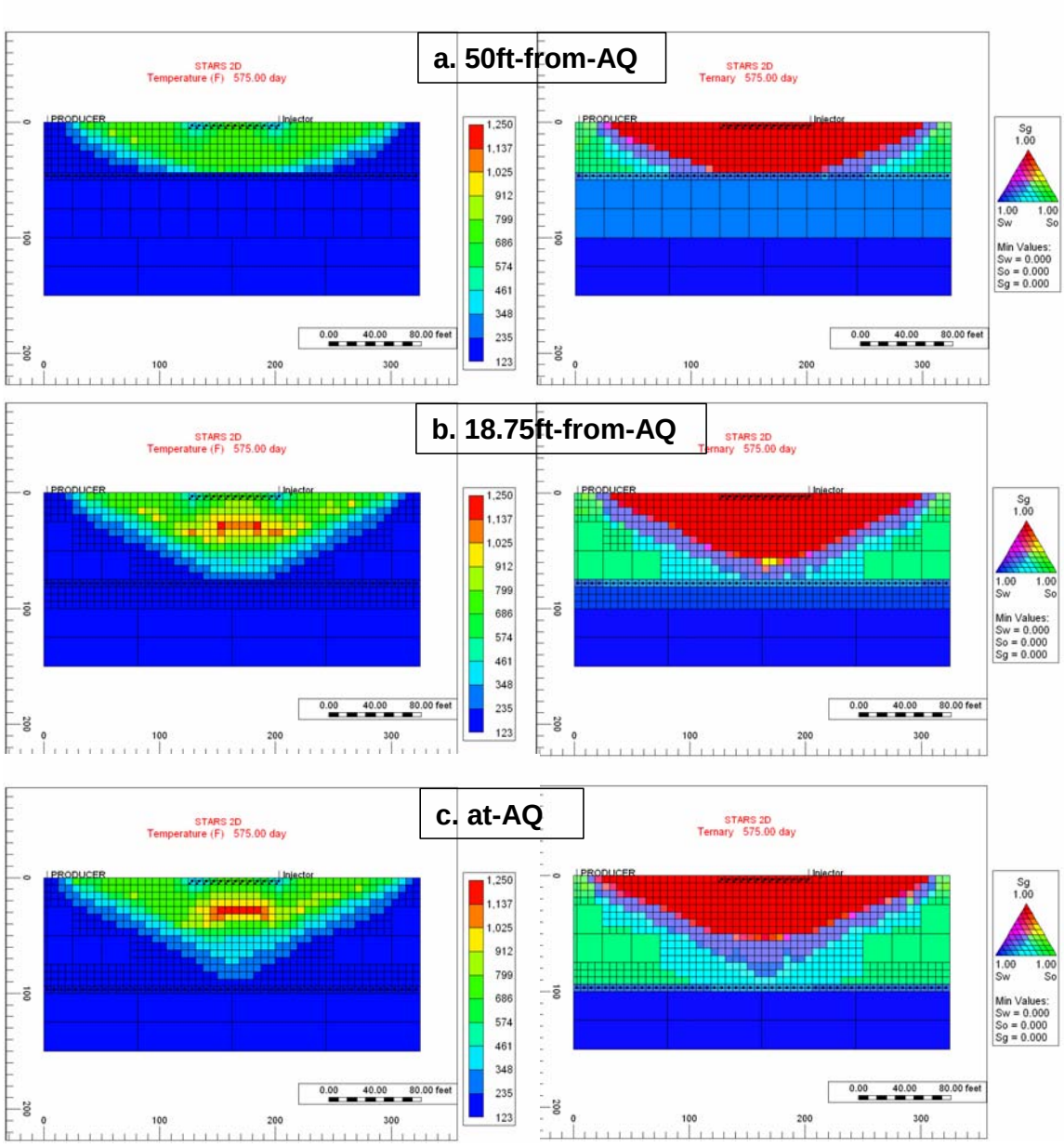

Figure 5.34: *Simulation results of temperature and ternary at 575 days: (a) 50ft-from-AQ, (b) 18.75ft-from-AQ, and (c) at-AQ*

5.8 Effect of horizontal producer length in top-down combustion process

An investigation to find the optimum horizontal producer length was conducted previously in section 5.4.2, where the horizontal producer was located in the top of the model and a vertical injector was used to initiate the fire front. The main outcome was

that the longer the horizontal producer, the earlier the fire front was quenched as a result of the early break through of the front. In this section, the effect of the horizontal producer length on the overall recovery process was investigated again, but this time using the top-down well configuration. Three models were used, and all the models had a 81.25ft (25%) horizontal injector completed in the top of the model. The horizontal producer length was 325ft (100%) in the first model (Figure 5.35a), 162.5ft (50%) in the second model (Figure 5.35b), and 81.25ft (25%) in the third model (Figure 5.35c).

The temperature distribution maps of the three models (Figure 5.36) show that the combustion fronts were initiated in all cases. The behaviour and the shape of the front vary depending on the pressure drawdown induced by the horizontal producer. For example at 90 days the fire front in the 25% long horizontal producer model mainly moved vertically as a result of the intense pressure drawdown applied by the short horizontal producer, which limited the fire front lateral spread. On the other hand, in the 100% horizontal producer model, the fire front moved laterally and spread faster than the two other cases, especially at 395 days. This was because using the longer horizontal producer helped to direct the combustion front to the model edges in order to recover the oil. Also, the horizontal producer acted as a barrier to prevent aquifer water from approaching the fire front and quenching it, in contrast to what happened in the two other short horizontal producer models. The front in the 25% long horizontal producer model was quenched after 340 days (Table 5.12) from the start of the process, and for the 50% horizontal producer model it was quenched after 635 days. This meant that the shorter the horizontal producer in the top-down well scenario was, the earlier the front was quenched as a result of the water being able to flow around the ends of the horizontal producer. This meant a smaller total volume of oil being produced by the shorter horizontal producer models (Figure 5.37). Figure 5.38 presents the cumulative oil produced relationship with the water cut in each of the three scenarios. The recovery factors from each case were shown in Table 5.12, with the 100% horizontal producer model leading to 6.1% and 12.3% higher recovery factor than the 50% and 25% horizontal producer length models, respectively.

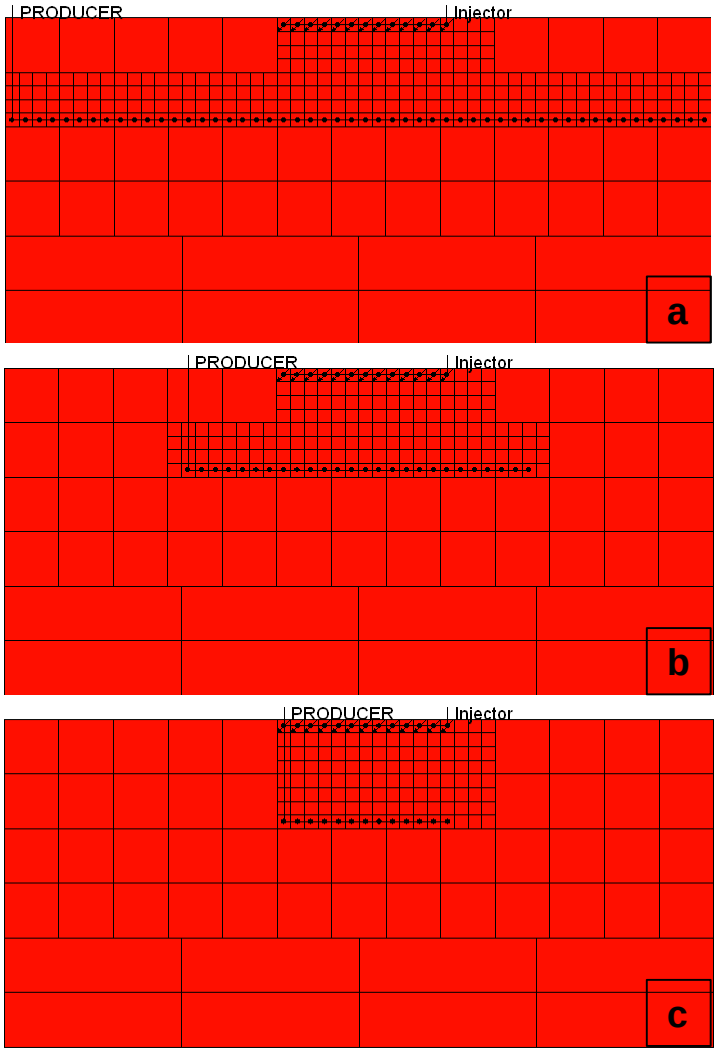

Figure 5.35: *Effect of horizontal producer length in top-down combustion process: (a) HP-100%, (b) HP-50%, and (c) HP-25%*

Model name	Recovery factor (%) @ 3095 days	Recovery factor @ quenched time (%)	Front quenched time (days)	So @ 3095 days (fraction)	So @ quenched time (fraction)
HP-100%	77.0	77.0	3095	0.10	0.10
HP-50%	70.9	61.8	635	0.15	0.20
HP-25%	64.7	38.5	340	0.18	0.33

Table 5.12: *Simulation results of effect of horizontal producer length in top-down combustion process*

The lower recovery factor in the shorter horizontal producer models was not only because of the fire front being quenched earlier, but it was also because the oil was been bypassed in the area swept by the water influx. This was due to the large difference between the heavy oil and water viscosities, which resulted in a very high mobility ratio, and oil being trapped behind the advancing water front. This was shown from the comparison between oil and water saturation maps (Figure 5.39) for all the three models at the final time step of the run (3095 days), especially in the upper area of the model, which resulted in a higher average oil saturation remaining in place in the model.

This sensitivity showed that the shorter the horizontal producer the earlier the front was quenched by the aquifer flow, which resulted in a lower recovery factor. Also, the influx of aquifer water into the oil zone results in trapping high oil saturations, and isolated those areas from being produced, especially areas away from the producer. Hence, for the top-down well configurations it was preferable to have a longer horizontal producer, since it produces with a higher recovery factor.

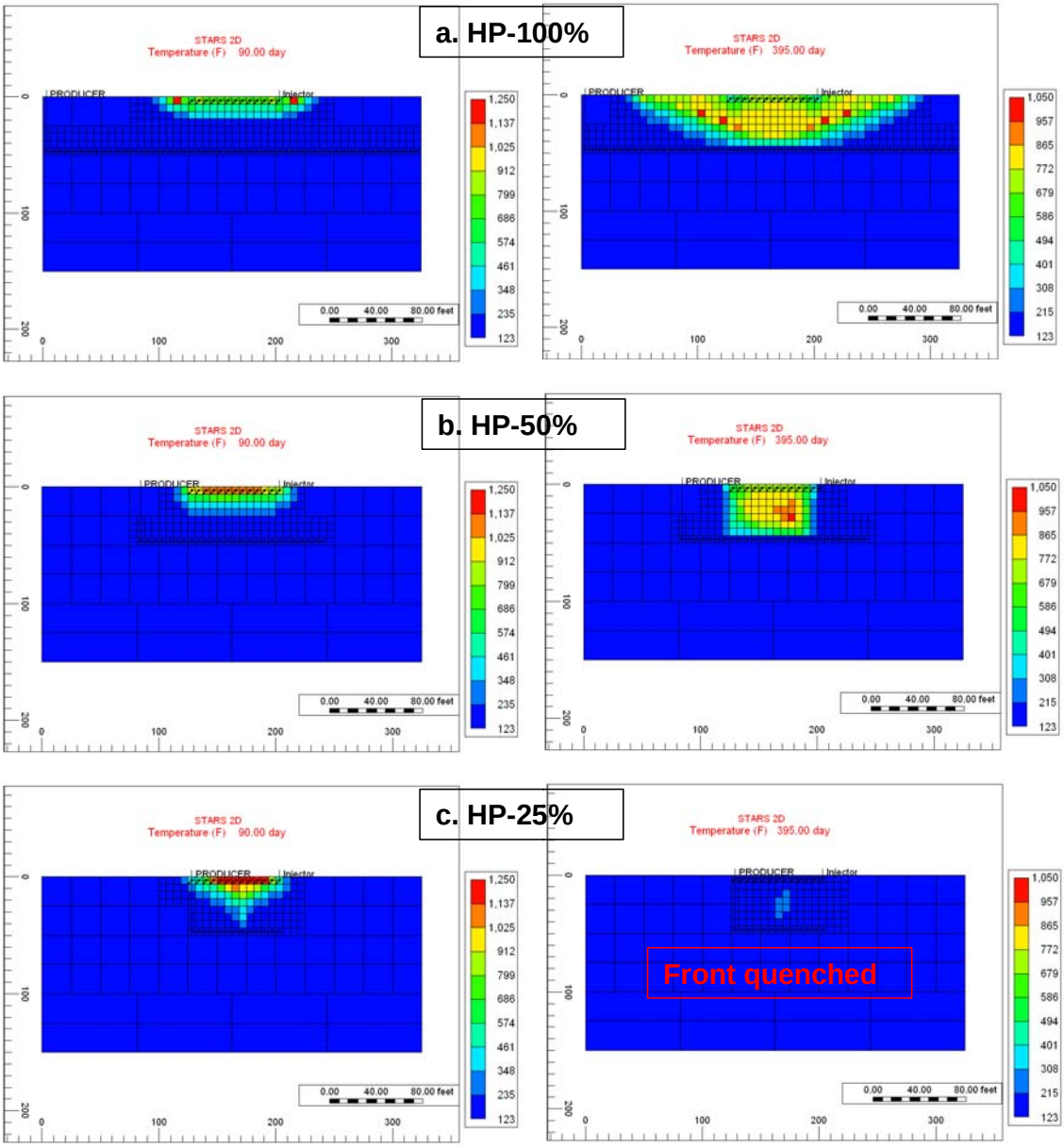

Figure 5.36: *Simulation results of temperature at 90 days and 395 days: (a) HP-100%, (b) HP-50%, and (c) HP-25%*

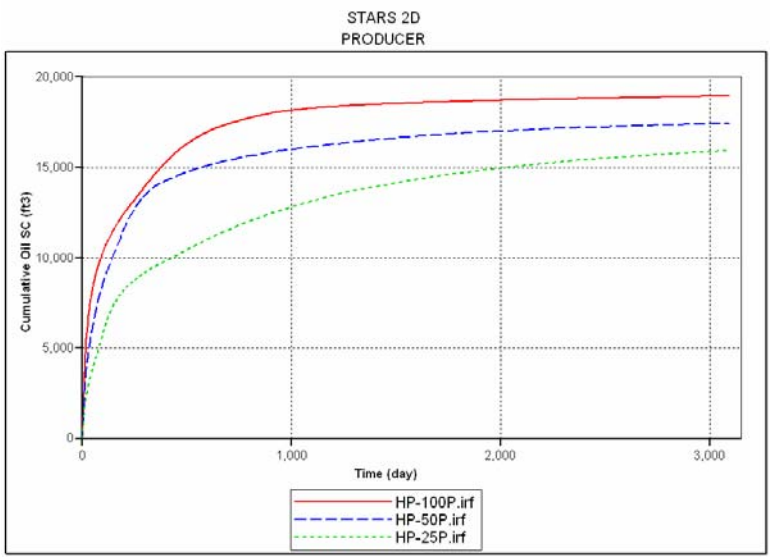

Figure 5.37: *Simulation results of cumulative oil produced for horizontal producer length in top-down combustion process sensitivity*

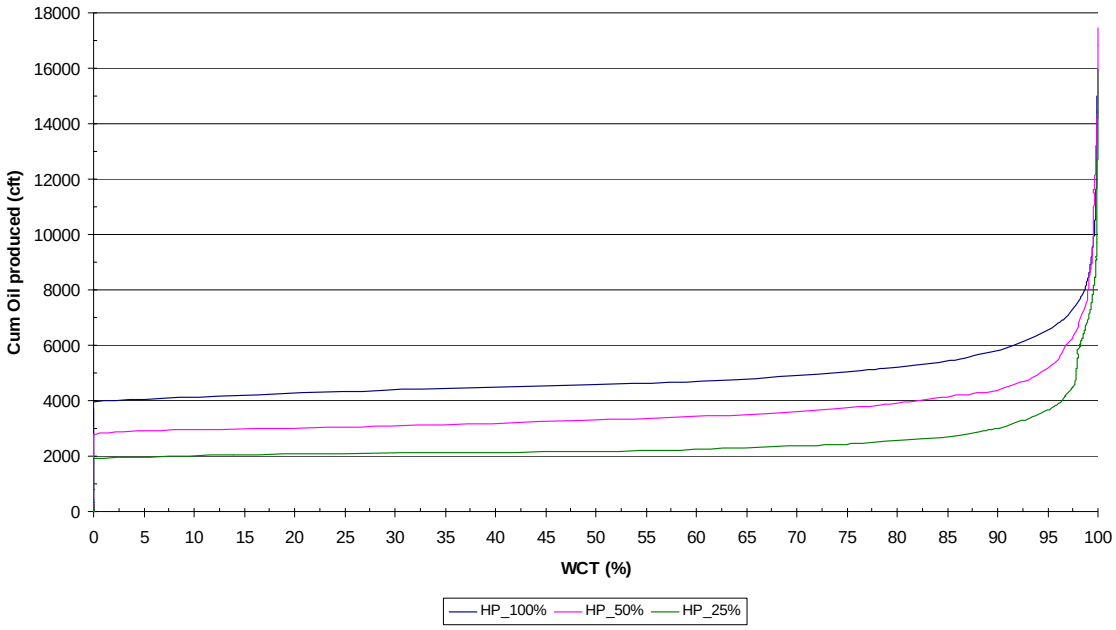

Figure 5.38: *Cumulative oil produced versus water cut.*

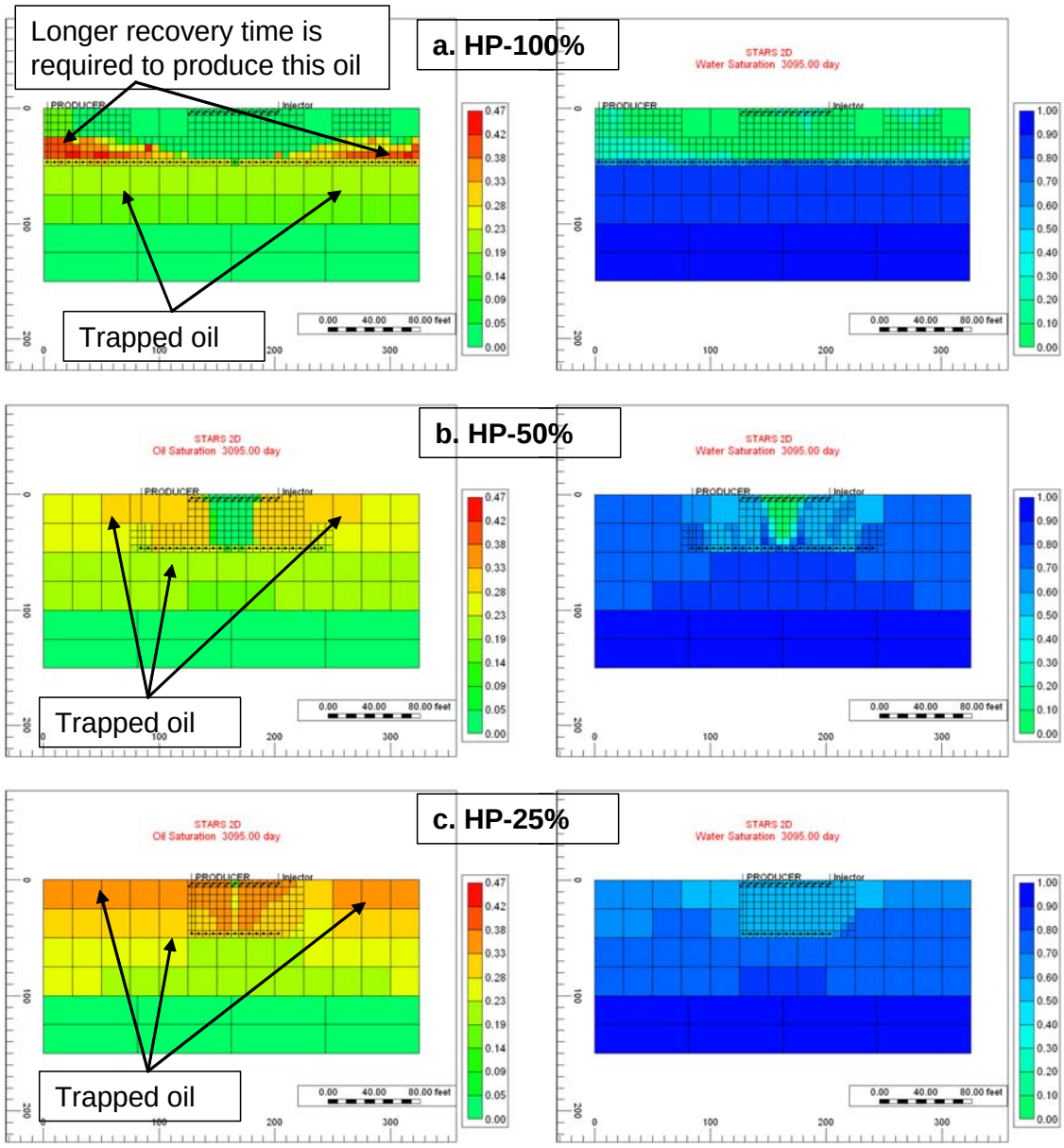

Figure 5.39: *Simulation results of oil and water saturations at 3095 days: (a) HP-100%, (b) HP-50%, and (c) HP-25%*

5.9 Application of partially completed horizontal wells

In Chapter 4, the use of partially completed horizontal wells increased the recovery factor from the combustion process. This was mainly due to the introduction of multiple fire fronts in the same system when using a partially completed horizontal injector, and resulted in a higher recovery and shorter recovery time. In this section, the use of

partially perforated horizontal injector and producer wells was investigated, and their affect on the combustion process was evaluated.

5.9.1 Effect of partially completed horizontal injector

In order to investigate the possibility of using a horizontal injector with multiple completions for in-situ combustion where there was strong bottom aquifer support, four models were developed. The first model had a fully completed horizontal injector with total length of 318.75 ft (Figure 5.40a). The second model had a horizontal injector which was completed in two intervals, each with a length of 18.75 ft (Figure 5.40b), and both the third and the fourth models had three (Figure 5.40c) and four (Figure 5.40d) completion intervals, respectively.

Figure 5.41 shows the temperature distribution of the fire fronts in each of the models at 200 days and at 665 days. The fire front in the fully completed horizontal injector model was initiated and propagated as a piston-like displacement, which improved the sweep efficiency of the front and resulted in production of the largest volume of oil (Figure 5.42). For the three partially completed horizontal injector models, the fire fronts gave similar behaviour in terms of each model producing multiple fire fronts which then propagated to recover the oil, and at a certain point in time all the fronts combined together near the horizontal producer. However, the cumulative oil produced by those models was less than the amount produced by the fully completed horizontal injector model. This was due to the fact that the multiple fire fronts for each model did not recover all the oil in the area between the injector and the producer, especially in the zones between the multiple fire fronts, in contrast to the fully completed horizontal injector case. Those areas were illustrated in Figure 5.43, where the high oil saturations were evident. Table 5.13 summaries the results of the four models in this sensitivity. It was observed that the fire fronts in all the four models were quenched before the end of the simulation. This was a result of the fire front in each case not moving away from the horizontal producer after it broke through, and also due to the lower remaining oil saturation in the area between the injector and producer which reduced the amount of fuel available for the front to consume and sustain itself. Also, from the comparisons of the recovery factor of the partially completed horizontal injector models, the model with

the horizontal injector completed in four sections gave the highest recovery factor (79.6%). This was because of the early merging of the four fire fronts, which in this case made the fire front act as a piston-like displacement, as in the case with the fully completed model, and thereby improved the combustion sweep efficiency. This sensitivity showed that the sweep efficiency of the combustion process can be improved when a partially completed horizontal injector was used, depending on the number of completion intervals. A higher recovery factor can be achieved in these cases, but not as high as the fully completed horizontal injector can offer.

Model name	Recovery factor (%) @ 3095 days	Recovery factor @ quenched time (%)	Front quenched time (days)	So @ 3095 days (fraction)	So @ quenched time (fraction)
HI-fully-completed	80.7	80.1	2000	0.08	0.08
HI-2parts	78.6	78.2	2248	0.09	0.09
HI-3parts	78.5	77.5	1657	0.09	0.09
HI-4parts	79.6	78.8	1733	0.08	0.08

Table 5.13: *Simulation results of effect of partially completed horizontal injector*

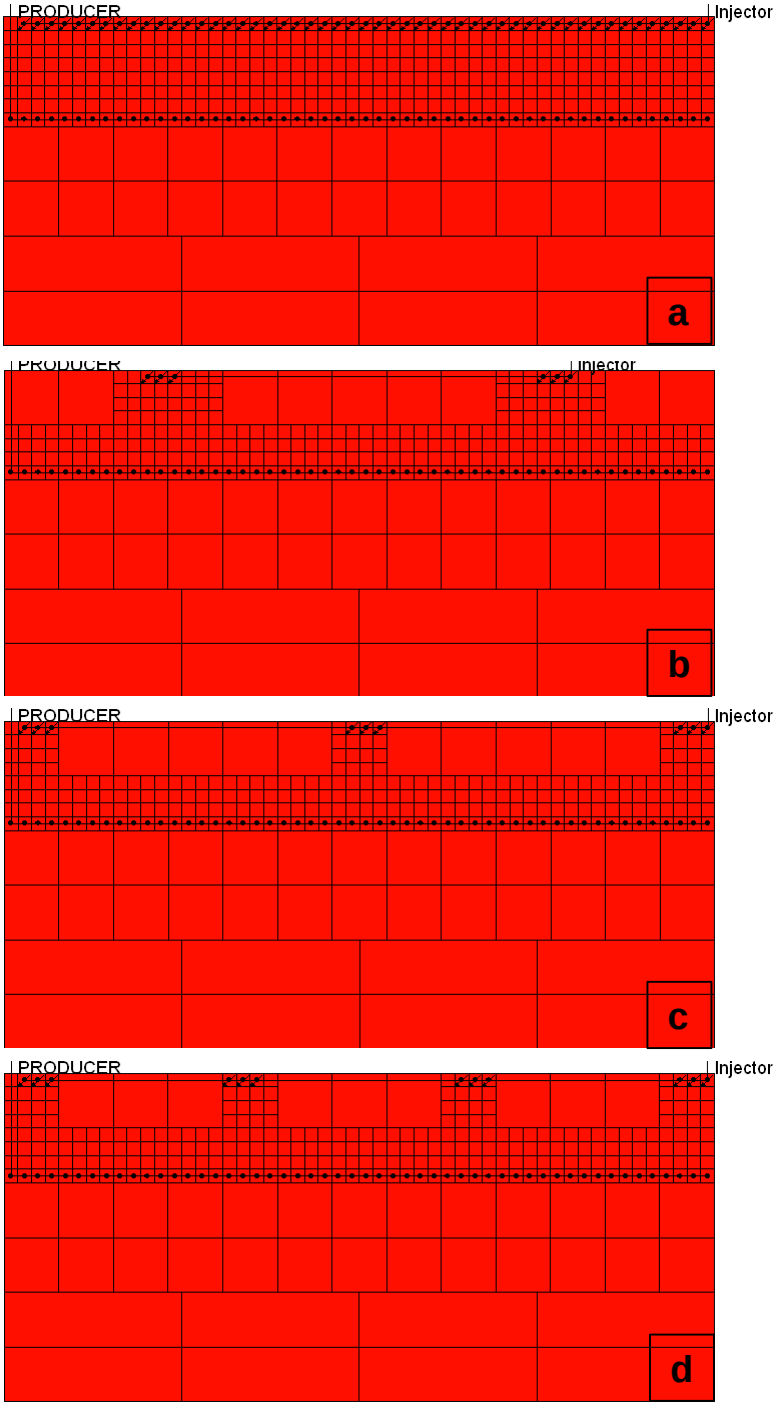

Figure 5.40: *Effect of partially completed horizontal injector: (a) HI-fully-completed, (b) HI-2parts, (c) HI-3parts, and (d) HI-4parts*

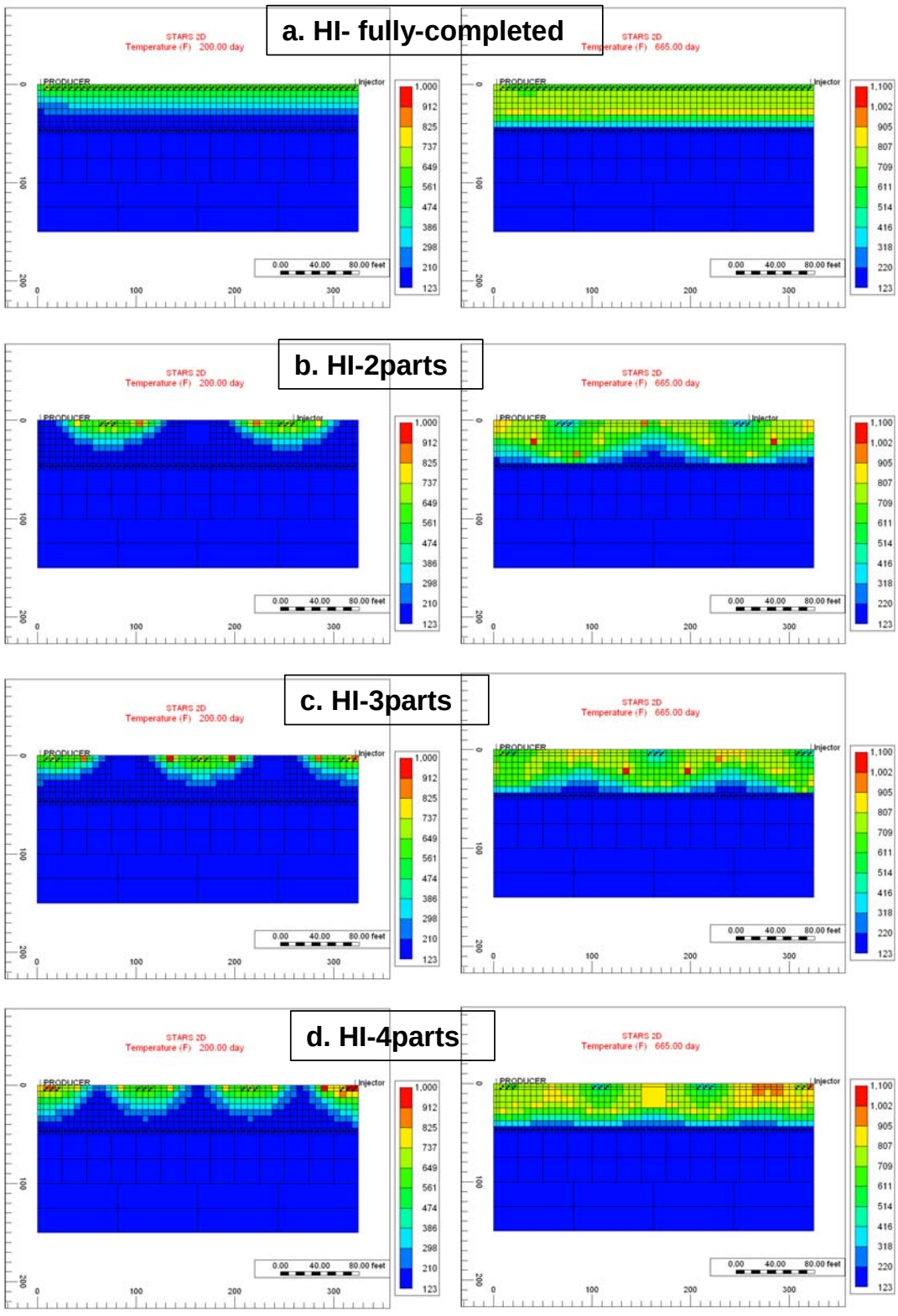

Figure 5.41: *Simulation results of temperature at 200 days and 665 days: (a) HI-fully-completed, (b) HI-2parts, (c) HI-3parts, and (d) HI-4parts*

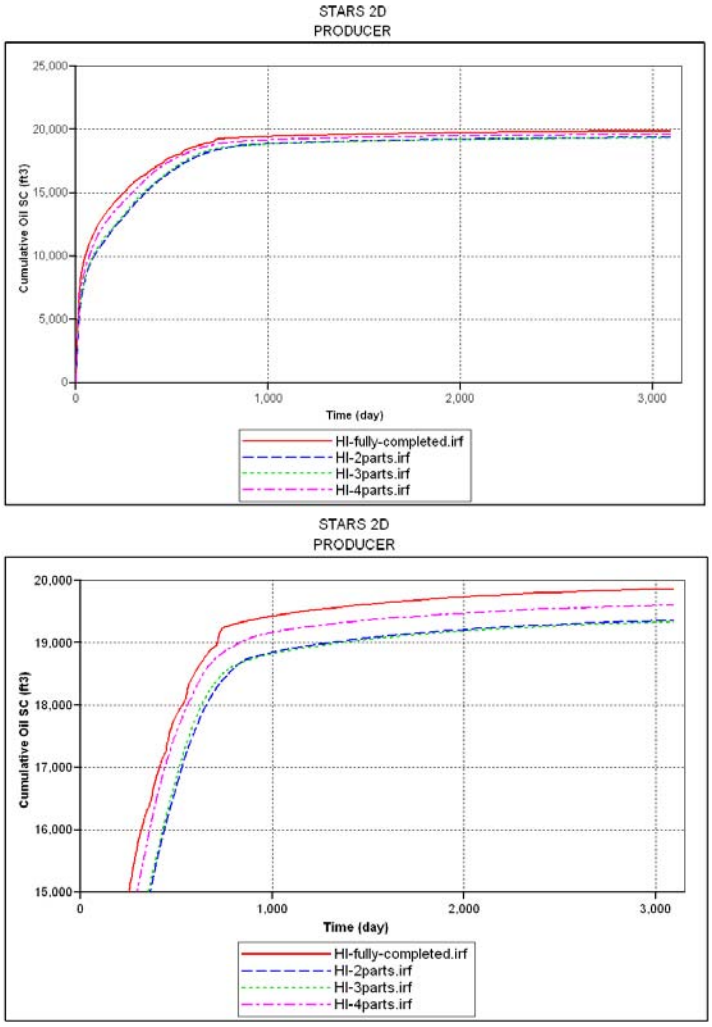

Figure 5.42: *Cumulative oil produced of partially completed horizontal injector*

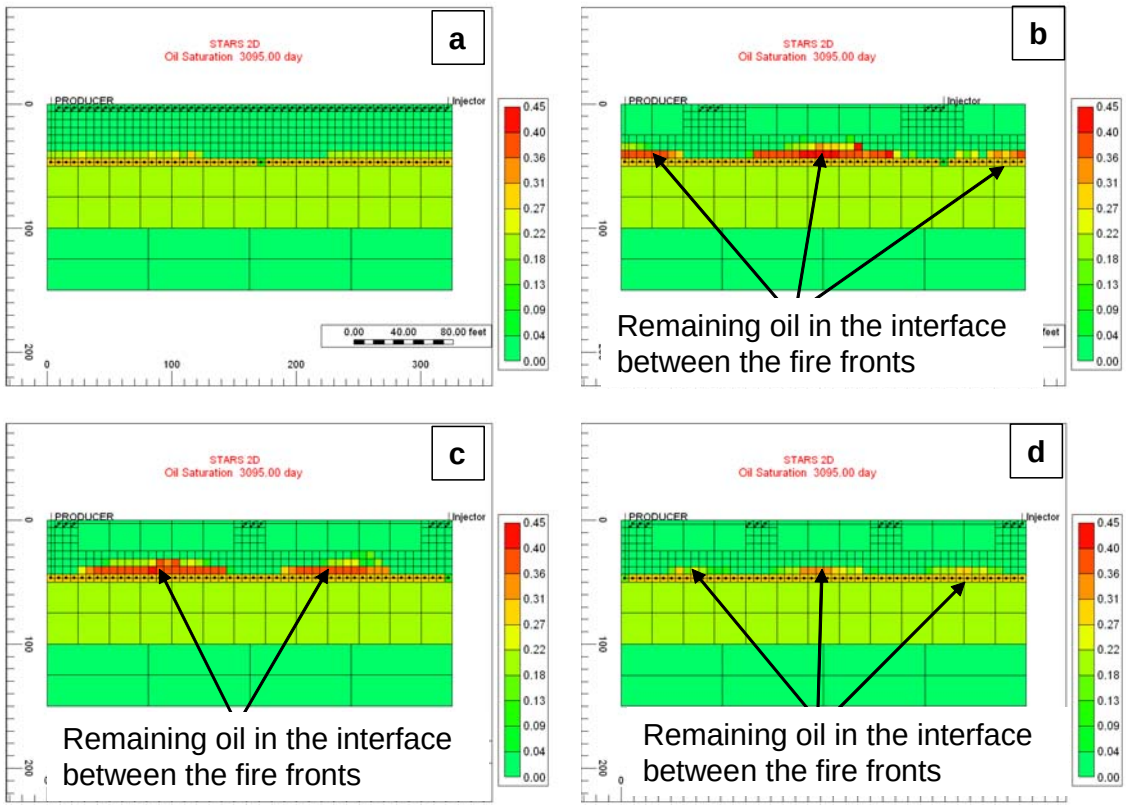

Figure 5.43: *Simulation results of oil saturations at 3095 days: (a) HI-fully-completed, (b) HI-2parts, (c) HI-3parts, and (d) HI-4parts. Note the high oil saturation neat the producer well in between the completed sections.*

5.9.2 Effect of partially completed horizontal producer

In all the previous sensitivities the horizontal producer used was fully completed, and the entire length of the well was perforated. This allowed for the production of more oil, but a large volume of aquifer water may be produced as well. The aim in this sensitivity was to investigate the performance of the in-situ combustion process when a partially completed horizontal producer was used. This way of completing the horizontal producer might help to reduce the amount of water produced. A new model was developed where the producer was completed with four perforation intervals, each 18.75ft long (Figure 5.44). The results from this sensitivity were compared with the results from a fully completed horizontal producer (Figure 5.40a).

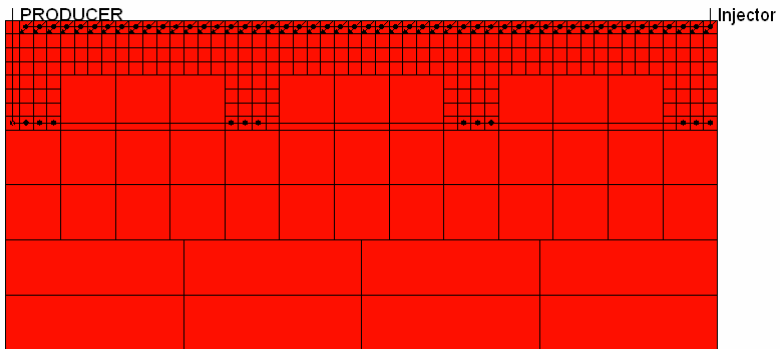

Figure 5.44: *Effect of partially completed horizontal producer*

The simulation results showed that the advantage of having a partially completed producer was to produce 35% less water compared to the fully completed horizontal producer case (Figure 5.45a), because of the lower number of perforations available in the partially completed well. However, the drawback of using the partially completed horizontal producer was the lower of cumulative volume of oil produced by such a well (Figure 5.45b), and the recovery factor achieved by this scenario was 12.5% less than the fully completed horizontal producer model. This was a result of the early quenching of the fire front (at around 190 days) because of water flowed through the gaps between the completion intervals, as both the temperature and ternary saturation maps show in Figure 5.46. Another reason for the lower recovery factor was the increase in the amount of oil trapped by the aquifer water influx in the partially completed horizontal producer model. This happened not only in the area below the horizontal producer, but also it occurred very significantly in the top area of the model between the horizontal injector and the partially completed horizontal producer, as the oil saturation plot shows (Figure 5.47) at the final time step of the run.

The use of a partially completed horizontal producer showed a good improvement in reducing the total volume of water produced when strong aquifer drive exists. However, this way of completing a horizontal producer did not allow the fire front to be sustained for a longer period of time, and as a result much of the oil in place was trapped by the influx of the aquifer, leading to a lower recovery factor.

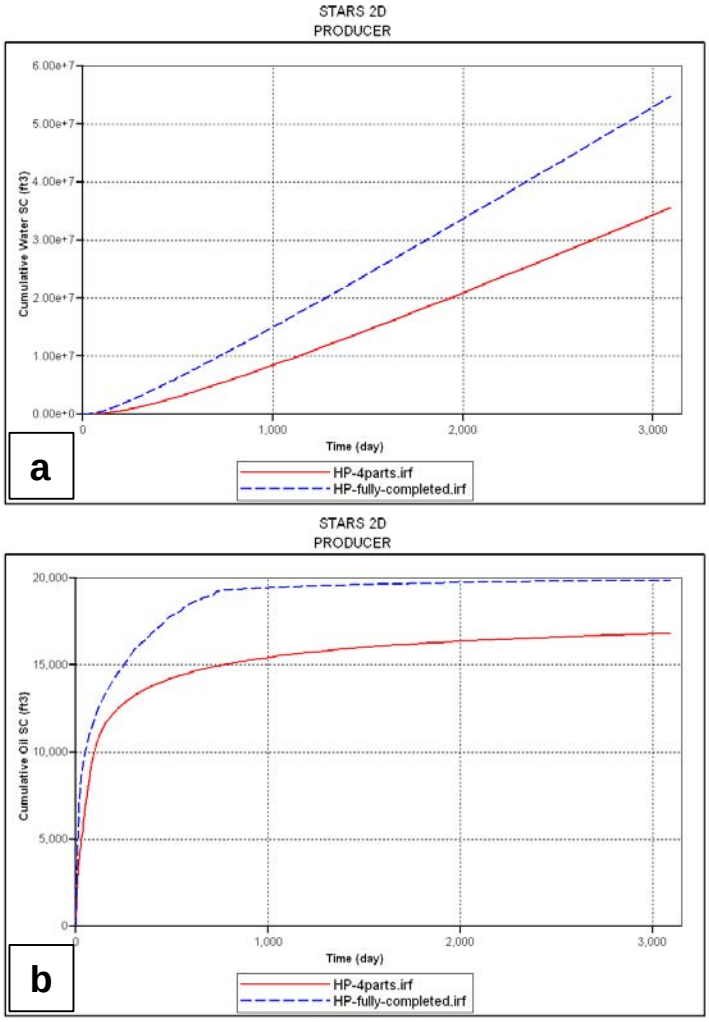

Figure 5.45: *Simulation results of effect of partially completed horizontal producer: (a) cumulative water produced, and (b) cumulative oil produced*

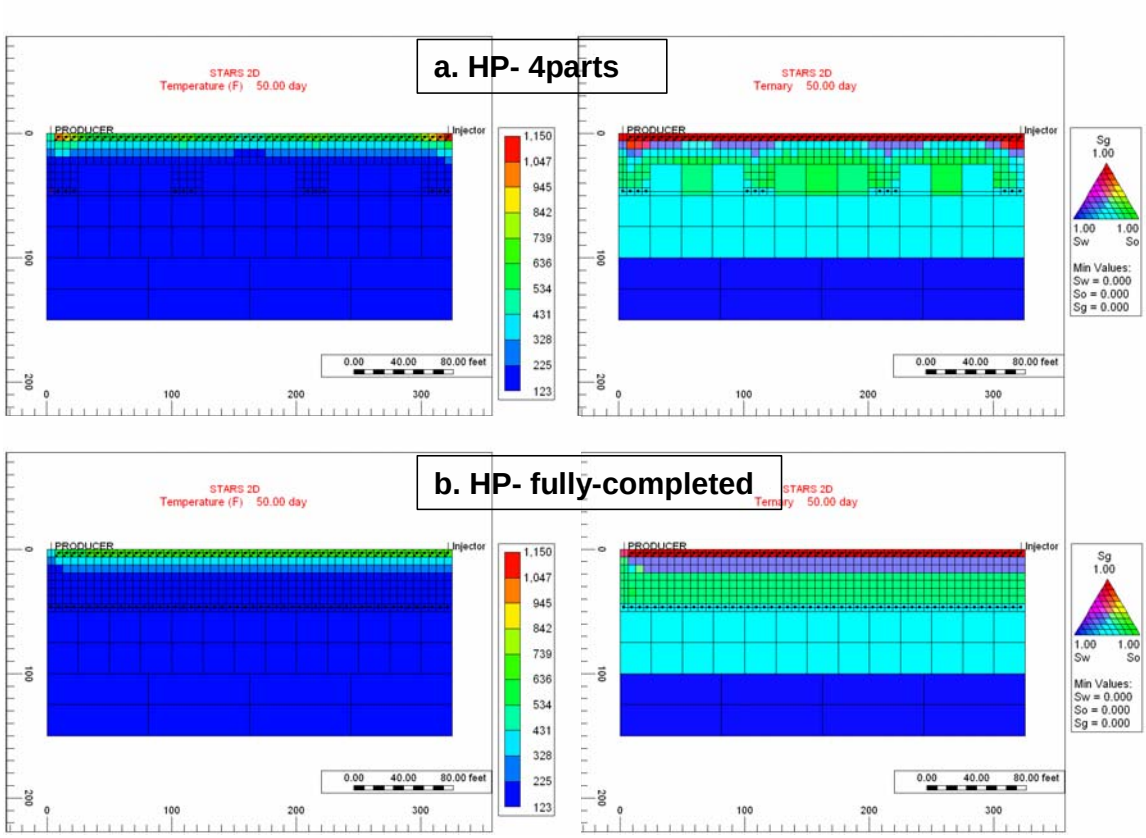

Figure 5.46: *Simulation results of temperature and ternary saturation plot at 50 days: (a) HP-4parts, and (b) HP-fully-completed*

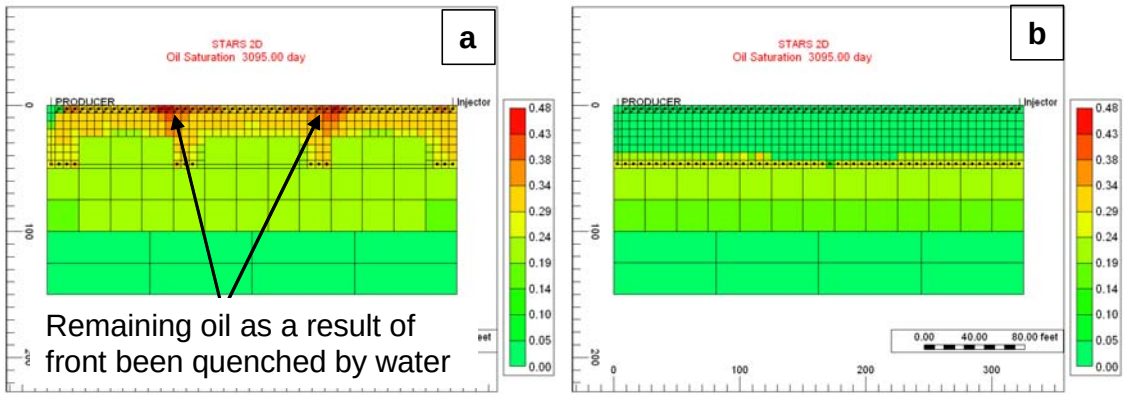

Figure 5.47: *Simulation results of oil saturations at 3095 days: (a) HP-4parts, and (b) HP-fully-completed*

5.10 Intelligent well completion in top-down in-situ combustion

Application of intelligent wells in Chapter 4 led to acceleration in oil production and reduced the required recovery time for the combustion process. In this chapter, introduction of strong bottom water aquifer support in the Nimr base case model resulted in a change in the in-situ combustion process behaviour, and affected the recovery factor achieved by the overall process. Use of smart well completions in the top-down well configuration, where a 81.25ft horizontal injector was completed in the bottom and a 325ft horizontal producer was completed in the middle (Figure 5.48), might be expected to result in an improved performance of the in-situ combustion process. This intelligent completion will enable the closure of the horizontal producer perforations when oxygen break through occurs, which will lead to the redirection of the fire front and air supplies being directed to the unswept area of the model. It also might help to reduce the total volume of water produced by the horizontal well. The aim in this sensitivity was to evaluate the in-situ combustion performance when intelligent well completions were used, and to estimate the improvement in the process due to the closure of the perforations in the horizontal producer.

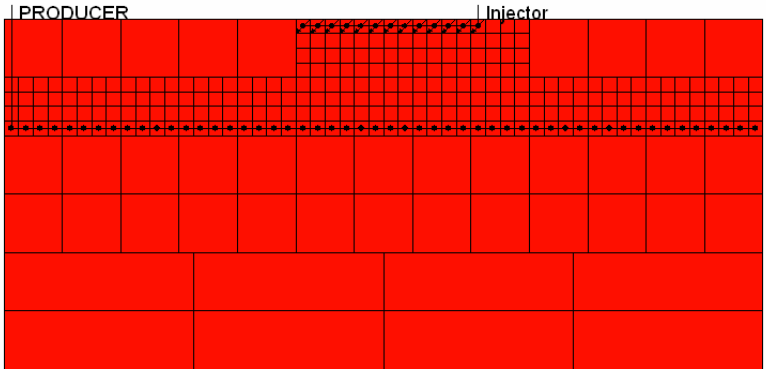

Figure 5.48: *Application of intelligent horizontal producer in top-down in-situ combustion process*

Figure 5.49 shows both the temperature and ternary saturation plots at 455 days for both scenarios. The closure of the horizontal producer perforations after the oxygen broke through (at 438 days) in the middle section of the well, and the flow of water from the aquifer, both resulted in the division of the fire front into two fronts, each moving

toward the model boundaries (Figure 5.49a). This resulted in a slight enhancement of the fire front velocity, and led to an acceleration of the oil production, as Figure 5.50a shows. However, the closure of the perforations in the intelligent completion of the producer allowed for greater water influx to the upper area of the model (Figure 5.49a) which quenched the front. Figure 5.50b shows the net coke in place, and it indicated that the fire front for the intelligent well system was quenched at around 730 days, compared to the long sustainability of the front in the other model. The smart completion model produces a smaller cumulative oil volume (Figure 5.50a), which made this model deliver a recovery factor 1.1% less compared to the normal horizontal producer completion case. However, the closure of the perforations in the intelligent producer case did result in the production of 36% less water when compared to the amount produced by the normal horizontal completion model (Figure 5.50c). This meant that the use of intelligent completion reduces the recovery factor by 1.1% in this case, but it also reduced the cost of handling 36% extra water, and it slightly accelerated the oil production in the early stage of the process. Table 5.14 summarises these sensitivity results. The main outcome of conducting this sensitivity was that the application of intelligent well technology, in terms of remotely closing the well perforations, led to an enhanced fire front velocity, and redirected the fire front to unswept area of the model. Also, using this well scenario results in a reduction in the rate of aquifer water production, and accelerated oil production. However, it could result in marginal reduction of the recovery factor of the overall process due to the early quenching of the combustion front as a result of water flow from the aquifer.

Model name	Recovery factor (%) @ 3095 days	Recovery factor @ quenched time (%)	Front quenched time (days)	So @ 3095 days (fraction)	So @ quenched time (fraction)
Intelligent-HP	75.9	73.8	730	0.11	0.12
HP-100%	77.0	77.0	3095	0.10	0.10

Table 5.14: *Simulation results of application of intelligent horizontal producer in top-down in-situ combustion process*

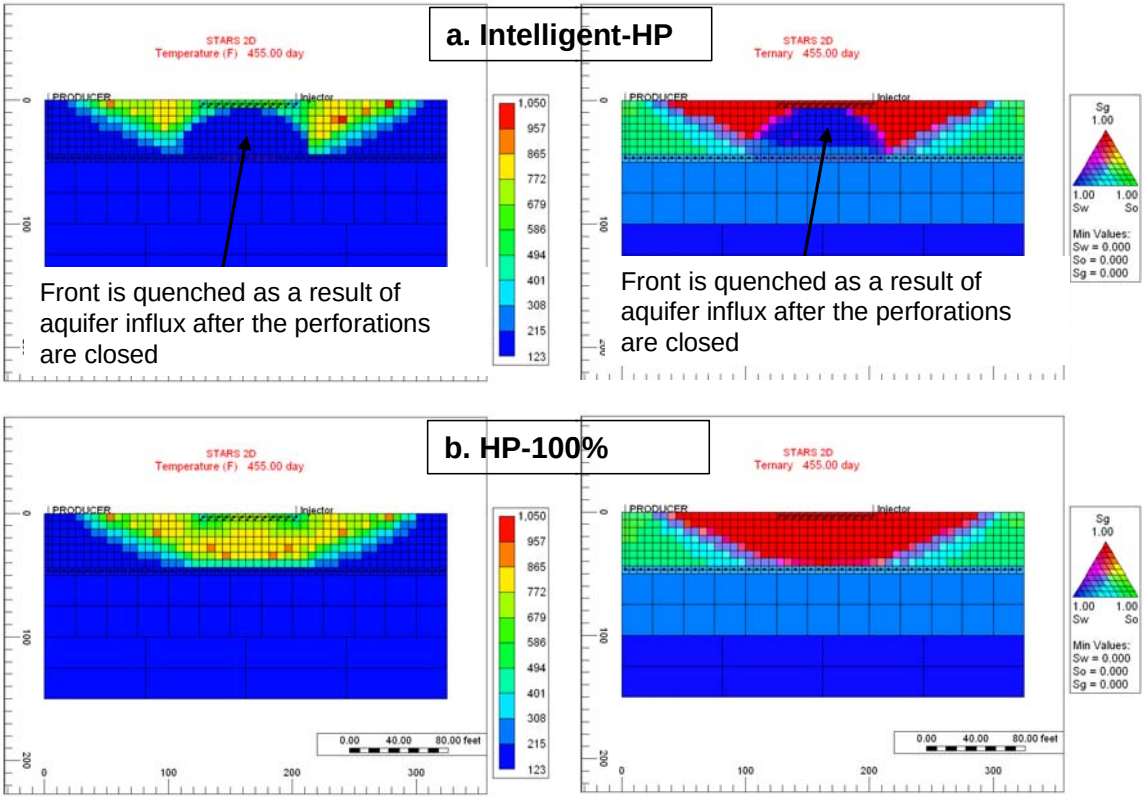

Figure 5.49: *Simulation results of temperature and ternary saturation plots at 455 days: (a) Intelligent-HP, and (b) HP-100%*

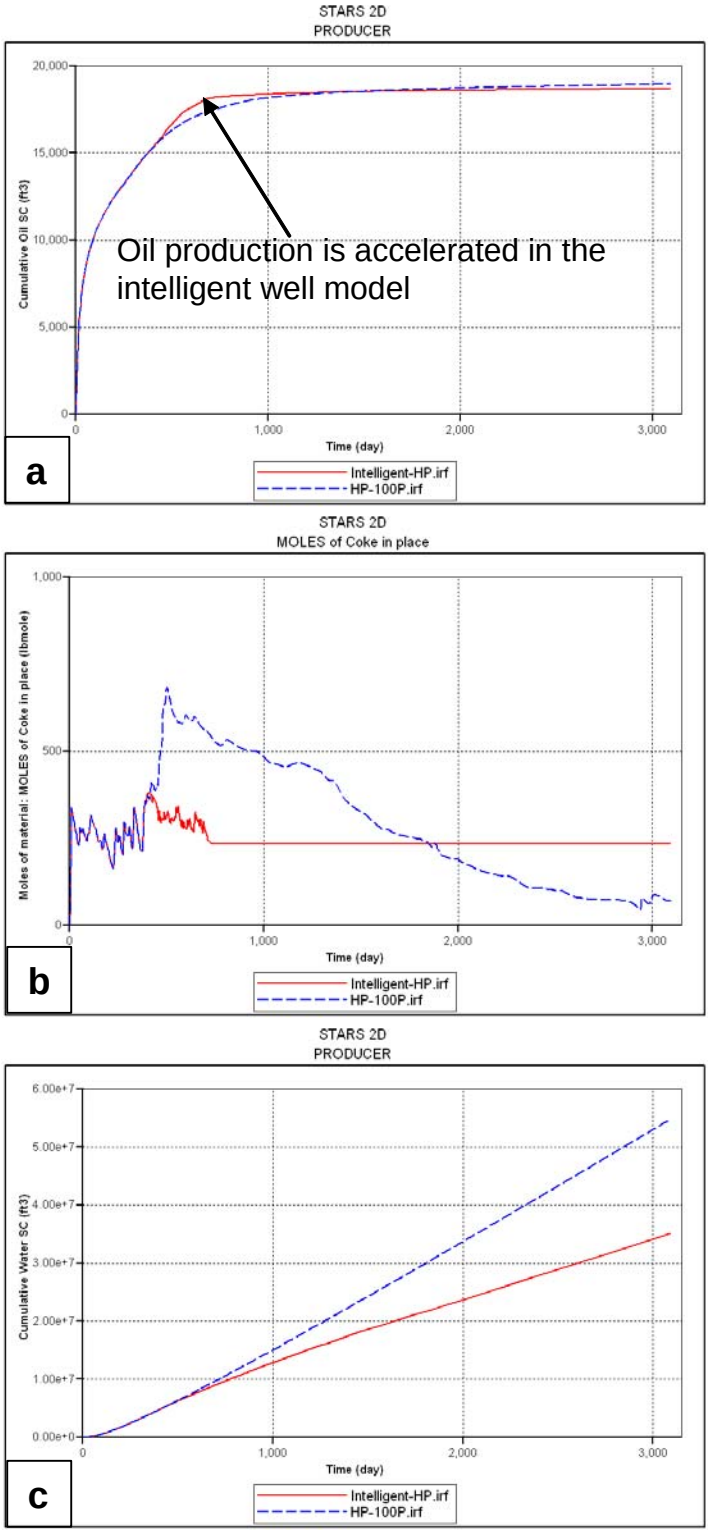

Figure 5.50: *Simulation results of application of intelligent horizontal producer in top-down in-situ combustion process: (a) cumulative oil produced, (b) net coke in place, and (c) cumulative water produced*

5.11 Delaying application of in-situ combustion

Both in-situ combustion and aquifer drive were the main forces leading to the recovery of oil in this study. A combination of both driving forces reduced the saturation of the majority of the hydrocarbons in place. In some cases, where the front was quenched at a later stage of the process, the recovery was mainly due to aquifer water influx. So far in this chapter, the plan was to introduce in-situ combustion from the beginning of each simulation. In this section, the possibility of delaying the use of in-situ combustion to a later stage was investigated. This meant that instead of igniting the fire front at the start of the simulation, it was postponed to a later stage of the model life. This made the production of oil in the initial period mainly due to aquifer drive, until later when the combustion process was established. Three different times were chosen for when the fire front was initiated: after one year, two years and four years. The top-down 81.25 ft horizontal injector and 325 ft horizontal producer well configuration was used (Figure 5.51).

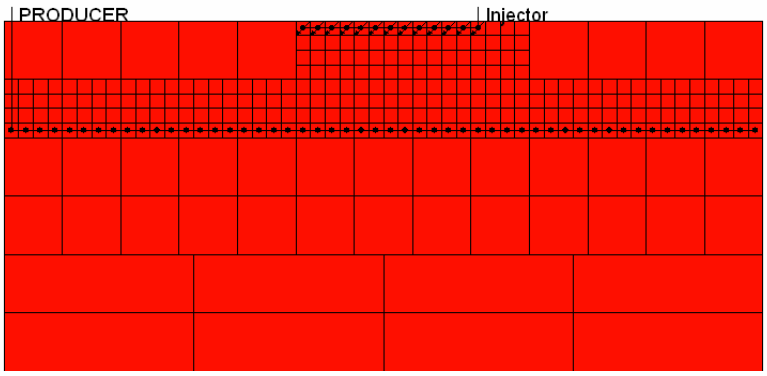

Figure 5.51: *Delaying in-situ combustion application well configurations*

The main outcome of this sensitivity was that the behaviour of the combustion fronts and the overall results from the four models were almost identical, except that there was a time delay in oil production, which was proportional to the delay in starting the in-situ combustion process. The net coke in place (Figure 5.52a) shows that all the models produced the same amount of coke. The total volume of oil produced was more or less the same in all cases (Figure 5.52b). For example, starting the in-situ combustion after one year led to the highest recovery factor at around 1600 days, whereas the four years

delay in starting the combustion process model meant that it took 2700 days to achieve the highest recovery. The main reason for the similarity in the final results of there four models were the use of the current top-down well configuration. The use of the 325 ft horizontal producer allows for oil recovery from the area between the producer and the aquifer, and at the same time it prevented water flow to the upper part of the model by producing it, which resulted in all the four models producing the same amount of water by the end of the run (Figure 5.52c) This meant that the area between the injector and the producer remains with its initial oil saturation until the fire front was introduced at a certain time for each case. Once this happened, similar behaviour of front propagation was observed for the different times in the four models, as both the temperature and saturation maps show (Figure 5.53). Also, because the area was the same in all the models, the final recovery factor was almost the same, and the saturation of the remaining oil in place at the end of the simulation was almost the same value (Figure 5.54) at both the top and bottom areas of the models.

This sensitivity showed that the performance, in terms of front propagation behaviour and the final recovery factor, were not affected by the delay in initiating the combustion process. The comparison in this section showed that the decision to apply in-situ combustion after one, two, or four years in a project depends in the economic viability of the process. To start recovering the oil in place with a water drive for the early stages of the project, and later on to introduce the combustion process will enhance the project feasibility by delaying the need for capital investment in the in-situ combustion infrastructure. In contrast, the delay of applying the combustion process will affect the project economics in terms of delaying the possibility of producing and recovering the oil in place in the shortest possible time frame (Figure 5.52b).

Figure 5.52b demonstrates the recovery that would be achieved if no fire front is initiated, since in the calculation where the fire front is initiated after four years, the recovery has reached a steady state value of about 10,000 ft^3 within those four years. (In the case where there is no aquifer present, then there is insufficient pressure to recover any significant volume of this viscous oil.

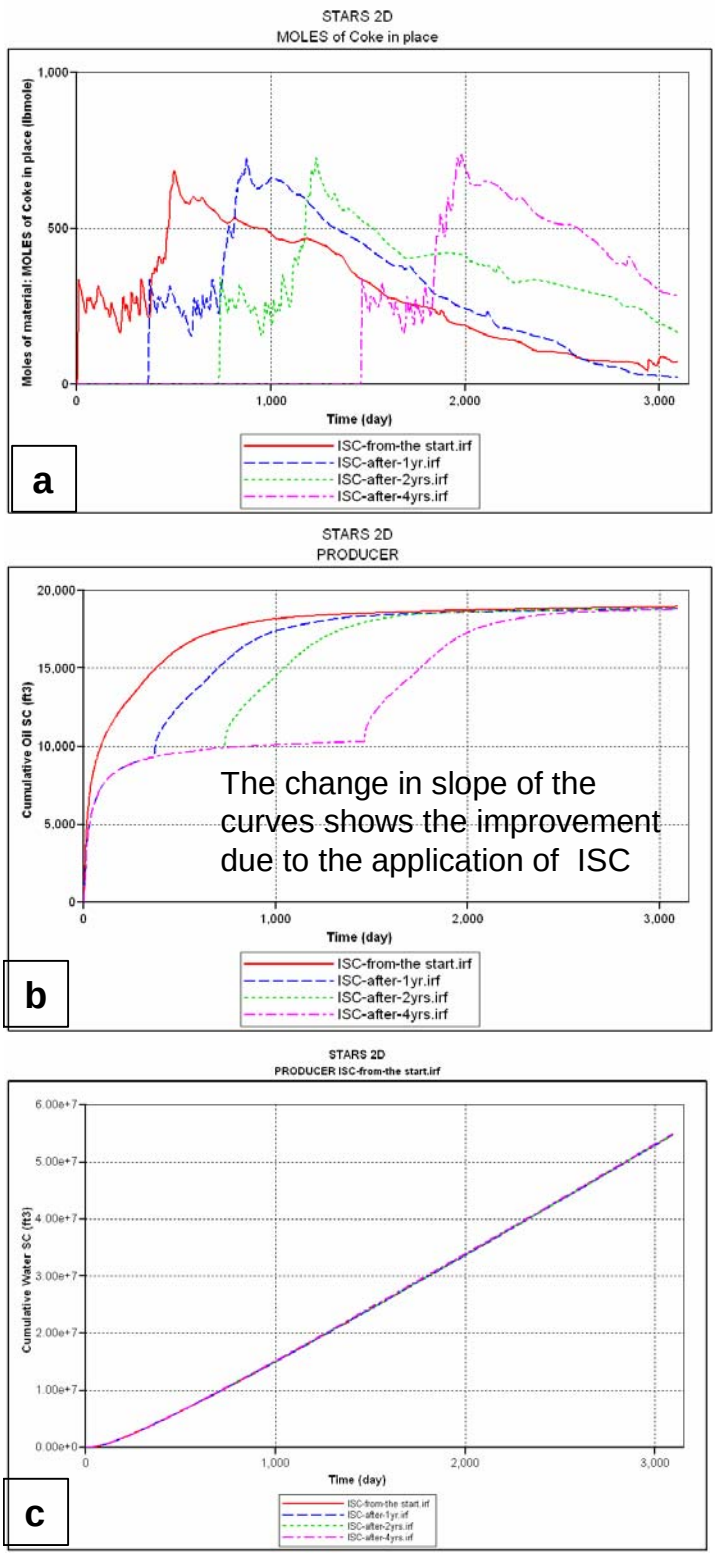

Figure 5.52: *Simulation results of delaying in-situ combustion application: (a) net coke in place, (b) cumulative oil produced, and (c) cumulative water produced.*

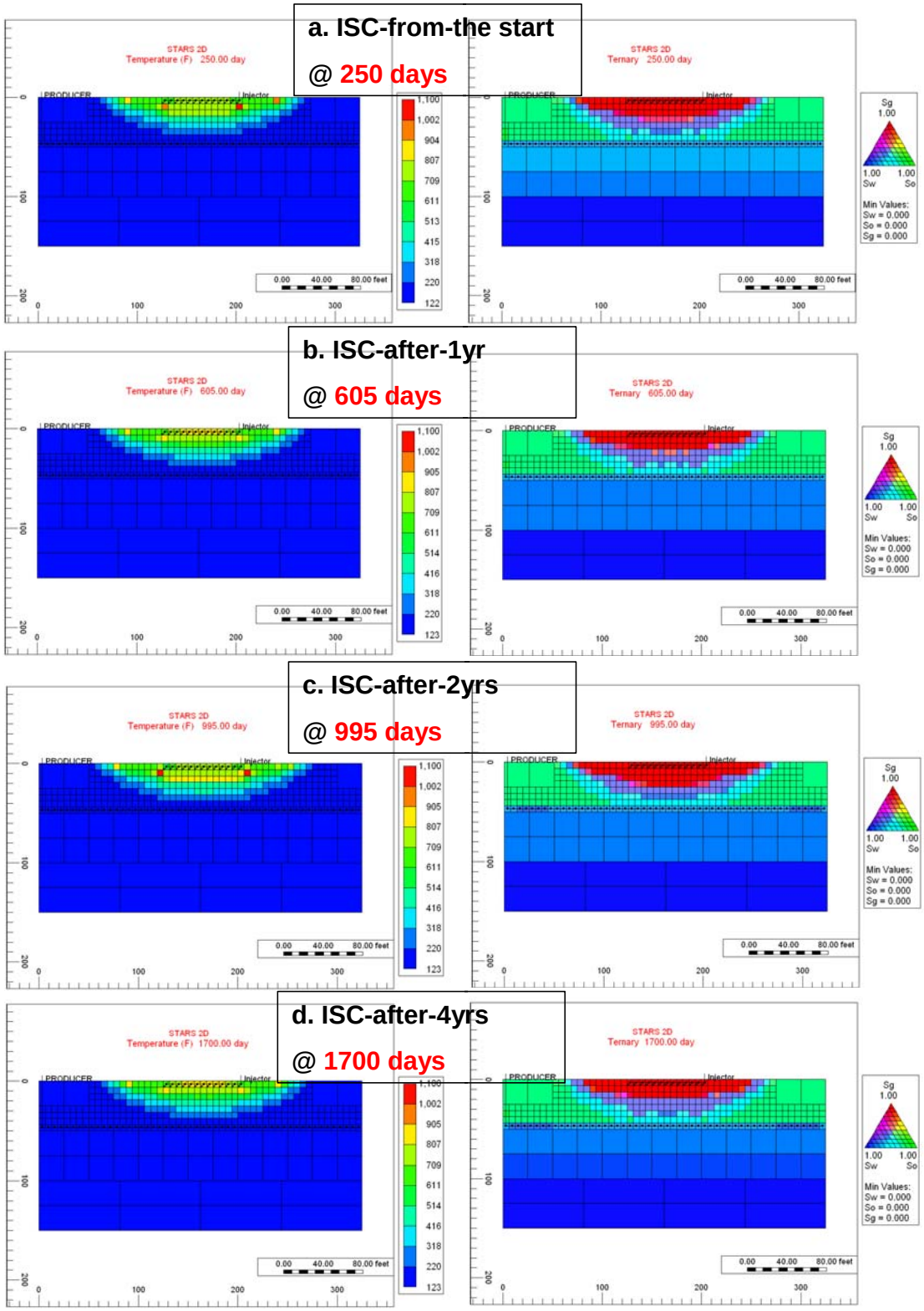

Figure 5.53: *Simulation results of temperature and ternary saturation plot at different time steps: (a) ISC-from-the start, (b) ISC-after-1yr, (c) ISC-after-2yrs, and (d) ISC-after-4yrs*

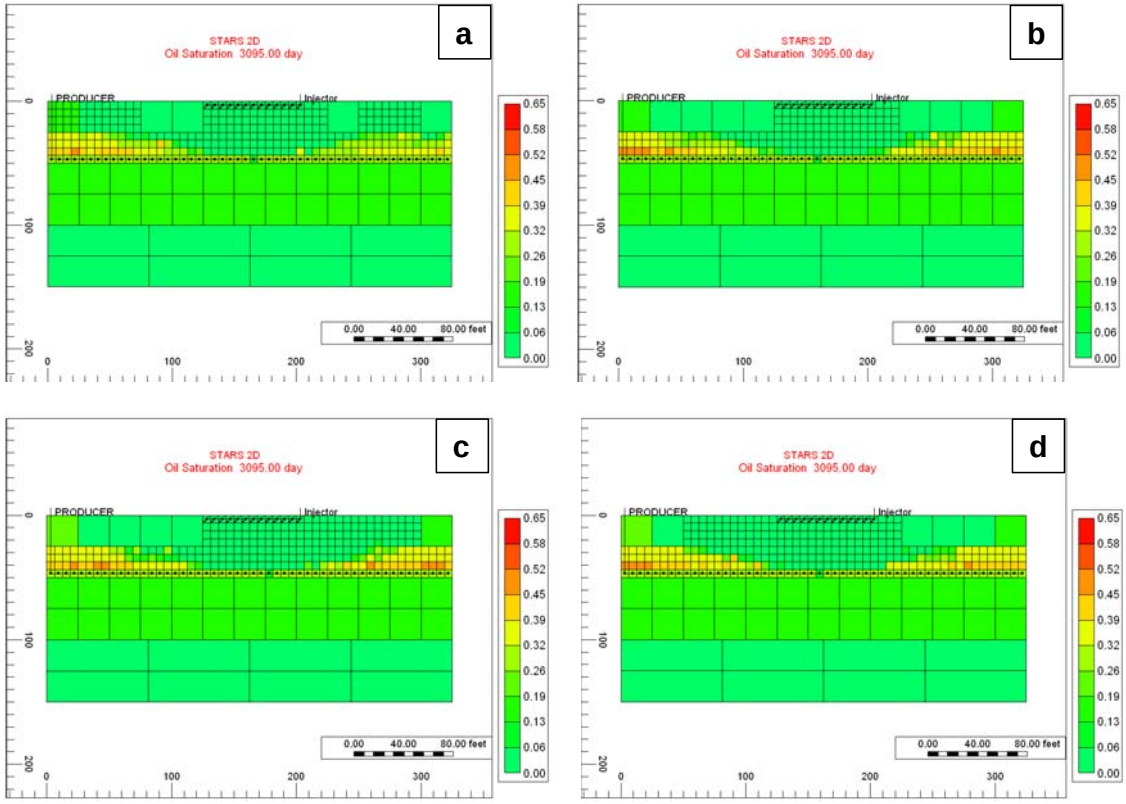

Figure 5.54: *Simulation results of oil saturations at 3095 days: (a) ISC-from-the start, (b) ISC-after-1yr, (c) ISC-after-2yrs, and (d) ISC-after-4yrs*

5.12 Summary

The base case model developed in this chapter has strong bottom aquifer support. There were two vertical wells, one injector and one producer. The sensitivity calculations around the configuration of the injector and producer wells showed the need to optimise the completion of both wells. This was required to successfully initiate the fire front and to sustain it for a longer time before it was quenched, and thereby to increase the recovery factor. Moreover, the results showed the need to avoid completing both wells near the aquifer, since this results in an early quenching of the combustion front and a significant volume of water was produced.

Several sensitivities were conducted to investigate the use of horizontal wells, and to optimise both their length and their location in the formation. The use of a horizontal

producer in the combustion process model resulted in a higher recovery factor when compared to the performance of the vertical producer. However, the fire front was quenched very early due to the short distance between the horizontal producer and the vertical injector, which allowed for early fire front break through into the producer. The optimisation of the horizontal producer length showed that the longer the horizontal producer, the more oil that was produced, and the more aquifer water that was produced also. As a result, in order to choose the optimum horizontal producer length, it was important to have a balance between the potential expected recovery factor and the cumulative water to be produced. For this specific sensitivity, this balance was achieved when a 162.5 ft (50%) horizontal producer length was used. Also, the location of the producer relative to the injector did affect the combustion process performance. For example, by locating the horizontal producer in the middle section of the model, this did help to sustain the fire front for the entire simulation. This was because the new location of the producer made it act as a barrier to prevent the aquifer water influx from reaching the combustion front and quenching it. However the drawback of lowering the horizontal producer was the rapid increase in water cut as soon as the modelling process started, due to the shorter distance between the producer and the aquifer. Furthermore, the use of a horizontal injector well in the combustion process while aquifer support exists was considered, and the location of the injector should be carefully chosen. In order to make the most of the horizontal injector, it was preferable that it be located far above the horizontal producer, which prevents the fire front from being quenched by the water flow from the aquifer. As a result, the sustained combustion front was able to efficiently sweep the top of the model area, and reduce the oil viscosity, which can then flow easily to the horizontal producer under gravity drainage. This well configuration was called the top-down well scenario.

In the top-down well configuration, the placement of the horizontal producer directly affected the recovery factor achieved by the in-situ combustion process. This was because the recovery factor was proportionally increased as the area of the model swept by the fire front increased. The horizontal producer was lowered to be closer to the aquifer in order to increase the distance between the horizontal producer and the injector. However, by doing so, the total amount of water produced also increased, which resulted in an increase in the cost of handling and treating the water. This meant

that the project economics plan for the top-down well scenario should decide the optimum horizontal producer location. In other words, to place the horizontal producer toward the bottom of the system near the aquifer, in order to achieve a higher recovery factor, may mean that at the same time more investment in water treatment facilities to handle the greater amount of water was required. Alternatively, to locate the horizontal producer away from the aquifer to reduce the need to invest in water treatment infrastructure will result in lower recovery factors. Moreover, the horizontal section length of the producer was considered to be crucial in top-down in-situ combustion. The sensitivity to optimise this length showed that the longer the horizontal section of the producer, the longer the fire front was sustained, and the more oil that was produced. This was not only because of the longer contact area between the producer and the formation, but also because the longer horizontal producer reduced, and in some case prevented, the water from the aquifer quenching the fire front.

Partially completed horizontal wells proved to be useful in improving the fire front performance in the case where there was no aquifer support in Chapter 4. The possibility of using a partially completed horizontal injector was investigated in this chapter. The results showed an improvement in the sweep efficiency of the combustion front as a consequence of introducing multi fire fronts in the same model. Also, the sensitivity showed that as the number of completion intervals increased, higher recovery factors were achieved. However, the use of a fully completed horizontal injector showed a better performance than the partially completed horizontal injector case because the fire front developed as a piston like advancement front to sweep the model area. Moreover, the use of partially completed horizontal producer was considered, but this scenario gives a poor performance in terms of producing 12.5% less oil compared to the fully completed horizontal producer case. This was mainly as a result of the water flow between the perforation intervals on the horizontal producer, and quenching of the combustion front too early. Another reason for the poor recovery in the use of the partially completed horizontal producer was the large volume of oil which was trapped by the aquifer water influx, especially in the upper area of the model between the horizontal injector and the horizontal producer. The only advantage achieved by having a partially completed horizontal producer was the reduction in the total amount of water produced by 35%, compared to the fully completed horizontal producer case.

Application of intelligent well completions in the top-down process showed a significant improvement in reducing the total amount of water produced by 36%. This was because the closure of the well perforations when oxygen breaks through resulted in limiting the amount of water that flowed into the producer. Also, this closure helped to redirect the combustion front to the unswept area of the formation and allowed for a faster front propagation velocity, as a result directing more air supplies to support the fire front instead of allowing this air to be produced from the break through perforations. However, the use of smart well completions led to early quenching of the fire front because of the water being able to flow through the part where the perforations were closed in the producer. This resulted in a slight decrease in the recovery factor of this well scenario (by 1.1%) compared to the normal horizontal producer well completion. Moreover, another sensitivity was conducted to investigate the possibility of delaying the use of the in-situ combustion process. It showed that the overall process performance was almost the same when using a 81.25ft horizontal injector and a 325ft horizontal producer top-down scenario. This was a result of the long horizontal producer keeping the area between the injector and the producer at initial oil saturation until the fire front was introduced at a later stage. The results of delaying the combustion process showed a similarity between the different cases, there only being a direct time shift of the outcomes depending on the time when the in-situ combustion was initiated.

Figure 5.55 presents a summary plot of the main sensitivity calculations conducted in this chapter. The use of a top-down 81.25ft horizontal injector and 325ft producer well scenario could be chosen to conduct the in-situ combustion process in formations where strong aquifer support was an issue. The choice of this well configuration was partially based on the high recovery factor which was achieved (77%), and also it could sustain the combustion front for a longer time. However, the main reason this well configuration was considered to be the optimum scenario was because of the balance between the recovery factor and the total amount of water produced. In work presented in this chapter there were other models (i.e. when the horizontal producer was completed near the aquifer) which produced higher recovery factors compared to the one chosen here, but they were considered as unfeasible because of the large volume of water associated with production in those cases.

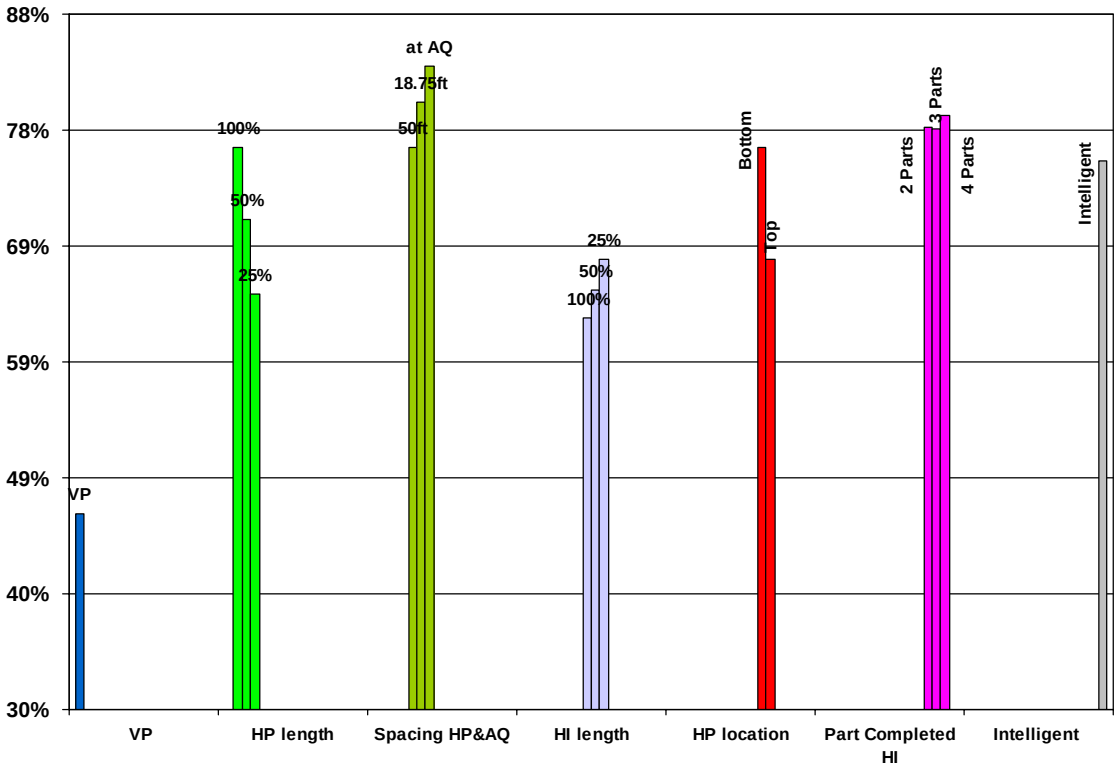

Figure 5.55: *Summary of the recovery factor achieved by some of the main scenarios which were considered in this chapter*

Chapter 6

Investigation of Heterogeneity Effect in In-Situ Combustion for the Nimr Field

6.1 Introduction

The requirements for the successful of initiation and sustaining of an in-situ combustion fire front were demonstrated in both Chapters 4 and 5, where a homogeneous simulation model of the Nimr field was used. A comprehensive evaluation and understanding of the effect of formation heterogeneity on in-situ combustion performance was also required. This chapter aimed to investigate the performance of the combustion process when various types of reservoir heterogeneity were introduced to the simulation model. To begin with, Kv/Kh ratio was investigated in order to evaluate the effect of changing the vertical permeability on the combustion front propagation and oil recovery. Moreover, the effect of heterogeneous multiple permeability layering was also investigated to determine the fire front behaviour in such heterogeneous environment. Finally, the effect of heterogeneous impermeable shale layers and shaley sand layers on in-situ combustion was studied and evaluated.

6.2 Heterogeneity

Heterogeneity is one of the main features of oil bearing formations. This feature introduces complexity to hydrocarbon extraction from such systems. This means a thorough investigate approach is required from the oil companies that develop heterogeneous reservoirs, which adds to the investment costs required for development and production. Also, the existence of heterogeneity leads to the development by oil companies of innovative approach and novel technologies, such as smart well

completions and the use of horizontal wells, to overcome the effects of heterogeneity in oil reservoirs and to maximise the oil production.

Heterogeneity in heavy oil reservoirs adds to the complex nature of oil recovery from such systems, and sometimes oil production may not be economically viable. Introducing the in-situ combustion process to heterogeneous heavy oil reservoirs could result in the fire front failing to initiate or be sustained, as it propagates throughout the reservoir. This is because the combustion process is affected by the dynamics of multi-phase flow, the reaction kinetics, heat transfer, and phase behaviour (Awoleke, 2007) and all of these parameters are affected by reservoir heterogeneity. This means the application of in-situ combustion in heterogeneous heavy oil reservoirs is considered a challenge, a challenge which will be investigated in this chapter.

The effect of heterogeneity in the combustion process was investigated using a total of four numerical Nimr models. From Chapter 4, where no aquifer support existed, two models were chosen. The first model had horizontal injector and producer well configuration (Figure 6.1a), and the second model had vertical injector and producer well configuration (Figure 6.1b). The other two models were from Chapter 5, where a strong bottom water aquifer was introduced. The first model had horizontal wells configuration (Figure 6.1c), and the second model had vertical wells (Figure 6.1d). Table 6.1 summaries the well control mode in the models. The choice of these four models was based on the objectives of achieving a high recovery factor, long fire front sustainability, and less cumulative water produced in the aquifer support case. The reason for considering both horizontal and vertical well configuration when evaluating the impact of heterogeneity is that the behaviour of the combustion front is strongly affected by the configuration of the wells.

Most of the heterogeneity modelling work conducted in this chapter was compared to a homogeneous model with an average permeability of 4000mD (since Nimr field is mainly a homogenous sandstone reservoir). However, there is evidence that a part of the field has a permeability distribution between 500mD and 5000mD (Leemput et al., 1997). Obviously, the average permeability for the heterogeneous system with this permeability range was not equal to 4000mD. As a result, for the sake of completeness

of the study at the end of this chapter (section 6.7) an example of a heterogeneous model with an average permeability of 4000mD will be presented. Furthermore, the multiple layers and discontinuous shale scenarios heterogeneities in this chapter were represented using one realisation only. In order to completely evaluate these heterogeneity effects in the in-situ combustion process five different realisations will be created and investigated in section 6.7.

Injector well	Air injection rate of 7,200ft^3/day for the first 240 days and 14,400 ft^3/day thereafter
Producer well without aquifer existence	Bottom hole pressure of 500psi
Producer well with aquifer existence	Bottom hole pressure of 1,300psi
Simulation duration	3095 days

Table 6.1: *Summary of the models well controls (no pressure limit on injector well)*

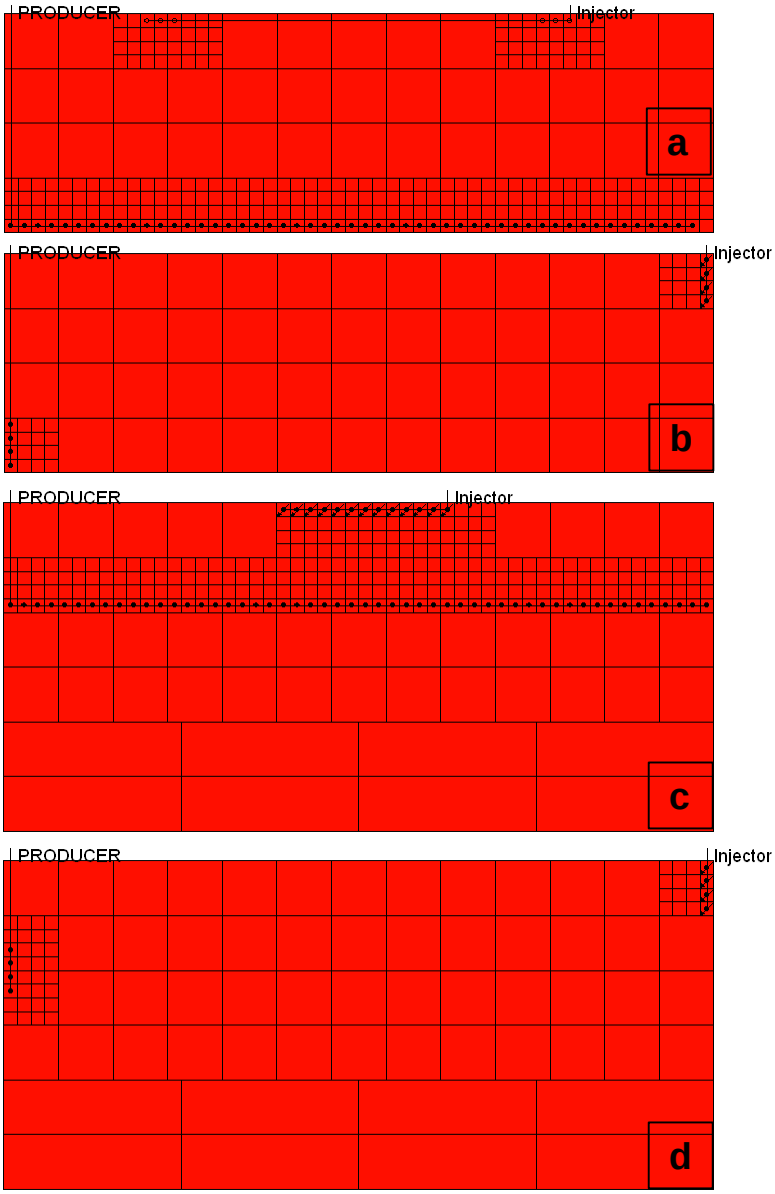

Figure 6.1: *Homogeneous well configuration base case models from Chapters 4 and 5: (a) horizontal well configuration without aquifer, (b) vertical well configuration without aquifer, (c) horizontal well configuration with aquifer, and (d) vertical well configuration with aquifer*

6.3 Kv/Kh ratio effect on in-situ combustion

The original homogenous base case 2D cross sectional model of the Nimr field had a Kv/Kh ratio of 1. This meant that the vertical permeability of the model was the same as

the horizontal permeability, both being 4,000mD. The reason for using Kv/Kh= 1 in the base case model at the beginning of the study was to reduce the base case model complexity in order to allow for the fire front initiation and to determine important combustion parameters such as air injection and ignition heat requirements. However, the actual Kv/Kh ratio in Nimr varies between 0.15 to 0.5, depending on the reservoir formation. In this section, both 0.15 and 0.5 Kv/Kh ratio were also modelled by changing the vertical permeability value to 600mD and 2000mD, respectively, instead of 4000md used in the base case model. The effect of Kv/Kh on the fire front process was investigated for both scenarios without and with aquifer support. Also, in each scenario both the horizontal and vertical well configuration was evaluated.

6.3.1 Kv/Kh ratio effect on combustion process without aquifer support

Reducing the Kv/Kh ratio from 1 to 0.5 and 0.15 would affect the fire front shape and performance because of the resistance introduced by having a lower vertical permeability in the model. The outcomes of such changes on the fire front might vary from case to case, depending on the vertical permeability value and the well configuration used in the model.

Horizontal well configuration: For the horizontal well configuration, lowering the Kv/Kh ratio results in no significant change in the final results for all three models in terms of total cumulative oil produced (Figure 6.2a) and average temperature profile (Figure 6.2b). The only effect of reducing the Kv/Kh ratio in the combustion process was that the fire front propagation was slower in the case of a low Kv/Kh ratio (i.e. 0.15) compared to the higher Kv/Kh ratio scenario (i.e. 1). This resulted in an increasing the time required to achieve the maximum total oil produced, as Table 6.2 shows. The slower fire front velocity was mainly as a result of the fact that the lower Kv/Kh ratio meant more resistance for the front, and the oil banks, obstructing its movement through the model layers, especially in the vertical direction as it approached the horizontal producer. Also, the model with the lower Kv/Kh ratio limited the combustion front from moving and spreading in the lateral direction, as both the temperature and ternary saturation plots for both models at 485 days show in Figure 6.3. This was because, as the vertical permeability decreased, the pressure gradient near the well induced by the

horizontal producer increased in this model, compared to the higher vertical permeability case. The higher pressure exacerbated the already instable air advancement within the system. This also explained the earlier oxygen break though in the lower Kv/Kh ratio model (Figure 6.4a) compared to the higher Kv/Kh ratio case. Moreover, Figure 6.4a shows that there was a crossover in the cumulative amount of oxygen produced in the Kv/Kh = 0.15 model at around 1800 days. This crossover meant less oxygen was produced in this model which indicated that more oxygen was consumed at 1800 days as a result of a large amount of coke that has been produced (Figure 6.4b) due to the slow fire front propagation. The main outcome from changing the Kv/Kh ratio in the horizontal well configuration was that when Kv/Kh was reduced, the fire front propagation velocity slowed down and more coke was produced, which resulted in a slight reduction in the recovery factor and a rapid increase in the required recovery time.

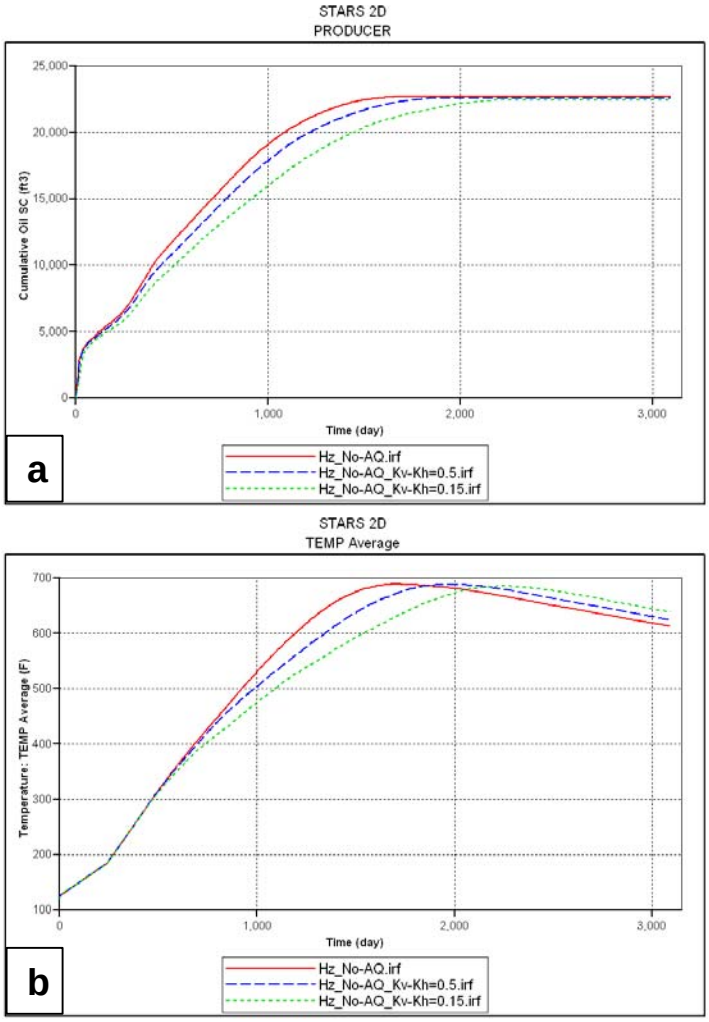

Figure 6.2: *Simulation results of effect of Kv/Kh ratio on combustion process using a horizontal well configuration without aquifer support: (a) cumulative oil produced, and (b) average temperature*

Model name	Recovery factor (%)	Time to recovery factor (days)	Oxygen break through (days)
Kv/Kh = 1	92.1	1631	855
Kv/Kh = 0.5	91.7	1876	717
Kv/Kh = 0.15	90.9	2136	657

Table 6.2: *Simulation results of effect of Kv/Kh ratio on combustion process using horizontal well configuration without aquifer support*

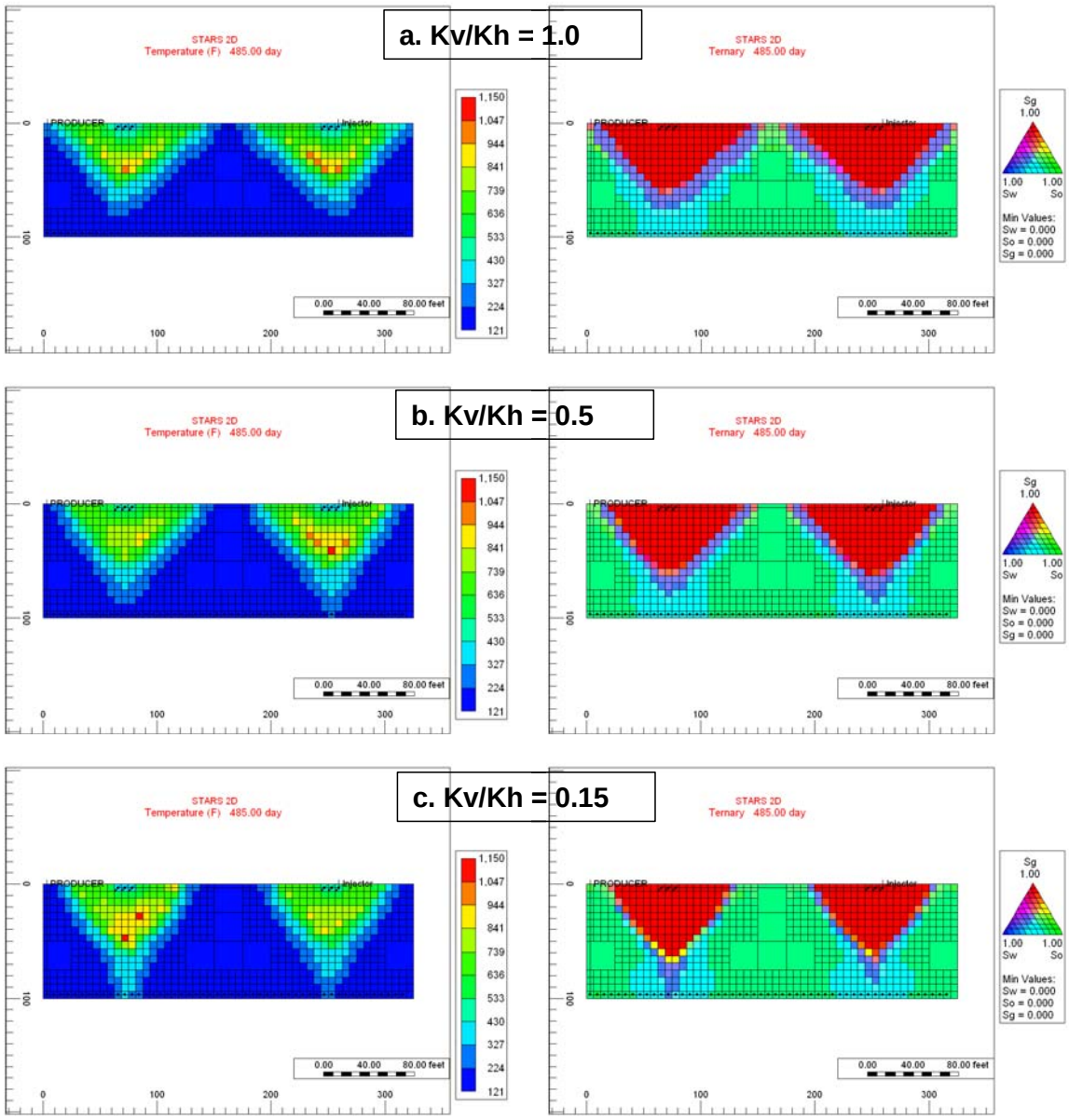

Figure 6.3: *Simulation results of temperature and ternary at 485 days: (a) Kv/Kh = 1, (b) Kv/Kh = 0.5, and (c) Kv/Kh = 0.15*

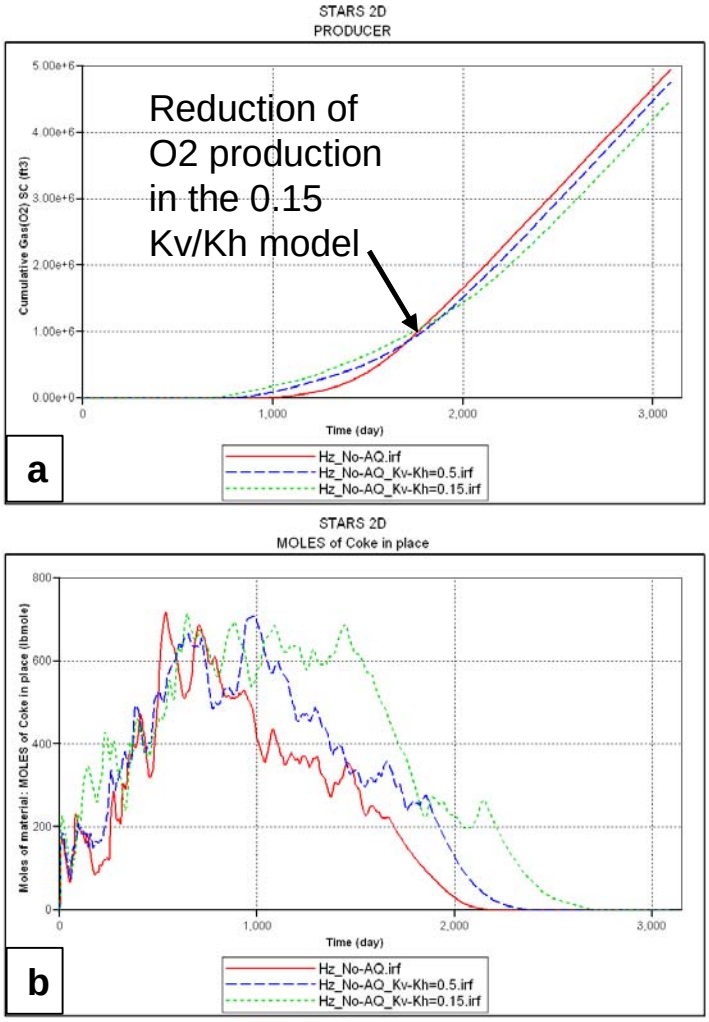

Figure 6.4: *Simulation results of effect of Kv/Kh ratio on combustion process using horizontal well configuration without aquifer support: (a) cumulative oxygen produced, and (b) net coke in place.*

Vertical well configuration: Reducing the Kv/Kh ratio in the vertical well configuration, where the vertical injector was completed at the top and the vertical producer was completed in the bottom 25ft of the model, results in an increase in the total amount of oil produced by the vertical producer (Figure 6.5a). The reason behind this improvement in recovery factor was the way the fire front developed and advanced in the vertical well configuration model. The temperature maps at 300 days (Figure 6.6) show how the fire front initiated and progressed in the model. For the high Kv/Kh ratio case (1), the fire front initiated near the injector perforations and then moved faster in the top of the model due to the gas override effect. On the other hand, in the lower Kv/Kh model (0.15), the fire front was initiated and then advanced in a more piston-like

displacement because the gas override effect was mitigated as a result of the lower vertical permeability, which limited air flow to the top of model. This may reduced the fire front propagation velocity, but at the same time it helped to improve the combustion front sweep efficiency and a higher recovery factor was achieved (Table 6.3). For both the models with 1.0 and 0.5 Kv/Kh ratios, the combustion front velocity was high as it propagated in the top of the model, and when it reached the model's lateral boundary it started to propagate vertically toward the vertical producer perforations. This change in front propagation direction resulted in a dramatic decrease in front velocity. As a result of the change between the lateral front velocity and vertical front velocity, a large mass of coke had been created (Figure 6.5b). However, for the 0.15 Kv/Kh model, the fire front advancement velocity was slow from the start of the process, because of the limitation in gas override effect. Since the combustion front moved in a piston-like displacement, it reached the vertical producer easily by breaking through from bottom part of the fire front as Figure 6.5c at 1055 days shows. Also, the lower Kv/Kh case delayed the oxygen break through (Table 6.3). The main outcome of this sensitivity was that when the Kv/Kh ratio was reduced in the vertical well configuration, the lower vertical permeability led to a reduced effect of gas override, which improved the combustion front sweep efficiency and led to high recovery factor.

Model name	Recovery factor (%)	Time to recovery factor (days)	Oxygen break through (days)
Kv/Kh = 1	80.4	2611	885
Kv/Kh = 0.5	83.6	2385	933
Kv/Kh = 0.15	86.4	1880	1270

Table 6.3: *Simulation results of effect of Kv/Kh ratio in combustion process using a vertical well configuration without aquifer support.*

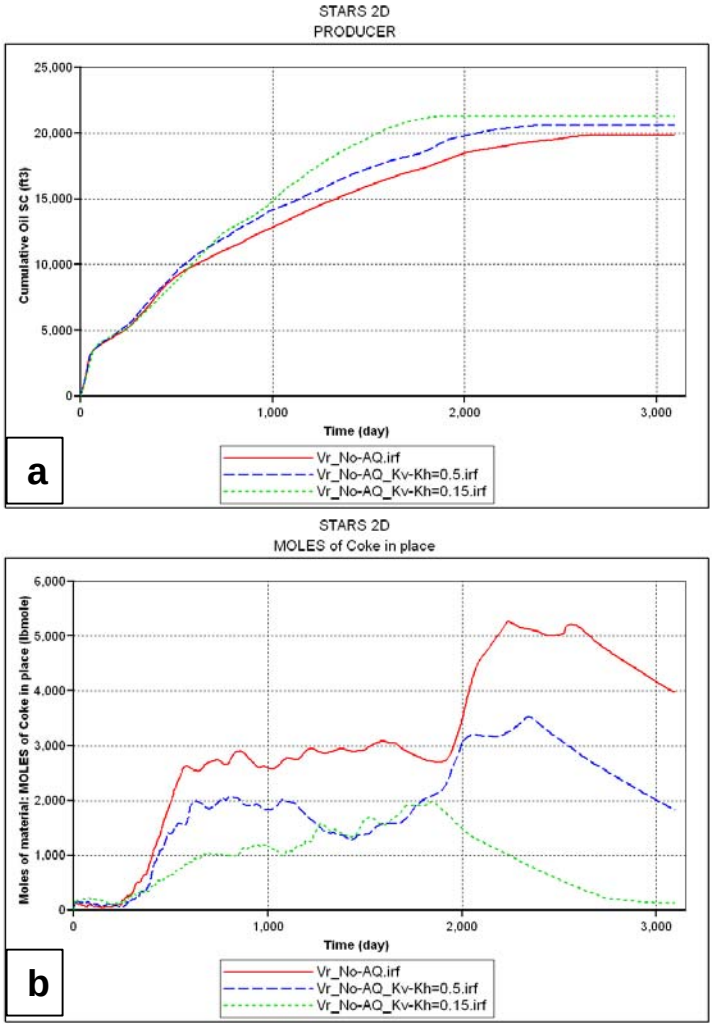

Figure 6.5: *Simulation results of effect of Kv/Kh ratio on combustion process using vertical well configuration without aquifer support: (a) cumulative oil produced, and (b) net coke in place*

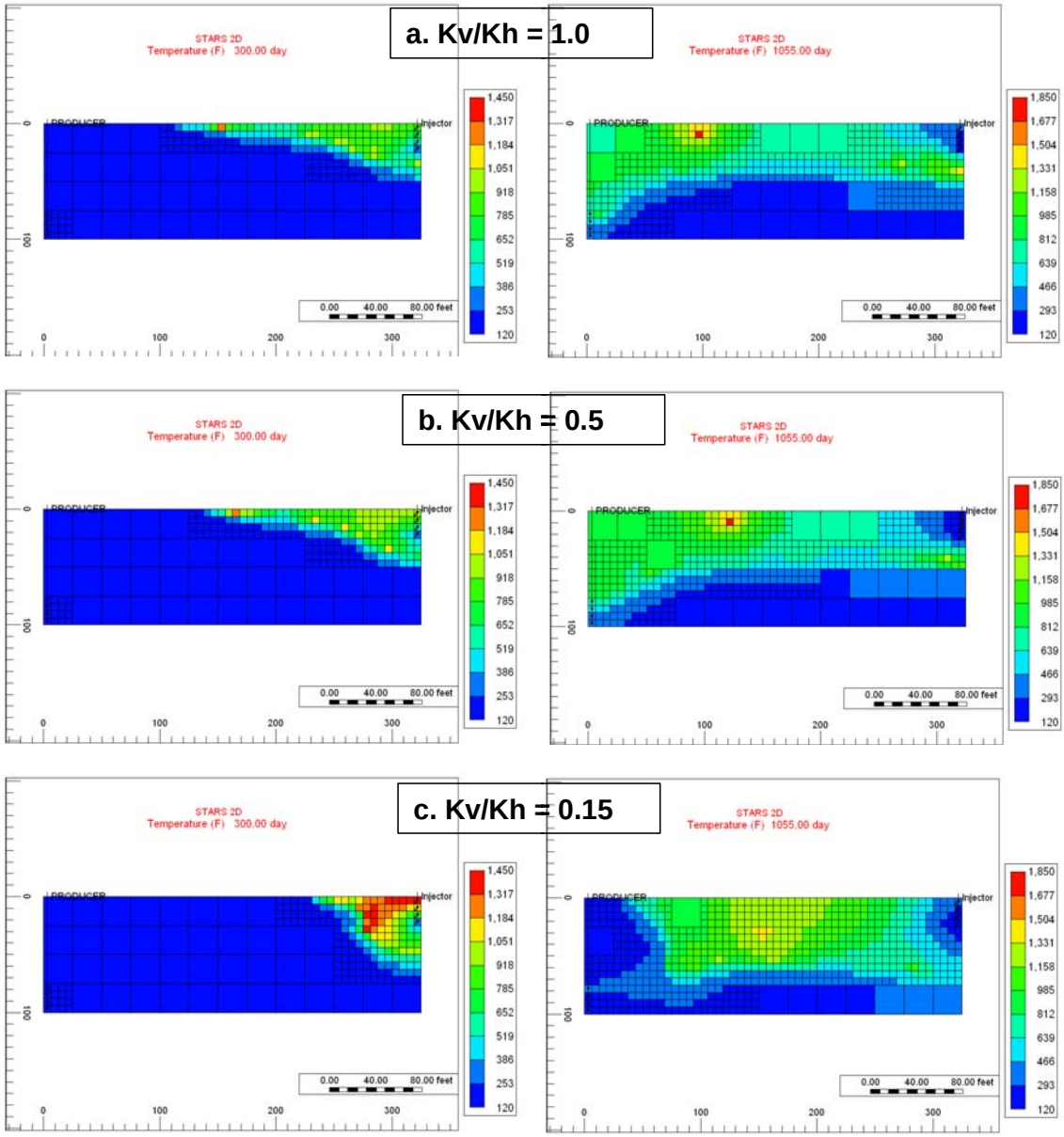

Figure 6.6: *Simulation results of temperature at 300days and 1055 days: (a) Kv/Kh = 1, (b) Kv/Kh = 0.5, and (c) Kv/Kh = 0.15*

<u>Comparison between Kv/Kh effect in horizontal and vertical well configuration:</u>

The reduction of the Nimr model homogeneity by lowering the Kv/Kh ratio changed the fire front process performance. For the horizontal well configuration, reducing Kv/Kh reduced the in-situ combustion process performance in terms of a slight decrease in recovery factor and increase in the recovery time required to achieve the maximum oil production. In contrast, in the vertical well configuration, lowering Kv/Kh results in an improvement in the combustion front sweep efficiency, and resulted in a higher

recovery factor compared to the higher Kv/Kh ratio model. This meant changing the Kv/Kh ratio in the combustion process resulted in changes to the process performance, and this variation depended on the type of well configuration used in the process.

6.3.2 Kv/Kh ratio effect on combustion process with aquifer support

Introducing strong bottom water aquifer into the combustion process model resulted in major changes in the recovery from the Nimr numerical model, as results in Chapter 5 showed. In this subsection, the effect of increasing the model heterogeneity through lowering the Kv/Kh ratio was investigated in both the horizontal and vertical well scenarios.

Horizontal well configuration: In this sensitivity, the effect of changing the Kv/Kh ratio from 1 in the base case model to 0.5 and 0.15 was studied, and the main observations of in-situ combustion performance under these scenarios were presented. Figure 6.7a shows cumulative oil produced by the three models with different Kv/Kh ratios. The lower the Kv/Kh ratio the lower the amount of oil that was produced by the combustion process. This was mainly as a result of low vertical permeability resulting in an increased the resistance that the fire front needed to overcome to propagate and sweep the formation. This led to slow combustion front propagation rate, which resulted in a low recovery factor being achieved in such cases (Table 6.4). The limitation in the fire front propagation as Kv/Kh was reduced was also shown on the temperature distribution maps for all three models at 360 days and 995 days (Figure 6.8). For the Kv/Kh=1 case, the fire front was able to spread laterally and vertically faster, unlike the low Kv/Kh ration case (0.15) where the fire front propagation velocity was slow, which resulted in more oil being converted to coke in place (Figure 6.7b). After 995 days, the combustion front swept almost the entire top area of the model, whereas the combustion front in the low Kv/Kh (0.15) model required a longer time to sweep a similar area of the model. As a result, the low Kv/Kh model had a higher final oil saturation than the case where Kv/Kh was high (Table 6.4). Also, Figure 6.9 shows that by reducing Kv/Kh ratio, the amount of oil remaining in place was higher because the fire front was not able to sweep the model area and recover all the oil in place by the end of the simulation (3095 days). However, the only advantage of having this kind of heterogeneity in the

model was that the cumulative water produced was dramatically decreased when Kv/Kh was reduced. The 0.15 Kv/Kh ratio model just produced 11% of the total volume of water produced by the Kv/Kh = 1 model (Figure 6.7c). This was because of the low vertical permeability leading to less water influx from the aquifer to the horizontal producer.

This sensitivity showed that reducing Kv/Kh in the horizontal well configuration resulted in a reduction in the in-situ combustion process sweep efficiency, which led to a reduction in the recovery factor for the process. This was as a result of the slow front propagation which allowed for more coke being produced, and a smaller area of the model being swept, which allowed for a higher final oil saturation remaining in place. By contrast, lowering the Kv/Kh ratio resulted in a reduction in the cumulative aquifer water produced by the horizontal well, and so reduced the handling cost of water production.

Model name	Recovery factor (%)	Front quenching time (days)	Oxygen break through (days)	So @ 3095 days (fraction)
Kv/Kh = 1	77	3095	454	0.10
Kv/Kh = 0.5	74.2	3095	398	0.12
Kv/Kh = 0.15	70.5	3095	342	0.13

Table 6.4: *Simulation results of effect of Kv/Kh ratio in combustion process using horizontal well configuration with aquifer support.*

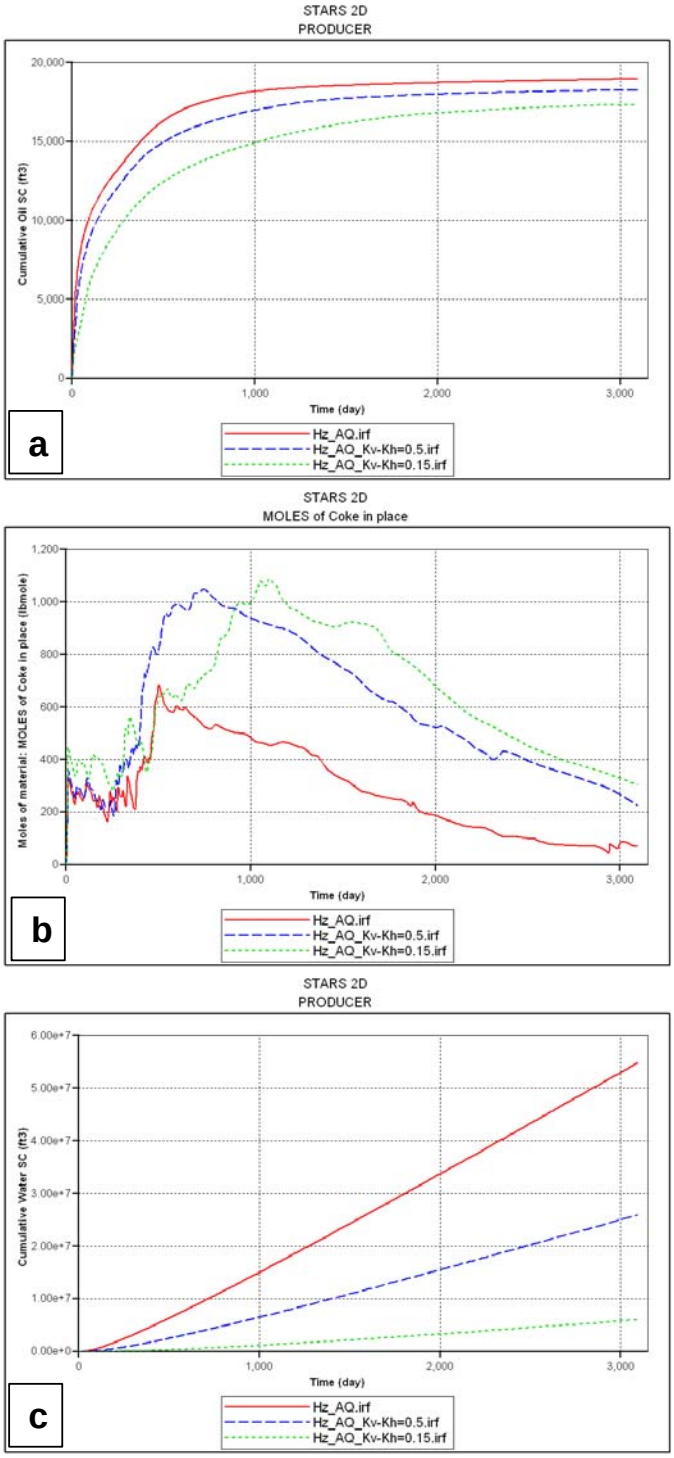

Figure 6.7: *Simulation results of effect of Kv/Kh ratio on combustion process using horizontal well configuration with aquifer support: (a) cumulative oil produced, (b) net coke in place, and (c) cumulative water produced*

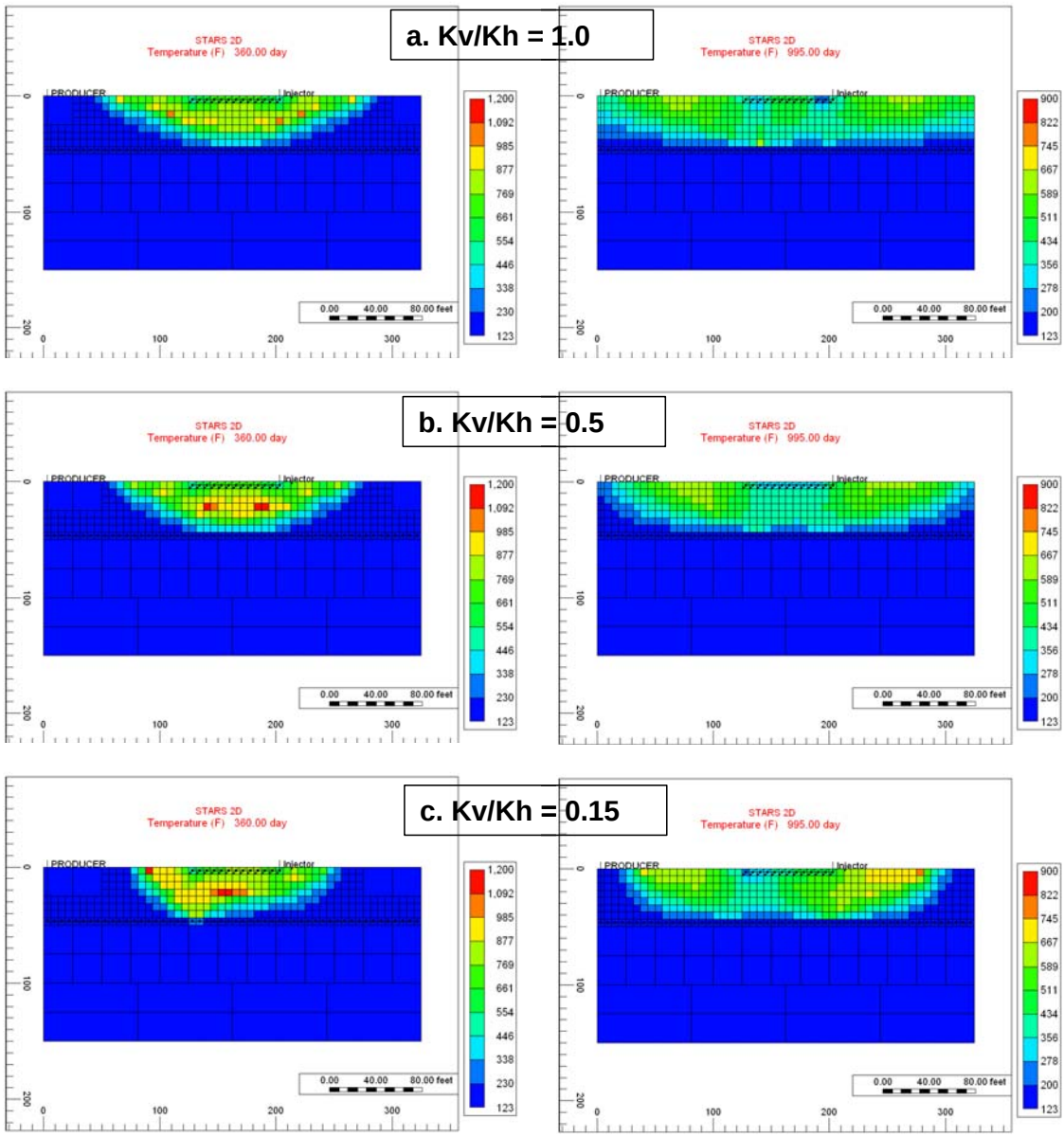

Figure 6.8: *Simulation results of temperature at 360 days and 995 days: (a) Kv/Kh = 1, (b) Kv/Kh = 0.5, and (c) Kv/Kh = 0.15*

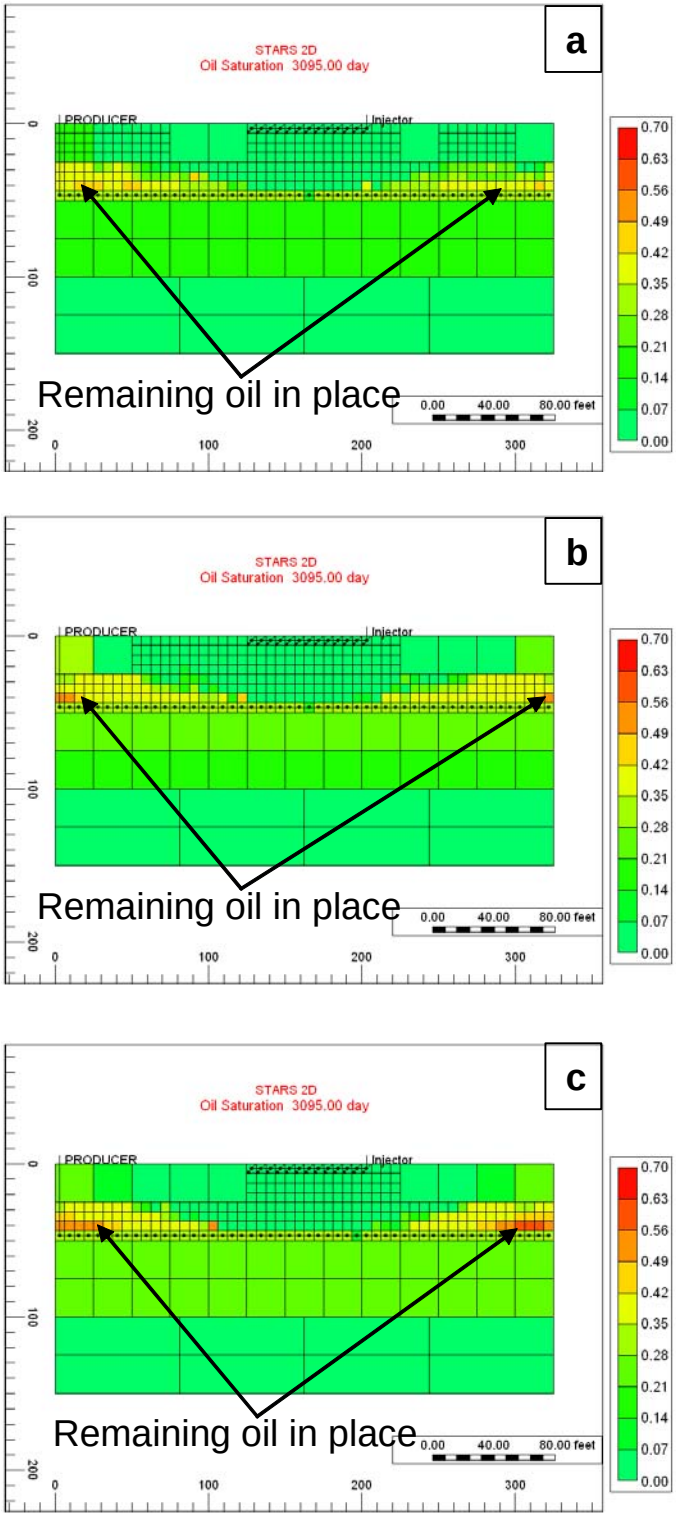

Figure 6.9: *Simulation results of oil saturation at 3095 days: (a) Kv/Kh = 1, (b) Kv/Kh = 0.5, and (c) Kv/Kh = 0.15*

Vertical well configuration: Using vertical wells, this sensitivity was performed to investigate the effect of lowering the Kv/Kh ratio on the combustion process. Table 6.5

summarises the main results for the three models when Kv/Kh equals 1, 0.5, and 0.15 respectively. The main observations were that when the Kv/Kh ratio was reduced, a higher recovery factor was achieved. The model with 0.15 Kv/Kh ratio produce 34% more oil than the model with Kv/Kh equals 1. This was because the low vertical permeability led to a limited gas override effect, which resulted in a delay in both the oxygen (Table 6.5) and fire front broke through into the vertical producer, and therefore the combustion front was sustained for a longer time. Also, the fire front propagation velocity was slower when Kv/Kh was lowered; this allowed for more coke to be produced (Figure 6.10), and resulted in the fire front being sustained for longer.

Figure 6.11 shows the temperature maps at 340 days and 635 days for the three models. For the Kv/Kh = 1 model, the fire front was ignited and then propagated faster in the top section of the model under the gas override effect, until it broke through into the producer and was quenched at around 1133 days. On the other hand, for the 0.15 Kv/Kh model, the front was initiated and then formed a position-like displacement combustion front which therefore propagated slowly through the model. This approach of the fire front in the lower Kv/Kh model enhanced the sweep efficiency, and resulted in a larger volume of oil produced. Also, some of the front heat spread to the top aquifer zone in the 0.5 (Figure 6.11b) and 0.15 (Figure 6.11c) cases. This was because part of the front was established and progressed near the aquifer zone, which allowed for heat transfer by both convection through the reservoir liquids and conduction through the reservoir rock.

From this sensitivity, the main effect of reducing the Kv/Kh ratio in a vertical well configuration when there was aquifer support was a longer sustained period of front propagation, which led to a more efficient sweep through the formation and a higher recovery factor.

Model name	Recovery factor (%)	Front quenching time (days)	Oxygen break through (days)	So @ 3095 days (fraction)
Kv/Kh = 1	34.6	1133	621	0.31
Kv/Kh = 0.5	47.6	1025	799	0.25
Kv/Kh = 0.15	52.6	1705	1507	0.14

Table 6.5: *Simulation results of effect of Kv/Kh ratio on combustion process using vertical wells with aquifer support*

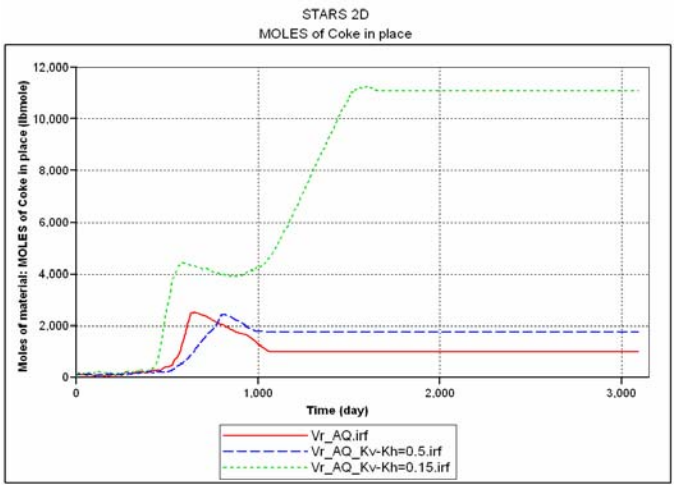

Figure 6.10: *Simulation results of net coke in place for effect of Kv/Kh ratio on combustion process using vertical wells with aquifer support*

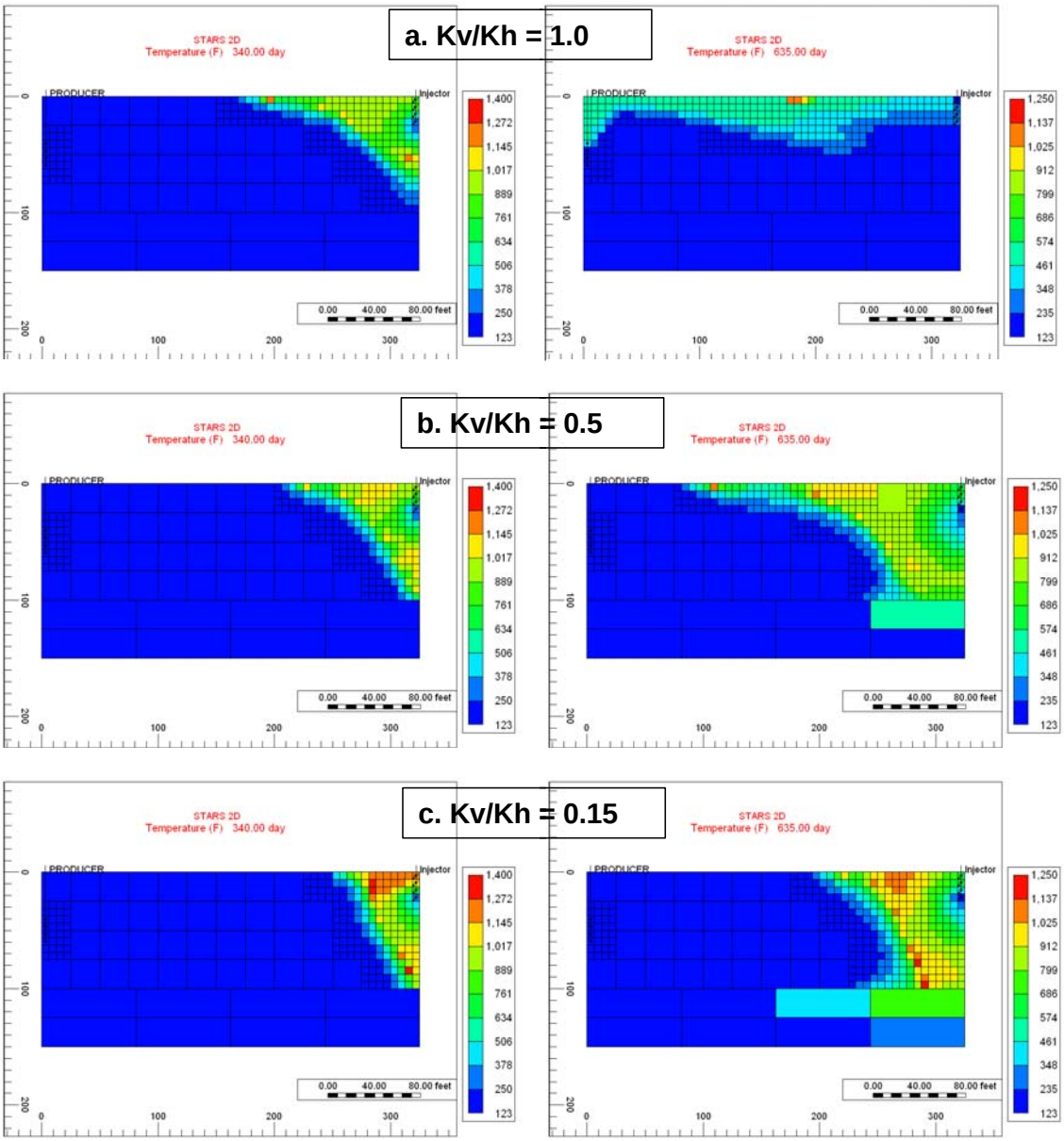

Figure 6.11: *Simulation results of temperature at 340 days and 635days: (a) Kv/Kh = 1, (b) Kv/Kh = 0.5, and (c) Kv/Kh = 0.15*

6.4 Multiple permeability layers effect on in-situ combustion

Propagation of the fire front in a reservoir with layers of varying permeabilities was expected to be different from that in a single layer model. The aim in this section was to evaluate the combustion front performance when different permeability values were

used in each layer of the model. In order to investigate this issue the base case Nimr model was modified, and permeability values between 0.5D to 5D were used in all 16 layers of the model (Figure 6.12b). This type of heterogeneity was expected to lead to variations in the fire front shape and rate of propagation, depending on the type of well configuration used and the existence or absence of the aquifer support. (Five more realisations were developed in section 6.7.1).

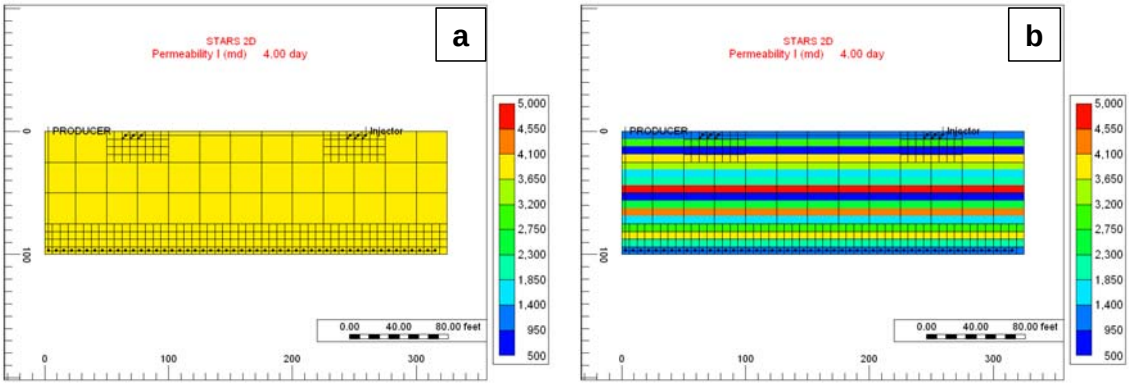

Figure 6.12: *Multiple permeability layers in combustion process: (a) homogeneous single permeability layer, and (b) distribution of multiple permeability layers*

6.4.1 Multiple permeability layers effect on combustion process without aquifer support

Horizontal well configuration: For the horizontal well scenario, the comparison between the single permeability layer model and the multiple permeability layers case showed that the fire front in the later model moved vertically faster compared to the movement in the lateral direction, as Figure 6.13b illustrates. This was mainly because the top layer of the multiple permeability model had a lower permeability value compared to the layer beneath it (layer two), which enhanced the fire front vertical propagation compared to its lateral movement in the low permeability layer. The homogeneity of the permeability in the single permeability model (Figure 6.13a) allowed for both the air and fire fronts to move to the top of the model, since the resistance to front propagation due to the formation was the same in both the vertical and lateral directions. The variation in permeability here led to faster combustion front propagation in the vertical direction, which led to early oxygen break through at 598

days (Table 6.6) into the horizontal producer, especially on the left hand side. This resulted in an increase in the time needed by the combustion process to sweep the model and to achieve the maximum possible oil production (Figure 6.14a). Also, a longer recovery time meant more coke was produced in place and less oil was available to be recovered (Figure 6.14b). However, the final recovery factor achieved by the multiple permeability layers model was just 0.6% less than the recovery factor achieved by the homogenous permeability case (Table 6.6), but with more than 400 additional days required to give that recovery factor.

The main outcome from this sensitivity was that to have multiple permeability layers in the combustion process might enhance the front's vertical propagation velocity as it approached the producer. This resulted in early oxygen break through which meant longer recovery time was required to achieve an almost similar recovery factor as in the homogeneous permeability model.

Model name	Recovery factor (%)	Time to recovery factor (days)	Oxygen break through (days)
homogeneous single permeability layer	92.1	1631	855
multiple permeability layers	91.5	2047	598

Table 6.6: *Simulation results of effect of multiple permeability layers on combustion process using horizontal well configuration without aquifer support*

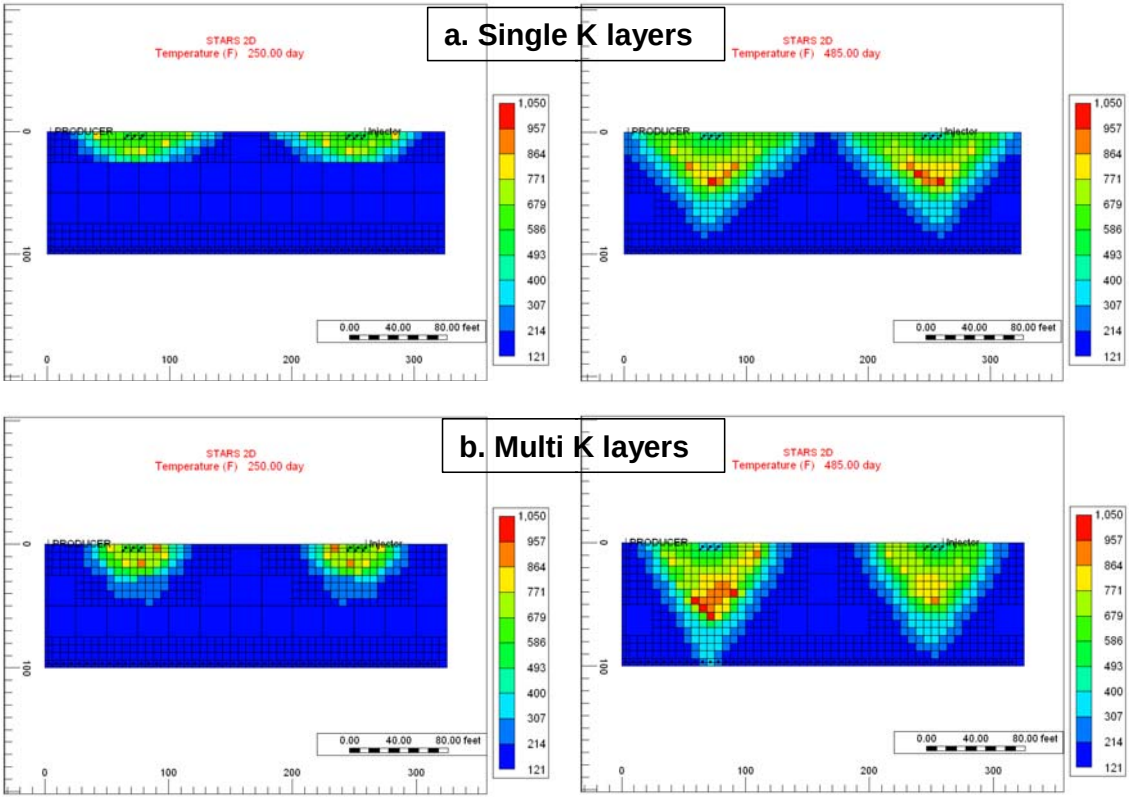

Figure 6.13: *Simulation results of temperature at 250 days and 485 days: (a) homogeneous single permeability layers, and (b) multiple permeability layers*

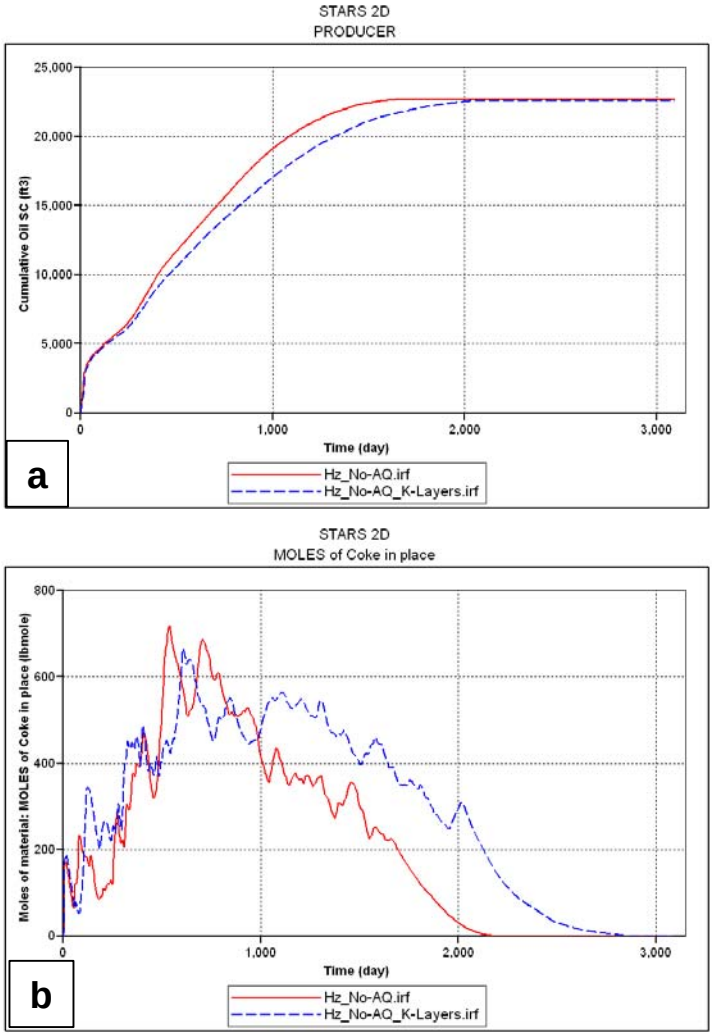

Figure 6.14: *Simulation results of effect of multiple permeability layers on combustion process using horizontal well configuration without aquifer support: (a) cumulative oil produced, and (b) net coke in place*

The temperature map of the multiple permeability layers model (Figure 6.13b) shows a non-symmetric combustion front shape (at 485 days) and the reason for that might be as a result of not completing the horizontal producer for the entire model length (including the last grid block in the bottom layer), or it could be a numerical simulator averaging error. To clarify the issue a model was developed and the horizontal producer was completed for the entire model length, which was achieved by including just one more grid block in the bottom right corner of the model. This resulted in a symmetric front shape (Figure 6.15b), which answered the question and showed how sensitive the modelling of the in-situ combustion process was to any minor change in the model properties. In other words, the asymmetry in this model was removed when the

horizontal producer was completed for the entire model length, which adjusted the producer well centre location (to be symmetric) and allowed for a more symmetric fire front development.

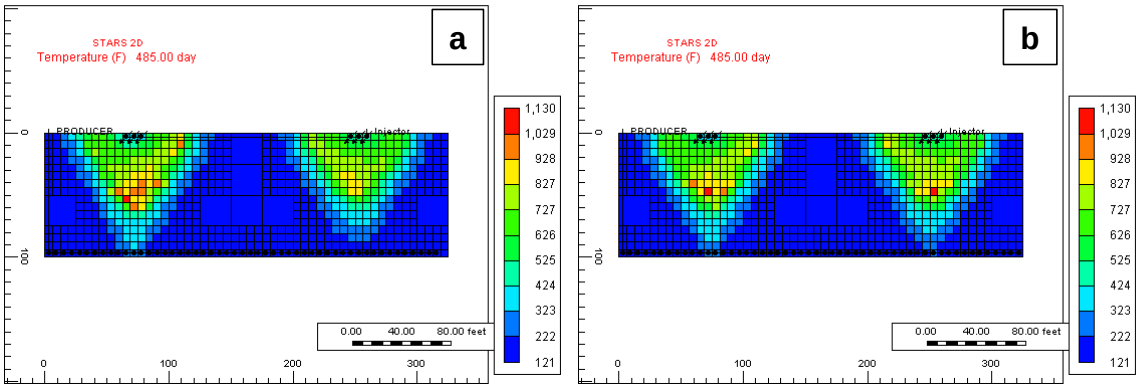

Figure 6.15: *Simulation results of temperature 485 days: (a) multiple permeability layers, and (b) multiple permeability layers model where the producer was completed for the entire model length*

Vertical well configuration: In the case where a vertical well configuration was used, the combustion process performance was more affected by heterogeneity of the multiple permeability layers compared to the horizontal well scenario in the previous sensitivity (Figure 6.13b). This was mainly because of the direction of the front movement in the horizontal well configuration, which was across the layers, which minimised their impact on the process; whereas for the vertical well configuration the main direction of the front was along the layers (Figure 6.16b). The temperature distribution maps of both the single permeability layers (Figure 6.16a) and the multiple permeability layers (Figure 6.16b) show the shape of the front development at 190 days and 725 days. For the homogeneous single permeability layers models, the fire front was initiated and then propagated in the top of model under the gas override effect, which allowed for a faster front propagation velocity, which resulted in early oxygen break through at around 885 days. In the heterogeneous multiple layer model, the front was initiated near the vertical injector, and then it started to propagate laterally faster through the higher permeability layers in the model (i.e. layer 4), and at the same time it propagated slowly in the low permeability layers, such as the top layer (layer 1). However, the overall front propagation velocity in this heterogeneous model was still slower than was the case in

the homogeneous single layer model, which led to a significant mass of coke being produced (Figure 6.17a). As a result, the cumulative amount of oil produced by the combustion front was 7.8% less than what was produced by the fire front in the homogeneous model (Figure 6.17b).

For the vertical well scenario, the presence of multiple permeability layers resulted in a reduction in the combustion front propagation velocity. This was because the main direction of the front propagation between the vertical injector and producer was the lateral direction, which meant that the fire front needs to move along the layers. This led to a slow overall combustion front propagation, and resulted in a large mass of oil being lost during convertion to coke in place. As a result, a lower recovery factor was achieved by the combustion process compared to the homogeneous permeability layers case.

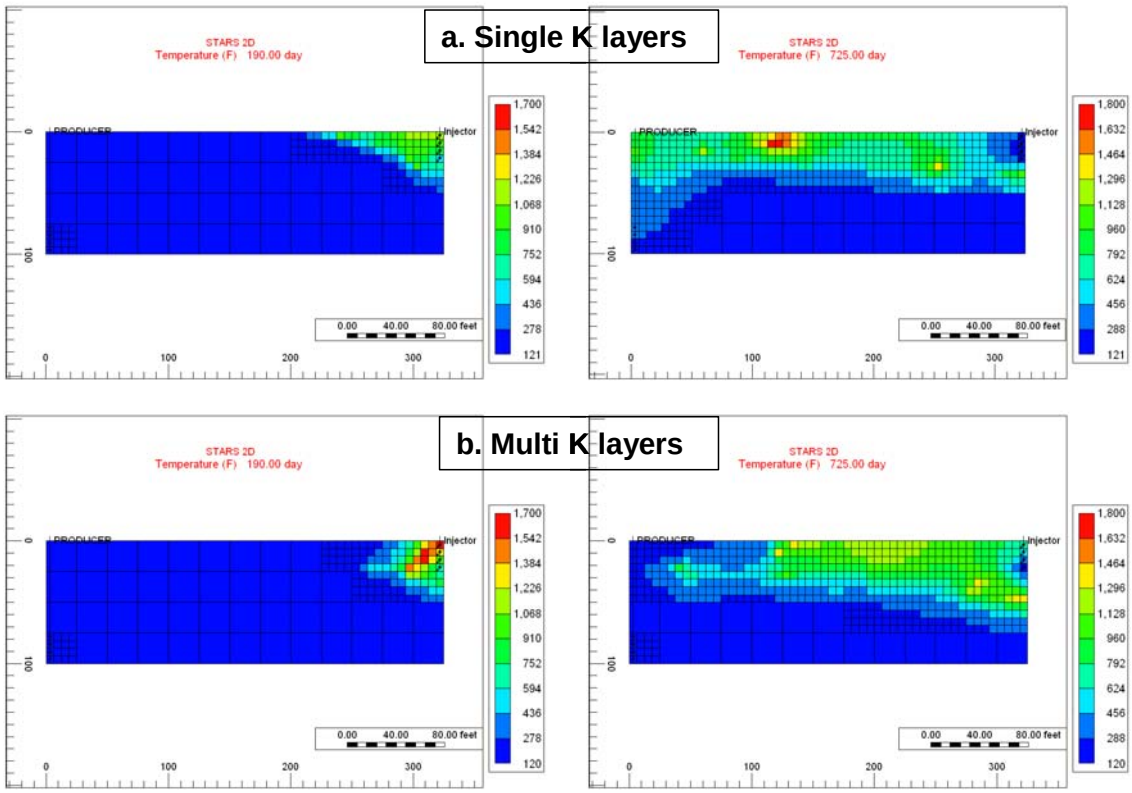

Figure 6.16: *Simulation results of temperature at 190 days and 725 days: (a) homogeneous single permeability layers, and (b) multiple permeability layers. Note how the fire front propagates in the heterogonous model (b) and how it follows the high permeability layer to be able to reaches the producer laterally.*

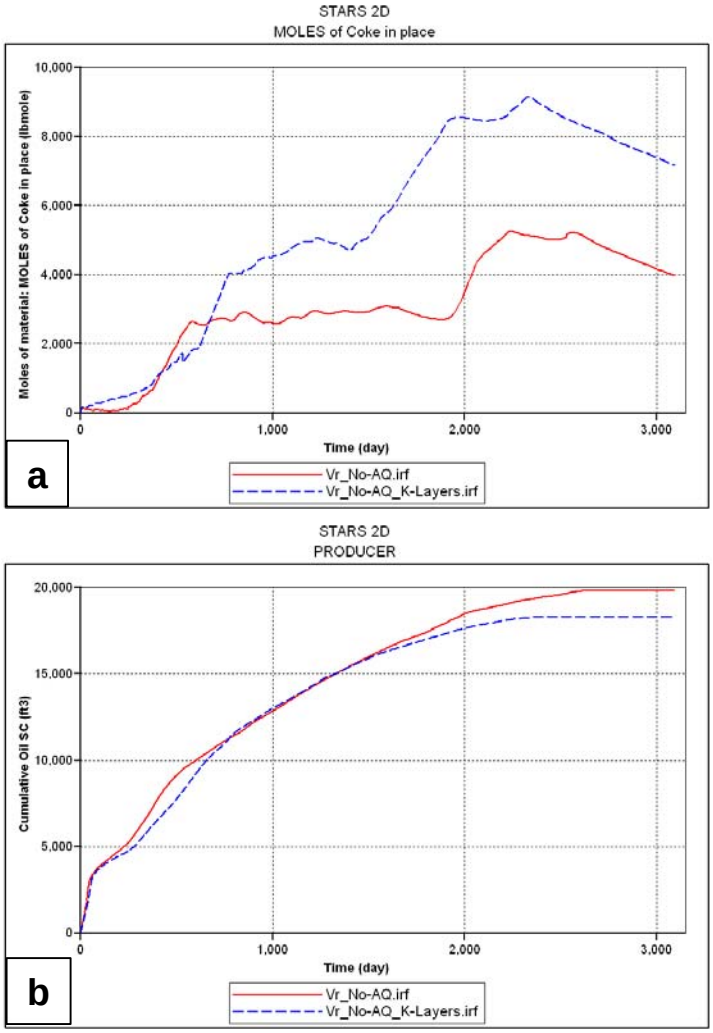

Figure 6.17: *Simulation results of effect of multiple permeability layers on combustion process using vertical well configuration without aquifer support: (a) net coke in place, and (b) cumulative oil produced*

6.4.2 Multiple permeability layers effect on combustion process with aquifer support

Horizontal well configuration: The effect of layered permeability heterogeneity was studied in this sensitivity using a horizontal well configuration in the presence of strong bottom water aquifer support. The combustion front behaviour for the multiple permeability layers model showed limited propagation of the front laterally along the layers, whereas the front propagated well in the vertical direction (Figure 6.18b). The contrast between the layers permeabilities led to variations in the behaviour of the front in both lateral and vertical directions. For example, the low permeability top layers

caused the front to move downwards and to flow through the high permeability layers beneath the middle of the model, which enhanced the vertical progression of the front and allowed for early oxygen break through into the horizontal producer. For the homogeneous single permeability layer (Figure 6.18a), the front propagation continued to flow in the top of the model and the fire front swept the area between the horizontal injector and producer efficiently, which led to a higher volume of oil produced (Figure 6.19a). This made the homogeneous single layer model achieved a 77% recovery factor, whereas the multiple heterogeneous layered model yielded 73.2%. Figure 6.20 shows that the poor sweep efficiency in the layered model results in a higher final oil saturation in the model after the final timestep (3095 days). This was mainly because of the early oxygen break through, due to the variations between the layer permeabilities, which reduced the combustion front performance as a result of the air being circulating between wells. There were thus limited air supplies available to enhance the front propagation to recover oil from boundaries of the model. Also, the permeability variation between model layers resulted in the total amount of water produced by the layered model being just 38% of what was produced by the homogeneous single permeability case (Figure 6.19b).

This sensitivity showed that the performance of the combustion process in a horizontal well configuration was poor if there was a significant variation in the permeability between the model layers. This type of heterogeneity led to early oxygen break through and restricted the front's lateral movement. As a result, more oil remained in place because of the poor sweep efficiency.

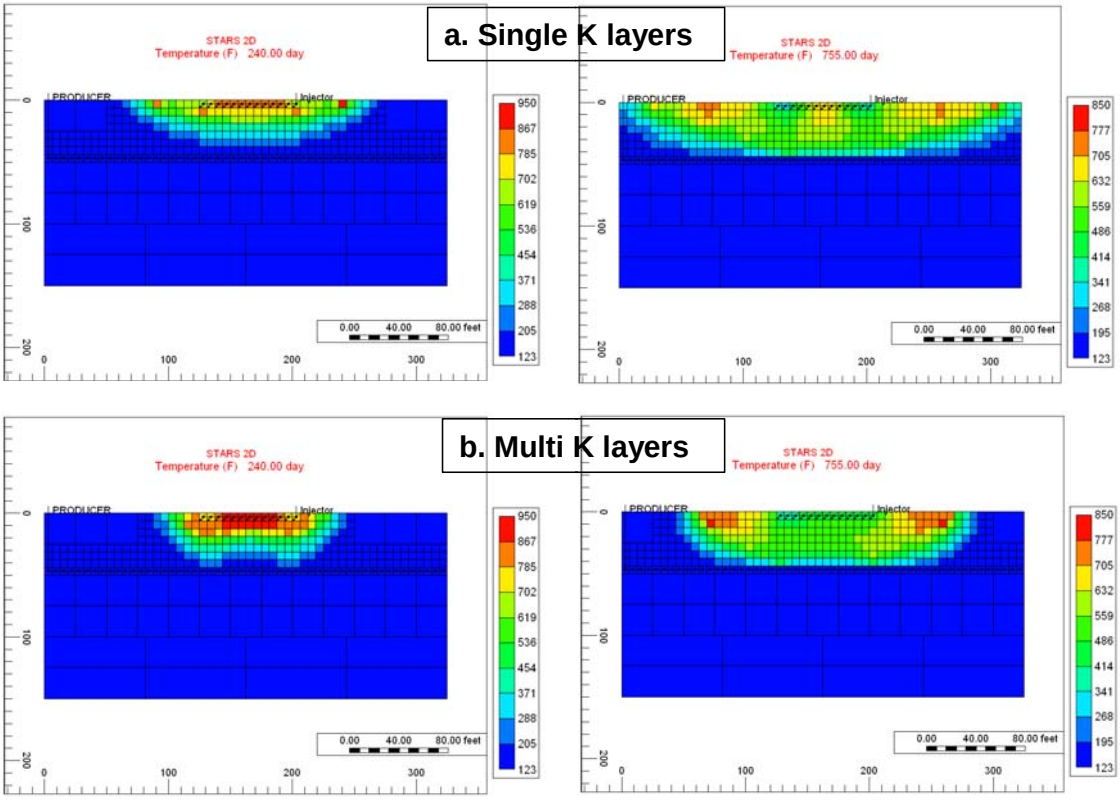

Figure 6.18: *Simulation results of temperature at 240 days and 755 days: (a) homogeneous single permeability layers, and (b) multiple permeability layers*

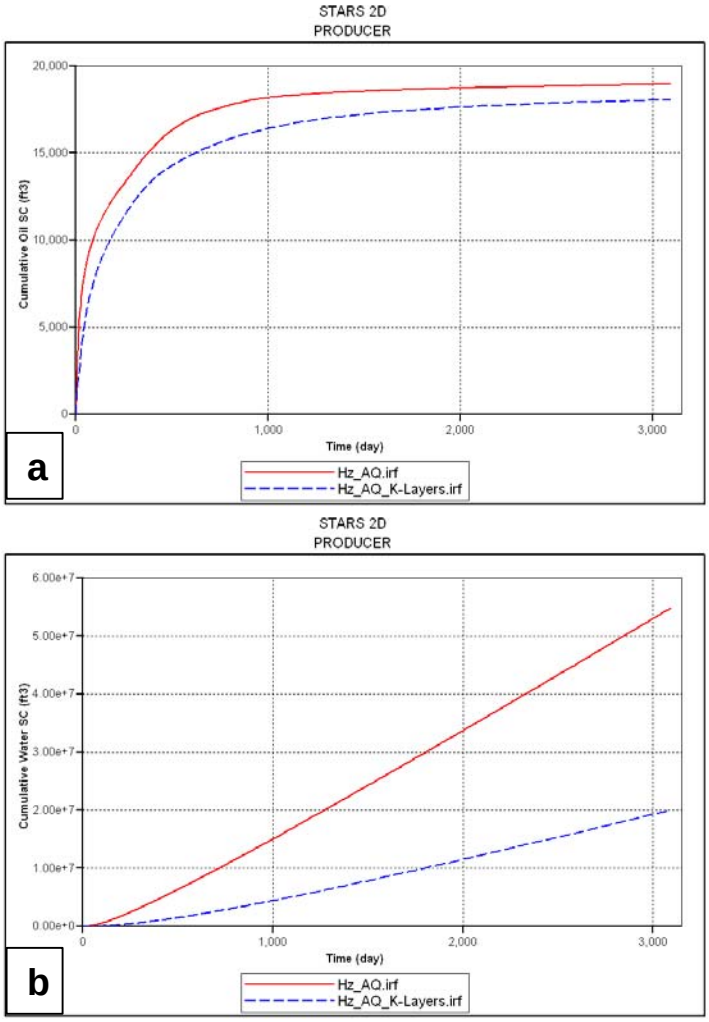

Figure 6.19: *Simulation results of effect of multiple permeability layers on combustion process using horizontal well configuration with aquifer support: (a) cumulative oil produced, and (b) cumulative water produced*

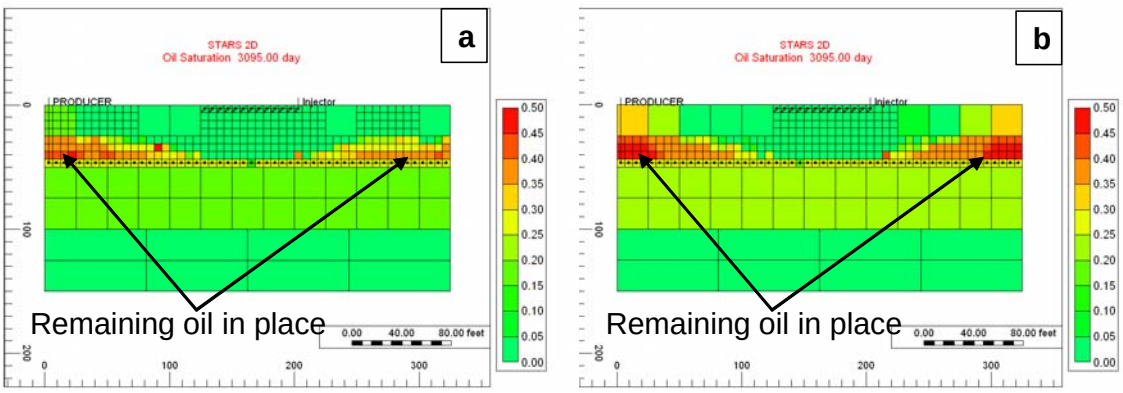

Figure 6.20: *Simulation results of oil saturation at 3095 days: (a) homogeneous single permeability system, and (b) multiple permeability layers*

Vertical well configuration: Further investigation of the effect of multiple permeability layers in the in-situ combustion process in the case with strong aquifer support was conducted in this sensitivity, where the vertical wells scenario was used. Figure 6.21 presents the comparison between the temperature distributions for both the homogeneous permeability model and the heterogeneous multiple permeability layers model at 240 days and 605 days. Initially, the combustion front for the layered model started to propagate along the layers with different velocities depending on each layer's permeability value. As time passed (i.e. at 605 days), the fire front interface with the cold oil zone started to develop a piston-like displacement (Figure 6.21b), which improved the combustion front overall sweep, whereas in the homogeneous permeability case the front was propagating in the top part of the model and bypassing oil in lower areas (Figure 6.21a). This resulted in more oil being produced by the combustion process in the heterogeneous model (Figure 6.22a) and a 47.5% recovery factor was achieved (Table 6.7). The fire front movement at the top of the system in the single permeability model led to a faster front velocity and early oxygen break through, which allowed for early fire front extinction (at 1133 days) as a result of both shortage in air supplies and a high water influx from the aquifer. On the other hand, the slow front propagation velocity sustained the combustion front for a longer time (1282 days) and delayed oxygen break through into the vertical producer. This also resulted in a better sweep efficiency and lower final average oil saturation of 24% compared to 31% in the homogeneous single permeability model (Table 6.7). Moreover, the permeability variation between the layers of the heterogeneous model resulted in a significant reduction in the total water produced, as Figure 6.22b shows.

The main outcome from this sensitivity was to show that for the vertical wells scenario, the combustion process performance was enhanced when multiple permeability layers exist in the reservoir where there was aquifer support. This was mainly because of the slow front propagation which delayed oxygen break through and allowed for better sweep efficiency and a higher recovery factor. Also, the permeability variation led to longer fire front sustainability, and less water being produced by such a system.

Model name	Recovery factor (%)	Front quenching time (days)	Oxygen break through (days)	So @ 3095 days (fraction)
homogeneous single permeability layer	34.6	1133	621	0.31
multiple permeability layers	47.5	1282	963	0.24

Table 6.7: *Simulation results of effect multiple permeability layers in combustion process using vertical well configuration with aquifer support*

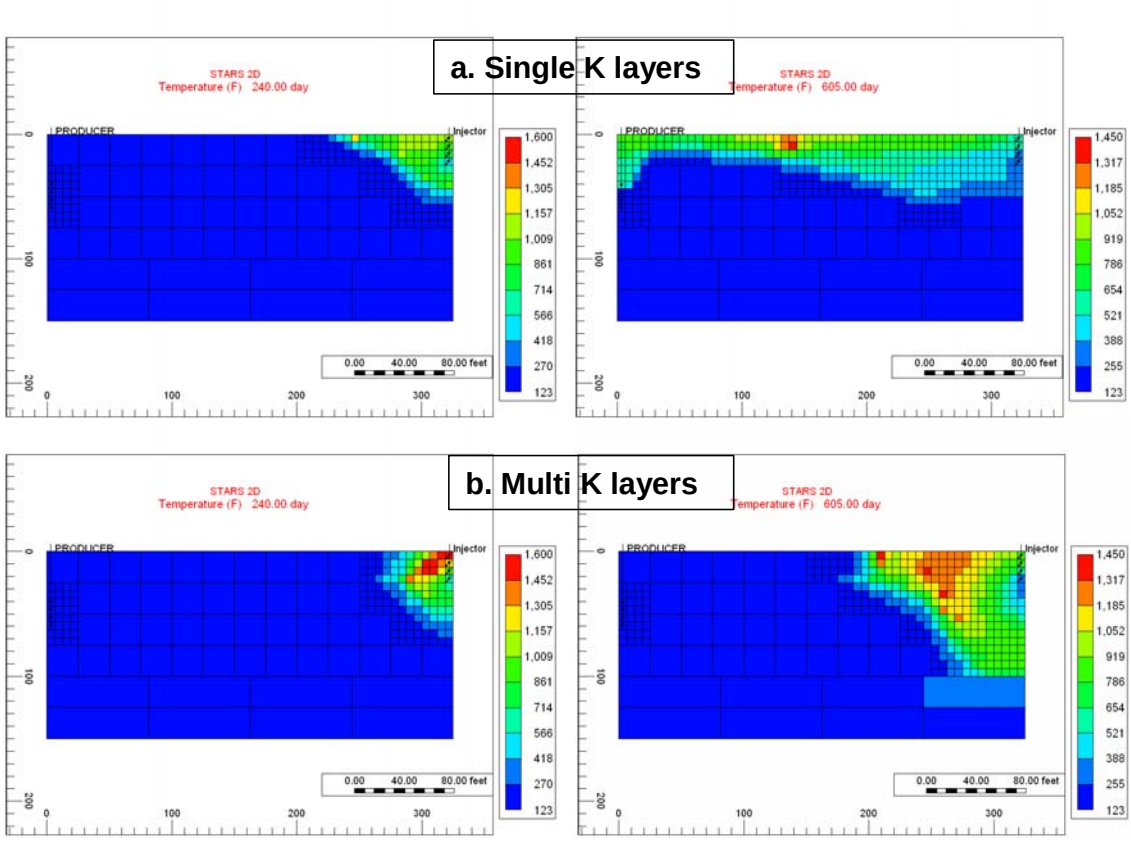

Figure 6.21: *Simulation results of temperature at 240 days and 605 days: (a) homogeneous single permeability layers, and (b) multiple permeability layers. Note the way the fire front development and the then propagates in the system.*

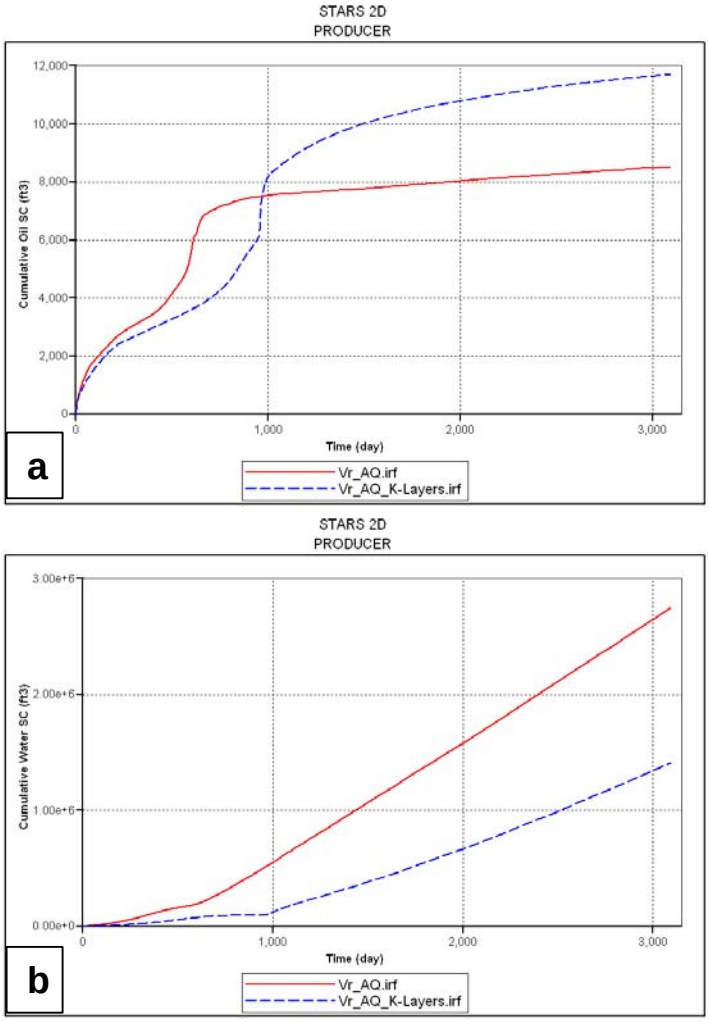

Figure 6.22: *Simulation results of effect of multiple permeability layers on combustion process using vertical well configuration with aquifer support: (a) cumulative oil produced, and (b) cumulative water produced*

6.5 Discontinuous impermeable shale layers effect on in-situ combustion

In this section, reservoir heterogeneity was introduced by having randomly distributed discontinues shale layers between the sand layers. The thin shale layers were laterally oriented, which severely reduced the vertical model permeability, but had no effect on the horizontal permeability. To represent the shale layers in the numerical model, the vertical transmissibility was reduced to zero (Figure 6.23b), which prevented fluid flow

across the shale layers but allowed heat to transfer through the impermeable layers. This kind of heterogeneity was expected to alter the in-situ combustion performance as the following sensitivities showed. (Four more realisations were developed in section 6.7.2).

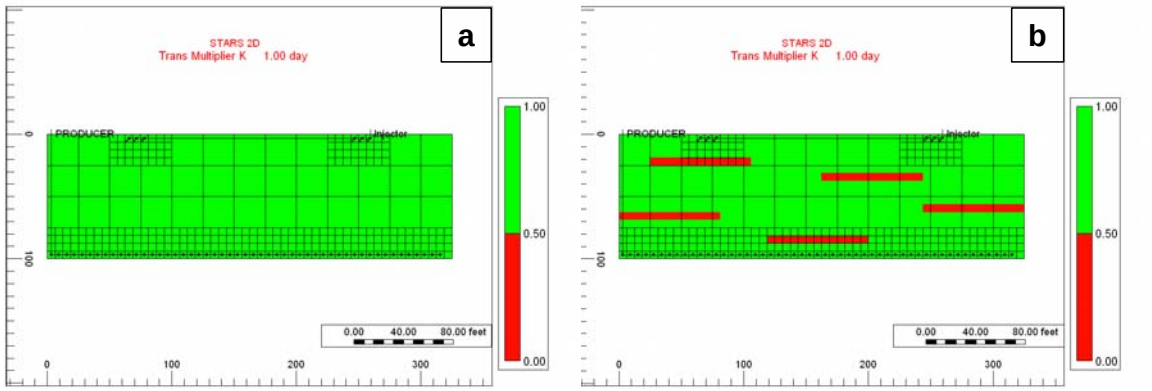

Figure 6.23: *Effect of discontinuous impermeable shale layers on the combustion process: (a) homogeneous clean sand (non-shale) model, and (b) heterogeneous shale layers model*

6.5.1 Discontinuous impermeable shale layers effect on combustion process without aquifer support

Horizontal well configuration: In the horizontal well configuration, the direction of the main fire front movement was vertically. This was because of the well placement in this scenario, where the horizontal injector was located at the top and the horizontal producer was completed at the bottom. This suggests that the existence of discontinuous shale layers will have a major impact on the way the combustion front develop and propagate between the wells. The comparison between the temperature and ternary saturation distribution maps of both models at 515 days (Figure 6.24) showed that the fire front in the shale layers model (Figure 6.24b) was retarded on the left hand side of the front propagation. This was mainly due to the existence of a shale layer directly under the left hand side of the perforated interval in the horizontal injector (Figure 6.23b). This led to a strictly limited fire front barely starting to move vertically to recover oil even though some heat did manage to transfer through the shale layer as temperature map shows (Figure 6.24b). The only way the combustion front could

propagate beyond that shale layer was to flowed around the edge of the shale layer, which resulted in a dramatic reduction in the overall front advancement velocity and allows for significant coke production (Figure 6.25a). The combustion front initiated from the right hand side perforations of the horizontal injector propagated around the shale layers, which enhanced the air fingering effect and led to early oxygen break through into the producer (Table 6.8), and resulted in a reduction in the sweep efficiency of the process. On the other hand, the clean sand model (Figure 6.24a) showed a smooth symmetric front propagating from the horizontal injector to the producer. This showed that the presence of shale layers did change the combustion font behaviour and performance.

The cumulative amount of oil produced by the heterogeneous shale model was lower than for the homogeneous clean sand case (Figure 6.25b) because of both the large volume of oil being converted to coke in the former case, and the poor sweep efficiency where the shale layers trap some oil beneath them. The total recovery factor achieved by the shale model was 89.3%, which was slightly lower than the homogeneous clean sand case recovery factor (Table 6.8). However, the main impact of shale heterogeneity was the length of time it took the combustion front to achieve that recovery factor, which was around 2609 days compared to the 1631 days needed in the clean sand case. This meant that the existence of shale layers led to a 978 days delay in the recovery time for the fire front to achieve an ultimately lower recovery factor than in the homogeneous clean sand model.

Model name	Recovery factor (%)	Time to recovery factor (days)	Oxygen break through (days)
homogeneous clean sand non-shale	92.1	1631	855
heterogeneous shale layers	89.3	2609	548

Table 6.8: *Simulation results of effect of discontinuous impermeable shale layers on combustion process using horizontal well configuration without aquifer support*

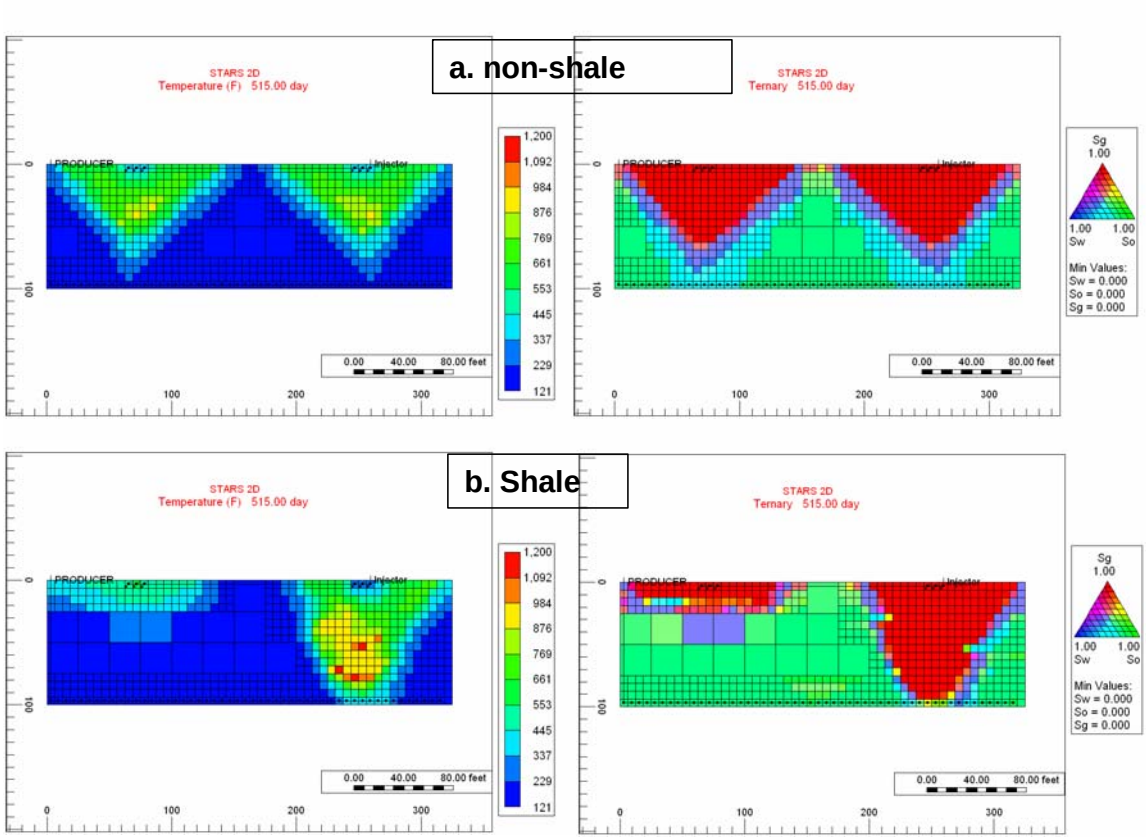

Figure 6.24: *Simulation results of temperature and ternary saturation at 515 days: (a) homogeneous clean sand non-shale model, and (b) heterogeneous shale layers model.*

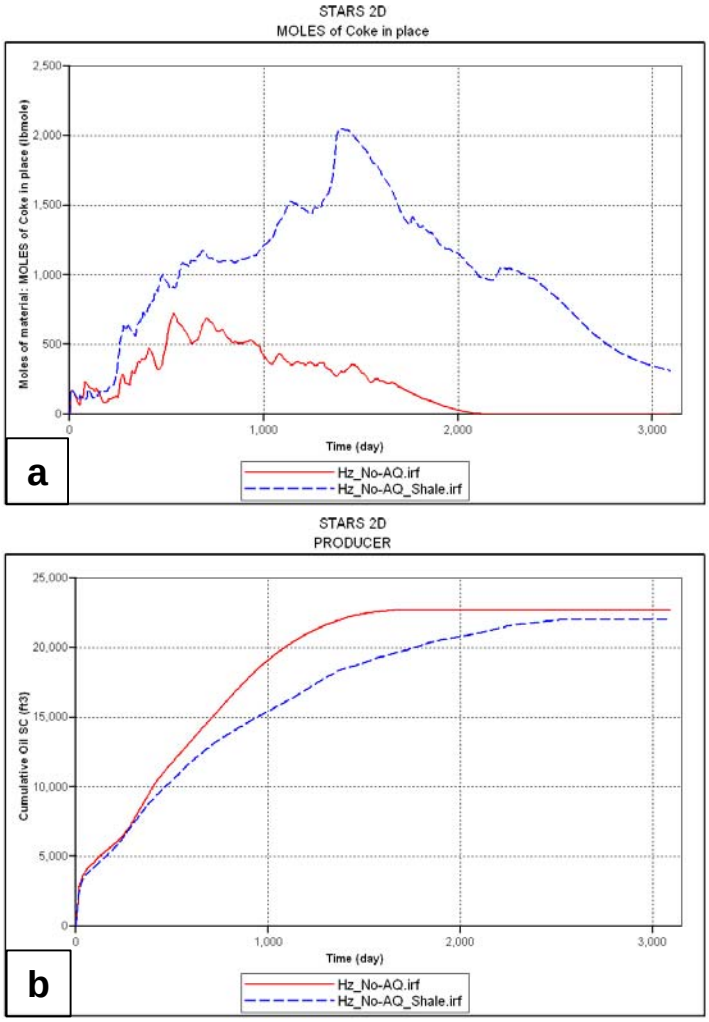

Figure 6.25: *Simulation results of effect of discontinuous impermeable shale layers on combustion process using horizontal well configuration without aquifer support: (a) net coke in place, and (b) cumulative oil produced*

Vertical well configuration: The fire front behaviour in the vertical well configuration in the presence of discontinuous shale layers was investigated in this sensitivity. The temperature maps at 425 days (Figure 6.26) for both scenarios showed almost an identical front, with the homogeneous clean sand model giving a slightly higher velocity. The main reason for the similarity of both these cases was the lateral orientation of the shale layers (Figure 6.23b), which did not affect the horizontal permeability of the system. Since the early combustion front movement in the vertical well configuration was mainly in the horizontal direction, the impact of the existence of shale layers on the process was minimised at the stage of lateral front propagation. When the fire front starts to propagate vertically to reach the vertical producer

perforations, the combustion behaviour in both models was changing, as the temperature maps show in Figure 6.26 at 905 days. For the homogeneous clean sand model, the front propagated vertically and broke through into the producer in a shorter time, as indicated by the cumulative oxygen produced curve in Figure 6.27a. On the other hand, for the shale layers model (Figure 6.26b), the front moved vertically until it reached the impermeable shale layer (Figure 6.23b) where its propagation rate was reduced significantly and a higher amount of coke has been produced at a later stage of the process, as shown by the net coke in place in Figure 6.27b. After that, the combustion front flowed around the shale layer until it reached the vertical producer perforations. The benefit of having the shale layers in this specific well scenario was that the fire front was able to sweep a larger area of the model, unlike the homogeneous clean sand model, because the front was forced to flow around the shale layers which improved the process sweep efficiency. However, even with this improvement in sweep efficiency, the cumulative oil produced by the heterogeneous model was slightly lower than the homogeneous model (Figure 6.27c) because of the higher amount of coke produced by the combustion front.

This study showed that the impact of including discontinuous shale layers in the combustion process was minimised when a vertical well configuration was used. This was mainly because of the front tending to propagate laterally for longer periods of the process. The process performance in both the clean sand and the shale layer models started to vary when the fire front propagated vertically at the later stage of the process. For the heterogeneous shale layers model, the combustion front propagates around the shale layers, which allowed a larger model area to be swept, but in the same time a larger amount of coke been produced due to the slow front propagation and the longer distance travelled by the fire front. However, the overall oil production for both scenarios was almost the same.

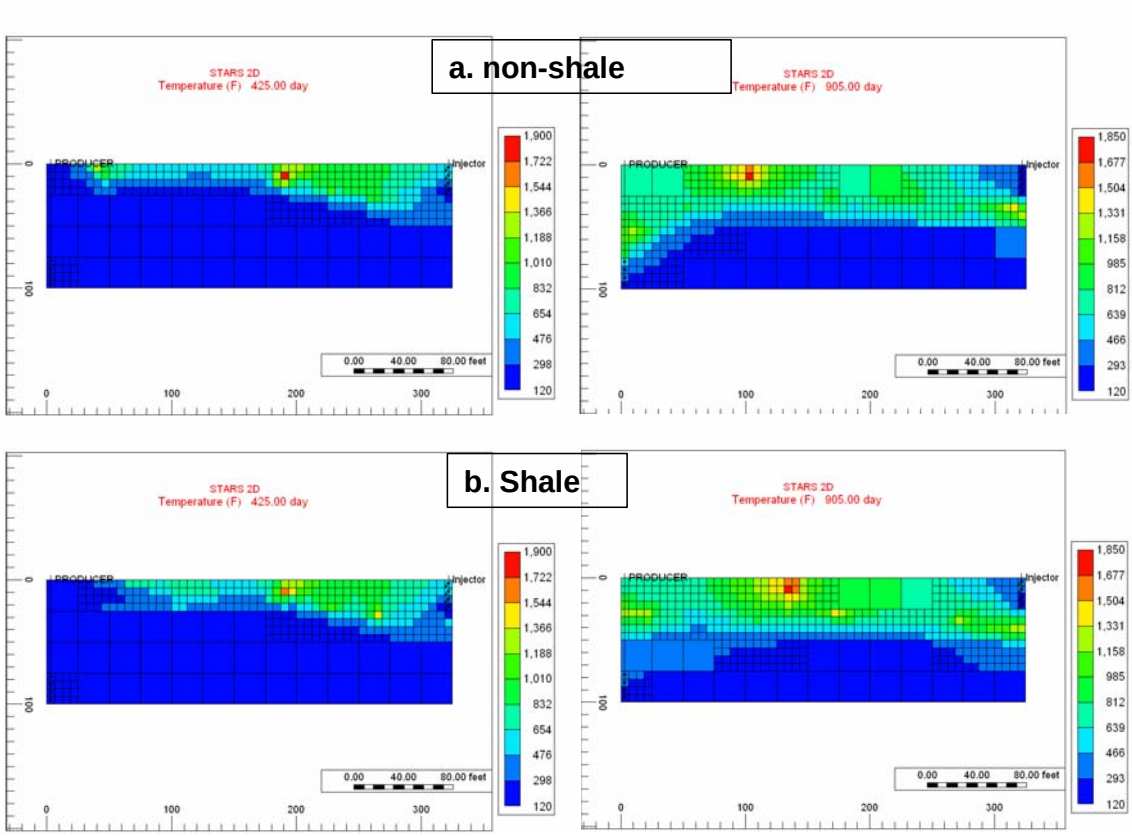

Figure 6.26: *Simulation results of temperature at 425 days and 905 days: (a) homogeneous clean sand non-shale model, and (b) heterogeneous shale layers model*

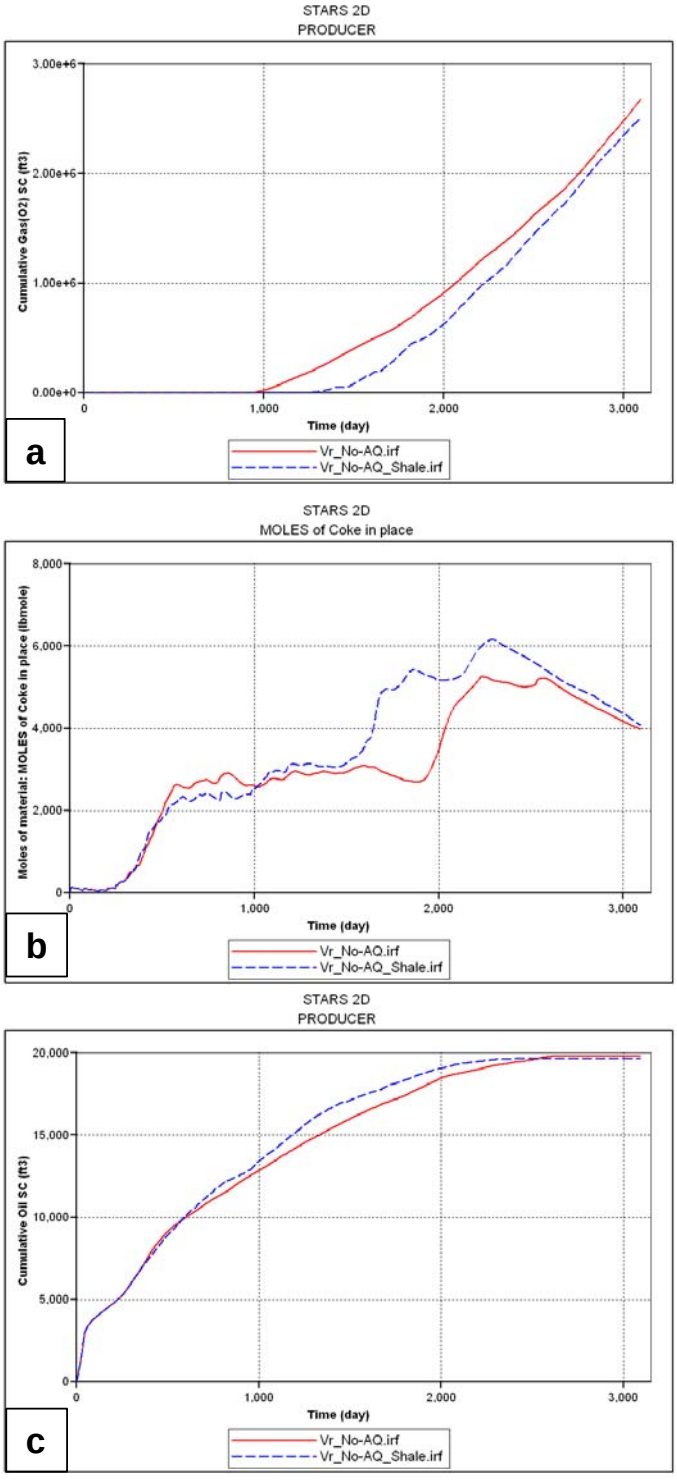

Figure 6.27: *Simulation results of effect of discontinuous impermeable shale layers on combustion process using vertical well configuration without aquifer support: (a) cumulative oxygen produced, (b) net coke in place, and (c) cumulative oil produced*

6.5.2 Discontinuous impermeable shale layers effect on combustion process with aquifer support

Horizontal well configuration: Introducing discontinuous impermeable shale layers into the horizontal well scenario with aquifer support resulted in a reduction of the effectiveness of the in-situ combustion process in terms of reducing the recovery factor. Table 6.9 shows the comparison between the non-shale homogeneous model and the heterogeneous shale layers model. The shale layers change the way the fire front was developed and propagated in the area between the two horizontal wells, especially when the horizontal injector perforations were located near the shale layer. In the heterogeneous model oil in place was swept, but achieved 4.3% lower recovery factor than in the homogeneous model. This was mainly as a result of the fire front propagation being retarded by the presence of the shale layers, which allowed for a significant volume of oil being wasted when it was converted to coke (Figure 6.28a). The resistance to flow around the shale layers led to a reduction in the front velocity compared to the homogeneous model scenario. Moreover, the occurrence of early oxygen break through (Table 6.9) in the heterogeneous case due to the effect of heterogeneity which enhanced gas fingering results in a poorer front sweep efficiency and less cumulative oil being produced (Figure 6.28b).

Model name	Recovery factor (%)	Front quenching time (days)	Oxygen break through (days)	So @ 3095 days (fraction)
homogeneous clean sand non-shale	77.0	3095	454	0.10
heterogeneous shale layers	72.7	3095	353	0.13

Table 6.9: *Simulation results of discontinuous impermeable shale layers on combustion process using horizontal well configuration with aquifer support*

The temperature distribution maps (Figure 6.29) show how the fire fronts developed and propagate in both models. The presence of shale layers made the front changed its direction of propagation around the layers (Figure 6.26b at 170 days), and allowed early

oxygen break through into the horizontal producer compared to the homogeneous model. At 605 days, the combustion fronts in both models swept the top of the model between the injector and the producer, but with a slightly lower velocity for the heterogeneous model. Also, in the upper model area, the shale layers acted like a shield to trap oil beneath them (Figure 6.30) and prevented the fire front from sweeping those protected areas up to the final time step. Figure 6.28c shows the total water produced from both scenarios, and it was clear both models produced the same amount of water at the end of the process, even though the shale layers existed in the area between the aquifer and the horizontal producer (Figure 6.31). This meant the shale heterogeneity did not reduce the aquifer influx to the oil zone, which might be as a result of the low water viscosity which allowed it to flow readily around the shale layers. Also, the large contact area between the long horizontal producer and the formation allowed for production of the same amount of water as in the heterogeneous model.

This sensitivity showed the impact of shale layers in reducing the in-situ combustion process performance. The obstruction of the fire front propagation by the shale layers resulted in a reduction of the front velocity, which allowed for significant production of coke in place. As a result, a lower recovery factor was achieved by the combustion front in this well scenario.

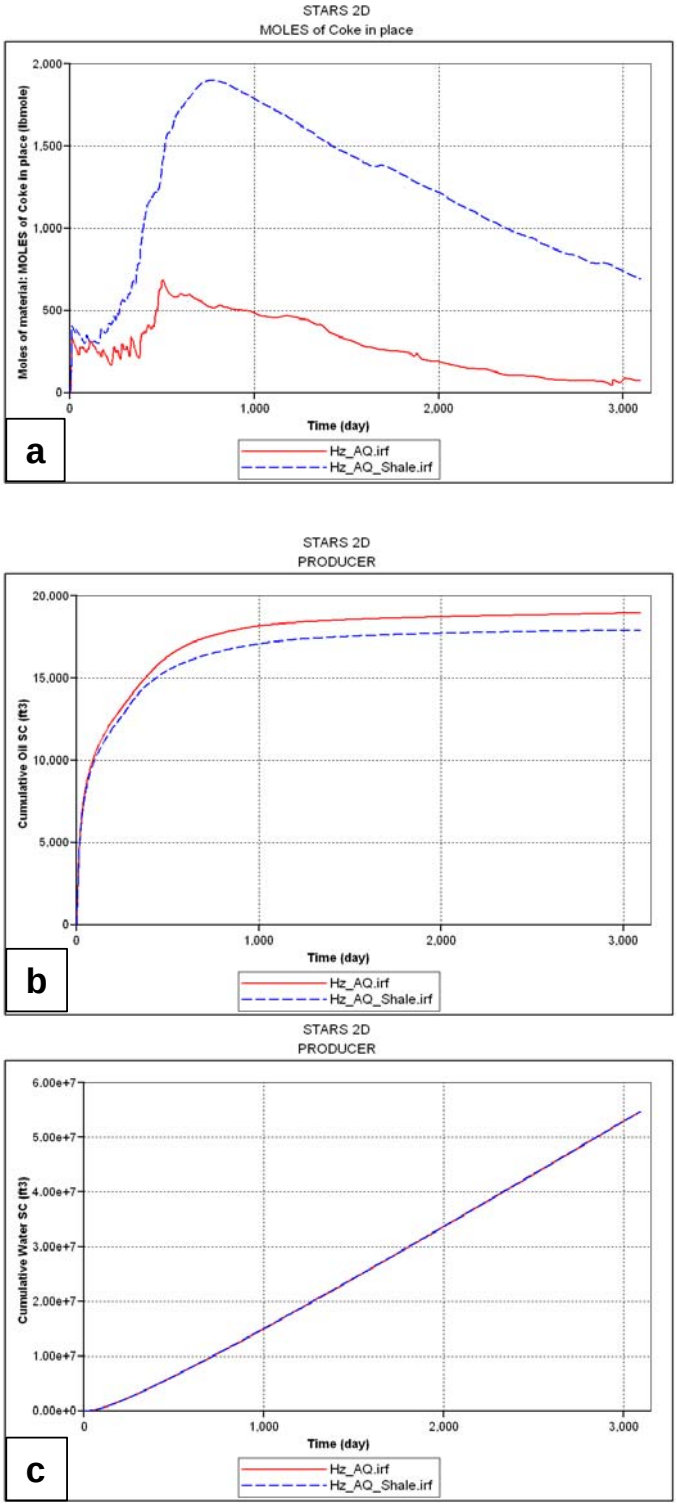

Figure 6.28: *Simulation results of effect of discontinuous impermeable shale layers on combustion process using horizontal well configuration with aquifer support: (a) net coke in place, (b) cumulative oil produced, and (c) cumulative water produced*

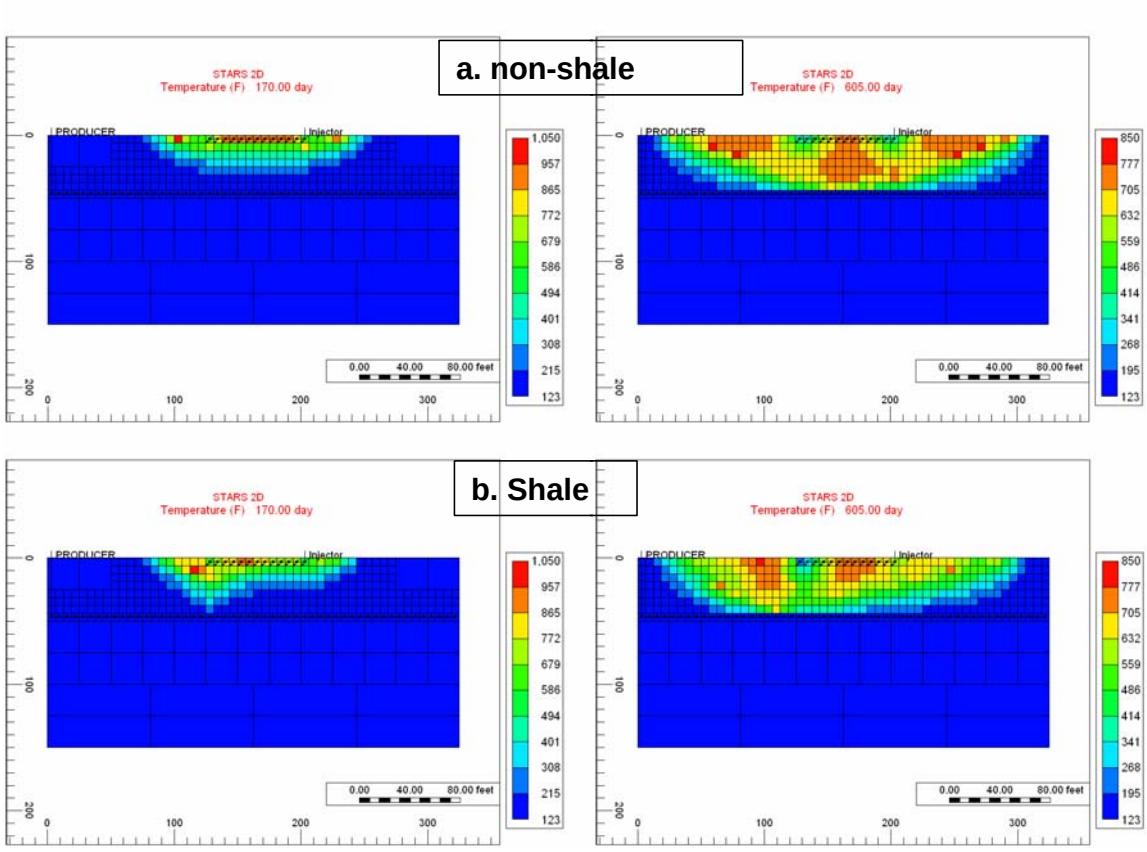

Figure 6.29: *Simulation results of temperature at 170 days and 605 days: (a) homogeneous clean sand non-shale model, and (b) heterogeneous shale layers model*

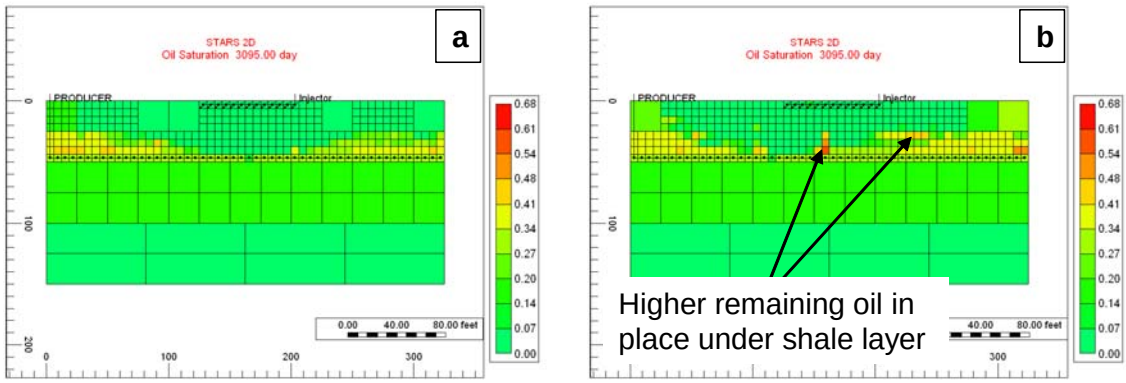

Figure 6.30: *Simulation results of oil saturation at 3095 days: (a) homogeneous clean sand non-shale model, and (b) heterogeneous shale layers model*

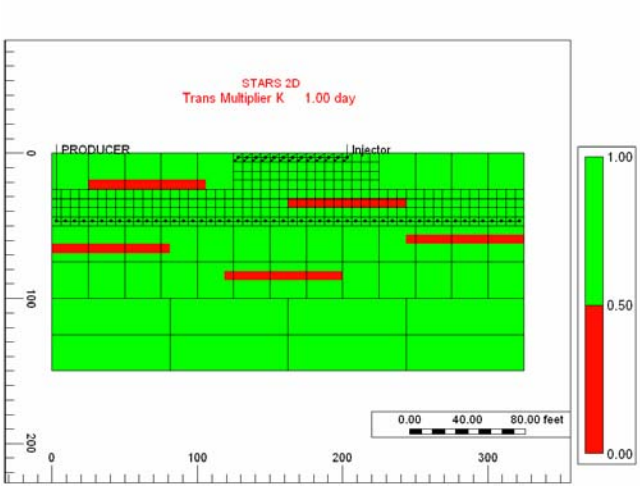

Figure 6.31: *Location of discontinuous impermeable shale layers in the horizontal well configuration with aquifer support*

Vertical well configuration: The existence of shale layers in the vertical well configuration led to termination of the calculation at around 785 days. The way the vertical injector and producer were completed and the location of the shale layers for this model (Figure 6.32) were the main reason for this termination. Introduction of heterogeneity to this well scenario would lead to further restriction to the propagating of the front and a significant reduction in its velocity, which resulted in a large mass of coke being deposited (Figure 6.33a). The coke was deposited ahead of the front in large quantities, which led to a rapid reduction to the model pore volume ahead of the front. As a result, the combustion front was not able to propagate further and the simulator run was terminated. Hence, the presence of shale layers in this specific well configuration could lead to failure in the application of in-situ combustion process.

In this sensitivity, the main comparison between the homogeneous non-shale model and the model with shale layers was based on the results up to the termination date (785 days). Figure 6.34 shows the temperature maps for the fire front for both models at 300 days and 545 days. The behaviour of the fronts were similar in both scenarios, but with some limitation to the fire font vertical progression in the heterogeneous shale layers model. This was because of the presence of a shale layer below the vertical injector perforations (Figure 6.32). Also, the vertical producer was located between two of the shale layers (Figure 6.32) which function as restrictions to front advancement. This led to a large mass of coke being deposited and lower cumulative oil production (Figure

6.33b) compared to the heterogeneous model. Moreover, the total water produced in the heterogeneous case was very low at the end of the run (785 days), which was as a result of both the existence of a shale layer between the vertical produced and the aquifer (Figure 6.33) which acted as a barrier to water flow, and because of the short perforation length of the vertical producer.

This sensitivity showed the possibility of failure of the fire front process when heterogeneity was present in the oil reservoir as discontinuous shale layers and when there was poor well placement, such as the vertical well configuration used in this model. The limitation of the fire front propagation due to the shale layers led to a rapid increase in coke in place, which dramatically reduced the formation pore volume and terminates the run.

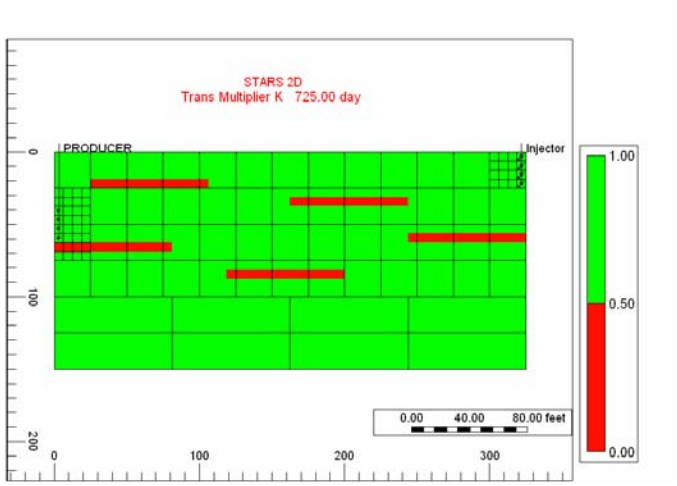

Figure 6.32: *Location of discontinuous impermeable shale layers in the vertical well configuration with aquifer support*

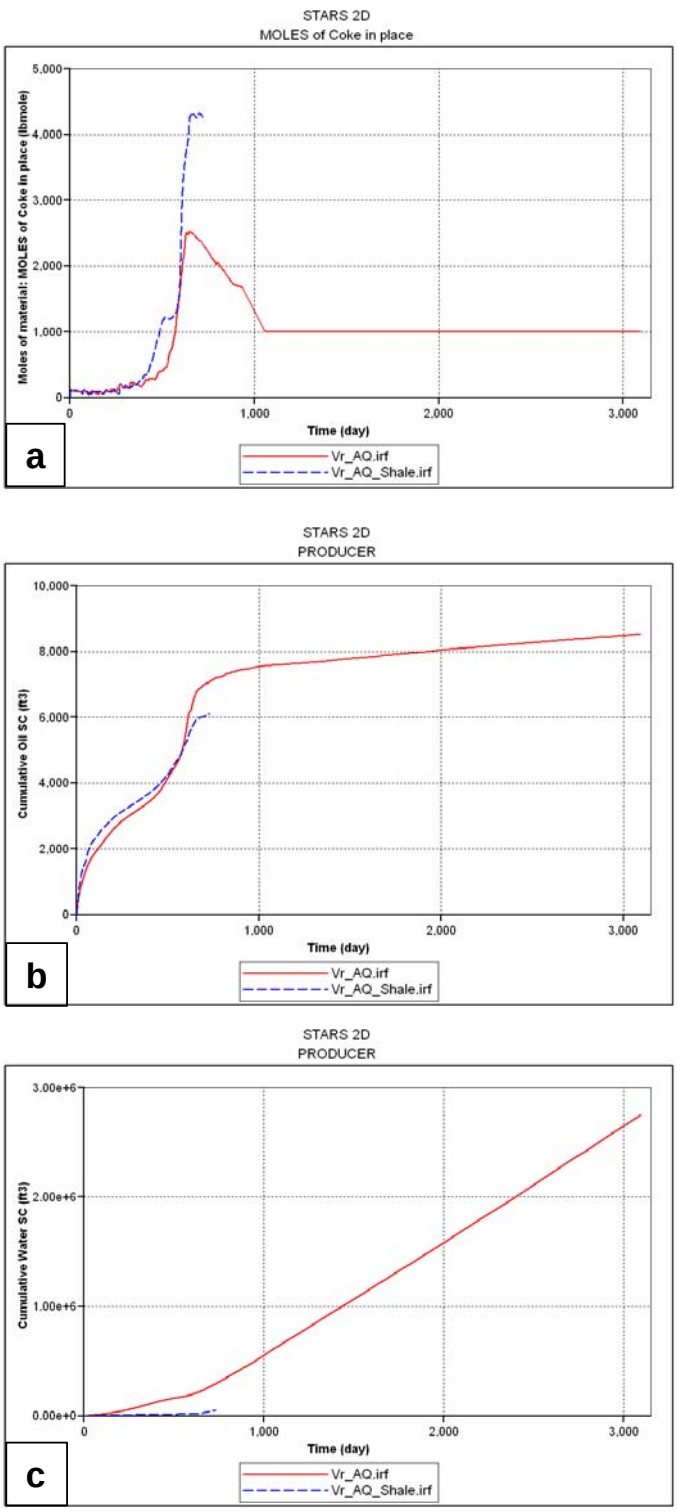

Figure 6.33: *Results of the effect of discontinuous impermeable shale layers in combustion process using vertical well configuration with aquifer support: (a) net coke in place, (b) cumulative oil produced, and (c) cumulative water produced*

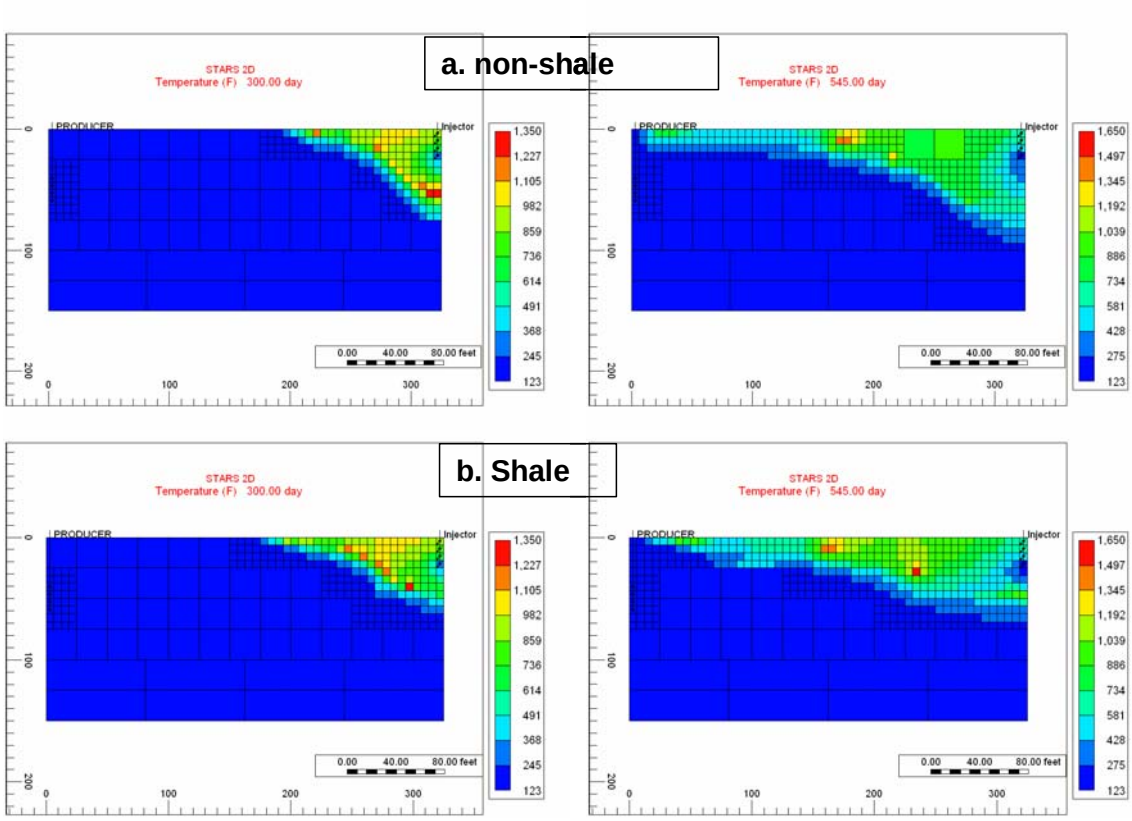

Figure 6.34: *Temperature at 300 days and 545 days: (a) homogeneous clean sand non-shale model, and (b) heterogeneous shale layers model*

In order to identify the specific cause of model termination in this sensitivity, there was a need to run the same model again, but with refined grid blocks. This should help to distinguish whether the reason behind the modelling process failure was a physical limitation of the combustion process as already explained or due to numerical instability. The new model was the same as the previous used model, except without the grid amalgamation option. This will ensure modelling the in-situ combustion process in a more accurate way. The process temperature maps, which were comparing the fire front propagation through both models, are shown in Figure 6.35 at 310 days and 485 days. The combustion front behaviour in both scenarios (amalgamated and refined) was the same in terms of the way the fire front was initiated, with the only exception being that the refined grid blocks led to a faster combustion front propagation (increase in the front velocity, particularly through the top layer). The refined model was terminated at around 550 days compared to the case of the amalgamated models, which terminated at 785 days (Figure 6.36). The reason behind the early process failure in the refined model

was due to the faster front propagation though the model until it was obstructed by the discontinuous impermeable shale layers.

This sensitivity comparison between the amalgamated and refined scenarios did confirm that the main cause of the in-situ combustion modelling failure was due to the physical limitation of the fire front propagation in such heterogeneous case (discontinuous impermeable shale layers). This meant that introduction this type of heterogeneity to this well scenario lead to further restriction to the propagating of the front and a significant reduction in its velocity, which resulted in a large mass of coke being produced. The coke was deposited ahead of the front in large quantities, which led to a rapid reduction to the model pore volume ahead of the front. As a result, the combustion front was not able to propagate further and the simulator run was terminated.

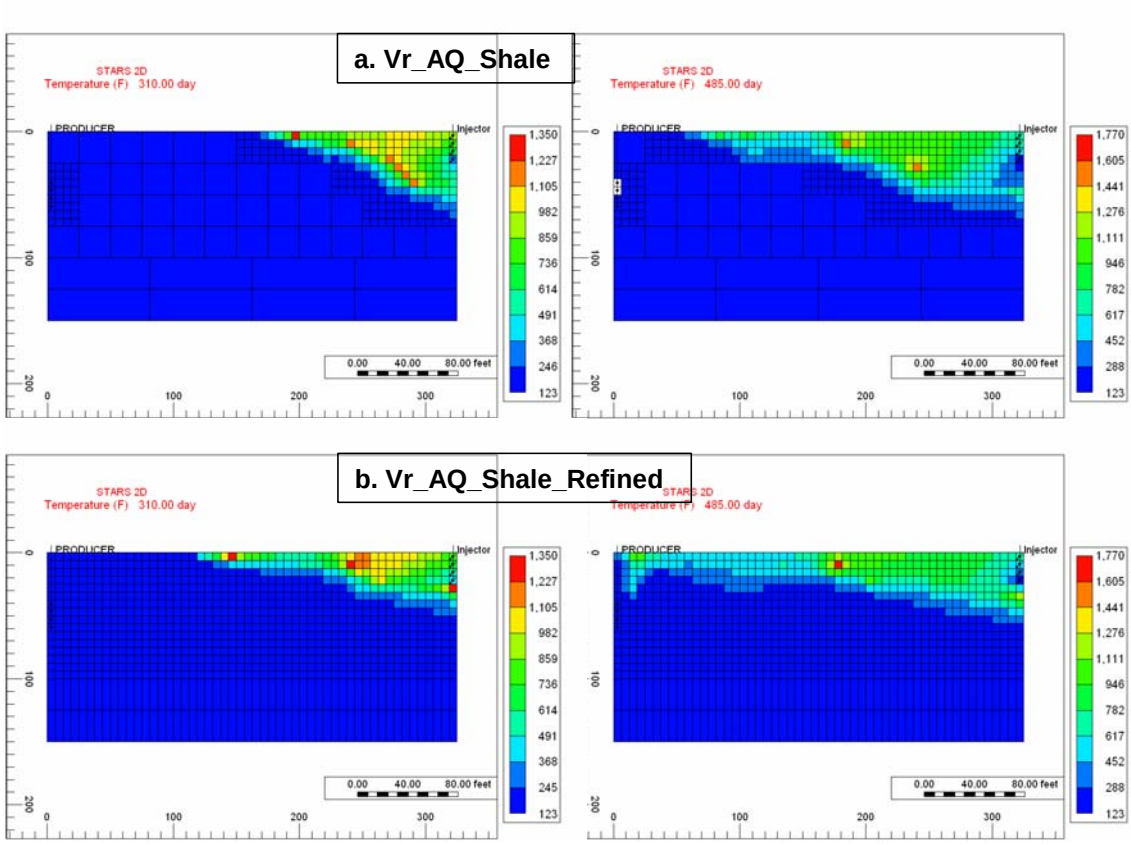

Figure 6.35: *Temperature at 310 days and 485 days: (a) amalgamated heterogeneous shale layers model, and (b) refined heterogeneous shale layers model*

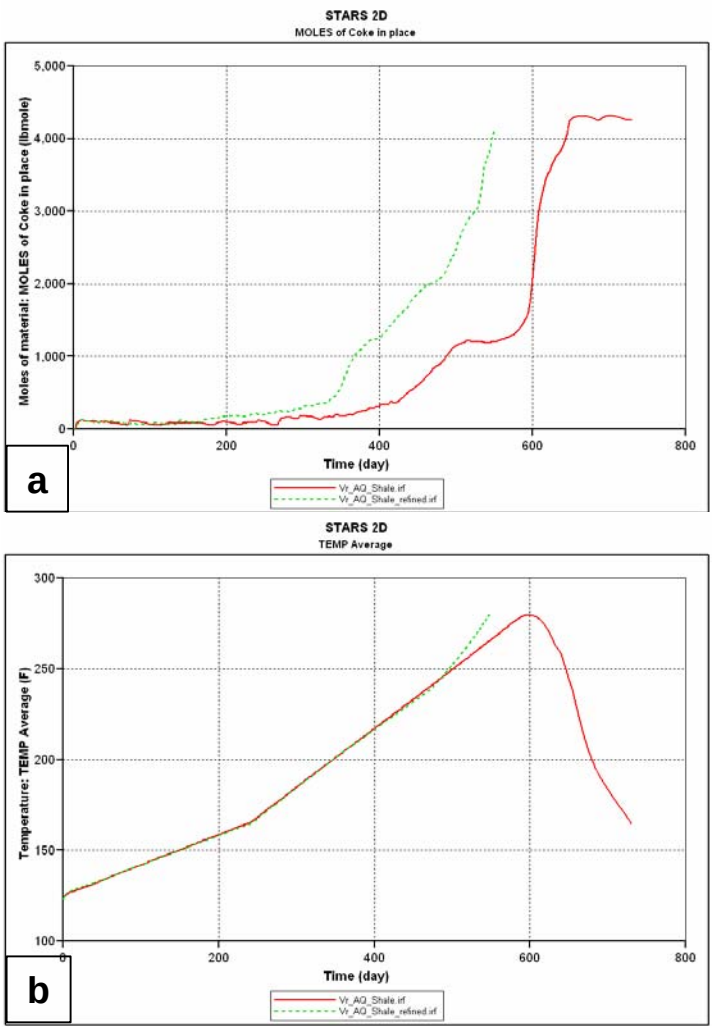

Figure 6.36: *Results of the comparison between the amalgamated (coarse) and refined models where the effect of discontinuous impermeable shale layers in combustion process was investigated using vertical well configuration with aquifer support: (a) net coke in place, (b) cumulative oil produced, and (c) cumulative water produced*

As already noted, more refined models tend to lead to more accurate calculations by reducing the effects of numerical dispersion. More refined models also allow for a more detailed reservoir description. In the case of dynamically amalgamated models, caution needs to be taken with respect to averaging of reservoir properties. If a shale layer lies at the boundary of amalgamated grid blocks it will be accurately represented in the model. However, if a shale layer lies in the middle of a zone of finer grid blocks that have been amalgamated, the effect of the shale may not be properly reproduced.

In these calculations, the grid blocks are not amalgamated in the vicinity of the fire front, and hence the impact of shales on the chemical and thermal reactions will be accurately represented, since reservoir description data will not be lost in these zones. However, some of the more general fluid flow calculations may be affected by the amalgamations that take place away from the fire front. In the context of in-situ combustion calculations this is a relatively minor effect compared to the chemical and thermal effects, which dominate the process. The impact of amalgamations (away from the fire front) on fluid flow is discussed in more detail in Appendix C.

6.6 Shaley sand layer effect on in-situ combustion

Modelling of the in-situ combustion process in the presence of impermeable shale layers showed variations in the process performance as sensitivities in previous section have highlighted. The impact of having those discontinuous shale layers was on the restriction of the fire front propagation through the model area. In this section, the effect on the combustion process of having a shaley sand layer the same length as the model was evaluated. This layer consists of 99% shale, which resulted in a significant reduction in the layer permeability to just 1% of the model permeability (4,000mD). The shaley sand layer thus had a permeability equals to 40mD (Figure 6.37b). The low permeability layer was expected to influence the in-situ combustion process in terms of limiting the fire front propagation. The impact of this type of heterogeneity was further investigated below, with different well configuration and with/without the presence of aquifer support.

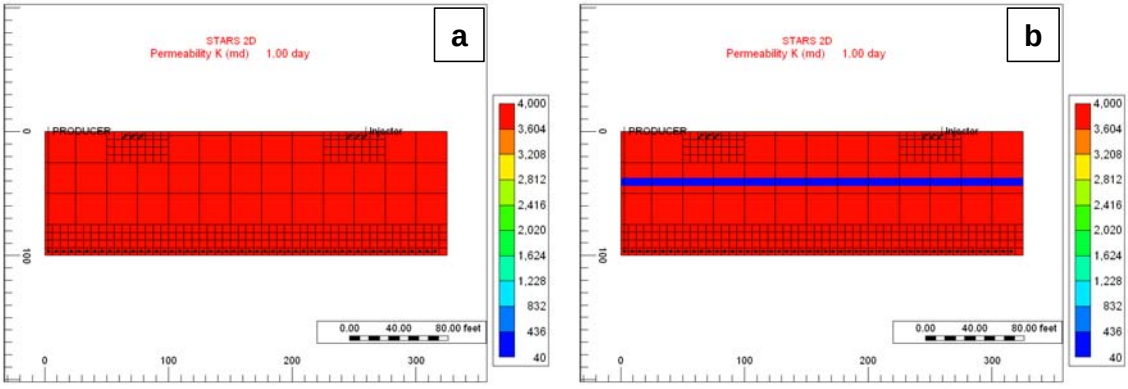

Figure 6.37: *Shaley sand layer effect on the combustion process: (a) homogeneous clean sand model, and (b) heterogeneous shaley sand layer model*

6.6.1 Shaley sand layer effect on combustion process without aquifer support

Horizontal well configuration: This sensitivity investigated the combustion performance using horizontal wells when a shaley sand layer with much lower permeability existed in the formation. The resulted of the shaley sand layer model were compared with the homogeneous clean sand model. Both the temperature and ternary maps (Figure 6.38) showed that the fire fronts in both models were initiated and propagated identically in the upper part of the models away from the shaley sand layer. At 455 days (Figure 6.38b), the combustion front in the heterogeneous shaley sand case reached the low permeability layer, which led to a reduced combustion front velocity. As a result, the front required longer time to advance through the shaley sand layer compared to the heterogeneous clean sand model. After the front broke through occurred in the lower permeability layer, it diffused laterally in the higher permeability layer below the shaley sand layer as the ternary saturation plots showed in Figure 6.38b. This led to a change the fire font behaviour before it stabilised again and continued vertical movement toward the horizontal producer. Hence, the main effect of the shaley sand layer in the combustion process was to slow the fire front propagation velocity when it reached that layer in the horizontal well scenario. Table 6.10 shows the main results of both the clean sand and shaley sand models. There was no significant variation between the two sets of results. The slightly lower recovery factor in the heterogeneous shaley sand layer model was due to the higher amount of coke being

produced (Figure 6.39) as a result of the front velocity reduction when the front approaches the lower permeability layer.

Model name	Recovery factor (%)	Time to recovery factor (days)	Oxygen break through (days)
homogeneous clean sand	92.1	1631	855
heterogeneous shaley sand layer	91.7	1700	815

Table 6.10: *Simulation results of effect of shaley sand layer in combustion process using horizontal well configuration without aquifer support*

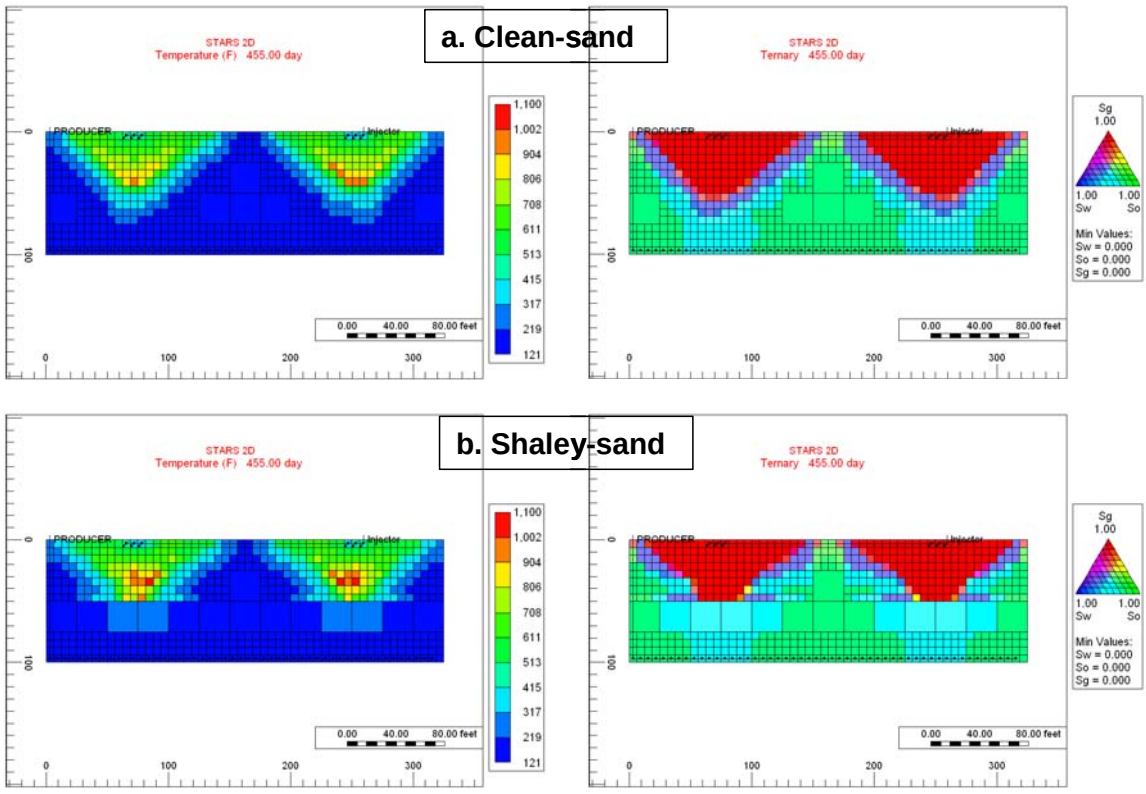

Figure 6.38: *Simulation results of temperature and saturation ternary plot at 455 days: (a) homogeneous clean sand model, and (b) heterogeneous shaley sand layer model*

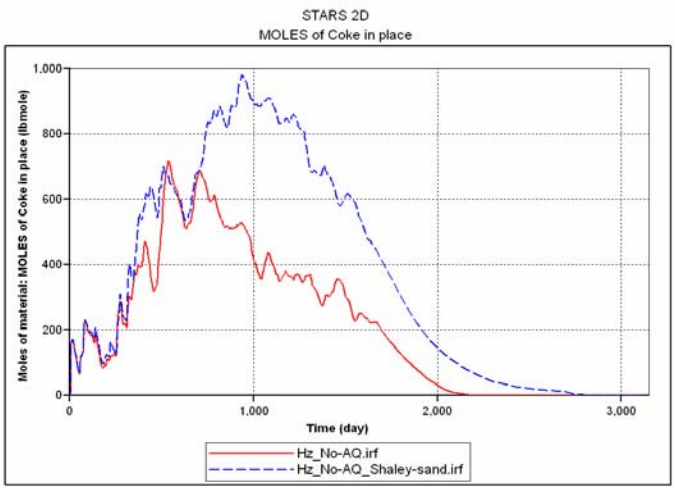

Figure 6.39: *Simulation results of net coke in place for the effect of shaley sand layer in combustion process using horizontal well configuration without aquifer support*

Vertical well configuration: In the vertical well scenario, the fire front movement in the model was dominated by the gravitational force. This meant the combustion front was propagating in the top of the model due to the gas override effect. Since the shaley sand layer was located almost in the middle section of the model, this allowed for similar behaviour of the fire fronts in both models (Figure 6.40) when the front was propagating laterally in the top of the model. However, the combustion front velocity was slower in the heterogeneous model, even when the front was propagating laterally away from the low permeability layers. This was because in the shaley sand layer model the flu gases and the oil bank ahead of the front were restricted by the low permeability layer when they started to move vertically to approach the vertical producer. This created a barrier in the model which reduced the front velocity in the lateral direction. This slow front velocity resulted in a slightly higher amount of coke being produced by the shaley sand model compared to the homogeneous model in the first 514 days (Figure 6.41a). On the other hands, after 514 days, the net amount of coke produced by the homogeneous clean sand model was much more in the case of the heterogeneous model. This occurred as a result of the behaviour of the front when a dramatic change in its velocity occurred in the clean sand scenario at the moment the front change its direction of movement from being fast in the lateral direction to becoming slower in the vertical direction.

In the case of the heterogeneous model, the fire front movement in the lateral direction was already slow, and when the combustion front started to propagate vertically, its velocity was further reduced, which produced more coke compared to the lateral front case (Figure 6.41a coke after 514 days). However, the change between front velocity in the clean sand case was much higher than the change in velocity for the shaley sand model fire front, which explained the increase in the net coke produced by the former scenario. As a result, the cumulative oil produced by the homogeneous model in this sensitivity was lower than that produced in the heterogeneous model (Figure 6.41b). This allowed the heterogeneous model to achieve a higher recovery factor (2.5% higher) than the homogeneous model (Table 6.11). Also, the shaley sand layer model delayed the oxygen break through by 116 days, which enhanced the sweep efficiency of the front and a higher recovery was achieved. However, the heterogeneous model needed a longer recovery time to yield its maximum recovery factor because of the slow front propagation.

This sensitivity showed that the presence of a shaley sand low permeability layer resulted in an improvement in the combustion front performance in a vertical well configuration. This was because of the slower fire font propagation, which delayed the oxygen breakthrough and improved the sweep efficiency. Also, the low front velocity helped to minimise the amount of coke being produced as a result of the change in the fire front velocity when the front movement was changed from a lateral to a vertical direction.

Model name	Recovery factor (%)	Time to recovery factor (days)	Oxygen break through (days)
homogeneous clean sand	80.4	2611	885
heterogeneous shaley sand layer	82.9	2824	1001

Table 6.11: *Simulation results of effect of shaley sand layer in combustion process using vertical well configuration without aquifer support*

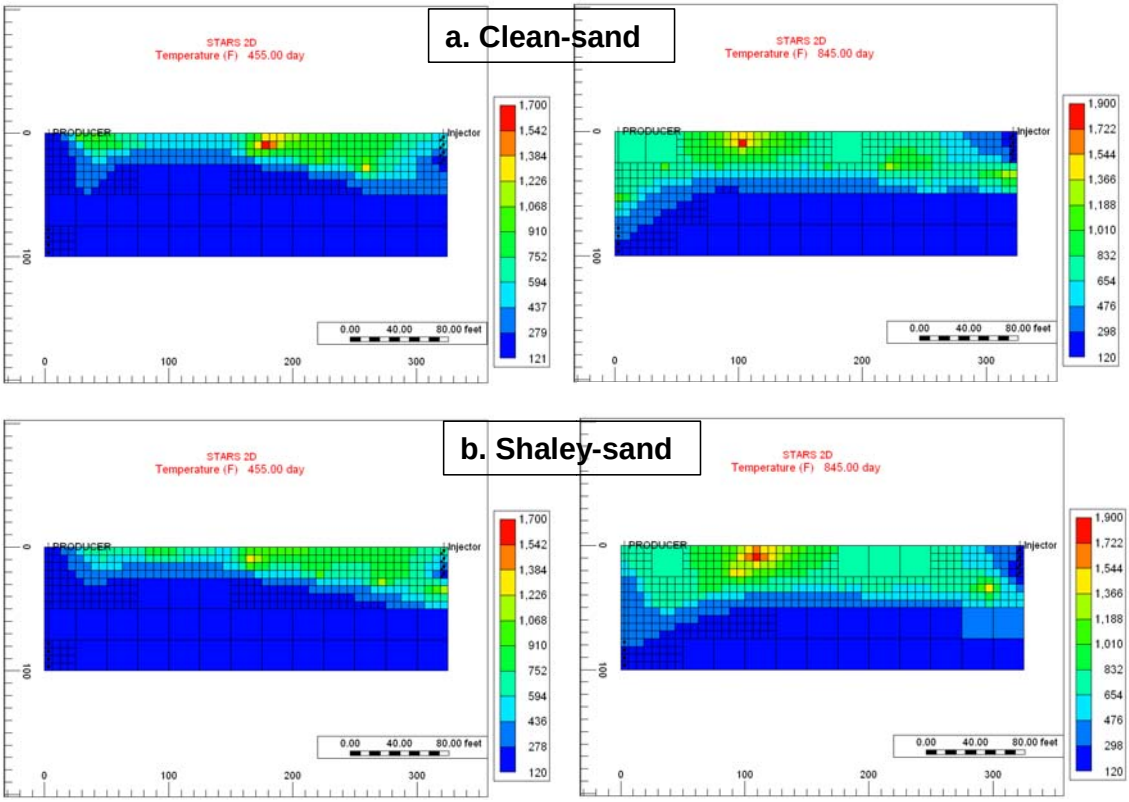

Figure 6.40: *Simulation results of temperature at 455 days and 845 days: (a) homogeneous clean sand model, and (b) heterogeneous shaley sand layer model*

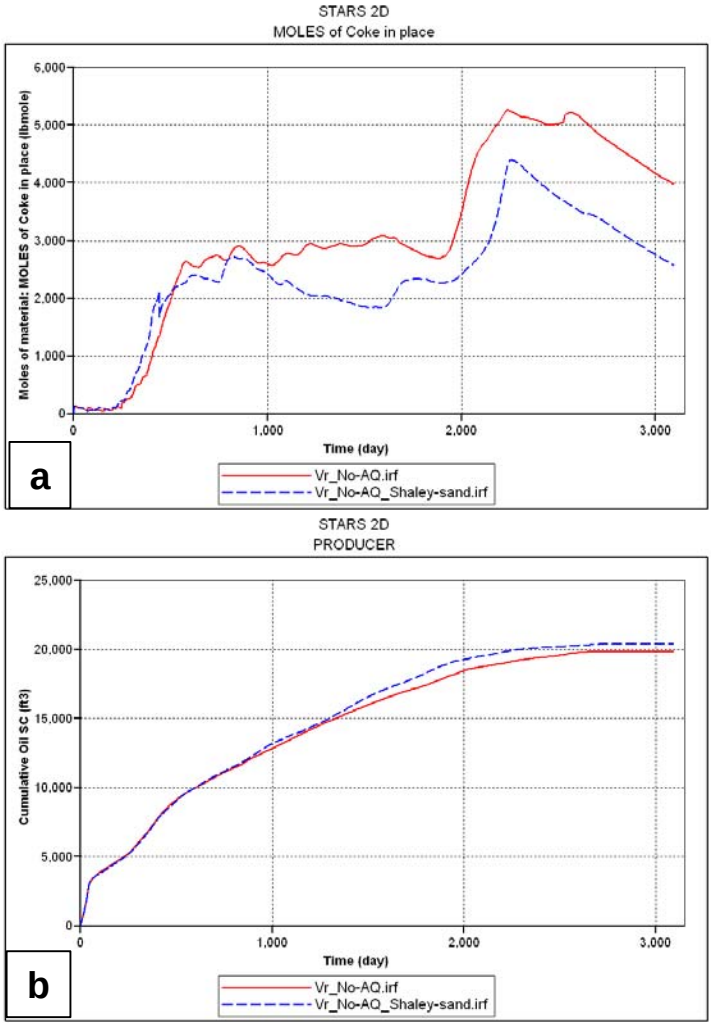

Figure 6.41: *Simulation results of the effect of shaley sand layer in combustion process using vertical well configuration without aquifer support: (a) net coke in place, and (b) cumulative oil produced*

6.6.2 Shaley sand layer effect on combustion process with aquifer support

Horizontal well configuration: The effect of shaley sand layer in the horizontal well configuration slowed the frontal velocity, which delayed the fire front propagation. The temperature distribution maps in Figure 6.42 for both the homogeneous and heterogeneous models at 360 days show the behaviour of the fronts within each model. The observation from the temperature maps was that the low permeability layer reduced the fire front propagation in the model, with some restraint to the lateral movement of the front as the ternary saturation plot showed as well. The slowness of the fire front in the shaley sand model could also be observed from the high amount of net coke

produced by the fire front (Figure 6.43a) from the start of the process. This led to a lower volume of oil being produced by this scenario compared to the clean sand case (Figure 6.43b). Moreover, the heterogeneity due to the shaley sand layer resulted in an enhancement of the air fingering effect, which led to earlier oxygen break through (Figure 6.43c). At the end of the combustion recovery process for both models, the amount of oil remaining in place for the heterogeneous models was much higher (Figure 6.44), especially near the model boundaries below the shaley sand layer. This reflected the low recovery factor (72.4%) achieved by the combustion process in this scenario (Table 6.12). Also, the overall average oil saturation at the end of the model run was 12% compared to 10% in the homogeneous model. Finally, the total water produced by both cases was the same; and the presence of the shaley sand layer heterogeneity did not reduce the water production. This was mainly because of the location of the low permeability layer in the upper part of the model away from the aquifer, between the injector and producer.

The investigation in this sensitivity showed that the total oil produced by the combustion front was lower in the shaley sand layer model when aquifer support existed. This was mainly due to the reduction of front velocity which led to higher production of coke in place. Also, because of the poor sweep efficiency of the front in this scenario, this allowed for a higher amount of oil left in place at the end of the process especially under the low permeability layer.

Model name	Recovery factor (%)	Front quenched time (days)	Oxygen break through (days)	So @ 3095 days (fraction)
homogeneous clean sand	77.0	3095	454	0.10
heterogeneous shaley sand layer	72.4	3095	372	0.12

Table 6.12: *Simulation results of effect of shaley sand layer in combustion process using horizontal well configuration with aquifer support*

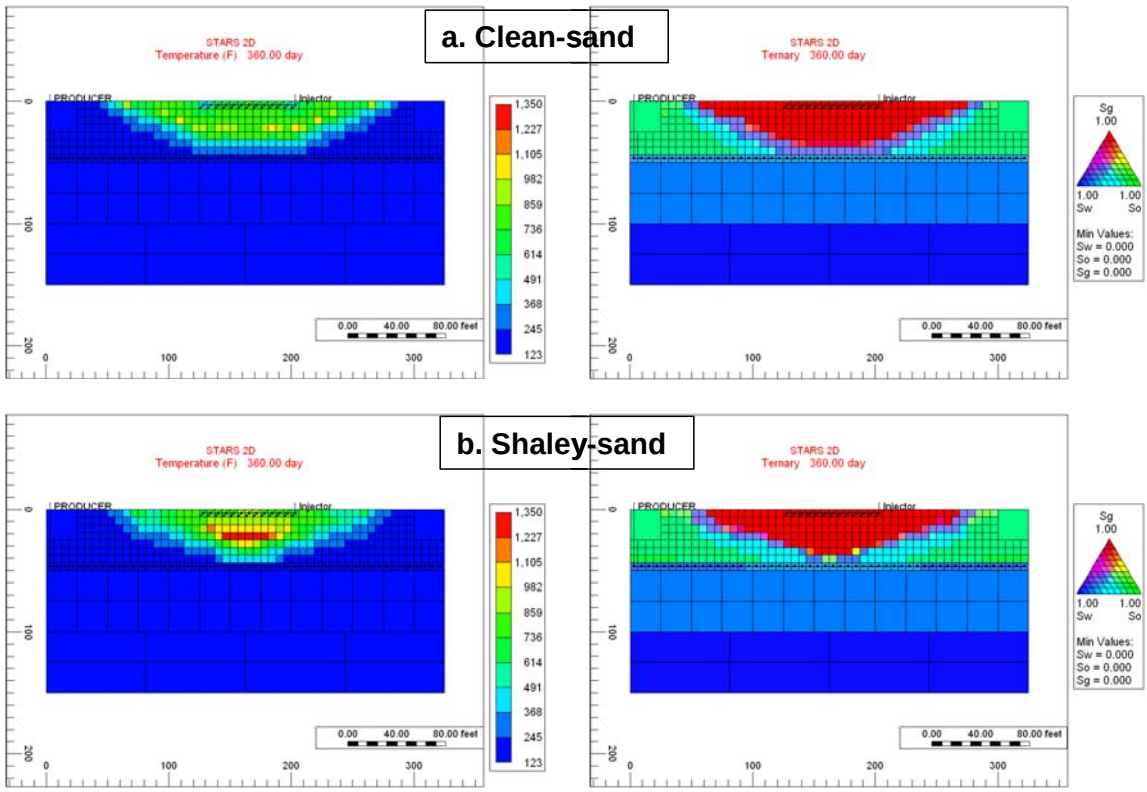

Figure 6.42: *Simulation results of temperature and ternary saturation plot at 360 days: (a) homogeneous clean sand model, and (b) heterogeneous shaley sand layer model*

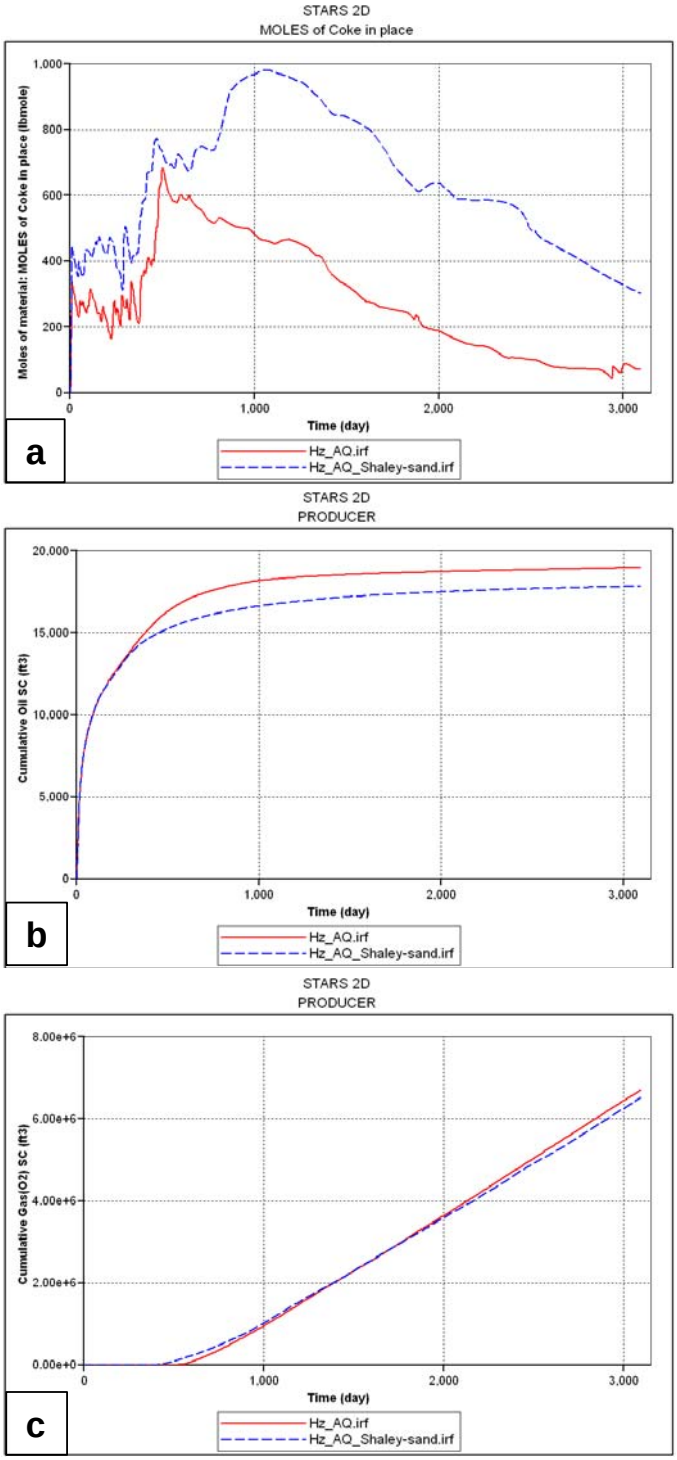

Figure 6.43: *Simulation results of the effect of shaley sand layer on combustion process using horizontal well configuration with aquifer support: (a) net coke in place, (b) cumulative oil produced, and (c) cumulative oxygen produced*

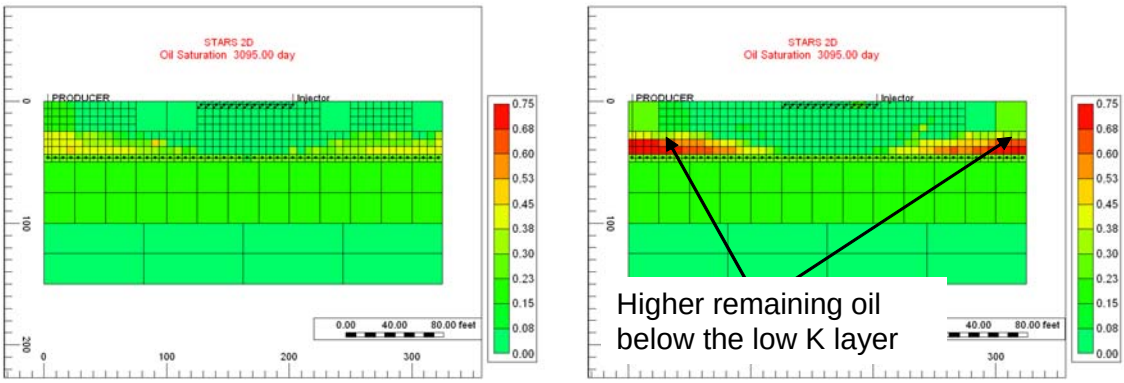

Figure 6.44: *Simulation results of oil saturation at 3095 days: (a) homogeneous clean sand model, and (b) heterogeneous shaley sand layer model*

Vertical well configuration: The result of having the shaley sand layer heterogeneity in the numerical model which was completed with a vertical well configuration led to termination of the model run at around 820 days. The presence of the low permeability layer results in a slowing of the fire front velocity to the point where a very large mass of coke was produced, as the steep increment shows in Figure 6.45a. This increase of coke led to a reduction in the porosity of the area ahead of the front, and blocked the pore space, which resulted in the front not propagating further to recover oil from the model. Figure 6.46 shows the temperature distribution of both scenarios at 425 days and 635 days. For the homogeneous models, the fire front propagation was faster in both lateral and vertical directions, whereas the shaley sand model has a limited frontal propagation in both directions, as Figure 6.46 shows.

At 635 days, the combustion front in the clean sand case managed to break through into the vertical producer, whereas in the heterogeneous models the fire front was still some distance away from the producer. However, the vertical sweep of the front in this scenario at this stage was much better than in the homogeneous case. This was mainly as a result of the presence of the low permeability layer, where it enhanced the front movement below it by reducing the gas flow to the top of the model. The total oil produced by both models was shown in Figure 6.45b, and up to the termination time for the shaley sand layer model. The cumulative oil produced by the combustion front for the homogeneous model was higher than that achieved by the heterogeneous scenario at 820 days.

The introduction of shaley sand layer heterogeneity to the model with the vertical well added to the complicity of the combustion process, and resulted in the simulation terminating much earlier than anticipated. The deposition of coke in place ahead of the front and the consequent reduction in pore volume was considered to be the main reason for this. The overall comparison of the results from both cases showed that the heterogeneous model produces less oil compared to the homogeneous scenario.

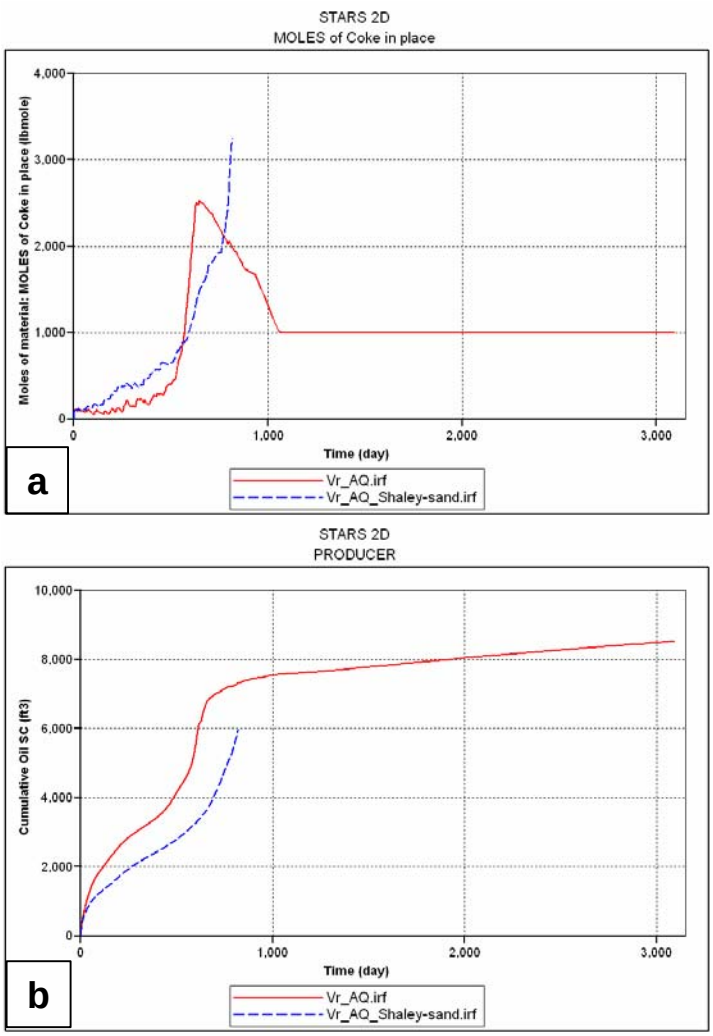

Figure 6.45: *Results of the effect of shaley sand layer on combustion process using a vertical well configuration with aquifer support: (a) net coke in place, and (b) cumulative oil produced*

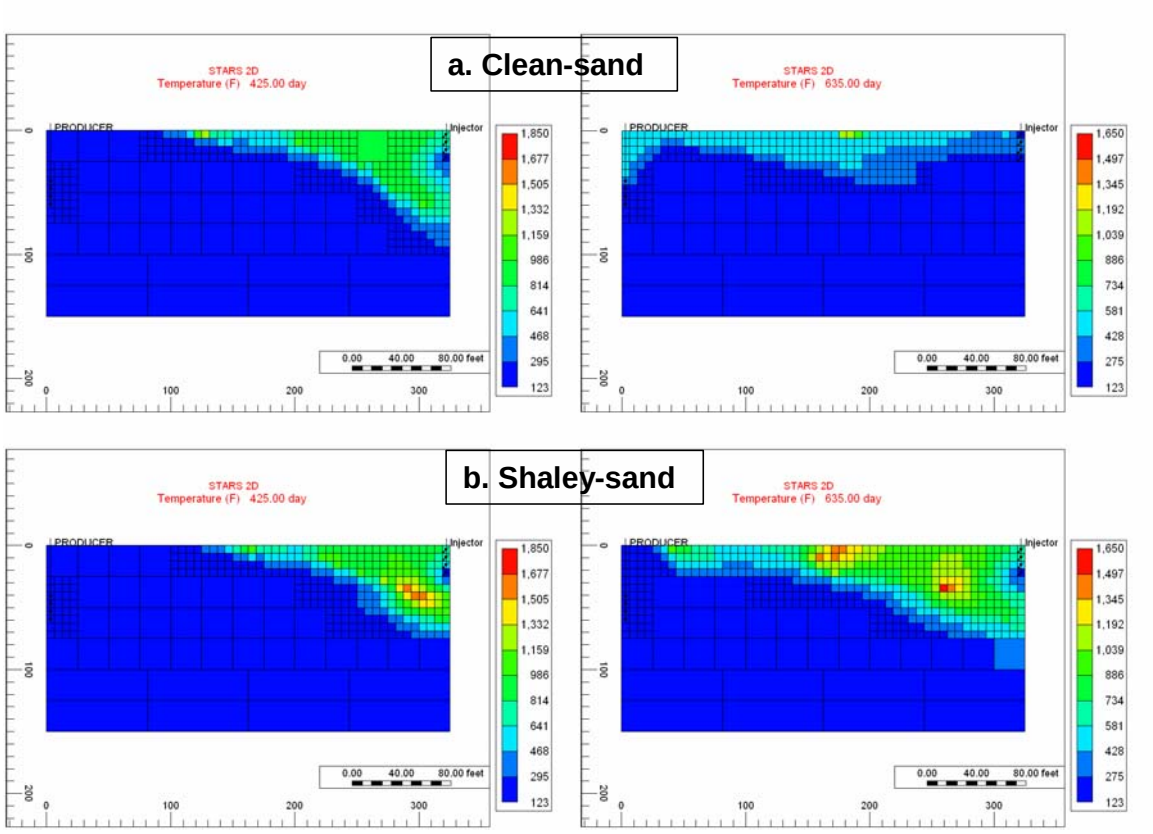

Figure 6.46: *Simulation results of temperature at 425 days and 635 days: (a) homogeneous clean sand model, and (b) heterogeneous shaley sand layer model*

6.7 Impact of multiple realisations

6.7.1 Multiple realisations for multiple permeability layers

So far in this chapter, the results of heterogeneous scenarios were compared to a homogeneous model with an average permeability of 4000mD. However, since the average permeability was less than that value (for the comparison in section 6.4), a comparison of the multiple permeability layers with an average permeability of 4000mD was presented in this section (Figure 6.47). The range of permeability used in the multiple permeability layers model was between 950mD and 9950mD. The mean permeability for the layered heterogeneous model was determined using the harmonic averaging method. This was used because the main fire front propagation direction was vertically between the horizontal injector (which was completed in the top of the model)

and the horizontal producer (which was completed in the bottom). The propagation was thus across the differnet permeability layers, and so the harmonic average was appropriate. The aim was to show the fire front performance in two different models where the average permeability was the same.

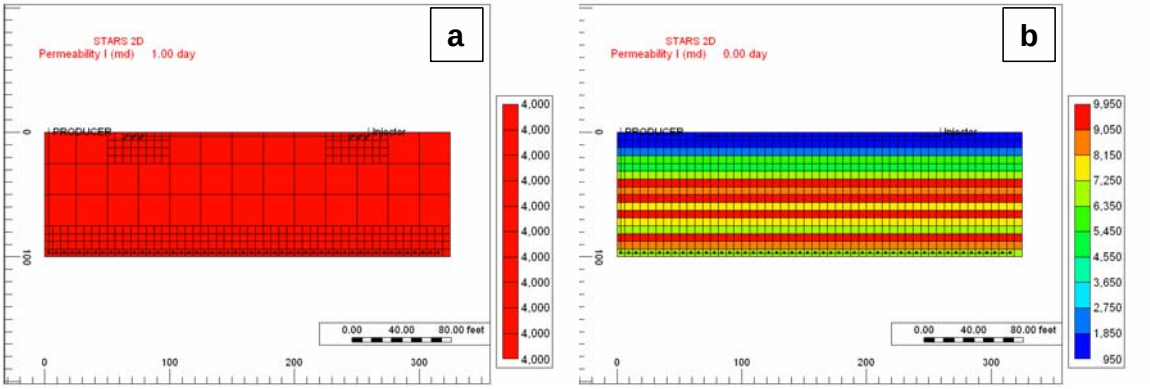

Figure 6.47: *Multiple permeability layers in combustion process: (a) homogeneous single permeability layer, and (b) distribution of multiple permeability layers*

Figure 6.48 shows the temperature maps of both models at 350days and 1025days. The fire front development and propagation in both cases were different in terms of that the front in the homogeneous model tends to move laterally more than vertically. On the other hand, the combustion front in the multiple permeability layers propagated vertically faster compared to its movement in the lateral direction (Figure 6.48b). This was mainly because of the lower permeability value of the model's top layers in the this scenario compared to the layers beneath them, which enhanced the fire front vertical propagation compared to its move in the lateral direction in the low permeability layers. The variation of the layers permeability did affect the in-situ combustion process performance, even though both scenarios (homogeneous and heterogeneous) have the same average permeability (4000mD). This was confirmed from the way the fire front started and propagated in both cases. Also, the comparison between the two cases results in Figure 6.49 shows the difference between the two scenarios. The multiple permeability layers model produced more net coke in place (Figure 6.49a) as a result of the variation in the front velocity due to the permeability variation from layer to layer. This led to slightly higher average temperature (Figure 6.49b) and less cumulative oil produced (Figure 6.49c). This sensitivity calculation showed that the variation in the

model layers permeability was the reason behind the change in the in-situ combustion performance rather than the change in the model's average permeability.

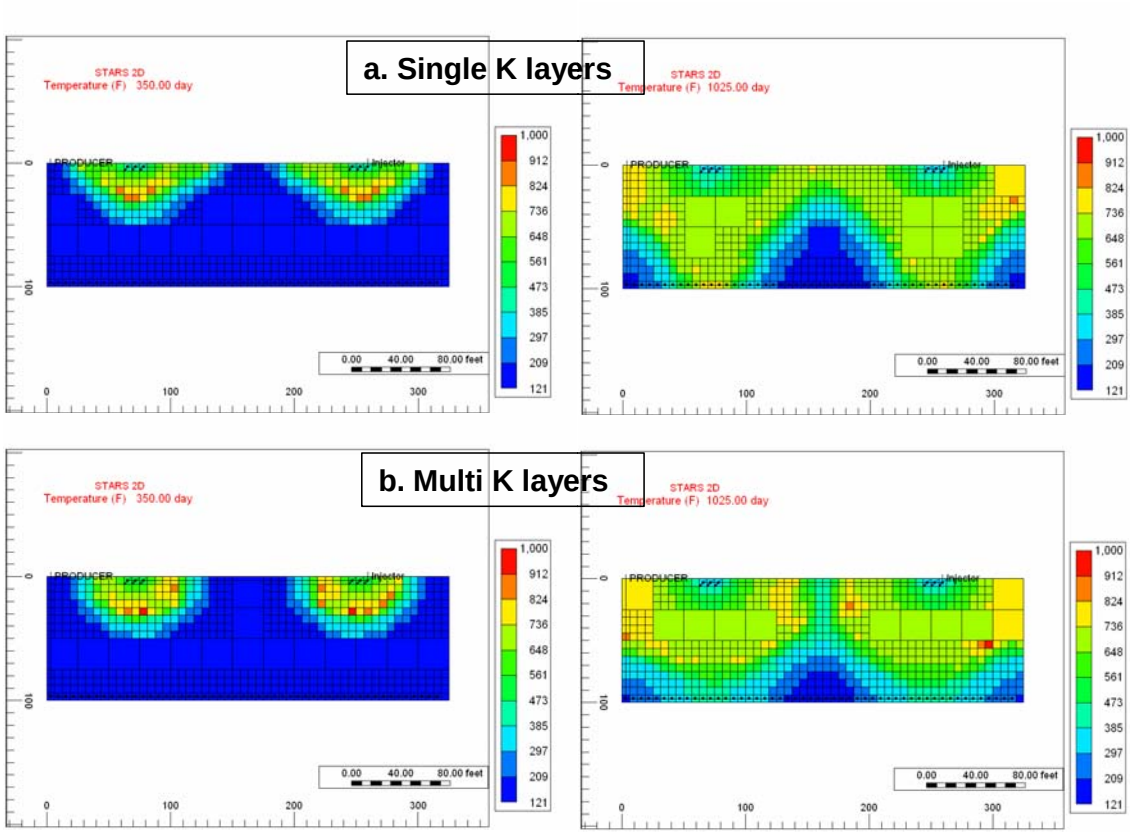

Figure 6.48: *Simulation results of temperature at 350 days and 1025 days: (a) homogeneous single permeability layers, and (b) multiple permeability layers*

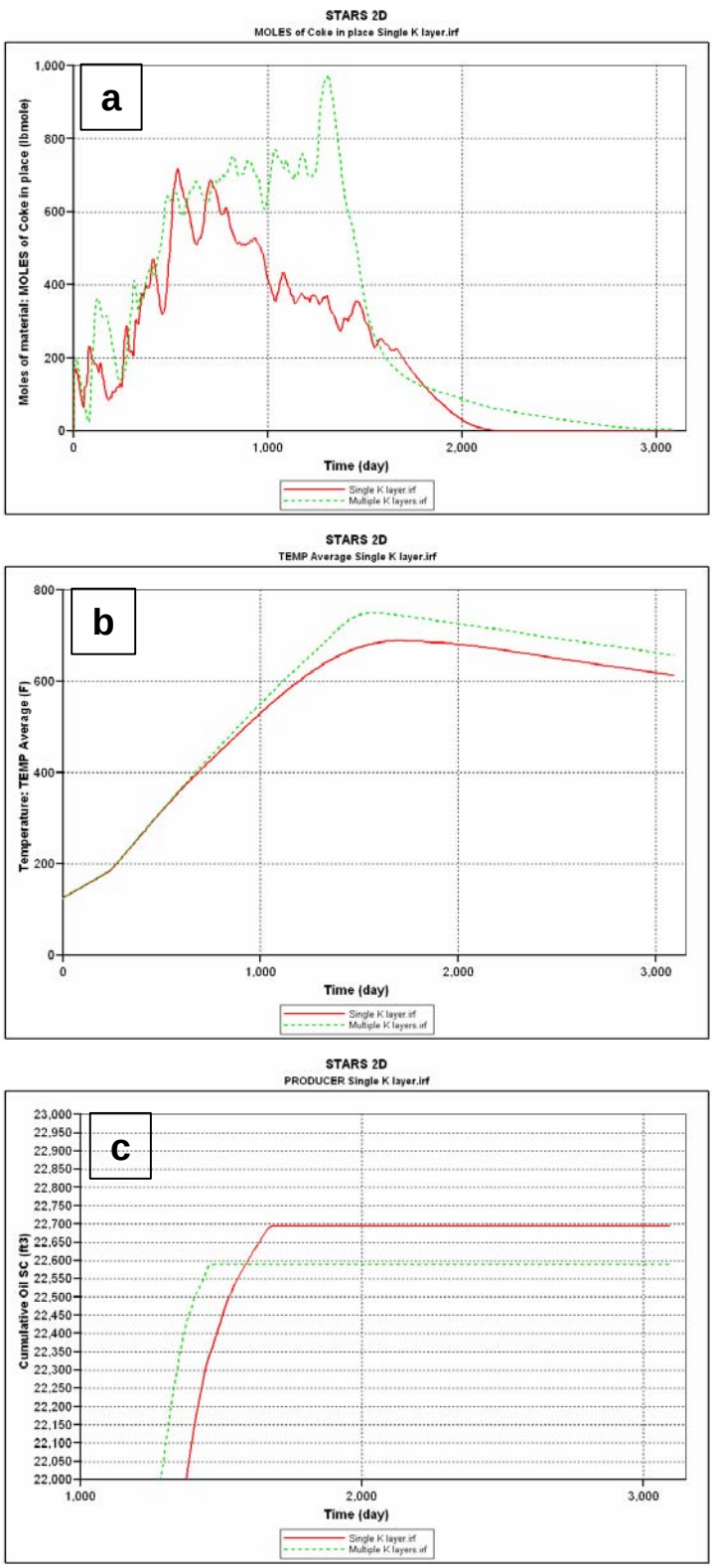

Figure 6.49: *Simulation results of effect of multiple permeability layers on combustion process: (a) net coke in place, (b) average temperature, and (c) cumulative oil produced*

In section 6.4, a detailed investigation of the impact of multiple permeability layers was presented. A single realisation of this heterogeneity was used. In this section five more realisations (Figure 6.50) were created in order to study the variation in the in-situ combustion process performance when such heterogeneity was presented. The permeability range for the five realisations was between 950mD and 9950mD with uniform distribution in each layer. A total of 16 uncorrelated permeability layers were used in each model and their locations in the model were manually changed from case to case (Figure 6.50) to produce the five realisations in this sensitivity. Also, the horizontal well configuration without the aquifer existence was used in this sensitivity. A horizontal well scenario was chosen because of the overall in-situ combustion performance using this configuration as the results from chapter 4 showed. The presence of the aquifer was not considered in this sensitivity since the main aim of this section was to investigate the impact of using multiple realisations in the combustion process, and by excluding the aquifer the modelling process complexity was reduced.

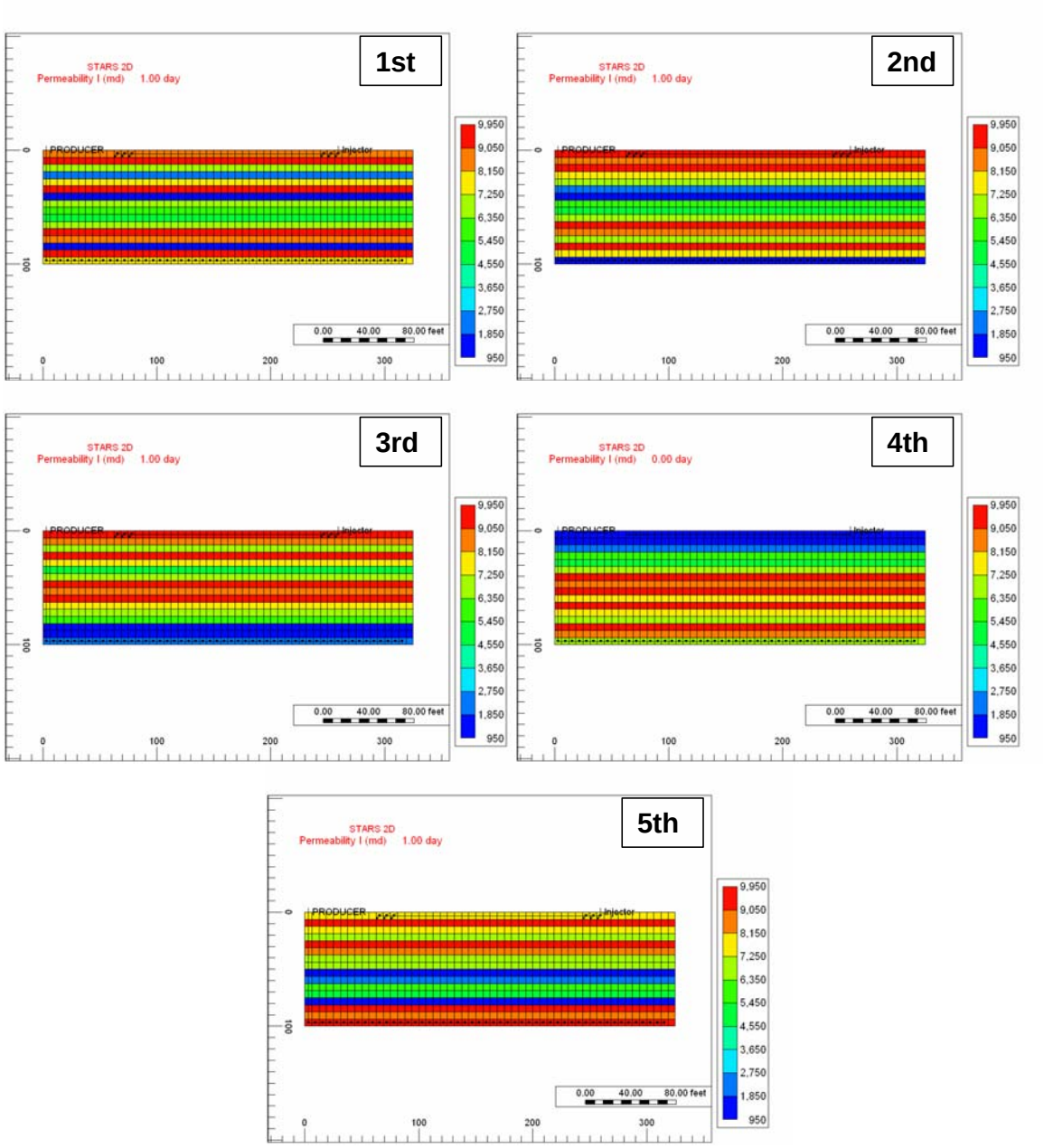

Figure 6.50: *Multiple permeability layers realisations*

The comparison of the temperature maps for the fire front initiation and propagation at 350 days (Figure 6.51) and 1025 days (Figure 6.52) showed variation in the fire front behaviour and the variation from case to case depends on the permeability differences in each realisation. However, the overall cumulative oil produced by these five realisations (Figure 6.53) was slightly different. To compare the variation between all the cases, the mean and the standard deviation of the cumulative oil for all the five scenarios was plotted together (Figure 6.54). From the comparison in Figure 6.54, the standard deviation was a small value, which suggested that a small variation in the in-situ

combustion process performance occurred when multiple realisations of permeability layers were used. This mainly due to the fact all the five realisations used in this section had the same number of layers and the fire front needed to propagate through these layers at different times depending on the layers order on each realisation. This sensitivity showed that a small amount of variation was expected in the combustion process when multiple permeability layers realisations were used.

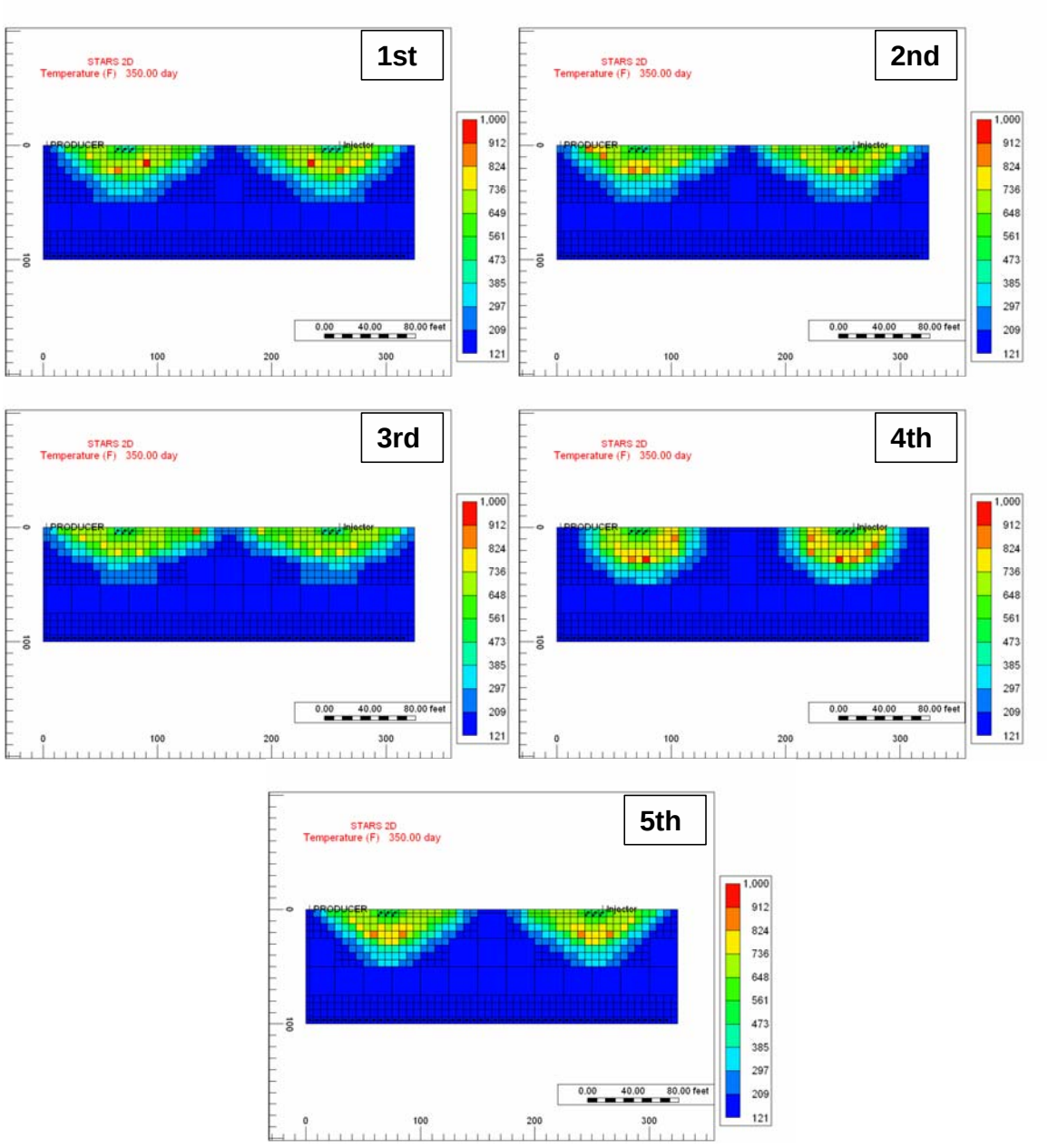

Figure 6.51: *Simulation results of temperature at 350 days for the five multiple permeability layers realisations*

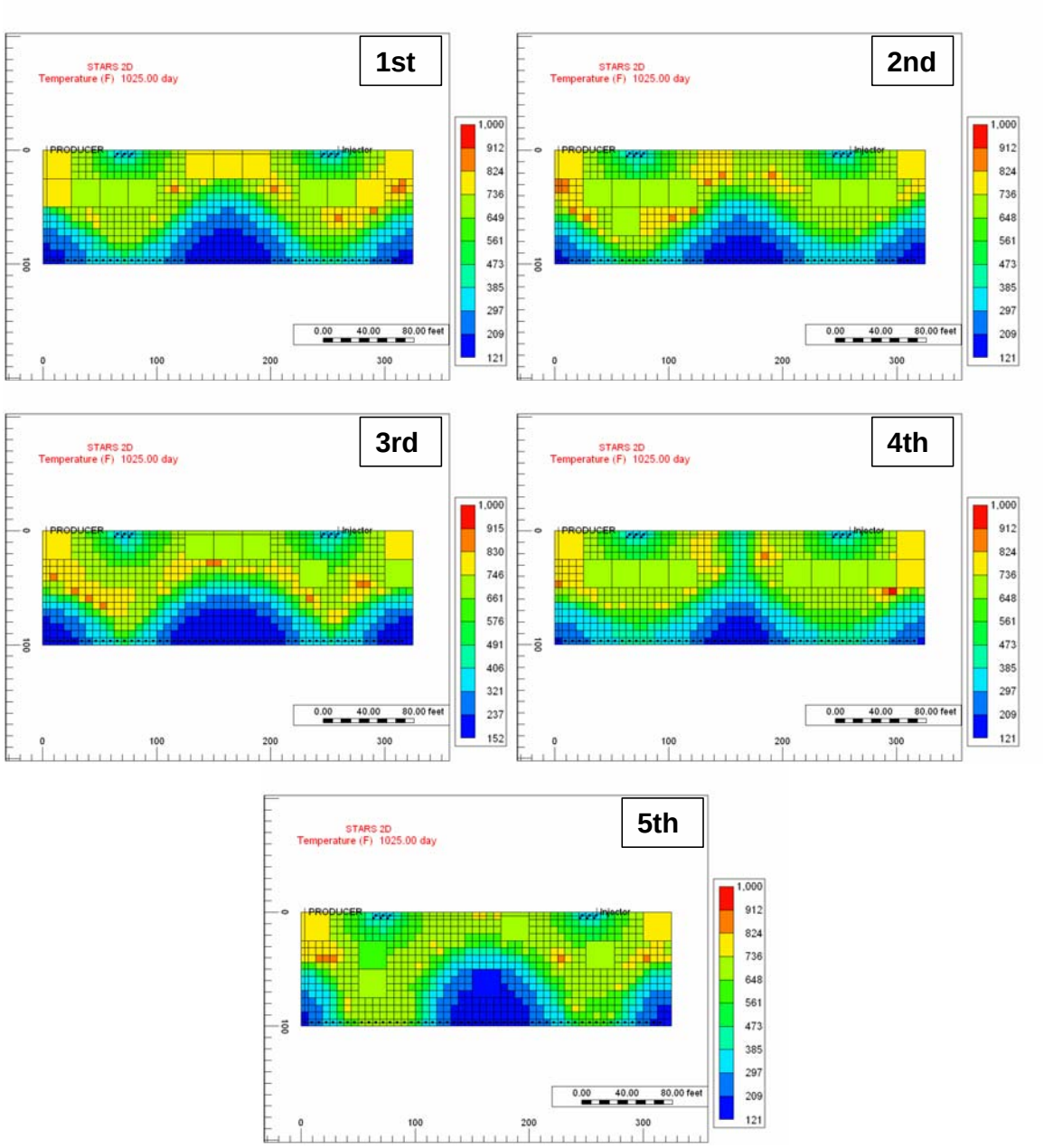

Figure 6.52: *Simulation results of temperature at 350 days for the five multiple permeability layers realisations*

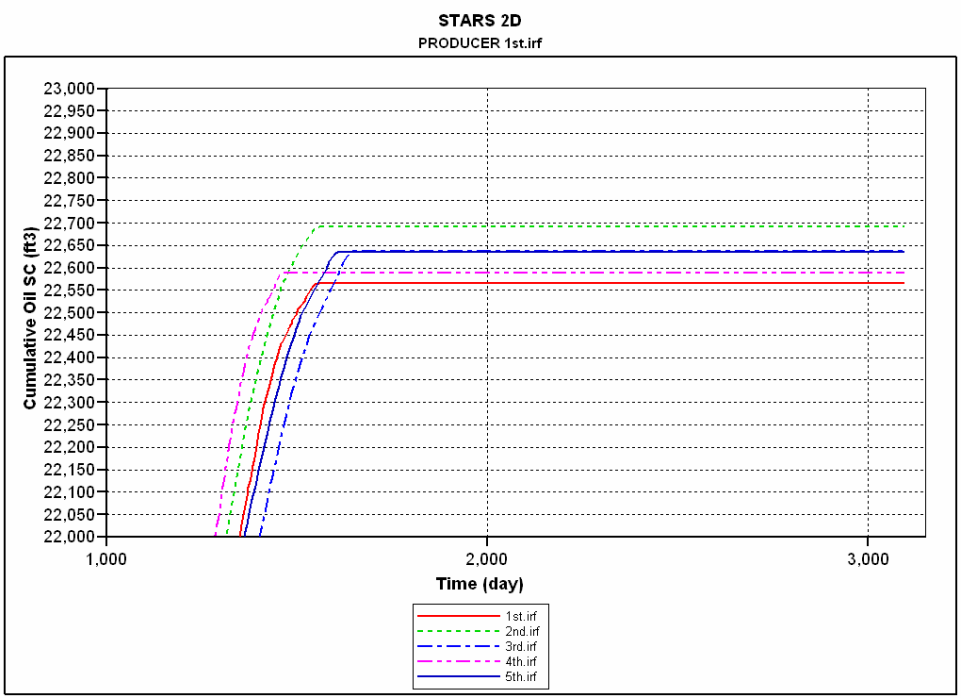

Figure 6.53: *Simulation results of the cumulative oil produced by the multiple permeability layers realisations.*

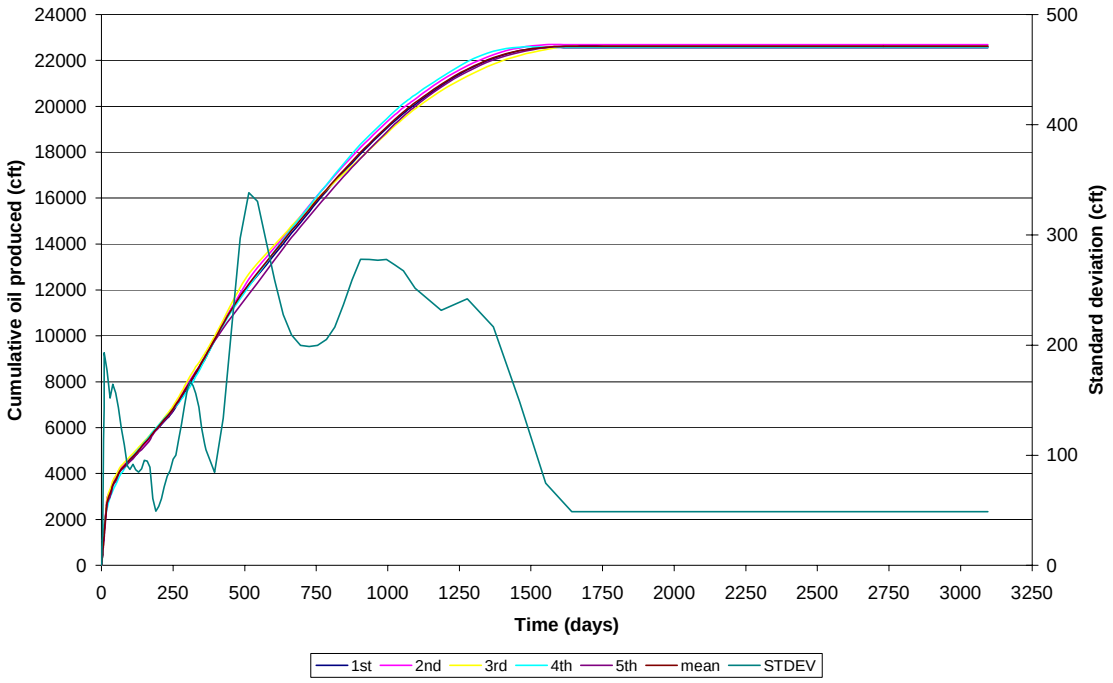

Figure 6.54: *The cumulative oil produced by the multiple permeability layers realisations with the mean and standard deviation.*

6.7.2 Multiple realisations for discontinuous impermeable shale layers

Section 6.5, presented a detailed investigation of the impact of discontinuous impermeable shale layers on in-situ combustion process. One realisation of the shale locations was developed. In this section four more realisations were developed in order to study the variation in the in-situ combustion process performance when such heterogeneity was presented. For sake of consistency, five discontinuous impermeable shale layers were used in each of the realisations and they were placed manually in the area between the horizontal injector and horizontal producer to identify the impact of their presence in the fire front performance. Each shale layer was 81.25 ft in length and had 100% shale content. Figure 6.55 shows the five used realisations in this subsection.

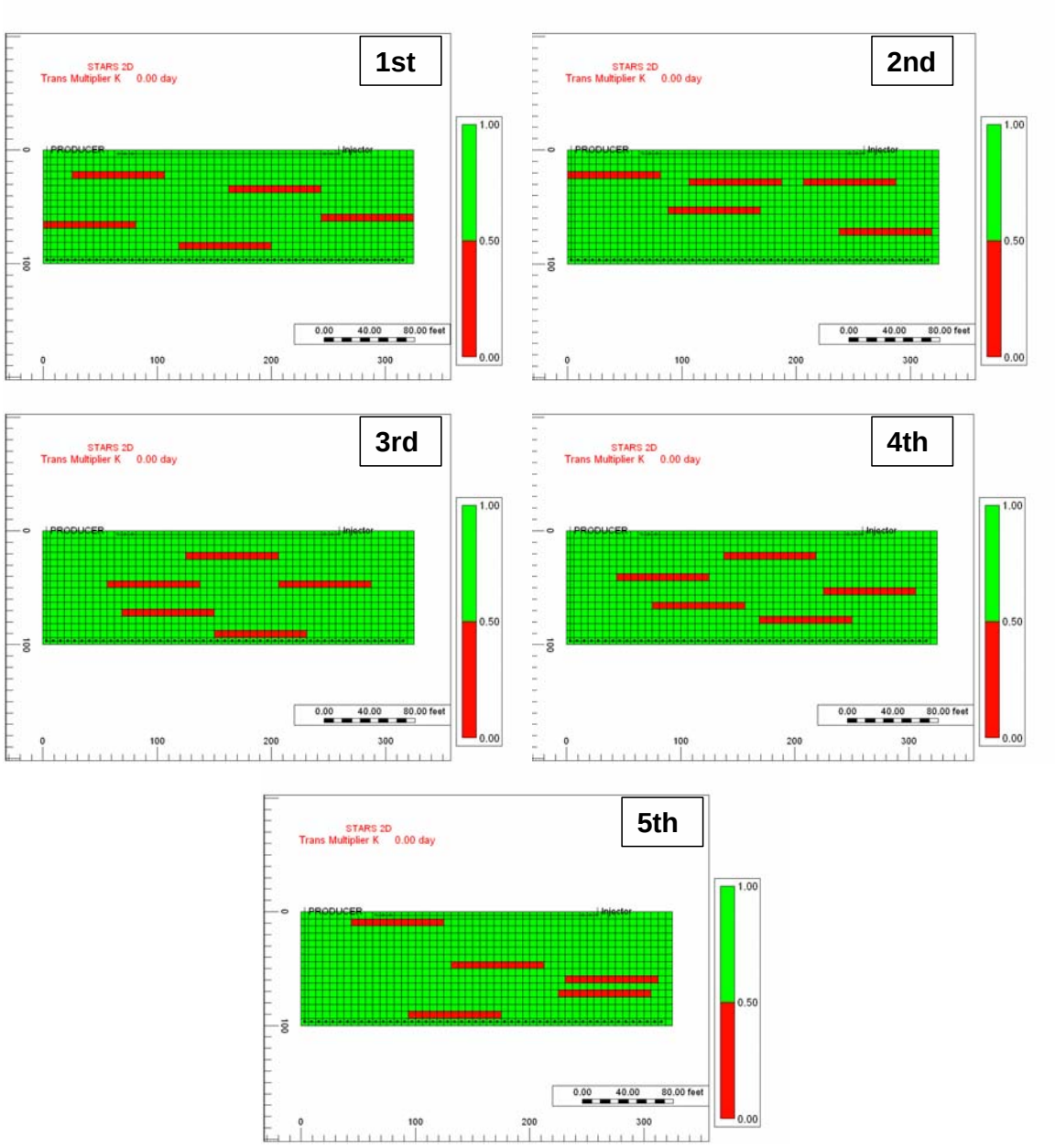

Figure 6.55: *Discontinuous shale layers realisations*

In the horizontal well configuration, the fire front propagation direction in the model was in the vertical direction from the injector in the model top to the producer in the bottom layer. This well orientation resulted in maximising the impact of the discontinuous shale layers in the in-situ combustion process. Using the five developed realisations in this sensitivity resulted in variation in the fire front behaviour depending in the location of the shale layer as the temperature maps in both Figure 6.56 and Figure 6.57 show at 350 days and 1095 days, respectively. The overall observation from all the five scenarios was that the fire front ignited near the injector perforations and then

moved toward the producer. When the front was obstructed by the shale layer, it started to move around the shale layer until it arrived to the producer. This resulted in that the combustion front needed to change its direction and velocity every time it faced a shale layer. This led to variation in the scenarios results as Figure 6.58 shows. In order to quantify the variation in the in-situ combustion process performance, when multiple shale layers realisations were used, the mean and standard deviation of the cumulative oil produced were calculated and plotted together. Figure 6.59 shows a small difference in the recovery factor between the various used cases and the standard deviation presented the amount of change to expect in the process recovery factor when the discontinuous impermeable shale layers location changed.

In summary, the sensitivity calculations conducted in this section (6.7) presented the impact of using multiple realisations for both the multiple permeability layers and the discontinuous impermeable shale layers cases. The main results suggested that various realisations did cause variation in the in-situ combustion performance. However, the amount of change for those both types of heterogeneity was small.

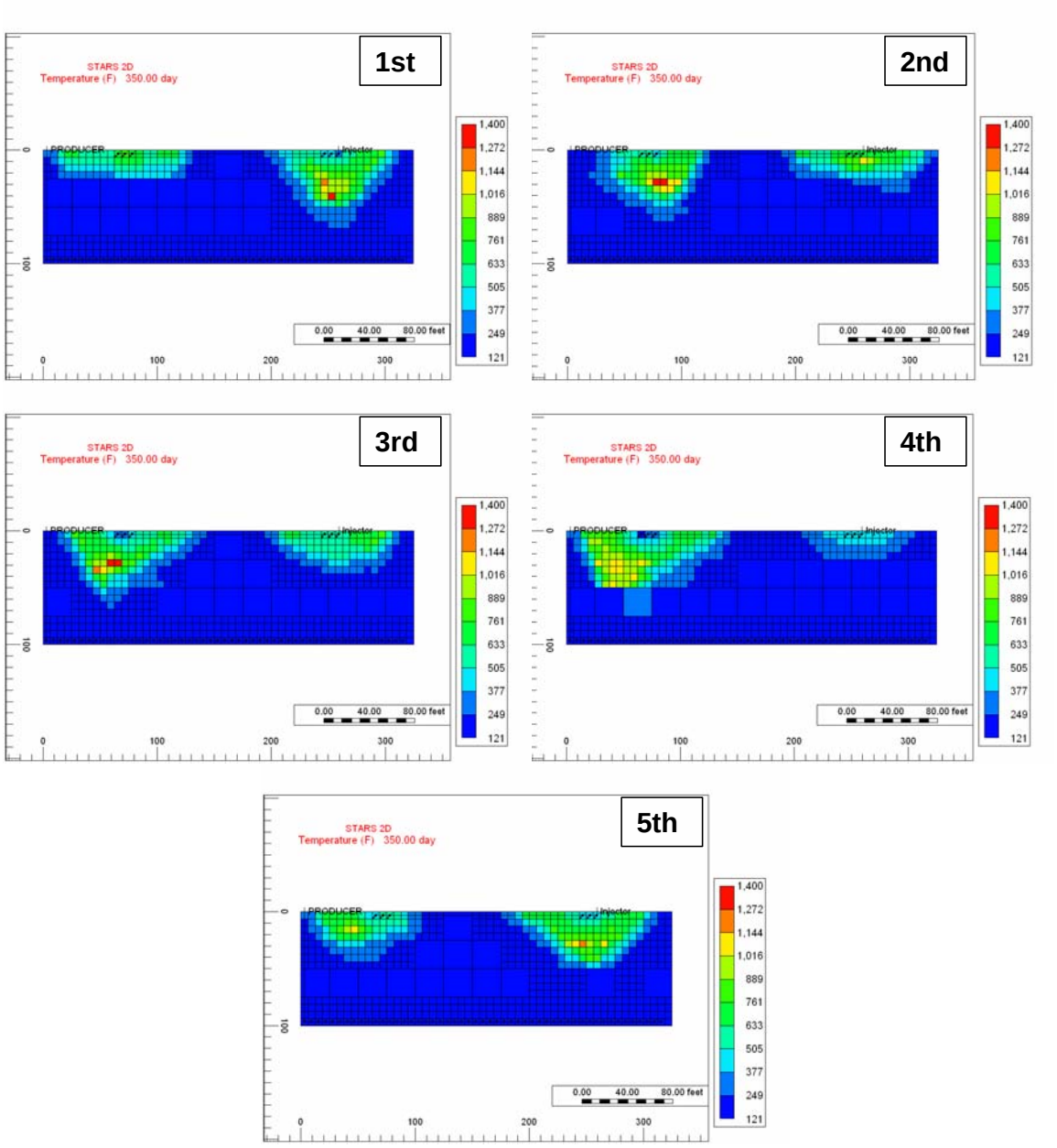

Figure 6.56: *Simulation results of temperature at 350 days for the five discontinuous shale layers realisations*

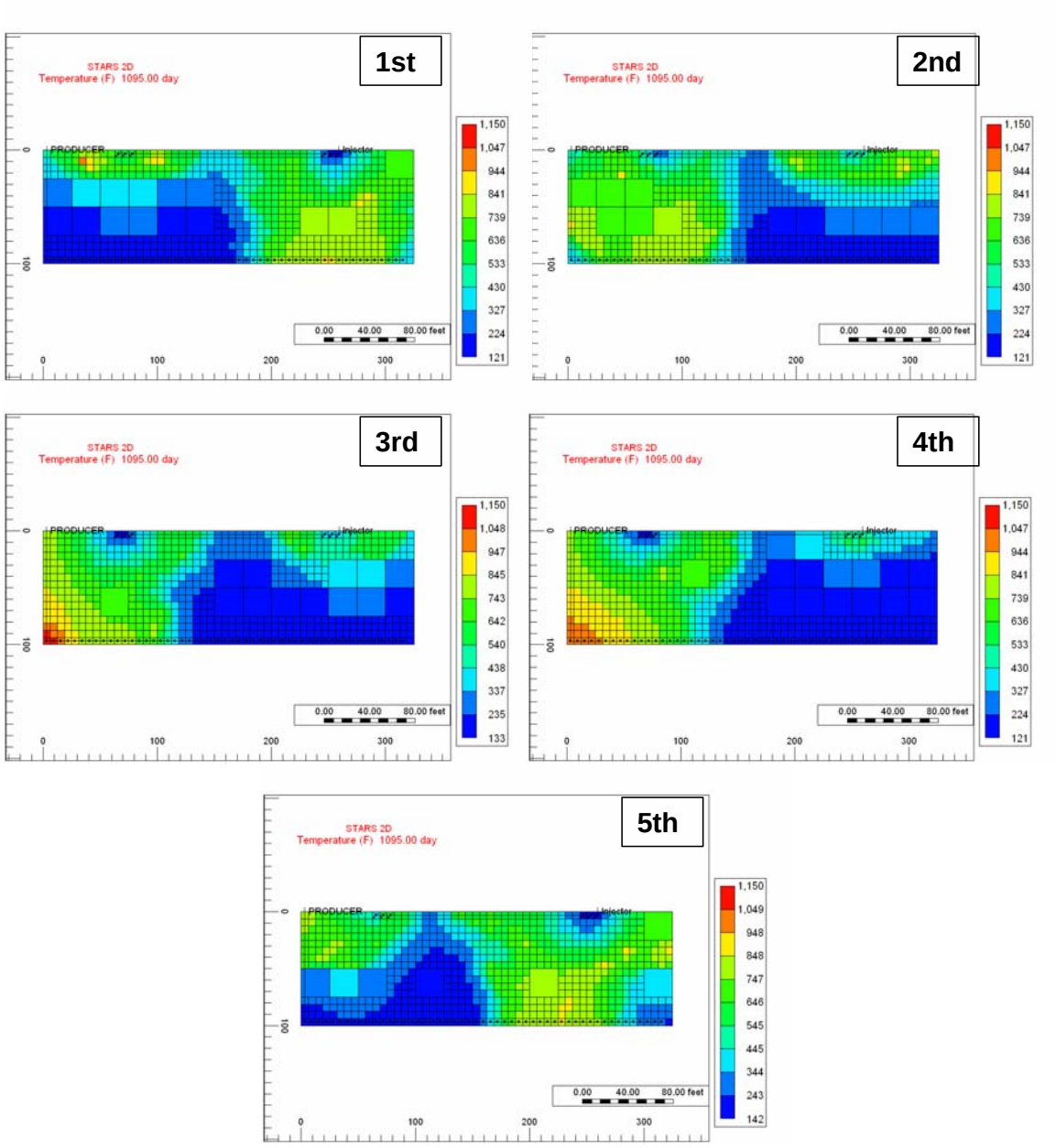

Figure 6.57: *Simulation results of temperature at 1095 days for the five discontinuous shale layers realisations*

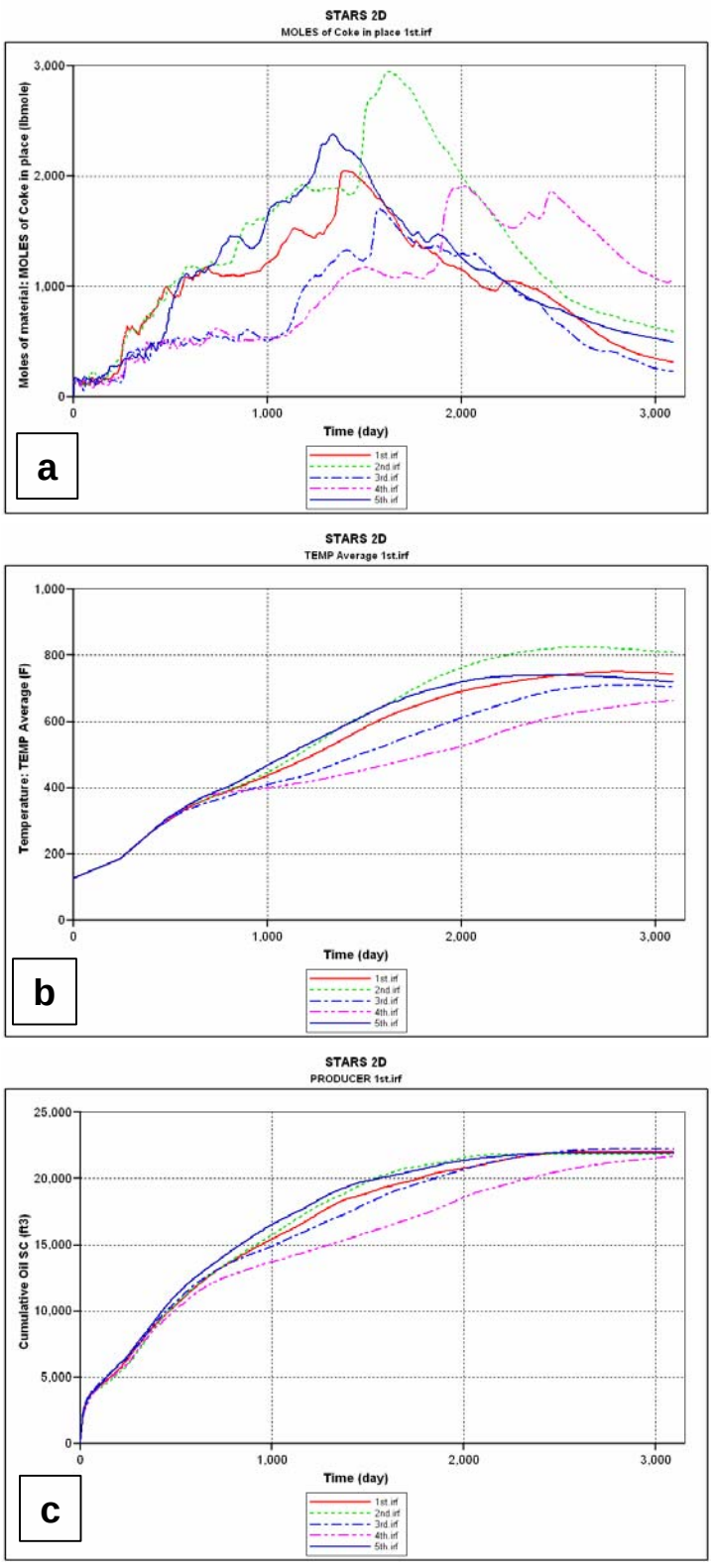

Figure 6.58: *Simulation results of the five discontinuous shale layers realisations: (a) net coke in place, (b) average temperature, and (c) cumulative oil produced.*

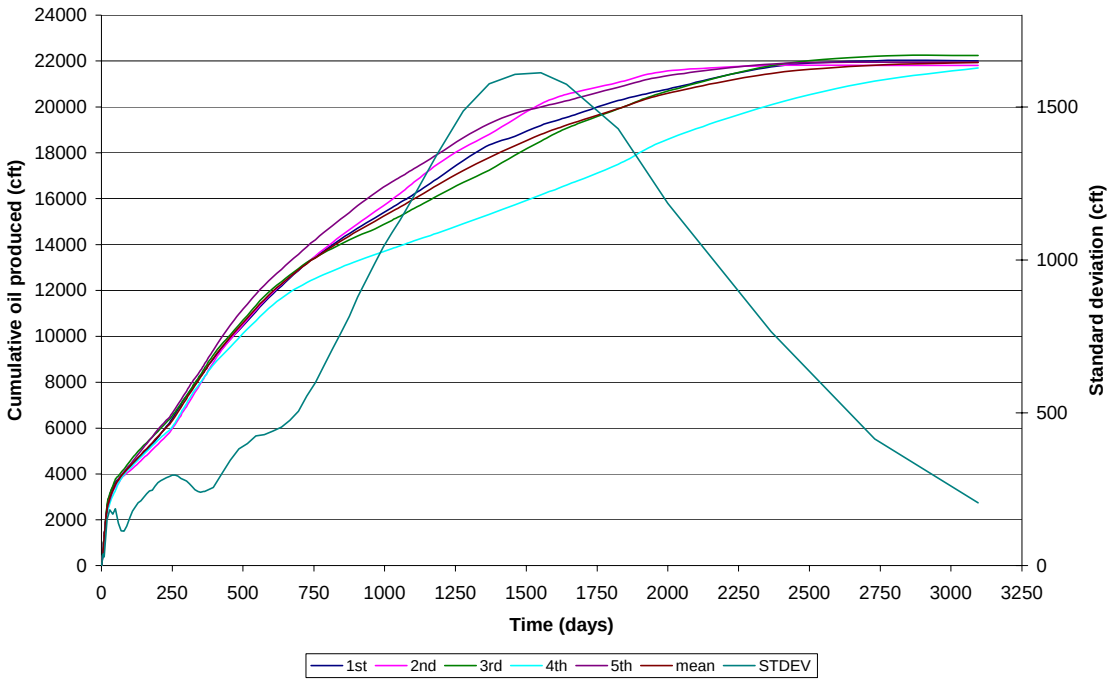

Figure 6.59: *The cumulative oil produced by the discontinuous shale layers realisations with the mean and standard deviation.*

6.8 Summary

The sensitivities in this chapter showed variations in in-situ combustion response to the various kinds of heterogeneities introduced to the simulation model. The way the combustion process performance was affected depends on the type of well configuration used. Also, the presence of a strong bottom aquifer had an impact on the fire front behaviour and the overall combustion process performance. In this section, the effect of each heterogeneity introduced was summarised for each of the four comparative models used in this chapter.

6.8.1 Horizontal well configuration without aquifer support

The behaviour of the combustion front in this specific well configuration was studied as a function of the variation of the four types of heterogeneity used in the study (Kv/Kh ratio, multiple permeability layers, discontinuous shale layers and shaley sand layer).

The main outcome from all the different heterogeneities in this scenario was that the recovery factor achieved by the combustion process decreases depending on the type of heterogeneity involve as Figure 6.60 shows. The introduction of discontinuous impermeable shale layers resulted in the biggest reduction in the recovery factor (by 2.8%) compared to the base case model. This was because of the way that both horizontal wells were located and completed, which resulted in the main fire front movement being in the vertical direction, and maximised the impact of having the discontinuous shale layers. As a result, the fire front velocity was decreased and more coke was produced. Furthermore, the shaley sand layer scenario reduced the recovery factor only by 0.4%, since the only affect of this heterogeneity was the slight increase of coke produced in place when the fire front was obstructed by the low permeability layer.

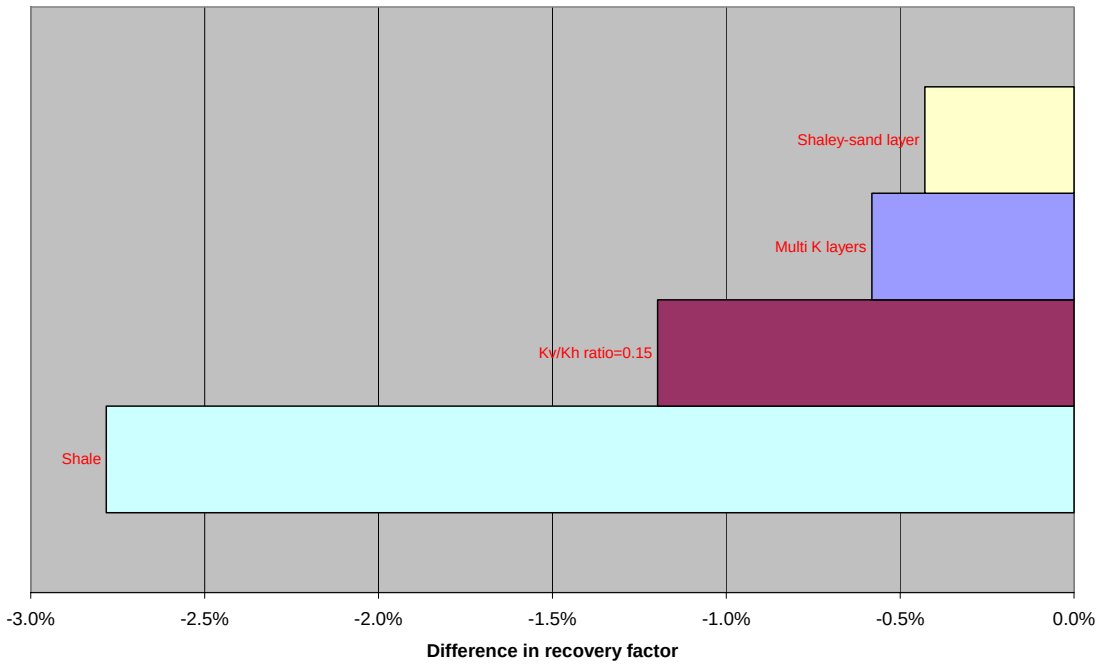

Figure 6.60: *Effect of heterogeneity on the combustion process recovery factor of the horizontal well configuration without aquifer support*

6.8.2 Vertical well configuration without aquifer support

The impact of heterogeneity on recovery factor when vertical wells were used depends on the type of heterogeneity, as Figure 6.61 shows. Whereas the presence of

heterogeneity in the horizontal well configuration always led to a reduction in the performance of the combustion front, this was not the case in the vertical well scenario. Both the Kv/Kh ratio (0.15) and shaley sand layer models showed an *improvement* in the process efficiency, and an increase in recovery factor values (6% and 2.5% respectively) were achieved compared to the base case model. This was because these two types of reservoir heterogeneity delayed oxygen breakthrough and improved the front sweep efficiency by producing a piston-like displacement, which resulted in more oil being produced. The permeability layers scenario reduced the recovery factor by 6.3% as a result of the main front propagation direction in this well configuration being the lateral movement along the layers. The front was moving due top the effect of gas override, which meant the front was propagating in the top layers of the model which have lower permeability values. This resulted in slower frontal movement and greater amounts of oil being converted to coke. The discontinuous impermeable shale layers mean that the process performance was reduced since the way the shale layers were oriented allows for easy lateral frontal propagation along those layers.

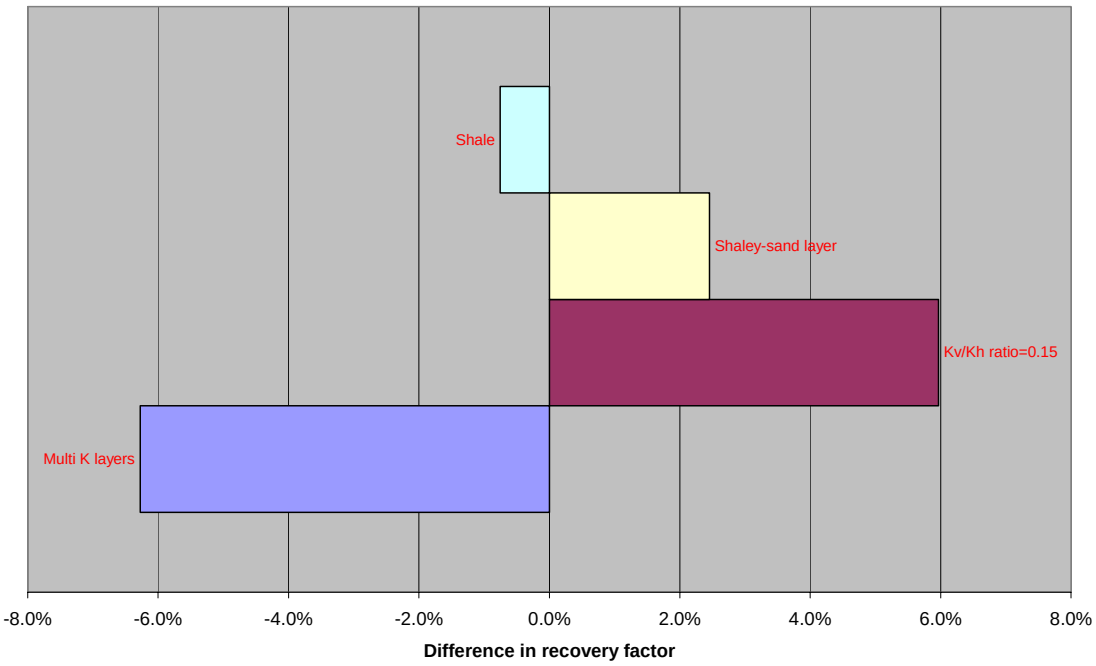

Figure 6.61: *Effect of heterogeneity on the combustion process recovery factor of the vertical well configuration without aquifer support*

6.8.3 Horizontal well configuration with aquifer support

The inclusion of a new driving force in the horizontal well configuration led to some variations in the performance of the in-situ combustion process. The overall recovery factors achieved in this model were decreased as a result of the various heterogeneity scenarios (Figure 6.62). For example, the reduction of the Kv/Kh ratio from 1 in the base case to 0.15 led to a significant decrease in the recovery factor by 6.5%. This was because of the orientation of the horizontal wells, which made the fire front moved vertically towards the horizontal producer. As a result, there was slow combustion front movement since the vertical permeability was decreased and more coke was produced. Also, the slow front movement led to a higher amount of oil being left in place by the end of the combustion process. Moreover, the other remaining types of heterogeneity in this well configuration slowed the fire front velocity and reduced the sweep efficiency. As a result, less oil was produced compared to the homogeneous base case model. The total amount of water produced was decreased, due to the reservoir heterogeneity, except for the shale layers and the shaley sand layer scenarios. This was because of the way they were introduced into the model, and also because of the low water viscosity which enabled easy water flow around the shale obstructions.

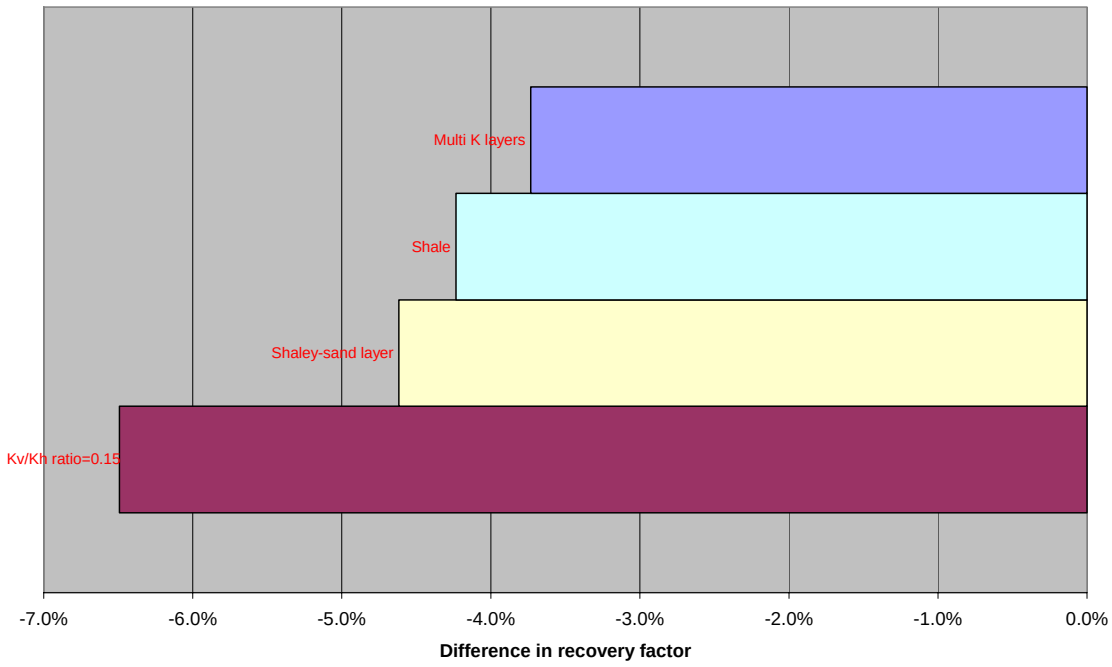

Figure 6.62: *Effect of heterogeneity on the combustion process recovery factor of the horizontal well configuration with aquifer support*

6.8.4 Vertical well configuration with aquifer support

The fire front process performance was improved when specific types of heterogeneity were involved in the vertical well configuration. For the successful model runs (Kv/Kh ratio, and multiple permeability layers), the fire front was sustained for a longer time compared to the homogenous base case scenario. As a result, a better sweep efficiency was achieved by the combustion front and more oil was produced in each of these three heterogeneity scenarios (Figure 6.63). The reduction of the Kv/Kh ratio (0.15) led to a 17.6% increase in the recovery factor compared to the base case model. This was mainly as a result of the low vertical permeability that reduced the gas override effect and improves the fire front shape, which led to better sweep efficiency and longer sustainability of the front. In this scenario more oil was produced even though a greater amount of coke has been produced. Moreover, both the discontinuous impermeable shale calculations layers and the shaley sand layer models led to termination of the combustion process earlier than anticipated. The main reason for this was that this kind of heterogeneity added to the combustion process complexity in terms of slower front propagation and formation of a large mass of coke in place which deposited ahead of the front. As a result, the model pore volume was reduced and the area ahead of the front was blocked, and this prevented further propagation of the front. The reductions in recovery factor shown in Figure 6.63 for both heterogeneity scenarios were up to the termination point and could not be considered as a representative of the recovery factor of the in-situ combustion process with this type of heterogeneity.

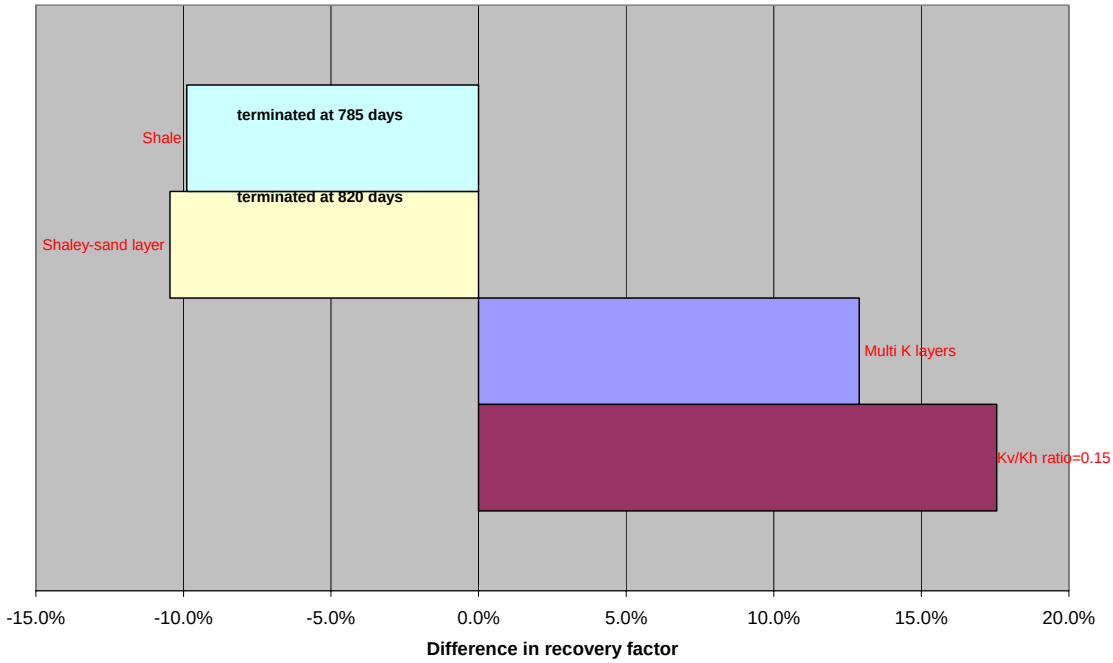

Figure 6.63: *Effect of heterogeneity in the combustion process recovery factor of the vertical well configuration with aquifer support*

In summary, this section showed that the performance of the in-situ combustion process in the horizontal well configuration with/without aquifer support was decreased in terms of achieving a lower recovery factor when heterogeneity was introduced. This was true in this study regardless of the type of heterogeneity involved in the horizontal well scenario. On the other hand, in the vertical well configuration, the recovery factor was increased by using a combustion process without aquifer support where the Kv/Kh ratio was reduced, and when shaley sand layer exist in the model. For multiple permeability layers and the discontinuous impermeable shale layer heterogeneities, the recovery factor of the combustion process decreases. The performance of the in-situ combustion process in the vertical well configuration with aquifer support showed an increase on the recovery factor when Kv/Kh and multiple permeability layers were used. On the other hand, the combustion process calculation was terminated prematurely when the shale layers and shaley sand layer heterogeneities were introduced to the model in this well configuration.

Chapter 7

Conclusions and Recommendations

7.1 Overall summary

This chapter presented a summary of the modelling work undertaken for this thesis and described in Chapters 3 to 6, which involved investigation into application of in-situ combustion process into heavy oil reservoirs. The development of the model used some available field data; however the results of the study are generic and can be applied to other heavy oil fields, especially with the presence of strong bottom aquifer. The identification and optimisation of the combustion processes had been described and the investigation of optimal well types, configurations, spacing and locations were carried out with and without aquifer support. Further process evaluations were conducted to determine the impact of reservoir heterogeneities on the combustion process. Finally, recommendations for future research are presented here.

7.2 Parameters to consider when implementing in-situ combustion process

Several parameters needed to be consider in the planning phase of applying in-situ combustion process. As a start, the reservoir rock and fluid properties needed to be obtained and then used in the experimental work in order to determine the main combustion process parameters. For example, information on in-situ combustion process design parameters such as the fuel availability, air requirements, peak combustion temperature, oxygen utilization efficiency, recovery factor, etc. obtained from combustion tube test (CTT). All of the outcomes from the experimental work helped to acquire the kinetic model, which is consider as the main core of the combustion process. After that, the uncertainty in the process parameters (such as

aquifer specifications, reservoir heterogeneity, etc.) needed to be highlighted and counted in the design phase. This will help to minimise their impact in the process at later stages. Furthermore, the means of igniting the fire front should be evaluated, since this is a key phase of the combustion process. This is important since it has a significant bearing on the ultimate success of the entire in-situ combustion process. Poor ignition may lead the process failure at early stages since the fire front was not ignited properly. In this study, electrical heating was considered since it considered as a reliable, safe and precise temperature control. However, there are many ignition techniques which can be used to start a combustion process. For example, gas burner, chemical ignition and high pressure steam. Moreover, well configurations, spacing, types, etc. were a very important parameter to consider in the planning of applying in-situ combustion process. In the case of well spacing, if well spacing is very close, the combustion front will break through very early, while if the well spacing is too large, the fire front will take longer time to sweep the area between the wells and results in delay in oil production and the project life will be longer, which makes the project economically unattractive.

7.3 Conclusions

This section provides the conclusions that were summarised at the end of each chapter. It is worth mentioning that while some of the data used in this study is field specific, the general simulation results are generic and can be applied to other heavy oil formations.

The work conducted in Chapter 3 led to the development of the simulation model, which was used as the main foundation of the study calculations. A number of conclusions could be gleaned from Chapter 3:

- The performance of the combustion process was strongly dependent on the kinetics model used. In this work the Belgrave kinetics model was used due to its detailed definition of the combustion process chemical reactions.
- Successful initiation of in-situ combustion in the model was achieved by optimising the air injection rate and optimisation of both the ignition heat rate and period.

- Numerical dispersion errors were considered to be the main challenge for modelling in-situ combustion. In order to reduce their effect in this work, a smaller 2D cross sectional model was used with the implementation of the dynamic gridding option. This minimised the dispersion error and more accurately mimicked the fire front propagation throughout the model.

Application of diverse well configurations and types did result in variations in the in-situ combustion process performance as the calculations in Chapter 4 showed, and as the following conclusions state:

- A change of well types, completion, number, spacing and locations may result in a very significant variation in the performance of in situ combustion due to the sensitive nature of the process.
- The use of horizontal producer wells resulted in the introduction of a Mobile Oil Zone (MOZ) to the combustion process, which accelerated oil production and allowed for instantaneous production of the upgraded oil fraction as a result of the heating at the combustion front.
- Occurrence of early oxygen breakthrough usually resulted in poor fire front sweep efficiency. To avoid this, the well placement plan was critical for a successful combustion process. In these sensitivity calculations, shorter well spacing between the injector and the producer led to early oxygen breakthrough.
- Increasing the number of vertical injectors in the combustion process led to acceleration of oil production and a reduction in the required recovery time for the process. However, the overall process recovery factor achieved was the same when compared to the case where a single vertical injector was used.
- The use of a horizontal well as an injector had the advantage of establishing a wider fire front compared to the normal vertical injector case when they were completed only in the upper layers. In the case where a partially completed horizontal injector was used, a greater mass of oil was produced, which was as a result of the several fire fronts which developed, one for each completed interval. Also, the viability of the combustion process was improved when a partially completed horizontal injector is used in deep reservoirs instead of drilling several vertical injectors to initiate fire fronts.

- Implementation of multi-lateral horizontal producers in the combustion front process led to poor performance, which was as a result of the air being circulated as soon the front broke through to one of the producer laterals. This limited how far the front propagated and hence the recovery of oil was poor due to unswept areas of the model. Also, the application of intelligent well completions for the horizontal producer led to a reduction in the recovery time needed by the combustion process. The closure of the producer perforations when oxygen broke through into the well led to a redirection of the front, enabling it to reach the unswept zones of the model and reduced overall recovery time.

While having aquifer support in light oil reservoirs is considered to be a favourable drive mechanism, this is not the case in heavy oil reservoirs. The sensitivity analysis conducted in Chapter 5 using the developed model with the presence of aquifer support resulted in the following conclusions:

- The presence of a strong bottom water aquifer was considered as a challenge for the application of in-situ combustion, since the water influx from the aquifer could quench the fire front as soon as it was ignited. In order to avoid that occurring, the fire front was initiated as far as possible away from the water zone, which allowed for longer process sustainability.
- The comparison between the use of vertical and horizontal producer wells in the presence of aquifer support showed the potential effect of using different well scenarios in the combustion process. More oil was produced when a horizontal producer was used, but with a large increase in the cumulative water production as well. Also, both the distance between the injector and producer wells and their location in the model were considered as important factors in the successful planning for combustion. The placement of the injector in the top of the model and the producer in the middle of the model (top-down) in the aquifer support combustion scenario did result in longer combustion front sustainability, which was reflected by a larger volume of oil being recovered. However, by using this well configuration, the horizontal producer was working as a barrier to prevent water influx from approaching and quenching the fire front. This led to a dramatic increase in the water production by the end of the process.

- The optimisation sensitivities for the top-down well configuration showed that as the well spacing between the injector and producer increased, the total oil produced by the front increased. At the same time, more water was able to break through to the producer, which increased water production. This meant that the project feasibility plan for in-situ combustion should decide the optimum horizontal producer placement depending in the balance between the potential recovery factor expected and the investment needed to handle and treat the produced water.
- The use of a partially completed horizontal injector well in top-down in-situ combustion with aquifer support provided an improvement on the process sweep efficiency because of the initiation of multiple fire fronts in this scenario. However, the fully completed horizontal injector did provide better combustion performance in terms of a higher recovery factor, which is mainly due to the piston like displacement shape of the front. Also, the use of a partially completed horizontal producer showed poor recovery compared to the fully completed horizontal producer system. This was because of the early extinguishing of the front as a result of water flow between the producer perforation intervals and also as a result of the high amount of oil that was trapped and bypassed due to the water influx in the model.
- For the aquifer support scenario, the closure of the perforations in the horizontal producer when an intelligent well system was used led to a 36% reduction in the total amount of water produced. This enhanced the viability of the combustion process, because of the lower handling cost required to treat water production. At the same time, the closure of the perforations led to a redirection of the fire front away from those closed perforations. This was achieved by enhancing the air supplies so the front can propagate to a wider area of the model. However, the total oil produced by the intelligent well completion was slightly less than that from the normally completed horizontal producer. This was as a result of the early quenching of the fire front due to the fast water influx from the aquifer zone.
- Attempts were made to delay the in-situ combustion by using a top-down well configuration. The results of this sensitivity showed similarity in the fire front

behaviour, with only some short delayed in production depending on the time when the process was applied.

Reservoir heterogeneity is one of the common characteristics of the majority of hydrocarbon bearing formations. Introduction of various types of heterogeneity to the simulation model did show the heterogeneity impact on the performance of in-situ combustion process. Here are the conclusions determined from the work in Chapter 6:

- The existence of reservoir heterogeneity had a major effect on the combustion process. The process performance changed between the horizontal and vertical well scenarios, and also in the presence of an active aquifer. The sweep efficiency varied from case to case, depending on the type of heterogeneity.
- The performance of the combustion process for the horizontal well configurations both with and without aquifer support was reduced in terms of a lower volume of oil being produced as a consequence of heterogeneity being introduced to the model.
- The vertical well configuration showed varying behaviour depending in the type of heterogeneity introduced to the system. For example, the presence of multiple permeability layering or of discontinuous shale layers decreased the recovery factor. However, the reduction in the Kv/Kh ratio or the introduction of shaley sand layers enhanced the fire front sweep efficiency. In the presence of aquifer support, the front behaviour again varied, depending in the type of heterogeneity. The reduction in Kv/Kh ratio and the multiple permeability layers all resulted in an improvement in the process recovery factor by the end of each simulation. On the other hand, both the discontinuous shale layers and the shaley sand layer resulted in early termination of the model runs due to failure to propagate the fire front.
- From the overall observations of all the sensitivities conducted in this study, the velocity with which the fire front propagated was clearly a critical parameter. A change in this velocity usually resulted in a change in the amount of coke being produced in-situ by the combustion reactions. For example, when the front propagation was slowed by the presence of shaley layers, a significant mass of coke was deposited, which resulted in lower recovery factor being achieved by the combustion process. Also, in some scenarios a higher frontal advance rate

led to more coke being produced and deposited. This was mainly observed when the fire front changed from moving quickly in a lateral direction to a slower vertical propagation. Also, the comparison between horizontal and vertical well scenarios showed that the later scenario usually produced *more* coke in place as a result of the *slow* propagation of the front associated with the way the wells were located and completed in this scenario.

At the end, it is important to highlight that, the recovery factors in this study were obtained using the 2D cross sectional simulation model which means that these factors are not representative the 3D effects and areal sweep efficiency. Therefore, they cannot be used to estimate the field recovery factor in the case of applying in-situ combustion process without further investigation using a 3D simulation model.

7.4 Recommendations

It is suggested that future work should consider:

- Development of kinetic reactions model based on experiments on the reservoir rock and fluid properties. This model would help to determine more accurate in-situ combustion process performance compared to the literature-based kinetics model used in this study.
- Further investigation of the effect of numerical dispersion on the upscaling of the kinetic model when simulating the in-situ combustion process.
- Evaluation of the combustion process when using enriched air injection, where a higher percentage of oxygen is used instead of the normal 21% oxygen used in this work. Also, an investigation of the combustion process performance is required where heat losses to the overburden and underburden are considered.
- Investigation of near wellbore front behaviour using discretized well modelling option available in STARS. Understanding of the front and its fluid behaviour near the wellbore will allow for better design of well completions.
- The sensitivity calculations in this study showed that, in general, the amount of coke in place increased as the front velocity decreased. A development of experimental work is required to investigate the relation between the change of the velocity and the amount of coke produced by the fire front.

- An experimental work to determine the relationship between the amount of coke deposited in the formation, as a result of the combustion process, and the formation permeability.
- Further investigation of the effect of heterogeneity on the in-situ combustion process is required, especially for fractured systems and random permeability distribution. In the case of fracture system, this will allow assessment of process performance in dual porosity and dual permeability systems. Also, it will help researchers to find possible ways to overcome the effect of heterogeneity and enhance the process performance.
- With better computing and data storage resources, a 3D simulation model is required. This would provide more accurate behaviour of the combustion process. Also, it would give a clearer view to the feasibility of implementing in-situ combustion, and provide a more accurate figure for the expected recovery factor.

Bibliography

ABOLHOSEINI, H. (2004) "Study on Ultimate Heavy Oil Recovery From Zaqeh Field in S. W. of Iran". SPE88861 presented at the 11th Abu Dhabi international Petroleum Exhibition and Conference. Abu Dhabi, U.A.E., 10-13 October.

ABU-KHAMSIN, S. A., BRIGHAM, W. E. & RAMEY JR, H. J. (1988) "Reaction Kinetics of Fuel Formation for In-Situ Combustion", SPE15736. SPE Reservoir Engineering, 1308-1316.

AKIN, S., BAGCI, S. & KOK, M. V. (2000) "Dry Forward Combustion with Diverse Well Configurations". SPE62551 presented at the 2000 SPE/AAGP Western Regional Meeting. Long Beach, California, 19-23 June.

AKRAM, F. (2008) "Effects of Well Placement and Intelligent Completions on SAGD in a Full-Field Thermal-Numerical Model for Athabasca Oil Sands". SPE117704 presented at the 2008 SPE International Thermal Operations and Heavy Oil Symposium. Calgary, Alberta, Canada, 20-23 October.

AL-ABRI, Y., LAMERS, E., ROSS, L., ZON, C. V. D., HERN, C., RIETHMULLER, G., CONSTANT, S. & EJIOGU, C. (Dec 2004) "Nimr A Field Development Plan Nimr Cluster, South Oman". Petroleum Development of Oman.

AL-KHARUSI, H. A. (1997) "Planning Optimal Horizontal Wells in Clastic Reservoirs: Case Histories from the South Oman Nimr Field". SPE37808 presented at the 1997 SPE 10th Middle East Oil Show & Conference. Manama, Bahrain, 15-18 March.

AL-WADHAHI, M., BOUKADI, F. & AL-BEMANI, A. (2005) "Nimr EOR Identification - Phase1". Department of Petroleum and Chemical Engineering, Sultan Qaboos University.

ALBAHLANI, A. M. & BABADAGLI, T. (2008) "A Critical Review of the Status of SAGD: Where Are We and What is Next?" SPE113283 presented at the 2008 SPE Western Regional and Pacific Section AAPG Joint Meeting. Bakerfield, California, U.S.A., 31 March-2 April.

ALEXANDER, J. D., MARTIN, W. L. & DEW, J. N. (1962) "Factors Affecting Fuel Availability and Composition During In Situ Combustion", SPE296. Journal of Petroleum Technology, 1154-1164.

ALGHUFAILI, A. (2008) "Impact of Grid Resolution on Modelling of Heavy Oil Recovery". Institute of Petroleum Engineering. Edinburgh, Heriot-Watt University.

ALKHELAIWI, F. & DAVIES, D. R. (2007) "Inflow Control Devices: Application and Value Quantification of a Developing Technology". SPE108700 presented at the 2007 International Oil Conference and Exhibition in Mexico. Veracruz, Mexico, 27-30 June.

AWOLEKE, O. G. (2007) "An Experimental Investigation of In-situ Combustion in Heterogeneous Media". SPE113022 presented at the 2007 SPE International Student Paper Contest at the SPE Annual Technical Conference and Exhibition. Anaheim, California, 11-14 November.

BAGCI, S. (2005) "Effect of Clay Content on Combustion Reaction Parameters". Energy Sources, 579-588.

BAGCI, S. & AYBAK, T. (2000) "A Laboratory Study of Combustion Override Split-Production Horizontal Well (COSH) Process". Journal of Canadian Petroleum Technology, August 2000, Volume 39, No. 8, 42-50.

BELGRAVE, J. D. M., MOORE, R. G., URSENBACH, M. G. & BENNION, D. W. (1993) "A Comprehensive Approach to In-Situ Combustion Modeling", SPE20250. SPE Advanced Technology Series, Volume 1, No. 1, 98-107.

BOBERG, T. C. (1988) "Thermal Methods of Oil Recovery", John Wiley & Sons.

BRESTON, J. N. (1958) "Oil Recovery by Heat From In Situ Combustion", SPE1087-G. Journal of Petroleum Technology, 13-17.

BROOKS, A. D., DE ZWART, A. H., BYCHKOV, A., AL-AZRI, N., HERN, C. Y., AL-AJMI, W. & MUKMIN, M. (2010) "Evaluation of EOR Techniques for Medium-Heavy Oil Reservoirs with a Strong Bottom Aquifer In South Oman". SPE129149 presented at the SPE EOR Conference at Oil & Gas West Asia. Muscat, Oman, 11-13 April.

BURGER, J., SOURIEAU, P. & MCOMBARNOUS, M. (1985) "Thermal Methods of Oil Recovery", Paris, Editions Technip.

BURGER, J. G. & SAHUQUET, B. C. (1972) "Chemical Aspects of In-Situ Combustion- Heat of Combustion and Kinetics", SPE3599. Society of Petroleum Engineers Journal, 410-422.

BUTLER, R. M. (1994) "Horizontal Wells for the Recovery of Oil, Gas and Bitumen", Petroleum Society, Canadian Institute of Mining, Metallurgy & Petroleum, Calgary.

CAMY, J. P. & EMANUEL, A. S. (1977) "Effect of Grid Size in the Compositional Simulation of CO2 Injection". SPE6894 presented at the 52nd Annual Fall Technical Conference and Exhibition of the Society of Petroleum Engineers of AIME. Denver, Colorado, 9-12 October.

CARCOANA, A. (1990) "Results and Difficulties of the World's Largest In-Situ Combustion Process: Suplacu de Barcau Field, Romania". SPE20248 presented in the SPE/DOE 7th Symposium on Enhanced Oil Recovery. Tulsa, OK, U.S.A., 22-25 April.

CHENGHUI, L., SHAOCHI, L., YAPING, C., JUNRONG, L. & QINLIN, W. (1998) "Study of Combustion Override, Split-Production Horizontal Well COSH Process in a Deep Extra Heavy Oil Reservoir of Leng41 Block in Liaohe Oil Field". The 7th UNITAR Conference on Heavy Crude and Tar Sands. Beijing, China.

CHICUTA, A. M. & TREVISAN, O. V. (2009) "Experimental Study on In-Situ Combustion of Brazilian Heavy Oil". SPE122036 presented at the 2009 SPE Latin American and Caribbean Petroleum Engineering Conference. Cartagena, Colombia, 31 May -3 June.

CHRISTENSEN, J. R., DARCHE, G., DECHELETTE, B. & SAMMON, P. H. (2004) "Applications of dynamic gridding to thermal simulations". SPE86969 presented at the SPE International Thermal Operations and Heavy Oil Symposium and Western Regional Meeting. Bakerfield, California, U.S.A., 16-18 March.

CHU, C. (1977) "A Study of Fireflood Field Projects", SPE5821. Journal of Petroleum Technology, 111-120.

CHU, C. (1982) "Current In-Situ Combustion Technology". SPE9994 presented in the 1982 SPE International Petroleum Exhibition and Technical Symposium. Beijing, China, 18-26 March.

CMG (2006) STARS Manual, Appendix D5. 2006.1 Revision 6 ed. Calgary, Canada.

COATES, R., LORIMER, S. & IVORY, J. (1995) "Experimental and numerical Simulations of a Novel Top Down In-Situ Combustion Process". SPE30295 presented in the International Heavy Oil Symposium. Calgary, Alberta, Canada, 19-21 June.

COATES, R. & TURTA, A. (2004) "Feasibility of Applying The In Situ Combustion (ISC) Process in Nimr-E Reservoir". Alberta Research Council.

CRISTOFARI, J., CASTANIER, L. M. & KOVSCEK, A. R. (2006) "Laboratory Investigation of the Effect of Solvent Injection on In-Situ Combustion". SPE99752 presented at the Fifteenth SPE Improved Oil Recovery Symposium in U.S.A. Tulsa, Oklahoma, U.S.A., 22-26 April.

CUNHA, L. B. (2005) "Recent In-Situ Oil Recovery-Technologies for Heavy-and Extraheavy-Oil Reserves". SPE94986 presented in the 2005 SPE Latin American and Caribbean Petroleum Engineering Conference. Rio de Janerio, Brazil, 20-23 June.

CURTIS, J. H. (1989) "Performance Evaluation of the MOCO In-Situ Combustion Project, Midway-Sunset Field". SPE18809 presented in the SPE California Regional Meeting. Bakersfield, California, U.S.A., 5-7 April.

DAYAL, H. S., BHUSHAN, B. V., MIRTA, S., SINHA, S. K. & SUR, S. (2010) "In-Situ Combustion: Opportunities and Anxieties". SPE126241 presented at the SPE Oil and Gas India Conference and Exhibition. Mumbai, India, 20-22 January.

DE ZWART, A. H., BAKKER, P., GLANDT, C. A., BROOKS, A. D. & VAN DROP, J. (2008) "A Thermal Recovery Method for Medium-Heavy Oil Reservoirs". SPE112876 presented at the 2008 SPE North Africa Technical Conference and Exhibition. Marrakech, Morocco, 12-14 March.

EMMONS, F. R., HUDSPETH, L. D., CLANCY, J. P., ZORNES, D. R. & PHILCOX, J. E. (1986) "Nitrogen Management at The East Binger Unit Using an Integrated Cryogenic Process". SPE15591 presented in the 61st Annual Technical Conference and Exhibition of the SPE. New Orieans, LA, U.S.A., 5-8 October.

ENERGY, H. (2006) "In Situ Production Technologies". published as a supplement to Hart Energy publications E&P Magazine and Oil and Gas Investor, July. Available at http://www.heavyoilinfo.com/feature_items/e-p_heavyoil_article-1.pdf/download, accessed February 16, 2010.

FAROUQ ALI, S. M. (1983) "Effect of Bottom Water and Gas Cap in Thermal Recovery". SPE11732 presented in the 53rd Annual California Regional Meeting of the Society of Petroleum Engineers of AIME. Ventura, California, U.S.A., 23-25 March.

FASSIHI, M. R., BRIGHAM, W. E. & RAMEY JR, H. J. (1980a) "Reaction Kinetics of In-Situ Combustion: Part 1-Observations". SPE8907 presented in the 1980 California Regional Meeting. Los Angeles, U.S.A., 9-11 April.

FASSIHI, M. R., BRIGHAM, W. E. & RAMEY JR, H. J. (1980b) "Reaction Kinetics of In-Situ Combustion: Part 2-Modeling". SPE9454 presented in the 1980 SPE Annual Technical Conference and Exhibition. Dallas, U.S.A., 21-24 September.

GADELLE, C. P., BURGER, J. G., BARDON, C. P., MACHEDON, V., CARCOANA, A. & PETCOVICI, V. (1981) "Heavy-Oil Recovery by In-Situ Combustion-Two Filed Cases in Romania", SPE8905. Journal of Petroleum Technology, 2057-2066.

GATES, C. F. & RAMEY JR, H. J. (1980) "A Method for Engineering In-Situ Combustion Oil Recovery Projects", SPE7149. Journal of Petroleum Technology, 285-294.

GATES, C. F. & SKLAR, I. (1971) "Combustion as a Primary Recovery Process-Midway Sunset Field", SPE3054. Journal of Petroleum Technology, 981-986.

GAVIRIA, F., SANTOS, R., RIVAS, O. & LUY, Y. (2007) "Pushing the Boundaries of Artificial Lift Applications: SAGD ESP Installations in Canada". SPE110103 presented at the 2007 SPE Annual Technical Conference and Exhibition. Anaheim, California, 11-14 November.

GHARSALLA, M. M. & ELGHMARI, M. B. (2008) "Multi Lateral Horizontal Well Application for Improving the Oil Recovery of a Mature Field, Intisar N. Field, Concession 103-Libya". SPE112125 presented at the 2008 SPE North Africa Technical Conference and Exhibition. Marrakech, Morocco, 12-14 March.

GOODLETT, G. O., HONARPOUR, M. M., CHUNG, F. T. & SARATHI, P. S. (1986) "The Role of Screening and Laboratory Flow Studies in EOR Process Evaluation". SPE15172 presented in the Rocky Mountain Regional Meeting of the SPE. Billings, MT, U.S.A., 19-21 May.

GREAVES, M., REN, S. R. & XIA, T. X. (1999) "New Air Injection Technology for IOR Operations in light and Heavy Oil Reservoirs". SPE57295 presented in the 1999 SPE Asia Pacific Improved Oil Recovery Conference. Kuala Lumpur, Malaysia, 25-26 October.

GREAVES, M., TUWIL, A. A. & BAGCI, A. S. (1993) "Horizontal producer wells in in situ combustion (ISC) processes". The Journal of Canadian Petroleum Technology, April 1993, Volume 32, No. 4, 58-67.

GREAVES, M., XIA, T. X., TURTA, A. T. & AYASSE, C. (2000) "Recent Laboratory Results of THAI and its Comparison with Other IOR Processes". SPE59334 presented in the 2000 SPE/DOE Improved Oil Recovery Symposium. Tulsa, OK, U.S.A., 3-5 April.

GREEN, D. W. & WILLHITE, G. P. (1998) "Enhanced Oil Recovery", SPE.

GUTIERREZ, D., MOORE, R. G., MEHTA, S. A., URSENBACH, M. G. & SKOREYKO, F. (2009) "The Challenge of Predicting Field Performance of Air Injection Projects Based on Laboratory and Numerical Modelling". Journal of Canadian Petroleum Technology, April 2009, Volume 48, No. 4, 23-34.

HALLIBURTON (2009) "Steam Valve: Optimize Production in Heavy Oil Reservoirs". Halliburton website http://www.halliburton.com/ps/Default.aspx?navid=1317&pageid=2602&prodid=PRN%3a%3aK4DJ6ELPT.

HAMMAWA, H., ABU, I. I., MEHTA, S. A., MOORE, R. G., URSENBACH, M. G. & ZALEWSKI, E. (2007a) "A Combustion Tube Test Report, Tube Test No. 345". Calgary, Canada, University of Calgary.

HAMMAWA, H., ABU, I. I., MEHTA, S. A., MOORE, R. G., URSENBACH, M. G. & ZALEWSKI, E. (2007b) "A Combustion Tube Test Report, Tube Test No. 347". Calgary, Canada, University of Calgary.

HELLER, J. P. & TABER, J. J. (1986) "Influence of Reservoir Depth on Enhanced Oil Recovery by CO2 Flooding". SPE15001 presented in the Permian Basin Oil and Gas Recovery Conference of the SPE. Midland, TX, U.S.A., 13-14 March.

HINKLE, A. & BATZLE, M. (2006) "Heavy oils: A worldwide overview". The Leading Edge, June 2006, 742-749.

HUFFMAN, G. A., BENTON, J. P., EL-MESSIDI, A. E. & RILEY, K. M. (1983) "Pressure Maintenance by In-Situ Combustion, West Heidelberg Unit, Jasper County, Mississippi", SPE10247. Journal of Petroleum Technology, 1877-1883.

ISLAM, M. R., CHAKMA, A. & FAROUQ ALI, S. M. (1989) "State-of-the-Art In-Situ Combustion Modeling and Operations". SPE18755 presented in the SPE California Regional Meeting. Bakersfield, California, U.S.A., 5-7 April.

JHA, K. N. & VERKOCZY, B. (1986) "The Role of Thermal Analysis Techniques in the In-Situ Combustion Process", SPE12677. SPE Reservoir Engineering, 329-340.

JOSHI, S. D. (1991a) "Horizontal Well Technology", Tulsa, OK, U.S.A, PennWell Books.

JOSHI, S. D. (1991b) "Thermal Oil Recovery With Horizontal Wells", SPE21751. Journal of Petroleum Technology, 1302-1304.

JU, B., DAI, S., FAN, T., WANG, X. & WU, H. (2005) "An Effective Method to Improve recovery of Heavy Oil Reservoir with Bottom water drive". IPTC1052 presented in the International Petroleum Technology Conference. Doha, Qatar, 21-23 November.

KISMAN, K. E. & LAU, E. C. (1994) "A New Combustion Process Utilizing Horizontal Wells and Gravity Drainage". Journal of Canadian Petroleum Technology, March 1994, Volume 33, No. 3, 39-45.

KOEDERITZ, L. F. "Relative Permeability Suite". 02038 ed. University of Missouri-Rolla, Missouri, U.S.A.

KRAGAS, T. K., SPEK, A. V. D. & AL HASHMI, K. M. (2002) "Field Trial of a Downhole, Fibre Optic, Two-phase Flowmeter in PDO's Nimr Field". SPE78306 presented at the SPE 13th European Petroleum Conference. Aberdeen, Scotland, 29-31 October.

KRISTENSEN, M. R., GERRITSEN, M. G., THOMSEN, P. G., MICHELSEN, M. L. & STENBY, E. H. (2008) "Impact of Phase Behaviour Modelling on In-situ Combustion Process Performance". SPE113947 presented at the 2008 SPE/DOE Improved Oil Recovery Symposium. Tulsa, Oklahoma, 19-23 April.

KUMAR, M. (1987) "Simulation and Laboratory In-Situ Combustion Data and Effect of Process Variations". SPE16027 presented at the Ninth SPE Symposium on reservoir Simulation. San Antonio, Taxes, 1-4 February.

KUMAR, M. (1991) "Heidelberg In-Situ Combustion Project", SPE16724. SPE Reservoir Engineering, 46-54.

LAKE, L. W. (1989) " Enhanced Oil Recovery", Prentice Hall, Amsterdam.

LANIER, D. (1998) "Heavy Oil- A Major Energy Source fro the 21st Century". The 7th UNITAR Conference on Heavy Crude and Tar Sands. Beijing, China.

LATIL, M. (1980) "Enhanced Oil Recovery", Paris, Editions Technip.

LAU, E. C. (2001) "Basal Combustion A Recovery Technology for Heavy Oil Reservoirs Underlain by Bottom Water". Journal of Canadian Petroleum Technology, August 2001, Volume 40, No.8, 29-36.

LAU, E. C., GOOD, W. K. & KANAKIA, V. (1995) "COSH Performance and Economic Predictions fro Six Filed Types in Western Canada". SPE30296 presented in the International Heavy Oil Symposium. Calgary, Alberta, Canada, 13-21 June.

LETHIEZ, P. A. & LEMONNIER, P. A. (1990) "An In-Situ Combustion Reservoir Simulator With a New Representation of Chemical Reactions", SPE17416. SPE Reservoir Engineering, 285-292.

LEEMPUT, B. V. D., GOODLAD, S., WEYRETER, C., MCKIM, N. & VERBRUGGEN, R. (1997) "Multiple reservoir models and multiple history matches: tools for finding reserves in a complex mature field". SPE38850 presented at the 1997 SPE Annual Technical Conference and Exhibition. San Antonio, Taxes, 5-8 October.

LIN, C. Y., CHEN, W. H. & CULHAM, W. E. (1987) "New Kinetic Models for Thermal Cracking of Crude Oils in In-situ Combustion Processes", SPE 13074. SPE Reservoir Engineering, 54-66.

LINDLEY, J. R. (1986) "NIPER's 1986 Enhanced Oil Recovery". The U.S. Department of Energy (DOE) EOR research program.

MAMORA, D. D. (1995) "New Findings in Low-Temperature Oxidation of Crude Oil". SPE29324 presented in the SPE Asia Pacific Oil & Gas Conference. Kuala Lumpur, Malaysia, 20-22 March.

MANRIQUE, J. F. (1996) "Optimization of Thermal Processes Through Combined Application of Horizontal Wells and Hydraulic Fracturing Technology". SPE37090 presented in the 2nd International Conference and Exhibition on Horizontal well Technology. Calgary, Alberta, Canada, 18-20 November.

MARJERRISON, D. M. & FASSIHI, M. R. (1992) "A Procedure for Scalling Heavy-Oil Combustion Tube Results to a Field Model". SPE24175 presented at the SPE/DOE Eighth Symposium on Enhanced Oil Recovery. Tulsa, Oklahoma, 22-24 April.

MEDEIROS, R. S., BISWAS, D. & SURYANARAYANA, P. V. (2004) "Impact of Thief Zone Identification and Shut-off on Water Production in Nimr Field". SPE91665 presented at the 2004 SPE/IADC Underbalanced Technology Conference and Exhibition. Houston, Texas, U.S.A., 11-12 October.

MOORE, R. G., LAURESHEN, C. J., URSENBACH, M. G., MEHTA, S. A. & BELGRAVE, J. D. M. (1999) "A Canadian Prospective on In Situ Combustion". Journal of Canadian Petroleum Technology, Special Edition 1999, Volume 38, NO. 13, 1-8.

NASR, T. N. & AYODELE, O. R. (2005) "Thermal Techniques for the Recovery of Heavy Oil and Bitumen". SPE97488 presented in the SPE International Improved Oil Recovery Conference in Asia Pacific. Kuala Lumpur, Malaysia, 5-6 December.

NELSON, T. W. & MCNIEL, J. S. (1961) "How to Engineer an In Situ Combustion Project". Oil and Gas Journal, (June 5, 1961), pp58-65.

NORTHROP, P. S., WILSON, J. L. & SOUSTEK, P. G. (1994) "Study of a Mature Fireflood: MOCO-T". SPE27889 presented at the Western Regional Meeting. Long Beach, California, 23-25 March.

ONYEKONWU, M. O., PANDE, K., RAMEY JR., H. J. & BRIGHAM, W. E. (1986) "Experimental and Simulation Studies of Laboratory In-Situ Combustion Recovery". SPE15090 presented at the 56th California Regional Meeting of the Society of Petroleum Engineers. Oakland, California, 2-4 April.

OPATA, J. T. (2008) "In-Situ Combustion - A Literature Review and Range of Applicability Evaluation". Institute of Petroleum Engineering. Edinburgh, Heriot-Watt University.

PANAIT-PATICA, A., SERBAN, D. & LLIE, N. (2006) "Suplacu de Barcau Field-A Case History of a Success in-Situ Combustion Exploitation". SPE100346 presented in the SPE Europec/EAGE Annual Conference and Exhibition. Vienna, Austria, 12-15 June.

PERRY, C. W. (1981) "The Economics of Enhanced Oil Recovery and Its Position Relative to Synfuels". SPE9562 presented in the SPE Economics and Evaluation Symposium. Dallas, U.S.A., 25-27 February.

PRATS, M. (1982) "Thermal Recovery", SPE, New York.

QIN, W. & WOJTANOWICZ, A. K. (2009) "Water Problems and Control Techniques in Heavy Oil With Bottom Aquifers". SPE125414 presented at the 2009 Americas E&P Environmental & Safety Conference. San Antonio, Texas, U.S.A., 23-25 March.

RAGHUNATHAN, M., GOKTUG, E., LIB, O., MOHR, P., GARIMELLA, S., SUTTON, D., VINOD, W. & PRADEEP, D. (Sep 2006) "Nimr E Field Development Plan Nimr Cluster, South Oman". Petroleum Development of Oman.

RANGEL-GERMAN, E. R., CAMACHO-ROMERO, S. & THEOKRITOFF, W. (2006) "Thermal Simulation and Economic Evaluation of Heavy-Oil Projects". SPE104046 presented in the First International Oil Conference and Exhibition in Mexico. Cancun, Mexico, 31 August-2 September.

ROBERTS, M. J. & TOLSTYKO, M. (1997) "Multi Lateral Rewards in Tern Field". SPE38496 presented at the 1997 Offshore Europe Conference. Aberdeen, Scotland, 9-18 September.

ROJAS, J., RUIZ, J. & VARGAS, J. (2010) "Numerical Simulation of an Enhanced Oil Recovery Process of Toe to Heel Air Injection (THAI)". SPE129215 presented at the SPE EOR Conference at Oil & Gas West Asia. Muscat, Oman, 11-13 April.

SAMMON, P. H. (2003) "Dynamic Grid Refinement and Amalgamation for Compositional Simulation". SPE79683 presented at the SPE Reservoir Simulation Symposium. Houston, Texas, U.S.A., 3-5 February.

SARATHI, P. S. (1998) "Nine Decades of Combustion Oil Recovery-A Review of In Situ Combustion History and Assessment of Geologic Environments on Project Outcome". The 7th UNITAR Conference on Heavy Crude and Tar Sands. Beijing, China.

SUN, K., CONSTANTIN, J. & COULL, C. (2008) "Interaction Between Intelligent Well Applications and Reservoir Management-A Comprehensive Thermal Modeling Technology for IWS Well". SPE115102 presented at the 2008 SPE Annual Technical Conference and Exhibition. Denver, Colorado, U.S.A., 21-24 September.

TABASINEJAD, F., KARRAT, R. & VOSSOUGHI, S. (2006) "Feasibility Study of In-Situ Combustion in Naturally Fractured Heavy Oil Reservoirs". SPE103969 presented in the First International Oil Conference and Exhibition in Mexico. Cancun, Mexico, 31 August-2 September.

TABER, J. J., MARTIN, F. D. & SERIGHT, R. S. (1996) "EOR Screening Criteria Revisited- Part 1: Introduction to Screening Criteria and Enhanced Recovery Field Projects". SPE35385 presented in the 1996 SPE/DOE Improved Oil Recovery Symposium. Tulsa, Oklahoma, U.S.A., 21-24 April.

TURTA, A. T., CHATTOPADHYAY, S. K., BATTACHARYA, R. N., CONDRACHI, A. & HANSON, W. (2007) "Current Status of Commercial In Situ Combustion Projects Worldwide". Journal of Canadian Petroleum Technology, November 2007, Volume 46, No. 11, 8-14.

TURTA, A. T., COATES, R. & GREAVES, M. (2009) "In-Situ Combustion in the Oil Reservoirs Underlain by Bottom Water. Review of the Field and Laboratory Tests". (Paper 2009-150) prepared to be presented at the Canadian International Petroleum Conference (CIPC) 2009. Calgary, Alberta, Canada, 16-18 June.

TURTA, A. T. & SINGHAL, A. K. (2004) "Overview of Short-Distance Oil Displacement Processes". Journal of Canadian Petroleum Technology, February 2004, Volume 43, No. 2, 29-38.

URSENBACH, M. G., MOORE, R. G. & MEHTA, S. A. (2010) "Air Injection in Heavy Oil Reservoirs - A Process Whose Time Has Come (Again)". Journal of Canadian Petroleum Technology, January 2010, Volume 49, No. 1, 48-54.

VOSSOUGHI, S., WILLHITE, G. P., KRITIKOS, W. P., GUVENIR, I. M. & EL SHOUBARY, Y. (1982) "Automation of In-Situ Combustion Tube and Study of the Effect of clay on the Is-Situ Combustion Process", SPE10320. Society of Petroleum Engineers Journal, 493-502.

WHITE, P. D. & MOSS, J. T. (1983) "Thermal Recovery Methods", Tulsa, OK, PennWell Books.

WU, C. H. (1977) "A Critical Review of Steamflood Mechanisms". SPE6550 presented in the 1977 47th Annual California Regional Meeting of the Society of Petroleum Engineers of AIME. Bakersfield, California, U.S.A., 13-15 April.

WU, C. H. & FULTON, P. F. (1971) "Experimental Simulation of the Zones Preceding the Combustion Front of an In-Situ Combustion Process", SPE2816. Society of Petroleum Engineers Journal, 38-46.

XIA, T. X. & GREAVES, M. (2000) "Upgrading Athabasca Tar Sand Using Toe-to-Heel Air Injection". SPE65524 presented in the 2000 SPE/Petroleum Society of CIM International Conference on Horizontal Well Technology. Calgary, Alberta, Canada, 6-8 November.

XIA, T. X. & GREAVES, M. (2001) "Downhole Upgrading Athabasca Tar Sand Bitumen Using THAI-SARA Analysis". SPE69693 presented in the 2001 SPE

International Thermal Operations and Heavy Oil Symposium. Porlamar, Margarita Island, Venezuela, 12 March.

XIA, T. X. & GREAVES, M. (2002) "Injection Well-Producer Well Combinations in THAI 'Toe-to-Heel Air Injection' ". SPE75137 presented in the SPE/DOE Improved Oil Recovery Symposium. Tulsa, Oklahoma, U.S.A., 13 - 17 April.

YANNIMARAS, D. V. & TIFFIN, D. L. (1995) "Screening of oils for In-Situ Combustion at Reservoir Conditions by Accelerating-Rate Calorimetry", SPE27791. SPE Reservoir Engineering, 36-39.

YOUNGREN, G. K. (1980) "Development and Application of an In-Situ Combustion Reservoir Simulator", SPE7545. Society of Petroleum Engineers Journal, 39-51.